Modulation of Proton Transfer and Charge Transfer Processes in few Azole Derivatives by Homogeneous and Heterogeneous Media

A dissertation

As partial fulfilment for the degree of

Doctor of philosophy in Chemistry

By

Minati Das
Roll No. 146122004

Department of Chemistry

Indian Institute of Technology Guwahati

Guwahati 781039

Assam, India

Statement

The work contained in this thesis entitled "**Modulation of Proton Transfer and Charge Transfer Processes in few Azole Derivatives by Homogeneous and Heterogeneous Media**" is the outcome of the research work carried out by me under the supervision of Prof. G Krishnamoorthy, Department of Chemistry, Indian Institute of Technology Guwahati, India.

In the present thesis the general practice of the scientific observations is reported and whenever needed, the work on the findings of other investigations are described and thus due acknowledgements have been made. This work has not been submitted elsewhere for the award of any degree.

22nd April, 2020

Minati Das

Department of Chemistry,
IIT Guwahati
Guwahati, Assam, India-781039

Dr. G. Krishnamoorthy
Associate Dean, Research & Development
& Professor of Chemistry

INDIAN INSTITUTE OF TECHNOLOGY GUWAHATI
Guwahati 781 039, Assam, India
Tel: +91 – 0361 – 258 2315 (W), 258 4315 (H)
Fax: +91 – 0361 – 2582349
E-mail: gkrishna@iitg.ernet.in, gkrishna_2000@yahoo.com

Certificate

It is certified that the work contained in thesis entitled "**Modulation of Proton Transfer and Charge Transfer Processes in few Azole Derivatives by Homogeneous and Heterogeneous Media**" by Minati Das is an authentic record of the results obtained from the research work carried out under my supervision in the Department of Chemistry, Indian Institute of Technology Guwahati, India.

Guwahati
22 April 2020

G. Krishnamoorthy

Dedicated

to

My Family

ACKNOWLEDGEMENT

First and foremost, I admire and thank the Almighty God, for His showers of blessings throughout my research work to complete the research successfully. I am overwhelmed in all humbleness and gratefulness to acknowledge my depth to all those who have helped me to put this thesis.

I would like to express my special thanks of gratitude to my thesis supervisor Prof. G Krishnamoorthy for giving me the opportunity to do research and providing invaluable guidance in all the time of research and writing this thesis. His immense knowledge, sincerity, enthusiasm and motivation have profoundly inspired me. I am extremely grateful for what he has offered me. It was a great privilege and honor to work and study under his guidance.

I would like to thank my doctoral committee members, Prof. Anil Kumar Saikia, Prof. Mohammad Qureshi, Department of Chemistry and Prof. K. Anki Reddy, Department of Chemical Engineering, for their encouragement, valuable suggestions and efforts during my thesis work. I wish to thank Prof. A. S. Achalkumar and Dr. Akshai Kumar A S, Department of Chemistry, for their valuable help during the course of my thesis work.

My heartfelt thanks to Dr. Saugata Sahu, Dr. Santosh K Behera, Dr. Ashim Malakar and Dr. Francis A S Chipem, alumni from our research group for their endless help in learning the basic concepts, experiments and computations, for their encouraging and stimulating discussions all the way through my PhD work. I express my special thanks to Ila for her genuine help and support in research and in every single need of mine and also for all the fun we have had during this PhD period. I am also thankful to Mongoli for helping me enormously in my research work. I thank my fellow lab mates Himadree, Aditya, Arup and Ashish for their incessant help in the lab. I like to thank my IIT Guwahati friends for making my stay in this beautiful campus unforgettable. Also I wish to thank my all other friends since my childhood for their constant love and encouragement.

I wish to thank all the faculty and staff members of Department of Chemistry and Central Instruments Facility, IIT Guwahati, for their supports and co-operations during all this time.

I am extremely grateful to my parents for their love, prayers, caring and sacrifices for educating and preparing me for my future. I am very much thankful to my brother for his love, understanding, prayers and continuing support to complete this research work. Also I express my thanks to other members of my family.

Finally, my thanks go to all the people who have supported me to complete the research work directly or indirectly.

Minati Das

SYNOPSIS

Modulation of Proton Transfer and Charge Transfer Processes in few Azole Derivatives by Homogeneous and Heterogeneous Media

Investigations on excited state intramolecular proton transfer (ESIPT), twisted intramolecular charge transfer (TICT) etc. leads to the new generation of fluorescence molecules for variety of applications in different field. ESIPT and TICT processes result in red shifted emission. ESIPT process happens in intramolecular hydrogen-bonded molecules. The acidity of the acidic group and basicity of basic group increases upon photoexcitation which results in PT. The process produces a keto tautomer with different electronic structure from the original excited enol state. The excited keto relaxes to the ground state radiatively. The emission that occurs from excited keto is known as tautomer emission and the emission that occurs from excited enol is known as normal emission. The large Stokes shift of ESIPT-active fluorophores effectively decreases self-absorption and hence plays a positive role in the emission intensity. TICT occurs upon photoexcitation in molecules that usually consist of a donor and an acceptor part linked by a single bond. In polar environments, such fluorophores upon excitation undergo fast intramolecular charge transfer from the donor to the acceptor part of the molecule. This electron transfer is accompanied by twisting of the donor around the single bond and produces a relaxed nearly perpendicular structure. The TICT state relaxes back to the ground state either through red-shifted emission or by nonradiative relaxation. The keto emission and TICT emission rely upon the nature of the solvents and are sensitive to heterogeneous environment. Modulation of dual emission generated by ESIPT or TICT process by solvent of different polarity or by other heterogeneous environment will be interesting as this will lead to various applications. The PT and charge transfer (CT) processes in a few azole derivatives and their behaviour in different environments are explored in this thesis. The thesis is divided into eight chapters and a summary of the chapters are briefed below:

Chapter 1: Introduction

Chapter 1 gives a brief description of excited state intramolecular PT, excited state intermolecular PT and excited state intramolecular CT processes with literature survey.

Factors affecting these excited state processes are also discussed in this chapter. The motivation for the present thesis work is also presented at the end of this chapter.

Chapter 2: Materials, method and instrumentation

Chapter 2 provides the details of the materials used, the procedures followed for the synthesis of the fluorophores and silver nanoparticles, the methods used for the preparation of the samples, the analysis and calculations of the present work. The details of theoretical calculations are also discussed in this chapter. Brief descriptions about important instruments used in the work are also presented.

Chapter 3: Host-Guest Interaction aided Zn^{2+} transport by ESIPT active 2-(2'-hydroxyphenyl)benzoxazole

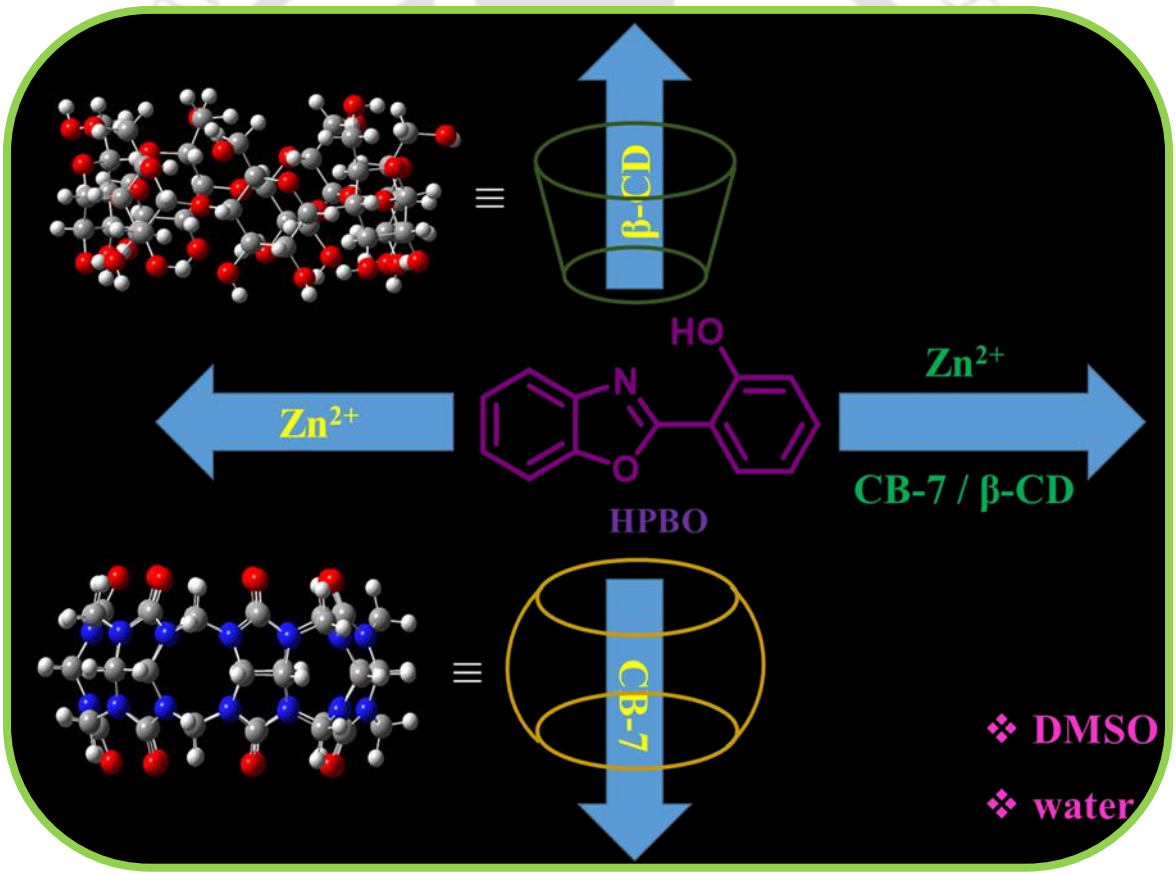

Figure 1: Graphical representation of interaction of HPBO with Zn^{2+}, β-CD and CB-7.

2-(2'-hydroxyphenyl)benzoxazole (HPBO) is a well-known ESIPT active molecule. The shorter wavelength emission of HPBO known as normal emission is obtained from the trans-enol conformer and the longer wavelength emission known as tautomer emission is

observed due to ESIPT of cis-enol. The binding sites of HPBO enables it to chelate with different metal ions (Figure 1). The fluorophore forms strong fluorescent complex with Zn^{2+} ion (Figure 2), but the ESIPT is blocked. In aqueous medium, the addition of β-CD or CB-7 breaks the HPBO–Zn^{2+} complex and encapsulate the freed fluorophore (Figure 2) and the ESIPT is recovered. Hence the photo physical properties of HPBO can be tuned by Zn^{2+} ion and these host molecules. Thus, HPBO can be used as a labeling and transport agent for Zn^{2+}.

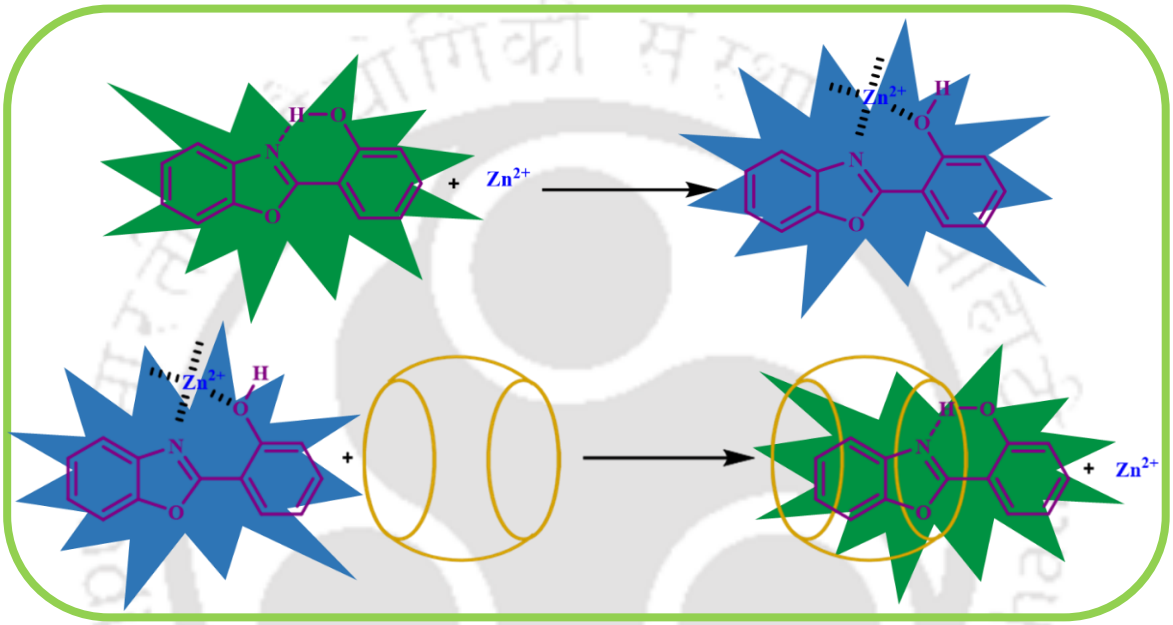

Figure 2: Schematic representation of formation of HPBO–Zn^{2+} complex and removal of Zn^{2+} by CB-7.

Chapter 4: Tweaking the proton transfer triggered proton transfer of 3,5-bis(2-hydroxyphenyl)-1H-1,2,4-triazole

3,5-Bis(2-hydroxyphenyl)-1H-1,2,4-triazole (bis-HPTA, Figure 3) has two ESIPT active sites (Figure 3). It was reported that in nonpolar solvents, initially, only the PT in α ring (ESIPT-I) is feasible and in β ring (ESIPT-II) it is not feasible due to annular tautomerism. Once the ESIPT occurs in α ring, it triggers the ESIPT in β ring giving the diketo emission and the proton transfer is leveled as proton transfer triggered proton transfer (PTTPT).

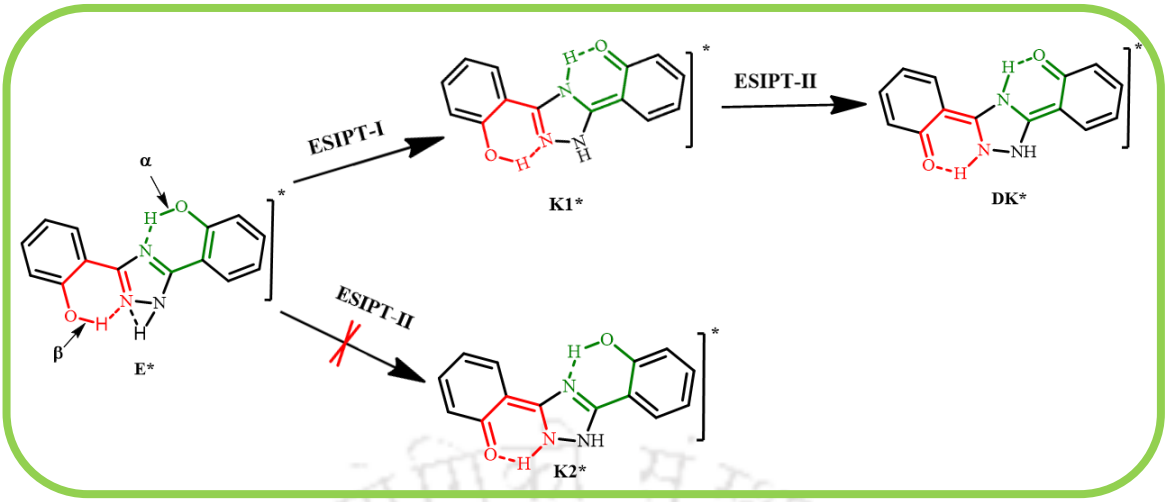

Figure 3: Proton transfer triggered proton transfer (PTTPT) in bis-HPTA-I.

N,*N*-dimethylformamide (DMF) is a good hydrogen bond acceptor. If this can inhibit the annular tautomerism, it may able to activate ESIPT-II without ESIPT-I. Therefore, the effect of DMF on the PT transfer of bis-HPTA is investigated. But, it is found that DMF alters the ground state conformers of bis-HPTA and also induces intermolecular proton transfer. The experimental and theoretical information reveals that out of 12 possible conformers of bis-HPTA, bis-HPTA-II and bis-HPTA-III are the most stable conformers in DMF. Upon excitation, the intermolecular proton transfer occurs from bis-HPTA-II to DMF molecule to form anion whereas bis-HPTA-III undergoes intramolecular proton transfer to form keto tautomer (Figure 4). Addition of silver nanoparticle reverses the conformation equilibrium that was altered by DMF. On the surface of the silver particle, the molecule again exists only as bis-HPTA-I, and upon excitation PTTPT takes place as like in other nonpolar solvents (Figure 4).

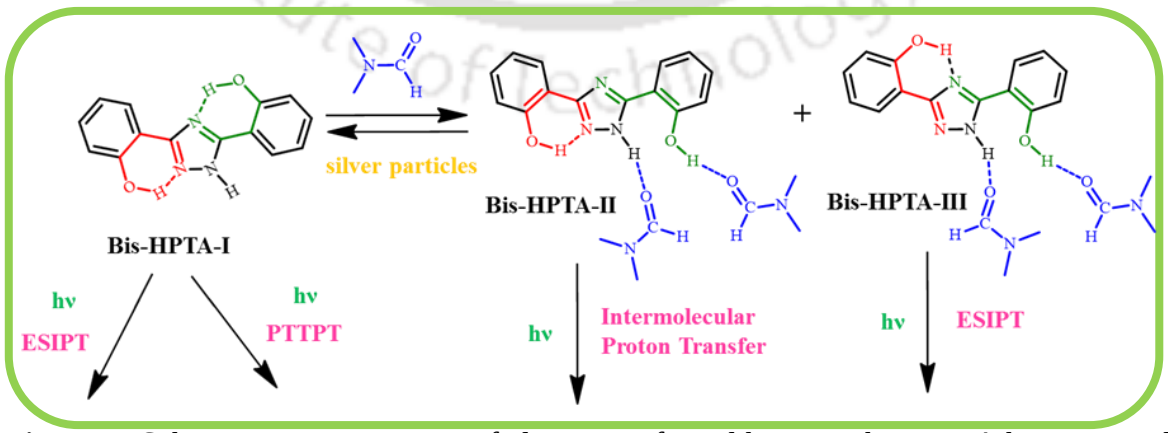

Figure 4: Schematic representation of alteration of equilibrium in bis-HPTA by DMF and restoration by silver particles.

Chapter 5: Tuning the triple emission of 2-(4′-diethylamino-2′-hydroxyphenyl)-1H-imidazo-[4,5-b]pyridine by solvent: ESIPT vs TICT

Multiple diverse reaction coordinates based photoswitches received attention in recent times. Therefore, 2-(4′-diethylamino-2′-hydroxyphenyl)-1H-imidazo-[4,5-b]pyridine (DEAHPIP-b, Chart 1) capable of both ESIPT and TICT was synthesized and studied. The hydrogen bonding capacity of the solvents was used as a tool to control the reaction path.

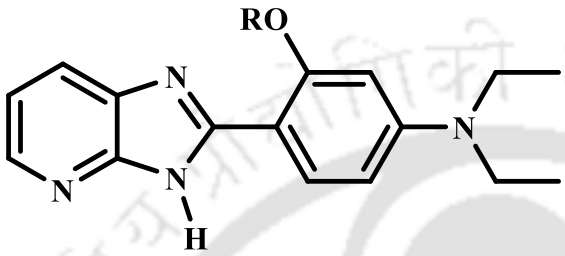

R = H **DEAHPIP-b**

R = CH3 **DEAMPIP-b**

Chart 1: Structure of 2-(4′-diethylamino-2′-hydroxyphenyl)-1H-imidazo-[4,5-b]pyridine (DEAHPIP-b) and 2-(4′-diethylamino-2′-methoxyphenyl)-1H-imidazo[4,5-b]pyridine (DEAMPIP-b).

DEAHPIP-b exists as cis-enol and trans-enol. In nonpolar solvent ether, polar aprotic solvent acetonitrile and polar protic solvents butanol, 2-propanol and 1-propanol trans-enol emits normal emission and the cis-enol undergoes ESIPT to emit tautomer emission (Figure 5). In a more polar solvent ethanol, along with the normal emission, two more emissions occur due to ESIPT and TICT (Figure 5). In polar solvent methanol, only the normal emission and TICT emission occur (Figure 5). Intermolecular proton transfer through solvents induced TICT emission in ethanol and methanol. ESIPT as well as TICT emission occurs from the same conformer, cis-enol. The methoxy derivative (DEAMPIP-b) in which the phenyl ring is twisted emits only normal emission in all these solvents. This suggests that not the phenyl ring it is the diethylamino group that is twisted to form TICT state in DEAHPIP-b. The conclusions were verified by DFT calculations.

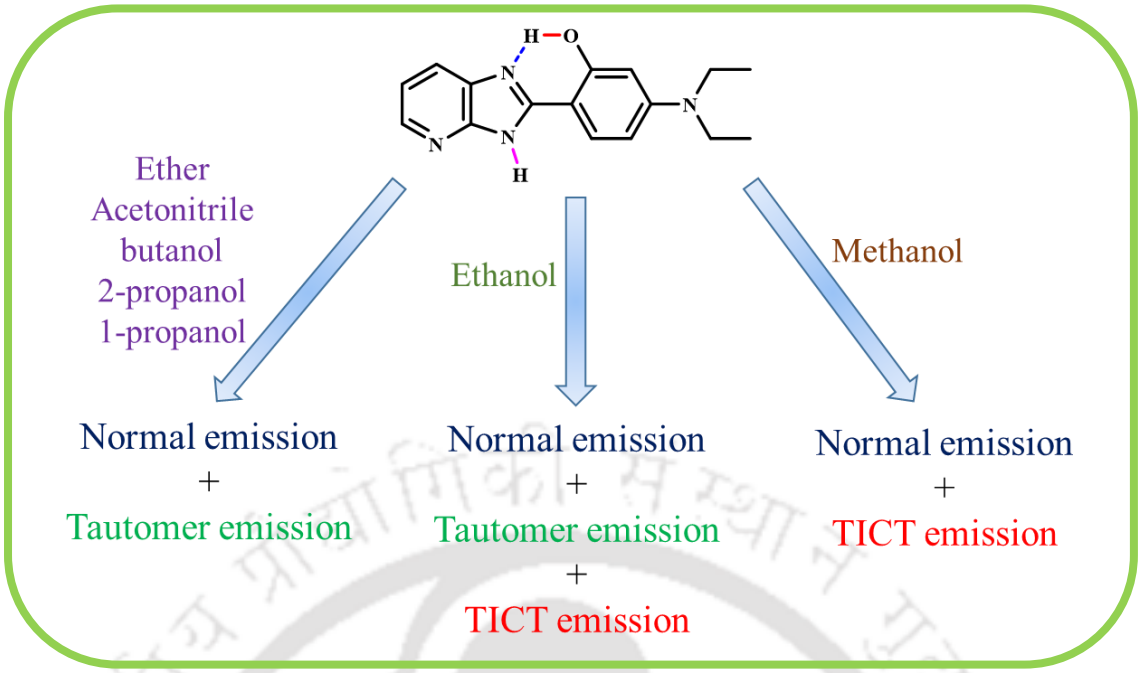

Figure 5: Mode of emissions in DEAHPIP-b in different solvents.

Chapter 6: Modulation of silver nanoparticle impelled TICT in 2-(4′-diethyl amino-2′-hydroxyphenyl)-1H-imidazo-[4,5-b]pyridine

The silver particles reverse the equilibrium between the conformers of bis-HPTA and restores the PTTPT path altered by DMF. Controlling the reaction path between the competing TICT and ESIPT paths of DEAHPIP-b was examined in DMF. In DMF, normal emission and tautomer emission occur from DEAHPIP-b. Silver nanoparticle induces the TICT emission in DEAHPIP-b (Figure 6). The ESIPT emission in DEAHPIP-b is again restored upon addition of surfactants to the nanoparticle-fluorophore complex (Figure 6). In the absence of surfactant, the fluorophore stabilizes the nanoparticle. Surfactants are known as good stabilizing agents for the silver nanoparticle. Upon addition of surfactants to the silver nanoparticle–fluorophore complex, the fluorophore become free and the emission occurs as usual in DMF. However, in DEAHPIP-b in presence of silver nanoparticle, till addition of 0.07 mM CTAB, the fluorophore remains free and exhibits ESIPT. At higher CTAB concentration, the free fluorophore remains inside the nanoparticle–CTAB composite and shows enhanced ESIPT.

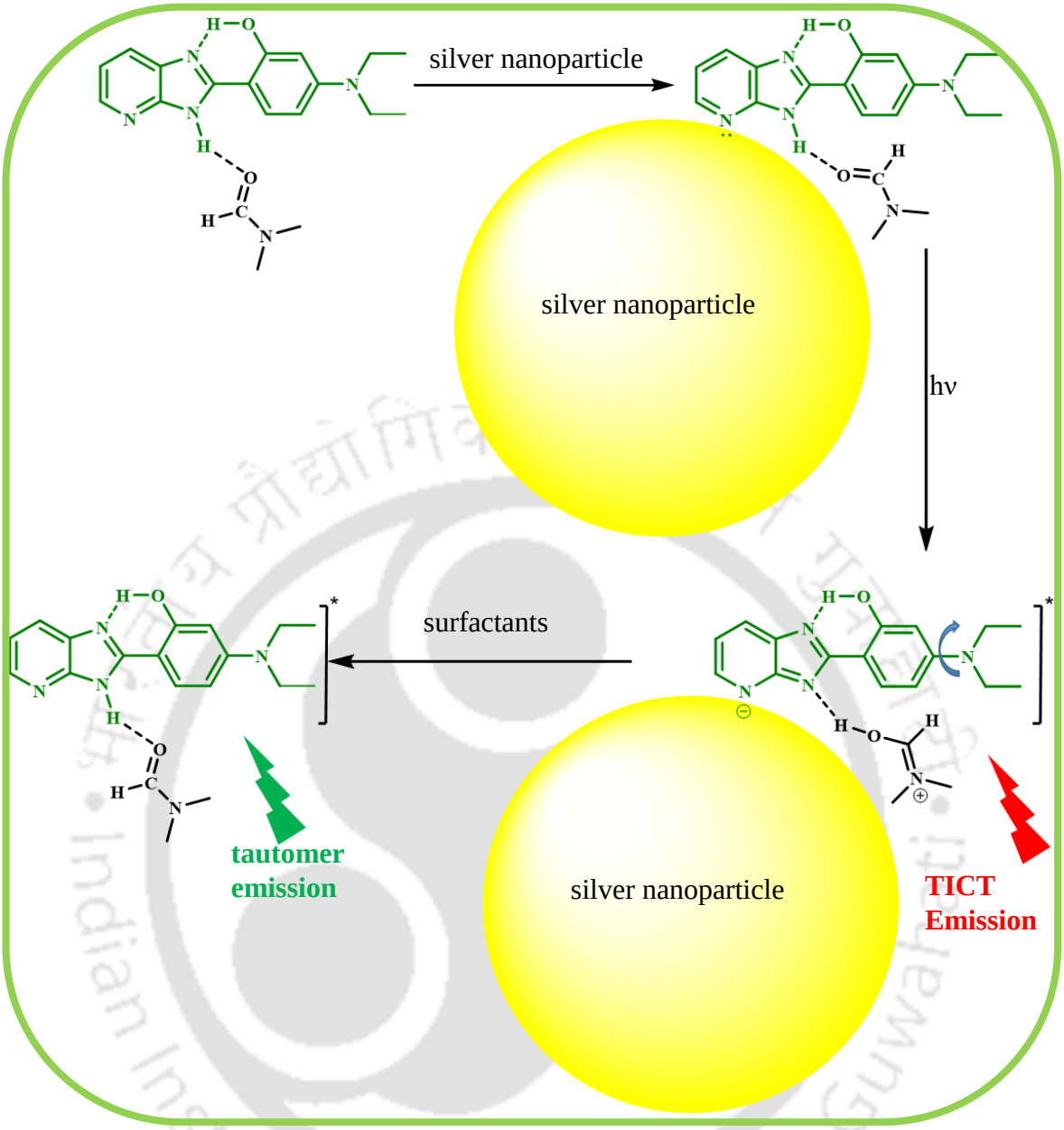

Figure 6: Schematic representation of silver nanoparticle induced TICT emission in DEAHPIP-b followed by removal of DEAHPIP-b from silver nanoparticle surface by surfactants in DMF.

Chapter 7: Effect of pH on 2-(4′-diethylamino-2′-hydroxyphenyl)-1H-imidazo-[4,5-b] pyridine and its methoxy analogous

Like the polarity and hydrogen bonding ability of the solvents, the pH of the solution also can influence the ESIPT and TICT processes (Figure 7).

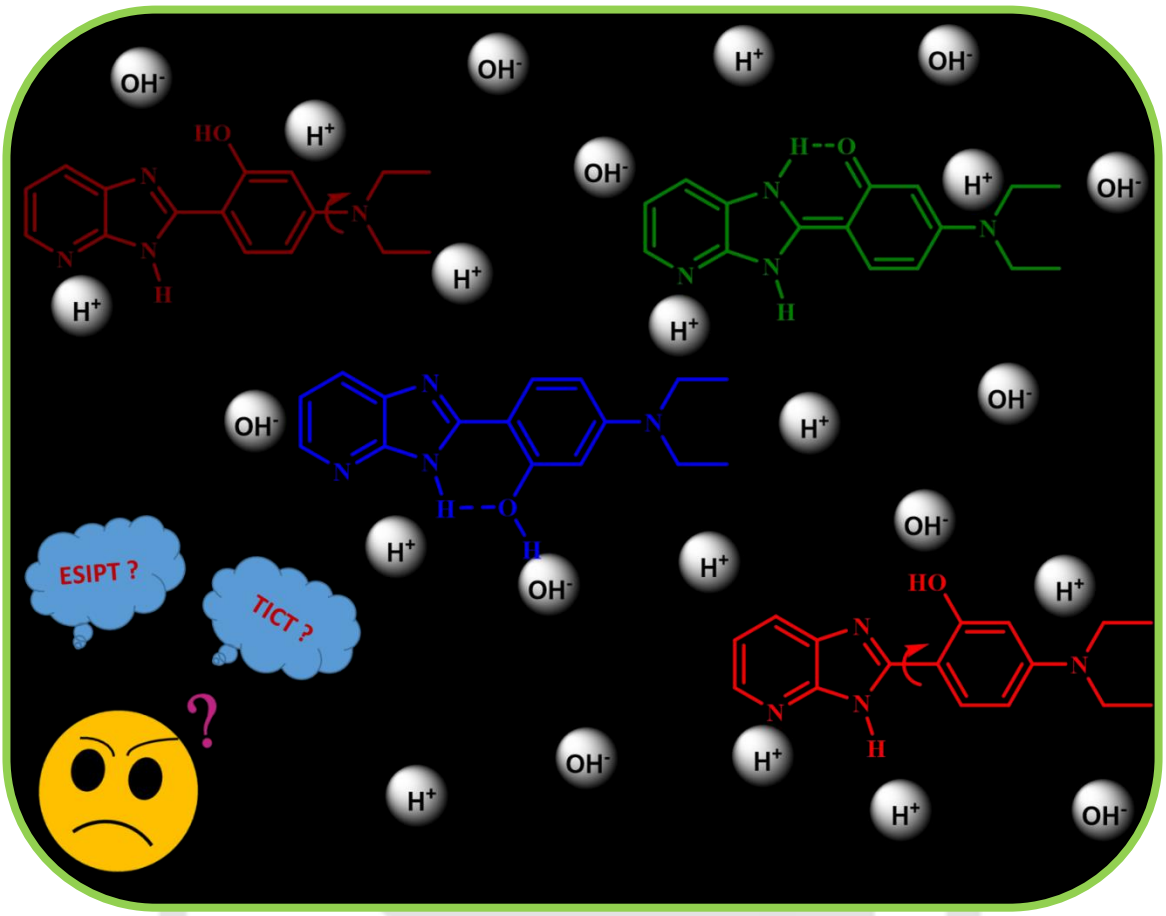

Figure 7: Different attainable states in DEAHPIP-b at different pH.

Neutral DEAHPIP-b may emit normal emission or tautomer emission or TICT emission or combination of any of the three emissions. However, the protonation of imidazole nitrogen or the deprotonation of hydroxyl group will eliminate the ESIPT process. Similarly, the protonation at pyridyl nitrogen may induce the TICT emission and at diethylamino nitrogen will prevent the TICT. Hence, the spectral properties of DEAHPIP-b and DEAMPIP-b are investigated over a broad range of pH. In neutral DEAHPIP-b, ESIPT predominates. In basic medium in DEAHPIP-b, normal emissions occur from the anionic species. In acidic medium different cationic species are formed, hence at different acid strength normal emission and keto emission are achieved. In DEAMPIP-b, only normal emissions are observed in neutral and acidic medium. Hence the spectral properties of the fluorophores can be modulated over a wide range of wavelength, as well the emission properties can be used to detect the pH.

Chapter 8: Summary and scope for future work

The thesis ends with a summary of the present work and scope for the future work.

Contents

List of Abbreviation

ADC	Analogue to digital converter
AHPIP-c	2-(4′-amino-2′-hydroxyphenyl)-1H-imidazo[4,5-c]pyridine
APIP-b	2-(4′-aminophenyl) imidazo[4,5-b]pyridine
APIP-c	2-(4′-aminophenyl) imidazo[4,5-c]pyridine
Bis-HPTA	3,5-bis(2-hydroxyphenyl)-1H-1,2,4-triazole
CB	Cucurbit
CD	Cyclodextrin
CT	Charge Transfer
CTAB	Cetyltrimethylammonium bromide
DEAHPIP-b	2-(4′-diethylamino-2′-hydroxyphenyl)-1H-imidazo-[4,5-b] pyridine
DEAMPIP-b	2-(4′-diethylamino-2′-methoxyphenyl)-1H-imidazo-[4,5-b] pyridine
DFT	Density functional theory
DK	Diketo
DLS	Dynamic Light Scattering
DMAPIP-b	2-(4′-N,N-dimethylaminophenyl) imidazo[4,5-b]pyridine
DMAPIP-c	2-(4′-N,N-dimethylaminophenyl) imidazo[4,5-c]pyridine
DMF	*N*,*N*-Dimethyl-formamide
DMSO	Dimethyl sulfoxide
ESIPT	Excited State Intramolecular Proton Transfer
ESIDPT	Excited State Intramolecular Double Proton Transfer
eV	electron volt
FC	Franck-Condon
FESEM	Field Emission Electron Microscopy
HPBI	2-(2′-hydroxyphenyl) benzimdazole
HPBO	2-(2′-hydroxyphenyl) benzoxazole
HPIP-b	2-(2′-hydroxyphenyl)-3H-imidazo-[4, 5-b] pyridine
HPIP-c	2-(2'-hydroxyphenyl)-3H-imidazo-[4,5-c] pyridine
HPLC	High-performance liquid chromatography
HRMS	High resolution mass spectrometry
ICT	Intramolecular Charge Transfer
IEFPCM	Integral equations formalism- polarizable continuum model
IRF	Instrument response function
LASER	Light Amplification by Stimulated Emission of Radiation
LE	Local Excited
LED	Light emitting diode
NMR	Nuclear Magnetic Resonance
PMT	photomultiplier tube
PICT	Planarized Intramolecular Charge Transfer
PT	Proton Transfer
PTTPT	Proton Transfer Triggered Proton Transfer
RICT	Rehybridized Intramolecular Charge Transfer
SDS	Sodium dodecyl sulfate
SPR	Surface Plasmon Resonance
TAC	Time to amplitude converter
TCSPC	Time-correlated Single Photon Counting

TDDFT	Time-dependent density functional theory
THF	Tetrahydrofuran
TICT	Twisted Intramolecular Charge Transfer
TRANES	Time resolved area normalized emission spectra
TX-100	Triton-X 100
UV	Ultra violet
WICT	Wagged Intramolecular Charge Transfer
˚C	˚Centigrade
$\in$	Extinction coefficient
λ_{max}^{ab}	Absorption maxime
λ_{max}^{ex}	Excitation maxima
λ_{max}^{fl}	Emission maxima
λ_{exc}	Excitation wavelength
λ_{em}	Emission wavelength
Φ_f	Quantum yield of fluorescence
τ	Fluorescence Lifetime

List of Charts

List of Figures

Chapter 4

Chapter 5

Chapter 6

Chapter 7

List of Schemes

List of Tables

Chapter 1

Introduction

1.0. Dual emission

Upon photoexcitation, several organic molecules emit from the lowest excited state to give normal fluorescence. The photochemical modification or electronic rearrangement leads to different species or conformational change in the excited state results in multiple fluorescence.[1-5] Excited state proton transfer (PT) and charge transfer (CT) are some of the common phenomena that lead to the generation of more than one emission.[6-10] Amongst these processes, the excited state intramolecular proton transfer (ESIPT) and the twisted intramolecular charge transfer (TICT) are most extensively studied.[11-20]

1.1. Excited state proton transfer

PT is a tautomerization process. In the field of photochemistry and photobiology, it is one of the most useful process.[21-25] Understanding the detailed mechanism of proton transfer by experimental and theoretical means has been a topic of research interest for several years. The proton transfer process can be classified as intramolecular and intermolecular process.

1.1.1. Excited state intramolecular proton transfer

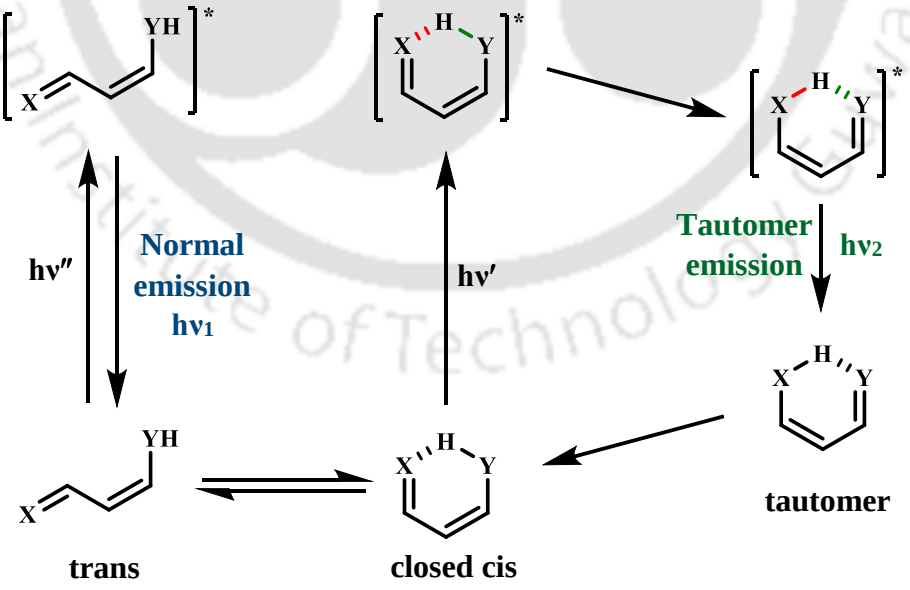

Scheme 1.1: Dual emission in ESIPT process.

The molecules having an acidic and a basic residue may exist as two different conformers cis and trans **[Scheme 1.1]**. In the cis conformer, the acidic and basic residue are in close proximity and intramolecular hydrogen bonding exists between them. This cis conformer upon excitation undergoes ESIPT to form a tautomer in the excited state which emits a largely Stokes shifted emission. Since in the trans conformer, the acidic and basic residue are not in close proximity no proton transfer occurs in the excited state and it emits normal emission. Weller first observed dual emission in salicylic acid **[Chart 1.1]** due to the ESIPT process.[11]

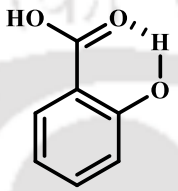

Chart 1.1: Structure of salicylic acid.

ESIPT in six-member intramolecular hydrogen bonded ring is most common.[11-15] However, the ESIPT process in four, five, seven and eight-member ring are also reported.[26-32] Due to steric effect the strength of the intramolecular hydrogen bond in the case of four-member ring is less compared to others. ESIPT process through eight-member ring are very rare. 7-hydroxy-2,3-dihydro-[1,2'-biindenylidene]-1',3'-dione is reported to exhibit ESIPT through eight-member hydrogen bonded ring **[Scheme 1.2]**.[32]

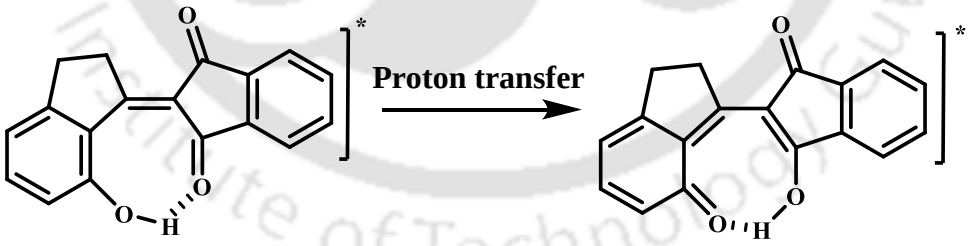

Scheme 1.2: ESIPT in 7-hydroxy-2,3-dihydro-[1,2'-biindenylidene]-1',3'-dione through eight-member hydrogen bonded ring system.

Excited state intramolecular double proton transfer (ESIDPT) active molecules are now-a-days a subject of interest as these processes are also perceived in biological systems, and understanding the detailed mechanism for these cases are essential.[33-37] In double proton transfer system, the protons can transfer in a concerted manner or a step by step process.

In 7-hydroxyquinoline-8-carboxylicacid, ESIDPT occurs in a concerted, asynchronous manner with a negligible potential barrier **[Scheme 1.3]**.[33]

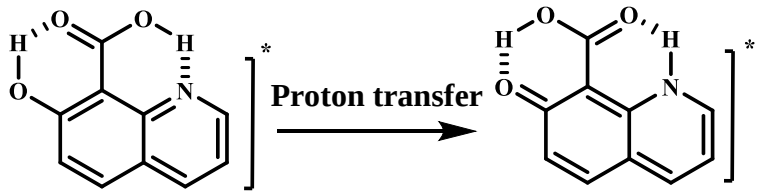

Scheme 1.3: Concerted ESIDPT in 7-Hydroxyquinoline-8-carboxylicacid.

In case of stepwise proton transfer, the molecule may have different donor-acceptor pair or one proton transfer site can produce the second proton transfer site making feasible of the second ESIPT process.[35-37] The anticancer drug doxorubicin possesses two pairs of proton donor-acceptor sites and goes through a stepwise double proton transfer reaction **[Scheme 1.4]**.[35] But the sequence of these two protons transfer is uncertain due to less difference between their potential barrier.

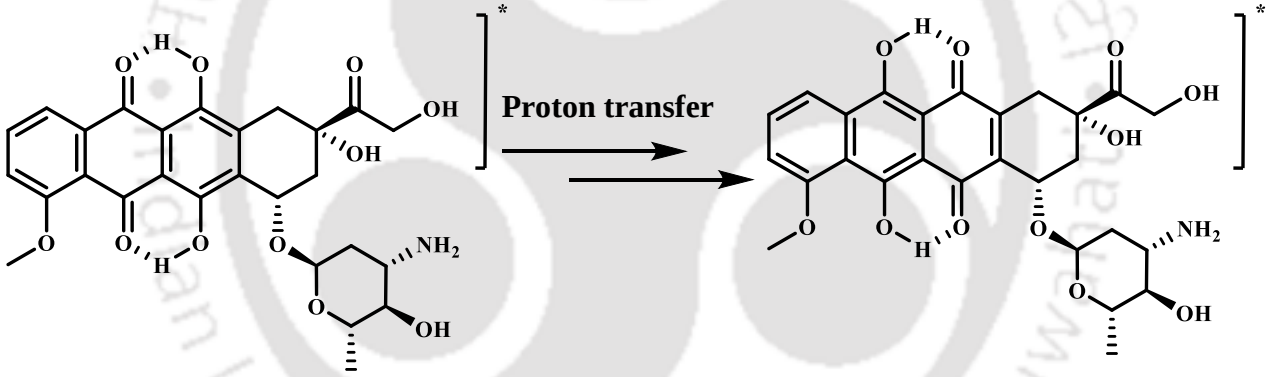

Scheme 1.4: Stepwise ESIDPT in doxorubicin.

In 1,8-dihydroxy-2-napthaldehyde, the first ESIPT process generates another pair of proton donor-acceptor pair which subsequently undergoes proton transfer leading to stepwise ESIDPT **[Scheme 1.5]**.[36]

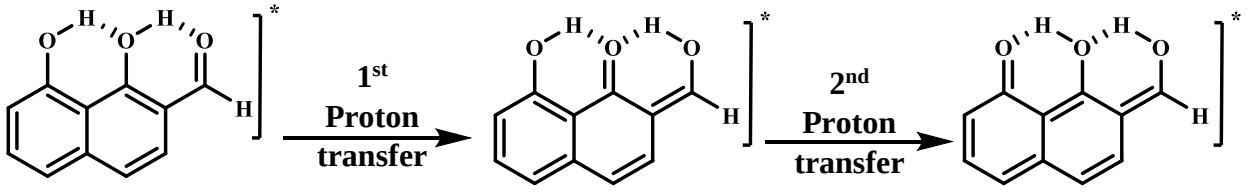

Scheme 1.5: Stepwise ESIDPT (one ESIPT making feasible of another ESIPT) in 1,8-dihydroxy-2-napthaldehyde.

Despite possessing more than one intramolecular hydrogen bonding system in some symmetric molecules, only single proton transfer occurs.[38, 39] It is reported that in bis-3,6-(2-benzoxazolyl)-pyrocatechol, a symmetric fluorophore having two ESIPT units, only one proton transfer is more prospective to occur **[Scheme 1.6]**.[38]

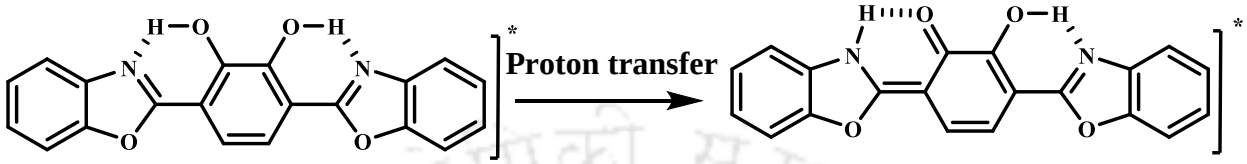

Scheme 1.6: ESIPT in bis-3,6-(2-benzoxazolyl)-pyrocatechol.

Though ESIPT process produces tautomer in the excited state, several reports dealt with ESIPT process can produce a zwitterion structure.[40, 41] 2-(imidazo[1,2-a]pyridin-2-yl)aniline upon photoexcitation generates a zwitterionic tautomer by ESIPT process **[Scheme 1.7]**.[40]

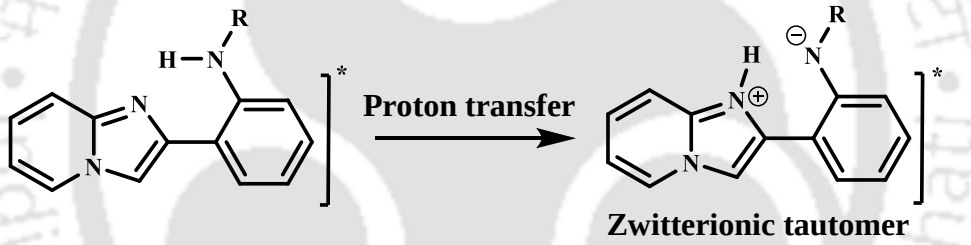

Scheme 1.7: Zwitterionic tautomer generated by ESIPT process in 2-(imidazo[1,2-a]pyridin-2-yl) aniline.

1.1.1.1. Factors affecting ESIPT

Polarity as well as hydrogen bonding ability of the solvents play an important role in modulating the ESIPT processes.[42-49] Polarity of the solvent affects the cis-trans equilibrium. Nonpolar and aprotic solvents favour the cis conformer whereas protic solvents favours trans conformer. Therefore, in nonpolar solvents, ESIPT is strong and the tautomer emission dominates.[44-47] In polar solvents the relative intensity of the normal emission increases as the equilibrium shifts from cis conformer towards trans conformer. Protic solvents disrupts the intramolecular hydrogen bond which hampers the ESIPT.[42, 43, 45] On the other hand, in some exceptional cases, ESIPT occurs utterly in polar solvents also.[48, 49] In 1- and 2-salicylidene-anthrylamine **[Chart 1.2]**, the tautomer emission occurs from the cis-keto in polar solvents,

acetonitrile and methanol, whereas in nonpolar solvent cyclohexane, the normal emission occurs from the locally excited trans-enol.[49]

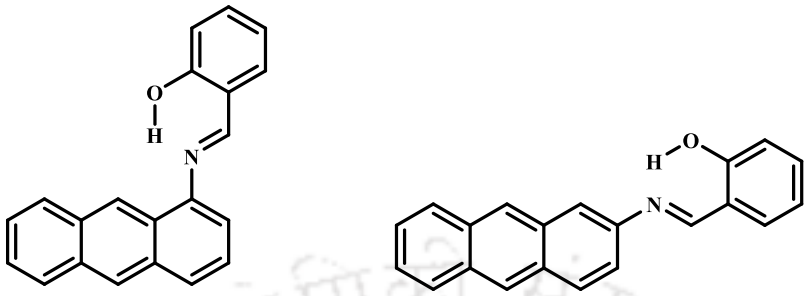

1-salicylideneanthrylamine **2-salicylideneanthrylamine**

Chart 1.2: Structure of 1- and 2- salicylideneanthrylamine.

The donor and acceptor sites present in ESIPT active fluorophores are also disturbed by the protonation or deprotonation in aqueous acidic or basic medium.[50-52] As a result, now-a-days these fluorophores are used as efficient pH probes.[53-55] Zhang et al. have reported a ratiometric fluorescent probe FR-Lys by implementing pH modulated ESIPT process for imaging the pH changes in lysosome **[Scheme 1.8]**.[53]

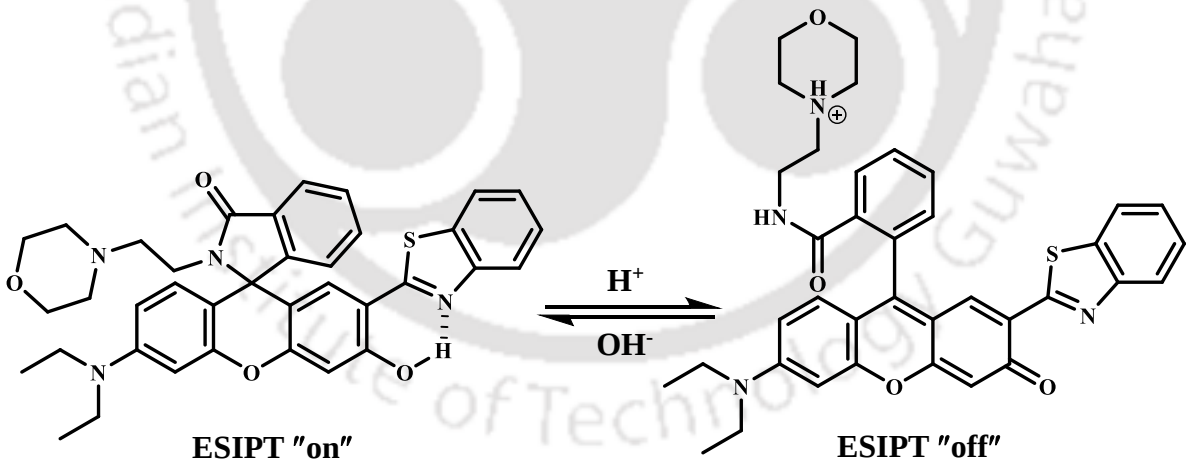

Scheme 1.8: pH response of FR-Lys.

Similar to H^+ ion, the metal ions also can coordinate with the active sites of the ESIPT fluorophore and affect the emission behavior.[56-59] Some metals are crucial elements for a number of physiological processes.[60-64] Hence, signaling of the metal ions is essential and ESIPT fluorophores due to their emission modulating behavior meet the necessity to a great extent.[56-59]

Pang et al. have reported an ESIPT active benzoxazole fluorescent probe which selectively detects and discriminates between Cr^{3+}, Al^{3+} and Fe^{3+} **[Scheme 1.9]**. In the presence of Cr^{3+} or Fe^{3+}, ESIPT is feasible while the addition of Al^{3+} inhibits ESIPT.[56]

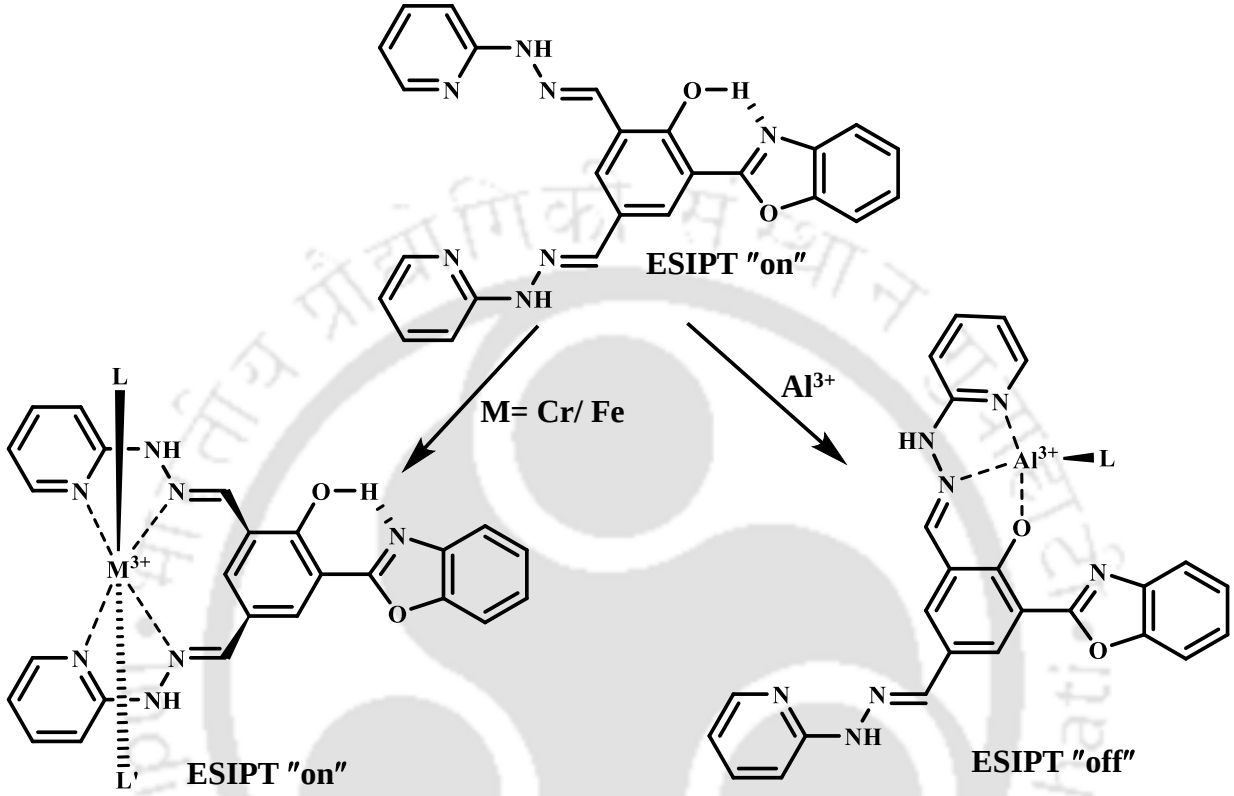

Scheme 1.9: Detection and distinction of Cr^{3+}, Al^{3+} and Fe^{3+} by a single benzoxazole derivative ESIPT probe.

The relatively low fluorescence quantum yield and solubility in aqueous medium limits the application of ESIPT active fluorophores. Supramolecular host molecules are well known to enhance the solubility and also the host-guest interaction can avoid the aggregation and retain the emission behavior of these fluorophores. The supramolecular host-guest interaction involves mainly the non-covalent type of interaction between organic fluorophores and macrocyclic hosts such as cyclodextrins (CDs), crown ethers, calixarenes, cucurbits (CBs), octa-acid etc.[65-67] The supramolecular host-guest interaction has wide applications in the field of food industry, molecular architectures, drug delivery, catalysis, fluorescence sensors and so on.[68-72] Also encapsulation of ESIPT fluorophores in various supramolecular host molecules in aqueous medium enhances the solubility of the fluorophores, making them more efficient candidate for various applications.[70-72]

The cavity size plays a major role in effective interaction with the guest molecules. Song et al. have studied the effect of CDs on an ESIPT active benzothiazole derivative fluorophore HBT-11 **[Chart 1.3]** and found it has weak enol and keto emissions in water. Complexation with α-CD predominantly improves the keto emission whereas β-CD mainly improves the enol emission of HBT-11.[73]

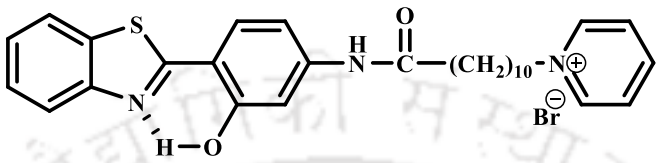

Chart 1.3: Structure of HBT-11.

The ESIPT of the oxazole derivatives **[Chart 1.4]** were enhanced upon encapsulation in octa-acid.[74] The interaction of benzimidazole moieties **[Chart 1.5]** with β-CD also shows the complexation with host reduced the nonradiative decay and favored the ESIPT process.[75] CB-7 was found to enhance the ESIPT of HPBI by encapsulation **[Chart 1.5.A]**.[76]

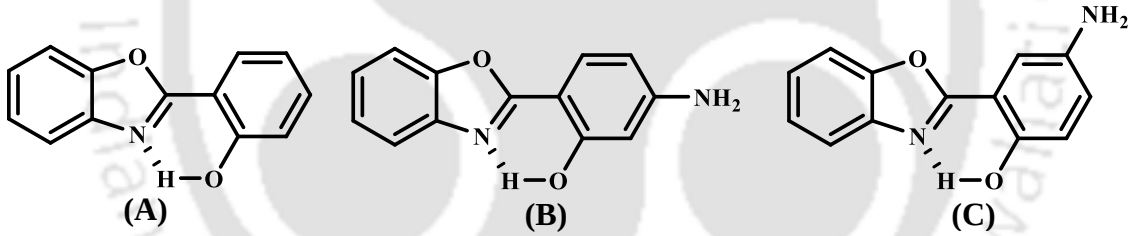

Chart 1.4: Structure of oxazole derivatives **(A)** 2-(2'-hydroxyphenyl)benzoxazole (HPBO), **(B)** 2-(4'-amino-2'-hydroxyphenyl)benzoxazole and **(C)** 2-(5'-amino-2'-hydroxyphenyl) benzoxazole.

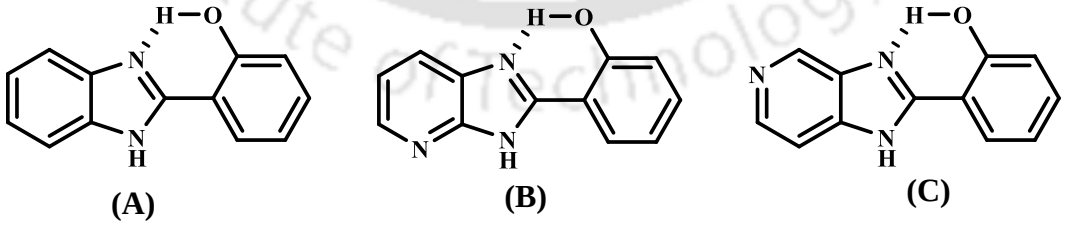

Chart 1.5: Structure of **(A)** 2-(2'-hydroxyphenyl)benzimidazole (HPBI), **(B)** 2-(2'-hydroxyphenyl)-3H-imidazo-[4,5-b]pyridine (HPIP-b) and **(C)** 2-(2'-hydroxyphenyl)-3H-imidazo-[4,5-c] pyridine (HPIP-c).

Like the solubility the aggregation of fluorophores limit the application, similarly, at physiological pH, the protonation or deprotonation of acidic or basic groups present in the fluorophores can limit their application. The use of surfactants brings encouraging solutions to the addressed issues. As surfactants possess hydrophilic head group and hydrophobic tail, they form micelle after a certain concentration known as critical micelle concentration and provides a microenvironment to the fluorophores. The micelle concentration, aggregation number and polarity of the surfactants play a major role in monitoring the photophysical properties of the fluorophores.[77-79] The self-assemblies of surfactants boost the solubility of organic molecules in aqueous medium and is a commonly used concept in drug industry to monitor the drug delivery.[80, 81] It is depicted that, the use of surfactants increases the solubility and stability of medicinal active curcumin **[Chart 1.6]** in water and ESIPT is the foremost photophysical process in curcumin in the presence of micelles.[82, 83] Sarkar et al. showed that the stability of the diketo tautomer of an ESIPT active fluorophore, 2,2′-bipyridine-3,3′-diol **[Chart 1.7]** increases on increasing the surfactant concentration.[78]

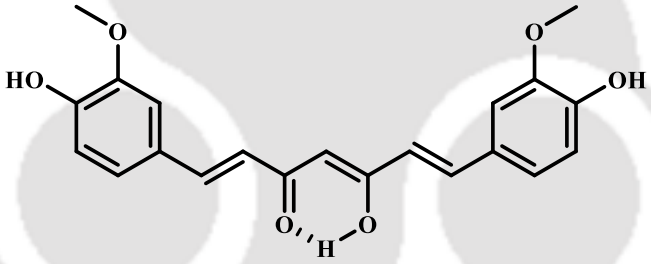

Chart 1.6: Structure of curcumin.

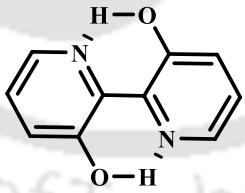

Chart 1.7: Structure of 2,2′-bipyridine-3,3′-diol.

The low polarity micellar medium favors the cis form, which in turn enhances the tautomer emission of the flavonol **[Chart 1.8]**.[79, 84] The rate of ESIPT of 2-(2′-furyl)-3-hydroxychromone **[Chart 1.9]** is slower in anionic micelles than in cationic micelles and in the nonionic micelles, the rate is in between that in anionic and cationic micelle.[77] Mitra et al. have reported that the tautomer fluorescence of 2-hydroxy-5-[(E)-(4 -ethoxyphenyl)diazenyl]benzoicacid **[Chart 1.10]**

was enhanced in the presence of surfactants.[85] Besides these benefit the wide-ranging use of surfactants in daily life as well as in industries are hazardous to the environment which needs serious attention and ESIPT active molecules can become a promising probe to detect the same at very low concentrations.[86]

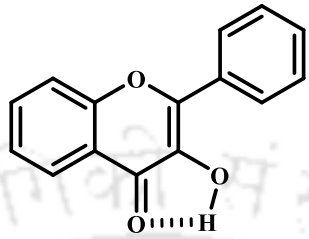

Chart 1.8: Structure of flavonol.

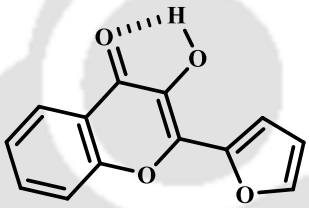

Chart 1.9: Structure of 2-(2′-furyl)-3-hydroxychromone.

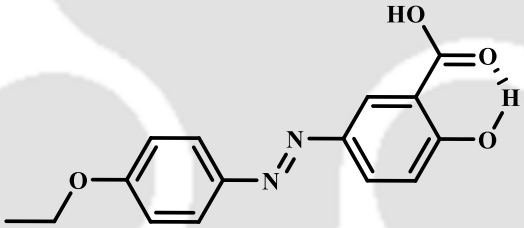

Chart 1.10: Structure of 2-hydroxy-5-[(E)-(4 -ethoxyphenyl)diazenyl]benzoicacid.

1.1.2. Excited state intermolecular proton transfer

The intermolecular proton transfer either can be bimolecular, when the proton transfer takes place between two molecules of the same kind, or of different kind or can be pseudo-unimolecular, when the proton transfers to the solvent molecule.[87-91] The proton transfer also happens in the same molecule through intermolecular proton transfer process via a solvent wire.[92-94] In indigo dye at dilute concentration, ESIPT occurs. But at millimolar concentration, excited state intermolecular proton transfer occurs in indigo dimer by generating an enol species which disappears with a time constant of 200−300 fs and returns to the ground state by a relatively slow nonradiative relaxation **[Scheme 1.10]**.[87]

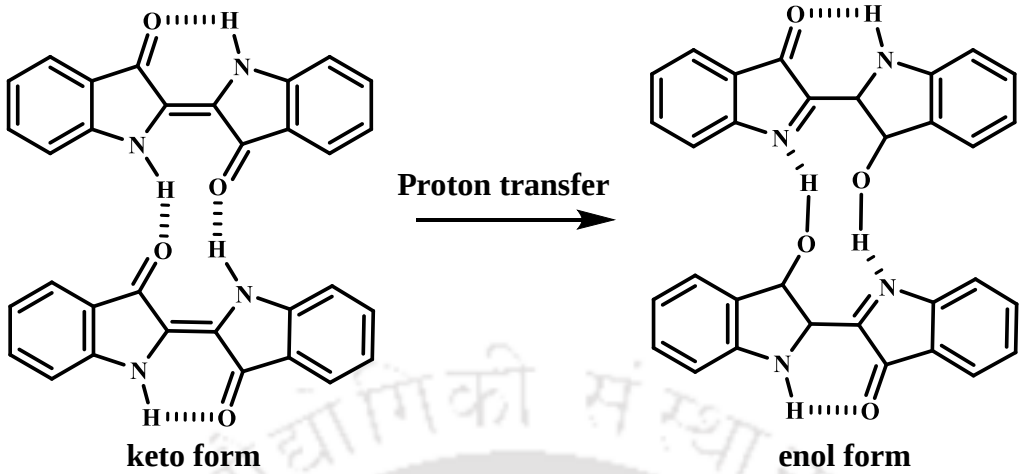

Scheme 1.10: Excited state intermolecular proton transfer in indigo dimer.

4-([2,2′-bipyridine]-4-yl)phenol produces a zwitterion photo tautomer by excited state intermolecular proton transfer process through HF molecule **[Scheme 1.11]**.[88] Brouwer et al. reported that the excited state intermolecular proton transfer occurs in N-methyl-3,6-dihydroxy-1,8-naphthalimide and other naphthalimide derivatives to alcohols and dimethyl sulfoxide (DMSO) **[Scheme 1.12]**.[90] 7-hydroxyquinoline was reported to produce photo tautomer by excited state intermolecular proton transfer process, which occurs via solvent methanol molecules **[Scheme 1.13]**.[92, 93]

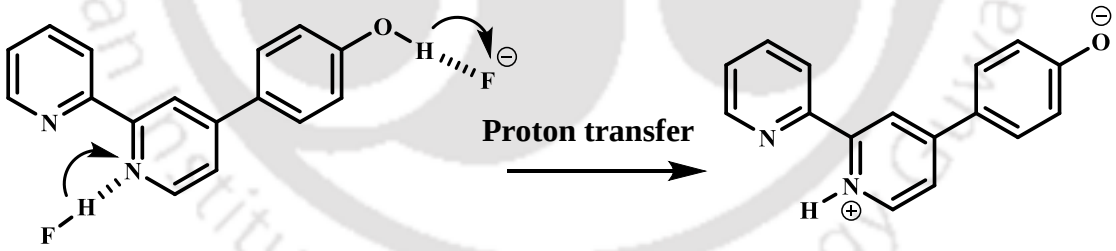

Scheme 1.11: Excited state intermolecular proton transfer in 4-([2,2′-bipyridine]-4-yl)phenol with HF molecule.

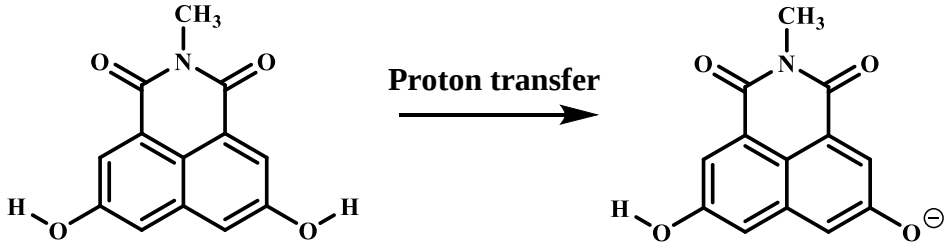

Scheme 1.12: Excited state intermolecular proton transfer in N-methyl-3,6-dihydroxy-1,8-naphthalimide to DMSO.

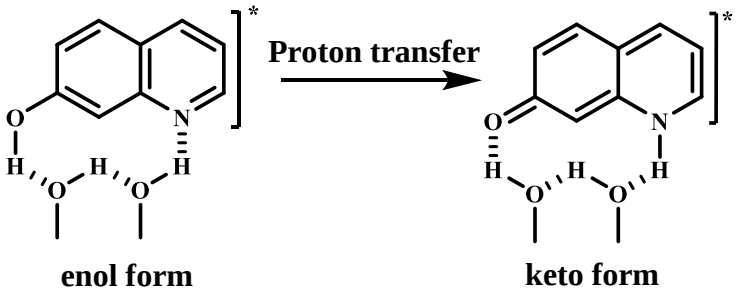

Scheme 1.13: Excited state intermolecular proton transfer in 7-hydroxyquinoline through methanol molecules.

1.1.2.1. Factors affecting excited state intermolecular proton transfer

Excited state intermolecular proton transfer mainly depends on the obtainability of a proton-acceptor and its ability to accept the proton from the proton-donor fluorophore. As in some cases, the proton transfer occurs to the solvent molecules, hence the strength of the hydrogen bonding ability of the solvent plays an important role. Ammonia was reported to favour the excited state intermolecular PT of a flavonol **[Chart 1.8]** more than methanol and water.[95] Arai et al. have studied the excited state intermolecular PT reaction between 1-(anthracen-2-yl)-3-(4-((2-methylundecan-2-yl)sulfonyl)phenyl)urea **[Chart 1.11]** and tetra butyl ammonium acetate in DMSO, acetonitrile, tetrahydrofuran (THF) and toluene and found that the PT occurs efficiently only in DMSO.[96]

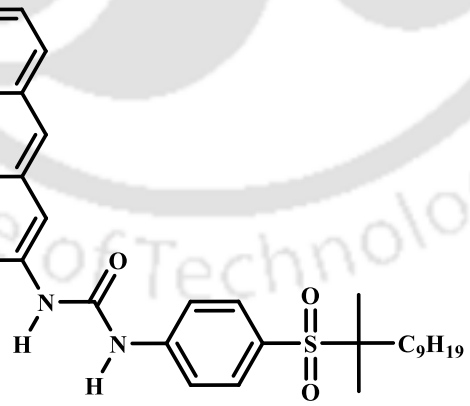

Chart 1.11: Structure of 1-(anthracen-2-yl)-3-(4-((2-methylundecan-2-yl)sulfonyl)phenyl)urea.

Bravo et al. have reported a bisguanidine naphthalene fluorophore **[Chart 1.12]** exhibits only neutral emission in hexane, monoprotonated emission in dichloromethane, both neutral and

monoprotonated emission in acetonitrile and THF, and a single red shifted monoprotonated emission in more polar protic solvent ethanol.[97] The monoprotonated emission is due to excited state intermolecular PT from the solvent molecule to the fluorophore.

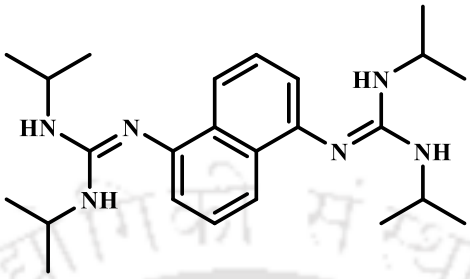

Chart 1.12: Structure of bisguanidine-naphthalene.

Like the homogeneous solvent medium, the heterogeneous media also affects the fate of excited state intermolecular proton transfer process.[98-100] According to Bhattacharyya et al. the intermolecular proton transfer from 8-hydroxypyrene-1,3,6-trisulfonate **[Chart 1.13]** to acetate becomes slower in the presence of γ-CD as compared to in the absence of γ-CD in bulk water.[98] Pina et al. have reported the complexation with CB-7 prevents the excited state PT in β-naphthol **[Chart 1.14]**.[101] Mukherjee et al. found that in the excited state, proton transfer occurs from the salicylidine-3,4,7-methyl amine to water leading to the formation of the anion **[Chart 1.15]**. But in the presence of β-CD, it forms hydrogen bonded complex with β-CD, and as a result, the anion emission was reduced.[99]

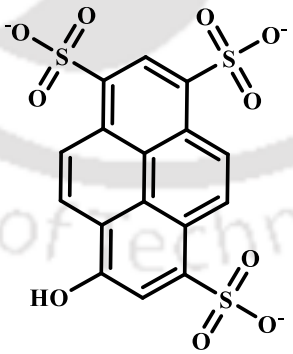

Chart 1.13: Structure of 8-hydroxypyrene-1,3,6-trisulfonate.

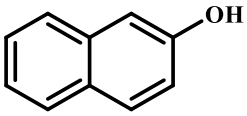

Chart 1.14: Structure of β-naphthol.

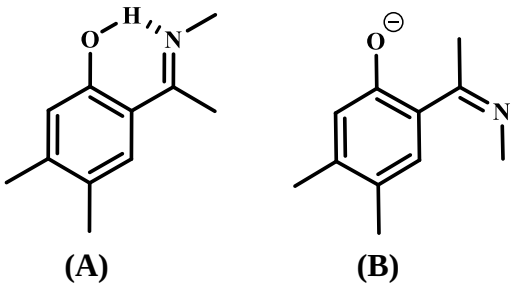

(A) **(B)**

Chart 1.15: Structure of **(A)** salicylidine-3,4,7-methylamine and **(B)** its anion.

Kuzmin et al. have reported that the anionic surfactant sodium dodecyl sulfate (SDS) suppresses the excited state intermolecular proton transfer of ω-(2-hydroxynaphthyl-1)-decanoicacid **[Chart 1.16]**.[100] Cetyl trimethyl ammonium bromide (CTAB) enhanced the excited state intermolecular proton transfer of 2-acetyl-4-chloro-6-nitrophenol **[Chart 1.17]**.[102]

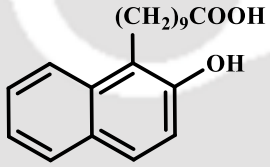

Chart 1.16: Structure of ω-(2-hydroxynaphthyl-1)-decanoicacid.

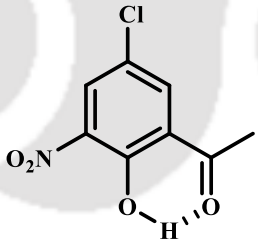

Chart 1.17: Structure of 2-acetyl-4-chloro-6-nitrophenol.

1.2. Excited state charge transfer

Like PT process, photo induced CT process is also an important phenomenon in photophysical, photochemical and photobiological processes.[103-105] Molecules having charge donor and acceptor units connected through a spacer, upon excitation exhibit low energy emission band in polar solvents.[106-109] Several mechanisms such as planarized intramolecular charge transfer (PICT), TICT, wagged intramolecular charge transfer (WICT), rehybridised intramolecular charge

transfer (RICT) have been proposed to explain this red shifted emission.[110-112] The ICT process was observed for the first time in 4-(dimethylamino)benzonitrile **[Chart 1.18]**.[113] Till date, the TICT mechaism is established as the most defensible mechanism to explain the photophysical property of 4-(dimethylamino)benzonitrile as well as of several other donor-acceptor molecules.[114]

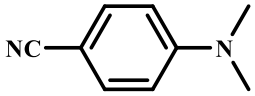

Chart 1.18: Structure of 4-(dimethylamino)benzonitrile.

1.2.1. Twisted intramolecular charge transfer

According to TICT mechanism, the intramolecular charge transfer from the donor to the acceptor is accompanying the twisting of the donor group to a perpendicular position and results in the twisted conformation **[Scheme 1.14]**. Upon photoirradiation the molecule is excited to the local excited (LE) state. The charge transfer and twisting of the donor in the excited state results in the more polar and highly stable TICT state. From the TICT state the excited molecules return to the ground state through emitting red-shifted emission or by nonradiative relaxation.

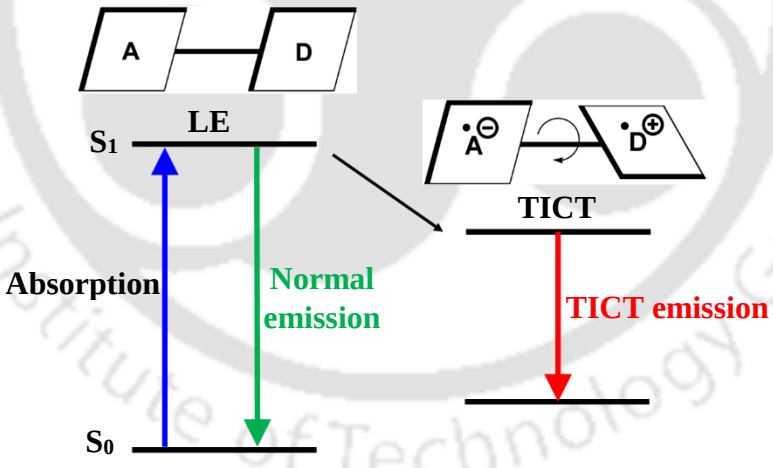

Scheme 1.14: Dual emission in TICT process.

1.2.1.1. Factors affecting TICT

Since, the TICT state is formed by charge transfer and twisting, the polarity and viscosity of the environment, as well as the position of the donor group plays a vital role in the formation and stabilization of the TICT state.[115-119] 3,5-Dimethyl-4-(dimethylamino)benzonitrile in *n*-hexane

[Chart 1.19.A] emits from both LE and TICT states, but in acetonitrile it emits single TICT emission. The meta-isomer of the fluorophore, i.e., 2,4-dimethyl-3-(dimethylamino)benzonitrile **[Chart 1.19.B]** in *n*-hexane, emits only from the LE state and in acetonitrile only from TICT state.[119]

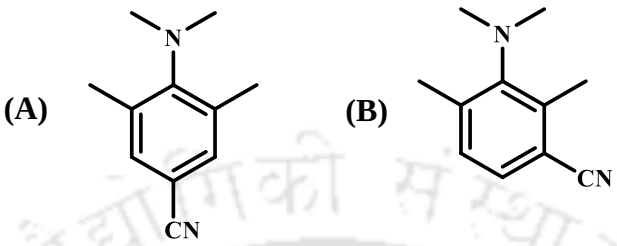

Chart 1.19: Structure of **(A)** 3,5-Dimethyl-4-(dimethylamino)benzonitrile and **(B)** 2,4-Dimethyl-3-(dimethylamino)benzonitrile.

Hydrogen bonding either with the donor group or with the acceptor group plays a significant role in the formation and stabilization of CT state.[20, 120-125] The hydrogen bonding with the donor weakens the CT state and the hydrogen bonding with the acceptor strengthens the CT state. Mitra et al. have demonstrated in *trans*-ethyl *p*-(dimethylamino)cinamate **[Chart 1.20]**, the hydrogen bonding with donor decreases the ICT emission in protic solvents.[120]

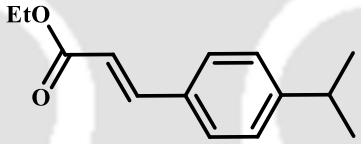

Chart 1.20: Structure of *trans*-ethyl *p*-(dimethylamino)cinamate.

The pH of the solution can modulate the emission behavior of TICT probes. Protonation of 1-methyl-2-(4′-*N*,*N*-diethylamino-2′-O-methoxyphenyl)benzimidazole **[Chart 1.21]** at acceptor ring led to formation of TICT state.[126] N-hydroxyethyl-4-guanidino-1,8-naphthalimide **[Chart 1.22]** is reported to produce ICT emission upon deprotonation.[127]

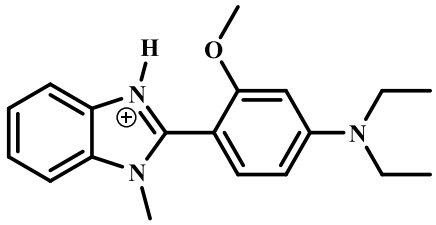

Chart 1.21: Structure of 1-methyl-2-(4′-*N*,*N*-diethylamino-2′-O-methoxyphenyl)benzimidazole.

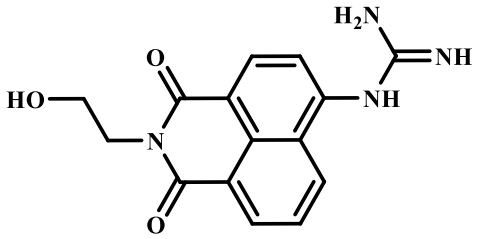

Chart 1.22: Structure of N-hydroxyethyl-4-guanidino-1,8-naphthalimide.

Like ESIPT, the TICT process is also modulated by metal ions. Das et al. reported in absence of metal ion 4-([2,2':6',2"-terpyridin]-4'-yl)-*N*,*N*-dimethylaniline emits TICT emission.[128] The complexation with Cr^{3+} inhibits the CT and the molecule emits a new blue shifted emission **[Scheme 1.15]**.[128]

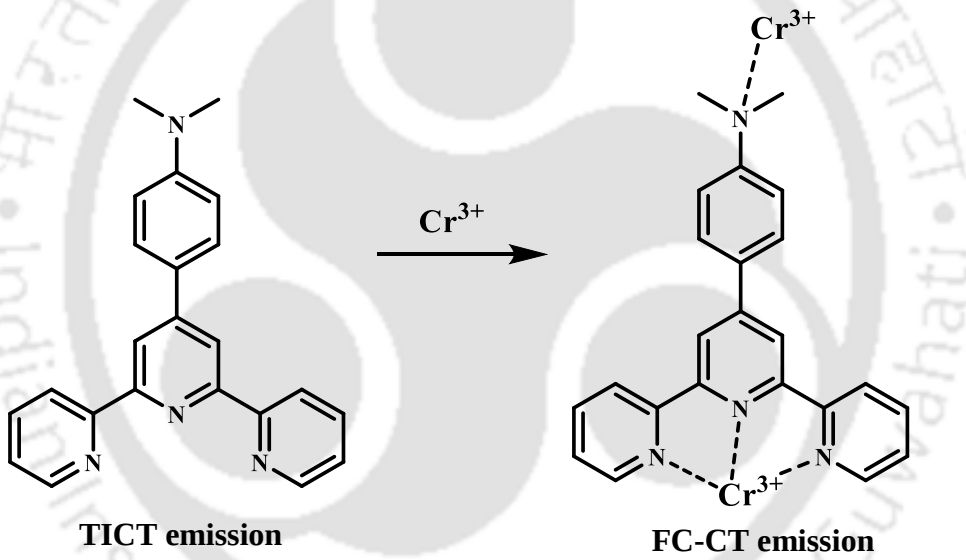

Scheme 1.15: Quenching of TICT emission in 4-([2,2':6',2"-terpyridin]-4'-yl)-*N*,*N*-dimethylaniline in presence of Cr^{3+}.

Same as homogeneous media, the heterogeneous host-guest interaction can modulate the TICT emission. The host molecules can trap the fluorophores inside their cavity and tweak the rotation of the donor group. The polarity inside the host also affects the TICT process. Seth et al. depicted with a gradual increase of the cavity size of CDs, the binding efficiency of coumarin molecule **[Chart 1.23]** with the hosts increases, and in the presence of γ-CD the non-emissive TICT state becomes highly emissive.[129] Rajendiran et al. have reported that labetalol **[Chart 1.24]**

shows TICT emission in polar solvents. The TICT emission was quenched upon encapsulation into β-CD cavity.[130]

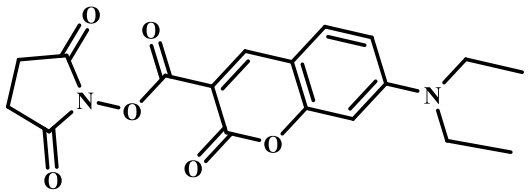

Chart 1.23: Structure of 7-(Diethylamino)coumarin-3-carboxylicacid-N-succinimidylester.

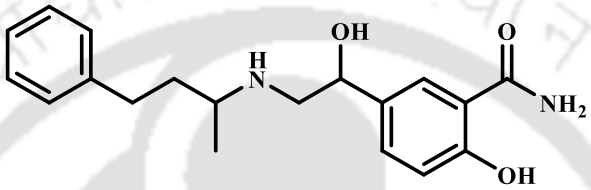

Chart 1.24: Structure of labetalol.

Similarly, the interaction of molecules with surfactants affect the TICT process. The surfactants CTAB and SDS enhance the TICT emission of 4-(dimethylamino)benzonitrile **[Chart 1.18]** more compared to its normal emission.[131] It is reported that the cationic surfactant CTAB enhances the TICT emission of p-dimethylaminobenzoicacid **[Chart 1.25]**.[132] The TICT emission of trans-2-[4-(dimethylamino)styryl]benzothiazole **[Chart 1.26]** was quenched in the anionic surfactant SDS.[133]

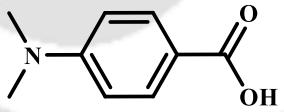

Chart 1.25: Structure of p-dimethylaminobenzoicacid.

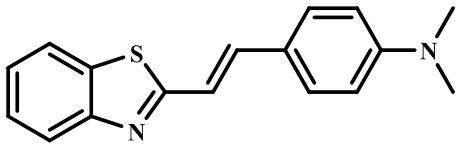

Chart 1.26: Structure of trans-2-[4-(dimethylamino)styryl]benzothiazole.

1.3. ESIPT vs TICT

Recently in contrast to the usual single reaction coordinate photoswitches, Dube et al. reported two diverse reaction coordinates based photoswitches.[134] The switching was between the mutually independent reaction coordinates, isomerization and TICT. Control over these two processes was attained by switching from nonpolar solvent cyclohexane to polar solvent DMSO. Depending on the polarity light can switch-on either the isomerization or TICT. Like photoisomerization, ESIPT is also an important photoprocess and can compete with TICT. TICT depends on the strength of the electron donor and the acceptor groups present in the fluorophore.[120-125] ESIPT depends on the acidity and basicity of the group those are connected by the intramolecular hydrogen bond.[135-140] Hence, the strength of the charge transfer and intramolecular hydrogen bond determines the emission properties of the fluorophores.[141-151] It is reported that in 4-(diethylamino)-2-hydroxybenzaldehyde and 2-(4′-diethylamino-2′-hydroxyphenyl)benzimidazole **[Chart 1.27]**, the ESIPT process suppresses the charge transfer process.[141, 142] But in case of 4-amino-2-hydroxybenzoicacid and 4-(dimethylamino)-2-hydroxy benzoicacid **[Chart 1.28]**, proton transfer process accelerates the charge transfer process.[143, 144] In 5-diethylamino-2-[(4-diethylamino-benzylidene)-hydrazonomethyl]-phenol and *N*,*N*′-bis(4-*N*,*N*-diethylaminosalisalidene)hydrazine Schiff bases **[Chart 1.29]**, Guchhait et al. have demonstrated that the proton transfer process assists the charge transfer process.[145]

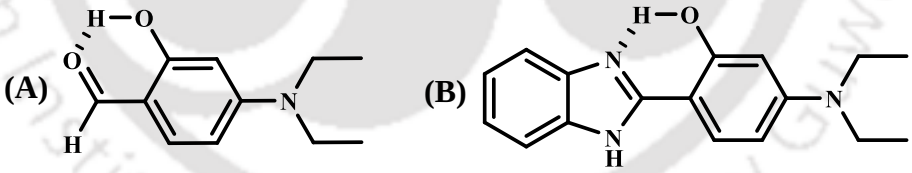

Chart 1.27: Structure of **(A)** 4-(diethylamino)-2-hydroxybenzaldehyde and **(B)** 2-(4′-diethylamino-2′-hydroxyphenyl)benzimidazole.

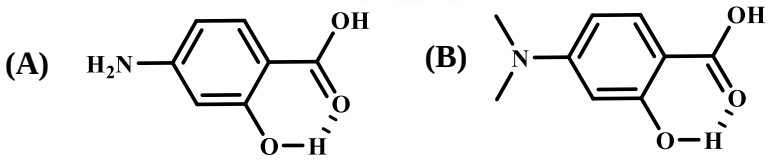

Chart 1.28: Structure of **(A)** 4-amino-2-hydroxybenzoicacid and **(B)** 4-(dimethylamino)-2-hydroxybenzoicacid.

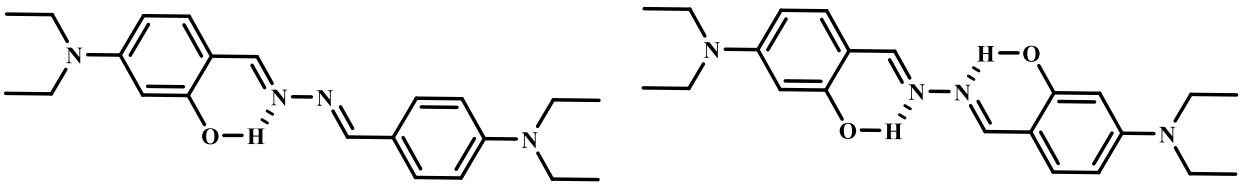

(A) **(B)**

Chart 1.29: structure of **(A)** 5-diethylamino-2-[(4-diethylamino-benzylidene)-hydrazonomethyl]-phenol and **(B)** *N,N′*-bis(4-*N*,*N*-diethylaminosalisalidene)hydrazine.

4-(dimethylamino)-2-hydroxybenzoate **[Chart 1.30]** reported to emit triple fluorescence.[146] One is normal fluorescence and another one is a composite fluorescence consisting of both tautomer emission and charge transfer emission. Flufenamic acid and mefenamic acid **[Chart 1.31]** were found to undergo ESIPT in non-polar solvent and TICT in polar aprotic solvents.[147]

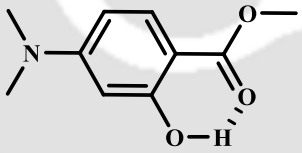

Chart 1.30: Structure of 4-(dimethylamino)-2-hydroxybenzoate.

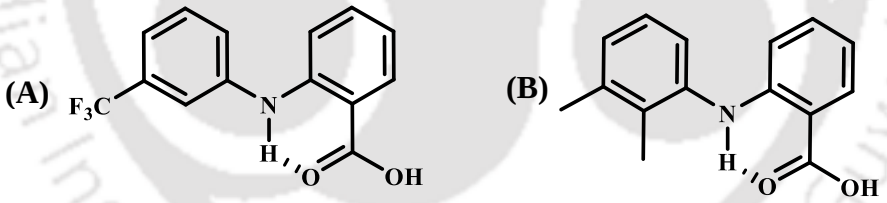

Chart 1.31: Structure of **(A)** flufenamic acid and **(B)** mefenamic acid.

N,N-dimethylanilino-1,3-diketone was stated to exist in two cis-enol forms **[Chart 1.32]**.[148] In low and medium polar solvents, one of the enol form undergoes ESIPT, followed by ICT. In polar solvents, another enol form undergoes TICT, and the ESIPT process gets reversed. Ultraviolet absorber 2-(2'-hydroxy-5'-methylphenyl)benzotriazole **[Chart 1.33.A]** attains the photostability through ESIPT, but its 6'-methyl substitution **[Chart 1.33.B]** changed the deactivation path to TICT.[149] In benzophenone derivatives, the derivatives possess strong electron donor followed the TICT path and the derivatives without such substituent, followed the ESIPT path.[150] Hu et al. reported that among a set of salicylideneaniline derivatives having ESIPT unit

[Chart 1.34], the derivatives having no substituents or having either electron donor or acceptor group exhibit only tautomer emission due to ESIPT. But the derivative having both electron donor and acceptor group, yields emissions both enol and keto emissions in non-polar solvents, and in polar solvents the enol emission was also red shifted due to ICT.[151]

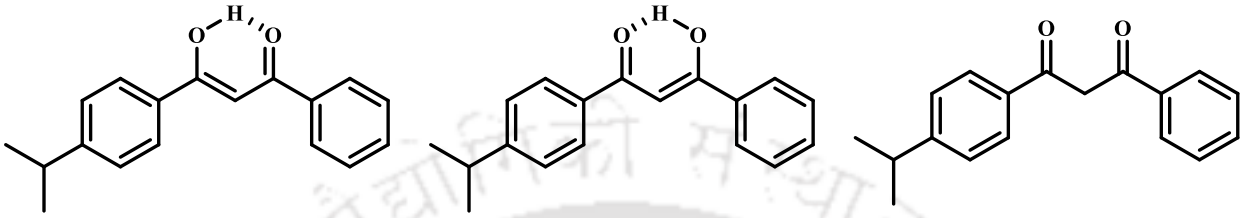

Enol-A **Enol-B** **Diketo**

Chart 1.32: Structure of *N*,*N*-dimethylanilino-1,3-diketone.

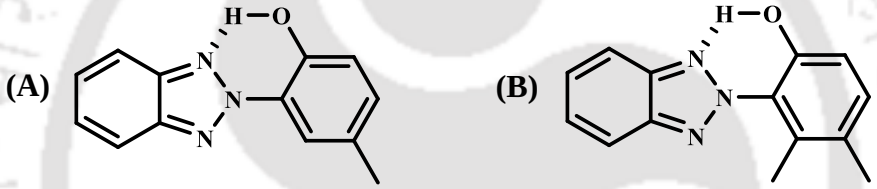

(A) **(B)**

Chart 1.33: Structure of **(A)** 2-(2'-hydroxy-5'-methylphenyl)benzotriazole and **(B)** 2-(2'-hydroxy-5',6'-dimethylphenyl)benzotriazole.

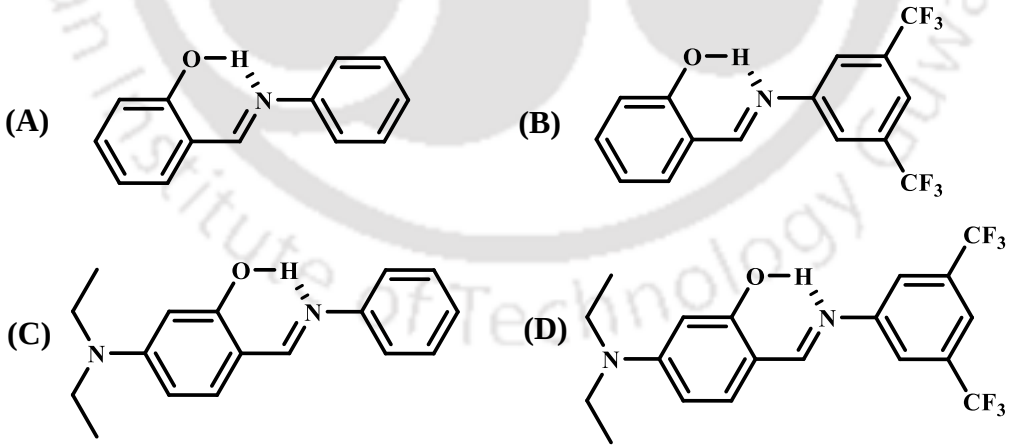

(A) **(B)** **(C)** **(D)**

Chart 1.34: Structure of **(A)** salicylideneaniline, **(B)** salicylidene-(3,5-bis-trifluoromethyl)-aniline, **(C)** 4-(*N*,*N*-diethyamino)-salicylideneaniline, **(D)** 4-(*N*,*N*-diethyamino)-salicylidene-(3,5-bis-trifluoromethyl)- aniline.

1.4. Proton transfer Induced TICT

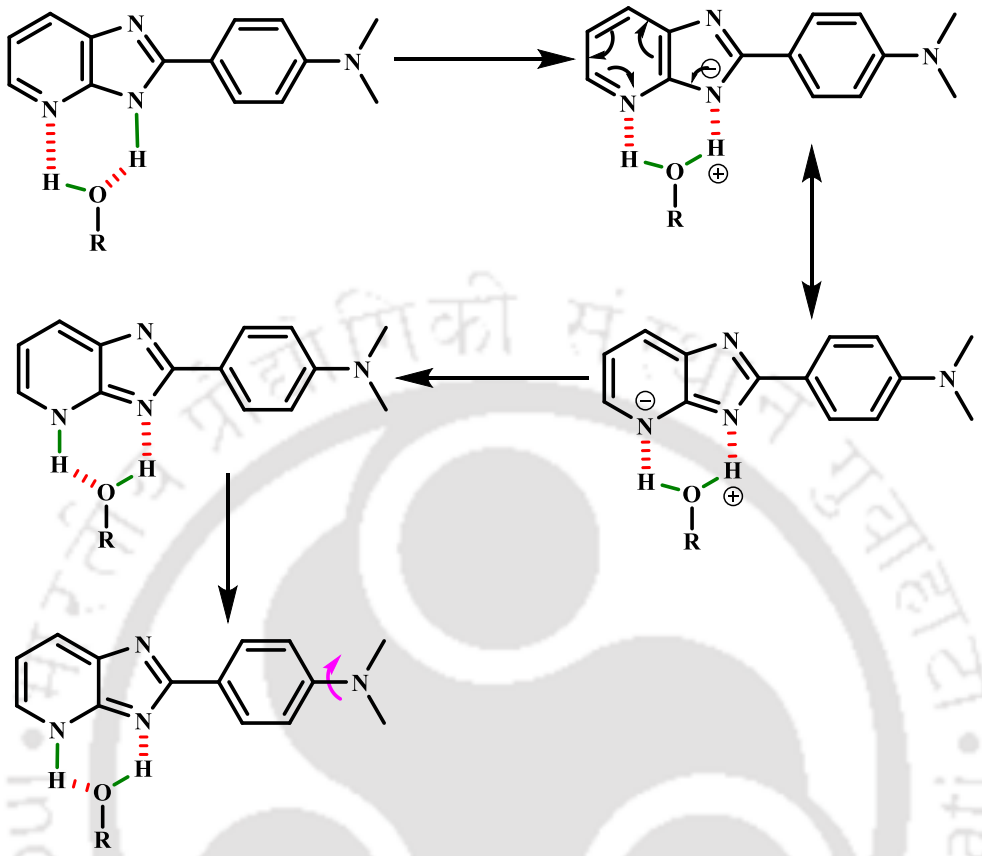

Scheme 1.16: Intermolecular proton transfer triggered TICT emission in 2-(4′-*N*,*N*-dimethylamino)phenylimidazo[4,5-b]pyridine (DMAPIP-b) in protic solvents.

In imidazopyridine derivatives, 2-(4′-*N*,*N*-dimethylamino)phenylimidazo[4,5-b]pyridine (DMAPIP-b), 2-(4′-amino)phenylimidazo[4,5-c]pyridine (APIP-c) and 2-(4′-*N*,*N*-dimethylamino) phenylimidazo[4,5-c]pyridine (DMAPIP-c) the hydrogen bonding between acceptor ring nitrogen atoms and protic solvent molecules induces the TICT emission.[20, 123-125] In this process, the imidazole 'NH' group transfers its' proton to solvent and negative charge is shifted to pyridyl nitrogen by resonance **[Scheme 1.16]**. The pyridyl nitrogen, in turn, accepts the proton from the solvent which enhances its' electron withdrawing capacity. This induces the intramolecular charge transfer from amino group to the imidazopyridine group that results in the TICT emission. This is evident from the fact that the TICT emissions of DMAPIPs were enhanced massively when their anion (formed by the deprotonation of 'NH' proton) is excited compared to the excitation of the neutral molecule. [123, 152] The normal emission of the anion is blue shifted compared to the neutral molecule. But the TICT emission maximum obtained from the excitation of anion as well as the

neutral molecule is same. This shows that the emitting species is the same in both cases. This further reinforced the proposed mechanism.

1.5. Motivation for the present work

The main objective of the present thesis work is to gain more knowledge on dual emission generated by ESIPT and TICT processes and to control these emission behaviors by external stimuli.

The organic molecules can bind with metal ions and it can act as metal carrier. As discussed, the ESIPT process is affected by the presence of metal ion. It can be used to follow the metal ion chelation. HPBO is well studied ESIPT exhibiting molecule,[153-156] The change in spectral property of HPBO due to chelation with metal ion can be used to detect or to deliver the metal ion. Also the host molecules are studied vastly as drug carriers as the host molecules are capable to encapsulate the drugs into its cavity.[157-160] Hence the use of host molecules may stimulate HPBO as a better deliver for the metal ion. Therefore, the effect of two host molecules β-CD and CB-7 on the HPBO metal complexation was studied.

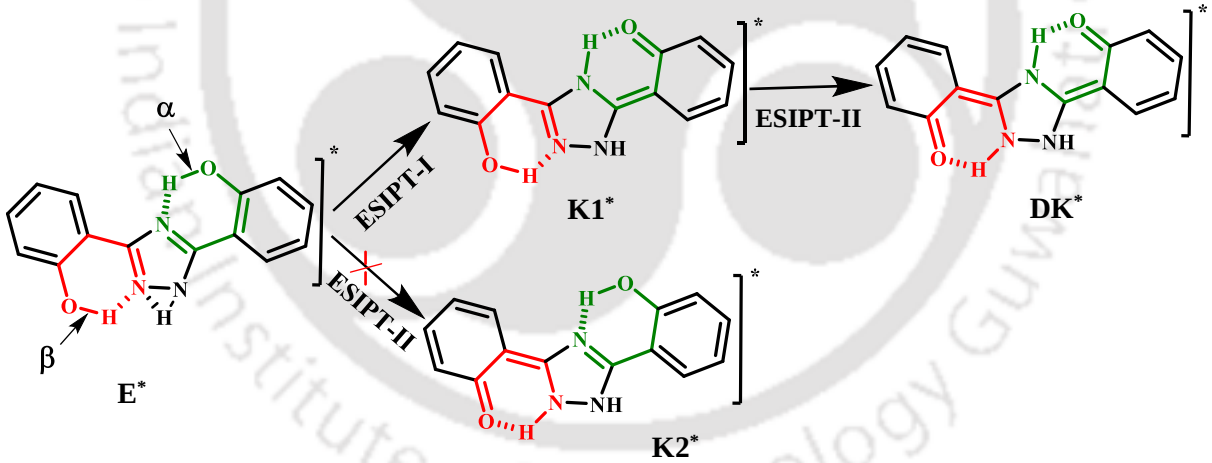

Scheme 1.17: Proton transfer triggered proton transfer (PTTPT) in bis-HPTA-I.

Recently, a new kind of excited state proton transfer process, proton transfer triggered proton transfer (PTTPT, **Scheme 1.17**) is reported in a triazole derivative fluorophore, 3,5-bis(2-hydroxyphenyl)-1H-1,2,4-triazole (bis-HPTA).[161] Though the fluorophore has two proton donor-acceptor pair, but initially only one pair is ESIPT (ESIPT-I) active. The shuttling of 'NH' proton between adjacent nitrogen atoms due to annular tautomerism prevents the ESIPT (ESIPT-II) in other pair. But ESIPT-I reduces the effectiveness of annular tautomerism. As a result, ESIPT-I

triggers ESIPT-II and gives a diketo tautomer and the process is labeled as proton transfer triggered proton transfer (PTTPT).

N.N-Dimethylformamide (DMF) is an interesting polar solvent. The C=O group present in a DMF molecule is a strong hydrogen bond acceptor and the CH/CH_3 groups are weak hydrogen bond donors.[162] Hence, the intermolecular hydrogen bonding of bis-HPTA with DMF could prevent annular tautomerism and ESIPT-II can be achieved without the assistance of ESIPT-I. Therefore, the effect of DMF on the spectral characteristics of bis-HPTA is investigated. Further DMF acts as a very good reducing and stabilizing agent to synthesize silver nanoparticle. Hence, the effect of silver particle on the ESIPT of bis-HPTA in DMF was also investigated.

The motivation for the next chapters was to tune the ESIPT and TICT with the external stimuli. In ESIPT and TICT combined system reported so far, depending on the system mostly either one of the processes or precursor/successor relationship was observed.[141-151] Exclusive switching between the mutually independent ESIPT and TICT state was scarcely reported so far. HPIPs are capable of undergoing ESIPT.[14, 163, 164] As discussed, APIPs and their *N,N*-dimethyl amino derivatives are interesting molecules, and they emit TICT emission only in protic solvents due to intermolecular proton transfer.[20, 123-125] On the other hand, the intermolecular proton transfer suppresses the ESIPT process. If the ESIPT moiety is introduced in APIP derivatives, it may be possible depending on the protic nature of the solvent light may switch on either the TICT or ESIPT process. APIP-c emits normal emission in aprotic solvents and emits TICT emission along with normal emission only in protic solvents.[125] Introduction of intramolecular hydrogen bonding moiety 'OH' suppress the TICT, and only ESIPT was observed from 2-(4'-amino-2′-hydroxyphenyl)-1H-imidazo[4,5-c]pyridine (AHPIP-c).[165] TICT depends upon the electron density of the charge donor and the withdrawing ability of the acceptor. Position of the pyridyl nitrogen plays a key role in the TICT process.[123, 124, 166, 167] It is observed that imidazo[4,5-b] pyridine is better charge acceptor than imidazo[4,5-c]pyridine. Therefore, imidazo[4,5-b]pyridine with ESIPT cable moiety and higher electron donating diethylamino group, 2-(4′-diethylamino-2′-hydroxyphenyl)-1H-imidazo-[4,5-b]pyridine (DEAHPIP-b) was synthesized and studied in aprotic and protic solvents. Further the methoxy analogous of DEAHPIP-b i.e. 2-(4′-diethylamino-2′-methoxyphenyl)-1H-imidazo-[4,5-b]pyridine (DEAMPIP-b) was also synthesized and studied to obtain a better understanding on the excited state nature of DEAHPIP-b.

Now-a-days nanoparticles also became a promising carrier in the field of drug delivery.[168, 169] The nanoscale materials have distinctive physical and chemical properties over their bulk counterparts due to their high surface area as well as great adsorption and liberating nature.[170, 171] These unique characteristics of nanoparticles mark them as pertinent candidates for numerous applications. From the ancient time silver, has been used as antimicrobial agent.[172, 173] Silver nanoparticles have substantial antimicrobial activity over silver ions.[174, 175] Similarly, metallic silver used in jewelry, in the field of electronics and catalysis requires a large amount of metal. In contrast, silver nanoparticles have extensive applications in the field of catalysis, chemical protections, tissue engineering, plasmon enhanced solar cells, photonics, drug delivery, waste water treatment, etc. requiring much smaller amounts of silver to complete the job.[171, 176-179] Silver nanoparticles display the highest efficacy of plasmon excitation compared to gold, copper, aluminum, lithium.[180, 181] Silver nanoparticles significantly change the photophysical properties of fluorophores as the surface plasmon resonance (SPR) band is usually observed in the visible region and overlays with the spectrum of the fluorophore and also is the only material whose plasmon resonance can be tweaked over a broad range of wavelength in the visible spectrum.[182, 183] Although other metal nanoparticles were investigated over the past decade, the silver nanoparticle has more advantages above other metal nanoparticles in terms of low environmental toxicity, high stability, material cost, wide-reaching plasmonic applications. Hence interaction of ESIPT active fluorophore with silver nanoparticles is interesting area to explore. The interaction of silver nanoparticles with a set of ESIPT fluorophores (HPBI, HPIP-b, HPIP-c) **[Chart 1.5]** has been studied and reported that the fluorophores stabilize the nanoparticles whereas the nanoparticle hampers the ESIPT process of the fluorophores.[184] Bojarski et al. have reported that on the silver nanoparticle surface, the ESIPT fluorescence of flavonol **[Chart 1.8]** was enhanced which enables it to determine the low-activity hydrolase enzymes.[185] The interaction of DMAPIPs with silver nanoparticle induces the TICT emission of these fluorophores.[166] Hence, the effect of silver nanoparticle on controlling the reaction coordinates of DEAHPIP-b is explored.

The hydrogen ion is an important external stimulus which can strongly influence the reaction path. The protonation of the nitrogen or deprotonation the hydroxyl group and the 'NH' group of DEAHPIP-b may impede or induce the ESIPT/TICT processes. Thus, the effect of pH on the spectral characteristics of DEAHPIP-b and its methoxy derivatives are examined.

Chapter 2

Materials, Methods and Instrumentations

2.0. Introduction

In the first part of this chapter, the details of the materials used for performing the work in the present thesis, and the synthetic procedures of the fluorophores and silver nanoparticles are described in this chapter. In the second part, the methodology used for sample preparation, theoretical calculations and analysis are discussed in detail. At the end of the chapter, a brief description of the instruments used in the present thesis work is given.

2.1. Materials

The details of the materials used are specified below.

2.1.1. Solvents

- Acetonitrile (HPLC grade, Spectrochem India)
- 1-Butanol (HPLC grade, Spectrochem India)
- *N*,*N*-Dimethylformamide (DMF, HPLC grade, Spectrochem India)
- Dimethylsulfoxide (DMSO, HPLC grade, Spectrochem India)
- Diethyl ether (ether, AR grade, Merck India)
- Ethanol (ACS grade, Merck India)
- Methanol (HPLC grade, Spectrochem India)
- Tetrahydrofuran (THF, HPLC grade, Spectrochem India)
- 1-Propanol (HPLC grade, Spectrochem India)
- 2-Propanol (HPLC grade, Spectrochem India)
- Water (Millipore water)

All the solvents were tested and found to be transparent in the region of spectral measurement before use.

2.1.2. Metal Salts

- Barium perchlorate hydrate, $Ba(ClO_4)_2.xH_2O$ (Sigma Aldrich)
- Cadmium nitrate hydrate, $Cd(NO_3)_2.xH_2O$ (Sigma Aldrich)
- Calcium perchlorate tetrahydrate, $Ca(ClO_4)_2.4H_2O$ (Sigma Aldrich)
- Chromium chloride hexahydrate, $CrCl_3.6H_2O$ (Sigma Aldrich)

- Cobalt chloride hexahydrate, $CoCl_2.6H_2O$ (Sigma Aldrich)
- Copper perchlorate hexahydrate, $Cu(ClO_4)_2.6H_2O$ (Sigma Aldrich)
- Iron perchlorate, $Fe(ClO_4)_2.xH_2O$ (Sigma Aldrich)
- Lead perchlorate hydrate, $Pb(ClO_4)_2.xH_2O$ (Sigma Aldrich)
- Lithium perchlorate, $LiClO_4$ (Sigma Aldrich)
- Magnesium perchlorate hexahydrate, $Mg(ClO_4)_2.6H_2O$ (Sigma Aldrich)
- Manganese nitrate hydrate, $Mn(NO_3)_2 \cdot xH_2O$ (Sigma Aldrich)
- Mercuric Chloride, $HgCl_2$ (Sigma Aldrich)
- Nickel perchlorate hexahydrate, $Ni(ClO_4)_2.6H_2O$ (Sigma Aldrich)
- Potassium perchlorate, $KClO_4$ (Sigma Aldrich)
- Silver nitrate, $AgNO_3$ (Sigma Aldrich)
- Sodium perchlorate monohydrate, $NaClO_4.H_2O$ (Sigma Aldrich)
- Zinc perchlorate hexahydrate, $Zn(ClO_4)_2.6H_2O$ (Sigma Aldrich)

2.1.3. Other Chemicals

- Cetyltrimethylammonium bromide (CTAB, Sigma Aldrich)
- Chloroform-d ($CDCl_3$, Sigma Aldrich)
- Cucurbit[7]uril hydrate (CB-7, Sigma Aldrich)
- β -Cyclodextrin (β-CD, Sigma Aldrich)
- 2,3-Diaminopyridine (Sigma Aldrich)
- Dimethylsulfoxide-d_6 (DMSO-d_6, Sigma Aldrich)
- Heavy water (D_2O, Sigma Aldrich)
- HPBO (Sigma Aldrich)
- Methyl iodide (CH_3I, Sigma Aldrich)
- 4-*N*,*N*-diethylamino salicylaldehyde (Sigma Aldrich)
- Potassium hydroxide, (KOH, Merck India)
- Silica gel (60-120 mesh) (Merck India)
- Silica gel for thin layer chromatography (Merck India)
- Silica gel GF254 (Merck India)
- Sodium dodecyl sulfate (SDS, Sigma Aldrich)
- Sodium hydroxide, (NaOH, Merck India)

- Sulphuric Acid, (H_2SO_4, AR grade, Rankem India)
- Triton X-100 (TX-100, Merck India)

2.1.4. Synthesis

2.1.4.1. Silver nanoparticles

1 mM silver nitrate was used to prepare silver nanoparticles by following the method reported by Pastoriza-Santos.[186] The ionic silver was reduced to nanoparticle by DMF at 100° C in an hour, in the absence of any other stabilizing agents by the following reaction.

$$HCONMe_2 + 2Ag^+ + H_2O \longrightarrow 2Ag^0 + Me_2NCOOH + 2H^+ \qquad (2.1)$$

The high temperature favors the decomposition of carbamic acid and subsequently favors the vaporization of ensued amine.

$$Me_2NCOOH \longrightarrow CO_2 + Me_2NH \qquad (2.2)$$

During the course of the reaction, the color of the solution changes with time. The color of the fresh solution of nanoparticles was golden yellow, and then it turns brown. In the absence of stabilizer with time, shiny metal particles were deposited on the wall of the container. The details of the stabilization of the silver particles by the fluorophores will be discussed in **Chapter 4** and **Chapter 6**.

2.1.4.2. 2-(4′-diethylamino-2′-hydroxyphenyl)-1H-imidazo-[4,5-b] pyridine (DEAHPIP-b)

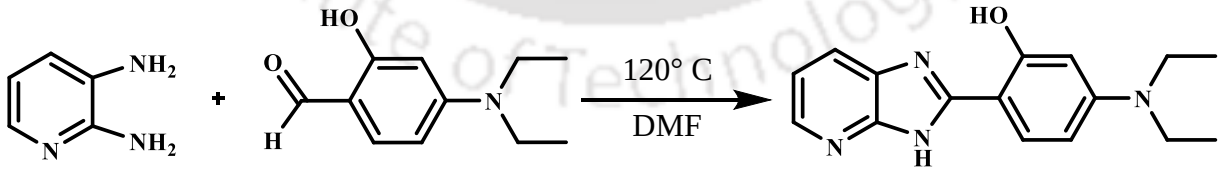

Scheme 2.1: Synthesis of DEAHPIP-b.

2-(4′-diethylamino-2′-hydroxyphenyl)-1H-imidazo-[4,5-b] pyridine (DEAHPIP-b) was synthesized by refluxing equimolar amount of 2,3-diaminopyridine and 4-*N*,*N*-diethyl amino salicylaldehyde in DMF at 120° C by following the procedure reported for similar molecules

[Scheme 2.1].[187] The compound was purified by column chromatography and confirmed by NMR and HRMS.

^{1}H NMR (600 MHz, DMSO-d6): δ 12.87 (s, 1H), 8.25 (dd, 1H), 7.94 (d, 1H), 7.86 (t, 1H), 7.20 (m, 1H), 6.38 (m, 1H), 6.20 (d, 1H), 3.39 (m, 4H), 1.12 (t, 6H).

HRMS (ESI) m/z: calculated 283.148, observed 283.156 [M + H^+]

2.1.4.3. 4-N,N-diethylamino-2-methoxybenzaldehyde

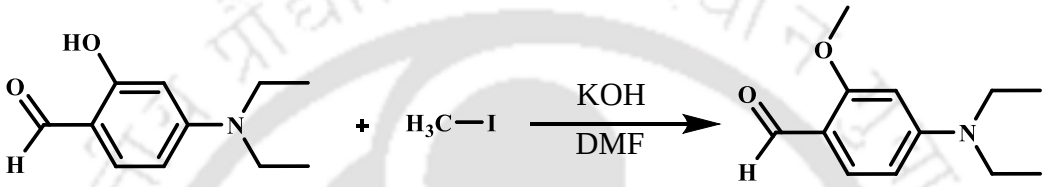

Scheme 2.2: Synthesis of 4-*N*,*N*-diethylamino-2-methoxybenzaldehyde.

4-*N*,*N*-Diethylamino-2-methoxybenzaldehyde was synthesized by methoxylation of 4-*N*,*N*-diethylamino salicylaldehyde in DMF with CH_3I in the presence of KOH **[Scheme 2.2]**.[188] The compound was purified by crystallization process in methanol and confirmed by NMR and HRMS.

^{1}H NMR (600 MHz, $CDCl_3$): δ 10.10 (s, 1H), 7.69 (d, 1H), 6.27 (d, 1H), 6.01 (s, 1H), 3.87 (s, 3H), 3.43 (q, 4H), 1.22 (t, 6H).

HRMS (ESI) m/z: calculated 208.125, observed 208.142 [M + H^+]

2.1.4.4. 2-(4′-diethylamino-2′-methoxyphenyl)-1H-imidazo-[4,5-b] pyridine (DEAMPIP-b)

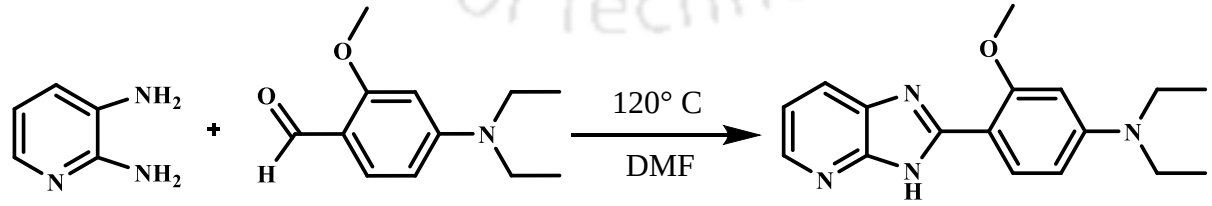

Scheme 2.3: Synthesis of DEAMPIP-b.

2-(4′-diethylamino-2′-methoxyphenyl)-1H-imidazo-[4,5-b]pyridine (DEAMPIP-b) was synthesized by refluxing 2,3-diaminopyridine and 4-*N*,*N*-diethylamino 2-methoxybenzaldehyde in DMF at 120° C **[Scheme 2.3]**,[187] and purified by column chromatography. The product was confirmed by NMR and HRMS.

^{1}H NMR (600 MHz, $CDCl_3$): δ 10.74 (s, 1H), 8.35 (d, 1H), 7.92 (s, 1H), 7.14 (s, 1H), 6.44 (d, 1H), 6.21 (s, 1H), 4.02 (s, 3H), 3.42 (t, 4H), 1.22 (t, 6H).

HRMS (ESI) m/z: calculated 296.163, observed 297.104 [M + H^+]

2.1.4.5. 3,5-bis(2-hydroxyphenyl)-1H-1,2,4-triazole (Bis-HPTA)

3,5-bis(2-hydroxyphenyl)-1H-1,2,4-triazole (Bis-HPTA) was present in the laboratory in pure form. The synthetic procedure for the synthesis of bis-HPTA was reported elsewhere.[161]

2.2. Preparation of Samples

2.2.1. In Solvents

The stock solutions of HPBO and bis-HPTA were prepared in acetonitrile and that of DEAHPIP-b and DEAMPIP-b were prepared in methanol. The strength of eah solution was 1 mM. The spectral measurements were performed in the concentration range of 3 to 5 μM depending on the absorbance of the fluorophore. The required volume of fluorophore solutions pipetted out from the stock solution to 10 ml volumetric flasks and dried. After drying the fluorophores, the solutions were prepared in different solvents as per requirement by adding the appropriate solvent upto the mark. The solution was then sonicated to completely dissolve the fluorophores in those solvents. For pH titration, the required amount of H_2SO_4 or NaOH solution was added to obtain the desired pH. For pK_a studies due to poor solubility of DEAHPIP-b, 5% methanol solution in water was used.

2.2.2. Fluorophore–metal solution

For metal ion titrations, stock solutions of metal salts were prepared in acetonitrile/DMSO/water in the presence of dried fluorophores. An appropriate amount of stock solution was mixed with an appropropriate amount of solvent to obtain the desired concentration.

2.2.3. Fluorophore–*β*-CD Solution

For *β*-CD titrations stock solutions of *β*-CD were prepared in DMSO/water in the presence of dried fluorophore in the absence and presence of Zn^{2+}. An appropriate amount of stock solution was mixed with an appropriate amount of solvent to obtain the desired concentration.

2.2.4. Fluorophore–CB-7 Solution

For CB-7 titrations stock solution of CB-7 solutions were prepared in DMSO/water in the presence of dried fluorophore in the absence and presence of Zn^{2+}. An appropriate amount of stock solution was mixed with an appropriate amount of solvent to obtain the desired concentration.

2.2.5. Fluorophore–silver nanoparticle solution

For silver particle titration stock solution of silver particles were prepared in DMF in the absence and presence of dried fluorophores. An appropriate amount of stock solution was mixed with an appropriate amount of solvent to obtain the desired concentration.

2.2.6. Fluorophore–surfactant solution

30 mM strength of each surfactant (CTAB/SDS/TX-100) solutions were prepared in the presence of dried DEAHPIP-b in the absence as well as in the presence 0.1 mM silver particle in DMF. The respective solutions without the fluorophore were prepared for recording reference absorption spectra.

2.3. Methods

2.3.1. Quantum Mechanical Calculation

All the density functional theory (DFT) and time-dependent density functional theory (TDDFT) calculations were performed by using Gaussian 09W program[189] and the input files were drawn in Gauss View 5.0. Ground state and excited state optimization for the geometries were performed by DFT and TDDFT, respectively.[190, 191] Integral equations formalism-polarizable continuum model (IEFPCM) was used to include the solvent effect in the calculations.[192] In proposed fluorophore–solvent complexes in **Chapter 4** and **Chapter 6**, the calculations were

accomplished adding solvent molecules at hydrogen bonding distance. Different functions and different basis sets were used to perform the calculations.[193, 194] The excitation energy and emission energy were obtained by performing TDDFT calculation on the respective optimized geometries.

2.3.2. Fluorescence Quantum Yield

Quantum yield of fluorescence (Φ_f) is defined as the ratio of the number of photons emitted to the total number of photons absorbed as shown in below:

$$\Phi_f = \frac{\text{Number of photons emitted}}{\text{Number of photons absorbed}} \tag{2.3}$$

The relative fluorescence quantum yields of the samples were determined with respect to a standard sample of known quantum yield by using the equation,

$$\Phi_S = \Phi_R \frac{n^2}{n_R^{\,2}} \times \frac{A_R}{A_S} \times \frac{I_S}{I_R} \tag{2.4}$$

I_S and I_R symbolize the area under the emission spectra of the sample and reference, respectively. A_S and A_R symbolize the absorbance values for the sample and reference, respectively. n_S and n_R denote the refractive indices for the solvent used for the sample and the reference solutions, respectively. In the present thesis, quinine sulphate in 1N sulphuric acid of quantum yield 0.55 is used as the reference.[195]

2.3.3. Determination of Ionization Constant

The acid dissociation constant (K_a) or the pK_a is the measure of the strength of an acid or a base. Hammett equation as shown below is employed for the determination of ionization constant of an acid in aqueous medium.

$$BH^+ + H_2O \rightleftharpoons B + H_3O^+ \tag{2.5}$$

$$H_0 = \mathrm{p}K_a + \log\frac{[B]}{[BH^+]} \tag{2.6}$$

where $[BH^+]$ and $[B]$ denote the molar concentration of conjugate acid and base respectively. H_0 is called Hammett's acidity function and is defined as follows

$$H_0 = -\log\frac{a_{H^+} f_B}{f_{BH^+}} \quad (2.7)$$

Where f_B and f_{BH^+} are the acidity coefficient of conjugate base and acid respectively. a_{H^+} is the activity of the proton. For dilute solution, H_0 is replaced by pH. The plot of pH versus $\log\frac{[B]}{[BH^+]}$ is a straight line with unit slope and the pH = pK_a when $[B] = [BH^+]$. $\frac{[B]}{[BH^+]}$ can be determined from the following relation.

$$\frac{[B]}{[BH^+]} = \frac{[A_B - A]}{[A - A_{BH^+}]} \quad (2.8)$$

where A_{BH^+} and A_B are the absorbance of the pure BH^+ and B respectively, and A is absorbance of any solution (at same wavelength) in which BH^+ is partially ionized.

$$\frac{[B]}{[BH^+]} = \frac{[B]}{[C]-[B]} \quad (2.9)$$

where $[C]$ is the molar concentration of the compound in the experimental solution.

$$[B] = \frac{A(\lambda_1)\varepsilon^+_{BH}(\lambda_2) - A(\lambda_2)\varepsilon^+_{BH}(\lambda_1)}{\varepsilon_B(\lambda_1)\varepsilon^+_{BH}(\lambda_2) - \varepsilon_B(\lambda_2)\varepsilon^+_{BH}(\lambda_1)} \quad (2.10)$$

ε is the molar extinction coefficient and for the calculation generally two wavelengths were considered (λ_1 and λ_2) at both sides of the isosbestic point of the absorption spectra at different pH.

2.3.4. Time resolved area normalized emission spectra

The emission spectra of the fluorophores were resolved by following the method reported by Periasamy et al.[196] The fluorescence decays were recorded at several wavelengths and fitted with multi-exponential function using reconvulation method. A corrected steady state emission spectrum was recorded at exciting at same wavelength that used as a light source to record the fluorescence decays. The fluorescence spectra at various times were constructed using both

emission spectrum and fluorescence decays data. Time resolved emission spectra at different wavelengths were constructed using the equation 2.11.

$$I(\nu, t) = I_{ss}(\nu)\frac{\sum_j \alpha_j(\nu)e^{-t/\tau_j(\nu)}}{\sum_j \alpha_j(\nu)\tau_j(\nu)} \qquad (2.11)$$

where $I_{ss}(\nu)$ is the steady state fluorescence intensity at ν, $\alpha_j(\nu)$ and $\tau_j(\nu)$ are the fit parameters. Time resolved area normalized emission spectra (TRANES) were constructed by normalizing the area of each emission spectra at different times.

2.4. Instruments

2.4.1. pH Meter

In the present thesis, the pH of the solutions was measured using a standard Jenway (model No 3510) pH meter having a glass electrode. The pH meter was calibrated by using three standard buffer solutions (pH 4, pH 7 and pH 10) within a range of ± 0.02 pH units to avoid the error. For preparing solutions of higher acidity (H_0) and basicity (H_) strength, i.e., out of pH range, Hammett's acidity scale and Yagil's basicity scale, respectively, were followed.[197, 198]

2.4.2. UV-visible Spectrophotometer

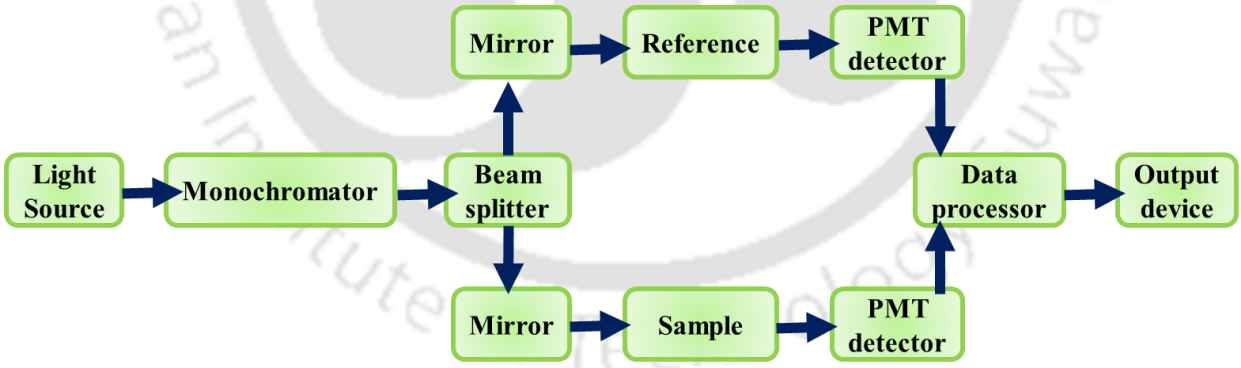

Figure 2.1: Block diagram of a double beam- UV-visible spectrophotometer.

The UV- visible Spectrophotometer provides information about the electronic transitions of the fluorophore. The absorption measurements were performed on the studied fluorophores with Perkin Elmer lambda-25 double beam spectrophotometer comprising of tungsten and deuterium lamps as excitation light source and diode as the detector. The block diagram of the UV-visible

spectrophotometer is shown in **Figure 2.1**. It consists of a light source, a monochromator, a sample holder, a detector, an amplifier and a recording device. A beam of polychromatic light source passes through a monochromator and is separated into components. The monochromatic beam is further splitted into sample and reference beam. The sample beam pass through the quartz cuvette with sample and the reference beam through the reference cuvette containing the reference solution and both reach the detector. The Spectrophotometer scans individual wavelength and provides the absorption spectra.

2.4.3. Steady State Spectrofluorimeter

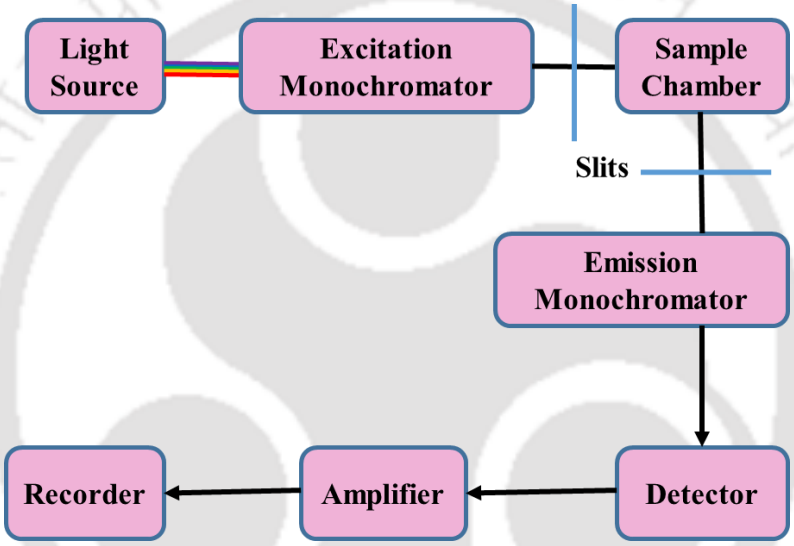

Figure 2.2: Block diagram of a Spectrofluorimeter.

Steady State Fluorescence measures the average fluorescence of a sample. In the present thesis the steady state fluorescence measurements were carried out with Jobin Yvon Spex Fluoromax 4 Spectrofluorimeter. The block diagram for steady state fluorimeter is shown in **Figure 2.2**.

The basic parts in the spectrofluorimeter include a light source, excitation monochromator, emission monochromator, sample holder, shutter, beam splitter, sometimes a polarizer, etc. Xenon arc lamp is the light source employed for carrying out the spectral measurement. Motorized monochromators are used for scanning each wavelength and these are controlled by computers.

Emission spectra can be obtained by keeping the excitation wavelength (λ_{exc}) fixed. In the same way excitation spectra can be measured by fixing the emission wavelength. The emission

spectra are largely dependent on monochromator efficiency and the response of the photo multiplier tube and are needed to be corrected. To get a corrected spectrum, a reference fluorophore with known corrected emission spectrum is considered for correction factor calculation or by a calibrated tungsten lamp. For Fluoromax 4 emission spectrum correction factors were provided by the manufacturer.

The excitation spectra are distorted due to difference in the intensity of the exciting source and the transmission efficiency of the monochromator. The quantum counter nullifies the sensitivity of wavelength dependence of sample and of reference photomultiplier. The ratio of fluorescence signal from sample to quantum counter or photodiode as a function of excitation wavelength provides the correction factor. However, this correction is not efficient; further correction factors can be obtained from the measurement of a known fluorophore, which absorbs in the same wavelength range as that of the sample to be studied gives more accurate results. In the present work, correction factors for Fluoromax 4 are supplied by the manufacturer.

2.4.4. Time Resolved Spectrofluorimeter

The fluorescence lifetimes were obtained using time correlated single photon counting (TCSPC) technique using the Edinburgh Instrument LifeSpec II. 308 nm LED from PicoQuant or 375 nm diode laser from Edinburgh were used as light source. The block diagram of a TCSPC instrument is shown in **Figure 2.3**. In this technique, the samples to be studied are excited with a pulsed short light LED or laser diode light source. Upon excitation with a laser diode or LED, the excited molecules emit photons with different relaxation time and a decay profile is obtained with a certain rate of occurrence. The basic principle of this TCSPC technique is the detection of single photons and measuring their arrival time with respect to instrument response function. A start signal and stop signal pulse are used to travel down to activate time-to-amplitude converter (TAC) and sample. The output obtained from TAC was amplified with an amplifier and this analogue pulse is further get converted to digital pulse with the help of analogue to digital converter (ADC). To accumulate sufficient numbers of photons for decay histogram, the time measurement of the start and stop sequence is repeated a number of times in the full range of delays between excitation and emission. The resulting histogram, counts versus time channels will represent the plot of fluorescence decay profiles.

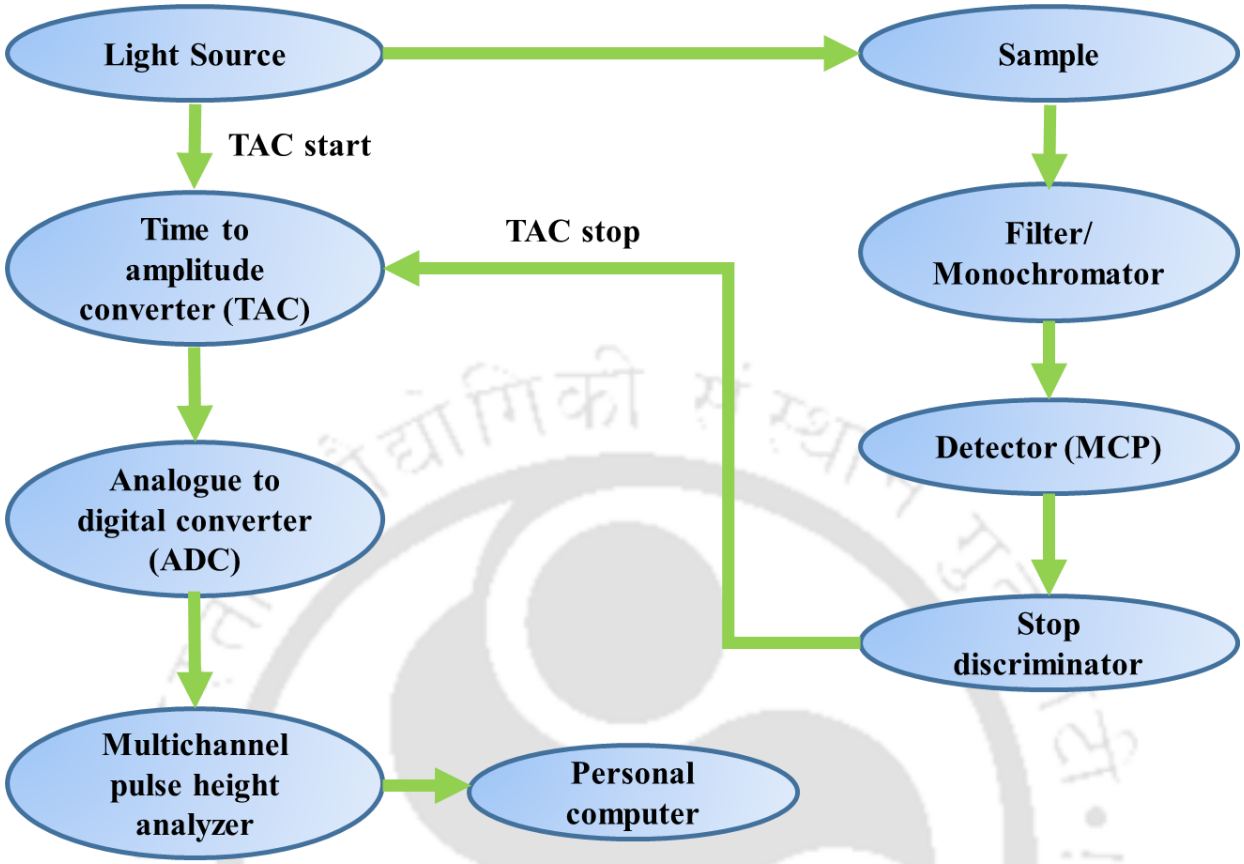

Figure 2.3: Block diagram of a TCSPC instrument.

The time resolved data were analyzed using the Reconvulation method from the FAST software provided by Edinburgh Instruments Ltd. Life Specs II operates in 50 ps response time with Hamamatsu MCP detector.

2.4.5. Other Instruments

The mass spectra of the synthesized fluorophore were recorded by using a high resolution mass spectrometry (HRMS) instrument of Agilent technologies Waters Instruments (Q-Tof Premier). Fourier transform NMR spectra were recorded on Bruker 600 MHz NMR spectrometer. To study the dimensions of silver nanoparticle in the absence and presence of the fluorophores and in presence of CTAB, the dynamic light scattering (DLS) measurements were performed in a Malvern Zetasizer ZS-90 instrument. The electron microscopic images of the particles were obtained using a Carl Zeiss, Gemini 300 field emission scanning electron microscope (FESEM). A drop of 10 µL from each sample was deposited on the glass slide covered with aluminum foil, dried and then sputter-coated with gold film using a sputter coater before proceeding for imaging.

Chapter 3

Host-Guest Interaction aided Zn^{2+} transport by ESIPT active 2-(2'-hydroxyphenyl)benzoxazole

3.0. Introduction

Zinc is a necessary micronutrient in daily life.[199-201] It is essential for the body's immune system. It is abundantly present in the brain and has various functions in neurological diseases.[202] Its deficiency in humans is an imperative malnutrition problem. Hence Zn carriers and delivery agents are essential and this has grabbed active research interest. In the present chapter, the feasibility of a well-studied ESIPT active fluorophore HPBO[50, 153, 154] as carrier for zinc was explored. The trans-enol conformer of HPBO upon photoexcitation gives normal emission at shorter wavelength whereas the cis-enol conformer undergoes tautomerisation giving the highly Stokes' shifted keto tautomer emission at longer wavelength **[Chart 3.1]**.[50, 153, 154] Besides the photophysical properties, HPBO has interesting applications.[203-205] Although some metal complexes of HPBO were reported in the literature,[206-208] in the present chapter, the sensitivity of HPBO towards some more metals was researched. Further, the host-guest complexes have remarkable application as drug carriers.[157-160] Hence the use of host molecules may help HPBO as a better deliver agent for zinc. In the present chapter, the effect of two host molecules *β*-CD **[Figure 3.1]** and CB-7 **[Figure 3.2]** on the HPBO zinc complex were studied. The interior of *β*-CD and CB-7 are hydrophobic in nature while the peripheral is hydrophilic.[209, 210] Generally, inclusion complexes are formed by noncovalent interactions such as hydrogen bonding, hydrophobic interactions and van der Waals interaction.[65-67]

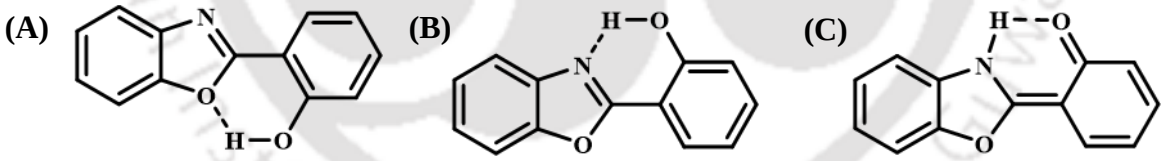

Chart 3.1: (A) trans-enol, **(B)** cis-enol conformers and **(C)** keto tautomer of HPBO.

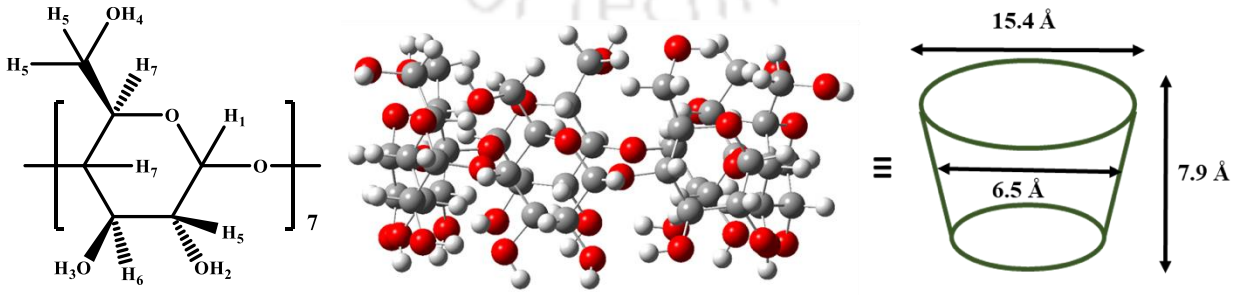

Figure 3.1: Different portrayals of *β*-CD.

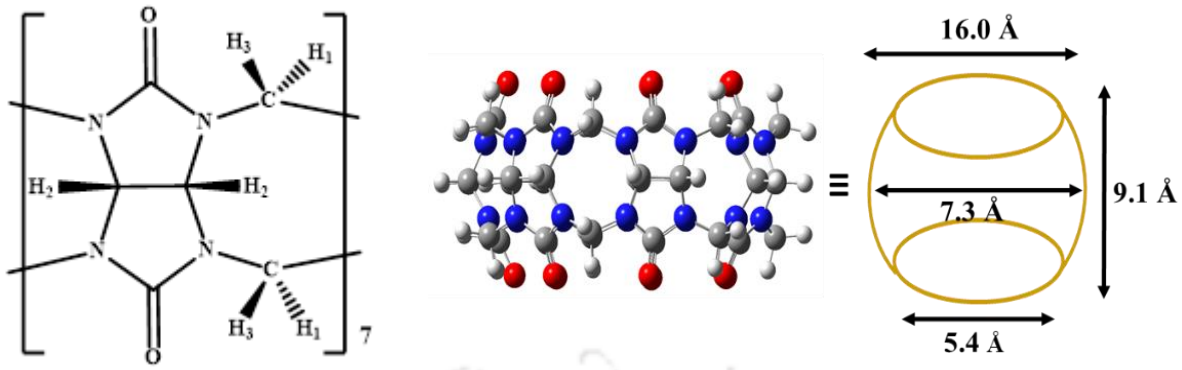

Figure 3.2: Different portrayals of CB-7.

3.1. Effect of metal ions

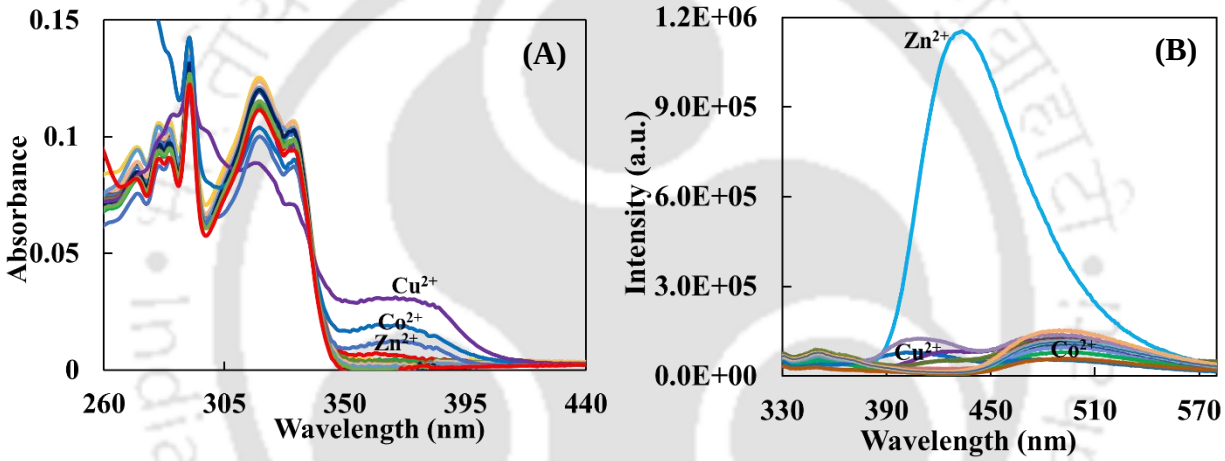

Figure 3.3: (A) Absorption spectra and **(B)** emission spectra of HPBO in acetonitrile in the absence and presence of different metal ions (1 mM concentration), λ_{exc} = 300 nm.

A systematic study of sensing of metal ion by HPBO was investigated using 1 mM concentration of different metal ions (Li^+, Na^+, K^+, Mg^{2+}, Ca^{2+}, Ba^{2+}, Cr^{3+}, Mn^{2+}, Fe^{2+}, Co^{2+}, Cu^{2+}, Ni^{2+}, Ag^+, Zn^{2+}, Cd^{2+}, Hg^{2+}, Pb^2) in acetonitrile. Acetonitrile, a polar aprotic solvent was used because of its noninterfering nature and good solubilizing ability. The absorption spectrum of HPBO has vibrational structures at 318 nm and 330 nm in its longer wavelength absorption band.[50] In the presence of Co^{2+}, Cu^{2+} and Zn^{2+} ions, the absorbance of the band at 318 nm and 330 nm decreases and a new red shifted band appears at 370 nm **[Figure 3.3.A]**. The effects of other metals are very little or negligible. In acetonitrile, HPBO emits the normal emission at 360 nm and the tautomer emission at 490 nm **[Figure 3.3.B]**. In the presence of Zn^{2+}, the new emission occurs at 435 nm with high intensity. The emission spectra under the conditions suggested that the spectral

changes in the presence of other metal ions are insignificant compared to that in the presence of Zn^{2+}. The bar diagram is plotted considering the emission intensity at 435 nm **[Figure 3.4]**. The spectral analysis shows that HPBO has a strong affinity towards Zn^{2+}. Henceforward, the detailed studies are performed on the interaction of Zn^{2+} with HPBO in three different solvents acetonitrile, DMSO and water.

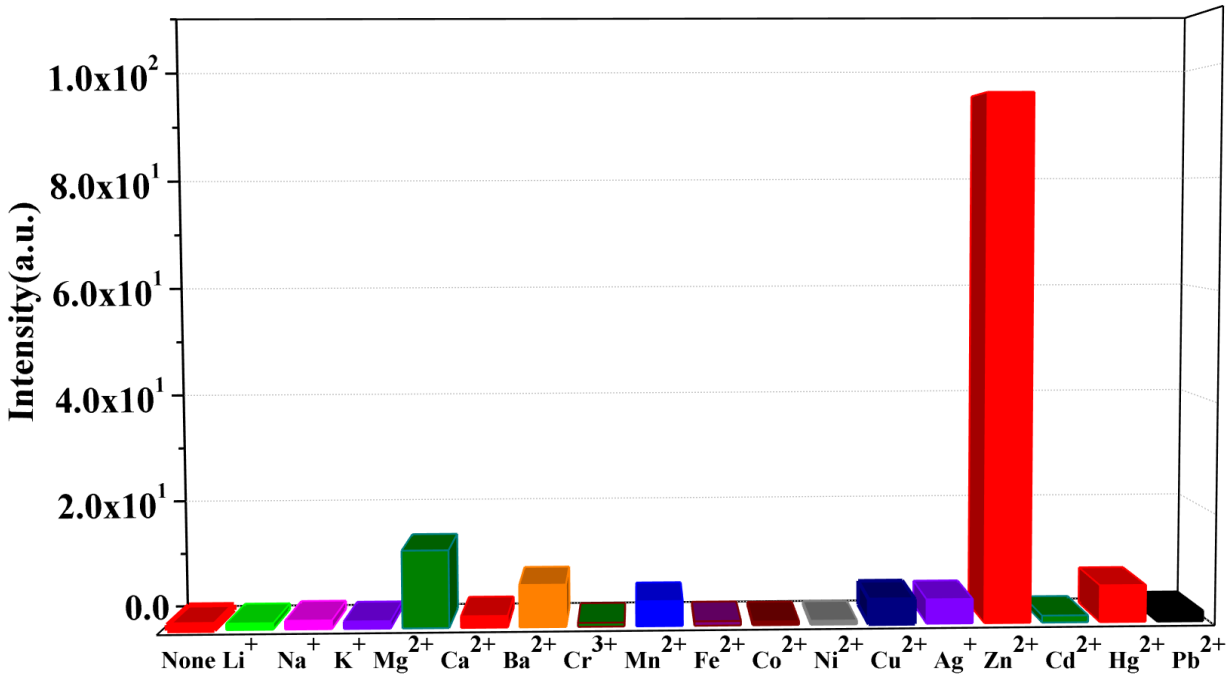

Figure 3.4: The histogram plot for the metal sensitivity of HPBO (considering the intensity at λ_{em} = 435 nm).

3.2. Effect of Zn^{2+} on HPBO

The absorption and emission spectra of HPBO were recorded in presence of different concentrations of Zn^{2+} in acetonitrile, DMSO and water and are shown in **Figure 3.5** to **3.7**. In acetonitrile on increasing Zn^{2+} concentration, the absorbance of the fluorophore decreases at 318 nm and 331 nm, and the absorbance at 370 nm increases due to the metal complex **[Figure 3.5.A]**. Upon addition of Zn^{2+}, initially, the tautomer band shifts hypsochromically and simultaneously the metal complex band at around 430 nm appears **[Figure 3.5.B]**. On further increasing Zn^{2+} concentration, the intensity at 435 nm increases sharply.

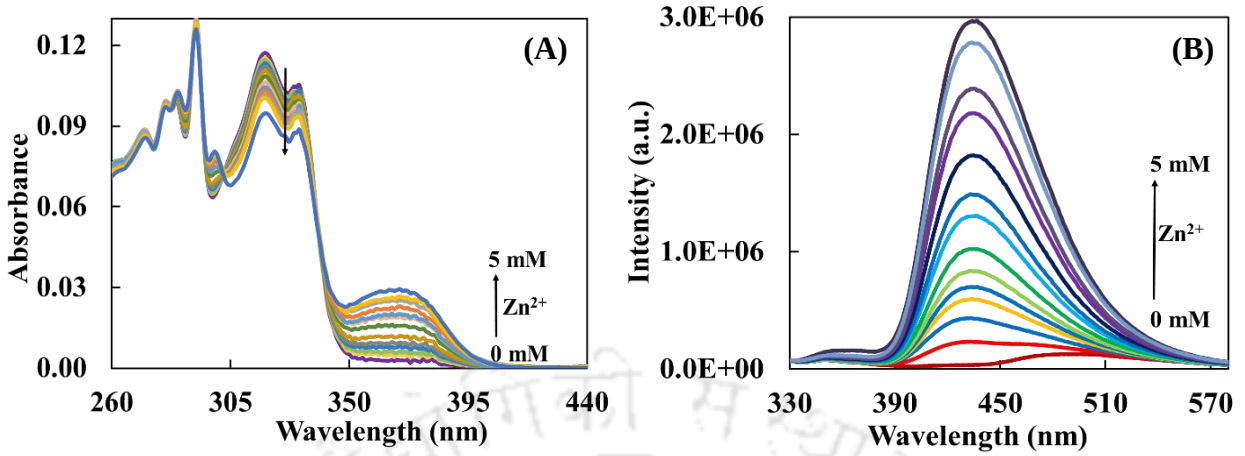

Figure 3.5: (A) Absorption spectra and **(B)** emission spectra of HPBO in presence of different concentration (0 to 5 mM) of Zn^{2+} in acetonitrile, λ_{exc} = 300 nm.

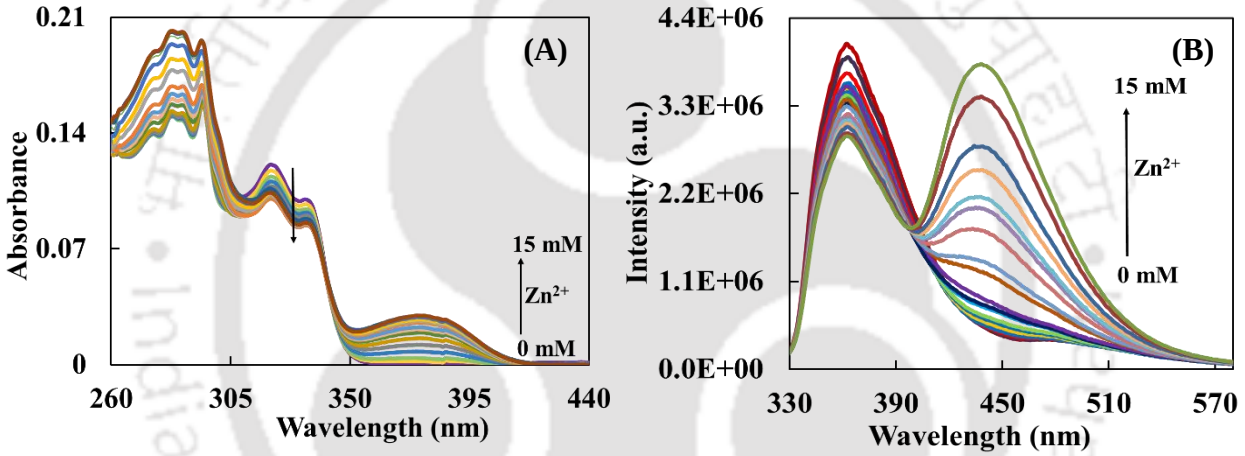

Figure 3.6: (A) Absorption spectra and **(B)** emission spectra of HPBO in presence of different concentration (0 to 15 mM) of Zn^{2+} in DMSO, λ_{exc} = 300 nm.

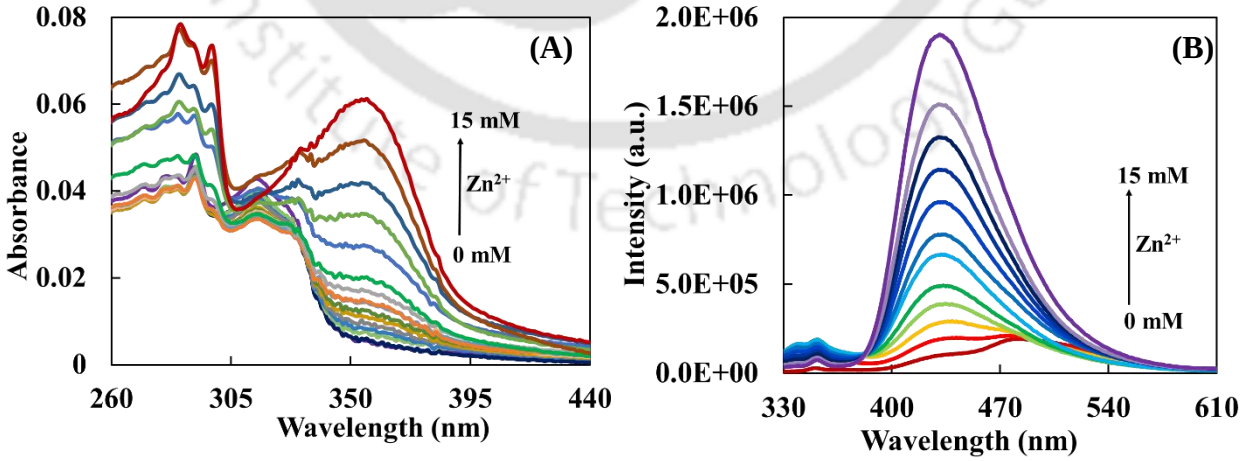

Figure 3.7: (A) Absorption spectra and **(B)** emission spectra of HPBO in presence of different concentration (0 to 15 mM) of Zn^{2+} in water, λ_{exc} = 300 nm.

Like in acetonitrile, in DMSO also the longer wavelength absorption band of HPBO has vibrational structure at 320 nm and 334 nm. On increasing Zn^{2+} concentration, the absorbance of the fluorophore decreases and the absorbance at 380 nm increases due to the formation of metal complex **[Figure 3.6.A]**. In DMSO, the normal emission of HPBO occurs at 360 nm and the tautomer emission occurs at 490 nm. The emission intensity of the normal and the tautomer emissions decrease and a new emissive band appears at ~ 440 nm **[Figure 3.6.B]**. HPBO remains neutral between pH 1.0 to pH 10.0.[50] Hence the experiments were carried out at physiological pH 7.0. In water (at pH 7.0) the absorbance of HPBO is less and the fluorophore absorbs at 316 nm and 328 nm. Gradually increasing Zn^{2+} concentration, the absorbance of HPBO decreases and the band responsible for metal complex appears at 360 nm **[Figure 3.7.A]**. Upon further addition of Zn^{2+}, the absorbance of the 360 nm band increases. In water at pH 7.0, HPBO emits dual emission **[Figure 3.7.B]**. According to Dorr et al.,[211] Fujimaza et al.,[212] Dogra et al.[50] reports, in aqueous medium neutral HPBO emits the normal emission from the trans-enol **[Chart 3.1.A]** and the tautomer **[Chart 3.1.C]** emission due to ESIPT of the cis-enol **[Chart 3.1.B]**. Upon addition of Zn^{2+}, a new band appears at 435 nm. The intensity of the band increases with an increase in concentration of Zn^{2+}, at 15 mM Zn^{2+} only single intense emission observed at 435 nm **[Figure 3.7.B]**.

The stoichiometric ratios and the association constants of HPBO and Zn^{2+} are determined using Benesi-Hildebrand equation in acetonitrile, DMSO and water. The emission intensity at 435 nm is considered to plot the double reciprocal plots of $1/(I-I_0)$ versus $1/[Zn^{2+}]$ in each case **[Figure 3.8]**. The general form of Benesi-Hildebrand equation for a 1:n complex formed between fluorophore and metal M is given below:

$$\frac{1}{I - I_0} = \frac{1}{I_\infty - I_0} + \frac{1}{K[M]^n\{I_\infty - I_0\}} \qquad (3.1)$$

Here [M] is metal ion Zn^{2+} concentration, I_0 and I are the fluorescence intensities in the absence and in the presence of Zn^{2+} respectively, I_∞ is the limiting intensity of fluorescence, *n* is the number of metal atoms binds to the molecule and *K* is the binding constant. The linear plot with good correlation coefficient ($r^2 \approx 0.99$) proposes the formation of 1:1 complex between the fluorophore and Zn^{2+}. The association constants in acetonitrile, DMSO and water are found to be 1.7×10^4 M^{-1}, 2.5×10^1 M^{-1} and 2.0×10^3 M^{-1} respectively.

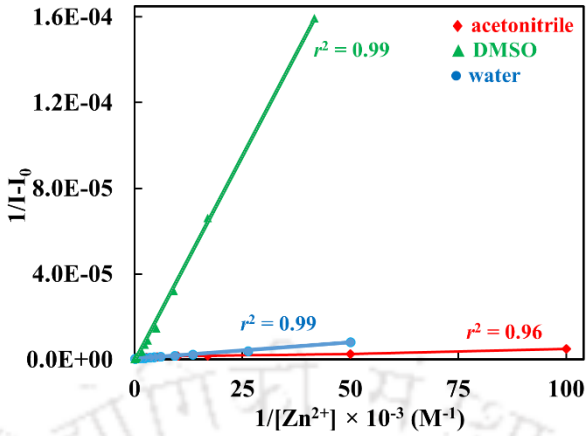

Figure 3.8: Benesi-Hildebrand plot of HPBO–Zn^{2+} in ♦ acetonitrile, ▲ DMSO and ● water.

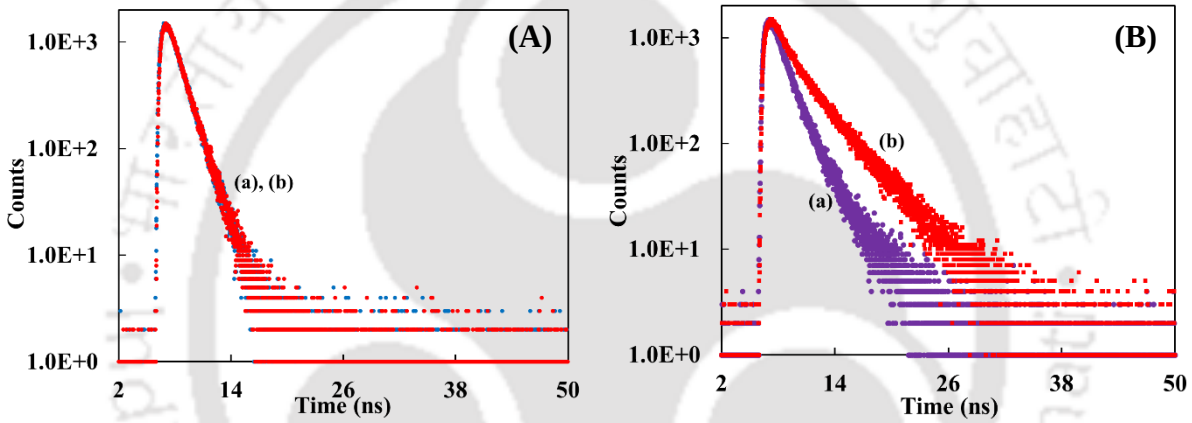

Figure 3.9: The fluorescence decays monitored at **(A)** shorter wavelength emission maxima and **(B)** longer wavelength emission maxima of HPBO in the (a) absence and (b) presence of Zn^{2+} in DMSO, λ_{exc} = 308 nm.

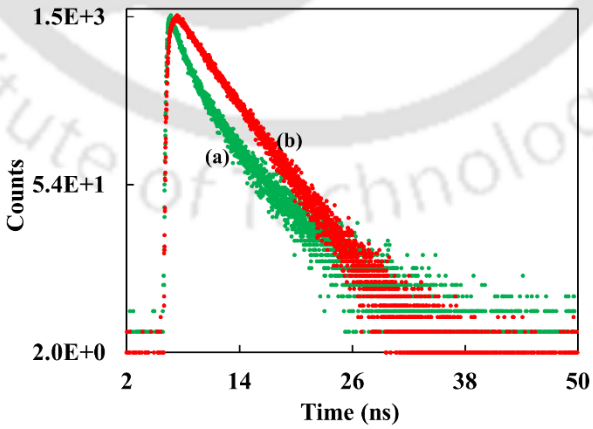

Figure 3.10: The fluorescence decays monitored at (a) tautomer emission maximum of HPBO in the absence of Zn^{2+} and (b) at 435 nm of HPBO–Zn^{2+} complex in water, λ_{exc} = 308 nm.

The fluorescence decays were monitored at emission maxima in both DMSO and water **[Figure 3.9** and **3.10]** and the lifetimes are compiled in **Table 3.1**. In DMSO, the lifetime of the excited trans-enol is 1.5 ns and the lifetime of tautomer is 3.4 ns. In presence of Zn^{2+}, along with the shorter lifetime, one more lifetime of 4.2 ns is obtained and this can be assigned to HPBO–Zn^{2+} complex. This shows still existence of trans-enol which gives normal emission while cis-enol forms the complex. In water, two lifetimes are obtained. The shorter lifetime, 1.5 ns matches with the lifetime of excited trans-enol and hence can be assigned to the same in water. The longer lifetime, 4.9 ns can be assigned to keto tautomer. In presence of Zn^{2+}, only one lifetime is obtained which is due to HPBO–Zn^{2+} complex in water.

Table 3.1: Absorption maxima (λ_{max}^{ab}, nm), emission maxima (λ_{max}^{fl}, nm) and fluorescence lifetime (τ, ns) of HPBO and HPBO complexes in DMSO and water.

	λ_{max}^{ab}	λ_{max}^{fl}		τ	
		Shorter wavelength	Longer wavelength	At shorter wavelength maximum	At longer wavelength maximum
In DMSO					
HPBO	320, 334	360	490	1.5	1.4 (77) 3.4 (23)
HPBO–Zn^{2+}	320, 334, 380	360	440	1.5	1.4 (28) 4.2 (72)
HPBO–*β*-CD	320, 334	360	490	1.5	1.3 (71) 3.1 (29)
HPBO–CB-7	323, 335	360	490	1.5	1.4 (77) 3.5 (23)
HPBO–Zn^{2+}–*β*-CD	322, 335, 380	360	440	1.5	1.4 (31) 4.1 (69)
HPBO– Zn^{2+}–CB-7	322, 335	360	490	1.4	1.4 (64) 3.7 (36)
In water					
HPBO	316, 328	360, 430	485		1.5 (57) 4.9 (43)
HPBO–Zn^{2+}	360		435		3.83
HPBO–*β*-CD	321, 332	367	490		0.8 (38) 2.7 (62)
HPBO–CB-7	313, 326, 351	372	470		0.5 (68) 4.8 (32)
HPBO–Zn^{2+}–*β*-CD	321, 333, 360	360	480		0.7 (57) 3.1 (43)
HPBO–Zn^{2+}–CB-7	315, 328	370	464		0.6 (70) 4.8 (30)

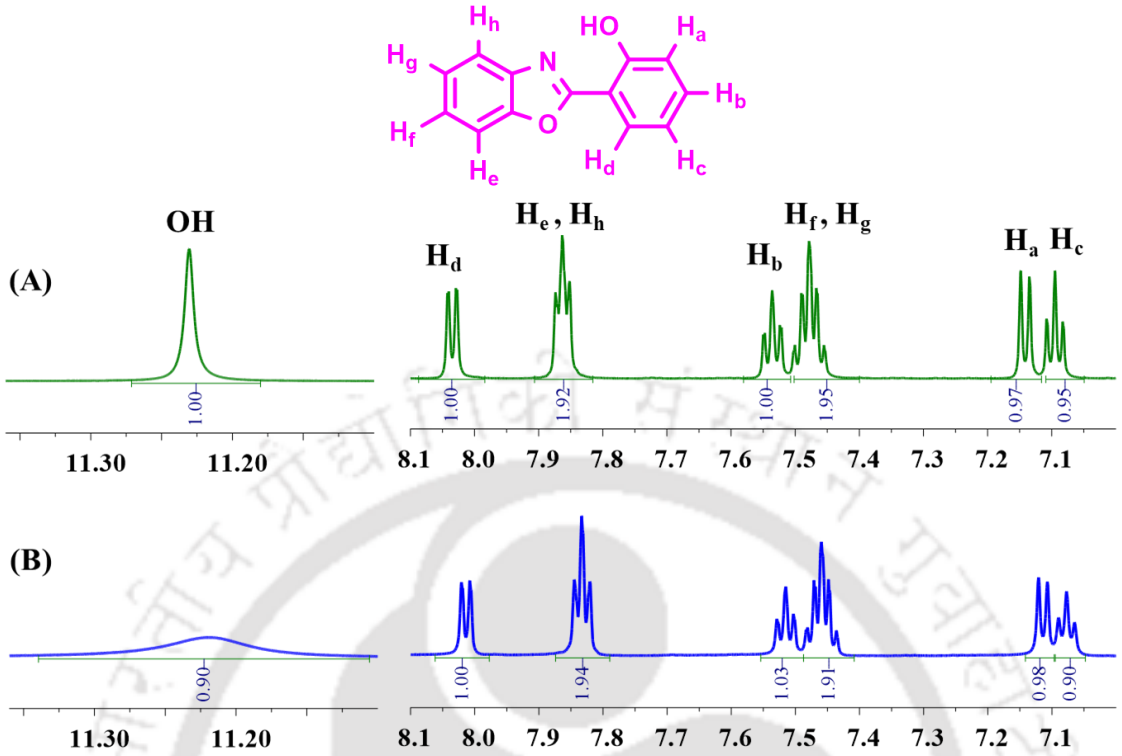

Figure 3.11: ^{1}H NMR spectra of HPBO in the **(A)** absence and **(B)** presence of Zn^{2+} (1:5 equivalent) in DMSO-d_6.

The ^{1}H NMR spectra of HPBO were recorded in the absence and presence of HPBO in DMSO-d_6 **[Figure 3.11]**. The NMR spectrum of HPBO was shifted up field in the presence of Zn^{2+}. The peak corresponds to 'OH' proton got broadened, indicating that 'OH' proton becomes labile in the presence of Zn^{2+}. Due to poor solubility of HPBO in D_2O, the NMR spectral measurements could not be performed. However, DFT calculations were performed in water for the 1:1 complex of HPBO:Zn^{2+} by coordinating through the imidazole nitrogen and 'OH' oxygen atoms using different functions **[Annexure-A]**. Theoretical excitation energy (3.5 eV) calculated by PBEPBE-321g method matches with experimental excitation energy (3.5 eV). Therefore, using the same functional and basis set, emission energy was also calculated. Theoretically calculated emission energy 2.9 eV is in excellent agreement with experimental emission energy 2.9 eV. The excitation energy (3.6 eV) and emission energy (2.9 eV) of HPBO–Zn^{2+} complex calculated in DMSO also, are in agreement with the experimental result (3.3 eV and 2.8 eV, excitation and emission energy respectively).

3.3. Effect of β-CD on HPBO

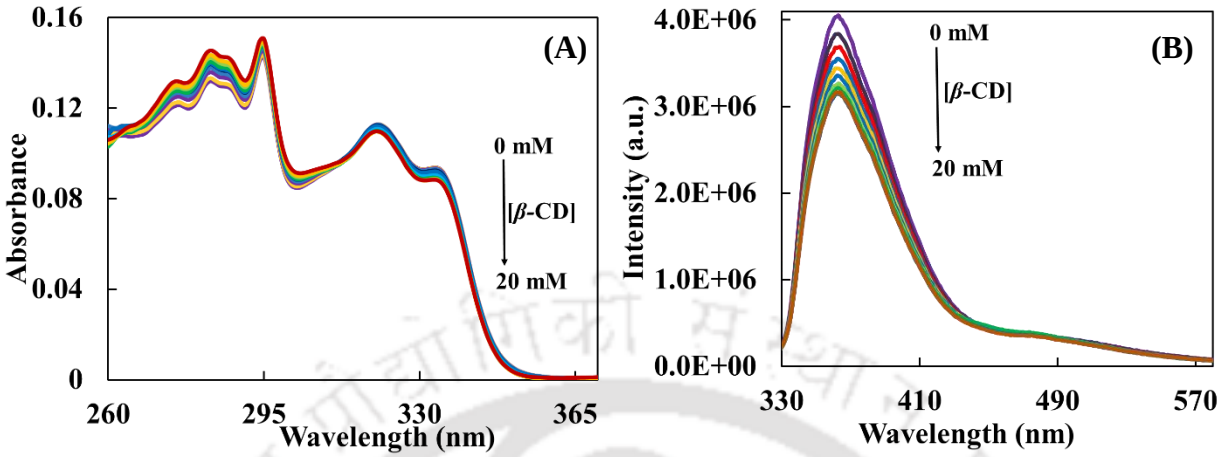

Figure 3.12: (A) Absorption spectra and **(B)** emission spectra of HPBO in presence of different concentration (0 to 20 mM) of β-CD in DMSO, λ_{exc} = 300 nm.

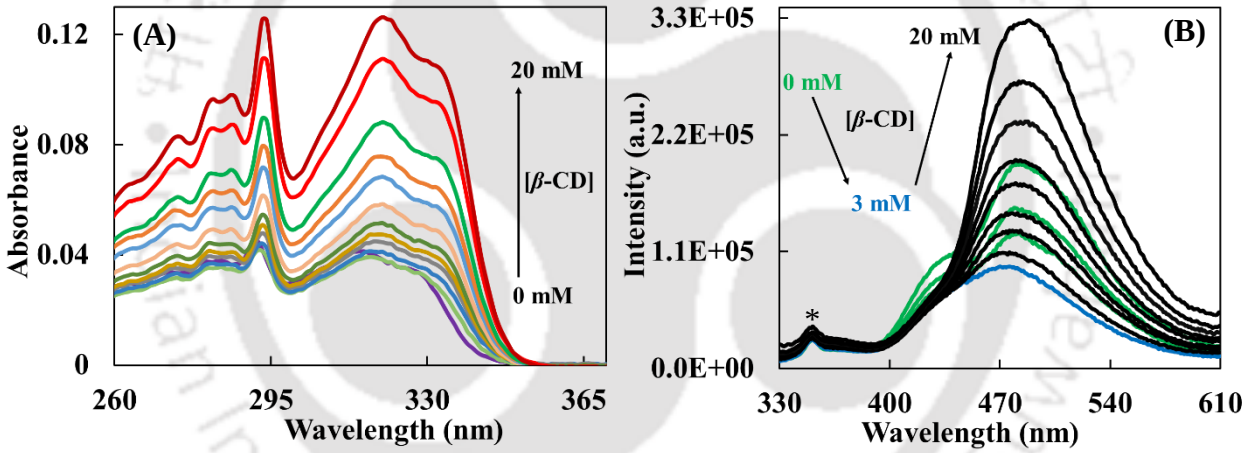

Figure 3.13: (A) Absorption spectra and **(B)** emission spectra of HPBO in presence of different concentration (0 to 20 mM) of β-CD in water, λ_{exc} = 300 nm.

Before evaluating the effect of β-CD and CB-7 on HPBO–Zn^{2+} complex, the effect of these host on HPBO in the absence of Zn^{2+} ion was investigated. Due to poor solubility of host molecules in acetonitrile, the experiments were carried out only in DMSO and water.

In DMSO, the absorbance as well as the emission intensities of HPBO decrease a little upon addition of β-CD **[Figure 3.12]**. On the other hand, significant changes are observed in both the spectra of HPBO in water **[Figure 3.13]**. Warner et al. have studied the effect of β-CD (till 8 mM) on HPBO in aqueous medium.[213] In the present work, it is extended up to 20 mM **(**the

solutions became turbid above this concentration). Upon addition of *β*-CD, the absorbance of HPBO increases and the absorption maximum shifts bathochromically **[Figure 3.13.A]**. *β*-CD has little effect on the normal emission. Upon addition of *β*-CD, initially, the keto emission intensity decreases. With further addition of *β*-CD, the keto emission intensity increases with continuous bathochromic shift **[Figure 3.13.B]**. The bathochromic shift of tautomer emission suggests that the molecule was encapsulated in the hydrophobic *β*-CD cavity. Such a bathochromic shift with decrease in polarity of the environment is a typical characteristic of tautomer emission.[214-216] This is due to fact that the ground state of the keto tautomer is more polar than its excited state. Therefore, in the less polar environment, the polar ground state is less stabilized which decreases the energy gap between the ground state and the excited state.

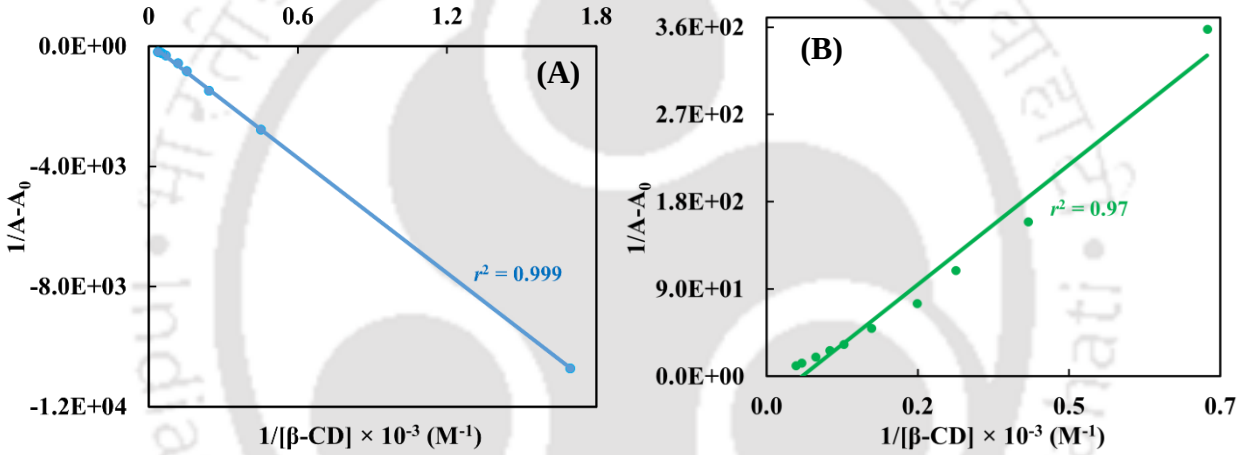

Figure 3.14: Benesi-Hildebrand plot of HPBO–*β*-CD complex in **(A)** DMSO and **(B)** water.

The stoichiometric ratios and the association constants are determined using Benesi-Hildebrand equation **[Equation 3.1]**. The Benesi-Hildebrand plots in both DMSO and water are shown in **Figure 3.14**. The linear plot with good correlation coefficient ($r^2 \approx 0.99$) suggests the formation of 1:1 complex. The association constants are found to be 16.9 M^{-1} and 55.7 M^{-1} in DMSO and water, respectively. This shows that HPBO has better inclusion ability in water. In presence of *β*-CD, the decays were recorded at emission maxima in both DMSO and water **[Figure 3.15** and **3.16]**. In DMSO, the fluorescence lifetimes of HPBO in HPBO–*β*-CD complex are close to that of free HPBO **[Table 3.1]**. But in water both normal and tautomer lifetime changes in the presence of *β*-CD **[Table 3.1]** which substantiates the conclusion that HPBO has more affinity towards *β*-CD in aqueous medium than in DMSO.

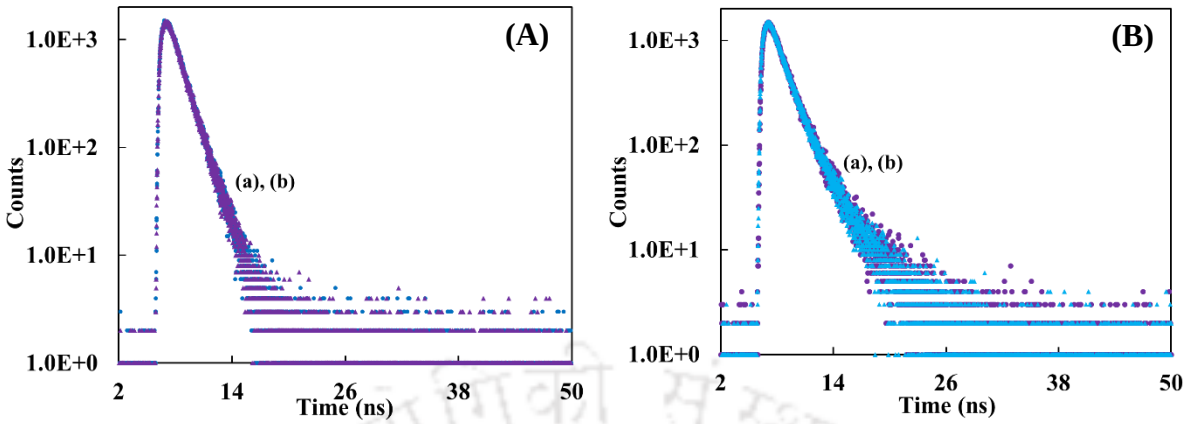

Figure 3.15: The fluorescence decays monitored at **(A)** shorter wavelength emission maxima and **(B)** longer wavelength emission maxima of HPBO in the (a) absence and (b) presence of *β*-CD in DMSO, λ_{exc} = 308 nm.

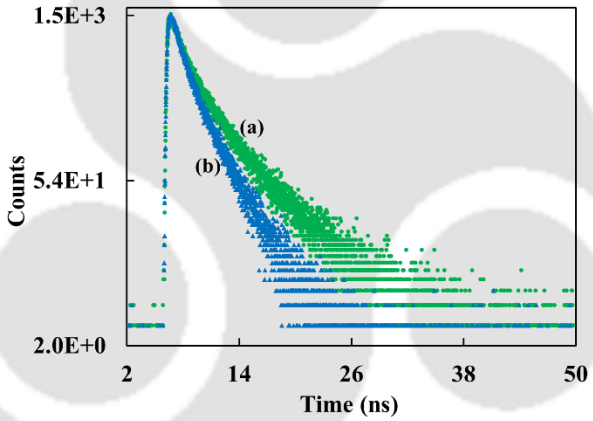

Figure 3.16: The fluorescence decays monitored at longer wavelength emission maximum of HPBO in the (a) absence and (b) presence of *β*-CD in water, λ_{exc} = 308 nm.

The ^{1}H NMR spectra were recorded to inspect the host-guest complexation. The ^{1}H NMR spectra of *β*-CD, HPBO and HPBO–*β*-CD complex were recorded for a better comparison. The spectra of the HPBO–*β*-CD complex show all the aromatic protons are up fielded and all the *β*-CD protons are down fielded compared to the spectra of neat solutions **[Table 3.2, Figure 3.17]**. This also confirms the interaction between *β*-CD and HPBO.

Table 3.2: Chemical shift (δ, ppm) of the protons of *β*-CD, HPBO, HPBO–*β*-CD, *β*-CD–Zn^{2+}, HPBO–Zn^{2+}, and HPBO–Zn^{2+}–*β*-CD in DMSO-d_6.

	β-CD	HPBO	HPBO–*β*-CD	*β*-CD–Zn^{2+}	HPBO–Zn^{2+}	HPBO–Zn^{2+}–*β*-CD
$H_1^{\beta\text{-CD}}$	5.77, 5.76		5.79	5.77, 5.76		
$H_2^{\beta\text{-CD}}$	5.71		5.73	5.71		5.74
$H_3^{\beta\text{-CD}}$	4.82		4.83	4.80		4.81
$H_4^{\beta\text{-CD}}$	4.543, 4.534, 4.525		4.56	4.57		
$H_5^{\beta\text{-CD}}$	3.63, 3.61, 3.60		3.66, 3.64, 3.63, 3.61, 3.60	3.61, 3.59, 3.58		3.64, 3.62, 3.60, 3.59
$H_6^{\beta\text{-CD}}$				3.53, 3.52		3.54, 3.52
$H_7^{\beta\text{-CD}}$	3.35, 3.34, 3.32, 3.31, 3.30		3.37, 3.35, 3.33, 3.31, 3.30	3.34, 3.32, 3.31 3.30		3.34, 3.33, 3.31, 3.29
H_a		7.15, 7.13	7.13, 7.12		7.12, 7.11	7.10, 7.09
H_b		7.55, 7.53, 7.52	7.54, 7.52, 7.51		7.53, 7.51, 7.50	7.51, 7.50, 7.49
H_c		7.11, 7.09, 7.08	7.10, 7.08, 7.07		7.09, 7.08, 7.06	7.07, 7.06, 7.05
H_d		8.04, 8.03	8.03, 8.01		8.02, 8.00	8.01, 7.99
H_e, H_h		7.87, 7.86, 7.85	7.85, 7.84, 7.83		7.84, 7.83, 7.82	7.83, 7.81, 7.80
H_f, H_g		7.50, 7.49, 7.48, 7.46, 7.45	7.49, 7.48, 7.47, 7.45, 7.44		7.48, 7.47, 7.46, 7.45, 7.44	7.47, 7.46, 7.45, 7.43, 7.42
-OH proton		11.23	11.23		11.22	11.22

The protons are defined as follows:

$H_1^{\beta\text{-CD}}$ to $H_7^{\beta\text{-CD}}$ are protons of *β*-CD. H_a to H_h and –OH proton are the protons in HPBO. For details refer **Figure 3.17**, **Figure 3.32** and **Figure 3.33**.

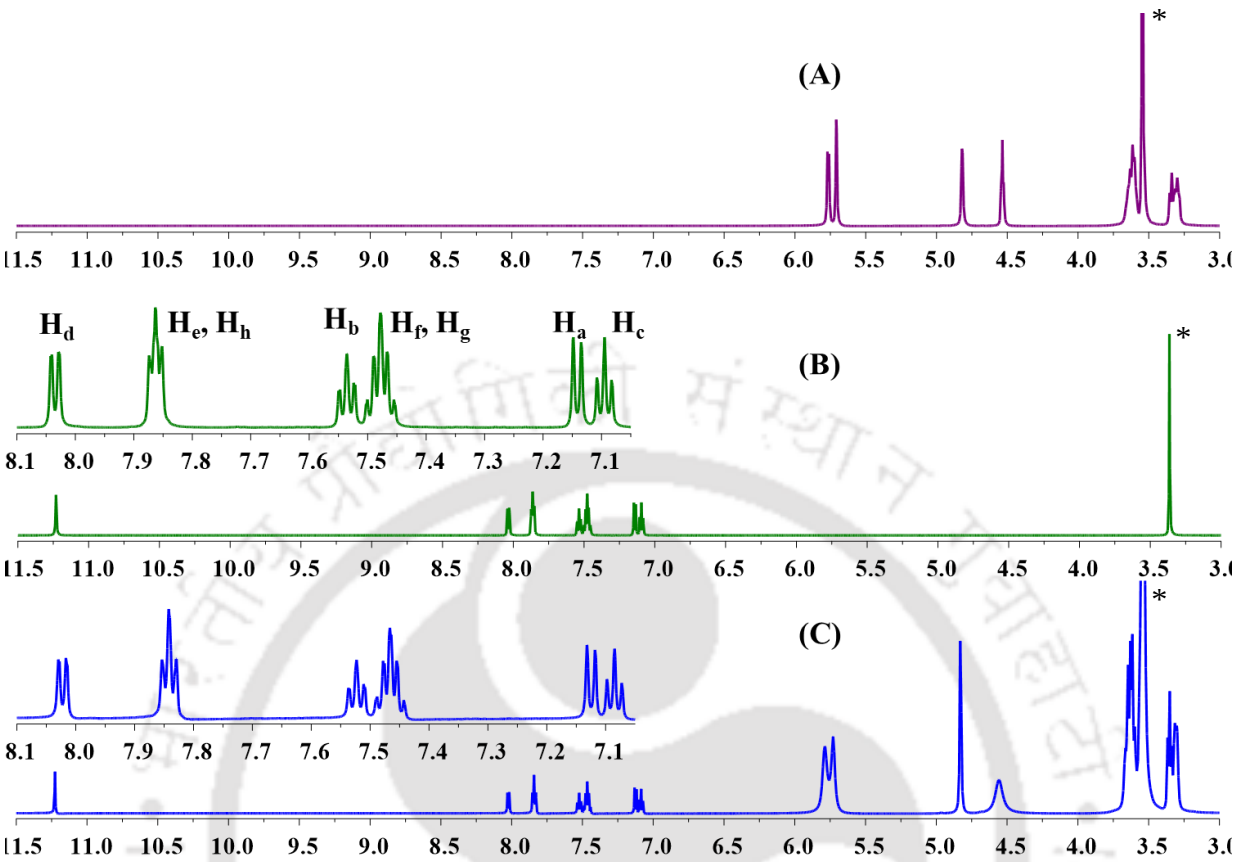

Figure 3.17: ^{1}H NMR spectra of **(A)** *β*-CD, **(B)** HPBO, **(C)** HPBO–*β*-CD complex (1: 5 equivalent) in DMSO-d_6.

The fluorophore can enter the cavity of *β*-CD either through its benzoxazole moiety or its phenol moiety. Hence, both the complexes were optimized in DMSO as well as in water. The molecule is more stable when the benzoxazole moiety is present inside the ring **[Table 3.3]**. Warner et al. also reported that HPBO axially enters into the *β*-CD cavity from the upper ring side of *β*-CD and the benzoxazole ring remains inside the cavity.[213] The trans-enol complex is also optimized in the same orientation. The excitation energy and emission energy of free HPBO and HPBO–*β*-CD complexes were calculated. The cis-enol conformer of HPBO optimized in the excited state resulted in the keto form. The ground state optimized structures of cis-enol (stable complex) and trans-enol HPBO–*β*-CD complexes in water are shown in **Figure 3.18** and **3.19**, respectively. Other structures and the Cartesian coordinates of all optimization are given in **Annexure-A**. The excitation energy and emission energy obtained theoretically are close to the experimental result **[Table 3.3]**.

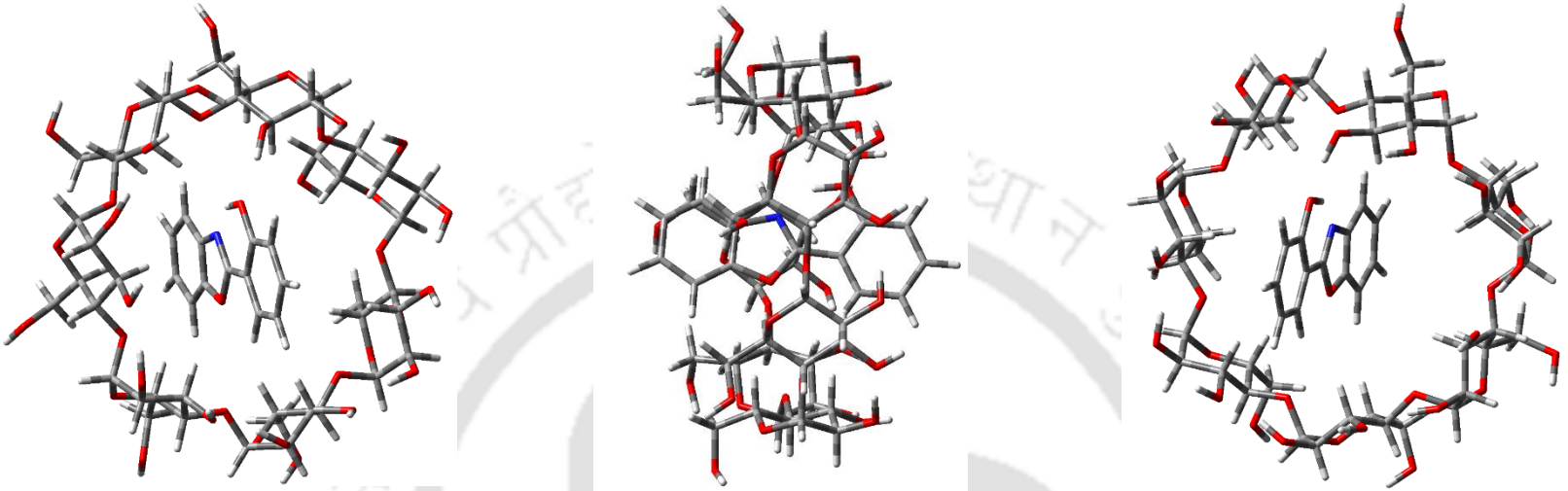

Figure 3.18: Ground state optimized geometry of cis-enol HPBO–*β*-CD complex by way of benzoxazole moiety inside the cavity in water (different view).

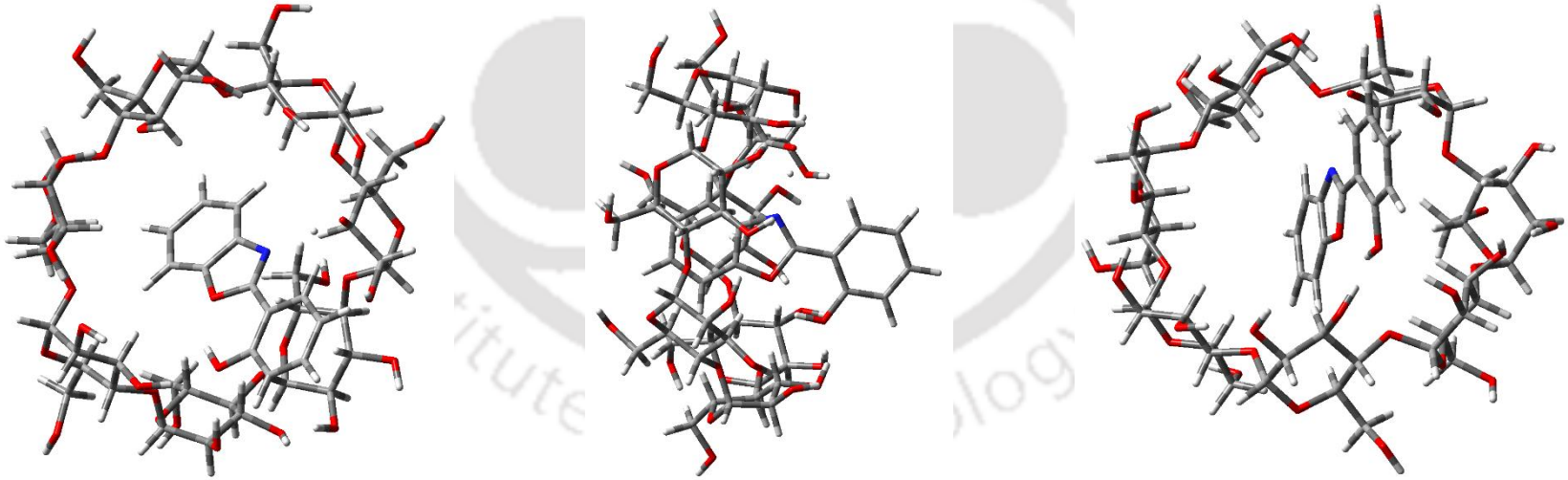

Figure 3.19: Ground state optimized geometry of trans-enol HPBO–*β*-CD complex by way of benzoxazole moiety inside the cavity in water (different view).

Table 3.3: Theoretically calculated **s**tabilization energy (E_s, kJ/mol), excitation energy (λ_{max}^{ex}, eV) and emission energy (λ_{max}^{fl}, eV) of HPBO, HPBO–*β*-CD and HPBO–CB-7 complexes in water and DMSO.

	water			DMSO		
	E_s	λ_{max}^{ex}	λ_{max}^{fl}	E_s	λ_{max}^{ex}	λ_{max}^{fl}
trans-enol HPBO[1]		3.9	3.2		3.9	3.2
		(3.9)	(3.4)		(3.9)	(3.4)
cis-enol HPBO[1]		3.8	2.6		3.8	2.6
		(3.8)	(2.6)		(3.7)	(2.5)
keto HPBO[1]			2.6			2.6
			(2.6)			(2.5)
cis-enol HPBO–*β*-CD[1]	-25.6	3.9	2.6	-25.7	3.9	2.6
(benzoxazole moiety inside cavity)		(3.7)	(2.5)		(3.7)	(2.5)
cis-enol HPBO–*β*-CD[1]	-9.0			-9.2		
(benzoxazole moiety outside cavity)						
trans-enol HPBO–*β*-CD[1]	-2.5	3.9	3.2	-2.4	3.9	
(benzoxazole moiety inside cavity)		(3.9)	(3.4)		(3.9)	
cis-enol HPBO–CB-7[1]	-5.4	3.8	2.6	-5.0	3.8	2.6
(benzoxazole moiety inside cavity)		(3.8)	(2.6)		(3.7)	(2.5)
cis-enol HPBO–CB-7[1]	1.7			3.5		
(benzoxazole moiety outside cavity)						
trans-enol HPBO–CB-7[1]	-10.6	3.9	3.2	-10.1	3.9	3.2
(benzoxazole moiety inside cavity)		(4.0)	(3.3)		(3.8)	(3.4)

[1]The values in parentheses are the experimental values.

3.4. Effect of CB-7 on HPBO

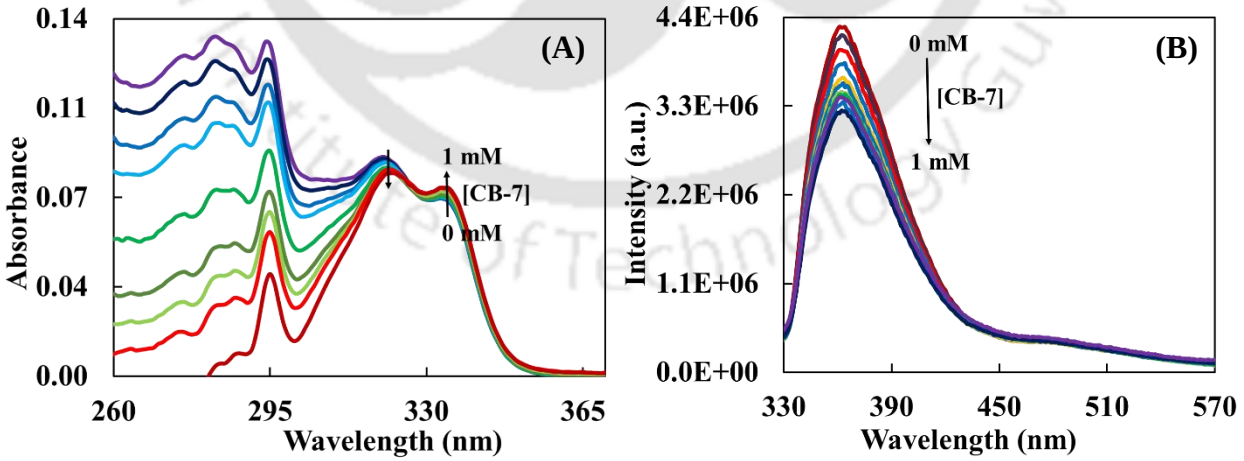

Figure 3.20: (A) Absorption spectra and **(B)** emission spectra of HPBO in presence of different concentration of CB-7 in DMSO, λ_{exc} = 300 nm.

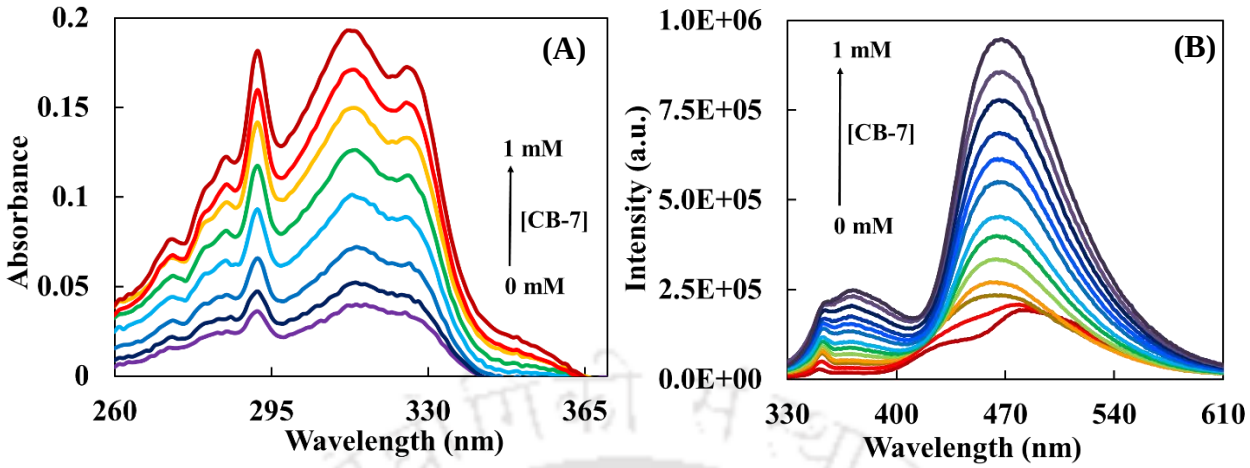

Figure 3.21: (A) Absorption spectra and **(B)** emission spectra of HPBO in presence of different concentration of CB-7 in water, λ_{exc} = 300 nm.

CB-7 has also a little influence on the spectral behavior of HPBO in DMSO, but significant in water. In DMSO, upon addition of CB-7, the absorbance at 320 nm decreases and at 335 nm increases **[Figure 3.20.A]**. In water, with gradual addition of CB-7, the absorbance increases and a very little blue shift is observed **[Figure 3.21.A]**. In DMSO, the normal emission intensity decreases in the presence of CB-7, whereas no significant change occurs at tautomer emission **[Figure 3.20.B]**. In water, the longer wavelength emission maximum shifts from 485 nm to 470 nm, and the shorter wavelength emission maximum shifts from 360 nm to 372 nm **[Figure 3.21.B]**. The intensities of both the emissions also increase with increasing CB-7 concentration. In ESIPT molecules, the blue shift in the tautomer emission and the red shift in the normal emission occurs when the polarity of the environment increases. Thus, the shift suggests that HPBO experience a less hydrophobic environment inside the CB-7 cavity. Both the absorption and emission spectral change show that the complexation ability in water is more compared to DMSO. The shift in spectra suggests CB-7 has strong interaction with the fluorophore as compared to β-CD. The stoichiometric ratios and the association constants were determined using the emission spectra. The double reciprocal plots of $1/(I-I_0)$ versus 1/[CB-7] were plotted using the emission intensities at shorter wavelength emission maxima 360 nm and 372 nm in DMSO and water, respectively **[Figure 3.22]**. The linear plot with good correlation coefficient ($r^2 \approx 0.98$) values propose the formation of 1:1 complex between the fluorophore and CB-7. The association constants are found to be 2.5×10^4 M^{-1} and 3.0×10^4 M^{-1} in DMSO and water respectively. In the presence of CB-7, the fluorescence decays were recorded at emission maxima in DMSO as well as in water **[Figure 3.23** and **3.24]**. In DMSO, the fluorescence lifetimes of HPBO in the presence and the absence of

CB-7 are close to each other **[Table 3.1]**. But in water they are different **[Table 3.1]** which shows CB-7 has more effect on HPBO in aqueous medium.

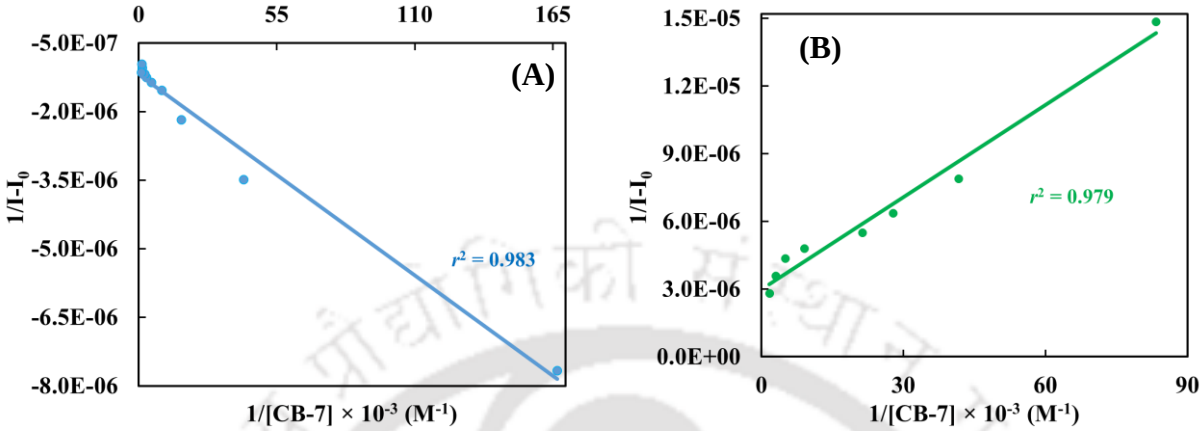

Figure 3.22: Benesi-Hildebrand plot of HPBO–CB-7 complex in **(A)** DMSO and **(B)** water.

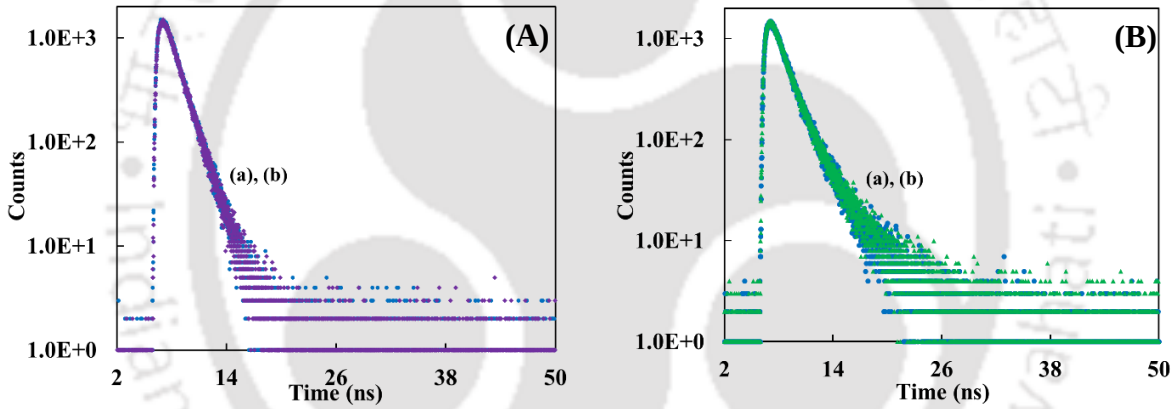

Figure 3.23: The fluorescence decays monitored at **(A)** shorter wavelength emission maxima and **(B)** longer wavelength emission maxima of HPBO in the (a) absence and (b) presence of CB-7 in DMSO, λ_{exc} = 308 nm.

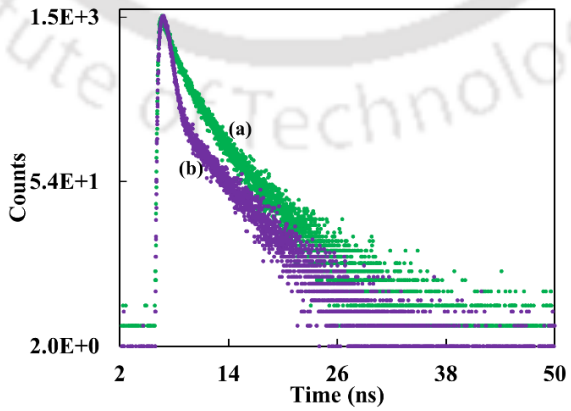

Figure 3.24: The fluorescence decays monitored at longer wavelength emission maximum of HPBO in the (a) absence and (b) presence of CB-7 in water. λ_{exc} = 308 nm.

The ^{1}H NMR spectra of CB-7, HPBO and the complex in DMSO-d_6 were obtained. The difference in the chemical shift of the free HPBO and the complexed HPBO is less **[Table 3.4]**. The splitting pattern of the aromatic protons was more sharp in absence of CB-7 **[Figure 3.25]**. But in presence of CB-7, the peaks correspond to H_e, H_g, H_f and H_h protons are more broaden compared to the other aromatic protons, while the –OH proton is unaffected. This suggests that the benzoxazole ring of HPBO is present inside the CB-7 cavity.

Table 3.4: Chemical shift (δ, ppm) of the protons of CB-7, HPBO, HPBO–Zn^{2+}, HPBO–CB-7 and HPBO–Zn^{2+}–CB-7 in DMSO-d_6.

	CB-7	HPBO	HPBO–CB-7	CB-7–Zn^{2+}	HPBO–Zn^{2+}	HPBO–Zn^{2+}–CB-7
H_1^{CB-7}	5.66, 5.64		5.66, 5.64	5.64, 5.62		5.64, 5.62
H_2^{CB-7}	5.39		5.39	5.39		5.39
H_3^{CB-7}	4.19, 4.16		4.19, 4.17	4.19, 4.17		4.18, 4.16
H_a		7.15, 7.13	7.15, 7.13		7.12, 7.11	7.13, 7.12
H_b		7.55, 7.53, 7.52	7.55, 7.53, 7.52,		7.53, 7.51, 7.50	7.53, 7.52, 7.51
H_c		7.11, 7.09, 7.08	7.11, 7.09, 7.08		7.09, 7.08, 7.06	7.10, 7.08, 7.07
H_d		8.04, 8.03	8.04, 8.03		8.02, 8.00	8.03, 8.01
H_e, H_h		7.87, 7.86, 7.85	7.86, 7.85		7.84, 7.83, 7.82	7.85, 7.84, 7.83
H_f, H_g		7.50, 7.49, 7.48, 7.46, 7.45	7.50, 7.49, 7.48, 7.46, 7.45		7.48, 7.47, 7.46, 7.45, 7.44	7.49, 7.48, 7.46, 7.45, 7.44
-OH proton		11.23	11.23		11.22	11.22

The protons are defined as follows: H_1^{CB-7} to H_3^{CB-7} are protons of CB-7. H_a to H_h and –OH protons are the protons in HPBO. For details refer **Figure 3.25**, **Figure 3.38** and **Figure 3.39**.

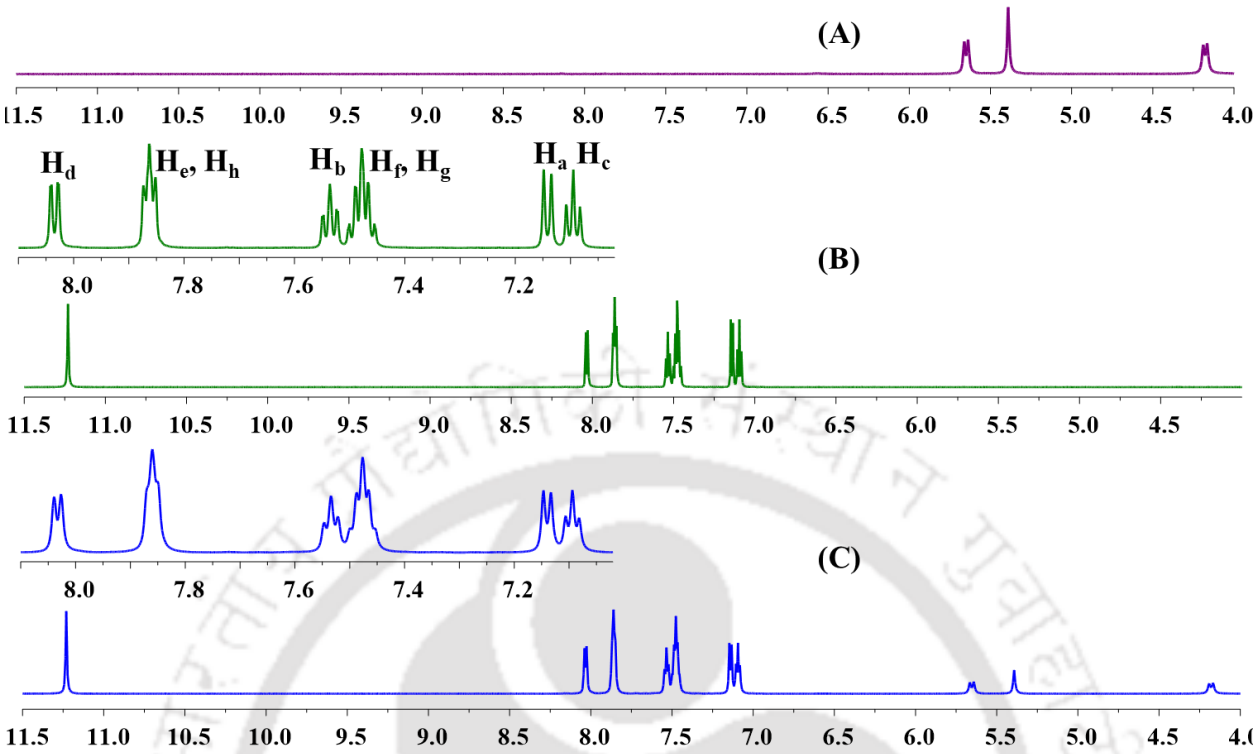

Figure 3.25: ^{1}H NMR spectra of **(A)** CB-7, **(B)** HPBO, **(C)** HPBO–CB-7 complex (1: 0.5 equivalent) in DMSO-d_6.

CB-7 cavity diameter is 7.3 Å, while HPBO molecule has length of ~10.0 Å and width of ~ 5.0 Å. Hence, in CB-7 cavity also the fluorophore can insert axially and partially. Like in *β*-CD, in CB-7, the fluorophore can insert into the cavity either through its benzoxazole moiety or phenolic ring. Hence, the cis-enol complexes were optimized in the ground state in both possible ways in water as well as in DMSO medium. Like in *β*-CD, in CB-7 also, the stabilization energy of the complex presenting benzoxazole moiety inside the cavity is more in both water and DMSO medium **[Table 3.3]**. This is consistent with the NMR spectral changes. Pal et al. reported that the benzimidazole moiety of HPBI, a fluorophore similar to HPBO, remains inside the cavity of CB-7.[76] The trans-enol complex was optimized in the ground state. The optimized structures of both cis-enol (stable complex) and trans-enol HPBO–CB-7 complexes in water are shown in **Figure 3.26** and **3.27**, respectively and other complexes with their Cartesian coordinates are given in **Annexure-A**. Theoretically calculated excitation energy and emission energies of the complexes are found to be close to the experimental energy **[Table 3.3]**.

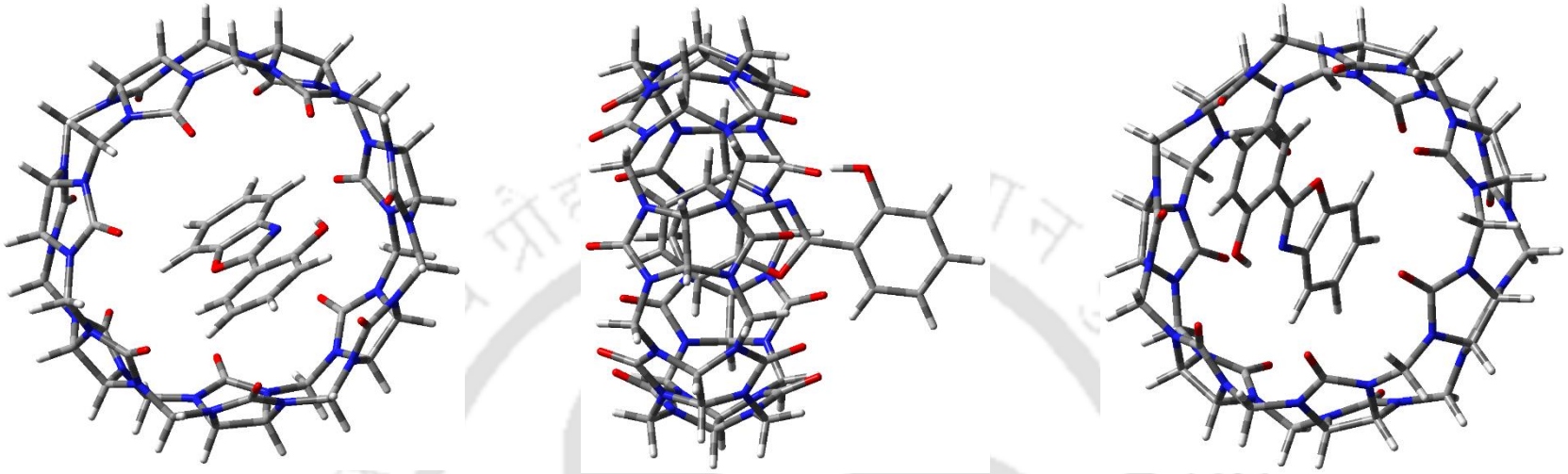

Figure 3.26: Ground state optimized geometry of cis-enol HPBO–CB-7 complex by way of benzoxazole moiety inside the cavity in water (different view).

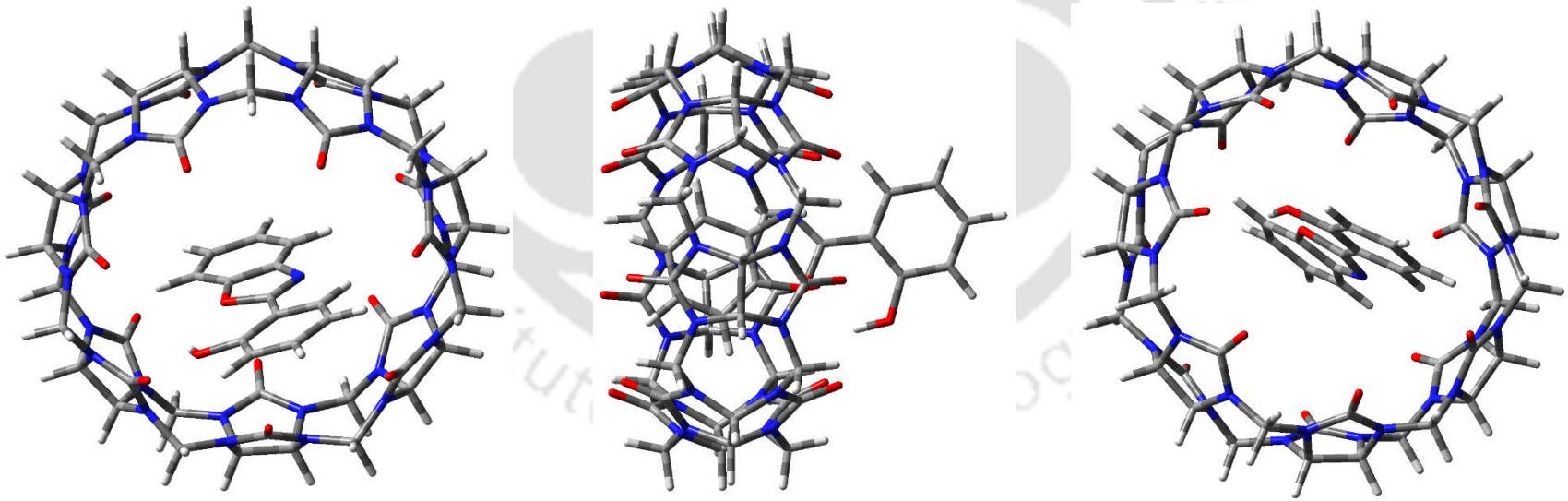

Figure 3.27: Ground state optimized geometry of trans-enol HPBO–CB-7 complex by way of benzoxazole moiety inside the cavity in water (different view).

3.5. Effect of β-CD on HPBO–Zn^{2+} complex

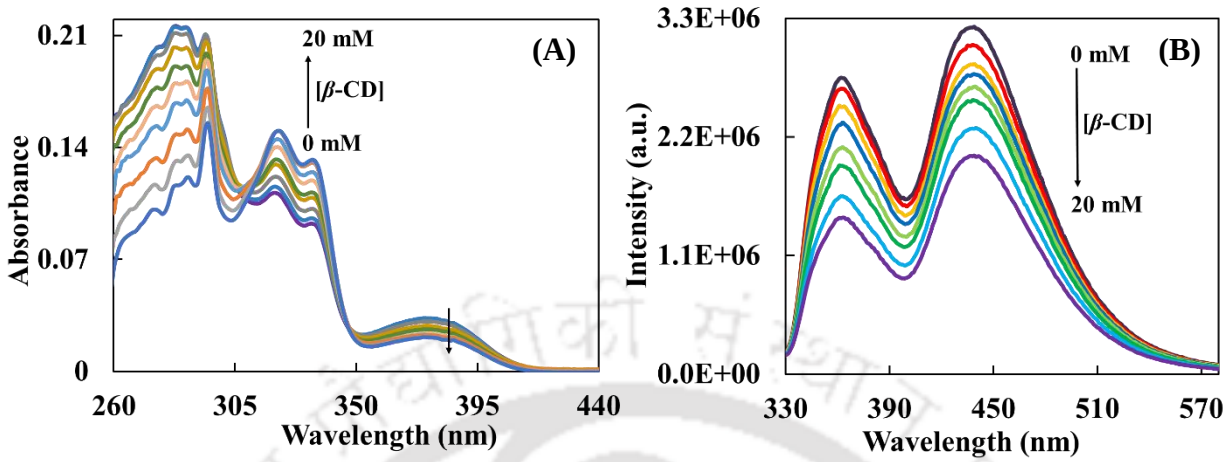

Figure 3.28: (A) Absorption spectra and **(B)** emission spectra of HPBO–Zn^{2+} complex in presence of different concentrations of β-CD (0 to 20 mM) in DMSO, λ_{exc} = 300 nm.

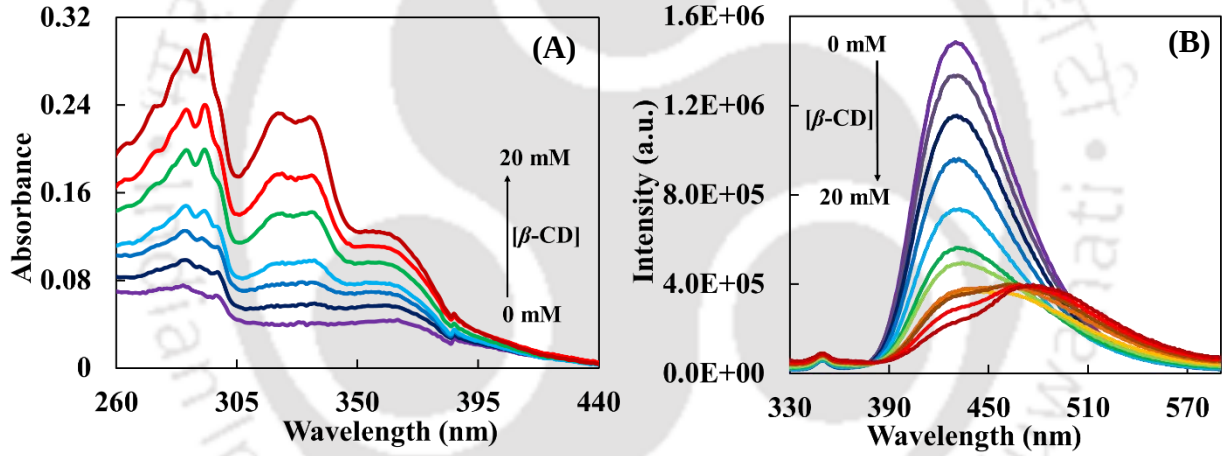

Figure 3.29: (A) Absorption spectra and **(B)** emission spectra of HPBO–Zn^{2+} complex in presence of different concentrations of β-CD (0 to 20 mM) in water, λ_{exc} = 300 nm.

The effect of β-CD on the HPBO–Zn^{2+} complex in DMSO as well as in water were studied. In DMSO upon addition of β-CD, the absorbance (at 380 nm) of the HPBO–Zn^{2+} complex decreases and the absorbance of the free fluorophore increases **[Figure 3.28.A]**. The emission intensities of both the bands at 360 nm and 440 nm decrease upon addition of β-CD **[Figure 3.28.B]**. In water, the HPBO–Zn^{2+} complex absorbs at 360 nm. But on gradual addition of β-CD, the band at ~ 320 nm and ~ 333 nm starts to appear and become prominent at higher concentration of β-CD **[Figure 3.29.A]**. In the same way, the emission intensity of HPBO–Zn^{2+} complex band decreases gradually and the longer wavelength band at around ~ 480 nm starts to appear **[Figure**

3.29.B]. The longer wavelength emission maximum is close to the longer wavelength emission of HPBO–β-CD complex. This suggests the fluorophore is detached from Zn^{2+} ion and it enters the host cavity.

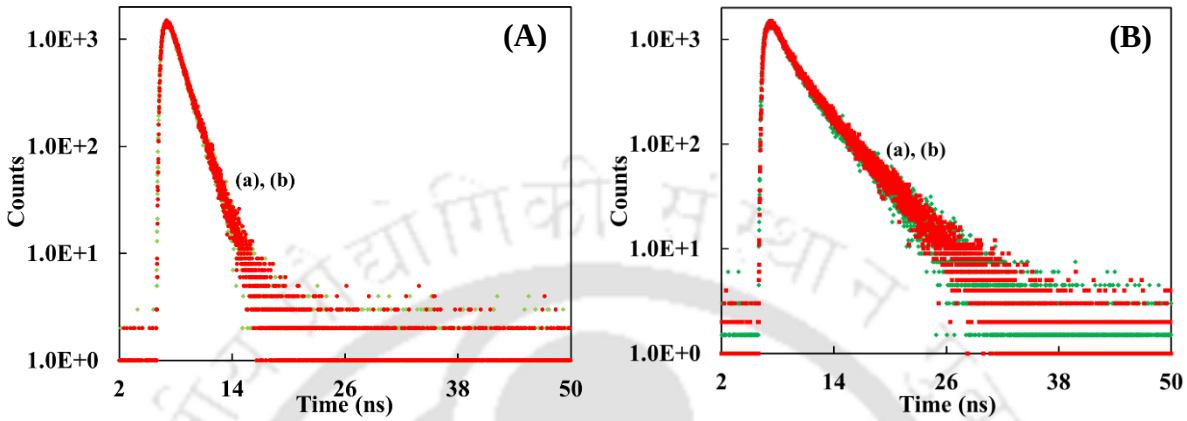

Figure 3.30: The fluorescence decays monitored at **(A)** shorter wavelength emission maxima and **(B)** longer wavelength emission maxima of HPBO in the presence of (a) Zn^{2+} and (b) both Zn^{2+} and β-CD in DMSO, λ_{exc} = 308 nm.

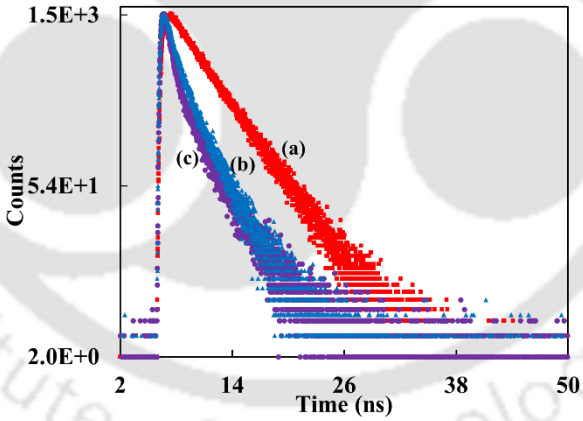

Figure 3.31: The fluorescence decays monitored at longer wavelength emission maximum of HPBO in the presence of (a) Zn^{2+}, (b) β-CD and (c) both Zn^{2+} and β-CD in water, λ_{exc} = 308 nm.

In DMSO, the fluorescence lifetime of HPBO in presence of (both) β-CD and Zn^{2+} are very close to that of HPBO–Zn^{2+} complex **[Table 3.1]**. But in water the fluorescence decay of HPBI in Zn^{2+} and β-CD solution matches with that of HPBO–β-CD complex **[Figure 3.31** and **Table 3.1]**. This substantiate the conclusion that β-CD breaks HPBO–Zn^{2+} complex and the free fluorophore

enters into the nanocavity of *β*-CD. Further ^{1}H NMR spectra in DMSO-d_6 were obtained for *β*-CD –Zn^{2+}, HPBO–Zn^{2+}–*β*-CD and the results are compared with *β*-CD, HPBO, HPBO–Zn^{2+} and HPBO–*β*-CD. Compared to the effect of Zn^{2+} on free *β*-CD, the change in chemical shift and of *β*-CD protons are more in HPBO–Zn^{2+}–*β*-CD solution **[Table 3.2, Figure 3.32]**. The chemical shift and spitting pattern for the aromatic protons of HPBO in HPBO–Zn^{2+}–*β*-CD solution is more likely to HPBO–Zn^{2+} solution **[Table 3.2, Figure 3.33]**. This shows in presence of the fluorophore, Zn^{2+} coordinates to both HPBO and *β*-CD.

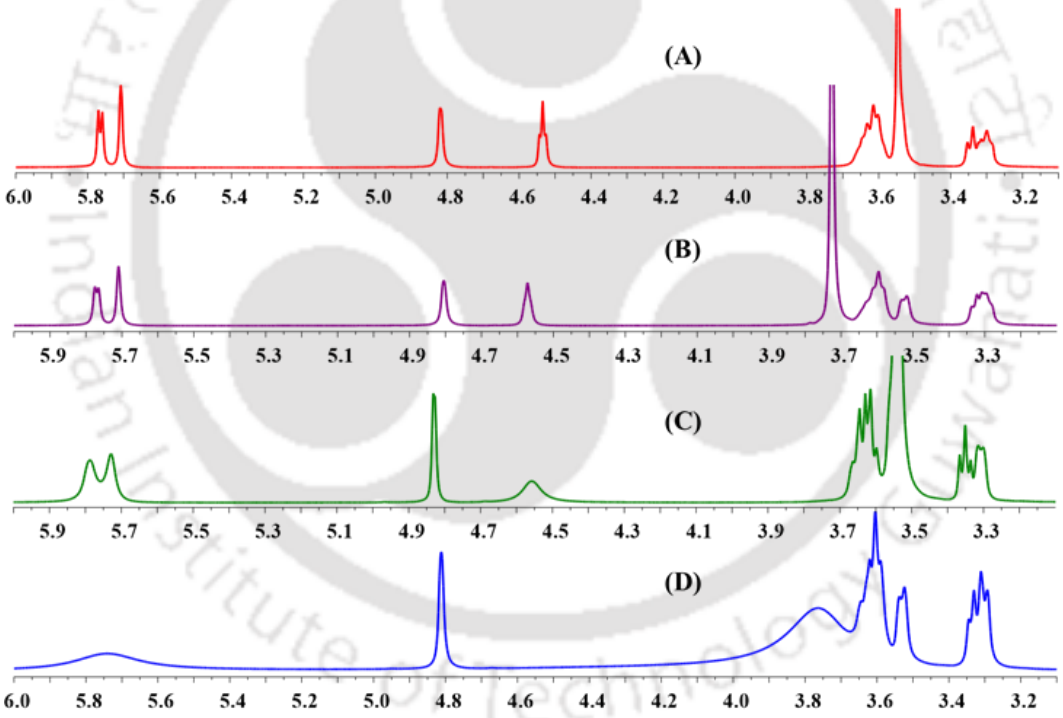

Figure 3.32: ^{1}H NMR (only *β*-CD protons) of **(A)** *β*-CD, **(B)** *β*-CD–Zn^{2+} (1:1 equivalent), **(C)** HPBO–*β*-CD (1:5 equivalent), and **(D)** HPBO–Zn^{2+}–*β*-CD (1:5:5 equivalent) in DMSO-d_6.

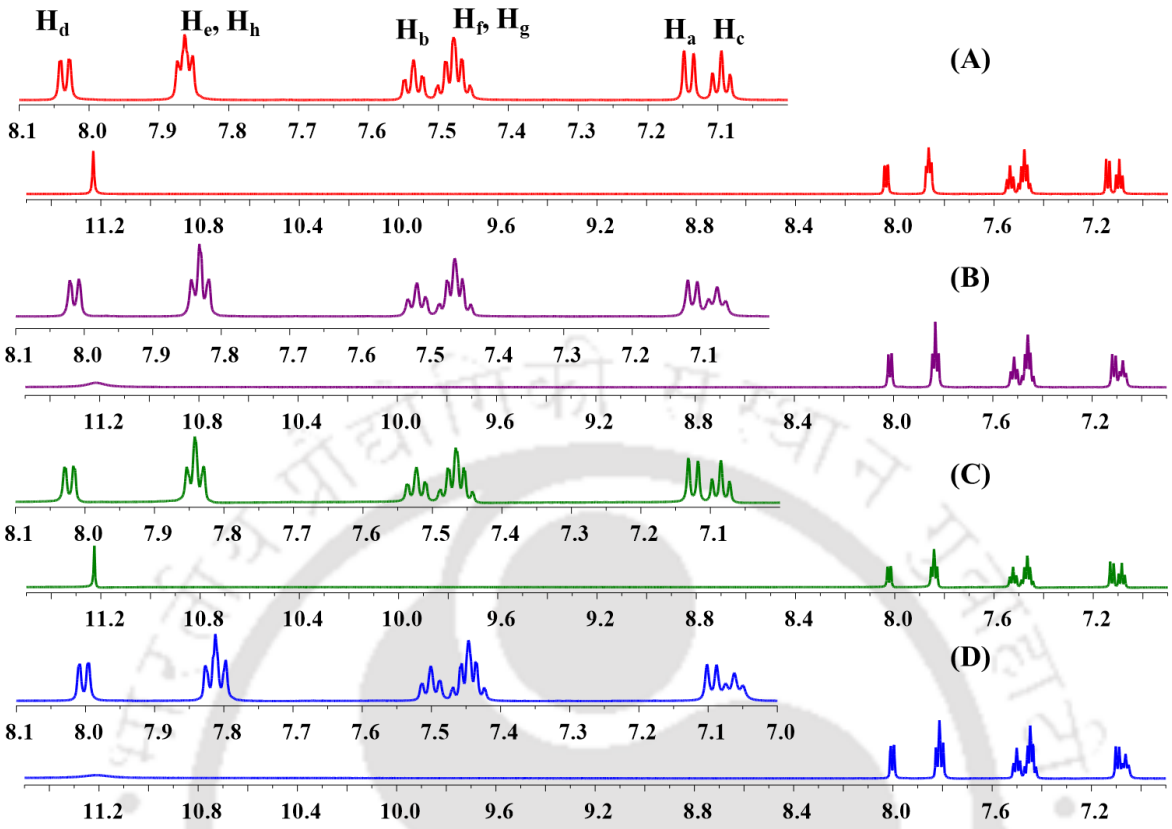

Figure 3.33: ^{1}H NMR spectra of **(A)** HPBO, **(B)** HPBO–Zn^{2+} (1:5 equivalent), **(C)** HPBO–*β*-CD (1:5 equivalent), and **(D)** HPBO–Zn^{2+}–*β*-CD (1:5:5 equivalent) in DMSO-d_6.

3.6. Effect of CB-7 on HPBO–Zn^{2+} complex

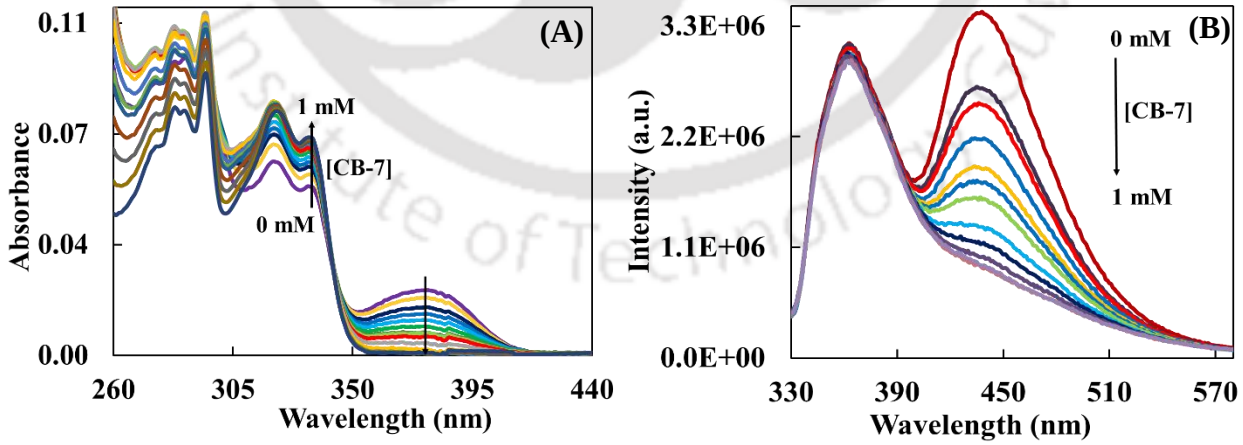

Figure 3.34: (A) Absorption spectra and **(B)** emission spectra of HPBO–Zn^{2+} complex in presence of different concentrations of CB-7 (0 to 20 mM) in DMSO, λ_{exc} = 300 nm.

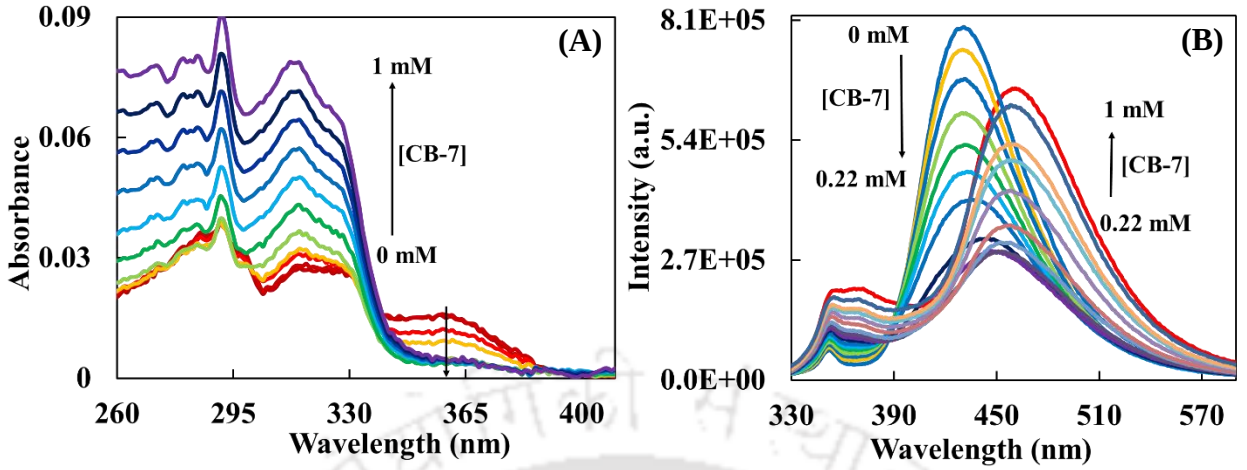

Figure 3.35: (A) Absorption spectra and **(B)** emission spectra of HPBO–Zn^{2+} complex in presence of different concentrations of CB-7 (0 to 20 mM) in water, λ_{exc} = 300 nm.

Unlike β-CD, upon addition of CB-7 to the HPBO–Zn^{2+} complex, the absorbance of the complex in DMSO at 380 nm completely disappears and the absorbance of the fluorophore at ~ 322 nm and ~ 335 nm increases **[Figure 3.34.A]**. Same as absorption spectra, the emission intensity at 440 nm emission of the HPBO–Zn^{2+} complex decreases **[Figure 3.34.B]**. In aqueous 1 mM CB-7 solution at higher concentration of Zn^{2+}, the solution turned turbid, therefore the spectra were recorded in presence of 3 mM of Zn^{2+}. In 3 mM of Zn^{2+} also the emission occurs at 435 nm which corresponds to HPBO–Zn^{2+} complex. Like in DMSO, in water also the absorbance at 360 nm decreases and at 315 nm, 328 nm increases **[Figure 3.35.A]**. For the initial addition of CB-7, the emission intensity at 435 nm decreases and the shorter wavelength emission intensity increases till 0.22 mM of CB. On further increasing the CB-7 concentration, the 435 nm band is bathochromically shifted to 464 nm **[Figure 3.35.B]**. On continuing the addition of CB-7, the emission intensity at both shorter wavelength and longer wavelength band increases. The fluorescence decays were recorded for HPBO–Zn^{2+}–CB-7 solution in both DMSO and water **[Figure 3.36** and **3.37]**. In DMSO, the longer lifetime is different from the keto lifetime of free and complexed HPBO **[Table 3.1]**. But in water the lifetimes are very close to that of HPBO–CB-7 complex **[Table 3.1]**.

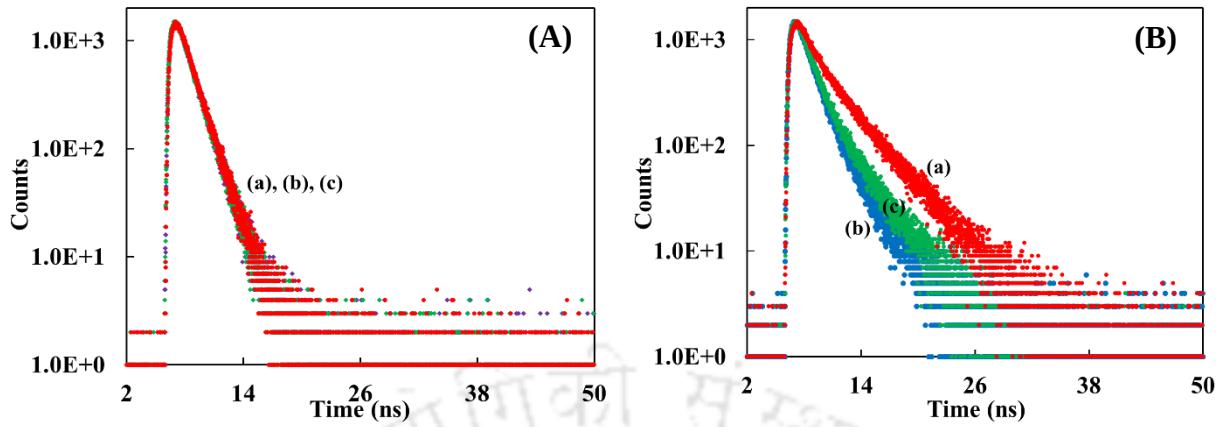

Figure 3.36: The fluorescence decays monitored at **(A)** shorter wavelength emission maxima and **(B)** longer wavelength emission maxima of HPBO in presence of (a) Zn^{2+}, (b) CB-7 and (c) both Zn^{2+} and CB-7 in DMSO. λ_{exc} = 308 nm.

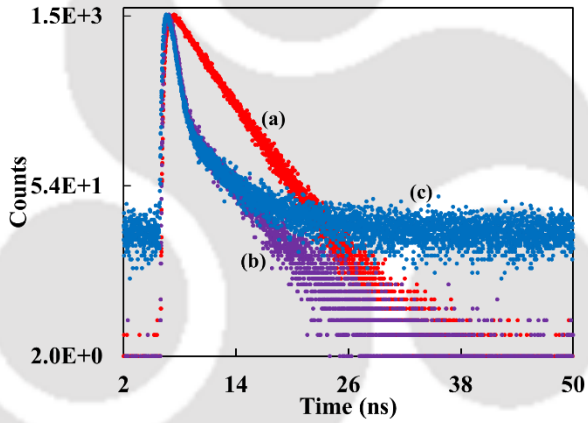

Figure 3.37: The fluorescence decays monitored at longer wavelength emission maximum of HPBO in presence of (a) Zn^{2+}, (b) CB-7 and (c) both Zn^{2+} and CB-7 in water. λ_{exc} = 308 nm.

^{1}H NMR spectra in DMSO-d_6 were obtained for CB-7–Zn^{2+}, HPBO–Zn^{2+}–CB-7 and the results are compared with CB-7, HPBO, HPBO–Zn^{2+} and HPBO–CB-7. **Figure 3.38** shows, CB-7 protons are not affected by the addition of Zn^{2+} in absence as well as in presence of HPBO. In presence of Zn^{2+}, the aromatic protons of HPBO are up fielded **[Table 3.4]**. Upon addition of CB-7 to HPBO–Zn^{2+} complex shifts back to downfield **[Table 3.4]** and the spectra become like the spectra of HPBO–CB-7 complex **[Figure 3.39]** which further supports the breaking of coordination between HPBO and Zn^{2+}.

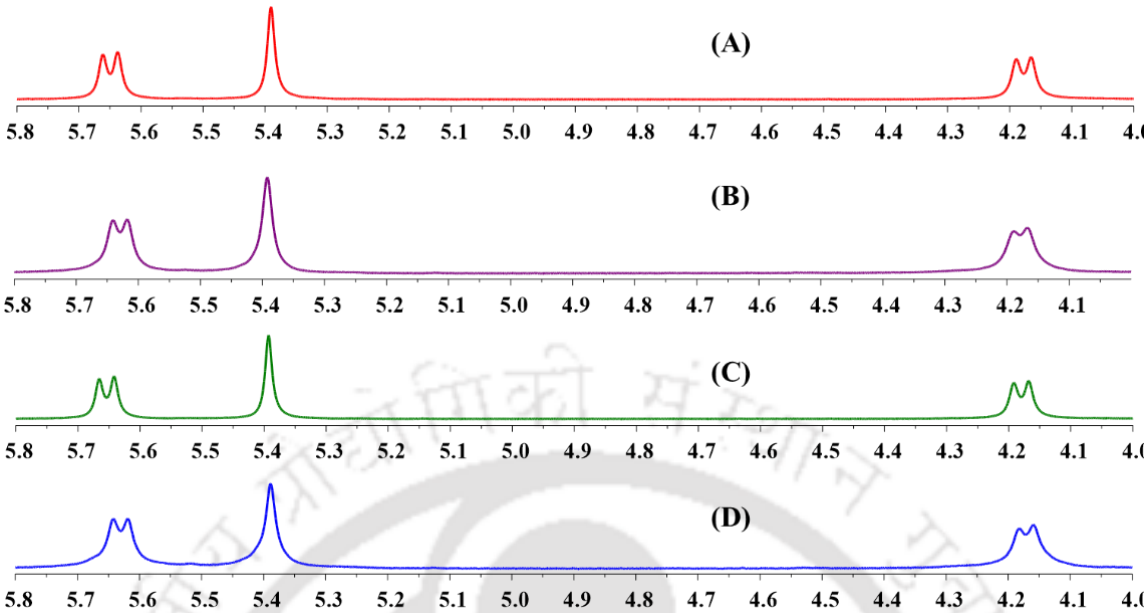

Figure 3.38: ^{1}H NMR of **(A)** CB-7, **(B)** CB-7–Zn^{2+} (1:10 equivalent), **(C)** HPBO–CB-7 (1:0.5 equivalent) and **(D)** HPBO–Zn^{2+}–CB-7 (1:5:0.5 equivalent) in DMSO-d_6.

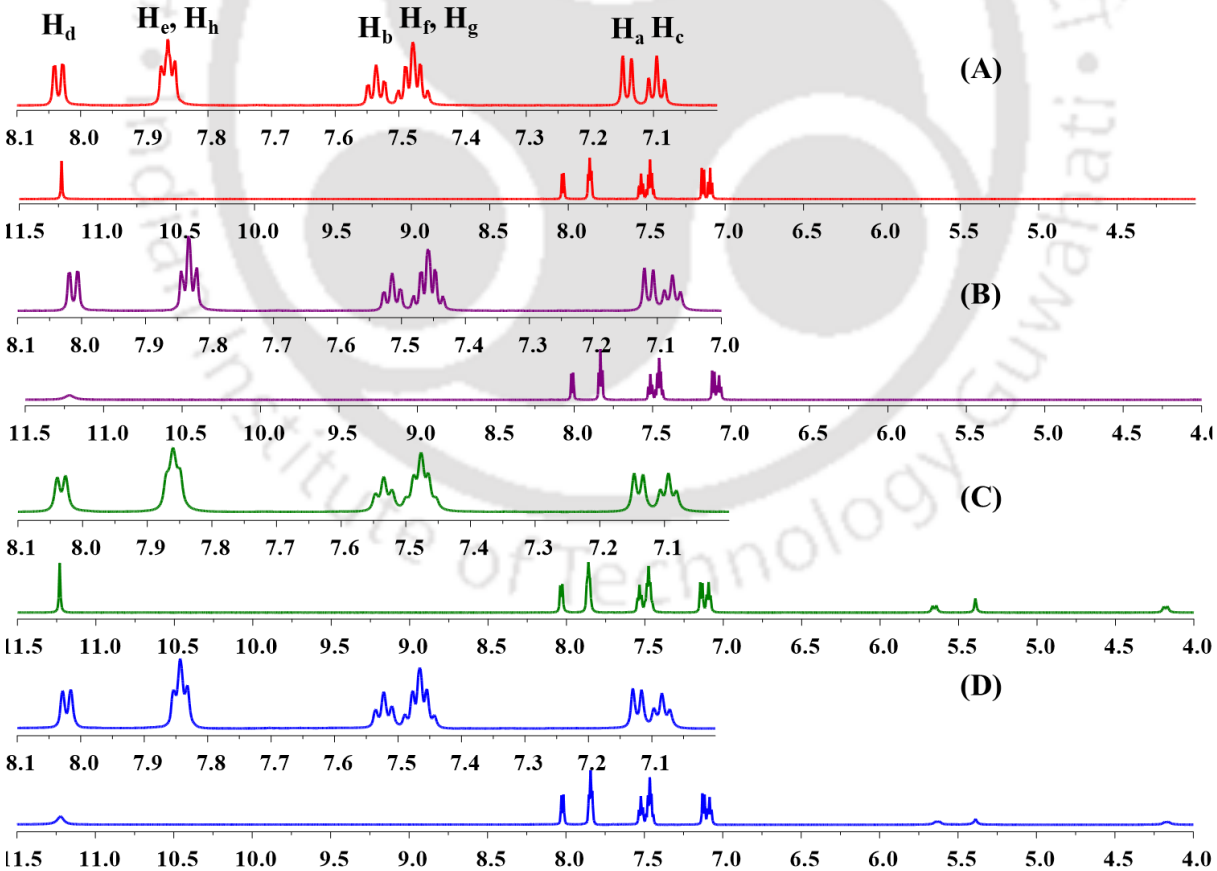

Figure 3.39: ^{1}H NMR of **(A)** HPBO, **(B)** HPBO–Zn^{2+}, **(C)** HPBO–CB-7 and **(D)** HPBO–Zn^{2+}–CB-7 in DMSO-d_6.

It is reported that in aqueous solution, the binding constant of cationic HPBI with CB-7 is more compared to the neutral or anionic species.[76] Further, it is reported that when there is a cationic guest – host interaction, use of inorganic cations compete with the guest molecules to enter into the cavity and in most cases, succeed. However, in case of neutral guest, the use of inorganic cations enhances the interaction.[217] It is also reported that inorganic cations not only compete with cationic guests but also collaborate the interaction depending on the stoichiometry of complexation between guest and host.[218, 219] When the stoichiometry is 1:1, inorganic cations help the molecule to release from the cavity and quench the emission but when the stoichiometry is 2:1, that cooperates the interaction and enrich the emission.[218, 219] It is also reported that the addition of organic or inorganic cationic stimuli to ESIPT probe 1′-hydroxy-2′-acetonaphthone and CB-7 complex, CB-7 interacts with cationic stimuli and the probe gets released from the cavity. [220] It was shown that in the presence of Ca^{2+}, a strongly hydrogen bonded 1′-hydroxy-2′-acetonaphthone–Ca^{2+} complex is formed within CB-7 cavity.[220] In contrary to all these report, CB-7 removes the cation (Zn^{2+}) form the fluorophore to encapsulate the fluorophore into its cavity **[Scheme 3.1]**. Therefore, it may be useful to deliver the zinc ion.

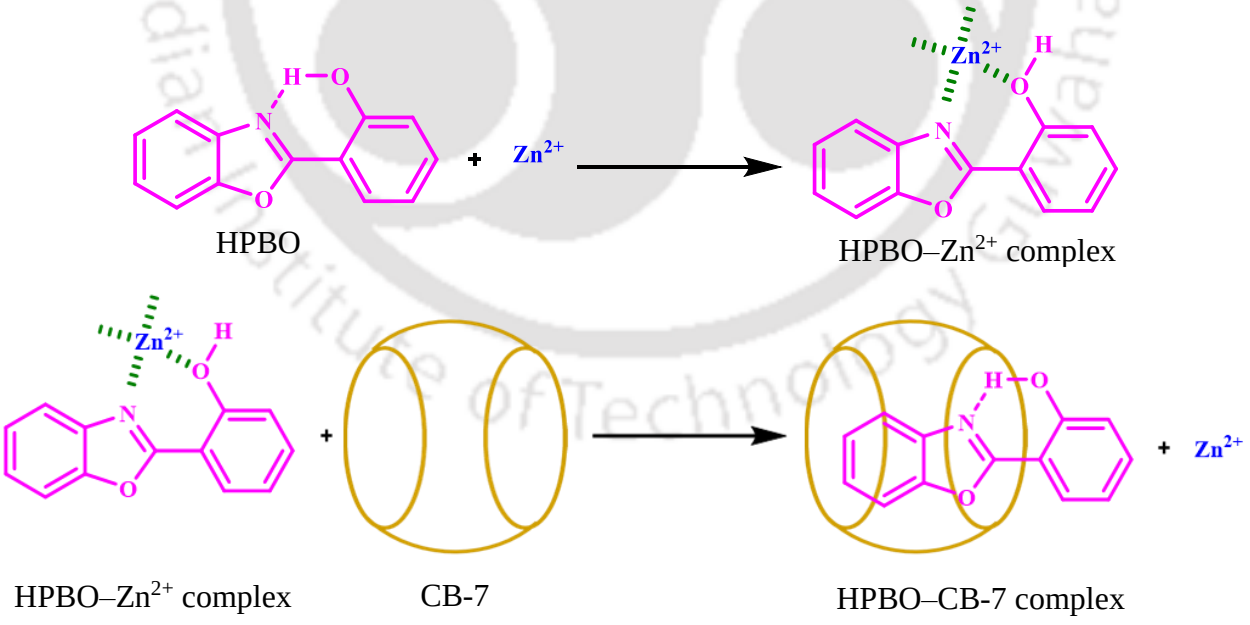

Scheme 3.1: Formation of HPBO–Zn^{2+} complex and release of Zn^{2+} in presence of CB-7.

3.7. Conclusion

Zn^{2+} forms a complex with HPBO which emits at 435 nm with very high intensity with respect to the free fluorophore emission in acetonitrile and water. In DMSO also, it forms complex with Zn^{2+} and the complex emits at 440 nm along with the normal emission. Free fluorophore forms 1:1 complex with both host molecules *β*-CD and CB-7. However, in aqueous medium the interaction is more compared to that in DMSO. In DMSO, *β*-CD could not break the HPBO–Zn^{2+} complex. But in aqueous medium, *β*-CD breaks the metal fluorophore complex and the free fluorophore enters into the nanocavity of *β*-CD. CB-7 has much greater effect on HPBO–Zn^{2+} complex and free the fluorophore from Zn^{2+} in both DMSO and water. The free fluorophore is encapsulated by CB-7 in water.

भारतीय प्रौद्योगिकी संस्थान गुवाहाटी
Indian Institute of Technology Guwahati

Chapter 4

Tweaking the proton transfer triggered proton transfer of 3,5-bis(2-hydroxyphenyl)-1H-1,2,4-triazole

4.0. Introduction

In the previous chapter, the influence of environment on the PT in a system with single proton donor-acceptor pair was shown. In the present chapter, the work is extended to a fluorophore 3,5-bis(2-hydroxyphenyl)-1H-1,2,4-triazole (bis-HPTA) containing two proton donor-acceptor pairs. Molecules having more than one intramolecularly hydrogen-bonded proton donor-acceptor pair not necessarily undergo multiple proton transfer simultaneously.[35-37] Also the polarity and hydrogen bonding ability of the solvent strongly affects the ESIPT process.[42-49] Recently, a new type of PT, proton transfer triggered proton transfer (PTTPT), was reported in bis-HPTA **[Scheme 1.17]**.[161] The molecule exists only as bis-HPTA-I in nonpolar solvents **[Chart 4.1]**. As shown in **Scheme 1.17**, initially, ESIPT-II is not achievable in bis-HPTA-I due to interfering annular tautomerism. ESIPT-I prevented the shuttling of 'NH' proton between two adjacent nitrogen and triggered ESIPT-II. Thus, ESIPT-II occurs as PTTPT. Hence, upon photoexcitation, K1 tautomer (formed by ESIPT-I) and Diketo (DK) tautomer (formed by PTTPT process) were observed in those solvents **[Scheme 1.17]**.[161] Polar protic solvents like methanol break the intramolecular hydrogen bond and form solvated bis-HPTA-Ic conformer, which exists in equilibrium with bis-HPTA-I.[161] Hence in polar protic solvents, apart from K1 and DK emissions, the normal emission occurs from the solvated enol.

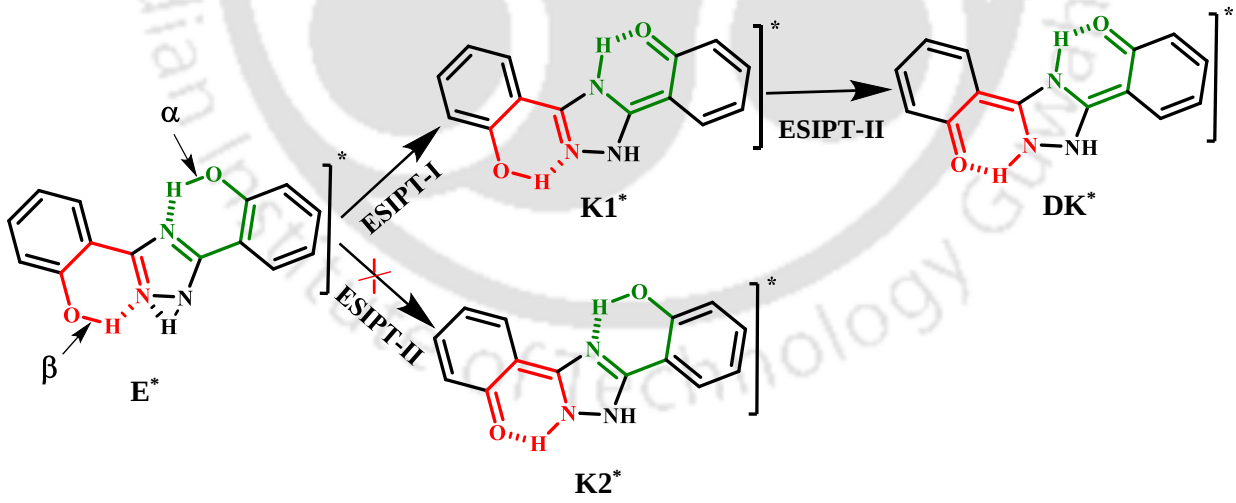

Scheme 1.17: Proton transfer triggered proton transfer (PTTPT) in bis-HPTA-I. (Scheme 1.17 is reproduced here for easy reference)

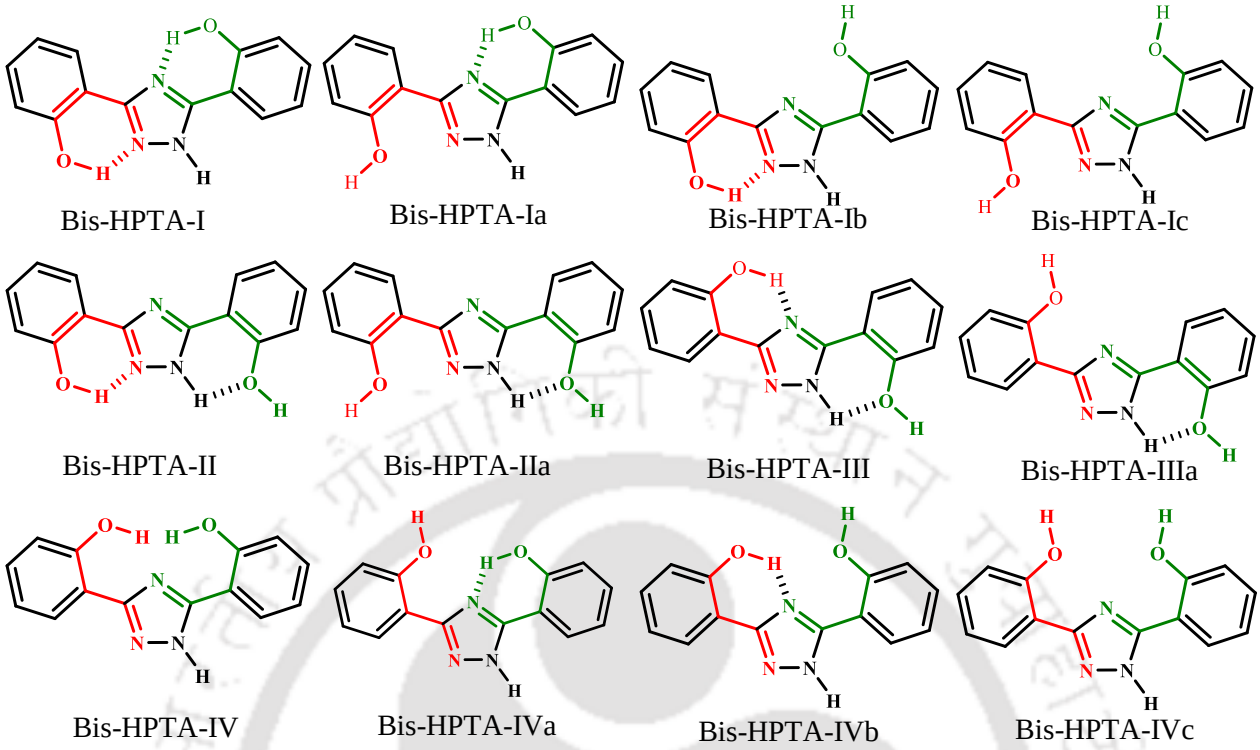

Chart 4.1: Different conformers of bis-HPTA.

DMF is an interesting polar solvent whose C=O group acts as a strong hydrogen bond acceptor and CH/CH_3 groups act as weak hydrogen bond donors. Therefore, it can form an intermolecular hydrogen bond with 'NH' proton of bis-HPTA and prevent the annular tautomerism. Consequently, ESIPT-II may be feasible without ESIPT-I **[Scheme 4.1]**.[221] Therefore, the effect of DMF on the ESIPT of bis-HPTA was investigated.

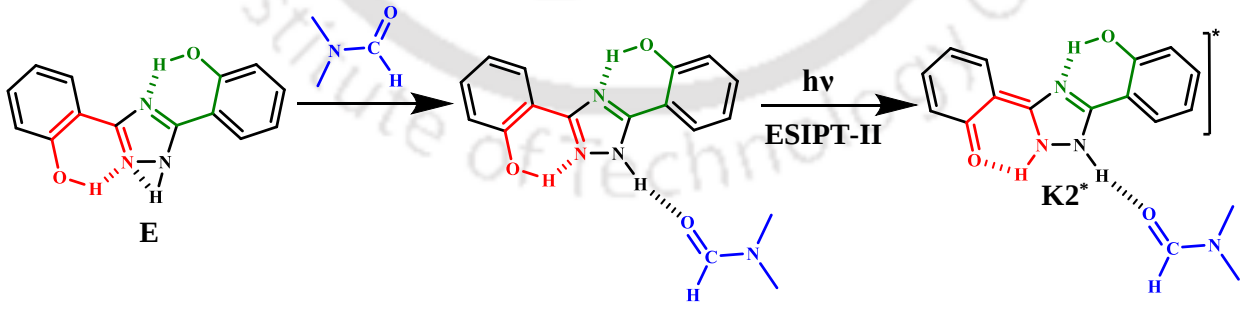

Scheme 4.1: A plausible way to attain ESIPT-II in bis-HPTA-I by preventing the annular tautomerism.

4.1. Perturbation of the ground state by DMF

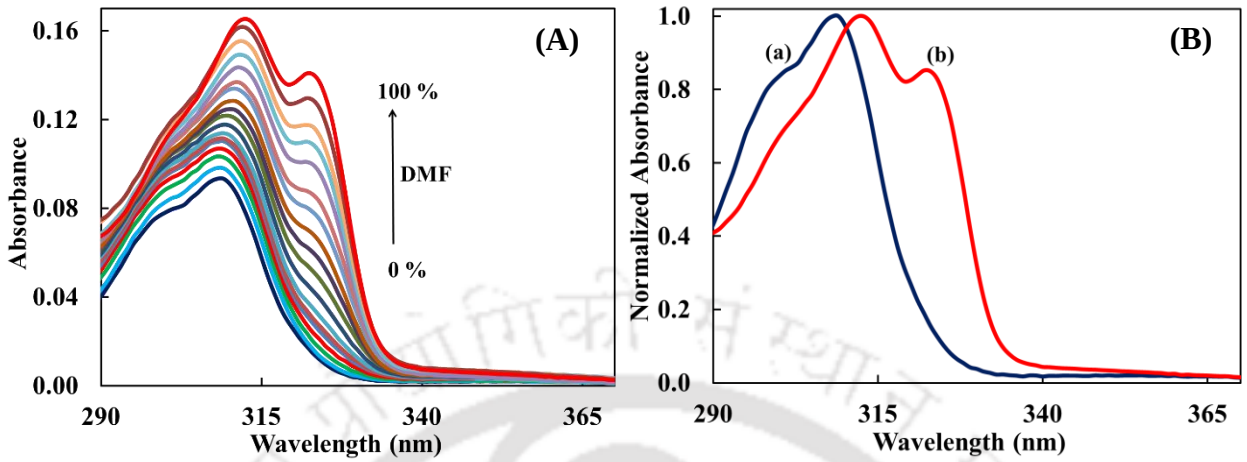

Figure 4.1: (A) Absorption spectra of bis-HPTA in THF-DMF mixture. **(B)** The normalized absorption spectra of bis-HPTA in THF (a) and DMF (b).

To obtain a better understanding of the spectral properties of bis-HPTA in DMF, the spectra of bis-HPTA were recorded at different concentrations of DMF in THF solution **[Figure 4.1.A]**. Bis-HPTA absorbs at 308 nm in THF,[161] and upon addition of DMF, the absorbance increases and the spectrum shifts bathochromically. The spectrum is more structured in DMF compared to the spectra in other solvents.[161] Bis-HPTA absorbs at 313 nm in DMF with a strong shoulder at 323 nm. A very weak broad band is also observed at ~ 350 nm **[Figure 4.1.A** and **4.1.B]**. It is reported that the absorption spectra of HPBI and its pyridoimidazole analogues were red shifted and well resolved due to the formation of hydrogen bond complex.[164, 222] Therefore, from the spectral change of bis-HPTA in DMF, one can infer the formation of similar kind of complex between the fluorophore and the solvent molecules.

Bis-HPTA emits normal emission at 350 nm. The tautomer emission of bis-HPTA is observed at 459 nm in THF **[Figure 4.2.A** and **4.2.B]**.[161] Upon addition of DMF, two emission bands are observed, one blue-shifted band at 410 nm and another red-shifted broad band at ~ 480 nm (with respect to the tautomer emission in THF) **[Figure 4.2.A** and **4.2.B]**. The relative intensity of 410 nm band to 480 nm band changes with the excitation wavelength. Upon excitation at 300 nm, the intensity of the 410 nm band is higher than that of 480 nm band. But when λ_{exc} = 300-330 nm, the relative intensity of the 480 nm band increases with respect to that of 410 nm with excitation wavelength. Again when λ_{exc} > 330 nm, the relative intensity of the 410 nm band

increases with respect to that of 480 nm **[Figure 4.3.A]**. The excitation spectra in DMF are also wavelength dependent. The excitation spectrum recorded at longer wavelength is more red shifted as compared to the excitation spectrum recorded at shorter wavelength **[Figure 4.3.B]**. The wavelength dependence of the spectra hint the existence of more than one species in the ground state. The fluorescence decays were recorded at both the emission maximum and the lifetimes are remarkably different **[Figure 4.4.A]**. The lifetime monitored at 410 nm is 3.4 ns and at 480 nm is 4.7 ns. TRANES spectra were also constructed by monitoring decays at different wavelengths and TRANES confirm the presence of two distinct bands at about 410 nm and 480 nm **[Figure 4.4.B]**.

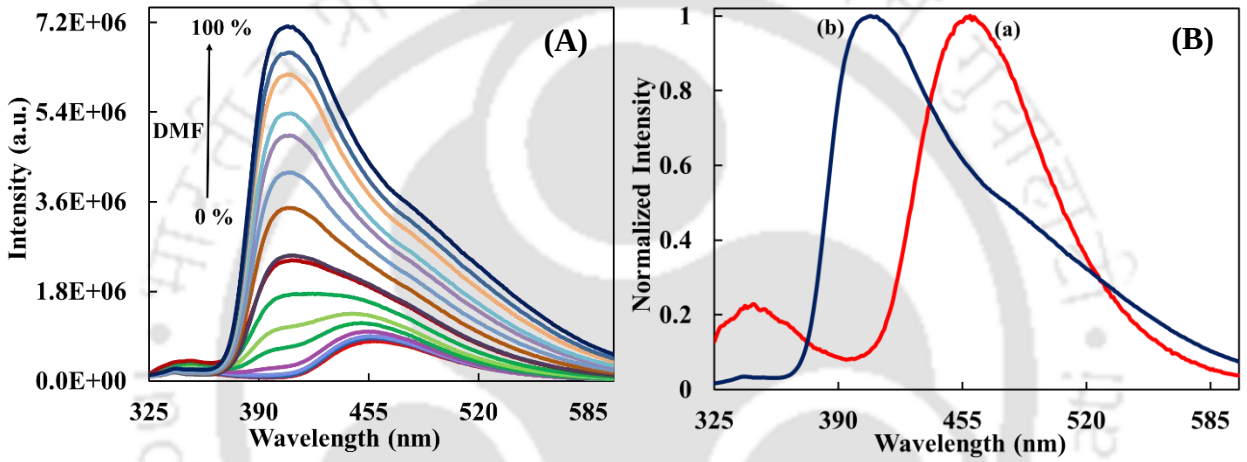

Figure 4.2: (A) Emission spectra of bis-HPTA in THF - DMF mixture. **(B)** Normalized emission spectra of bis-HPTA in (a) THF and (b) DMF, λ_{exc} = 310 nm.

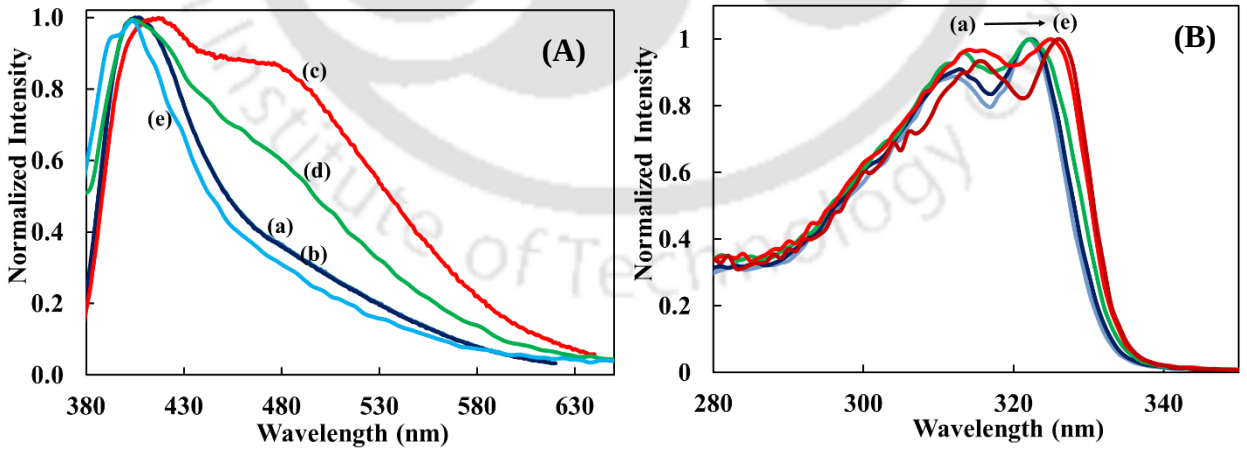

Figure 4.3: (A) Normalized emission spectra of bis-HPTA in DMF at different excitation wavelength (a) 310 nm, (b) 320 nm, (c) 330 nm, (d) 340 nm, (e) 350 nm. **(B)** Normalized excitation spectra of bis-HPTA in DMF at different emission wavelength (a) 400 nm, (b) 420 nm, (c) 460 nm, (d) 480 nm, (e) 500 nm.

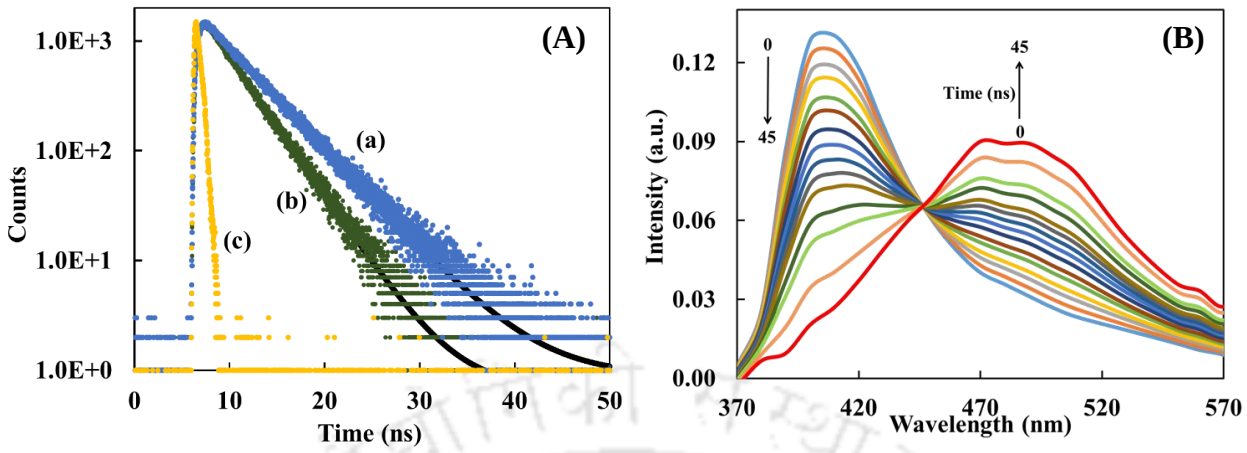

Figure 4.4: (A) The fluorescence decays of bis-HPTA in DMF (a) monitored at 480 nm, (b) monitored at 410 nm and (c) the instrument response function, λ_{exc} = 308 nm. **(B)** TRANES of bis-HPTA in DMF obtained at different times 0 ns to 45 ns, λ_{exc} = 308 nm.

4.2. Theoretical calculations

In all the solvents studied earlier (including THF), though tautomer emission appears as single band, TRANES revealed two keto emissions are present at about 455 nm and 465 nm.[161] The keto species responsible for the emissions are K1 and DK. But, both the keto emissions have same ground state precursor. As stated earlier, bis-HPTA can exist as different conformers **[Chart 4.1]**. Earlier, theoretical calculations performed in THF predicted bis-HPTA exists predominantly as bis-HPTA-I and the relative populations of other conformers are negligible.[161] K1 and DK are formed from bis-HPTA-I by ESIPT-I and PTTPT.

The excitation wavelength dependence of emissions in DMF shows both 410 nm and 480 nm emissions originated from different ground precursor. Theoretical calculations have been performed to get a better understanding on the distinct spectral nature of bis-HPTA in DMF with respect to other solvents. First the geometries of the different conformers were optimized in the ground state using DMF as solvent in IEFPCM. The result concludes that bis-HPTA-I is the most stable conformer followed by bis-HPTA-III and then bis-HPTA-II **[Table 4.1]**. The population of bis-HPTA-III conformer is only 4.9% with respect to the most stable conformer and that of bis-HPTA-II is only 1.5% with respect to the most stable conformer. However, the excitation spectra clearly show the substantial presence of second conformer in the ground state.

Table 4.1: The ground state optimized energy of different conformers in DMF.

Conformer	Relative energy (eV)
Bis-HPTA-I	0
Bis-HPTA-III	0.076
Bis-HPTA-II	0.107
Bis-HPTA-IV	0.116
Bis-HPTA-IVb	0.271
Bis-HPTA-Ia	0.277
Bis-HPTA-IVa	0.283
Bis-HPTA-Ib	0.313
Bis-HPTA-IIa	0.412
Bis-HPTA-IIIa	0.459
Bis-HPTA-Ic	0.610
Bis-HPTA-IVc	0.635

Table 4.2: The ground state optimized energy of bis-HPTA-DMF complexes in DMF.

Bis-HPTA DMF complex	Relative energy (eV)
Bis-HPTA-III	0
Bis-HPTA-II	0.028
Bis-HPTA-I	0.070
Bis-HPTA-IVb	0.076
Bis-HPTA-IIa	0.078
Bis-HPTA-IIIa	0.079
Bis-HPTA-Iva	0.090
Bis-HPTA-Ia	0.104
Bis-HPTA-Ib	0.126
Bis-HPTA-Ic	0.169
Bis-HPTA-IV	0.221
Bis-HPTA-IVc	0.236

As stated earlier, the interaction between the fluorophore and DMF is strong and they form complexes. IEFPCM does not include the specific interactions. To account for these specific interactions, the addition of explicit DMF molecules are needed in the calculations. Considering the hydrogen bonding ability of bis-HPTA and DMF, three DMF molecules were added near the three acidic centers (two 'OH' and one 'NH' protons) of bis-HPTA and performed the calculations. The calculations predicted that bis-HPTA-III is the most stable conformer followed by bis-HPTA-II with 25% relative population. The relative energy of all the conformers are given in **Table 4.2** and the optimized structures of bis-HPTA-II and bis-HPTA-III DMF complexes are shown in

Figure 4.5 and **4.6**, respectively. All the input and output geometries are given in **Annexure-B**. The Cartesian coordinates of the optimized geometries are also given in **Annexure-B**. Though inputs were given by adding three DMF molecules within the hydrogen bonding distance, one of the DMF molecule moves away **[Figure 4.5** and **4.6]**. It may be due to the intramolecular hydrogen bond. The other two protons have strong hydrogen bonding interaction with DMF.

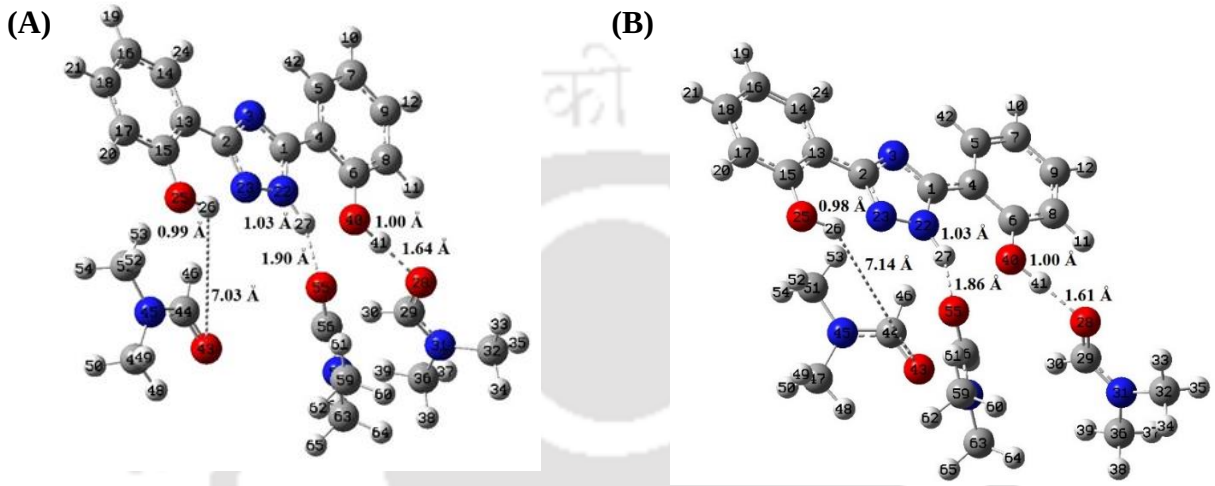

Figure 4.5: The optimized geometries of bis-HPTA-II-DMF complex in **(A)** ground state and **(B)** excited state in DMF. The dashed lines represent the hydrogen bond (the corresponding distances are labeled).

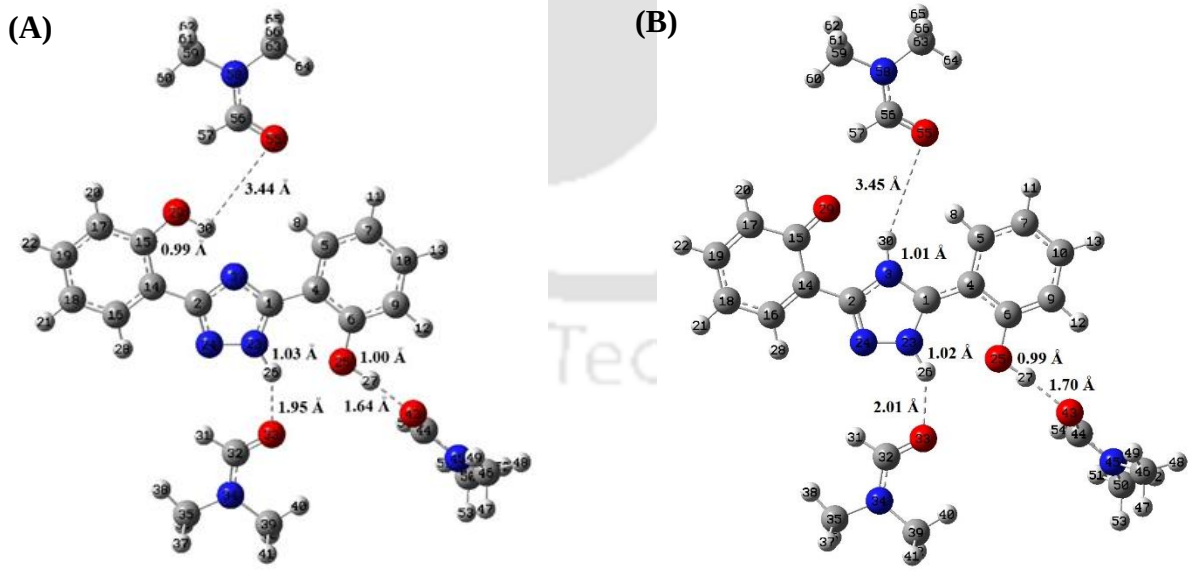

Figure 4.6: The optimized geometries of bis-HPTA-III-DMF complex in **(A)** ground state and **(B)** excited state in DMF. The dashed lines represent the hydrogen bond (the corresponding distances are labeled).

In nonpolar solvents like THF, bis-HPTA-I is the most stable conformer due to the presence of the intramolecular hydrogen bond between both the proton donor-acceptor pairs **[Chart 4.1]**. Theoretically, it has been seen that the intramolecular hydrogen bonding in the α ring is stronger as compared to that in β ring in bis-HPTA-I in THF.[161] As explained earlier, annular tautomerism plays an essential role in preventing ESIPT-II and hence weakens the hydrogen bond in β ring. Nevertheless, in DMF, the intermolecular hydrogen bonding between the 'NH' proton and DMF molecule weakens the annular tautomerism, subsequently strengthens the intramolecular hydrogen bonding in β ring. On the other hand, the complexation with DMF molecules breaks the intramolecular hydrogen bond in the α ring. As a result, bis-HPTA-III and bis-HPTA-II become the most stable conformers **[Table 4.2]**. The relative population of other conformers is negligible. Theoretically, finding of presence of two conformers agrees with the excitation spectral results. For both bis-HPTA-II and bis-HPTA-III DMF complex, the excitation energies were calculated using the optimized structures. The excitation energy of bis-HPTA-II complex (4.2 eV) is more like that of bis-HPTA-III complex (4.1 eV). Hence, the shorter wavelength excitation spectrum can be assigned to bis-HPTA-II complex (3.9 eV) and the longer wavelength excitation spectrum can be assigned to bis-HPTA-III complex (3.8 eV).

4.3. Benesi-Hildebrand plot

Theoretical calculations performed in presence of DMF molecules in DMF as solvent medium revealed, out of three acidic protons of bis-HPTA, only two protons form an intermolecular hydrogen bond with two DMF molecules. To confirm this, the stoichiometric ratio between bis-HPTA and DMF was calculated by plotting Benesi-Hildebrand plot using spectral data. The absorbance at 323 nm, the emission intensities at 410 nm and 480 nm, the intensities at 313 nm of excitation spectra (λ_{em} = 410 nm), and 323 nm of excitation spectra (λ_{em} = 480 nm) are considered to acquire the plot **[Figure 4.7.A-4.7.E]**. In each plot, better fitting is found for n = 2. Thus, the experimental results and the theoretical calculations together confirm the formation of 1 (bis-HPTA): 2 (DMF) complex.

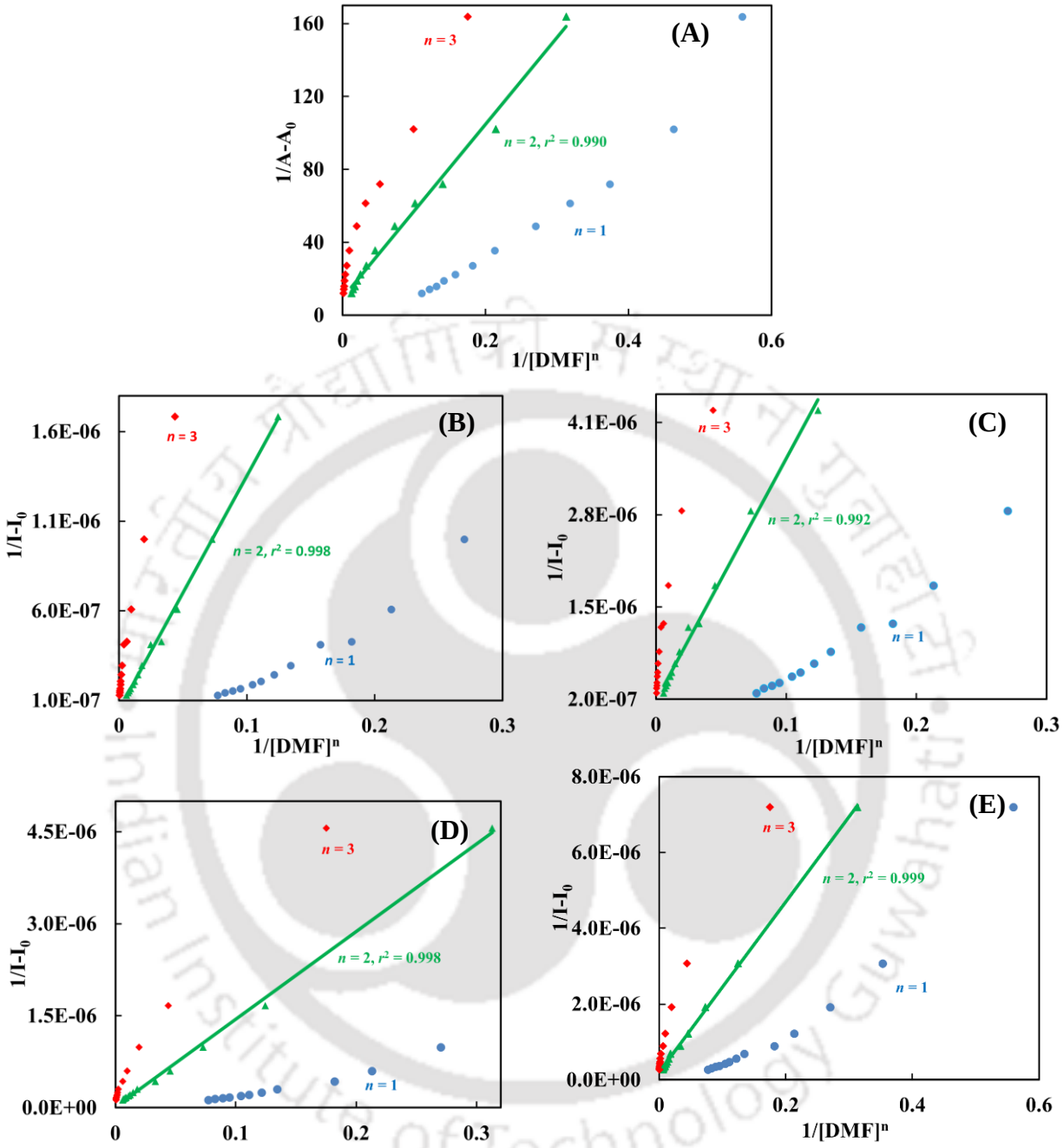

Figure 4.7: Benesi-Hildebrand plot using **(A)** the absorbance at 323 nm, **(B)** emission intensity at 410 nm, **(C)** emission intensity at 480 nm, **(D)** intensity at 313 nm of excitation spectra (λ_{em} = 410 nm), **(E)** intensity at 323 nm of excitation spectra (λ_{em} = 480 nm) (*r* - regression).

4.4. Intermolecular and intramolecular proton transfer

Upon excitation at 350 nm, only one emission band is observed at 410 nm **[Figure 4.3.A]**. In the earlier studies, the broad absorption band at ~340 nm and the emission band at 410 nm of

bis-HPTA in polar solvents were assigned to anion formed by the deprotonation of hydroxyl proton and was confirmed by studying in basic methanol.[161] Hence, it is clear that 340 nm and 410 nm bands in the absorption spectrum and emission spectrum of bis-HPTA in DMF, respectively, are due to the formation of the anion. When excited at shorter wavelengths (310 nm and 320 nm), also the anionic emission (410 nm emission) is predominantly observed **[Figure 4.3.A]**. This suggests that the shorter wavelength absorbing complex, bis-HPTA-II-DMF produces the anion in the excited state. The 480 nm emission does not match with tautomer emission observed in nonpolar solvents.[161] The relative intensity of 480 nm band increases when excited at 330 nm compared to 310 nm and 320 nm excitations.

Bis-HPTA-II forms complex with two DMF molecules through intermolecular hydrogen bond between 'OH' and 'NH' protons of bis-HPTA with the carbonyl oxygen of DMF **[Figure 4.5]**. The intermolecular hydrogen bond distances of H41….O28, H27….O55, and the intramolecular hydrogen bond distance H26….O25 decrease in the excited state **[Figure 4.5.A** and **4.5.B]**. It is well acknowledged that in the excited state, the acidic protons become more acidic and the same is observed in bis-HPTA-II DMF complex and it is evident from the decrease in the hydrogen bond lengths in the excited state. These decrease in intermolecular hydrogen bond length, simulate intermolecular proton transfer from bis-HPTA-II to DMF, which results in anion **[Scheme 4.2]**. The emission energy of the anion was calculated theoretically (2.9 eV) and is found to be in good agreement with the experimental emission energy (3.0 eV).

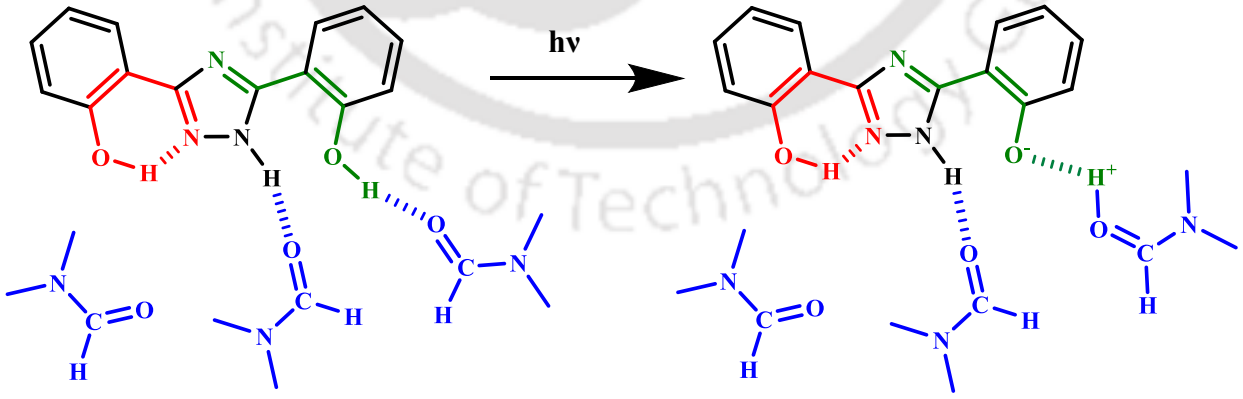

Scheme 4.2: Intermolecular proton transfer in bis-HPTA-II-DMF complex.

The longer wavelength (480 nm) emission is much red-shifted compared to the keto emissions in other reported solvents.[161] This advocates that 480 nm emission cannot be a normal emission from the enol form. On the other hand, it can be a keto emission but not from the K1 tautomer. The normalized emission intensity at 480 nm increases on increasing the excitation wavelength up to 330 nm **[Figure 4.3.A]**. This advocates bis-HPTA-III-DMF complex, which absorbs at longer wavelength compared to bis-HPTA-II, is the one which is accountable for longer wavelength emission. As only one pair proton donor-acceptor are intramolecular hydrogen bonded in bis-HPTA-III-DMF complex, the only possible ESIPT outcomes as K3 keto tautomer, which is a zwitterion **[Scheme 4.3]**. In few other fluorophores also, the ESIPT lead to the zwitterionic keto tautomer.[223, 40, 41] Finally, bis-HPTA-III-DMF complex was optimized in the excited state to verify the hydrogen bond distances, but it resulted in the keto form **[Figure 4.6.A** and **4.6.B]**. This further supports the assignment of 480 nm emission to keto emission.

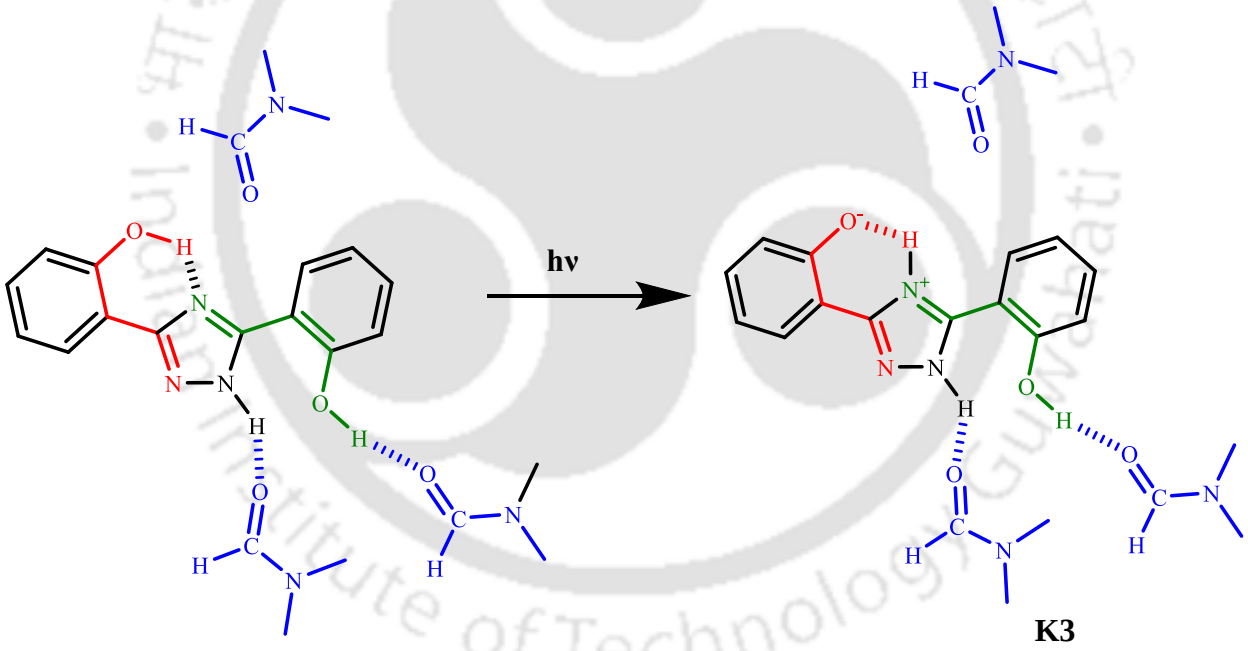

Scheme 4.3: Intramolecular proton transfer in bis-HPTA-III-DMF complex.

4.5. Reversing the equilibrium

As stated earlier, DMF acts as a reducing agent as well as stabilizing agent to synthesize silver nanoparticle,[186] henceforth, the effect of silver nanoparticle on bis-HPTA-DMF complex was studied. In presence of silver particle, the absorption spectrum of bis-HPTA is blue-shifted

with respect to the absorption spectrum recorded in the absence of silver particle in DMF and the absorption maximum (308 nm) matches with the absorption maximum in THF. The characteristic SPR band of silver nanoparticle is observed at ~ 430 nm and in presence of bis-HPTA, the band shifted to 460 nm **[Figure 4.8.A** and **4.8.B]**. Usually, the SPR band of silver nanoparticle is observed at ~ 430 nm and the band position shifts based on the size and shape of the particles.[166] Though DMF acts as a stabilizer, the particles become less stable with time in DMF, in absence of any other stabilizer.[166, 186] The particles precipitate and stick to the surface of the container as black coating and the solution becomes colorless. However, when the fluorophores stabilize the particles the solutions retain their golden yellow color for a long time.[166] The color of silver nanoparticle solution in DMF is yellow and in presence of bis-HPTA, the color becomes pale pink **[Figure 4.9]**. The absence of black coating on the surface of the container suggests the particles are still present in the solution **[Figure 4.10.B]**. However, the shift in SPR band and change in color of the solution suggests the change in particle size or shape, in the presence of bis-HPTA. The DLS studies were performed and images were captured by FESEM. DLS study indicates in the absence of bis-HPTA, the size of the particles are in the range of 100-200 nm and in the presence of bis-HPTA, particles size increase to 300-1000 nm **[Figure 4.11]**. FESEM images also confirm that in the presence of bis-HPTA, the particles size enhanced **[Figure 4.12.A** and **4.12.B]**. This shows that though bis-HPTA prevents the precipitation of the particles, it admits the particles to agglomerate.

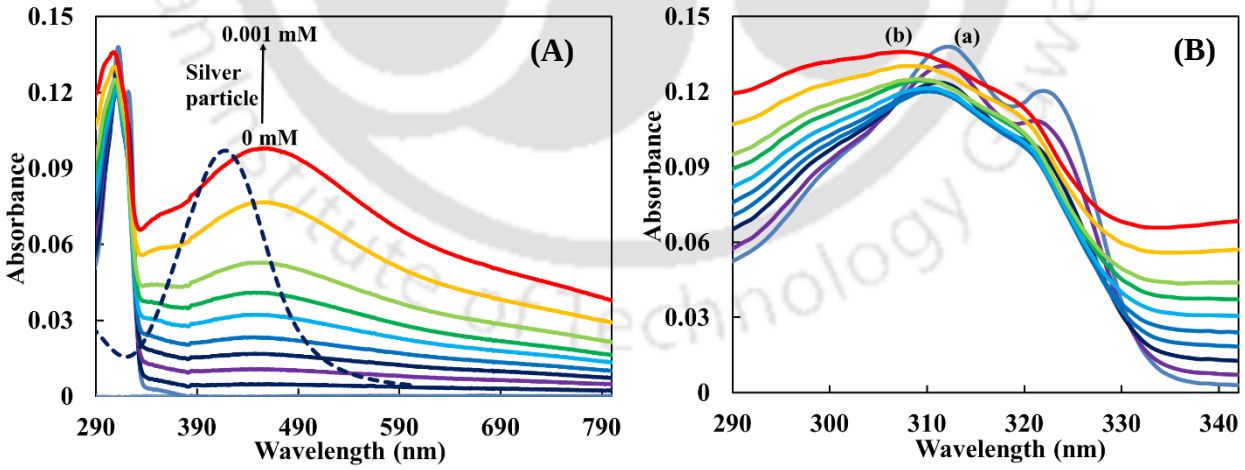

Figure 4.8: (A) Absorption spectra of bis-HPTA in the presence of silver particle (0 – 0.001 mM of silver) in DMF, and the dashed line is the normalized absorption spectrum of silver nanoparticle (0.001 mM) in DMF in the absence of bis-HPTA. **(B)** The normalized absorption spectra from 290 nm to 340 nm: (a) in the absence of silver particle, (b) in the presence of 0.001 mM silver particle.

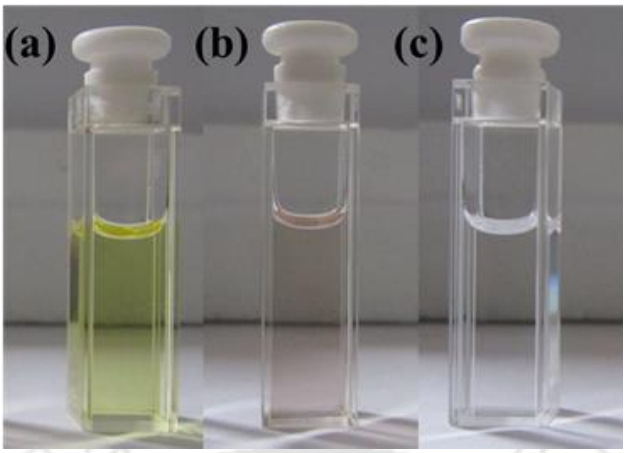

Figure 4.9: Images of (a) 0.5 mM silver nanoparticles solution in DMF, (b) bis-HPTA with 0.5 mM silver particles solution in DMF, (c) bis-HPTA solution in DMF.

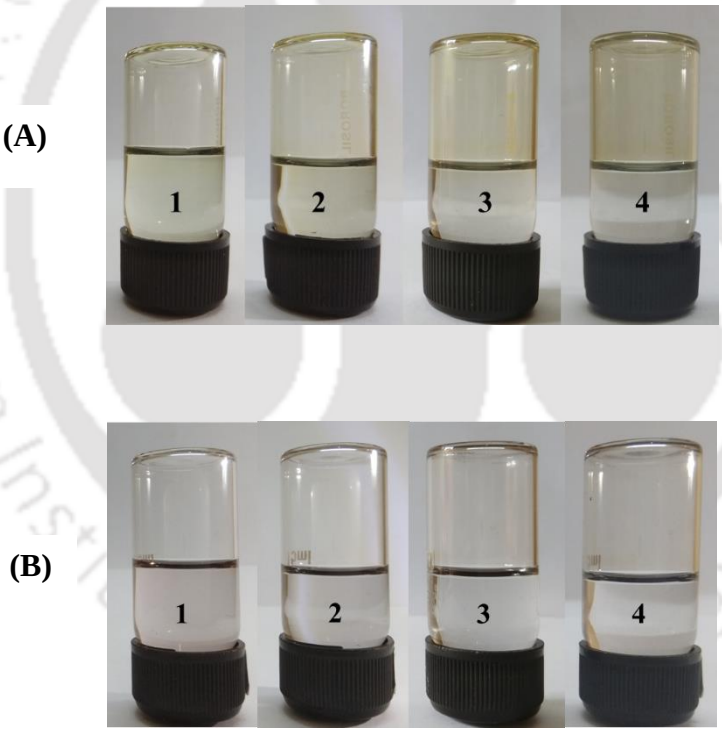

Figure 4.10: Images at different times after preparation of the solution (1) 5 min, (2) 5 hrs., (3) 12 hrs., (4) 24 hrs of **(A)** 0.5 mM silver nanoparticles solution in DMF (silver sticks at the side of the inverted vial and the colour deepens with time), **(B)** bis-HPTA with 0.5 mM silver particles solution in DMF (no silver sticks at the side of the inverted vial).

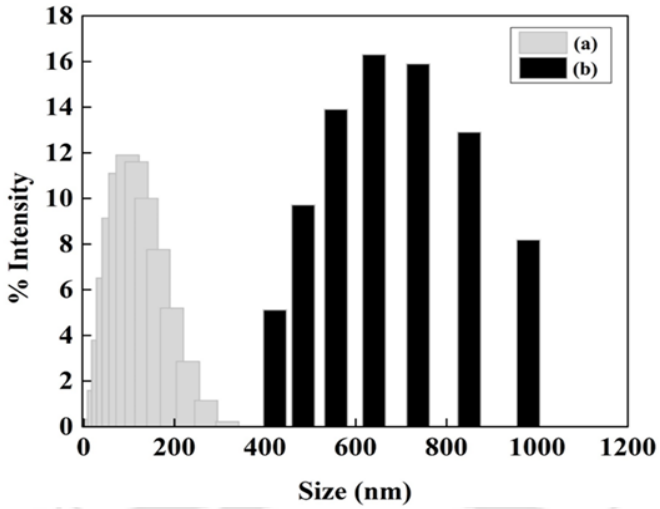

Figure 4.11: DLS plot of silver particles (a) in the absence and (b) in the presence of bis-HPTA.

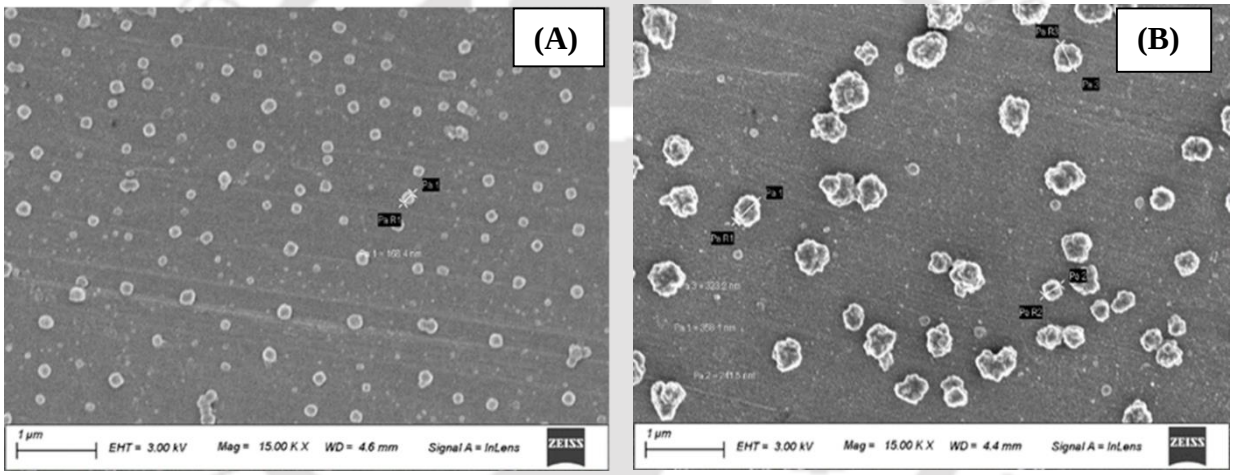

Figure 4.12: FESEM images of silver particles **(A)** in the absence of bis-HPTA and **(B)** in the presence of bis-HPTA.

The steady state emission spectra were also recorded in the presence of silver particles. On increasing the silver particle concentration, initially, the emission intensity of both the emission decreases. For further increase in silver particle concentration, the 450 nm band appears at the cost of 410 nm and 480 nm bands **[Figure 4.13.A]**. At 0.5 mM concentration of silver, the 450 nm band completely replaces the 410 nm and 480 nm bands **[Figure 4.13.B]**. Unlike in DMF, in presence of silver particles, the emission maxima as well as the excitation maxima are independent of excitation and emission wavelengths, respectively **[Figure 4.14.A** and **4.14.B]**. The fluorescence decay was monitored at 450 nm and found to be biexponential **[Figure 4.15]**. The lifetimes are 0.9 ns and 4.2 ns, are close to the lifetimes of K1 and DK tautomer in nonpolar solvents.[161]

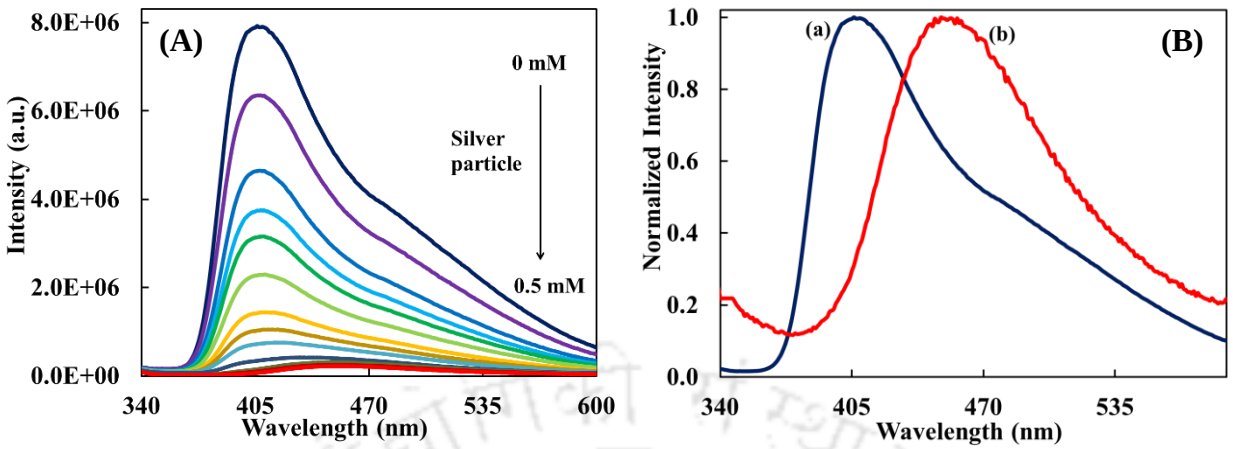

Figure 4.13: (A) Emission spectra of bis-HPTA in the presence of silver particle (0 – 0.5 mM of silver) in DMF. **(B)** The normalized emission spectra (a) in the absence of silver particle and (b) in the presence of 0.5 mM silver particle.

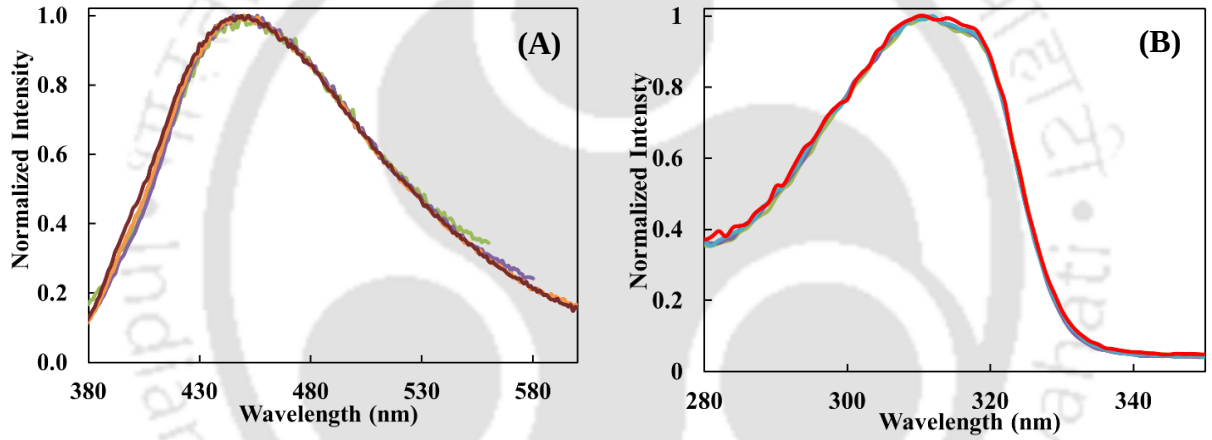

Figure 4.14: (A) Normalized emission spectra of bis-HPTA in presence of (0.5 mM) silver particle. λ_{exc} = 290 nm, 300 nm, 310 nm, 320 nm. **(B)** Normalized excitation spectra of bis-HPTA in presence of (0.5 mM) silver particle. λ_{em} = 430 nm, 450 nm, 480 nm, 500 nm.

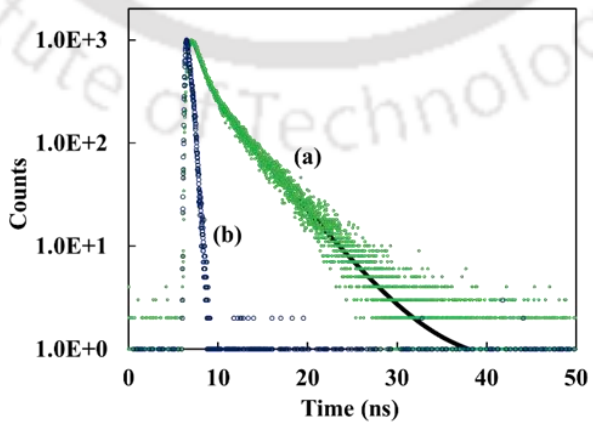

Figure 4.15: The fluorescence decay of (a) bis-HPTA in the presence of 0.05 mM silver particle in DMF recorded at 450 nm (b) the instrument response function, λ_{exc} = 308 nm.

The characteristics of bis-HPTA in the presence of silver particles match with the characteristics observed in THF. This shows that the equilibrium shifts towards bis-HPTA-I in the presence of silver particles. In the absence of silver particles in DMF, the formation of intermolecular hydrogen bond between bis-HPTA and DMF lead to the formation of bis-HPTA-II and bis-HPTA-III. Nevertheless, in presence of silver particles, the fluorophore is adsorbed on the surface of silver particles. As a result, the intermolecular hydrogen bond with DMF molecules is interrupted. As a consequence, the equilibrium shifts toward bis-HPTA-I. Thus, the silver nanoparticles reactivate the annular tautomerism that is prevented by DMF through the intermolecular hydrogen bond. As a result, the intramolecular hydrogen bond in the β ring gets weakened and ESIPT-I is observed in bis-HPTA-I as in other solvents **[Scheme 1.17]**. Subsequently, ESIPT-I retards the annular tautomerism and enables the ESIPT-II. Thus, PTTPT is reestablished by the addition of silver particles.

4.6. Conclusion

In contrary to the anticipation (proposed in **Scheme 4.1**) that DMF may promote ESIPT-II, DMF completely alters the ESIPT paths of bis-HPTA by tweaking the ground state conformers. Bis-HPTA forms 1:2 hydrogen bonded complex with DMF. The intermolecular hydrogen bond breaks one of the intramolecular hydrogen bond. Breaking of intramoleular hydrogen bonding leads to the formation of bis-HPTA-II and bis-HPTA-III. In the excited state, while bis-HPTA-III undergoes intramolecular proton transfer to form keto tautomer, bis-HPTA-II undergoes intermolecular proton transfer to form anion. By adding silver particle to DMF solution bis-HPTA-I can be regenerated, thereby, the self-assisted twin proton transfer PTTPT can be restored. Bis-HPTA induces agglomeration of silver nanoparticles to form particle of bigger size. However, it prevents the precipitation of the silver metal by getting adsorbed on the surface of the silver particles. In summary, ESIPT process in bis-HPTA can be modulated by DMF and again can be restored as in THF by using silver particles.

Chapter 5

Tuning the triple emission of 2-(4′-diethylamino-2′-hydroxyphenyl)-1H-imidazo-[4,5-b]pyridine by solvent: ESIPT *vs* TICT

5.0. Introduction

In the previous chapter, it was shown, that the complexation with solvent modified the ground state conformers, which in turn changed the ESIPT paths. In this chapter, it is shown that how the complexation with solvent molecule not just changed the ESIPT path, but it can completely alter the reaction itself to promote TICT emission.

As stated earlier, like ESIPT, TICT is also an important excited state phenomenon which leads to dual emission and has applications in various fields.[17-20, 224-226] TICT depends on the polarity and the hydrogen bonding ability of the solvent. The effect of aprotic and protic solvents on the emission characteristics of DEAHPIP-b and DEAMPIP-b **[Chart 5.1]** are discussed.

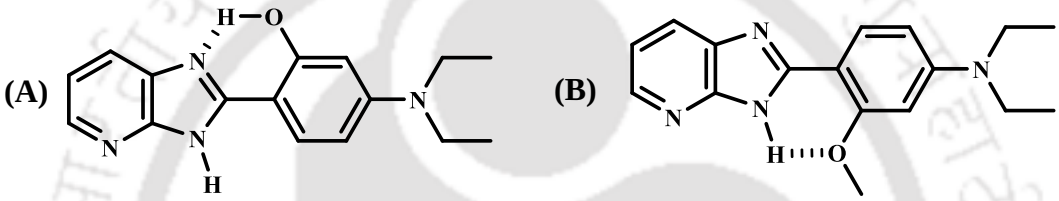

Chart 5.1: Structure of **(A)** DEAHPIP-b and **(B)** DEAMPIP-b.

5.1. Effect of aprotic solvents

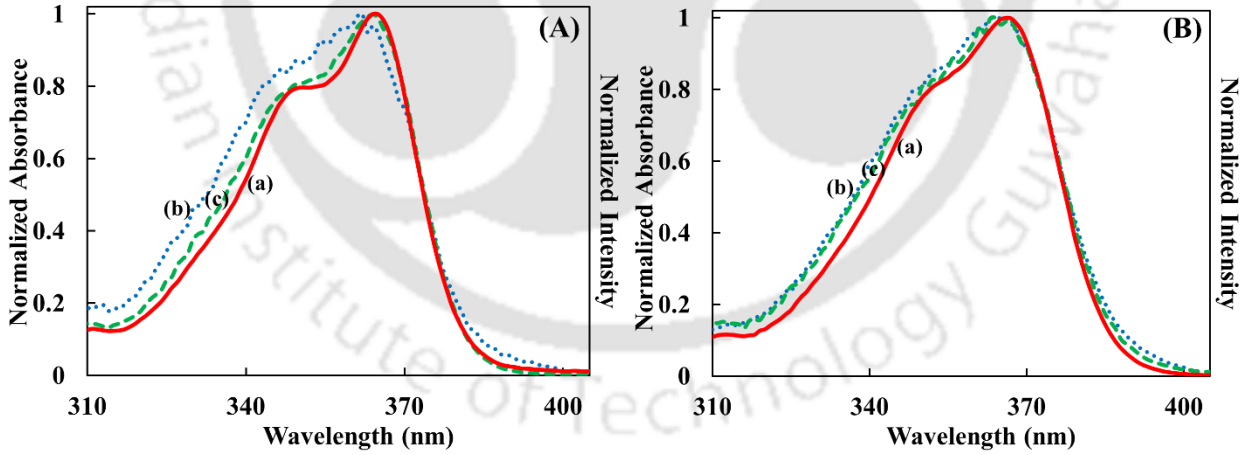

Figure 5.1: Normalized (a) absorption spectrum, (b) excitation spectra of DEAHPIP-b monitored at shorter wavelength emission maximum and (c) at longer wavelength emission maximum in **(A)** ether and **(B)** acetonitrile.

To understand the effect of aprotic solvents, the spectral characteristics of DEAHPIP-b and its methoxy derivative are studied in ether, a nonpolar aprotic solvent and acetonitrile, a polar aprotic solvent. In ether, DEAHPIP-b absorbs at 365 nm with a shoulder at 350 nm **[Figure 5.1.A]**.

The absorption band maxima are red-shifted compared to DMAPIP-b and HPIP-b. This is due to the presence of both hydroxyl group and diethylamino group together and stronger electron donating capacity of the diethylamino group.[227, 123, 125] In polar acetonitrile, a small red shift is observed in the absorption spectrum of DEAHPIP-b compared to that in ether **[Figure 5.1.B, Table 5.1]**. The absorption spectra of methoxy derivative are blue shifted with respect to DEAHPIP-b and the relative absorbance of the shorter wavelength shoulder is also increased **[Figure 5.2, Table 5.1**]. This shift may be due to the absence of intramolecular hydrogen bond in the methoxy derivative.

Table 5.1: Absorption maxima (λ_{max}^{ab}, nm), extinction coefficient ($\in_{max}$, M^{-1} cm^{-1}) emission maxima (λ_{max}^{fl}, nm), fluorescence quantum yield (ϕ_f) and fluorescence lifetime (τ, ns) of DEAHPIP-b and DEAMPIP-b in ether and acetonitrile.

	λ_{max}^{ab} (log $\in_{max}$)	λ_{max}^{fl} (ϕ_f)		τ^b	
		Shorter wavelength	Longer wavelength	At shorter wavelength maximum	At longer wavelength maximum
Ether					
DEAHPIP-b	350 (4.18), 365 (4.29)	390 (0.006)[a]	480 (0.046)[a]	0.4 (57) 1.0 (43)	0.5 (76) 0.9 (24)
DEAMPIP-b	348 (4.27), 362 (4.27)	390 (0.62)		1.3 (100%)	
Acetonitrile					
DEAHPIP-b	351 (4.18), 367 (4.28)	410 (0.025)[a]	470 (0.01)[a]	0.2 (87) 1.3 (13)	0.2 (95) 1.5 (5)
DEAMPIP-b	353 (4.25), 365 (4.28)	413 (0.69)		1.5 (100%)	

[a]Relative fluorescence yield. [b]The relative amplitude.

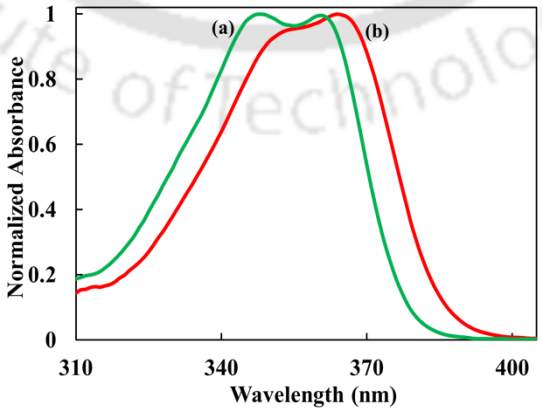

Figure 5.2: Normalized absorption spectra of DEAMPIP-b monitored in (a) ether and (b) acetonitrile.

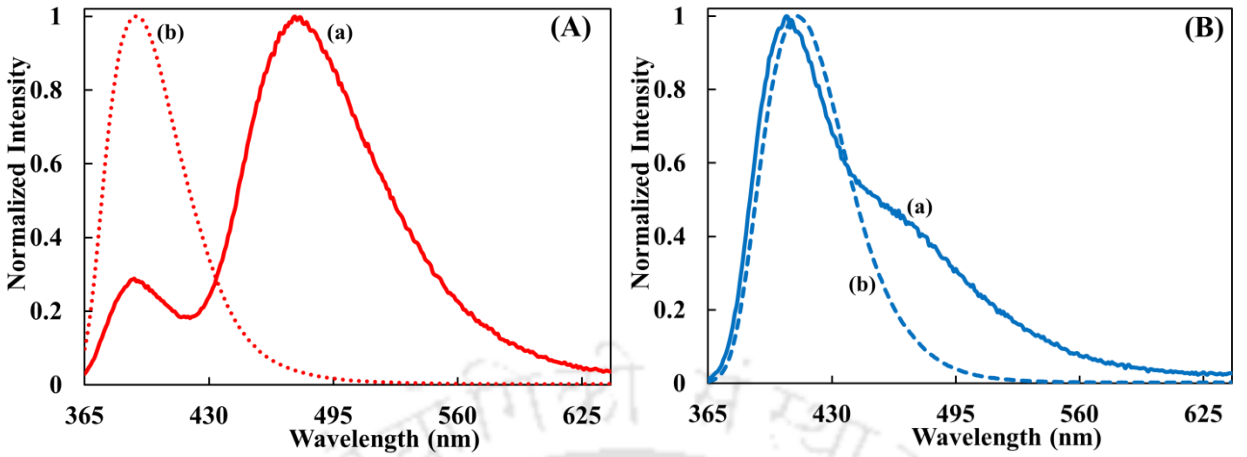

Figure 5.3: Normalized emission spectra of (a) DEAHPIP-b and (b) DEAMPIP-b in **(A)** ether and **(B)** acetonitrile, λ_{exc} = 350 nm.

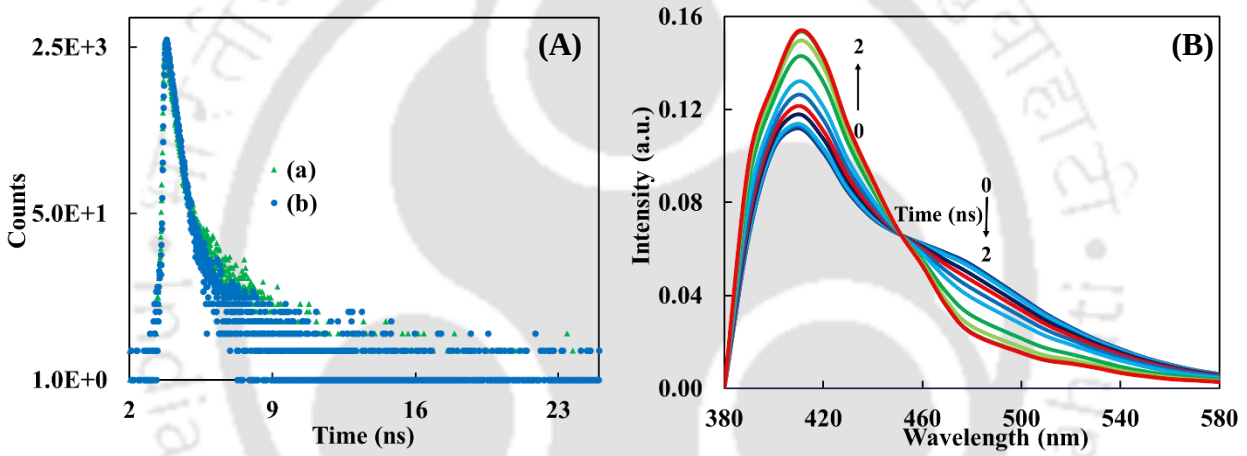

Figure 5.4: (A) Fluorescence decays monitored at ▲ (a) 410 nm, ● (b) 470 nm and **(B)** TRANES obtained at different times 0 ns to 2 ns of DEAHPIP-b in acetonitrile, λ_{exc} = 375 nm.

DEAHPIP-b emits dual emission. In ether, the longer wavelength emission is more strong than the shorter wavelength emission **[Figure 5.3.A]**. But in polar aprotic solvent acetonitrile, the shorter wavelength emission band predominates over longer wavelength emission **[Figure 5.3.B]**. The large Stokes shift and decrease in relative intensity of the longer wavelength emission with increasing polarity are the emission characteristics of tautomer emission in typical ESIPT capable molecules. The emission of methoxy derivative which cannot undergo ESIPT is single and nearly matches with that of shorter wavelength emission of hydroxyl derivative **[Figure 5.3]**. It substantiates the fact that the longer wavelength emission of DEAHPIP-b is due to tautomer emission. Two different fluorescence lifetimes were obtained when monitored at emission maxima of normal as well as tautomer emission in both the solvents **[Table 5.1]**. One of the decay

corresponds to normal emission and the other corresponds to tautomer emission. The relative amplitude of the shorter decay increases at longer wavelength and that of the longer decay decreases at longer wavelength. Unlike in ether, the steady state emission spectra of DEAHPIP-b are not well resolved in acetonitrile **[Figure 5.3.B]**. The emission spectra were resolved by time resolved method, the TRANES thus obtained in acetonitrile are represented in **Figure 5.4.B**. The relative intensity of the normal emission increases with decay time and the relative intensity of the tautomer emission decreases with decay time. Hence, the longer decay and shorter decay can be assigned to normal and the tautomer emissions, respectively. The decay of the methoxy derivative is single exponential and it is close to that of the longer decay of the hydroxyl derivative **[Table 5.1]**. This is consistent with the assigned fluorescence lifetimes. On the other hand, the lifetime of the tautomer emission of HPIP-b is longer than its normal emission.[227] Though, lifetime of the normal emission of DEAHPIP-b is comparable with the normal emission of HPIP-b, the lifetime of the tautomer emission is much shorter compared to the tautomer lifetime of HPIP-b. In HPIP-b and related molecules, the keto tautomer is reported to undergo non-radiative decay via the formation of ICT state by torsional rotation of the phenyl ring in the excited state.[163, 167, 227, 228] Substitution of charge donating diethylamino group is expected to enhance this non-radiative decay. This explains the smaller relative fluorescence yields of DEAHPIP-b than those of HPIP-b.[227] A similar enhancement in the non-radiative decay of AHPIP-c compared to HPIP-c was reported when the charge donating amino group was attached to HPIP-c.[165, 229]

To identify the ground state precursor for both emission, the excitation spectra were recorded by monitoring at both emission maxima. In ether, the excitation spectra of both the emission are different **[Figure 5.1.A]**. This shows that both the emissions originate from different ground state species. DEAHPIP-b can exist in two different conformers, cis-enol and trans-enol **[Scheme 5.1]**. Cis-enol has intramolecular hydrogen bond which upon excitation undergoes ESIPT **[Scheme 5.1]**. The trans-enol does not have the intramolecular hydrogen bond, therefore it cannot undergo ESIPT and it emits normal emission **[Scheme 5.1]**. The excitation spectrum of the tautomer emission is red shifted compared to the excitation spectrum of the normal emission and more close to that of the absorption spectrum **[Figure 5.1]**. From this, it can be concluded that the cis-enol is the dominating species in the ground state. The difference between two excitation spectra decreases in acetonitrile compared to that in ether **[Figure 5.1]**.

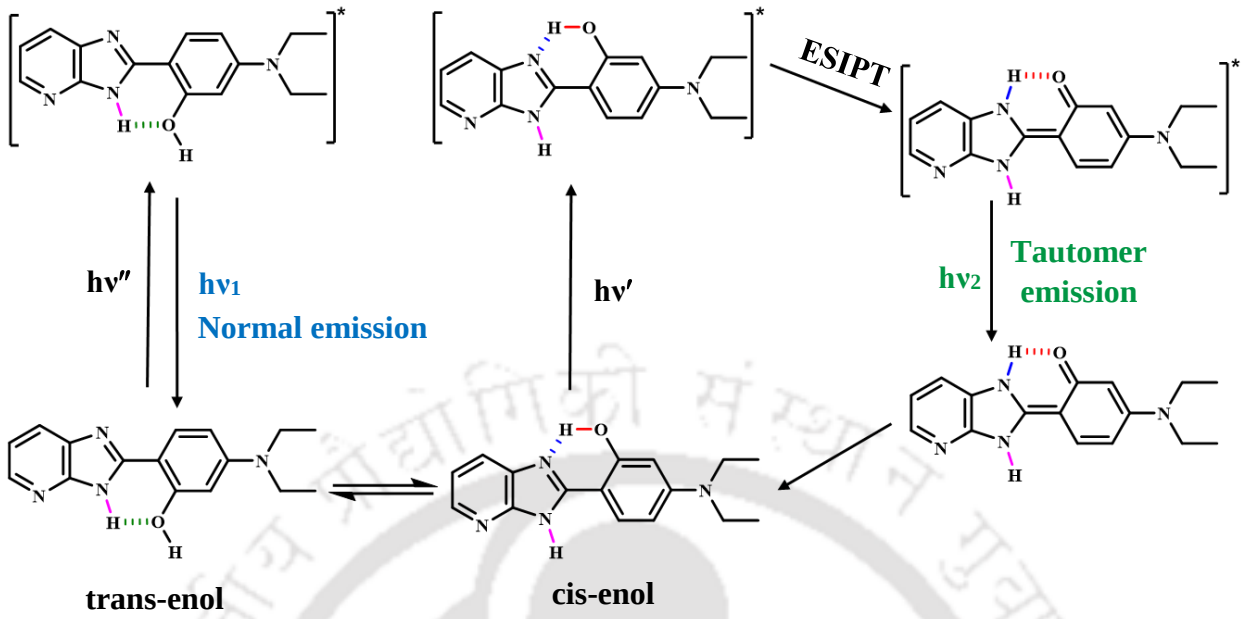

Scheme 5.1: Schematic representation of normal emission and tautomer emission in DEAHPIP-b.

5.2. Effect of protic solvents

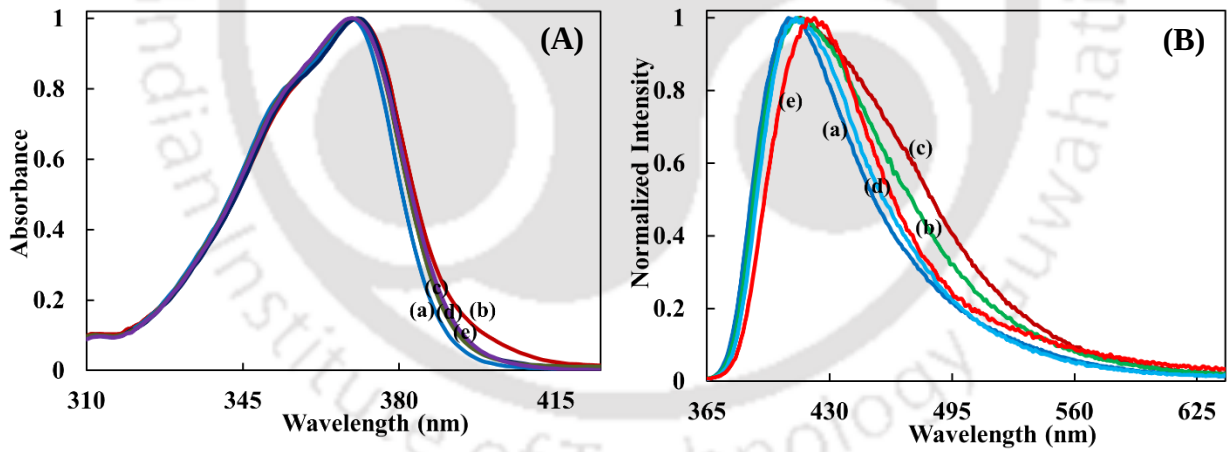

Figure 5.5: Normalized **(A)** absorption spectra and **(B)** emission spectra of DEAHPIP-b at λ_{exc} = 350 nm in (a) 2-propanol, (b) 1-propanol, (c) 1-butanol, (d) ethanol and (e) methanol.

The absorption spectra of both DEAHPIP-b and DEAMPIP-b are red shifted in protic solvents with respect to those in aprotic solvents **[Figure 5.5.A** and **5.6.A]**. The fluorescence in protic solvents are broad which suggests the presence of more than one band **[Figure 5.5.B]**. In methanol along with the shorter wavelength emission, long tailing towards longer wavelength is also observed **[Figure 5.5.B]**. In all the protic solvents except ethanol, the fluorescence decay is

biexponential **[Table 5.2]**. To get better insight, fluorescence decays were recorded at different wavelengths and TRANES were constructed in these solvents. Both emission maxima thus obtained are compiled in **Table 5.2**. In the methoxy derivative, a single emission is found in all these solvents **[Figure 5.6.B]**, which is supported by the single exponential fluorescence decay **[Table 5.3, Figure 5.12.A]**. In 1-propanol, 2-propanol and 1-butanol, the shorter wavelength emission maxima of DEAHPIP-b are close to that methoxy derivative **[Table 5.2** and **5.3]**. Therefore, the shorter wavelength emissions in these solvents are normal emissions. The longer wavelength emissions are blue shifted with respect to the tautomer emission in aprotic solvents. Such blue shift with increase in polarity and hydrogen bonding capacity of the solvent is a typical characteristic of the tautomer emission.[214-216] This is due to more stabilization of the keto ground state than its excited state. Hence, the longer wavelength emission in these solvents are tautomer emission formed by ESIPT. Like aprotic solvents, in these solvents also the relative intensity of the normal emission increases and that of the tautomer emission decreases with an increase in emission decay time **[Figure 5.7.B-5.9.B]**.

Table 5.2: Absorption maxima (λ_{max}^{ab}, nm), extinction coefficient ($\in_{max}$, M^{-1} cm^{-1}) fluorescence maxima (λ_{max}^{fl}, nm), relative fluorescence yield (**F**) and fluorescence lifetime (τ, ns) of DEAHPIP-b in protic solvents.

solvent	λ_{max}^{ab} ($\log \in_{max}$)	λ_{max}^{fl} (**F**)		τ^a	
		Shorter wavelength	Longer wavelength	At shorter wavelength maxima	At longer wavelength maxima
2-Propanol	354 (4.20), 369 (4.30)	410 (0.019)	460 (0.043)	0.3 (36) 1.5 (64)	0.4 (90) 1.7 (10)
1-Butanol	355 (4.19), 371 (4.29)	420 (0.026)	460 (0.048)	0.5 (42) 1.4 (58)	0.5 (90) 1.6 (10)
1-Propanol	356 (4.18), 371 (4.28)	420 (0.027)	450 (0.042)	0.4 (45) 1.3 (55)	0.4 (87) 1.5 (13)
Ethanol	354 (4.18), 370 (4.28)	420 (0.028)	440, 560	0.3 (49) 1.3 (51)	0.3 (87) 1.4 (13) **[at 440 nm]** 0.3 (54) 1.2 (26) 2.3 (21) **[at 560 nm]**
Methanol	354 (4.19), 370 (4.29)	430 (0.011)	570	0.3 (100 %)	0.2 (89) 0.7 (11)

[a]The relative amplitude.

Table 5.3: Absorption maxima (λ_{max}^{ab}, nm), extinction coefficient ($\in_{max}$, M^{-1} cm^{-1}), emission maxima (λ_{max}^{fl}, nm), fluorescence quantum yield (ϕ_f) and fluorescence lifetime (τ, ns) of DEAMPIP-b in protic solvents.

Solvent	λ_{max}^{ab} (log $\in_{max}$)	λ_{max}^{fl} (ϕ_f)	τ
2-Propanol	355 (4.25), 368 (4.26)	405 (0.70)	1.5
1-Butanol	356 (4.25), 369 (4.27)	403 (0.66)	1.4
1-Propanol	356 (4.22), 369 (4.24)	410 (0.66)	1.4
Ethanol	356 (4.18), 369 (4.20)	418 (0.56)	1.3
Methanol	356 (4.17), 369 (4.19)	418 (0.16)	0.3

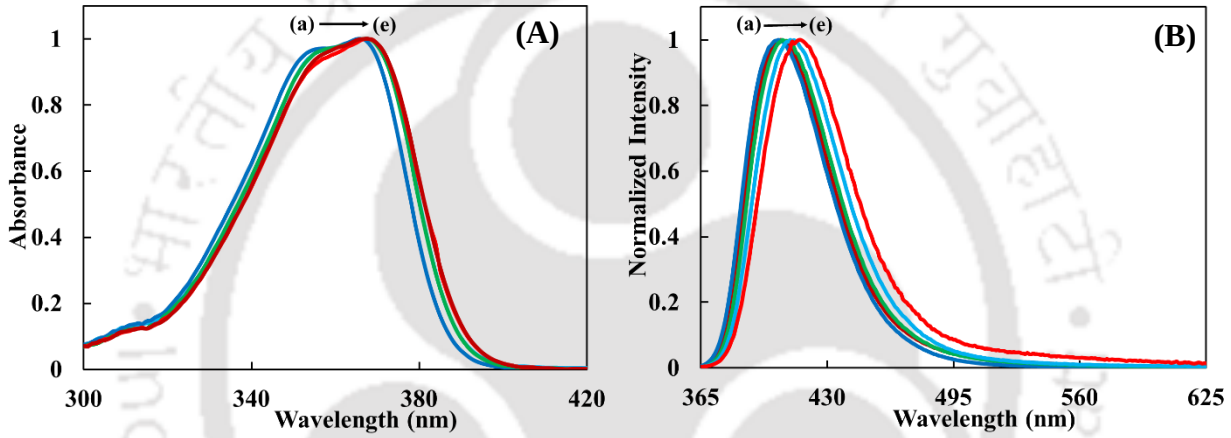

Figure 5.6: Normalized **(A)** absorption spectra and **(B)** emission spectra at λ_{exc} = 350 nm of DEAMPIP-b in (a) 2-propanol, (b) 1-propanol, (c) 1-butanol, (d) ethanol and (e) methanol.

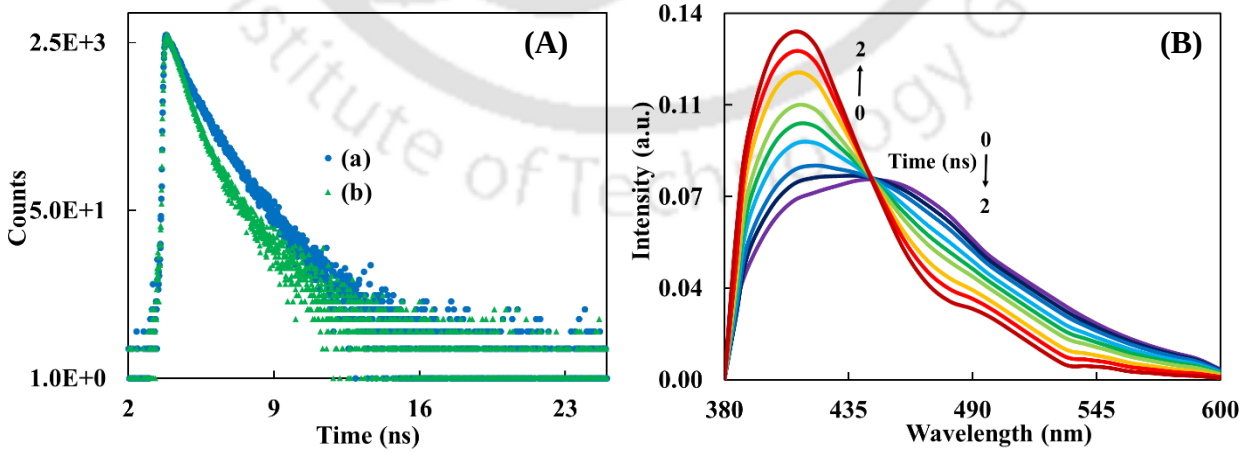

Figure 5.7: (A) The fluorescence decays monitored at ● (a) 410 nm, ▲ (b) 460 nm and **(B)** TRANES obtained at different times 0 ns to 2 ns of DEAHPIP-b in 2-propanol, λ_{exc} = 375 nm.

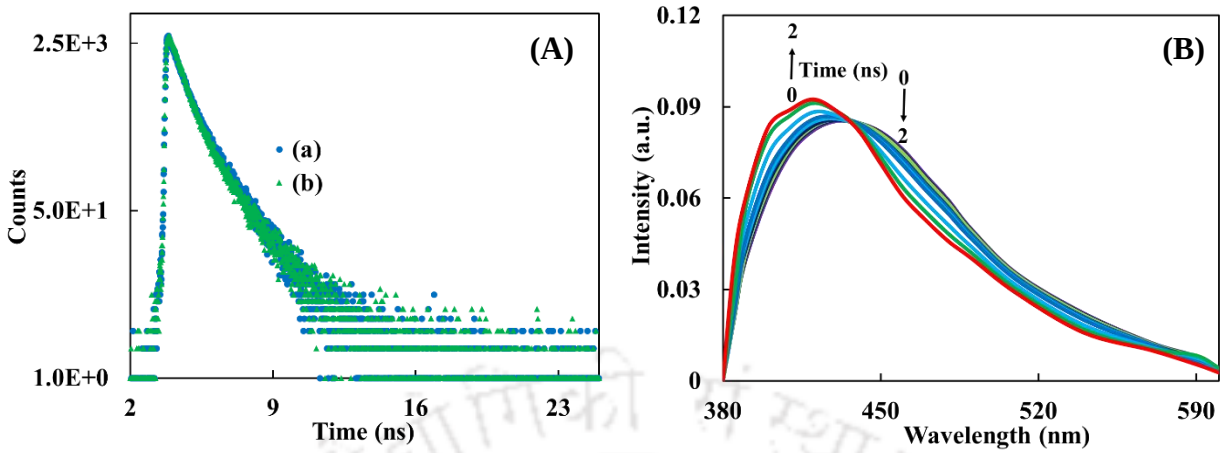

Figure 5.8: (A) The fluorescence decays monitored at ● (a) 420 nm, ▲ (b) 450 nm and **(B)** TRANES obtained at different times 0 ns to 2 ns of DEAHPIP-b in 1-propanol, λ_{exc} = 375 nm.

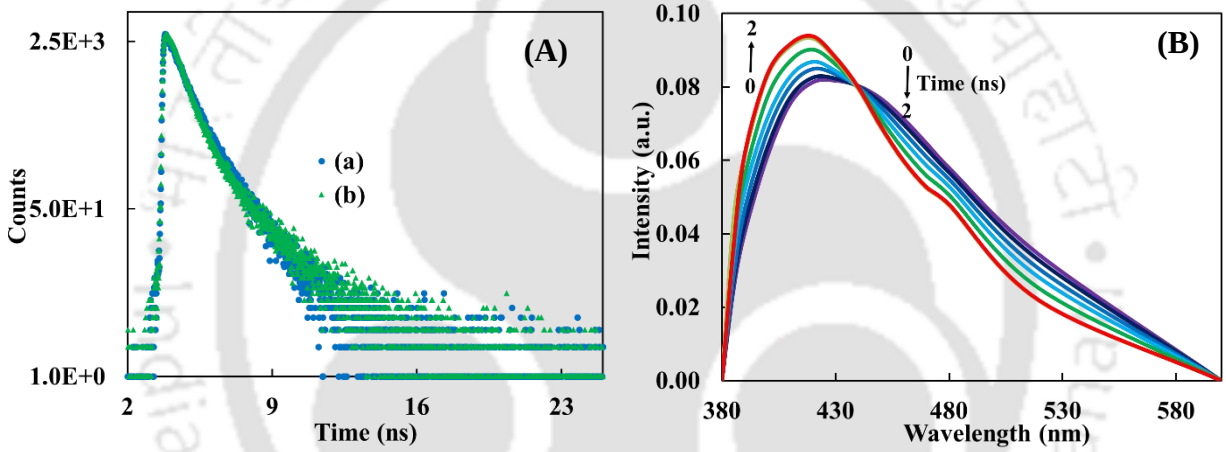

Figure 5.9: (A) The fluorescence decays monitored at ● (a) 420 nm, ▲ (b) 460 nm and **(B)** TRANES obtained at different times 0 ns to 2 ns of DEAHPIP-b in 1-butanol, λ_{exc} = 375 nm.

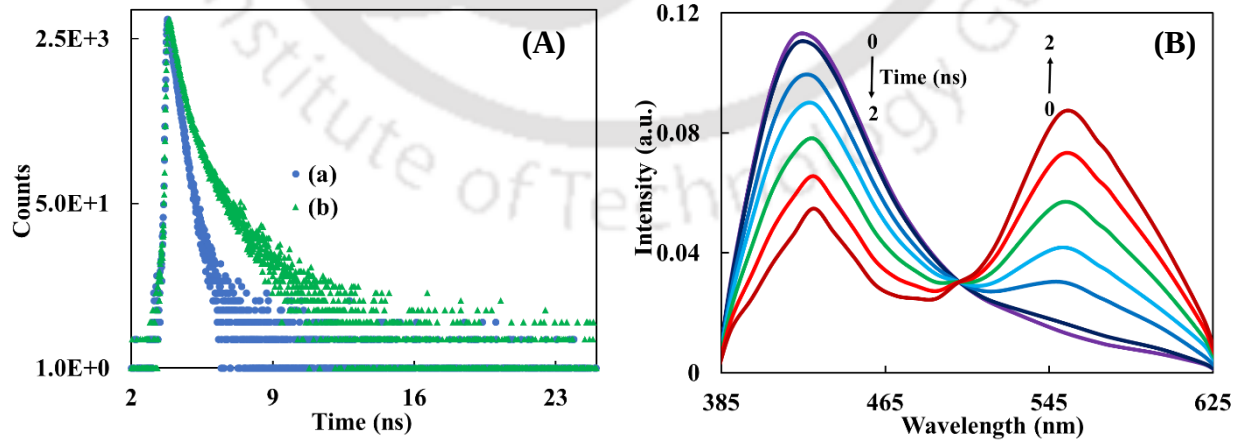

Figure 5.10: (A) The fluorescence decays monitored at ● (a) 430 nm, ▲ (b) 570 nm and **(B)** TRANES obtained at different times 0 ns to 2 ns of DEAHPIP-b in methanol, λ_{exc} = 375 nm.

Although in methanol biexponential decay is observed, the relative intensity of normal emission (shorter wavelength emission) decreases and that of longer wavelength emission increases with longer decay time **[Figure 5.10.B]**. This trend is just opposite to that observed in propanols and butanol. The longer wavelength emission maximum is also red shifted with respect to those in aprotic and other protic solvents. This is a typical behavior of TICT emission which will red shift with an increase in polarity and hydrogen bond capacity of the solvent. Since, the ICT increases in the excited state (TICT state), it has much higher dipole moment than the ground state. Therefore, the TICT state is more stabilized than the corresponding ground state. This emission is also red shifted with respect to the TICT emission observed in DMAPIP-b. This is due to the presence of hydroxyl group and diethylamino group in DEAHPIP-b. The TICT emission of 2-(4′-amino-2′-hydroxyphenyl)-1H-imidazo[4,5-c]pyridine is also red shifted compared to that of 2-(4′-aminophenyl)imidazo[4,5-c]pyridine.[165, 124] As stated earlier, in DMAPIP-b, the intermolecular proton transfer triggers the TICT emission **[Scheme 1.16]**.[123] However, DMAPIP-b emits TICT emission in other protic solvents such as propanol and butanol also.[20] DMAPIP-b does not have a 'OH' group to form intramolecular hydrogen bond to compete the ESIPT and therefore it emits TICT emission. DEAHPIP-b has stronger intramolecular hydrogen bond and in butanol or propanol, the intramolecular proton transfer dominates over the intermolecular proton transfer in the excited state. Hence, ESIPT overcomes TICT. Since methanol has higher polarity and hydrogen bonding capacity, it forms strong intermolecular hydrogen bond. Therefore, the intermolecular proton transfer dominates the intramolecular proton transfer which triggers the TICT emission in DEAHPIP-b, same as in DMAPIP-b **[Scheme 5.2]**.

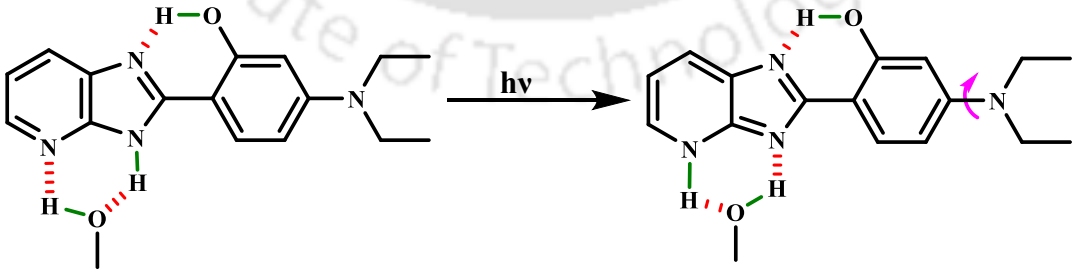

Scheme 5.2: Intermolecular proton transfer triggered TICT emission in DEAHPIP-b in methanol.

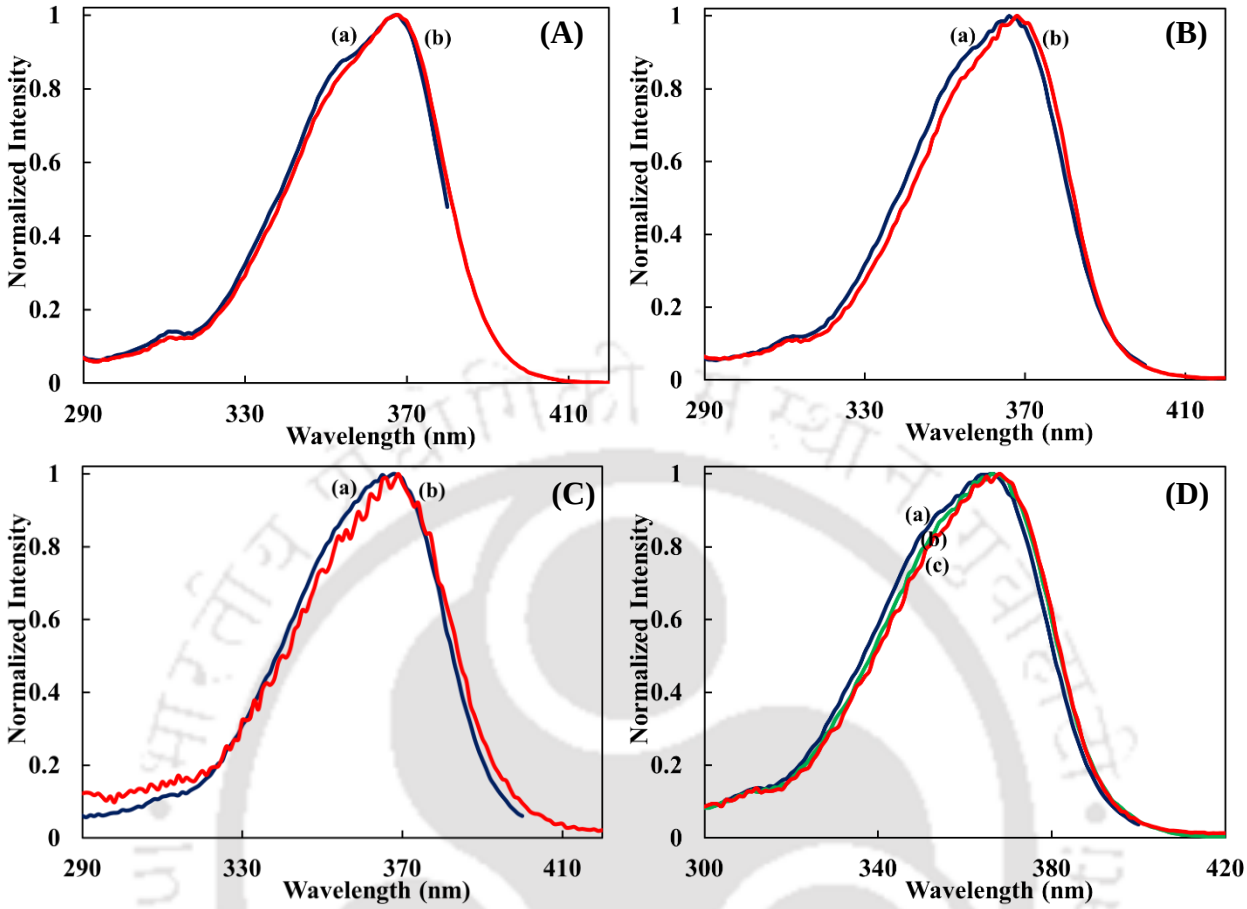

Figure 5.11: Normalized excitation spectra of DEAHPIP-b monitored at (a) shorter wavelength emission maximum and (b) longer wavelength emission maximum in **(A)** 1-propanol, **(B)** butanol, **(C)** methanol and **(D)** in ethanol at (a) λ_{em} = 420 nm, (b) λ_{em} = 440 nm, (c) λ_{em} = 560 nm.

The excitation spectra recorded at the shorter and the longer wavelength emission maxima in all these protic solvents including methanol are different **[Figure 5.11]**. Hence, it is clear that both the emissions originate from different ground state species. DEAHPIP-b can exist as two conformers, cis and trans enols **[Scheme 5.1]**. The excitation spectrum is red shifted at longer wavelength than at shorter wavelength. The cis-enol has the intramolecular hydrogen bond. Usually, its excitation spectrum is red shifted compared to that of trans-enol.[165, 230] Therefore, the trans-enol is the ground state precursor for the normal emission (shorter wavelength emission) and cis-enol is the ground state precursor for the tautomer emission (longer wavelength emission) in butanol and propanols as well as for the TICT emission (longer wavelength emission) in methanol. Like in aprotic solvents, the emission of methoxy derivative is single exponential in all these protic solvents **[Table 5.3, Figure 5.12.A]**. The excitation spectra recorded at different emissions overlap with each other. This indicates the presence of single species **[Figure 5.12.B]**.

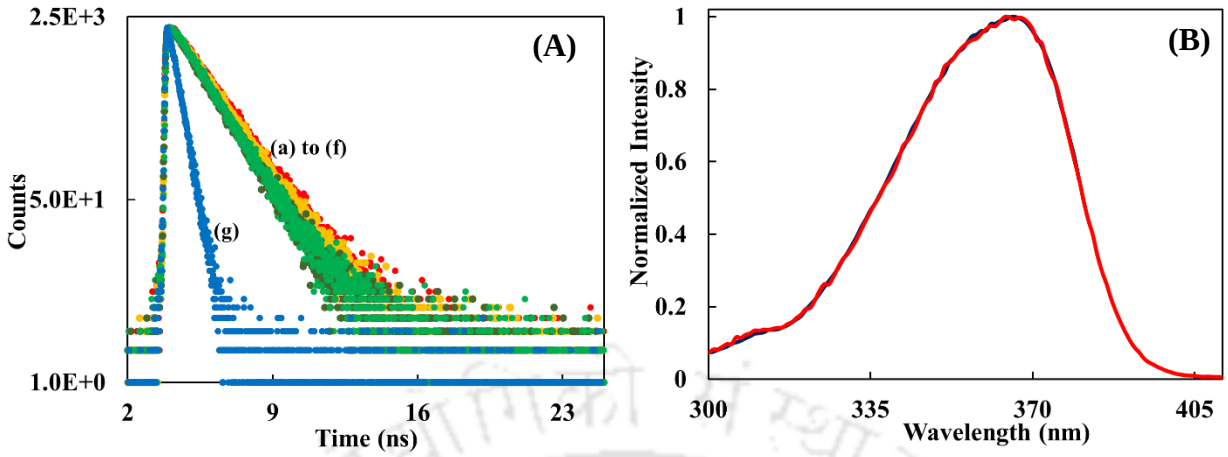

Figure 5.12: (A) The fluorescence decays of DEAMPIP-b at emission maxima in (a) ether, (b) acetonitrile, (c) 2-propanol, (d) 1-propanol, (e) 1-butanol, (f) ethanol and (g) methanol. **(B)** Normalized excitation spectra of DEAMPIP-b in methanol at λ_{em} = 420 nm and 520 nm.

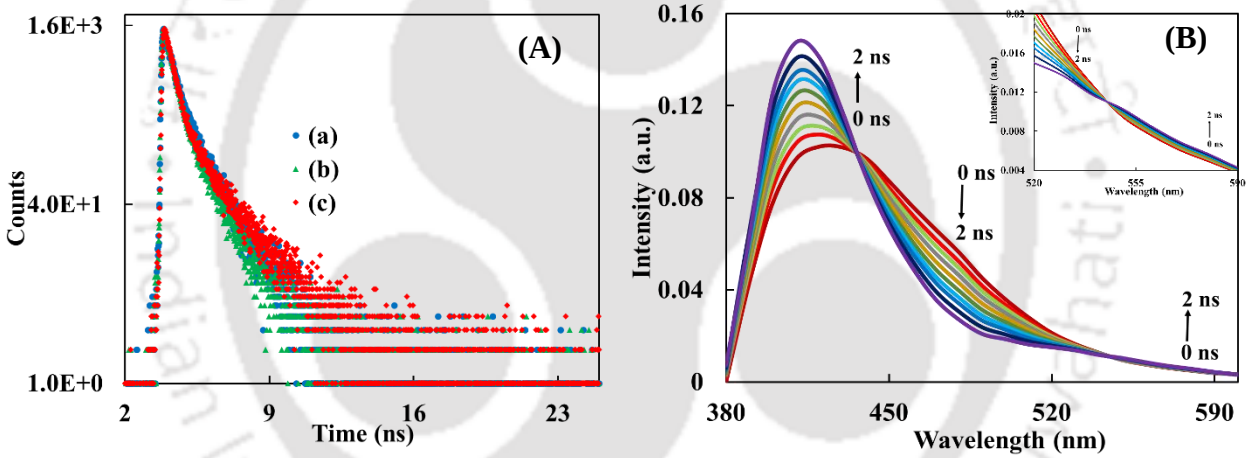

Figure 5.13: (A) The fluorescence decays of DEAHPIP-b in ethanol monitored at (a) 420 nm, (b) 440 nm and (c) 560 nm. **(B)** TRANES obtained at different times 0 ns to 2 ns using λ_{exc} = 375 nm. The inset figure shows expanded spectra from 520 nm to 590 nm.

DEAHPIP-b exhibits triple emission in ethanol **[Figure 5.13.B]**. The emission decay is biexpoential when monitored at 420 nm and 440 nm with lifetime 1.3 ns and 0.3 ns and triexpoential when monitored at 560 nm **[Table 5.2]**. Additional decay of 2.3 ns is observed along with 1.3 ns and 0.3 ns decays. In all other solvents by TRANES, the spectra resolved into two bands with single isoemissive point. In ethanol, three bands are obtained at 420 nm, 440 nm and 560 nm with two isoemissive points at 440 nm and 550 nm **[Table 5.2, Figure 5.13.B]**. The intensity of the 420 nm and 560 nm bands increase and the intensity of the 440 nm decreases with (decay) time. This behavior is also a combination of those observed in methanol and other protic

solvents. Therefore, the 420 nm, 440 nm and 560 nm emissions are due to normal enol emission, the keto tautomer emission and the TICT emission, respectively. The 440 nm emission in ethanol is blue shifted with respect to the tautomer emission in less polar solvents, propanols and butanol **[Table 5.2]**. Similarly, the 560 nm emission is also blue shifted to TICT emission in more polar protic solvent, methanol. This is consistent with the fact that the excited state keto tautomer is less polar than its ground state and the excited TICT state is more polar than the corresponding ground state. The excitation spectra monitored at different emission again states the presence of different conformers in the ground state **[Figure 5.11.D]**. The excitation spectra recorded at tautomer emission maximum (440 nm) and TICT emission maximum (560 nm) are more close to each other than that of the one that is recorded at normal emission maximum (420 nm). These are also red shifted compared to excitation spectrum recorded at normal band emission maximum. As shown earlier, the excitation spectrum of the cis-enol is red shifted compare to that trans-enol. This indicates that trans-enol is ground state precursor for the normal emission and the cis-enol is the ground state precursor for both tautomer and TICT emissions. When the solvent is less polar and less protic, the intramolecular proton transfer dominates over the intermolecular proton transfer, then the excited cis-enol undergoes ESIPT and the molecule exhibits tautomer emission. This is the case in propanols and butanol. When solvent is more polar and more protic (methanol), the intermolecular proton transfer dominates, then the molecule emits the TICT emission. Since, ethanol is less polar and less protic than methanol but more polar and more protic than propoanols/butanol, the molecule emits from both (keto) tautomer and TICT states. Like in other solvents, in ethanol also the methoxy molecule emits only normal emission.

5.3. Theoretical investigation

To support the experimental findings and to get a better understanding of PT and CT emission in DEAHPIP-b, theoretical calculations were performed in nonpolar solvent ether, in polar aprotic solvent acetonitrile and in polar protic solvents ethanol and methanol. Both cis and trans conformers were optimized in the ground state and the excited state in acetonitrile and ether **[Table 5.4]**. The cis conformer is the stable conformer in the ground state. Theoretically, calculated excitation energy of cis-enol is also red shifted than that of trans-enol. Since the ‘OH’ group is acidic and azole nitrogen is basic, intramolecular hydrogen bond exists between these groups which stabilize the cis-enol more than the trans-enol. In the excited state, the ‘OH’ group becomes

more acidic and azole nitrogen becomes more basic. The excited state optimized geometry of cis-enol also suggests that the O–H bond length increases and N·····H hydrogen bond distance decreases **[Figure 5.14]**. This suggests the strengthening of intramolecular hydrogen bond in the excited state which results in ESIPT. The keto structure was also optimized in the excited state and the emission energy was also obtained. The emission energy of keto tautomer in ether and acetonitrile obtained theoretically (2.58 eV, 2.74 eV, respectively) are in good agreement with the experimental result (2.58 eV, 2.64 eV, respectively) **[Table 5.4]**. The methoxy derivative was also optimized in the ground and excited states **[Table 5.5]**. The transition energies obtained theoretically match the experimental values **[Table 5.5].**

Table 5.4: The relative energy and transition energies (in eV), the dihedral angle between the imidazopyridine ring and phenyl ring (θ), the dihedral angle between the phenyl ring and the diethylamino group (φ) of cis-enol and trans-enol of DEAHPIP-b in ether and acetonitrile.

	Ether		Acetonitrile	
	cis	trans	cis	trans
Enol				
Relative energy	0	0.23	0	0.20
θ^1	0.12 (0.06)	0.33 (0.08)	0.69 (0.28)	0.54 (0.17)
φ^1	3.37 (1.8)	3.59 (0.73)	3.94 (1.1)	3.88 (1.05)
Excitation energy[2]	3.45 (3.40)	3.55 (3.42)	3.43 (3.39)	3.49 (3.40)
Emission energy[2]	3.16	3.18 (3.18)	3.05	3.04 (3.02)
Keto				
Emission energy[2]	2.58 (2.58)		2.74 (2.64)	

[1]The values in parentheses are in the excited state.
[2]The values in parentheses are the experimental values.

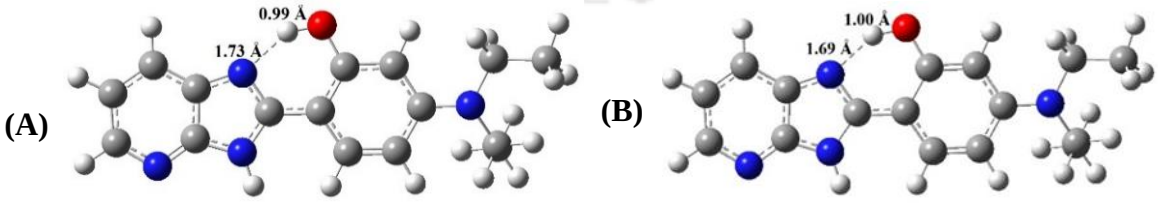

Figure 5.14: The optimized geometries of cis conformer in **(A)** ground state and **(B)** excited state.

Table 5.5: The dihedral angle between the imidazopyridine ring and phenyl ring (θ), the dihedral angle between the phenyl ring and the diethylamino group (φ), transition energies (in eV) of DEAMPIP-b in ether and acetonitrile.

	Ether	Acetonitrile
θ[1]	0.71 (0.15)	0.87 (0.39)
φ[1]	3.68 (0.01)	3.89 (0.56)
Excitation energy[2]	3.50 (3.42)	3.45 (3.40)
Emission energy[2]	3.14 (3.15)	3.01 (3.00)

[1]The values in parentheses are in the excited state.
[2]The values in parentheses are the experimental values.

Table 5.6: Relative energy (in eV), the dihedral angle between the imidazopyridine ring and phenyl ring (θ), the dihedral angle between the phenyl ring and the diethylamino group (φ), hydrogen bond lengths (in Å) and excitation energies (in eV) in cis-enol, trans-enol, open-enol conformers of DEAHPIP-b – methanol and ethanol complexes.

	In methanol			In ethanol		
	cis-enol	trans-enol	open-enol	cis-enol	trans-enol	open-enol
relative energy	0	0.14	0.33	0	0.14	0.33
θ	0.6	2.8	34.8	0.04	0.8	33.1
φ	4.0	4.9	4.6	5.2	4.1	4.3
$N_{py}\cdots H_{sol}$	1.99	1.91	1.97	1.98	1.94	2.00
$O_{sol}–H_{sol}$	0.98	0.98	0.98	0.98	0.98	0.98
$O_{sol}\cdots H_{im}$	2.08	2.41	2.13	2.10	2.35	2.10
$N_{im}–H_{im}$	1.02	1.01	1.02	1.01	1.01	1.02
$N_{im}\cdots H_{ph}$	1.69			1.69		
$O_{ph}–H_{ph}$	1.00	0.96	0.96	1.00	0.96	0.96
$O_{ph}–H_{im}$		2.04			2.05	
excitation energy[1]	3.38 (3.35)	3.42 (3.36)	3.46	3.38 (3.36)	3.42 (3.39)	3.47

[1]The values in parentheses are the experimental values.
The bond lengths are defined as follows:
$N_{py}\cdots H_{sol}$ is hydrogen bond distance between pyridyl nitrogen and hydrogen of the solvent. $O_{sol}–H_{sol}$ is bond length of oxygen and hydrogen in solvent molecule. $O_{sol}\cdots H_{im}$ is hydrogen bond distance between oxygen of solvent molecule and imidazole 'NH' proton. $N_{im}–H_{im}$ is bond length of imidazole 'NH'. $N_{im}\cdots H_{ph}$ is the hydrogen bond distance between imidazole nitrogen and phenol hydrogen. $O_{ph}–H_{ph}$ is bond length of phenol 'OH'. $O_{ph}\cdots H_{im}$ is hydrogen bond distance between phenol oxygen and imidazole 'NH' proton. For details refer **Figure 5.15** and **5.16**.

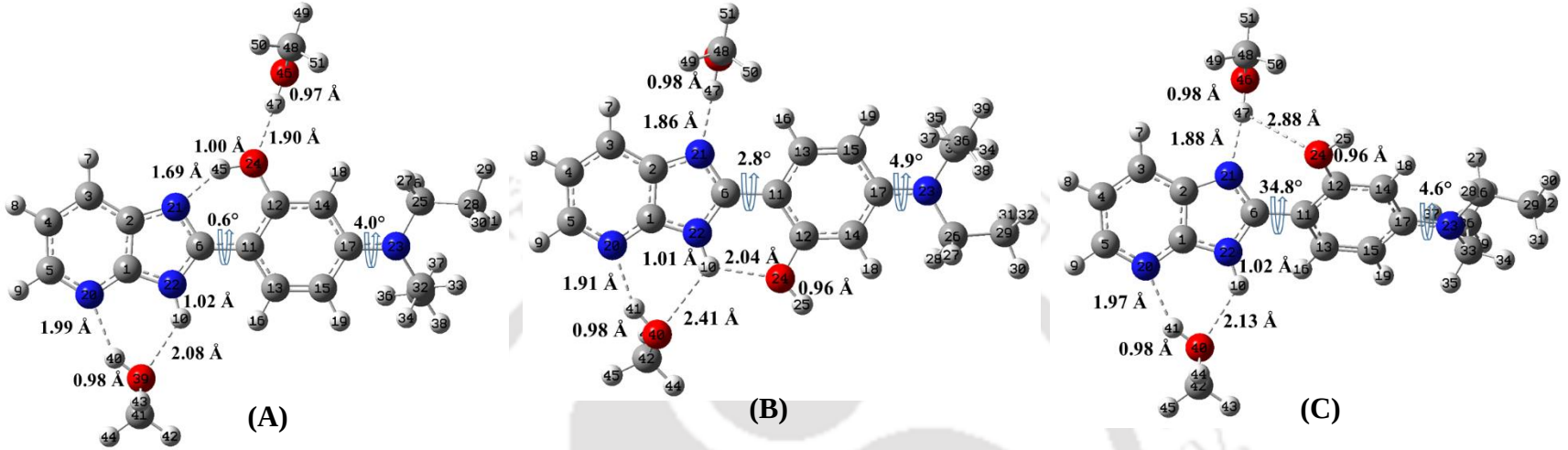

Figure 5.15: The ground state optimized geometries of **(A)** cis-enol, **(B)** trans-enol and **(C)** open-enol conformers of DEAHPIP-b – methanol complexes.

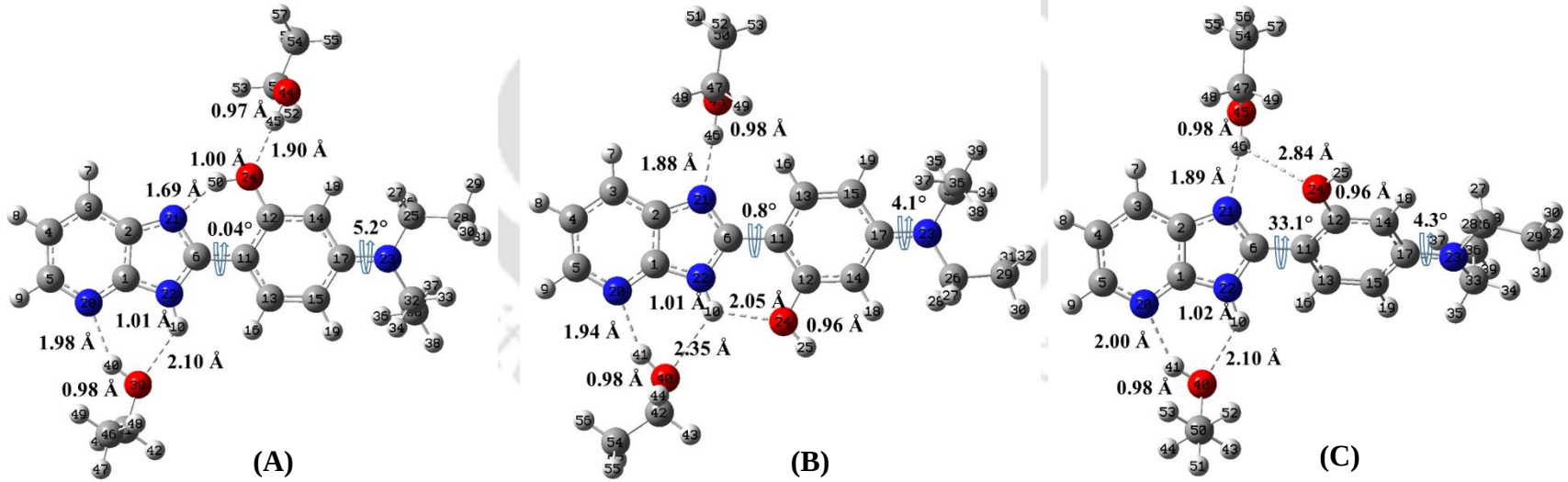

Figure 5.16: The ground state optimized geometries of **(A)** cis-enol, **(B)** trans-enol and **(C)** open-enol conformers of DEAHPIP-b – ethanol complexes.

In methanol, intermolecular hydrogen bond exists between the fluorophore and the solvent molecule. To take into account the intermolecular hydrogen bond, explicit solvent molecules were added and the structure of the complexes were optimized. The cis-enol hydrogen bonded complex is more stable than the trans-enol hydrogen bonded complex **[Table 5.6]**. Though, open enol **[Figure 5.15** and **5.16]** is also possible, but energetically it is not favored and its relative population is negligible. This supports the experimental observation of two conformers, cis and trans enols. In DMAPIP-b, the intermolecular proton transfer from imidazole 'NH' group to pyridyl nitrogen induces the TICT.[123] Like, DMAPIP-b, protic environment is a necessary condition for DEAHPIP-b also to emit TICT emission. Therefore, in DEAHPIP-b also the intermolecular proton transfer from imidazole 'NH' proton to pyridyl nitrogen might have induced TICT emission. TICT state is formed by the twisting of the charge donor with respect to other part of the molecule.[231] In DMAPIPs, the intermolecular proton transfer from the imidazole 'NH' group to the pyridyl nitrogen is accompanying the charge transfer and twisting of donor group to form a TICT state. DEAHPIP-b has diethylamino group as charge donor instead of dimethylamino group. Kim et al. stated that the planarization of the acceptor with phenyl ring increase the charge flow from the phenyl ring to the acceptor, thereby enhances the TICT emission in diethylaminobenzoicacid.[232,233] The geometry of the intermolecular proton transfer induced TICT was also optimized with twisting of diethylamino group in the excited state and the transition energy was calculated **[Figure 5.17]**. The TICT emission energy thus obtained matches with the experimental value. This supports the mechanism.

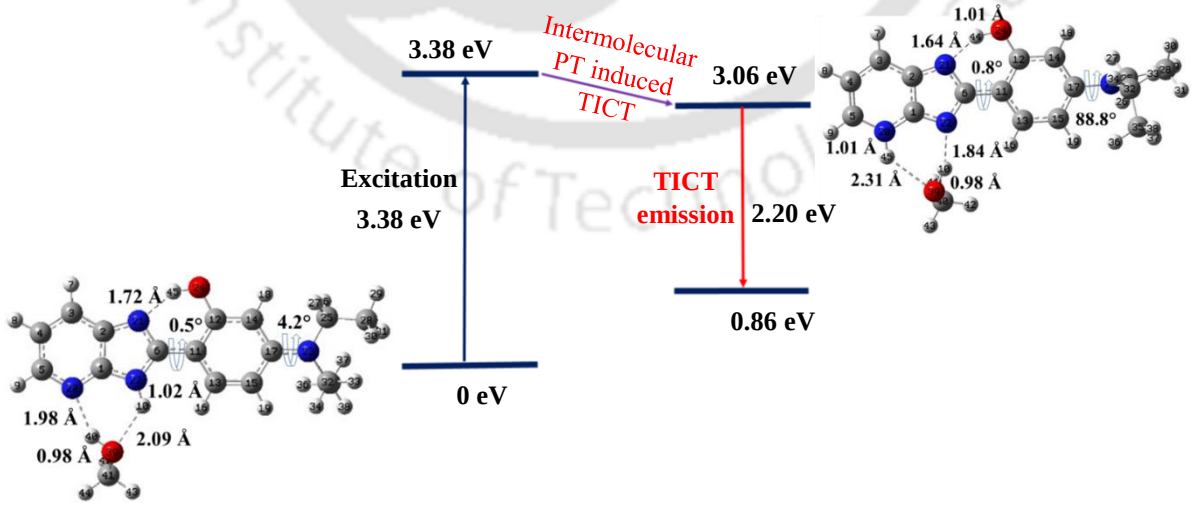

Figure 5.17: Formation of intermolecular proton transfer triggered TICT state in cis-enol DEAHPIP-b – methanol complex in methanol.

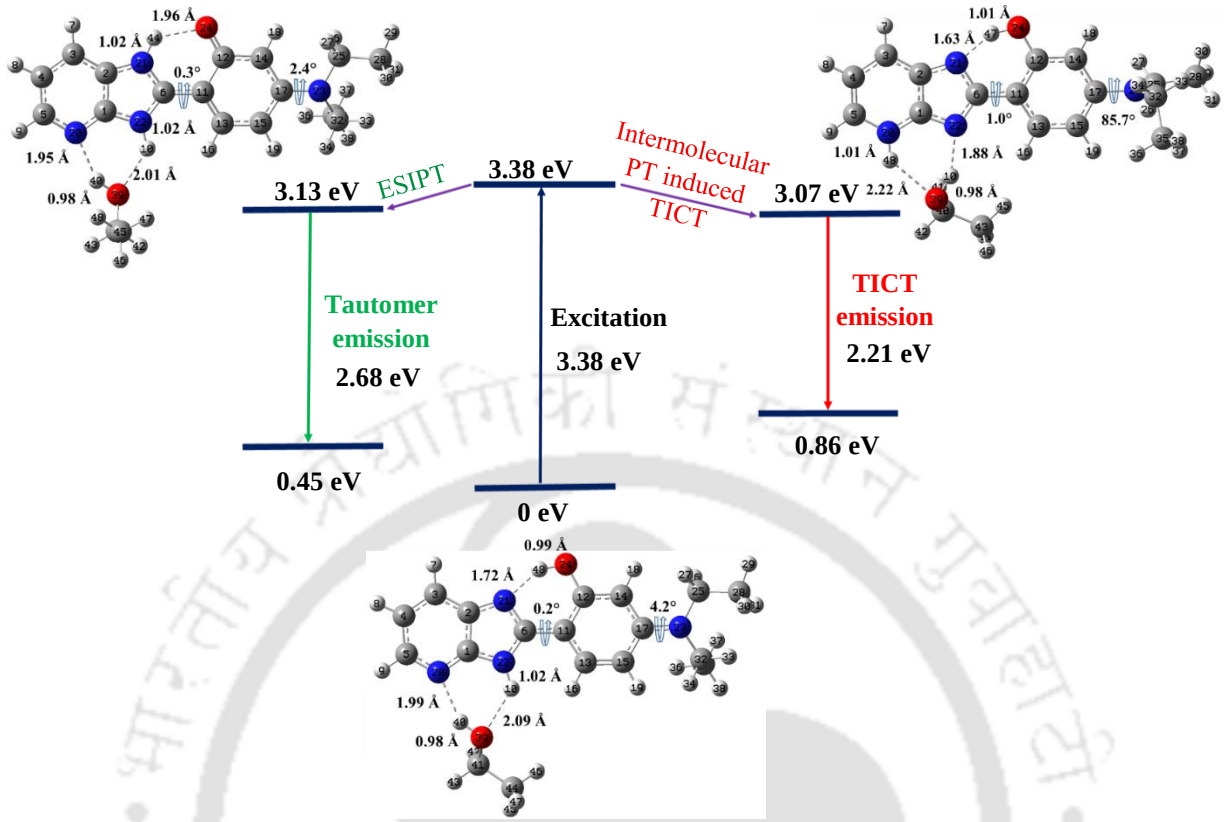

Figure 5.18: Formation of keto excited state and intermolecular proton transfer triggered TICT state in cis-enol DEAHPIP-b – ethanol complex in ethanol.

The theoretical calculations were performed for cis-enol ethanol complex in ethanol **[Table 5.6]**. Likewise, in ethanol also the longer wavelength emission occurs due to twisting of diethyl amino group in the cis conformer and the transition energies obtained theoretically (2.21 eV) as well experimentally (2.21 eV) are matching with each other. Experimentally it is shown, three emissions are feasible in ethanol. Theoretically, the transition energy calculated for keto is 2.68 eV which is close to one of the experimental emission energy (2.81 eV). Thus, the emission at 440 nm in ethanol assigned to the keto emission formed by ESIPT process is further substantiated. In ethanol also the excitation spectra suggest the presence of two ground state conformers **[Figure 5.11.D]**. The transition energy of the optimized geometry of the trans conformer (3.02 eV) is close to the shorter wavelength emission (2.95 eV). This supports the assignment of shorter wavelength emission to the normal emission. As ethanol, has relatively weak hydrogen bonding ability compared to methanol, the intramolecular proton transfer competes with the intermolecular proton transfer **[Figure 5.18]**. ESIPT of cis-enol results in keto form which emits the tautomer emission and the intermolecular proton transfer results in twisting of diethylamino group which results in

TICT emission. Excellent agreement between the theoretically predicted emission energies with the experimental emission energies substantiates the conclusion.

Unlike, the cis-enol, the trans-enol does not undergo ESIPT due to a lack of intramolecular hydrogen bond. But, the absence of TICT emission from trans-enol is surprising. Therefore, to understand the absence of TICT from trans enol, the solvated complex of trans enol was optimized with two molecules of alcohol (methanol/ethanol). One of the solvent molecules forms hydrogen bond with azole nitrogen and other forms hydrogen bond with pyridyl nitrogen and azole 'NH' group, like earlier as in cis-enol. The optimized structures are shown in **Figure 5.19** and **Figure 5.20**. In cis-enol methanol complex, the hydrogen bond length between the azole 'NH' hydrogen and methanol oxygen is 2.08 Å **[Table 5.6]**. Whereas, in trans-enol methanol complex that intermolecular hydrogen bond is weaker and the distance between the azole 'NH' hydrogen and the methanol oxygen increases to 2.41 Å **[Table 5.6]**. In trans-enol ethanol complex also that intermolecular hydrogen bond is weaker compared to in cis-enol ethanol complex **[Table 5.6].** As a consequence, the transfer of 'NH' proton to solvent is not feasible. Therefore, trans enol does not exhibit TICT emission in methanol or ethanol but gives only normal emission.

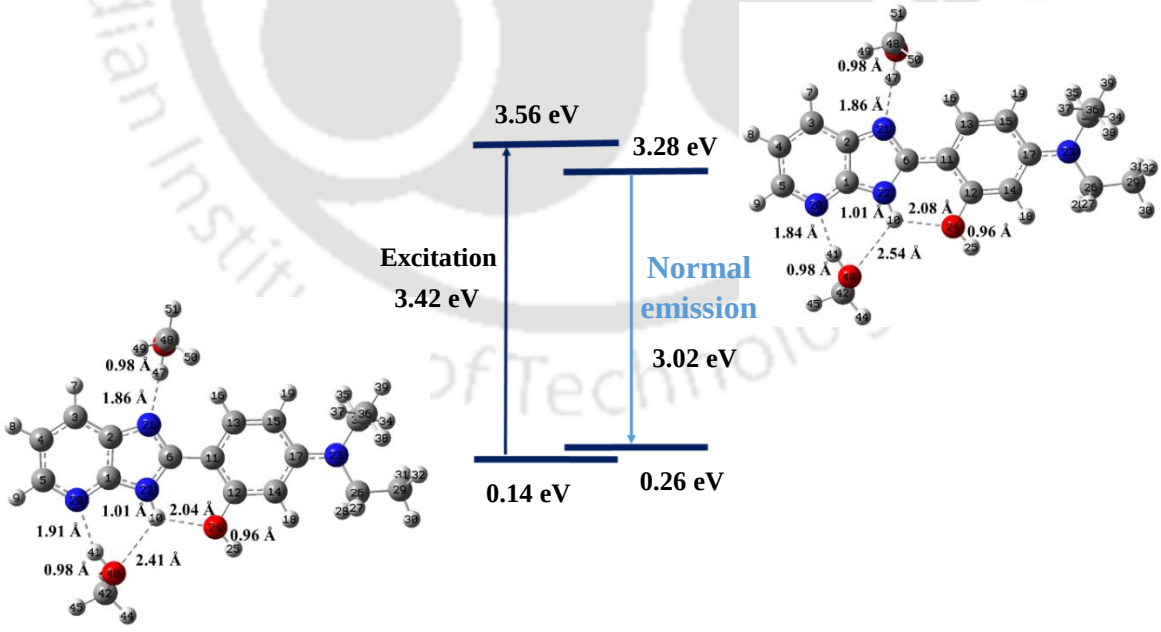

Figure 5.19: Normal emission from trans-enol DEAHPIP-b in methanol.

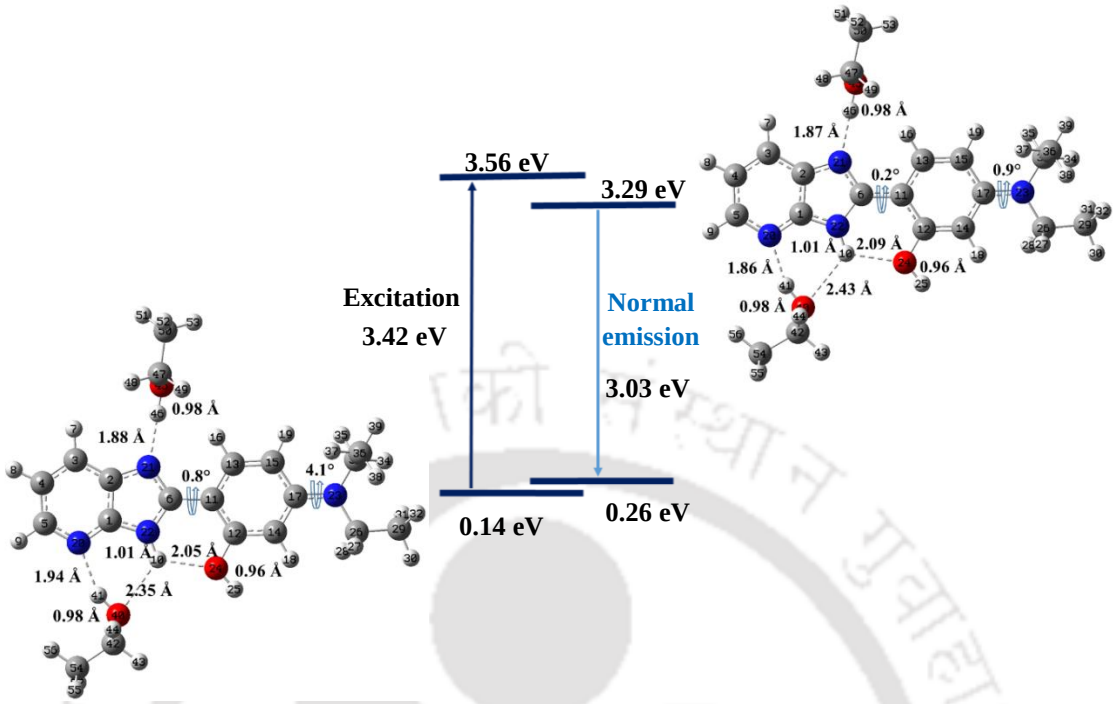

Figure 5.20: Normal emission from trans-enol DEAHPIP-b in ethanol.

5.4. Conclusion

In this chapter, control over excited state PT and CT processes are obtained by changing the solvent system. Dual fluorescence is observed in DEAHPIP-b in nonpolar and polar aprotic solvents. The excited trans enol emits the normal emission at a shorter wavelength, and the cis enol undergoes intramolecular proton transfer yielding the keto tautomer emission at a longer wavelength. In the polar protic solvents, butanol, 2-propanol and 1-propanol, dual emission is also observed from the normal excited state and keto excited state. In all these solvents, the ESIPT process suppresses the TICT process and the solvent polarity affects the tautomer to normal emission intensity ratio. In ethanol, a relatively more polar solvent, ESIPT competes with TICT and triple emission is observed from the trans-enol excited state, keto excited state and the TICT state. In much more polar and protic solvent, methanol having strong hydrogen-bonding ability, intermolecular proton transfer predominates and the TICT process suppresses the ESIPT. Only TICT emission is observed at a longer wavelength along with the normal emission. Intermolecular proton transfer induced the ICT which accompanies the twisting of diethylamino group to produce the TICT state. The reaction coordinate can be tuned by choosing an appropriate solvent. Unlike DEAHPIP-b, DEAMPIP-b exhibits only normal emission in all the solvents.

भारतीय प्रौद्योगिकी संस्थान गुवाहाटी
Indian Institute of Technology Guwahati

Chapter 6

Modulation of silver nanoparticle impelled TICT in 2-(4′-diethylamino-2′-hydroxyphenyl)-1H-imidazo-[4,5-b] pyridine

6.0. Introduction

In the previous chapter, it was shown that complexation with methanol changes the reaction coordinate of DEAHPIP-b from ESIPT to TICT. In chapter 4, it is found that silver particle breaks the complex formed between bis-HPTA and DMF and restores the ESIPT path altered by DMF. Therefore, silver nanoparticle may also modulate the reaction path of DEAHPIP-b. In this chapter, the effect of silver nanoparticle on DEAHPIP-b is demonstrated. It is reported that addition of stabilizing agents like surfactants, tunes the surface properties of metal nanoparticles by eluding agglomeration of nanoparticles.[234-236] Also it has been reported that ionic surfactants have greater encapsulation ability over nonionic surfactants.[237-239] Hence, the effects of cationic CTAB, anionic SDS and nonionic TX-100 surfactant on nanoparticle DEAHPIP-b complex were investigated. The photophysics of DEAHPIP-b were also investigated under same environments to understand the effect of surfactants.

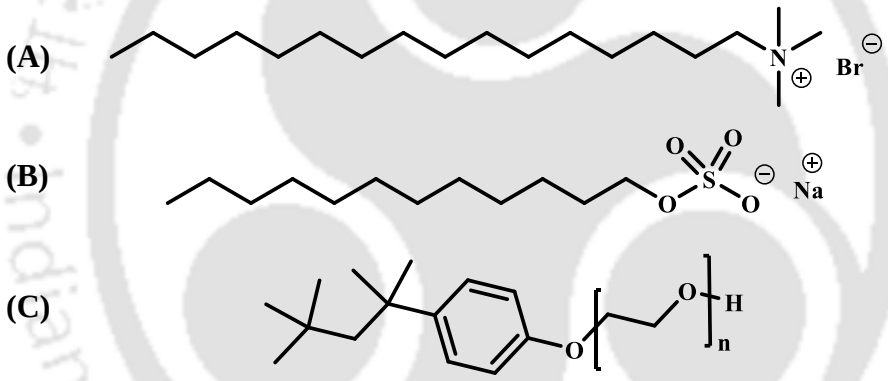

Chart 6.1: Structure of **(A)** CTAB, **(B)** SDS and **(C)** TX-100.

6.1. Silver nanoparticle triggered TICT

Like in other solvents, the longer wavelength absorption band of DEAHPIP-b has vibrational structure at 353 nm and 370 nm in DMF **[Figure 6.1.A].** For initial addition of silver nanoparticle up to 0.04 mM, the absorbance of fluorophore decreases. For more addition, the spectra become structure less and red shifted **[Figure 6.1.A]**. The characteristic SPR band of silver nanoparticle appears at ~ 450 nm. DEAHPIP-b emits dual emission at 406 nm and 460 nm in DMF **[Figure 6.1.B]**. The fluorophore exhibits ESIPT process in aprotic and some protic solvents **[Chapter 5]**. The emission at 406 nm is close to normal emission and the emission at 460 nm is close to keto tautomer emission. The fluorescence decays monitored at both the emission are biexponential. The amplitude of the shorter lifetime increases and that of the longer lifetime

decreases when monitoring wavelength changes from 406 nm to 460 nm **[Table 6.1]**. This shows that the longer wavelength emission has shorter lifetime than shorter wavelength emission. The shorter and the longer fluorescence decays are also close to those of tautomer and normal emissions, respectively **[Table 5.1]**. Hence, it can be concluded that DEAHPIP-b undergoes ESIPT in DMF to exhibit dual emission.

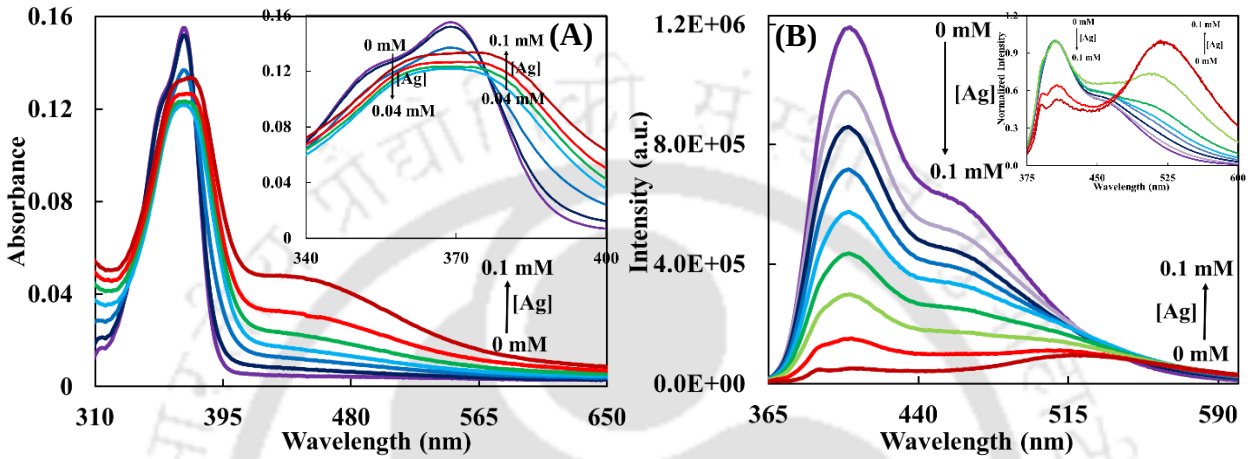

Figure 6.1: (A) Absorption spectra (the inset shows expanded region from 340 nm to 400 nm) and **(B)** emission spectra (the inset shows normalized emission spectra) of DEAHPIP-b at different concentrations of silver nanoparticle (0 to 0.1 mM) in DMF, λ_{exc} = 350 nm.

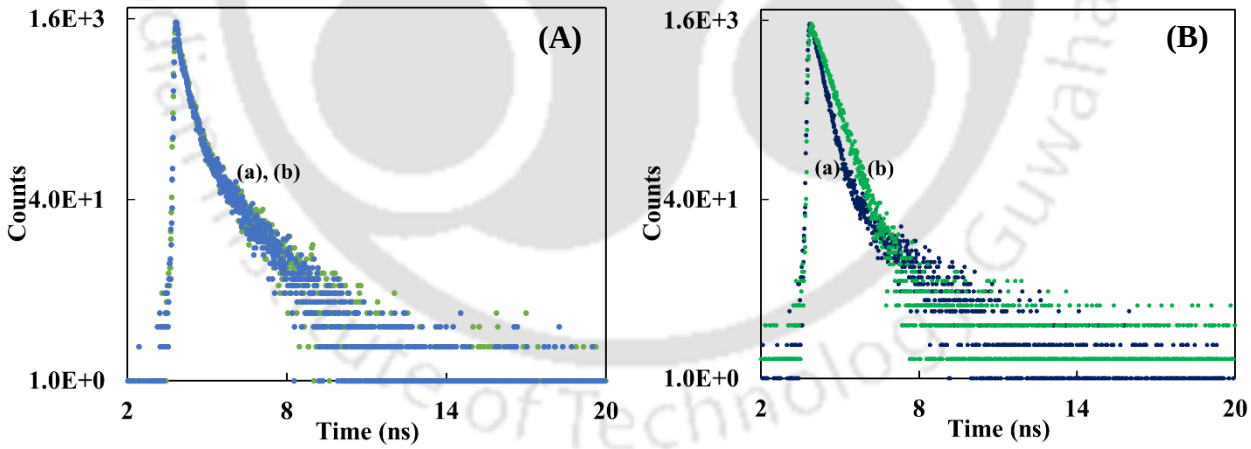

Figure 6.2: The fluorescence decays of DEAHPIP-b in (a) absence and (b) presence of nanoparticles at **(A)** shorter wavelength emission maximum and **(B)** longer wavelength emission maximum in DMF, λ_{exc} = 375 nm.

For initial addition of silver nanoparticles, the emission intensity of both bands of DEAHPIP-b decrease **[Figure 6.1.B]**. With further addition of the nanoparticle, along with 406 nm and 460 nm bands, a hump appears around ~ 500 nm. At 0.1 mM silver concentration, a clear band appears at 530 nm and becomes the intense band than other bands **[Figure 6.1.B]**. Unlike in

the absence of silver nanoparticles, the decay recorded at 530 nm in presence of 0.1 mM silver nanoparticles **[Figure 6.2.B]** turned into a single exponential with a lifetime 0.6 ns **[Table 6.1]**. This lifetime is distinctly different from the decays of normal and tautomer emissions and is close to that of TICT emission in methanol. Thus, the emission at 530 nm in presence of nanoparticle can be assigned to TICT emission.

Table 6.1: Absorption maxima (λ_{max}^{ab}, nm), emission maxima (λ_{max}^{fl}, nm) and fluorescence life time (τ, ns) of DEAHPIP-b in absence and presence of silver nanoparticle in DMF.

	λ_{max}^{ab}	λ_{max}^{fl}		τ	
		Shorter wavelength	Longer wavelength	At shorter wavelength maximum	At longer wavelength maximum
In absence of nanoparticle	353, 370	406	460	0.2 (63) 1.3 (37)	0.3 (82) 1.5 (18)
In presence of nanoparticle	375, 450 (SPR)	406	530	0.2 (63) 1.2 (37)	0.6

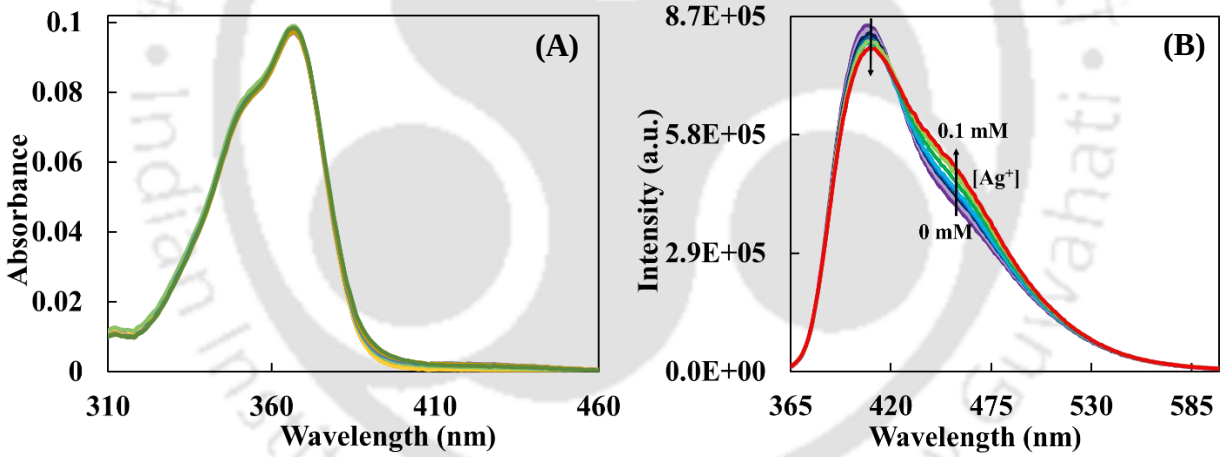

Figure 6.3: (A) Absorption spectra and **(B)** emission spectra of DEAHPIP-b in presence of different concentration of Ag^+ ion (0 to 0.1 mM) in acetonitrile, λ_{exc} = 350 nm.

Since DMF reduces the silver ion to silver, to verify the effect of silver ion, the experiments have been performed in acetonitrile. Unlike silver nanoparticle, the silver ion has little effect on the absorption spectra **[Figure 6.3.A]**. As shown in the last chapter, in acetonitrile DEAHPIP-b exhibits ESIPT. Therefore, the normal and tautomer emissions are observed at 410 nm and 470 nm, respectively **[Figure 6.3.B]**. Addition of silver ion did not cause any shift in the emission spectra. However, the emission intensity decreases at shorter wavelength emission and increases at longer wavelength. But the effect is very little. The absence of red shifted longer wavelength

emission spectrum at the same concentration of ions suggests that the TICT emission is induced by nanoparticles in DMF not by silver ion.

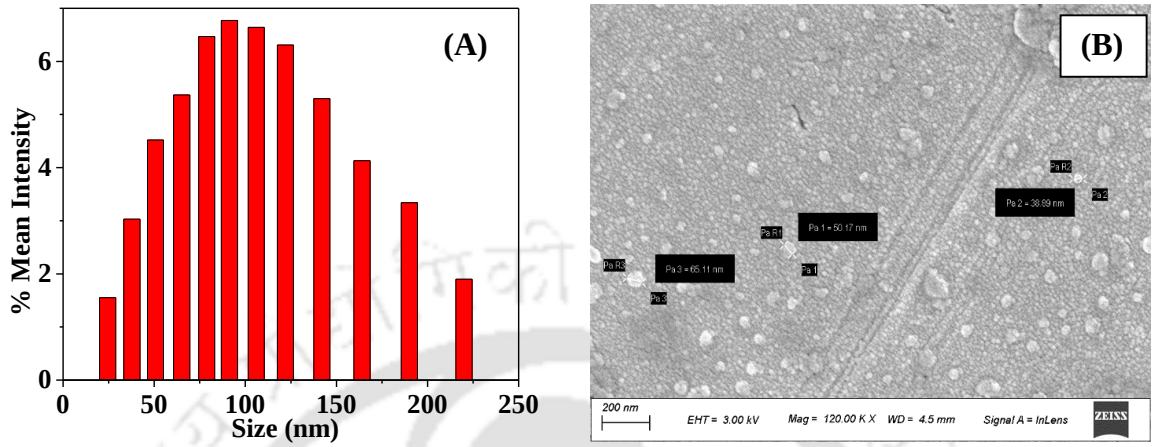

Figure 6.4: (A) DLS plot and **(B)** FESEM image of silver nanoparticles in presence of DEAHPIP-b.

As stated earlier **[Chapter 4]**, the SPR band of silver nanoparticle is usually observed at ~ 430 nm and the size and shape of the particles influences the band position.[166] Further it is shown that in presence of bis-HPTA, silver nanoparticles aggregate to form particles of size 300-1000 nm which were otherwise in size of 100-200 nm in absence of bis-HPTA. The SPR band of silver nanoparticle in presence of DEAHPIP-b is observed at 450 nm. Hence, DLS measurements and FESEM images were attained for silver nanoparticle in presence of DEAHPIP-b. The DLS studies reveal that the average size of the nanoparticles are ~ 60 nm in presence of DEAHPIP-b **[Figure 6.4.A]**. The FESEM image also supports it **[Figure 6.4.B]**. Unlike bis-HPTA, in presence of DEAHPIP-b, the nanoparticles do not agglomerate rather remain as nanoparticle.

It is known that silver nanoparticle behaves as electron acceptor for the nucleophiles and electron donor for the electrophiles.[240-242] The orientation of fluorophores around the nanoparticle surface can control the emission properties of fluorophores. DEAHPIP-b possess electrophilic nitrogens and the interaction may occur through these. The interaction can occur through diethylamino nitrogen on electron donor and nitrogens on the acceptor. The interaction through the nitrogen on the donor decreases the charge transfer and it will produce blue shift. That through the electron acceptor increases the charge transfer and it will produce red shift. The red shift in the absorption spectrum of DEAHPIP-b suggests that the increase in ICT. This shows that the interaction occurs through the ring nitrogen. If it would have occurred through the donor nitrogen,

then the absorption spectrum is expected to shift blue due to decrease in charge transfer. In DEAHPIP-b, nanoparticle also simulated the TICT emission. As shown earlier, the hydrogen bonding with the pyridyl nitrogen is necessary for DEAHPIP-b to emit TICT emission. This shows that DEAHPIP-b is attached to the nanoparticle through the pyridyl nitrogen. It was reported that the ICT emission was quenched and the normal emission was enhanced when trans-2-[4-(dimethylamino)styryl]benzothiazole attached to nanoparticle through its electron donating nitrogen.[243] On the other hand, in DMAPIP-b and DMAPIP-c, the interactions occur through pyridine nitrogen and it induces the TICT emission.[166]

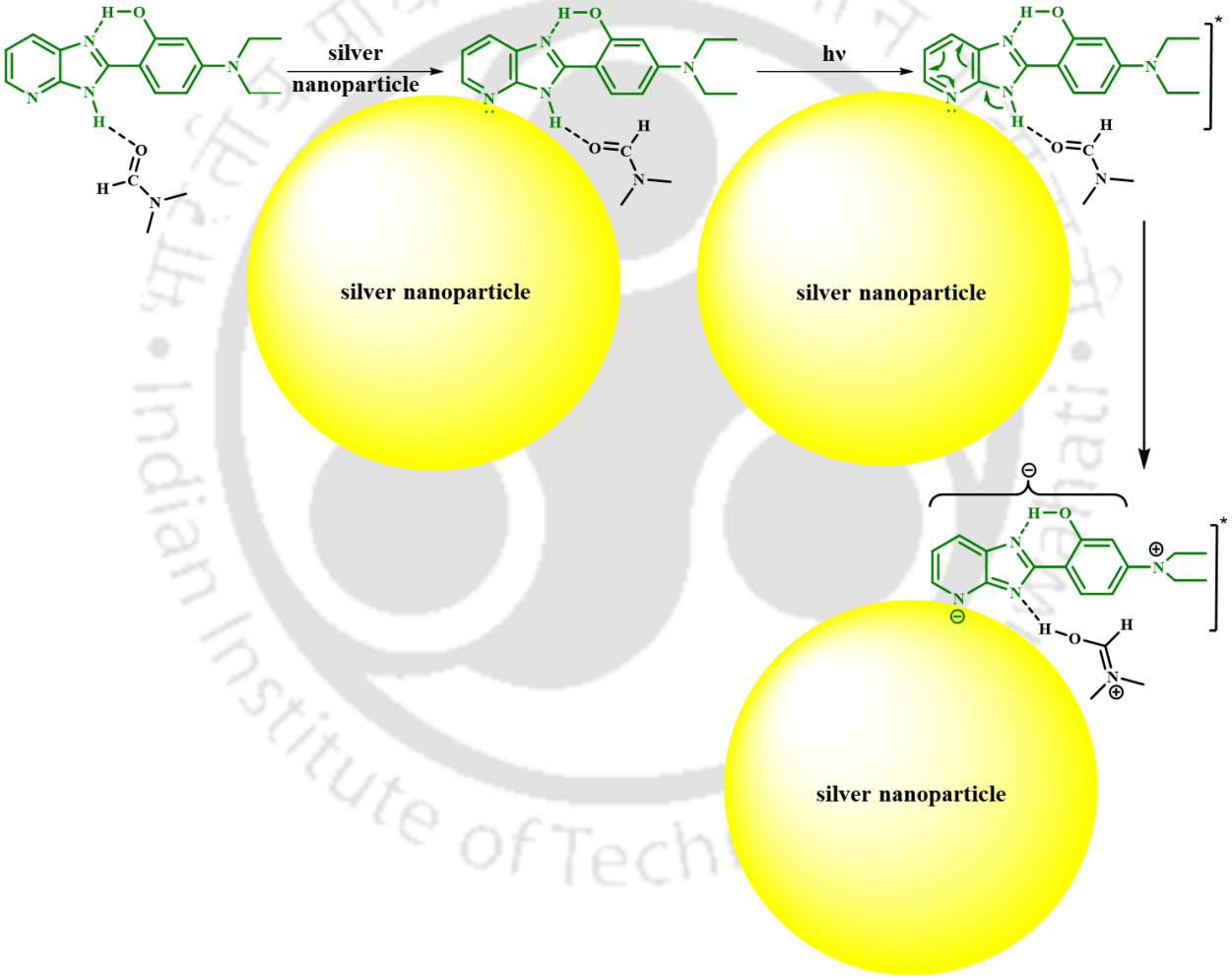

Scheme 6.1: Schematic picture of silver nanoparticle triggered TICT process in DEAHPIP-b.

The tautomer emission of DEAHPIP-b is due to the transfer of intramolecular proton of 'OH' group to imidazole nitrogen in the excited state. On the other hand, the TICT emissions of DEAHPIP-b and DMAPIPs are induced by excited state intermolecular proton transfer from

imidazole nitrogen (NH) to pyridyl nitrogen **[Scheme 1.16]**.[20, 123-125] When DEAHPIP-b is adsorbed on the surface of the nanoparticle, the TICT emission is induced at the expense of ESIPT. As discussed earlier, DEAHPIP-b is attached on the surface of the nanoparticle through pyridyl nitrogen. The interaction of nanoparticle through pyridyl nitrogen withdraw the charge on that nitrogen. This will in turn reduce the charge on the imidazole nitrogens. This will enhance the acidity of the 'NH' proton. Since DMF is a good hydrogen bond acceptor, 'NH' forms hydrogen bond with DMF. As shown earlier **[Chapter 4]**, DMF can accept the proton, upon excitation, the acidity of the 'NH' proton enhances, this lead to intermolecular proton transfer from DEAHPIP-b to DMF. The negative charge thus generated shifts to pyridyl nitrogen by resonance. The charge is accepted by nanoparticle which strengthens the interaction. As nanoparticle, can play the role of proton in protic solvent, hence the charge transfer from diethylamino group to imidazopyridine ring gets enhanced. This can result in TICT emission as shown in **Scheme 6.1**.

6.2. Effect of surfactants

Before evaluating the effect of surfactant on DEAHPIP-b nanoparticle complex, the effect of surfactants in absence of silver nanoparticle on the fluorophore in DMF were experimented. Neither the ionic surfactant, SDS and CTAB nor nonionic surfactant, TX-100 produces any shift in the absorption spectrum or fluorescence spectrum of DEAHPIP-b, only small increase in absorbance and emission intensity are observed **[Figure 6.5, 6.6, 6.7]**. The tautomer to normal emission intensity ratio increase a little in CTAB, but no significant change is observed in the ratio of tautomer to normal emission in SDS and TX-100. The fluorescence lifetimes of both the emissions are less affected by the surfactants **[Figure 6.8** and **Table 6.2]**.

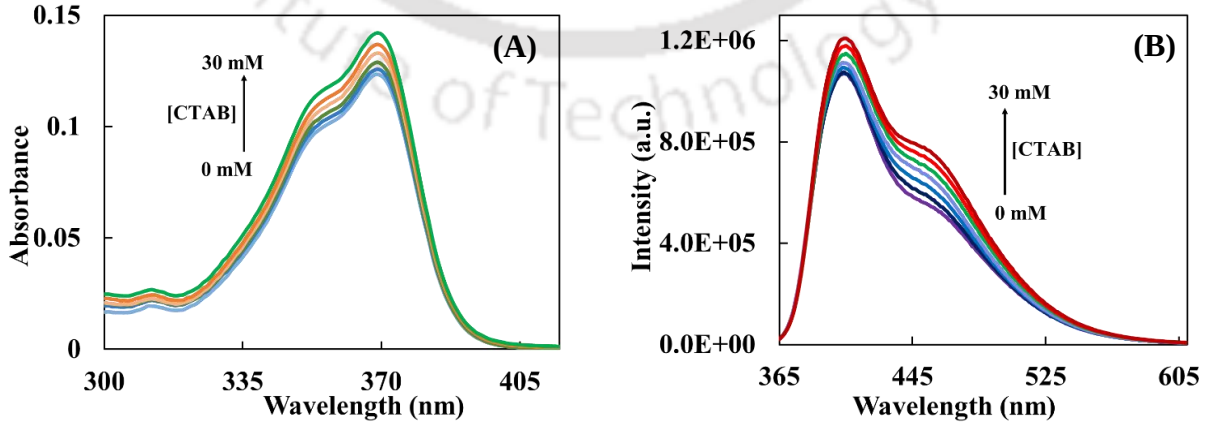

Figure 6.5: (A) Absorption spectra and **(B)** emission spectra of DEAHPIP-b in presence of different concentrations of CTAB (0 to 30 mM), λ_{exc} = 350 nm.

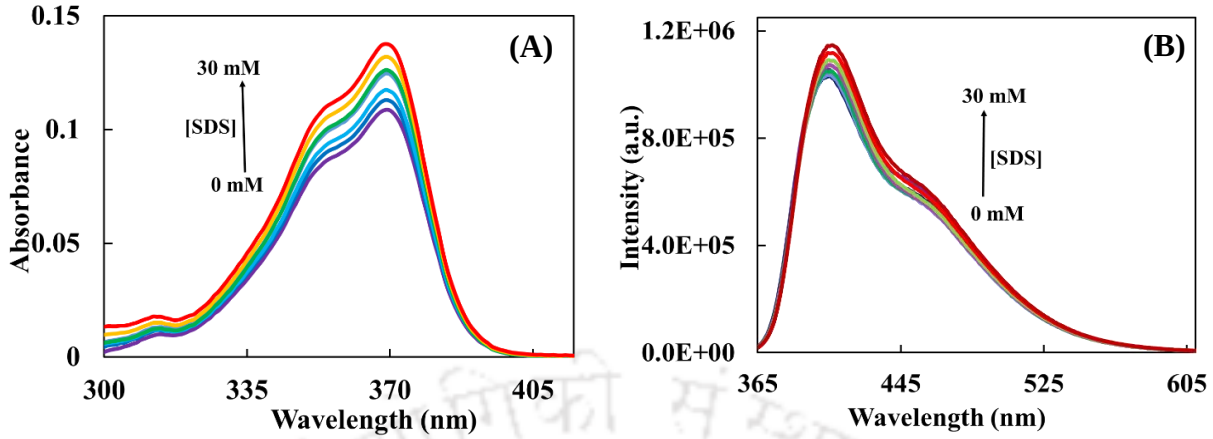

Figure 6.6: (A) Absorption spectra and **(B)** emission spectra of DEAHPIP-b in presence of different concentrations of SDS (0 to 30 mM), λ_{exc} = 350 nm.

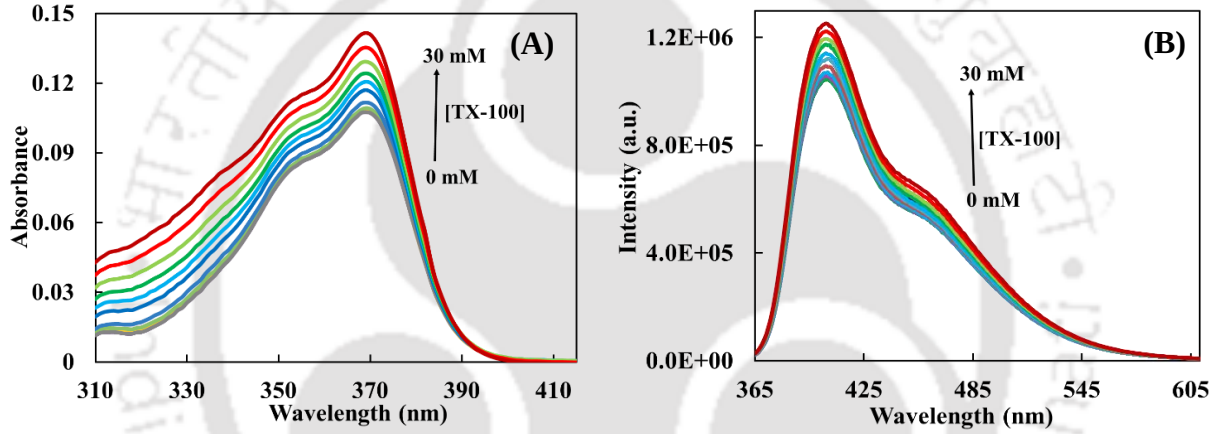

Figure 6.7: (A) Absorption spectra and **(B)** emission spectra of DEAHPIP-b in presence of different concentrations of TX-100 (0 to 30 mM), λ_{exc} = 350 nm.

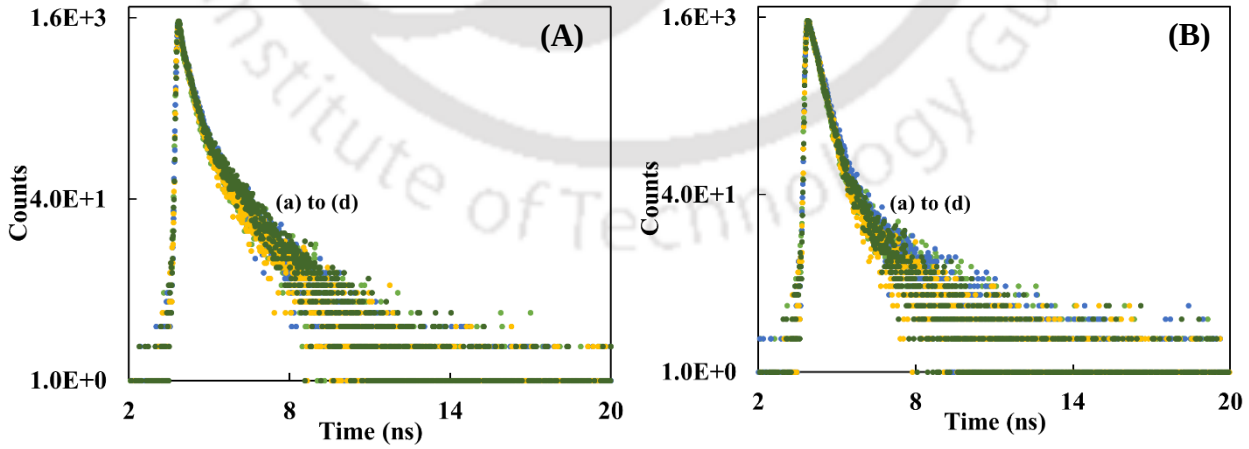

Figure 6.8: The fluorescence decays of DEAHPIP-b (a) in absence of surfactants, (b) in presence of 30 mM CTAB, (c) in presence of 30 mM SDS and (d) in presence of 30 mM TX-100 at **(A)** λ_{em} = 406 nm and **(B)** λ_{em} = 460 nm in DMF, λ_{exc} = 375 nm.

Table 6.2: Absorption maxima (λ_{max}^{ab}, nm), emission maxima (λ_{max}^{fl}, nm) and fluorescence life time (τ, ns) of DEAHPIP-b in absence and presence of surfactants in DMF.

	λ_{max}^{ab}	λ_{max}^{fl}		τ	
		Shorter wavelength	Longer wavelength	At shorter wavelength maximum	At longer wavelength maximum
In absence of surfactants	353, 370	406	460	0.2 (63) 1.3 (37)	0.3 (82) 1.6 (18)
In presence of 30 mM CTAB	353, 370	407	460	0.2 (58) 1.2 (42)	0.4 (91) 1.7 (9)
In presence of 30 mM SDS	354, 370	408	460	0.2 (64) 1.2 (36)	0.3 (85) 1.4 (15)
In presence of 30 mM TX-100	354, 370	406	460	0.2 (58) 1.3 (42)	0.3 (78) 1.1 (22)

6.3. Switching back to ESIPT

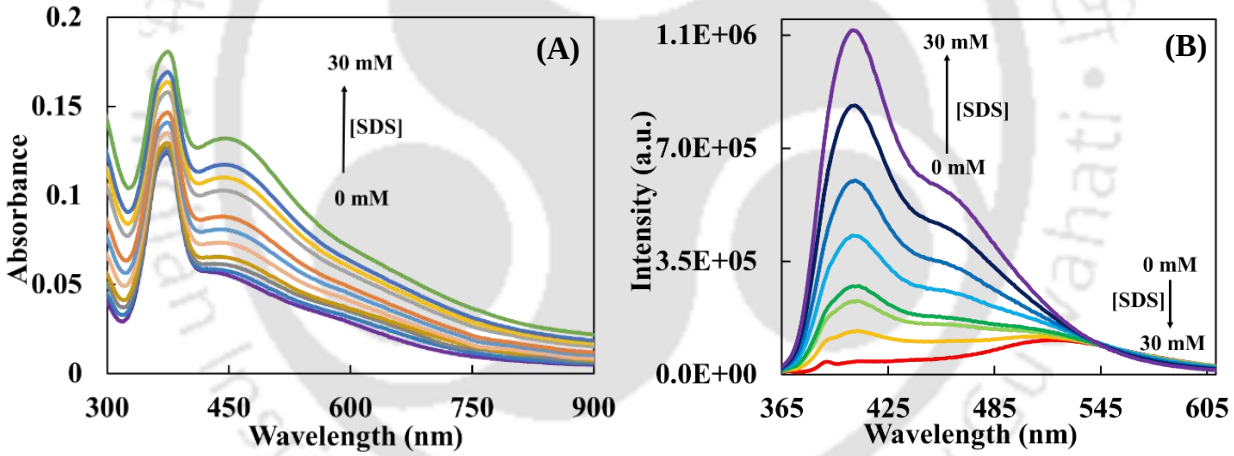

Figure 6.9: Effect of SDS on **(A)** absorption spectra and **(B)** emission spectra of DEAHPIP-b with 0.1 mM silver nanoparticle in DMF, λ_{exc} = 350 nm.

In presence of silver nanoparticle, DEAHPIP-b absorbs at 375 nm and the SPR band is observed at 450 nm. The absorbance of both the bands increase with addition of SDS **[Figure 6.9.A]**. Nanoparticle induced the TICT emission (530 nm emission) of DEAHPIP-b. With addition of SDS, the normal emission at 406 nm gains intensity and the 460 nm tautomer emission intensity slowly increases at the expense of TICT emission **[Figure 6.9.B]**. At higher concentration, only normal and tautomer emission are observed. The emission maxima also match with those of free

fluorophore in DMF **[Table 6.3]**. The fluorescence decays also match with those of normal and tautomer emission of DEAHPIP-b in DMF **[Figure 6.10]**.

Table 6.3: Absorption maxima (λ_{max}^{ab}, nm), emission maxima (λ_{max}^{fl}, nm) and fluorescence life time (τ, ns) of DEAHPIP-b in different environments in DMF.

	λ_{max}^{ab}	λ_{max}^{fl}		τ	
		Shorter wavelength	Longer wavelength	At shorter wavelength maximum	At longer wavelength maximum
in DMF	353, 370	406	460	0.2 (63) 1.3 (37)	0.3 (82) 1.6 (18)
in presence of 0.1 mM nanoparticle and 30 mM SDS	375, 450 (SPR)	407	460	0.2 (61) 1.2 (39)	0.3 (76) 1.5 (24)
in presence of 0.1 mM nanoparticle and 30 mM Tx-100	370, 422 (SPR)	406	460	0.2 (66) 1.2 (34)	0.3 (79) 1.1 (21)
in presence of 0.1 mM nanoparticle and 0.07 mM CTAB	353, 370, 420 (SPR)	406	460	0.2 (67) 1.3 (33)	0.3 (88) 1.4 (12)
in presence of 0.1 mM nanoparticle and 30 mM CTAB	355, 370, no clear SPR	406	480	0.2 (64) 1.1 (36)	0.3 (77) 0.7 (23)

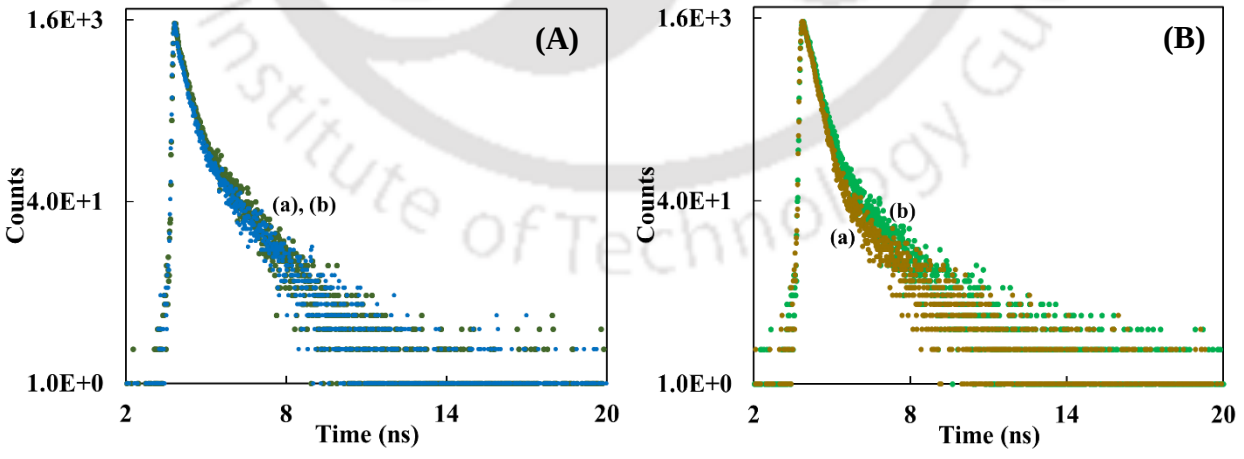

Figure 6.10: The fluorescence decays of DEAHPIP-b in (a) absence and (b) presence of 0.1 mM nanoparticle and 30 mM SDS at **(A)** λ_{em} = 406 nm and **(B)** λ_{em} = 460 nm in DMF, λ_{exc} = 375 nm.

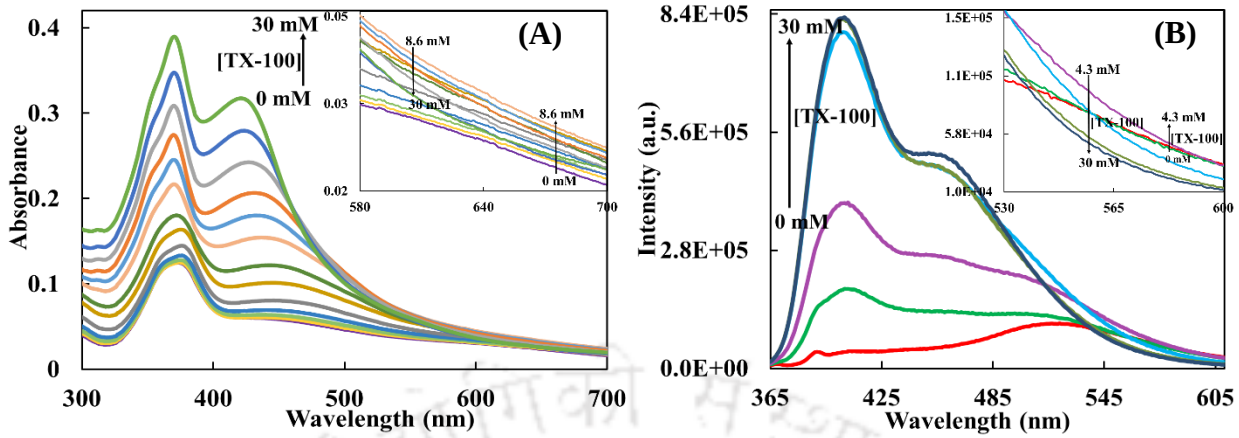

Figure 6.11: Effect of TX-100 on **(A)** absorption spectra and **(B)** emission spectra of DEAHPIP-b with 0.1 mM silver nanoparticle in DMF.

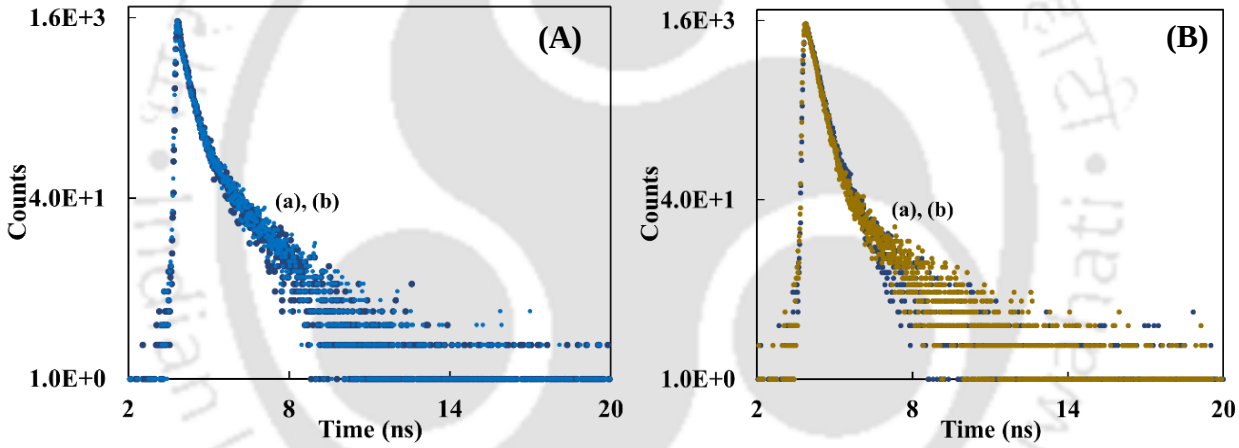

Figure 6.12: The fluorescence decays of DEAHPIP-b in (a) absence and (b) presence of 0.1 mM nanoparticle and 30 mM TX-100 at **(A)** λ_{em} = 406 nm and **(B)** λ_{em} = 460 nm in DMF, λ_{exc} = 375 nm.

When TX-100 was added to nanoparticles-DEAHPIP-b complex, the absorption band of DEAHPIP-b enhanced **[Figure 6.11.A]**. The SPR band of the silver nanoparticles shifted from 450 nm to 420 nm. For initial addition of TX-100, the TICT emission is enhanced and the 460 nm tautomer emission started to appear **[Figure 6.11.B]**. At higher concentration, the TICT emission is completely replaced by the tautomer emission. Same as in SDS, the lifetimes of normal and tautomer emission also agree with those in DMF **[Figure 6.12]**.

These spectral changes show that the surfactants detached the fluorophore from the nanoparticles and release it to the solution. Initially, DEAHPIP-b interacts with nanoparticle and stabilize it. SDS interacts with nanoparticle and replaces the DEAHPIP-b and release it **[Scheme 6.2]**. Therefore, the molecule switch back to ESIPT from TICT. However, at lower concentration of TX-100, unlike SDS, TX-100 does not completely replace DEAHPIP-b. Thus, DEAHPIP-b exhibits both TICT emission and tautomer emission. The enhancement in TICT emission of DEAHPIP at lower concentration of TX-100 is due to the reduction in the nonradiative decay. This suggest that some DEAHPIP-b molecules are interacting with the nanoparticles along with surfactant molecules. The less polar and constrained environments decrease the nonradiative decay of TICT emission. The TICT emissions of DMAPIPs were also enhanced in constrained less polar environments such as CD, proteins, surfactants including TX-100.[244-246] At higher concentrations, TX-100 replaces DEAHPIP-b completely. The broadening of the SPR band of silver nanoparticle were also decreased and shifted hypsochromically compared to that in SDS or without surfactant. This indicates the formation of more uniform distribution of smaller nanoparticle. This will also push DEAHPIP-b out due to competition. The changes are illustrated schematically in **Scheme 6.3**. It was reported that the host α-CD entraps the free heterocyclic acceptor group of ICT molecule trans-2-[4-(dimethylamino)styryl]benzothiazole and detaches the fluorophore from the silver nanoparticle surface.[243]

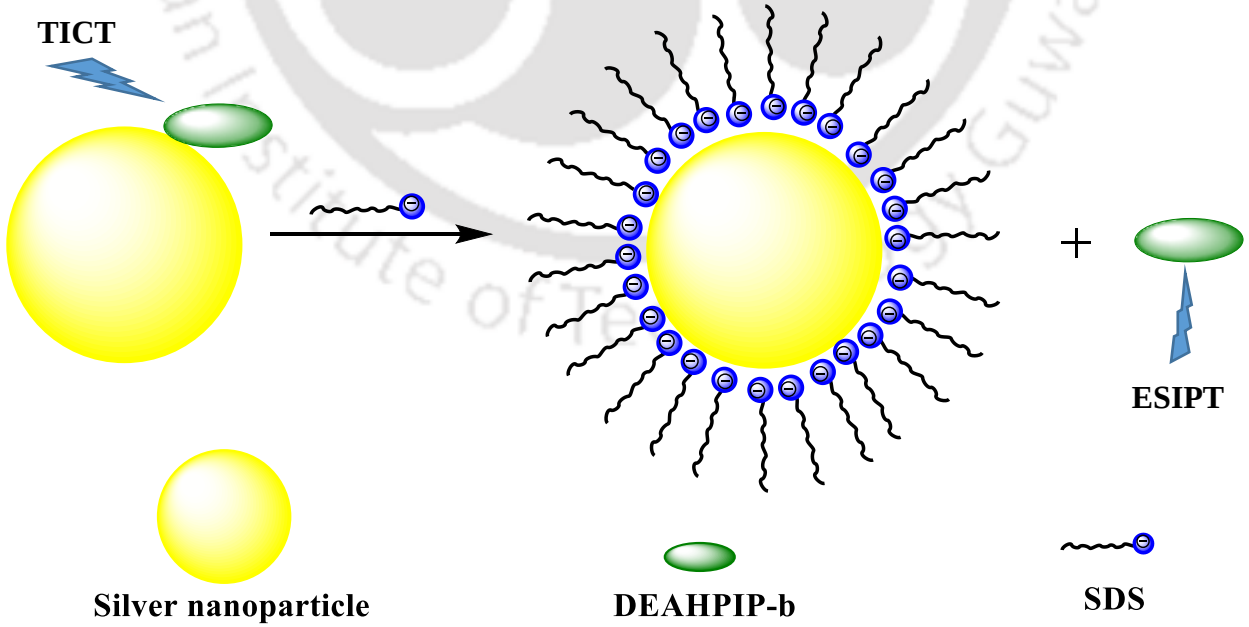

Scheme 6.2: Effect of SDS - Switching back of silver nanoparticle induced TICT to ESIPT.

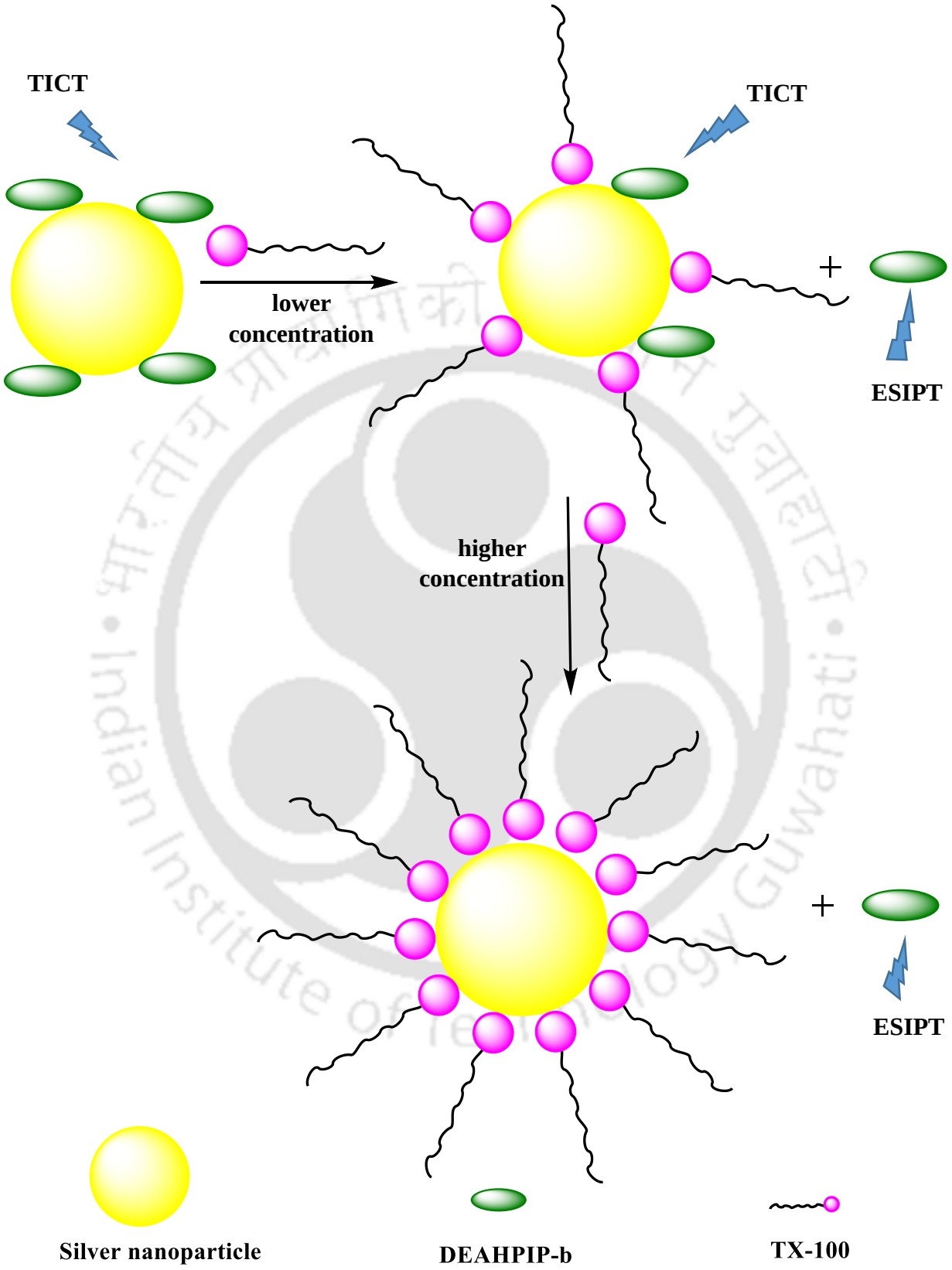

Scheme 6.3: Effect of TX-100 - Modulation of silver nanoparticle triggered TICT to ESIPT.

6.4. Switching back and enhancing ESIPT

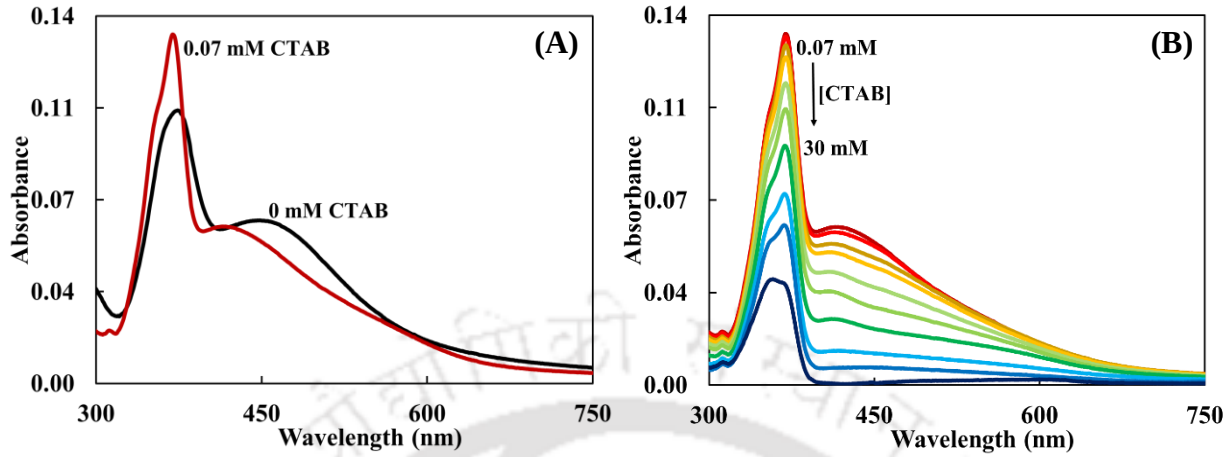

Figure 6.13: Effect of CTAB on absorption spectra of DEAHPIP-b with 0.1 mM silver nanoparticle in DMF.

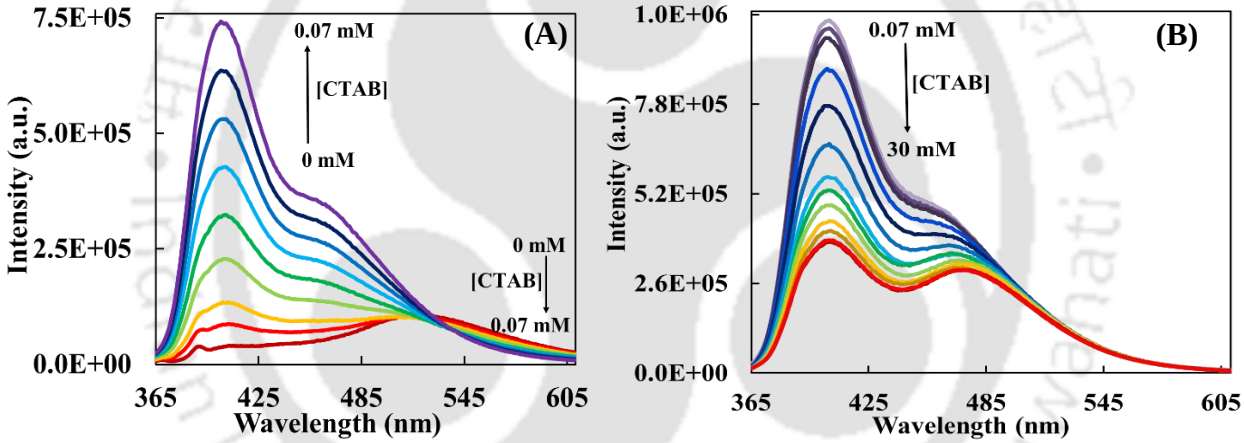

Figure 6.14: Emission spectra of DEAHPIP-b containing 0.1 mM silver nanoparticle in presence of **(A)** 0 to 0.07 mM and **(B)** 0.07 mM to 30 mM CTAB in DMF.

For initial addition of CTAB to DEAHPIP-b-nanoparticle complex, the absorbance of DEAHPIP-b increases with a blue shift and vibrational structure also become prominent **[Figure 6.13.A]**. Upon further increasing the CTAB concentration, the absorbance of DEAHPIP-b decreases and the vibrational structure also become less resolved. DEAHPIP-b in presence of nanoparticle emits at 406 nm and 530 nm due to normal emission and TICT emission, respectively. On increasing the CTAB concentration, the intensity at 406 nm increases and the longer wavelength emission is blue shifted. In presence of 0.07 mM CTAB the emission occurs at 406 nm and 460 nm like the emission observed in free fluorophore in DMF **[Figure 6.14.A]**. On further increasing the CTAB concentration, the emission intensity at 406 nm decreases and bathochromic

shift is observed for longer wavelength emission. Finally, the emission occurs at 480 nm **[Figure 6.14.B]**. In presence of 0.07 mM CTAB, the fluorescence lifetimes are more close to the excited state lifetimes of free fluorophore **[Table 6.3** and **Figure 6.15]**. In presence of 30 mM CTAB, the lifetimes obtained when monitored at shorter wavelength emission maximum are close to the lifetime obtained at shorter wavelength emission in DMF **[Table 6.3]**. When monitored at longer wavelength emission maximum, the short lifetime is the predominant species. The predominant species lifetime is much shorter than normal emission and TICT emission and close to tautomer's lifetime. Therefore, the emission at 480 nm band is assigned to the tautomer emission from the keto species formed by ESIPT.

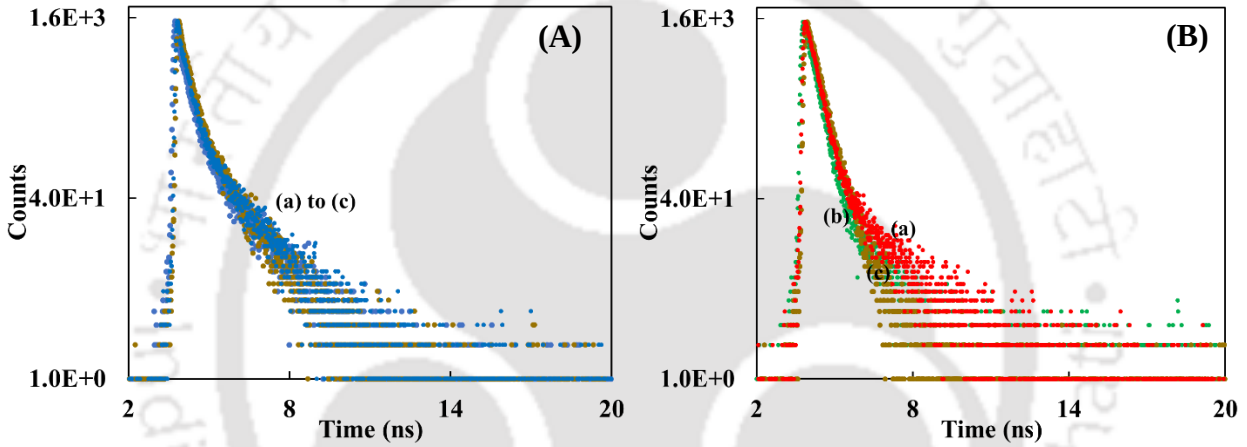

Figure 6.15: The fluorescence decays of DEAHPIP-b in (a) absence, (b) presence of 0.1 mM nanoparticle and 0.07 mM CTAB, (c) presence of 0.1 mM nanoparticle and 30 mM CTAB at **(A)** shorter wavelength emission maximum and **(B)** longer wavelength emission maximum in DMF, λ_{exc} = 375 nm.

Both the absorption and fluorescence spectra suggest that the initial changes are different from the final changes. Upon addition of CTAB up to 0.07 mM, DEAHPIP-b is detached, this led to diminishing of TICT and restoration of ESIPT. For further addition CTAB both the absorption and emission spectra of DEAHPIP-b undergo significant change. This shows that the environment of the fluorophore changed significantly. With the increase in concentration of surfactant, the surfactants aggregate to form molecular aggregates. To confirm the aggregation in DMF, the effect of concentration on the size of aggregates were examined by performing DLS study **[Figure 6.16]**. DLS study predicts that till 0.07 mM CTAB, the size of particles remains close to that of particles in absence of CTAB i.e. ~ 80 nm. Upon further addition of CTAB, the size of the particle in the

solution increases. At 1 mM CTAB, the size becomes ~ 160 nm and at 30 mM CTAB that of ~ 500 nm. Increase in size suggest the aggregation of surfactant molecules. The significant change in tautomer emission maximum suggest the fluorophore is not free, but present inside the aggregates. The red shift in the tautomer emission also supports the fact that the molecule is present in a relative less polar environment than in DMF. However, CTAB in the absence of silver has little effect on the emission spectrum of DEAHPIP-b. Therefore, it may be concluded that in presence of silver nanoparticle, an aggregate of silver nanoparticle-surfactant is formed and DEAHPIP-b is present inside the aggregate. This not only restored the ESIPT, but also enhanced the ESIPT. The absence of SPR band suggest that silver is not present as nanoparticle in this complex.

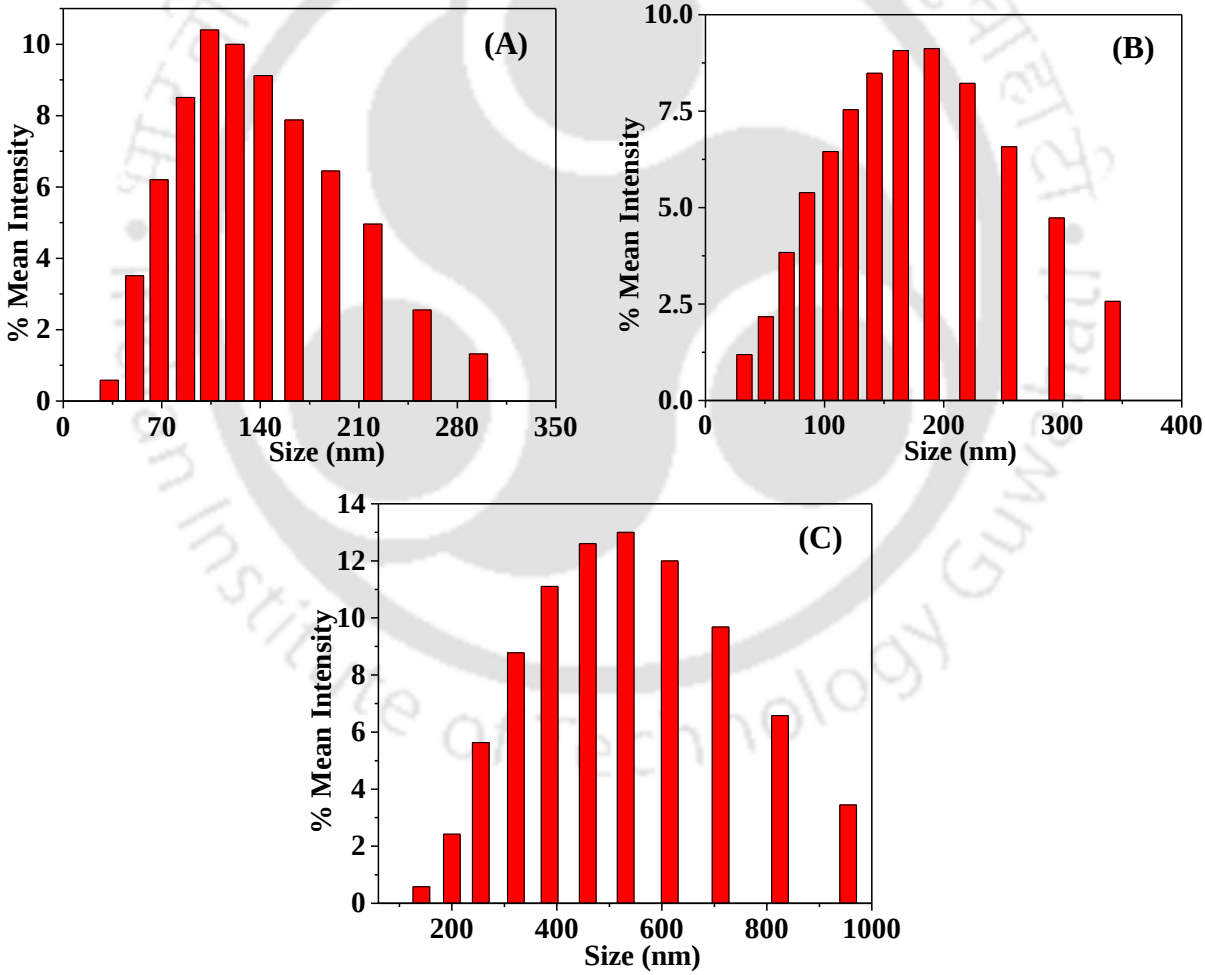

Figure 6.16: DLS plot of DEAHPIP-b with 0.1 mM nanoparticle in presence of **(A)** 0.07 mM, **(B)** 1 mM CTAB and **(C)** 30 mM CTAB.

6.5. Conclusion

DEAHPIP-b exhibits normal and tautomer emission in DMF. Silver nanoparticles induce the TICT emission. In the absence of silver nanoparticle, the surfactants have negligible effect on the fluorophores. However, the photophysics of the fluorophore as well as the morphologies of silver nanoparticles are different at different type of surfactants. The ESIPT can be restored by the addition of either ionic or non-ionic surfactant. The anionic surfactant SDS simply restores the ESIPT in DEAHPIP-b by detaching the fluorophore and the surfactant. Nonionic TX-100 at lower concentration did not completely replace the molecules. The stabilization of nanoparticle along with DEAHPIP-b led to enhancement of TICT emission. However, at higher concentration, it completely free the fluorophore to DMF. The lower concentration of cationic surfactant CTAB restores the ESIPT process in DEAHPIP-b by altering the nanoparticle triggered TICT emission. At higher CTAB concentration, the fluorophore present insides the nanoparticle-surfactant aggregates and exhibits enhanced ESIPT.

Chapter 7

Effect of pH on 2-(4′-diethylamino-2′-hydroxyphenyl)-1H-imidazo-[4,5-b] pyridine and its methoxy analogous

7.0. Introduction

The prototropic study is always an attractive area of research. The nature of the substituent and its' position in the molecule strongly affects the spectral characteristics. For example, both benzimidazole and indazole molecules have basic center, =N- atom. But the equilibrium constant of benzimidazole is 5.53 and for indazole is 1.24.[247-249] Molecules containing multiple acidic and basic centers are much more interesting. DEAHPIP-b possesses two acidic protons, the phenolic 'OH', the imidazole 'NH' and three basic nitrogens, the imidazole nitrogen, the pyridyl nitrogen and the diethyl amino nitrogen. These centers can be either deprotonated or protonated in basic/acidic conditions. Consequently, this affects the ESIPT and TICT process in DEAHPIP-b. Therefore, the prototropic studies of DEAHPIP-b will be further exciting. In the previous two chapters the protic nature of the solvents and the nanoparticles surface was used to control the excited state reaction coordinate of DEAHPIP-b. In this chapter, the pH is used to control the emission characteristics by tuning the prototropic species.

The different prototropic species of DEAHPIP-b are presented in **Chart 7.1**. As DEAHPIP-b has two acidic centers, it can form two anions. The monoanion (MA) formed by the deprotonation of the phenolic 'OH' and the imidazole 'NH' are labeled as MA1 and MA2, respectively. Deprotonation of both the acidic protons leads to the formation of dianion (DA). The monocation (MC) produced by the protonation of diethylamino 'nitrogen', imidazole 'nitrogen' and pyridyl 'nitrogen' are marked as MC1, MC2 and MC3, respectively. Three different kinds of dications (DCs) are also possible. DC formed by the protonation of diethylamino and imidazole nitrogens is labeled as DC1, protonation of diethylamino and pyridyl nitrogens as DC2 and protonation of imidazole and pyridyl nitrogens as DC3. Protonation of all three basic centers results in trication (TC). However, DEAMPIP-b lacks the 'OH' proton, so it can produce only one MA. All other species of the methoxy analogous DEAMPIP-b can exist, same as in the hydroxy molecule. There the chapter is divided into two parts. In the first part, the protropic species of the hydroxyl compound is discussed and in the second part, the prototropic species of the methoxy derivatives are presented.

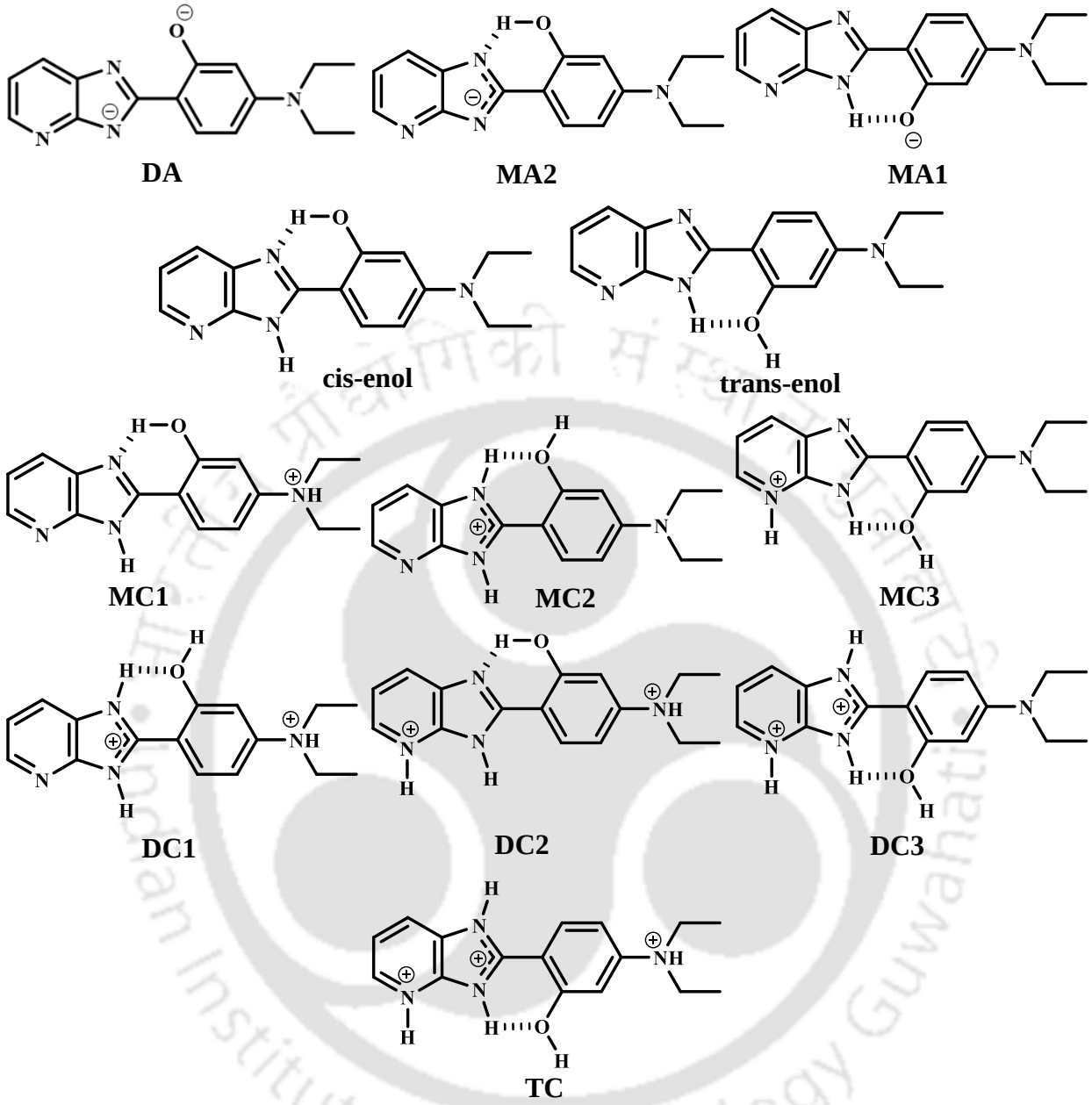

Chart 7.1: All possible species in DEAHPIP-b.

7.1. Effect of pH on 2-(4′-diethylamino-2′-hydroxyphenyl)-1H-imidazo-[4,5-b]pyridine

7.1.1. Neutral molecule

At neutral pH (7.0), the absorption band maximum of DEAHPIP-b is at 367 nm **[Table 7.1]**. The very low absorbance in water suggests that the low solubility of the molecule in water **[Figure 7.2.A in section 7.1.2, see later]**. The neutral molecule may have low solubility, but the ionic forms should have significant solubility.

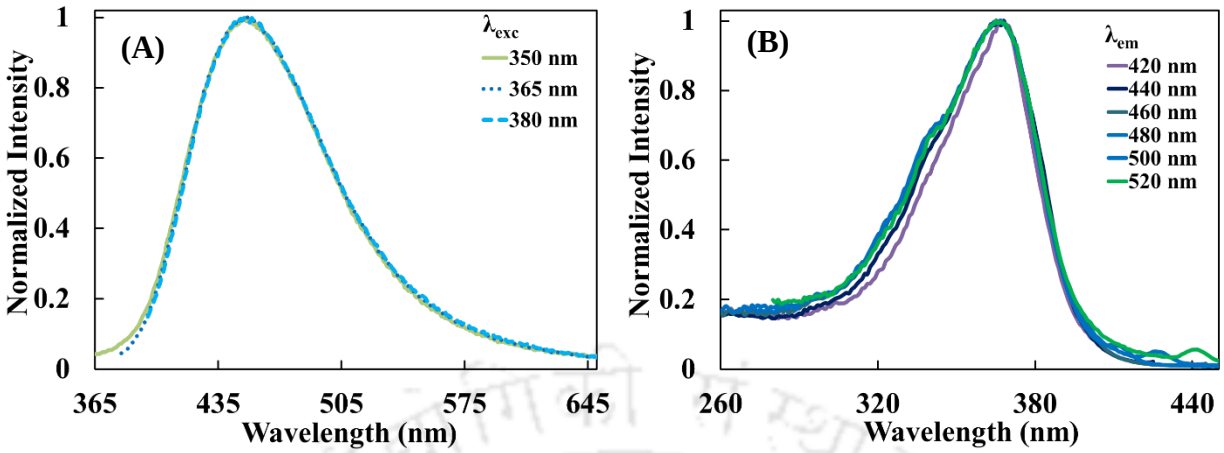

Figure 7.1: (A) Normalized emission spectra recorded at different excitation and **(B)** normalized excitation spectra recorded at different emission of DEAHPIP-b at pH 7.0.

Excitation at 367 nm led to emission at 454 nm **[Figure 7.1.A]**. The emission spectra are independent of the excitation wavelength **[Figure 7.1.A]**. The excitation spectra obtained monitoring at different emission also have only one maximum at ~ 367 nm **[Figure 7.1.B]**. This suggests presence of only one species in the ground state. Further, theoretical calculations were performed. Both cis and trans enol in neutral form were optimized in the ground state and found that the cis-enol is more stable (0 eV) than the trans-enol (0.2 eV) which supports the experimental result that presence of only one species. Theoretically obtained excitation energy and keto emission energy are also in good agreement with the experimental result at pH 7.0 **[Table 7.2]**.

Table 7.1: Absorption maxima **(**λ_{max}^{ab}, nm), excitation maxima (λ_{max}^{ex}, nm), emission maxima (λ_{max}^{fl}, nm) of different species in DEAHPIP-b.

Species	H_/pH/H_0	λ_{max}^{ab}	λ_{max}^{ex}	λ_{max}^{fl}
DA	16.2	370	370	466
MA2	12		335	375
MA1	12	378	375	475
Neutral	7.0	367	367	454
MC1	3.0		335	465
MC2	3.0	390	390	450
MC3	3.0	410	410	560
DC1	–0.6	336	350	430, 550
DC2	–0.6	352	357	465
DC3	–0.6		420	520
TC	–10.0	360	360	442

Table 7.2: Experimental and theoretical excitation energies (λ_{max}^{ex}, eV) and emission energies (λ_{max}^{fl}, eV) of different species in DEAHPIP-b.

Species	H_/pH/H_0	λ_{max}^{ex} (experimental)	λ_{max}^{ex} (theoretical)	λ_{max}^{fl} (experimental)	λ_{max}^{fl} (theoretical)
DA	16.2	3.3	3.2	2.7	2.8
MA2	12	3.7	3.6	3.3	3.0
MA1	12	3.3	3.2	2.6	2.8
Neutral	7.0	3.4	3.4	2.7	2.7
MC1	3.0	3.7	3.8	2.7	2.7
MC2	3.0	3.2	3.3	2.7	2.9
MC3	3.0	3.0	2.8	2.2	2.3
DC1	–0.6	3.6	3.8 (of DC1)	2.2 (rearrangement of DC1 to DC2-keto)	2.1 (DC2-keto)
DC2	–4.5	3.5	3.5	2.9	2.9
DC3	–4.5	2.9	2.8	2.4	2.3
TC	–10.0	3.4	3.4	2.8	2.9

7.1.2. Neutral-Monoanion equilibrium

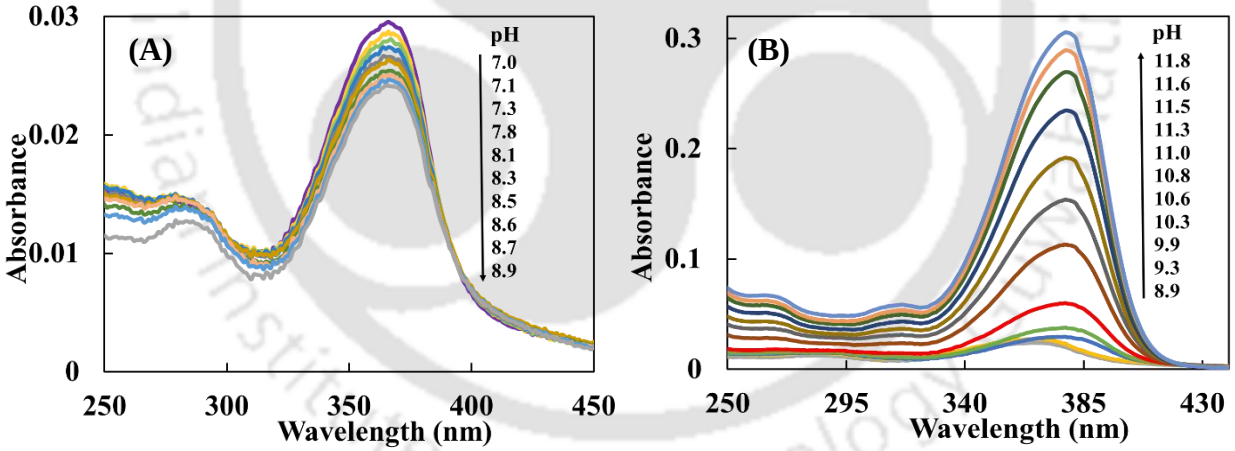

Figure 7.2: Absorption spectra of DEAHPIP-b in basic medium at pH **(A)** 7.0 to 8.9 and **(B)** 8.9 to 11.8.

In pH range 7.0 to 8.9, the shift in the spectrum is negligible and a small change in absorbance was observed **[Figure 7.2.A]**. When the pH increases from 8.9 to 11.8 gradually, the absorption spectrum is red shifted with significant increase in absorbance **[Figure 7.2.B]**. The increase in absorbance may be due to increase in solubility of the ionic species in water. Therefore, to dissolve the neutral fluorophore completely, 5% methanol was added to water. In 5% methanol solution, the absorbance increased significantly **[Figure 7.3]**. When the pH was increased from

7.0 to 12.0, like earlier, the absorption spectrum is red shifted indicating the formation of the same prototropic species. In basic solution, the acidic protons are deprotonated. Deprotonation of 'OH' proton increases the conjugation and produce red shift.[222, 250, 251] The monoanion thus formed is labeled as MA1 **[Chart 7.1]**. The monoanion formed by the deprotonation of 'NH' proton is labeled as MA2. In this, the charge flow from the donor diethylaminophenyl ring to acceptor imidazopyridine ring reduces and results in blue shift.[123, 124, 152] The red shift is more pronounced here, this suggests the formation of MA1.

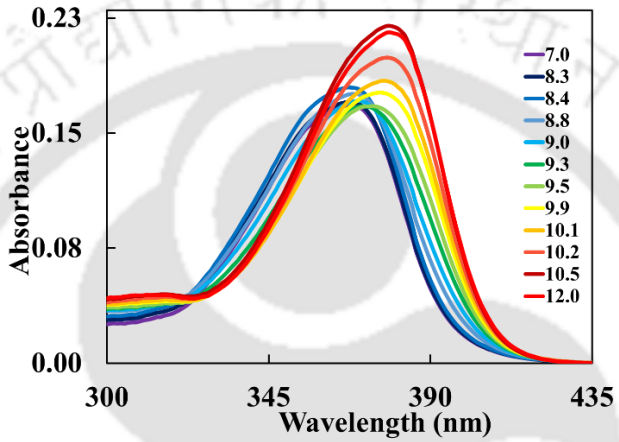

Figure 7.3: Absorption spectra of DEAHPIP-b in 5% methanol-water mixture at pH 7.0 to 12.0.

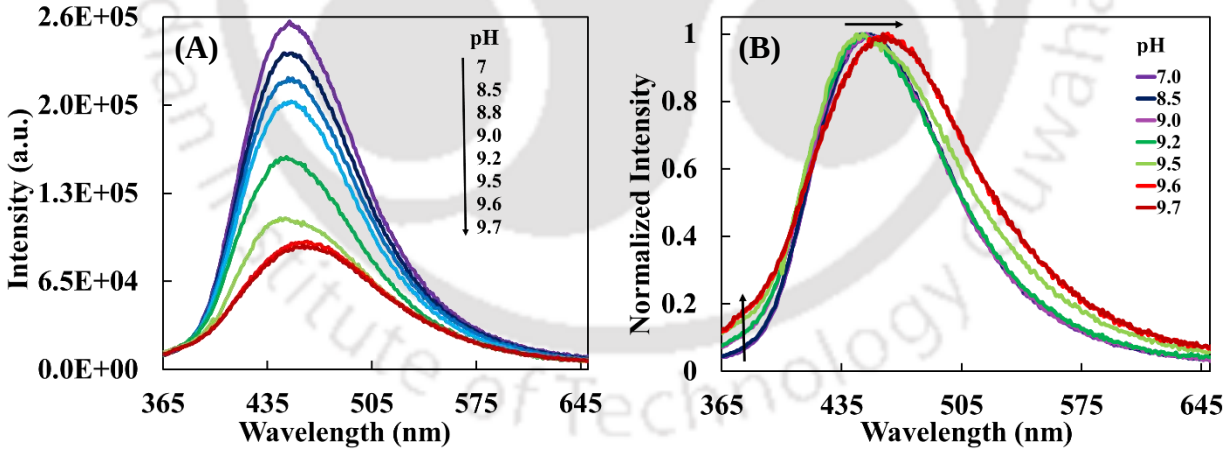

Figure 7.4: (A) Emission spectra and **(B)** normalized emission spectra of DEAHPIP-b at pH 7.0 to 9.7, λ_{exc} = 350 nm.

On increasing the pH of the solution from 7.0 to 9.7, the emission intensity decreases, but the maximum does not change much up to pH 9.2 **[Figure 7.4.A** and **7.4.B]**. Then the maximum shifts towards longer wavelength as well as a small band appears around 375 nm **[Figure 7.4.B]**. This shows the deprotonation of the molecule.

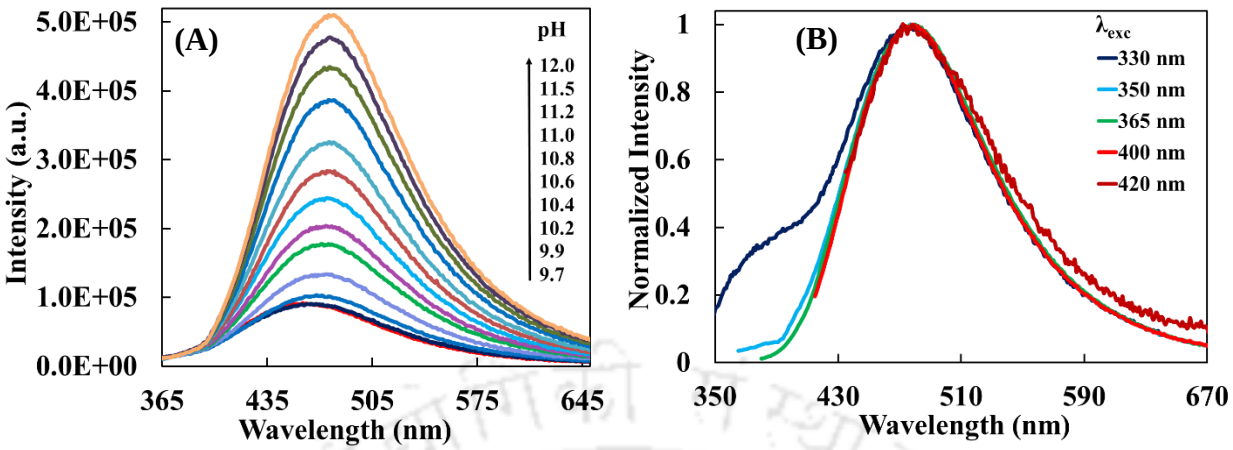

Figure 7.5: (A) Emission spectra of DEAHPIP-b at pH 9.7 to 12.0, λ_{exc} = 350 nm and **(B)** normalized emission spectra of DEAHPIP-b recorded at different excitation at pH 12.

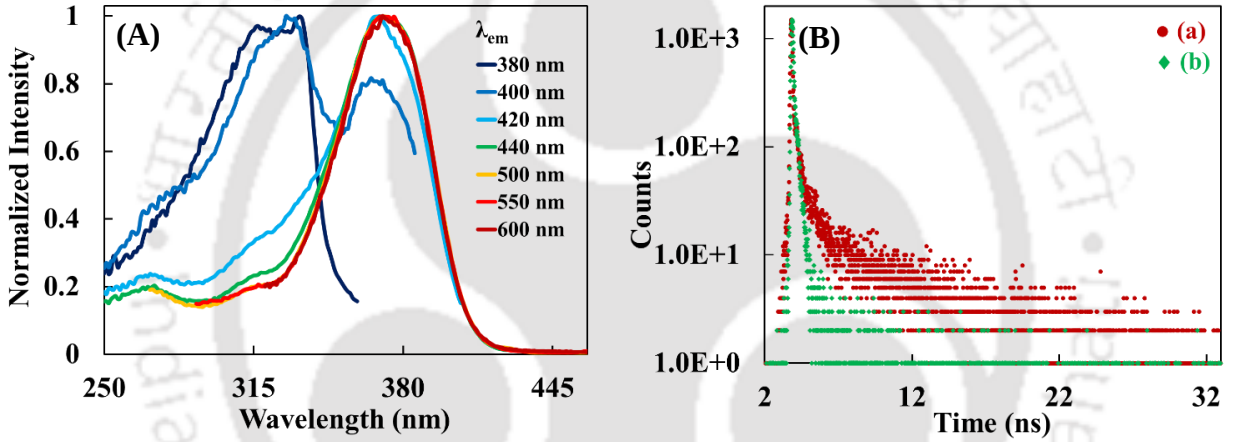

Figure 7.6: (A) Normalized excitation spectra of DEAHPIP-b recorded at different emission at pH 12.0. **(B)** The fluorescence decays of DEAHPIP-b at pH 12.0 monitored at ● **(a)** 390 nm and ♦ **(b)** 475 nm, λ_{exc} = 375 nm.

On further increasing the pH up to 12.0, the spectra continuously shift towards longer wavelength with increase in intensity **[Figure 7.5.A]**. The normalized emission spectra at pH 12.0 show the bands at 375 nm and 475 nm **[Figure 7.5.B]** and the normalized excitation spectra monitored at those emission maxima display the bands at 335 nm and 375 nm **[Figure 7.6.A]**. The fluorescence lifetime also suggests the presence of two different species with 4.6 ns (57 %) and 0.3 ns (43 %) when monitored at 390 nm **[Figure 7.6.B]**. It becomes single exponential with 0.2 ns when monitored at 475 nm. As described earlier, the spectra of MA1 will be red shifted compared to neutral and the spectra of MA2 will be blue shifted compared to neutral species. The emission at 375 nm is blue shifted compared to the normal emission observed even in nonpolar solvent. Theoretically calculated emission energy of MA2 is close to the experimental value

[Table 7.2]. Corresponding 335 nm excitation band is also blue shifted compared to neutral. Therefore, the 375 nm emission with 4.6 ns decay time and the corresponding 335 nm excitation spectrum can be assigned to MA2. The 475 nm emission with 0.2 ns decay time and the 375 nm excitation spectrum are red shifted related to corresponding emission and excitation band of neutral species, therefore, corresponds to MA1. Theoretically calculated excitation and emission energies of the MA1 are also close to experimental values **[Table 7.2]**.

7.1.3. Monoanion-Dianion equilibrium

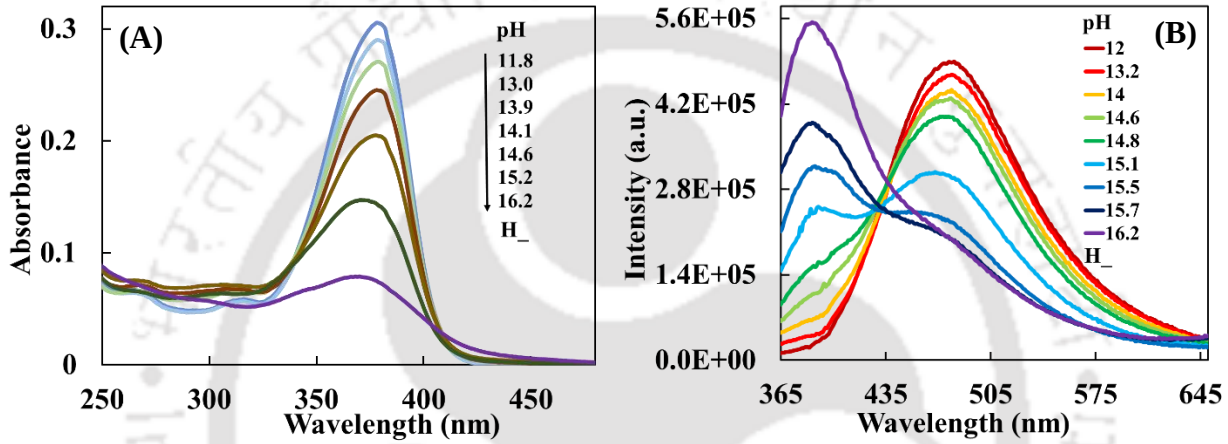

Figure 7.7: (A) Absorption spectra and **(B)** emission spectra of DEAHPIP-b at λ_{exc} = 350 nm in the basic solutions at pH 12 to H_ 16.2.

Upon increasing the basicity from pH 11.8 to H_ 16.2, the absorbance at 378 nm decreases and blue shifted to 370 nm **[Figure 7.7.A]**. The emission intensity at 475 nm decreases and shifted to 466 nm **[Figure 7.7.B]**. However, the intensity at 375 nm (MA2 emission) increases **[Figure 7.7.B]**. The emission spectra at H_ 16.2 (maximum basicity) recorded at different excitation display the bands at 380 nm and 466 nm **[Figure 7.8.A]**. Similarly, the normalized excitation spectra at H_ 16.2 show the bands at 335 nm and 370 nm **[Figure 7.8.B]**. The new bands at 466 nm in the emission spectra and at 370 nm in the excitation spectra indicate the appearance of DA along with MA2. As stated earlier, the 370 nm excitation spectrum and 466 nm emission spectrum of DA are blue shifted compared to corresponding excitation and emission spectra of MA1 and red shifted compared to the corresponding excitation and emission spectra of MA2 **[Table 7.1]**. Theoretically calculated spectral energies of the DA also match with the experimental values **[Table 7.2]**. Henceforth the 370 nm excitation and 466 nm emission can be assigned to DA. However, at H_ 16.2 biexponential decay with two different lifetimes, 0.2 ns (69 %) and 2.0 ns

(31 %) were obtained when the fluorescence decay was monitored at 460 nm **[Figure 7.9]**. The 0.2 ns indicates the presence of MA1 along with DA having lifetime 2.0 ns. This shows that at H_ 16.2, the DA formation is not completed, both MA1 and MA2 are also present in the solution.

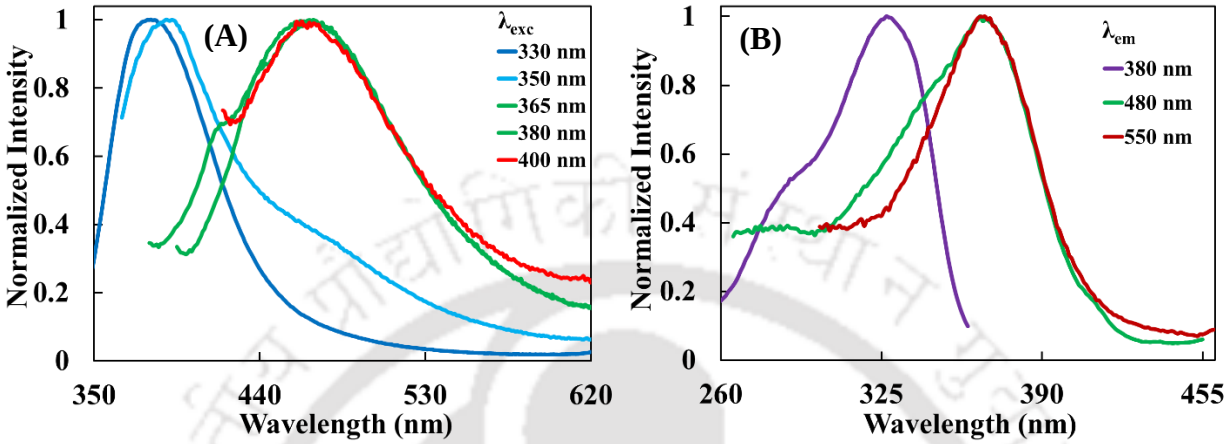

Figure 7.8: (A) Normalized emission spectra recorded at different excitation and **(B)** normalized excitation spectra recorded at different emission at H_ 16.2.

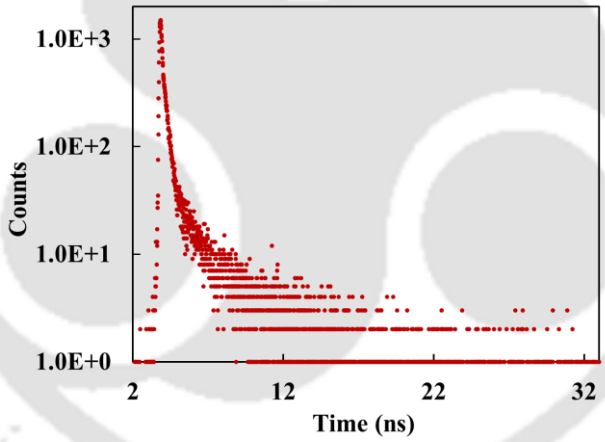

Figure 7.9: The fluorescence decay of DEAHPIP-b at H_ 16.2 at λ_{em} = 460 nm.

7.1.4. Neutral-Monocation equilibrium

The absorption spectra are red shifted on decreasing the pH below 7.0, also a band emerges at 390 nm along with another band at ~ 410 nm **[Figure 7.10.A]**. In pure water the absorbance increases significantly, with decrease in pH and no isosbestic point was found. In 5 % methanol, no such significant increase in absorbance was observed. However, the spectral shift and the formation of new bands are same as that of pure water **[Figure 7.10.B]**. Unlike, in pure water a quasi isosbestic point was observed. This difference again suggests the less solubility of the neutral

molecule and higher solubility of the cationic species in water. In 5% methanol, neutral molecules as well as the cations are completely soluble. As the electron density over donor (–NEt_2) decreases upon protonation, the absorption band of MC1 **[Chart 7.1]** should be blue shifted compared to the neutral species.[152, 252, 253] The absorption band of MC2 should be red shifted as compared to the absorption band of the neutral species as protonation of imidazole ring nitrogen will cause the charge deficiency over the acceptor ring making the charge flow from donor to the acceptor increases.[152, 252] Similarly, the absorption band of MC3 should be further red shifted as compared to MC2, as in MC3, the protonation at pyridyl nitrogen will increase the conjugation more.[152, 252, 253] Hence, the absorption band at 390 nm and ~ 410 nm are due to the formation of MC2 and MC3, respectively.

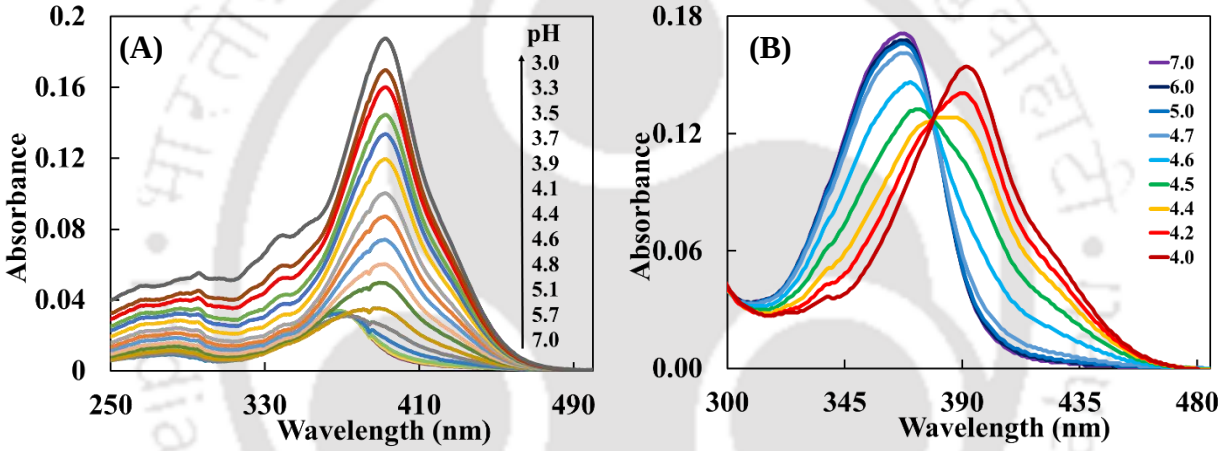

Figure 7.10: Absorption spectra of DEAHPIP-b **(A)** in water at pH 7.0 to 3 and **(B)** in 5% methanol-water mixture at pH 7.0 to 4.0.

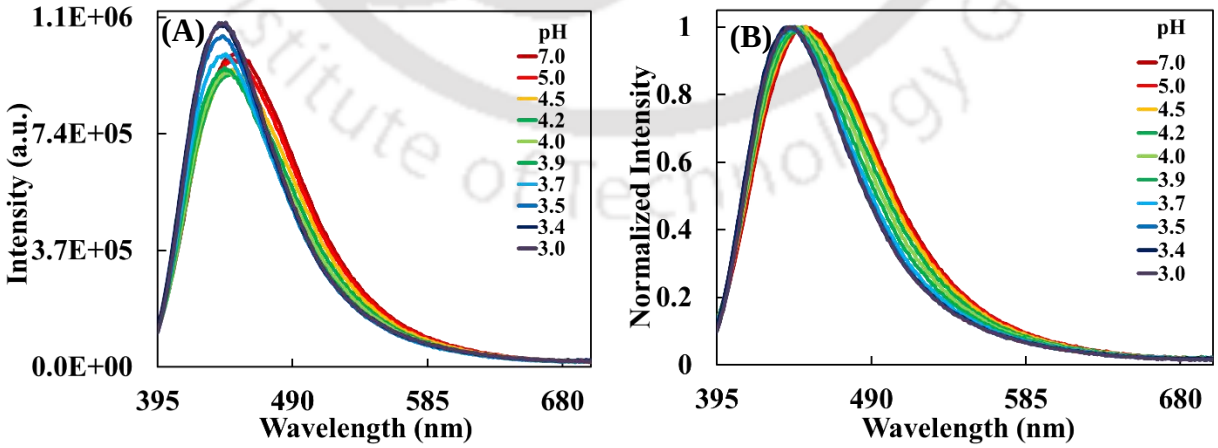

Figure 7.11: (A) Emission spectra and **(B)** normalized emission spectra of DEAHPIP-b at pH 7 to 3.0, λ_{exc} = 380 nm.

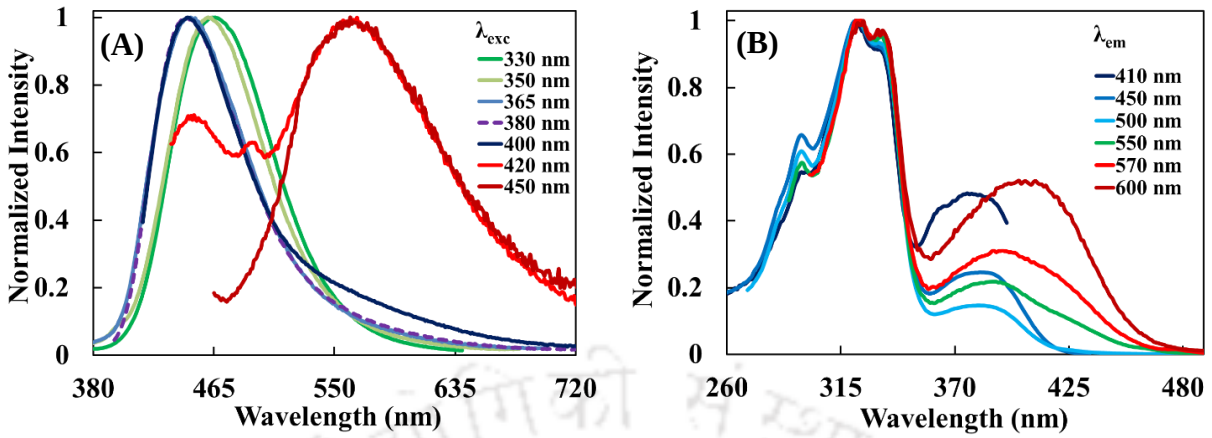

Figure 7.12: (A) Normalized emission spectra recorded at different excitation and **(B)** normalized excitation spectra recorded at different emission of DEAHPIP-b at pH 3.0.

The emission spectra were obtained by exciting at the quasi isosbestic point **[Figure 7.11.A]**. The fluorescence spectrum is blue shifted with a small change in intensity due to the formation of MCs. The normalized emission spectra show the continuous shift in the spectra **[Figure 7.11.B]**. To get insight information about the presence of different MC, at pH 3.0 the emission spectra were recorded at different excitation and the excitation spectra were recorded at different emission **[Figure 7.12]**. When excited at 330 nm and 350 nm, predominantly emission was observed at 465 nm. Excitation at 365 nm and 380 nm resulted in emission at 450 nm. Though excitation at 400 nm also yielded the 450 nm emission, a weak emission started to emerge at 560 nm. The relative intensity of the 560 nm emission increase upon excitation at longer wavelength. The excitation spectra are also consistent with the emission spectra. The structured excitation band observed at 335 nm gives the 465 nm emission. The broad bands at 390 nm and 410 nm produce the 450 nm and 560 nm emissions. As assigned in the absorption spectra, the 390 nm and 410 nm correspond to MC2 and MC3, respectively. Therefore, the corresponding emission at 450 nm and 560 nm are the emission bands of MC2 and MC3, respectively. The structured excitation band at 335 nm is blue shifted to the neutral band and therefore, can be assigned to MC1. The Stokes shift of MC1, MC2 and MC3 are 8345, 3750 and 6650 cm^{-1}, respectively. The higher Stokes shift of MC3 compared to MC2 is not surprising as the protonation at the pyridyl nitrogen is expected to increase the ICT. But the large Stokes shift in shorter wavelength emission suggest that MC1 is not emitting the normal emission. With proton on the charge donor, diethylamino group, the TICT emission is ruled out. Unlike, the excitation spectra, the emission spectrum is broad and structure less. Therefore, indicate that MC1 is not emitting the normal emission, but the tautomer emission.

The Stokes shift observed in the MC1 of methoxy derivative is much less **(see later in section 7.2.2)**. This is because the methoxy derivative which cannot undergo ESIPT, emit the normal emission and MC1 of DEAHPIP-b which is capable of ESIPT emits the tautomer emission. Thus, the protonation study on methoxy derivative support this.

The fluorescence decays were monitored at 450 nm, 465 nm, 550 nm at pH 3.0 using λ_{exc} = 375 nm **[Figure 7.13]**. The lifetimes are at 450 nm, 0.2 ns (48 %) and 1.7 ns (52 %), at 465nm, 0.2 ns (44 %) and 2.1 (56 %) ns and at 550 nm, 0.2 ns (38 %) and 2.5 ns (62 %). The shorter lifetime at each wavelength is close to tautomer lifetime. Also, it has been established that the emission at 465 nm is due to the tautomer of MC1. Hence, the 1.7 ns lifetime at 450 nm should be the lifetime of MC2 emission. The 2.5/2.1 ns lifetime has to be that of MC3. The increase in its relative percentage when monitored at longer wavelength (550 nm) also supports this. The excitation and emission energies of the MCs were also obtained theoretically and observed that a great correlation exists between theoretical calculations and experimental findings **[Table 7.2]**.

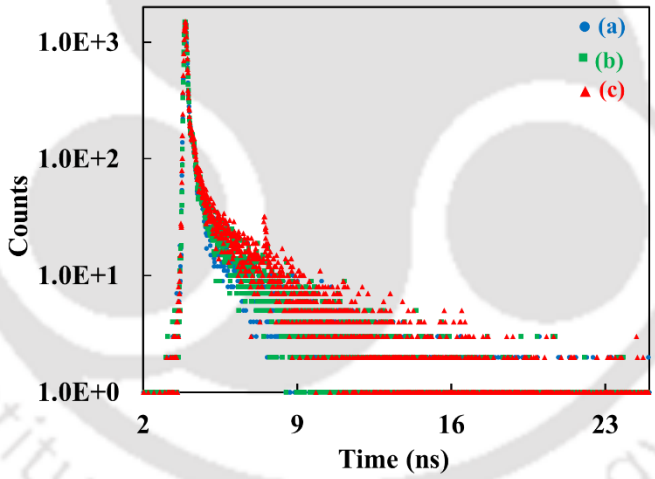

Figure 7.13: The fluorescence decays of DEAHPIP-b monitored at ● **(a)** 450 nm, ■ **(b)** 460 nm and ▲ **(c)** 550 nm at pH 3.0, λ_{exc} = 375 nm.

7.1.5. Monocation-Dication equilibrium

On further increasing the acidity from pH 3.0 to H_0 –0.6, the absorbance at 390 nm and 410 nm decreases and a clear band appears at 336 nm with a quasi isosbestic point at 360 nm **[Figure 7.14.A]**. The existence of equilibrium indicates the formation of DCs. Both the DC1 and DC2 will be red shifted compared to MC1 and blue shifted compared to MC2 and MC3 **[Chart 7.1]**. The DC3 will be red shifted compared to all other cations as both the ring nitrogens are

protonated. Therefore, the absorption band at 336 nm is due to the formation of DC1. However, the 336 nm structured absorption band is identical to the excitation band of MC1 obtained at pH 3.0. To confirm this band at H_0 –0.6 whether is due to MC1 or DC1, theoretically the excitation energy of DC1 was calculated and found that the excitation energies of both MC1 and DC1 are very close to each other **[Table 7.2]**. Further the presence of a quasi isosbestic point at 360 nm suggests the equilibrium between the MCs and DCs. This can be confirmed further from the emission spectra of MC1 and DC1. On increasing the acidity from H_0 –0.6 to –4.5, the absorbance decreases at 336 nm, the spectra become a little broad **[Figure 7.14.B]**, a bathochromic shift is observed from 336 nm to 352 nm and there is no clear isosbestic point. This suggests the appearance of DC2 along with DC1. The absorption band of DC2 (352 nm) is blue shifted compared to that of MC3 (as it can be formed due to protonation at diethylamino nitrogen of MC3) and red shifted compared to that of MC1 (as it can be formed due to protonation at pyridyl nitrogen of MC1).

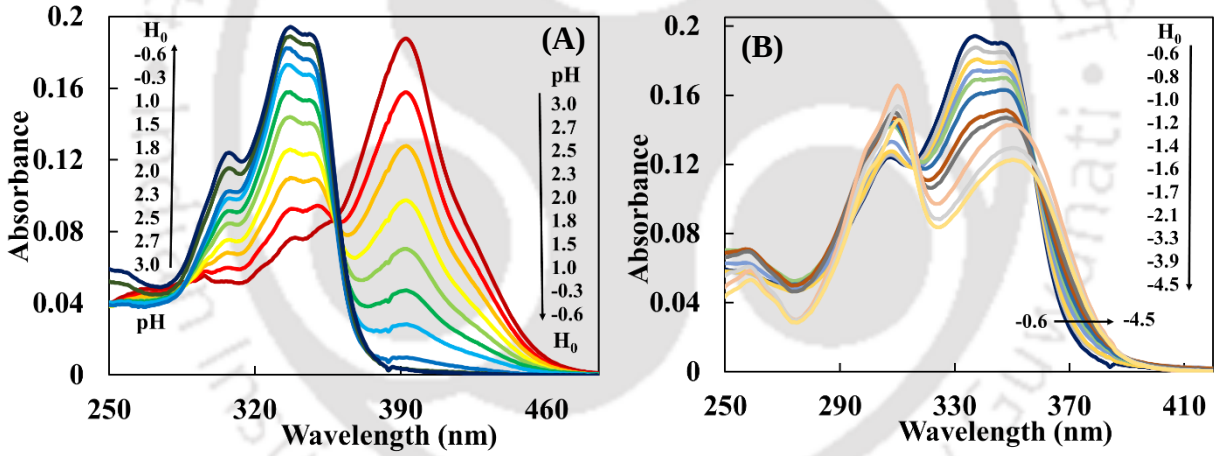

Figure 7.14: Absorption spectra of DEAHPIP-b at **(A)** pH 3.0 to H_0 – 0.6 and **(B)** H_0 –0.6 to –4.5.

Upon increasing the acidity of the solution from pH 3.0, the emission intensity decreases up to H_0 –0.6 **[Figure 7.15.A]**. The normalized emission spectra show that the spectrum at H_0 –0.6 is blue shifted compared to the spectrum at pH 3.0 and it is also accompanied by another band at around ~ 550 nm **[Figure 7.15.B]**. The new emissions suggest the formation of DCs. Further increasing the acidity till H_0 –4.5, the emission bands become prominent **[Figure 7.16]**.

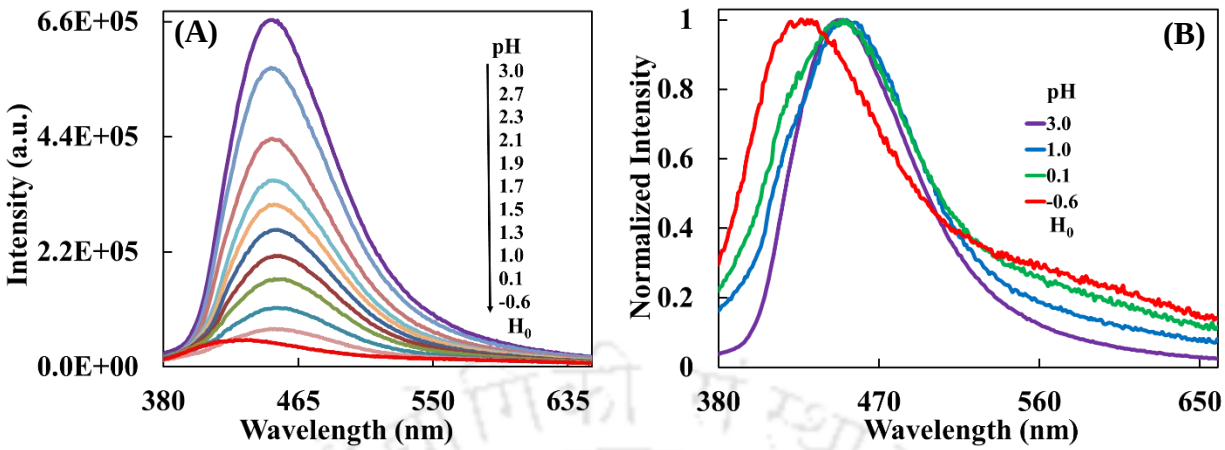

Figure 7.15: (A) Emission spectra and **(B)** normalized emission spectra of DEAHPIP-b at pH 3.0 to H_0 –0.6, λ_{exc} = 365 nm.

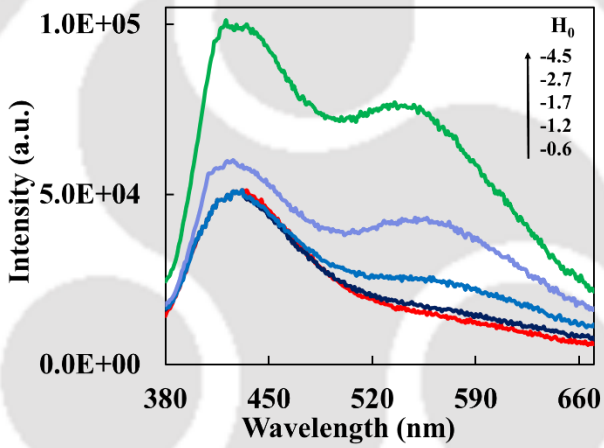

Figure 7.16: Emission spectra of DEAHPIP-b at H_0 –0.6 to –4.5, λ_{exc} = 365 nm.

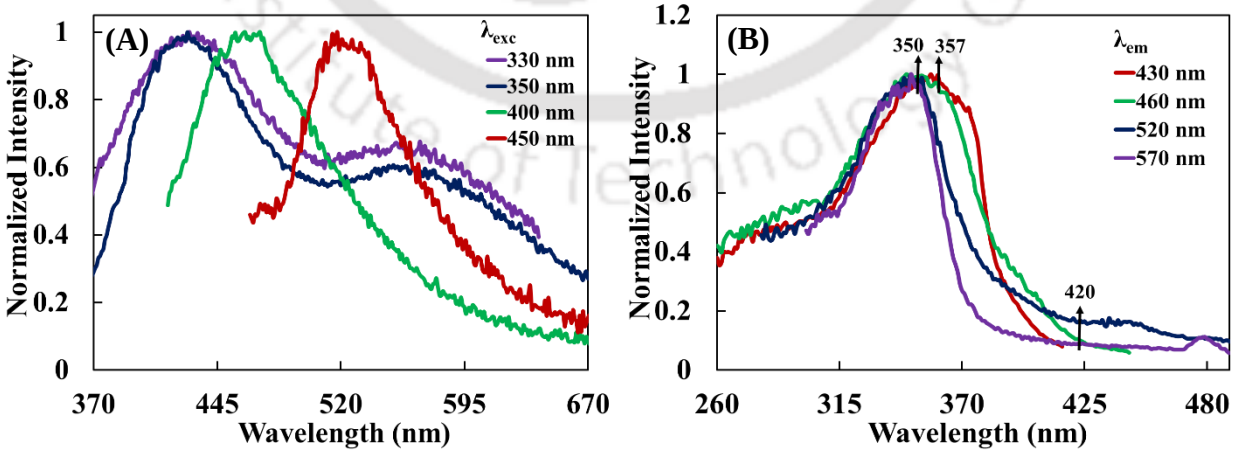

Figure 7.17: (A) Normalized emission spectra of DEAHPIP-b recorded at different excitation and **(B)** normalized excitation spectra of DEAHPIP-b recorded at different emission, at H_0 –0.6.

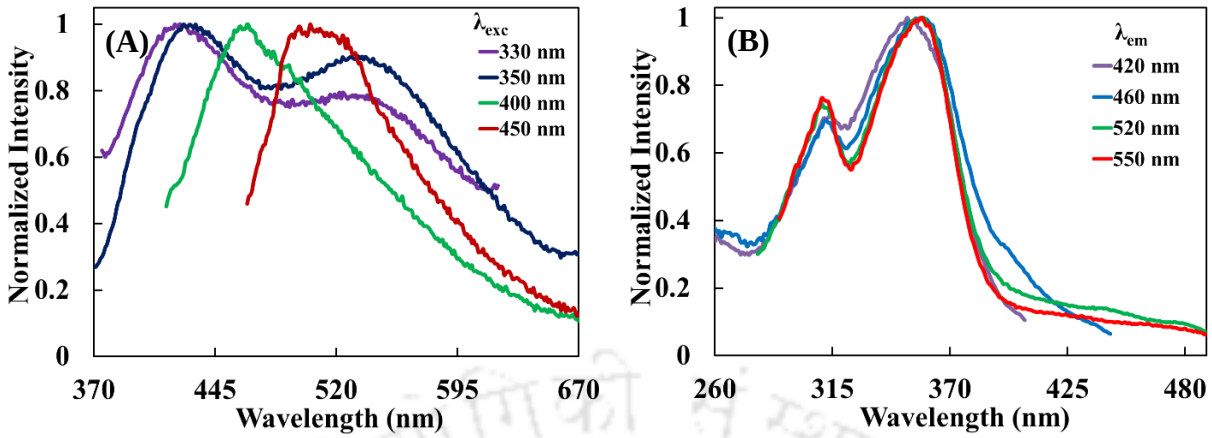

Figure 7.18: (A) Normalized emission spectra of DEAHPIP-b recorded at different excitation and **(B)** normalized excitation spectra of DEAHPIP-b recorded at different emission, at H_0 –4.5.

The normalized emission spectra obtained using different excitation at H_0 –0.6 and H_0 –4.5 show the bands at 430 nm, 465 nm, 520 nm and 550 nm **[Figure 7.17.A** and **7.18.A]**. The normalized excitation spectra obtained at H_0 –0.6 and H_0 –4.5 using different emission indicate the bands at ~ 350 nm and ~ 357 nm and a broad band at ~ 420 nm **[Figure 7.17.B** and **7.18.B]**. From the spectral shift the bands at 350 nm, 357 nm and 420 nm can be assigned to DC1, DC2 and DC3, respectively. Four emission band from three DCs shows the formation of at least one tautomer. Dual emissions 430 nm and 550 nm are observed upon excitations at short wavelengths, this shows the formation of this normal and tautomer from DC1. The 430 nm normal band can be assigned to normal emission of DC1. Similarly, from the shift, other red shifted bands 465 nm and 520 nm can be assigned to normal emission of DC2 and DC3, respectively. Further, it confirms that the 336 nm absorption band is due to DC1 as the emission spectrum (430 nm) obtained by exciting at 336 nm is different from MC1 emission (465 nm). The emission spectrum of DC1 is supposed to be red shifted to that of MC1 emission. However, since the MC1 is emitting from the tautomer (keto) form and not from the enol form, the emission spectrum of DC1 is blue shifted compared to MC1.

Among DCs, only in DC2, ESIPT is probable, therefore assigning 550 nm emission to tautomer of DC1 is not possible, but it can be assigned to the tautomer of DC2. Theoretically predicted tautomer emission of DC2 is 576 nm and is also close to 550 nm. The absence of 550 nm emission in methoxy derivative, which is incapable of ESIPT **(see later in section 7.2.3)**, further supports the assignment of 550 nm band to tautomer emission of DC2. But the corresponding excitation spectrum matches with DC1. The formation of DC2 tautomer from DC1

can be explained as follows. As discussed earlier, upon excitation the acidity of the 'OH' proton increases and it undergoes intermolecular proton transfer. The DC1 rearranged to form DC2 tautomer via biprotonic phototautomersism is explained in **Scheme 7.1**.[152, 254] Theoretically obtained excitation and emission energies of DCs are close to experimental values **[Table 7.2]** which supports the assignments.

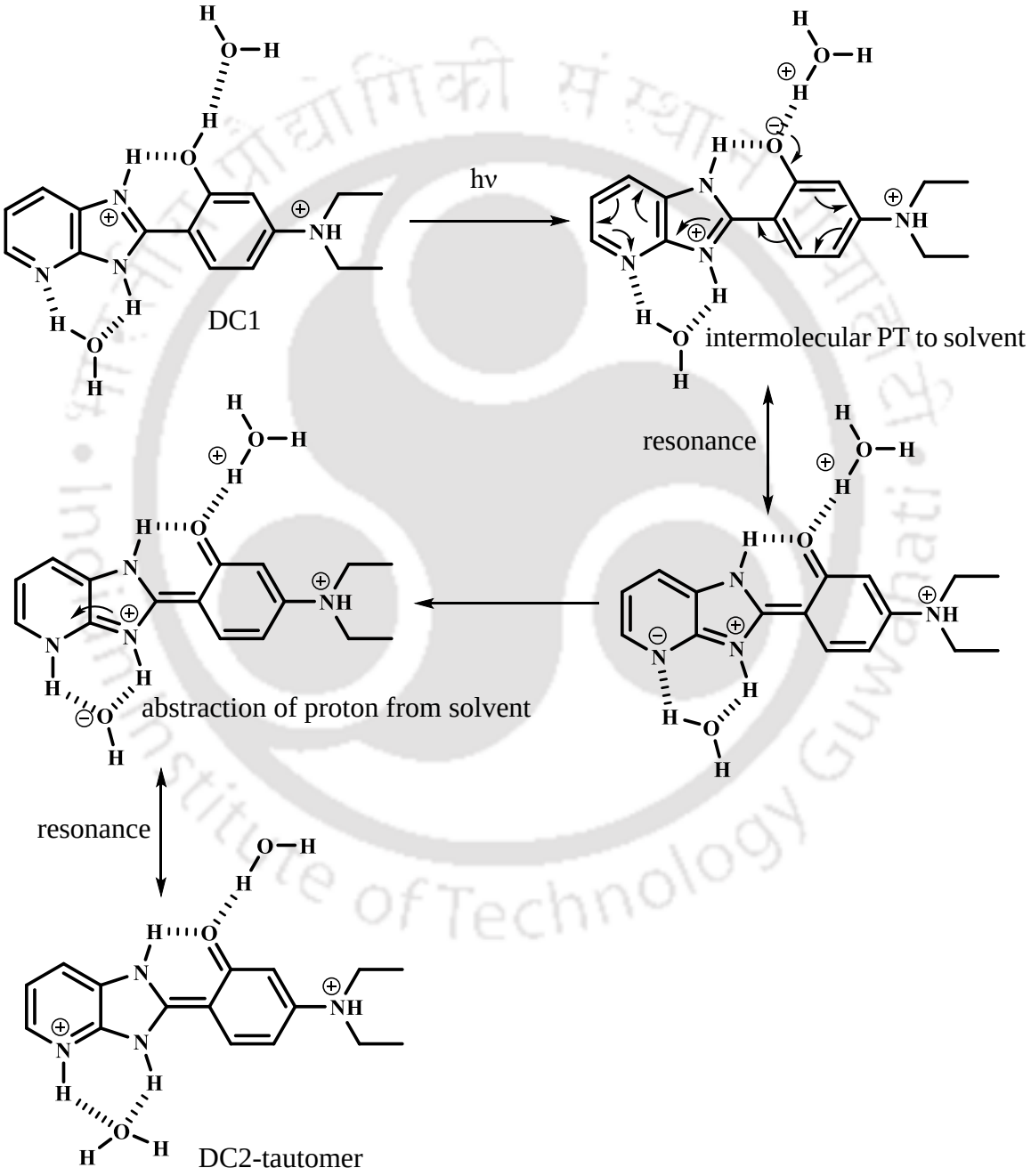

Scheme 7.1: Excited state rearrangement of DC1 to DC2 tautomer by solvent mediated proton transfer and resonance.

7.1.6. Dication-Trication equilibrium

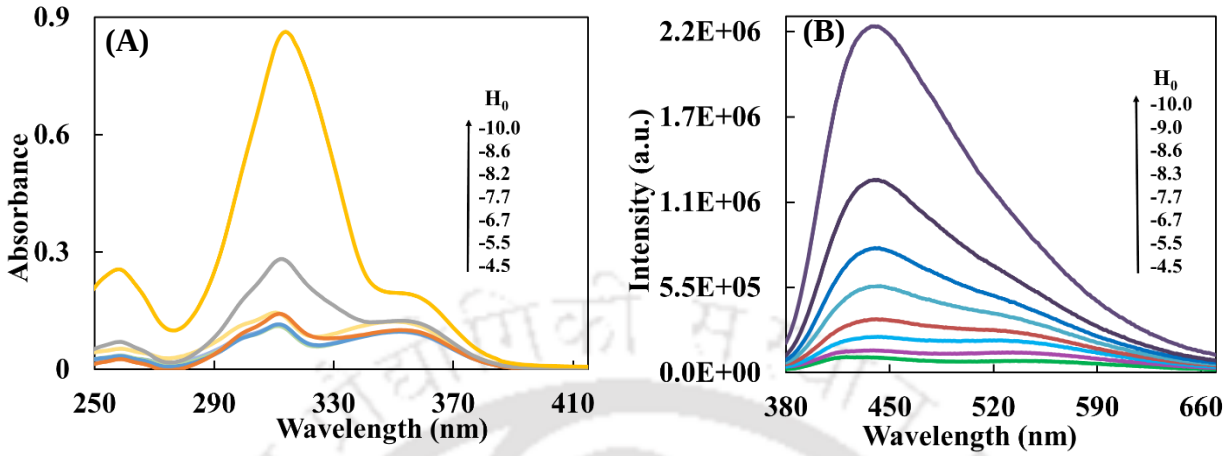

Figure 7.19: (A) Absorption spectra and **(B)** emission spectra of DEAHPIP-b at H_0 –4.5 to –10.0, λ_{exc} = 365 nm.

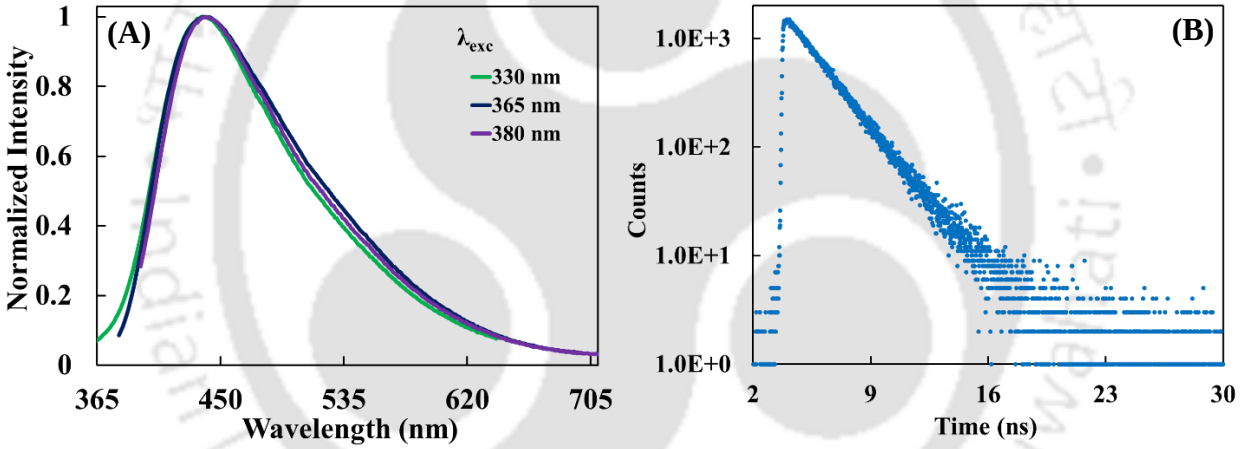

Figure 7.20: (A) Normalized emission spectra of DEAHPIP-b at H_0 –10.0 at different excitation. **(B)** The fluorescence decay of DEAHPIP-b monitored at 440 nm at H_0 –10.0.

On further increasing the acidity to H_0 –10.0 (concentrated sulphuric acid), the absorbance shifts to 360 nm **[Figure 7.19.A]**. The emission intensity also increases with increase in acidity **[Figure 7.19.B]**. A single emission is observed at 442 nm, which is independent of excitation wavelength **[Figure 7.20.A]** and is single exponential decay with 2.2 ns lifetime **[Figure 7.20.B]**. The TC band should be red shifted compared to DC1 (due to protonation at pyridyl nitrogen of DC1) and blue shifted compared to DC3 (due to protonation at diethylamino nitrogen of DC3). Hence the 442 nm band with 2.2 ns lifetime at H_0 –10.0 can be assigned to TC. Theoretically the excitation and emission energies were obtained for TC and are close to the experimental result **[Table 7.2]**.

7.1.7. pK_a of DEAHPIP-b

The pK_a values of the equilibria between different species of DEAHPIP-b were calculated using the absorption spectral data. The pK_a values between the equilibria between different species are given in **Figure 7.21**. The neutral-MA pK_a value of HPIP-b is 8.6,[255] whereas of DEAHPIP-b is 9.2. The neutral-MC pK_a value of HPIP-b is 4.0,[255] and that of DMAPIP-b is 5.4[20] and of DEAHBI is 6.3,[126] whereas of DEAHPIP-b is 4.5. The MC-DC pK_a value of HPIP-b is –1.6[255] and of DEAHBI is 2.3,[126] whereas of DEAHPIP-b is 2.0. The substitution of electron donating 'OH' and 'NEt$_2$' groups ease the protonation and make difficult the deprotonation in DEAHPIP-b.

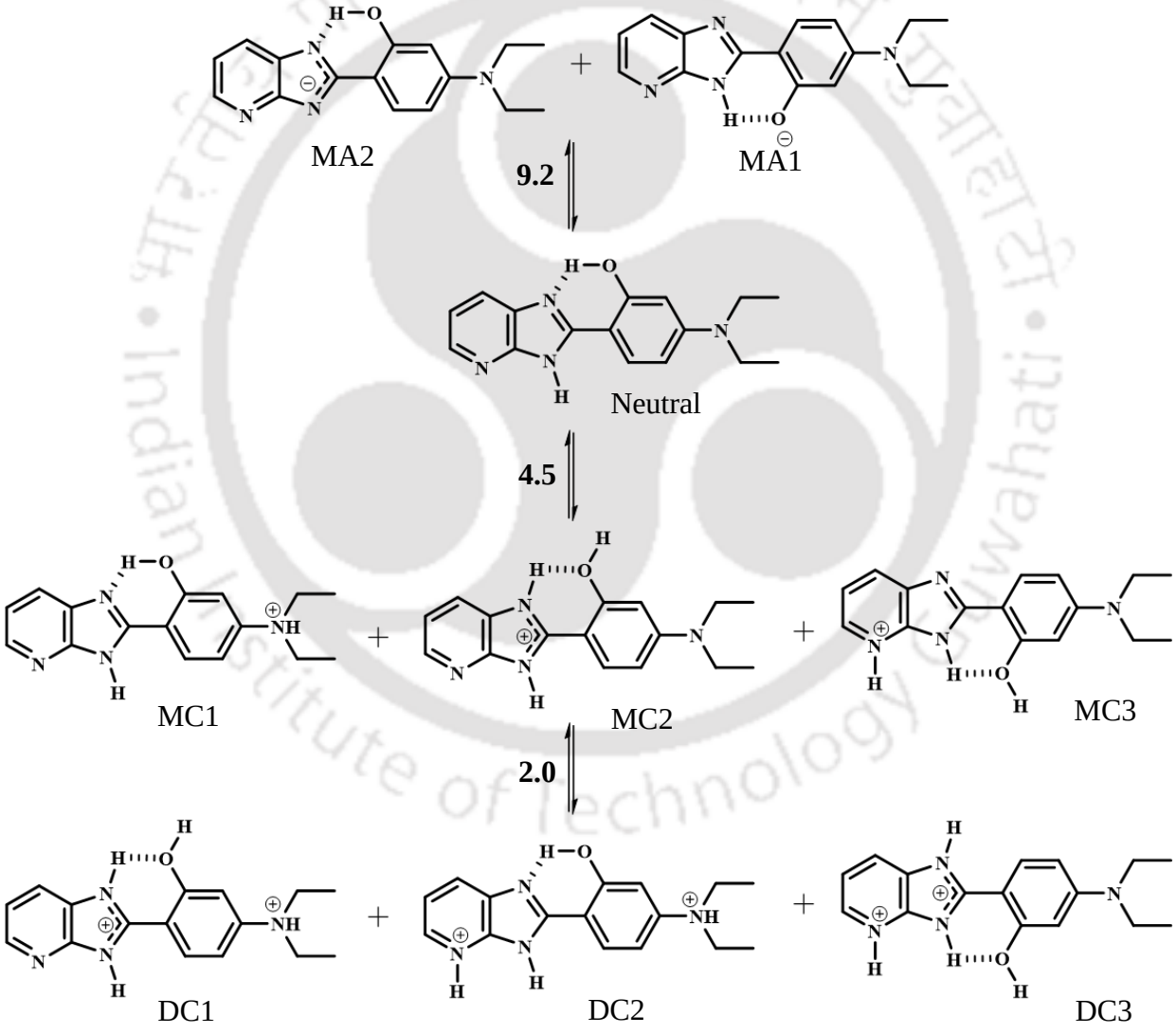

Figure 7.21: The pK_a of the equilibria between different species of DEAHPIP-b.

7.2. Effect of pH on 2-(4′-diethylamino-2′-methoxyphenyl)-1H-imidazo-[4,5-b]pyridine

7.2.1. Neutral

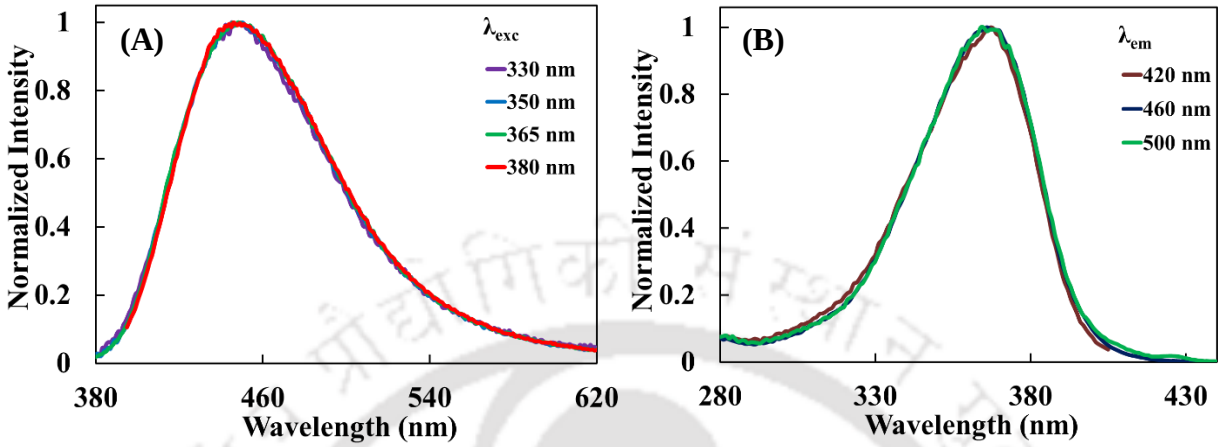

Figure 7.22: (A) Normalized emission spectra recorded at different excitation and **(B)** normalized excitation spectra recorded at different emission of DEAMPIP-b at pH 7.0.

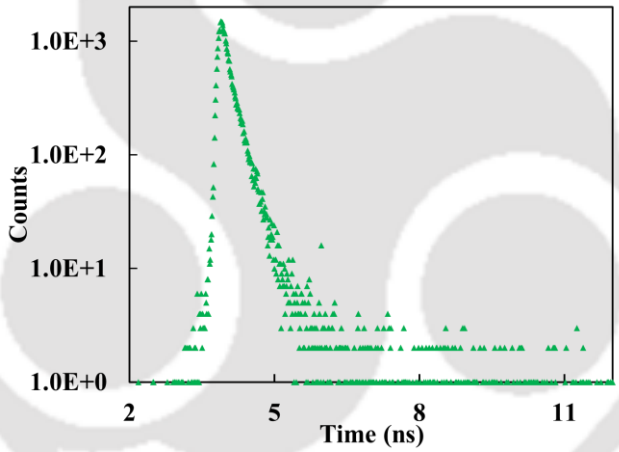

Figure 7.23: The fluorescence decay of DEAMPIP-b at pH 7.0 monitored at 445 nm, λ_{exc} = 375 nm.

Like the hydroxy derivative, the methoxy derivative is also in the neutral form at pH 7.0. At pH 7.0, DEAMPIP-b absorbs at 366 nm **[Table 7.3]**. At pH 7.0, the molecule emits single emission at 445 nm and independent of excitation wavelength **[Figure 7.22.A]**. Similarly, the excitation spectra monitored at different emission wavelength shows only one maximum at 366 nm, which is matching with the absorption maximum **[Figure 7.22.B]**. The fluorescence decay is also single exponential **[Figure 7.23]**. Both the excitation and the emission spectra suggest the presence of single species. The emission maximum in water at pH 7.0 is red shifted due to increase in polarity of the solvent compared to other solvents **[Table 5.3** and **7.4]**. Unlike DEAHPIP-b, in

DEAMPIP-b, the keto emission is not possible. The Stokes shift is similar to that normal emission of the hydroxy molecule, therefore can be assigned to normal emission rather than the TICT emission. The excitation and emission energies calculated theoretically for neutral DEAMPIP-b also agrees with the experimental results **[Table 7.4]**.

Table 7.3: Absorption maxima (λ_{max}^{ab}) of different species in DEAMPIP-b.

pH/H_0	λ_{max}^{ab}	species
7.0	366	Neutral
3.0	395	MC2
3.0	430	MC3
-0.6	336	DC1
-7.7	356	DC2
-10.0	360	TC

Table 7.4: Experimental and theoretical excitation energies (λ_{max}^{ex}, eV) and emission energies (λ_{max}^{fl}, eV) of different species in DEAMPIP-b.

Species	pH/H_0	λ_{max}^{ex} (experimental)	λ_{max}^{ex} (theoretical)	λ_{max}^{fl} (experimental)	λ_{max}^{fl} (theoretical)
Neutral	7.0	3.4	3.4	2.8	3.0
MC1	1.0	3.7	3.8	3.2	3.1
MC2	1.0	3.2	3.3	2.8	2.9
MC3	1.0	2.9	2.8	2.2	2.3
DC1	–0.6	3.7	3.7	2.8	3.1
DC2	–7.7	3.5	3.6		3.1
DC3	–7.7	2.9	2.8	2.5	2.3
TC	–10.0	3.4	3.3	2.9	2.9

7.2.2. Neutral – Monocations equilibrium

Upon decreasing the pH of the solution from 7.0 to 4.2, same as that of DEAHPIP-b, the absorption spectrum of DEAMPIP-b is shifted bathochromically. Two new bands are observed at around ~ 395 nm and ~ 430 nm with a quasi isosbestic point at 376 nm **[Figure 7.24]**. On further decreasing the pH to 3.0, the absorbance increases sharply at 395 nm and the 430 nm band appears like a hump. Same as in DEAHPIP-b, in DEAMPIP-b based on the spectral shift, the 395 nm and the 430 nm bands can be assigned to MC2, the monocation formed by the protonation of imidazole nitrogen and MC3, the monocation formed by the protonation of pyridyl nitrogen, respectively **[Chart 7.2]**. The pK_a value of N-MC equilibrium is 4.5.

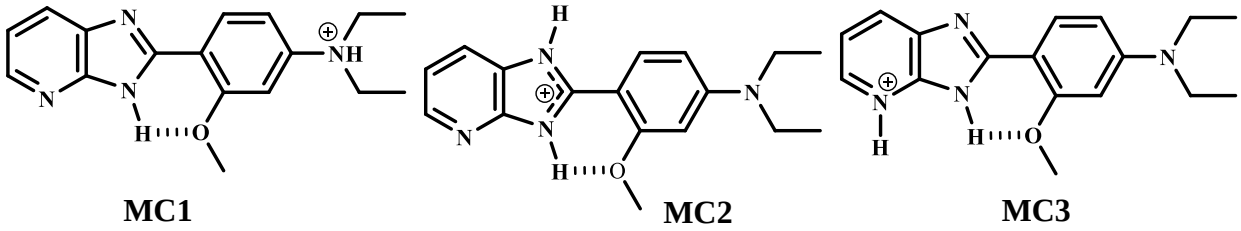

Chart 7.2: The monocations of DEAMPIP-b.

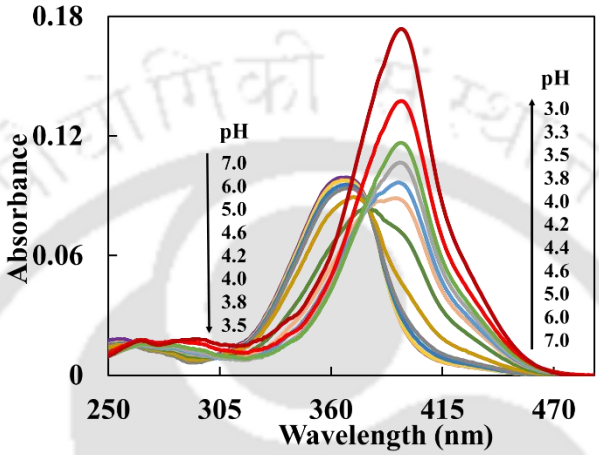

Figure 7.24: Absorption spectra of DEAMPIP-b in acidic medium at pH 7.0 to 3.0.

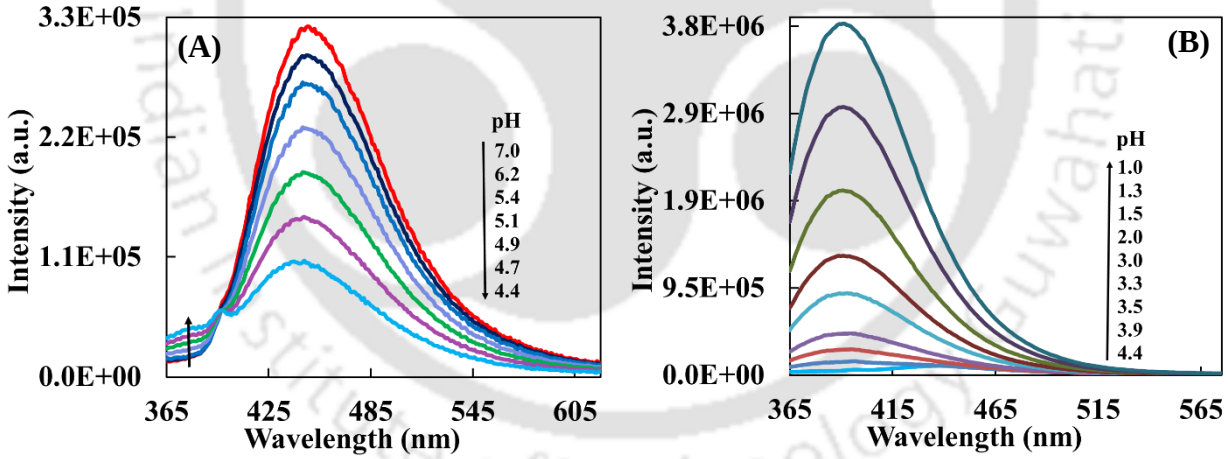

Figure 7.25: Emission spectra of DEAMPIP-b at pH **(A)** 7.0 to 4.4 and **(B)** 4.4 to 1.0, λ_{exc} = 350 nm.

On exciting at 350 nm, the emission intensity of DEAMPIP-b at 448 nm decreases and the intensity at 390 nm increases from 7.0 to 4.4 **[Figure 7.25.A]**. On further increasing the acidity up to pH 1.0, the intensity at 380 nm increases without any shift **[Figure 7.25.B]**. This indicates the conversion of the neutral molecule to monocations. On exciting at isosbestic point 376 nm, the emission intensity at 445 nm decreases hypsochromically **[Figure 7.26.A]** and in the normalized spectra, a small hump at 395 nm is visible **[Figure 7.26.B]**.

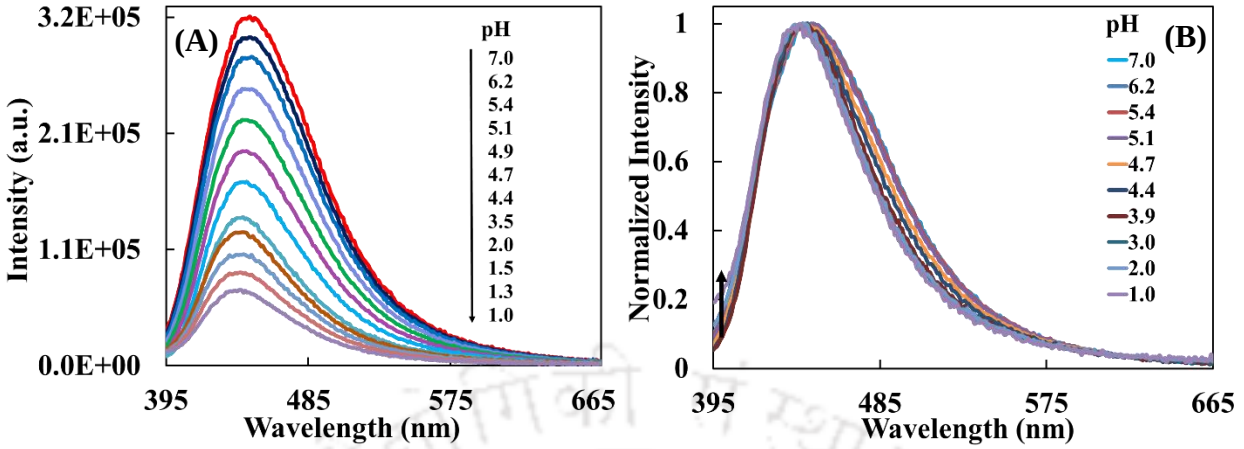

Figure 7.26: (A) Emission spectra and **(B)** normalized emission spectra of DEAMPIP-b at pH 7.0 to 1.0, λ_{exc} = 376 nm.

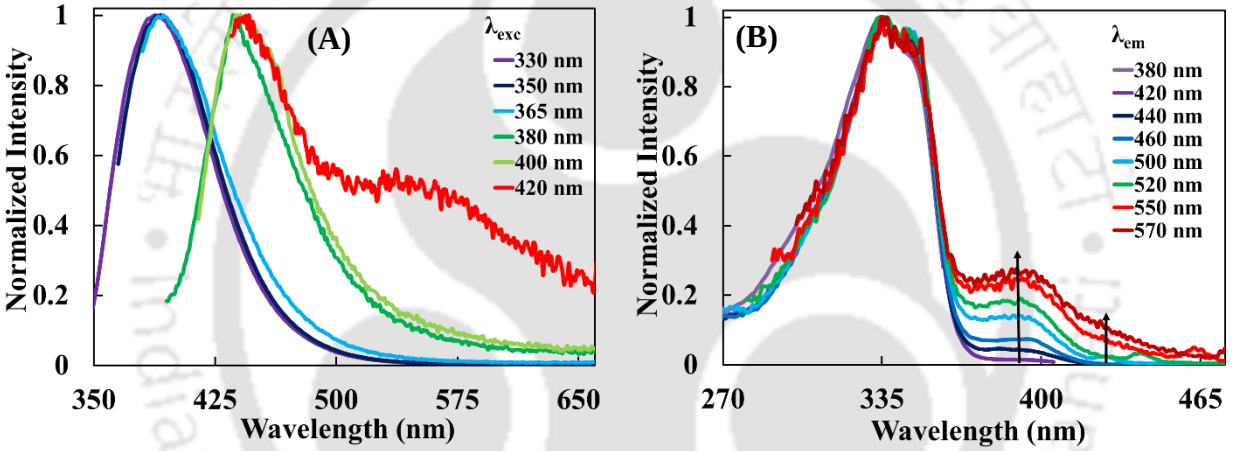

Figure 7.27: (A) Normalized emission spectra recorded at different excitation and **(B)** normalized excitation spectra recorded at different emission of DEAMPIP-b at pH 1.0.

At pH 1.0, the emission spectra of DEAMPIP-b obtained by exciting at different wavelength clearly show three emission maxima at 390 nm, 442 nm and 550 nm **[Figure 7.27.A]**. The excitation spectra recorded at different emission wavelength is dominated by a band at 336 nm **[Figure 7.27.B]**. When monitored at 440 nm or 460 nm, one small band appears at 395 nm. When monitored at longer wavelength, the relative intensity of the 395 nm band increases, but still the 336 nm band dominance continues and another small band appears at 430 nm **[Figure 7.27.B]**. The 395 nm and 430 nm excitation spectral band are same as in that of the absorption spectrum, shows the presence of MC2 and MC3 **[Chart 7.2]**. Same as in the absorption spectrum based on the spectral shift, 550 nm can be assigned to MC3. The 442 nm band at this pH is close to the emission maximum of the neutral molecule. But the excitation maximum as well as excitation spectral pattern are different at pH 7.0 and pH 1.0. Also this 442 nm band is close to MC2 emission

in DEAHPIP-b (450 nm). Further, theoretically obtained emission energy of MC2 is close to this energy **[Table 7.4]**. Again the lifetime obtained on monitoring the decay at 440 nm is 1.3 ns, different from the lifetime of neutral species (0.2 ns). Hence, the 442 nm emission can be assigned to MC2. The 380 nm emission and the corresponding excitation spectra at 336 nm are blue shifted with respect to neutral molecule, therefore can be assigned to MC1. In the absorption spectrum, bands of MC2 and MC3 are observed, but no clear band was observed for MC1. It is buried under predominating 390 nm absorption band of MC2. However, the emission spectrum is dominated by MC1. This suggests that the radiative decay of MC1 is higher than that of MC2 and MC3. Since, the absorption spectra of all three cations are overlapping, it was not feasible to measure the quantum yields of the MCs.

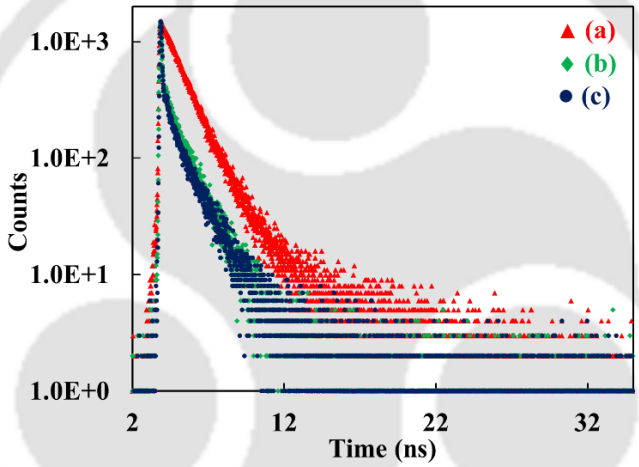

Figure 7.28: The fluorescence decays of DEAMPIP-b monitored at ▲ **(a)** 390 nm, ♦ **(b)** 440 nm and ● **(c)** 550 nm at pH 1.0, λ_{exc} = 375 nm.

The fluorescence decays were also monitored at 390 nm and 550 nm **[Figure 7.28]**. The lifetimes are 1.4 ns (93 %), 7.4 ns (7 %) at 390 nm and 0.4 ns (47 %), 1.6 ns (53 %) at 550 nm. From the monitoring wavelength, the 7.4 ns and 0.4 ns lifetimes can be assigned to MC1 and MC3, respectively. The lifetimes, 1.4 ns and 1.6 ns are same within the error limit and can be assigned to MC2 from the fact that the 442 nm band overlaps with 390 nm and 550 nm emission. Theoretically obtained excitation energies and emission energies of MCs are also close to experimental energies **[Table 7.4]** The 380 nm emission of MC1 of DEAMPIP-b also confirms that the 465 nm emission is the tautomer emission of MC1 of DEAHPIP-b rather than its normal emission.

7.2.3. Monocations - Dications equilibrium

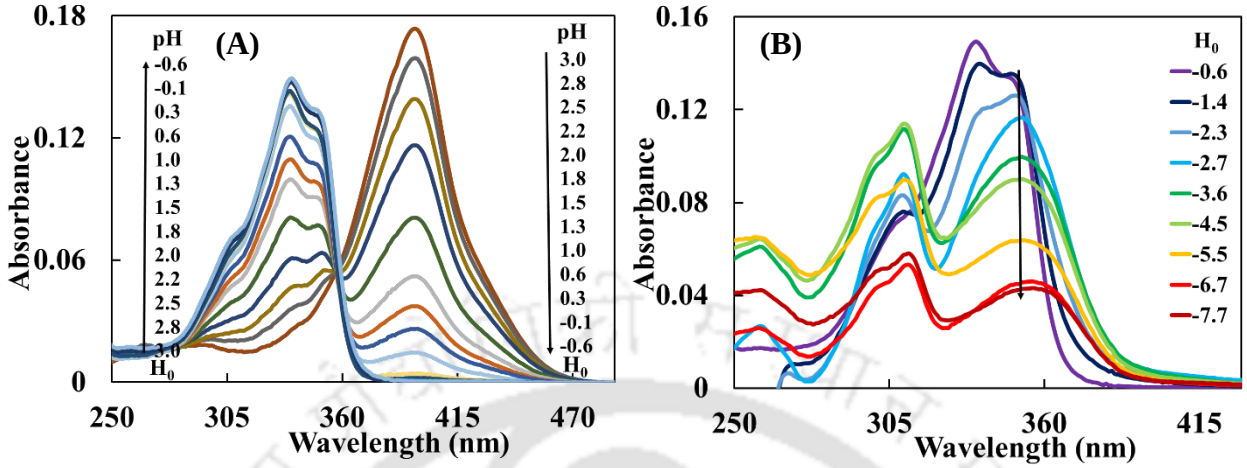

Figure 7.29: Absorption spectra of DEAMPIP-b in acidic medium at **(A)** pH 3.0 to H_0 –0.6 and **(B)** H_0 –0.6 to –7.7.

Similar to the absorption spectra of DEAHPIP-b, on decreasing the pH from 3.0 to H_0 –0.6, the absorption spectra of DEAMPIP-b are slowly blue shifted and a more structured band appear at 336 nm with a quasi isosbestic point at 359 nm **[Figure 7.29.A]**. Further decreasing till H_0 –7.7, the absorbance decreases with a red shift to 356 nm and gradually the spectra become structure less **[Figure 7.29.B]**. As discussed in **section 7.1.5**, based on the spectral shift, the 336 nm and 356 nm bands can be assigned to DC1 and DC2, respectively **[Chart 7.3]**. Theoretically calculated excitation energies of DC1 and DC2 are close to experimental excitation energies **[Table 7.4]**.

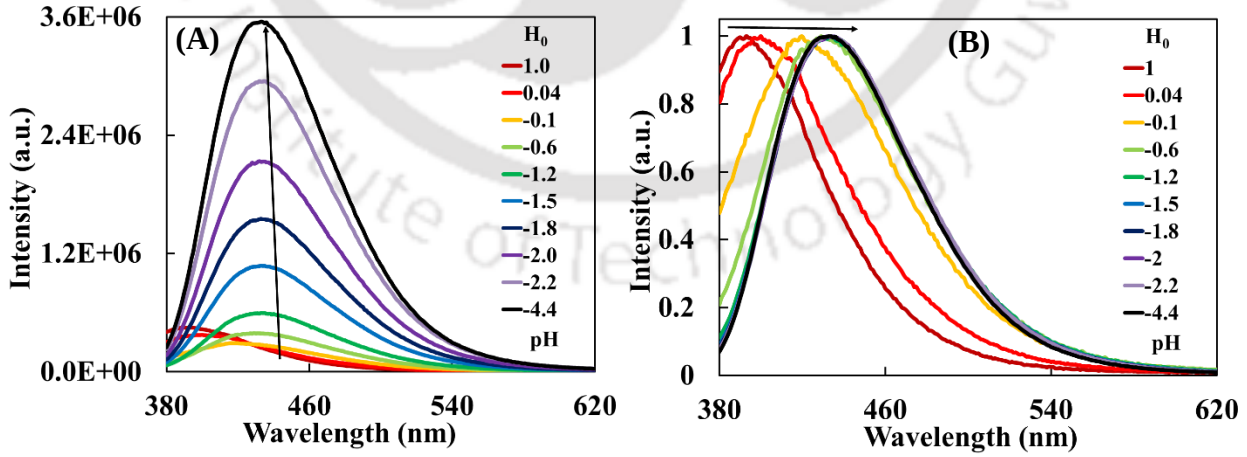

Figure 7.30: (A) The emission spectra and **(B)** normalized emission spectra of DEAMPIP-b at pH 1.0 to H_0 –4.4, λ_{exc} = 360 nm.

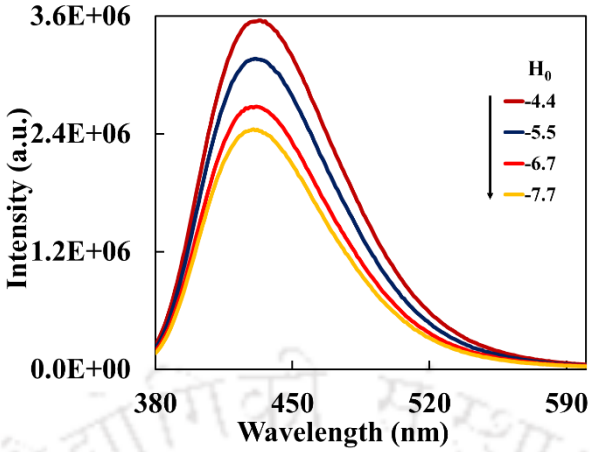

Figure 7.31: (A) The emission spectra of DEAMPIP-b at H_0 –4.4 to –7.7, λ_{exc} = 360 nm.

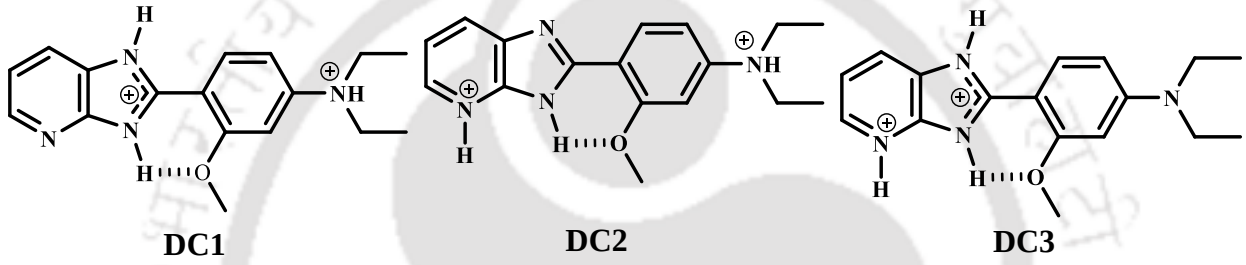

Chart 7.3: The dications of DEAMPIP-b.

Upon increasing the acidity of the solution from pH 1.0 to H_0 –4.4, the emission intensity at 390 nm decreases and at 435 nm increases **[Figure 7.30.A]**. Also, the spectrum continuously shifts bathochromically **[Figure 7.30.B]**. Further increasing the acidity till H_0 –7.7, the emission intensity at 435 nm only decreases a little **[Figure 7.31]**. At H_0 –0.6 and –7.7, the emission spectra at different excitation show the presence of two bands at 435 nm and 490 nm **[Figure 7.32.A** and **7.33.A]**. The emission band at 435 nm is strong and at the 490 nm is very weak. At H_0 –0.6, the excitation spectra are independent of emission wavelength and the excitation maximum is 336 nm **[Figure 7.32.B]**. At H_0 –7.7, the excitation maximum is at 356 nm when monitored at shorter wavelengths and one small hump around ~ 420 nm along with 356 nm is observed when monitored at longer wavelength **[Figure 7.33.B]**. The excitation maximum and absorption maximum at H_0 –0.6 and –7.7 match with each other. Hence, the 336 nm and 356 nm excitation bands are due to DC1 and DC2, respectively **[Chart 7.3]**. The small broad band at 420 can be assigned to DC3 **[Chart 7.3]**. The spectral shifts also consistent with the assignment. The 435 nm emission maximum obtained on exciting at shorter wavelength can be assigned to DC1 of methoxy derivative. The emission is also close to the normal emission of DC1 of DEAHPIP-b **[Table 7.1]**

and the theoretically obtained emission energy of DC1 is also close to the experimental result **[Table 7.4]**. The emission maximum at 490 nm attained on exciting at longer wavelength and the excitation maximum at around 420 nm can be assigned to DC3 **[Chart 7.3]**. As stated earlier, the energy of DC3 should be red shifted with respect to other DCs, theoretical data also exclaims the same.

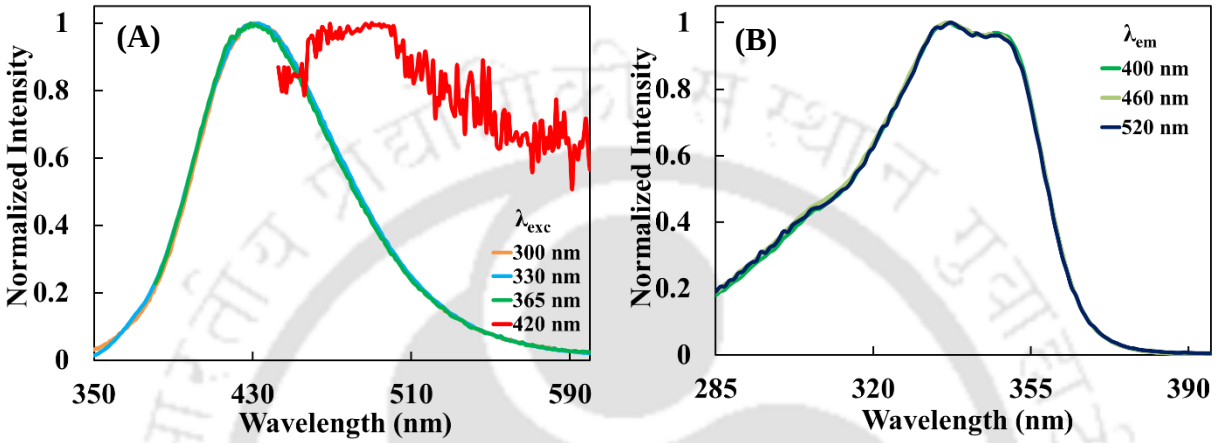

Figure 7.32: (A) Normalized emission spectra recorded at different excitation and **(B)** normalized excitation spectra recorded at different emission of DEAMPIP-b at H_0 −0.6.

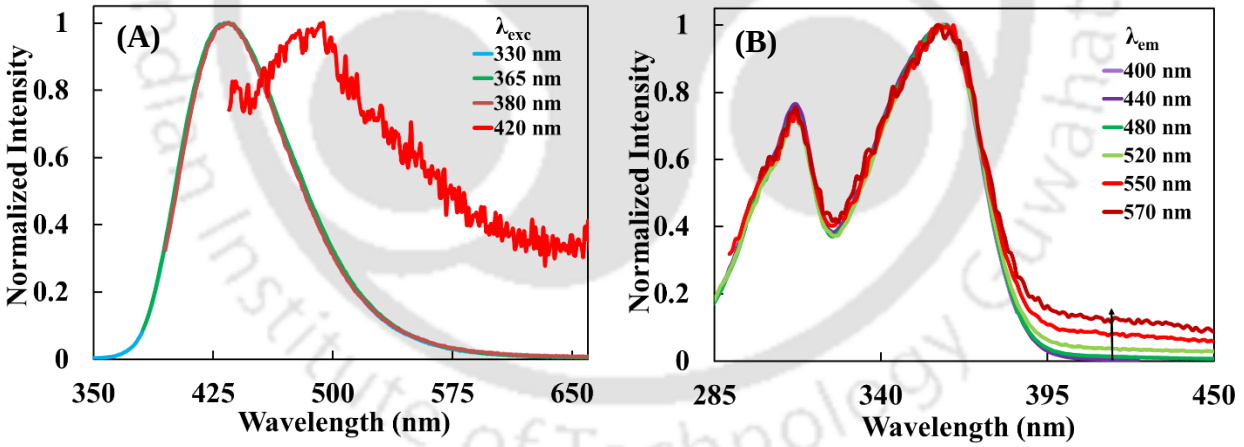

Figure 7.33: (A) Normalized emission spectra recorded at different excitation and **(B)** normalized excitation spectra recorded at different emission of DEAMPIP-b at H_0 −7.7.

The fluorescence decays **[Figure 7.34]** obtained at emission maxima of DCs show at 435 nm, the lifetimes are 2.7 ns (92 %) and 4.8 ns (8 %). The shorter lifetime which is having higher relative amplitude can be assigned to DC1. The deacys at 490 nm are 2.7 ns (97 %) and 6.8 ns (3 %). The longer lifetime 6.8 ns can be assigned to DC3. The presence of shorter lifetime with higher relative amplitude shows DC1 is the predominating species. The existence of another

lifetime 4.8 ns when monitored at 435 nm shows there is presence of DC2, which is buried under the spectra of DC1 and DC3 and no clear emission band for DC2. Theoretically obtained emission energies of DC1 and DC2 are also close, which further supports the experimental result that the emission spectrum of DC2 is buried under the spectra of DC1 and DC3. The single normal emission from DC1 of DEAMPIP-b confirms that the longer emission from the hydroxyl derivative corresponds to tautomer emission of dication.

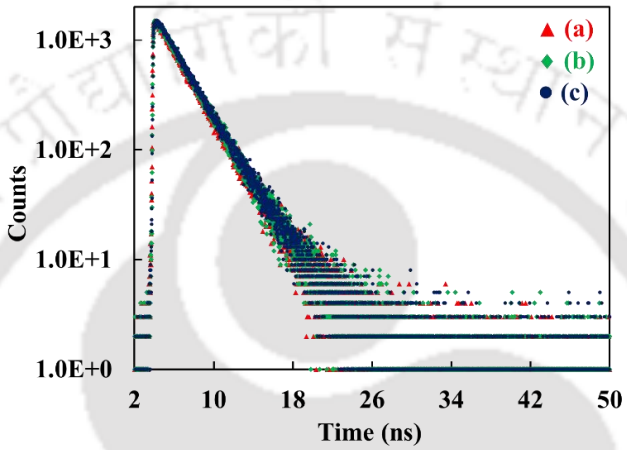

Figure 7.34: The fluorescence decays of DEAMPIP-b monitored ▲ (**a**) 435 nm, ♦ (**b**) 445 nm and ● (**c**) 490 nm at H_0 –7.7, λ_{exc} = 375 nm.

7.2.4. Dications - Trication equilibrium

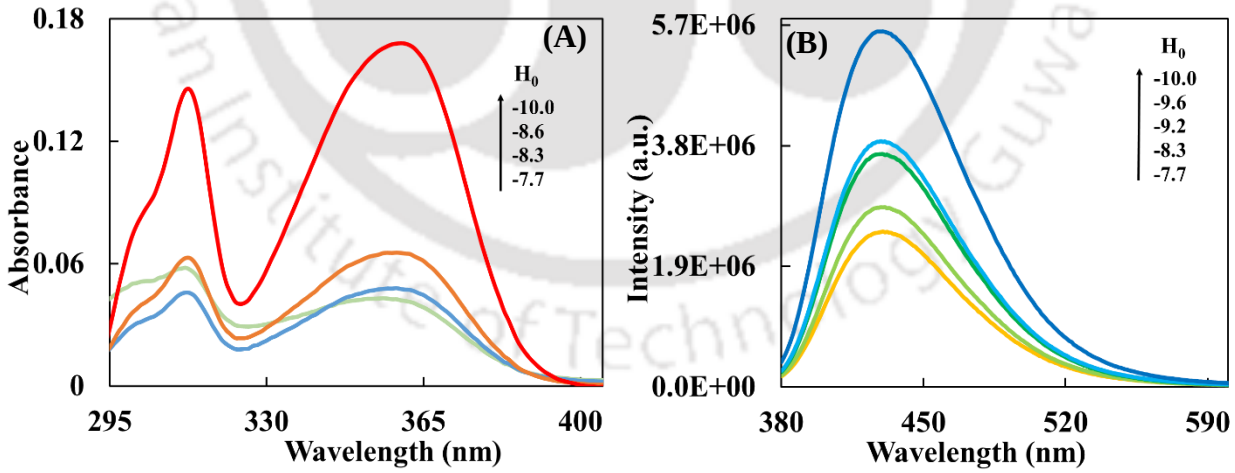

Figure 7.35: (A) Absorption spectra and **(B)** emission spectra of DEAMPIP-b in acidic medium at H_0 –7.7 to –10.0 at λ_{exc} = 350 nm.

On increasing the acidity of the solution from H_0 –7.7 to –10.0, the absorption spectra of DEAMPIP-b further shift a little towards longer wavelength to 360 nm and the absorbance increases **[Figure 7.35.A]**. This is due to the formation of TC. The emission intensity also increases

on increasing the acidity of the solution from H_0 −7.7 to −10.0 **[Figure 7.35.B]**. A single emission is observed at 430 nm which is independent of excitation wavelength **[Figure 7.36.A]** and is single exponential decay with 4.7 ns lifetime **[Figure 7.36.B]**. This emission energy is exactly matching to theoretical emission energy of TC **[Table 7.4]**. Hence the emission at 430 nm having lifetime 4.7 ns at H_0 −10.0 can be assigned to the normal emission of TC.

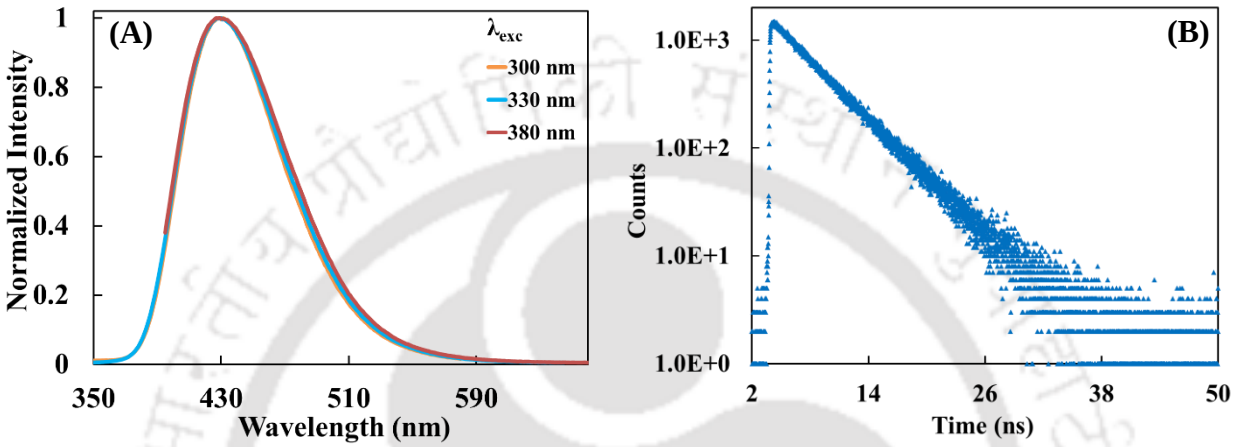

Figure 7.36: (A) Normalized emission spectra recorded at different excitation and **(B)** the fluorescence decay of DEAMPIP-b monitored at 430 nm at H_0 −10.0, λ_{exc} = 375 nm.

7.3. Conclusion

The hydroxy derivative, DEAHPIP-b emits only tautomer emission in neutral form. Upon deprotonation it forms both the monoanions. When protonated it also forms all three possible monocations. While MC2 and MC3 emit normal emission, MC1 emits exclusive tautomer emission. DEAHPIP-b also forms all three different possible dications. DC2 and DC3 exhibit single emission. Interestingly upon excitation DC1 emits both normal and tautomer emissions. The keto tautomer of the neutral and the monocation are formed by intramolecular proton transfer in the excited state. But the keto tautomer of the dication is formed by intermolecular proton transfer in the excited state. Though 'OH' proton is transferred in all the proton transfer processes, in neural form and monocationic form it is transfer to imidazole nitrogen, in dicationic form it is transferred to pyridyl nitrogen. Hence, DC1 rearrange to form DC2 keto tautomer. The spectral data of different prototropic species of the methoxy derivatives and the theoretical calculations substantiate the assignments to different species.

Chapter 8

Summary and Scope for Future Work

8.1. Summary of the Present Thesis Work

In the present thesis, the modulation of ESIPT and ICT by different environments is investigated using few azole derivatives as model systems **[Scheme 8.1]**. In chapter 3, the modulation of ESIPT by metal ion and its regaining using inclusion host CD and CB were reported. In chapter 4, the effect of solvent on PT of a molecule with additional PT unit and its recovery using silver particle were presented. In the next three chapters, the modulation of a system with both PT and CT units was studied. In chapter 5, modulation/tuning of PT and CT system by solvents was shown. In chapter 6 and 7, tuning the competitive paths by nanoparticles and pH were respectively, presented.

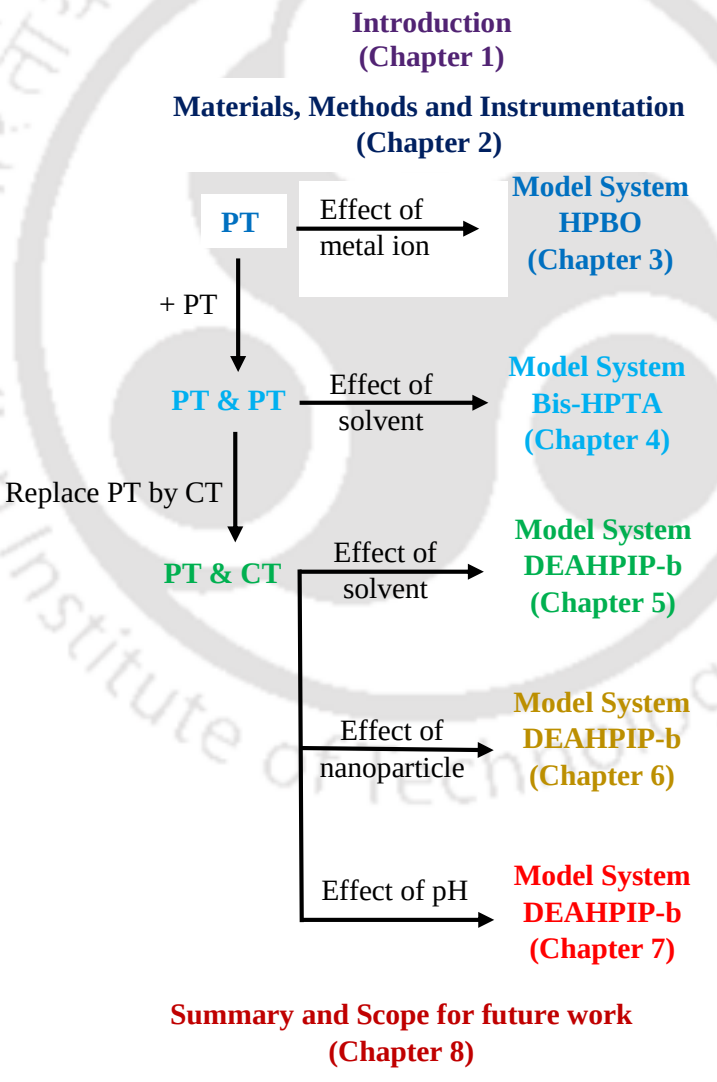

Scheme 8.1: Organization of the thesis.

HPBO is a simple and one of the most studied ESIPT active azole derivative. Modulation of the ESIPT process of HPBO was presented. Initially, the ESIPT process is blocked by chelating with Zn^{2+} ion, and then ESIPT process is restored by forming an inclusion complex with the host molecules. HPBO exhibits normal emission at around ~ 360 nm and stokes' shifted tautomer emission at around ~ 500 nm in polar solvents acetonitrile, DMSO and water. The fluorophore forms fluorescent metal complex only with Zn^{2+} giving blue emission. According to literature survey, CB-7 has greater binding affinity towards the cationic guests compared to neutral ones. Hence, to get enhanced fluorescence emission from HPBO–Zn^{2+} complex, the effect of CB-7 on this complex was investigated. Contrary to the common expectation, instead of enhancing the metal complex interaction, CB-7 breaks the complex and sets HPBO free by restoring its ESIPT emission in both DMSO and aqueous medium. Effect of another host molecule β-CD was also investigated. Unlike CB-7, β-CD was incapable to break the fluorophore metal complex in DMSO. However, in aqueous medium, β-CD also breaks the fluorophore metal complex, and restores its ESIPT.

The photophysics of fluorophores having dual ESIPT system are more interesting. In nonpolar solvents THF, amongst twelve possible conformers, bis-HPTA exist only as bis-HPTA-I. In bis-HPTA-I, among two proton donor-acceptor pairs, initially, only one pair is ESIPT (ESIPT-I) active and another pair is ESIPT (ESIPT-II) inactive due to shuttling annular tautomerism. ESIPT-I triggers the ESIPT-II. In contrary to our anticipation DMF will help to prevent annular tautomerism; DMF completely alters the conformational equilibrium of bis-HPTA. Bis-HPTA forms complex with DMF and exists as bis-HPTA-II and bis-HPTA-III DMF complexes. The excited bis-HPTA-II complex undergoes intermolecular proton transfer and emits anionic emission at shorter wavelength. On the other hand, upon excitation bis-HPTA-III undergoes intramolecular proton transfer and gives tautomer emission. Silver particle removes the DMF from the complex and the equilibrium shifts back to bis-HPTA-I and restores its photophysics as in nonpolar solvent.

The competitive reactions coordinates, ESIPT and TICT of DEAHPIP-b can be controlled by solvents. While the trans-enol emits normal emission, the cis-enol emits tautomer or/and TICT emission depending on the solvent. In nonpolar and polar aprotic solvents and less protic solvents (butanol, 2-propanol, 1-propanol) ESIPT process predominates over TICT. In more polar strong

protic solvent, methanol TICT suppresses the ESIPT. In a relatively less protic solvent, ethanol, both ESIPT and TICT compete with each other. This is because of the competition between the intramolecular proton transfer and intermolecular proton transfer. In less protic environment, intramolecular proton transfer leads to tautomer emission. In more protic solvents, the intermolecular proton transfers from imidazole nitrogen to pyridyl nitrogen through solvent molecule induces the TICT emission. Thus, the reaction coordinates switches between ESIPT and TICT depending on the solvents. Theoretically calculated emission energies also match with the experimental values.

The competing processes ESIPT and TICT of DEAHPIP-b can be tuned by nanoparticle. In the polar aprotic solvent DMF, DEAHPIP-b exhibits dual emission due to normal and tautomer emission. Silver nanoparticle forms complex with DEAHPIP and switches the reaction path from ESIPT to TICT. Further addition of surfactants to DEAHPIP-b silver nanoparticle solution in DMF alters the process. The anionic surfactant SDS restores the ESIPT process by completely detaching the molecule from the nanoparticle. The nonionic surfactant TX-100, at lower concentration, enhances the TICT emission and the ESIPT process is also observed due to the release of some fluorophore from the nanoparticle complex. But at higher concentration all the fluorophores are released and it completely restores the ESIPT process. The cationic surfactant CTAB, at lower concentration, simply restores the ESIPT process by releasing the fluorophore. But at higher CTAB concentration, DEAHPIP-b enters the nanoparticle-CTAB aggregate and shows enhanced ESIPT.

The emissions of DEAHPIP-b were modulated over a broad range of wavelengths in aqueous medium by varying the pH. The fluorophore contains three basic nitrogens and two acidic protons. Hence, at different pH, the protonation/deprotonation at the basic/acidic sites led to the formation of different species. In some species, due to decrease in charge flow from donor to acceptor, the emissions are blue shifted while in some species due to increase in charge flow from donor to acceptor, the emission are red shifted. Among the possible species of DEAHPIP-b, the normal emission occurs from DA, MA2, MA1, MC2, MC3, DC1, DC2, DC3 and TC. Neutral and MC1 undergo ESIPT to emit tautomer emissions. DC1 in the excited state rearranges to DC2 tautomer and emits tautomer emission along with the normal emission. When the pH of the

solution is varied, DEAMPIP-b also emits over a broad range of wavelengths. However, all the species emit only normal emission.

8.2. Scope for the Future Work

Azole derivatives are interesting molecules with anti-cancer, anti-malarial, anti-bacterial activity and widely used for various applications in different fields. The modulation of fundamental processes, PT and CT by different environments are mainly focused in the present thesis using model systems.

The ESIPT active fluorophore HPBO studied in the present work shows it forms strong fluorescent complex with Zn^{2+}. The addition of CB-7 breaks the complex and release the Zn^{2+} ion. Hence, the study may be extended in live cells to study the possible feasibility of using HPBO as a zinc carrier.

The twin ESIPT capable, bis-HPTA has been studied only in organic solvents system and the equilibrium between only three conformers were restored by using silver particle. As a total, 12 conformers are possible in bis-HPTA, hence further these ESIPT processes, as well as the possibility of tuning the ESIPT can be explored in different media as well as in aqueous solvent. Also, the utility of the modulating emission properties for biological sensing and to construct molecular logic gates can be explored.

The ESIPT and TICT coordinates in DEAPIP-b are controlled by solvent medium, silver particle and surfactants. The reason for the low quantum yield of this fluorophore can be explored by performing a comprehensive theoretical study on conical intersection. The utility of DEAHPIP-b–nanoparticle composite in sensing the surfactants can be investigated. The studies may be extended to look into the feasibility of these nano-composites for biochemical sensing. The variation in emission in DEAHPIP-b over a broad range of wavelengths at different pH can be investigated to signal the pH change in the living system. The strong blue-green emissions in all these fluorophores can be explored for possible utility in optoelectronic devices.

References

1. D. K. Das, K. Makhal, S. Singhal and D. Goswam, *Chem. Phys. Lett.*, 2013, **579**, 45-50.
2. Y.-J. Lee, S. Datta and J.-P. Pellois, *J. Am. Chem. Soc.*, 2008, **130**, 2398-2399.
3. S. H. Mostafavi, M. Mettry, A. D. Gill, C. J. Easley, R. J. Hooley and C. J. Bardeen, *Chem. Phys. Lett.*, 2020, **741**, 137059-137064.
4. X. Wang, Y. Chen, J. Gong and J. Hou, *Org. Biomol. Chem.*, 2019, **17**, 3409-3415.
5. K. Liu, Y. Chen, H. Sun, S. Wang and F. Kong, *J. Mater. Chem. B*, 2018, **6**, 7060-7065.
6. M. Cotlet, J. Hofkens, M. Maus, T. Gensch, M. V. Auweraer, J. Michiels, G. Dirix, M. V. Guyse, J. Vanderleyden, A. J. W. G. Visser and F. C. D. Schryver, *J. Phys. Chem. B*, 2001, **105**, 4999-5006.
7. Q. J. Meisner, A. H. Younes, Z. Yuan, K. Sreenath, J. J. M. Hurley and L. Zhu, *J. Phys. Chem. A*, 2018, **122**, 9209-9223.
8. P.-T. Chou, M. L. Martinez and W. C. Cooper, *Chem. Phys. Lett.*, 1992, **198**, 188-192.
9. W. Rettig and E. A. Chandross, *J. Am. Chem. Soc.*, 1985, **107**, 5617-5624.
10. S. Sreejith, K. P. Divya, T. K. Manojkumar and A. Ajayaghosh, *Chem. Asian J.*, 2011, **6**, 430-437.
11. A. Weller, *Naturwissenschaften*, 1955, **42**, 175-176.
12. H.-Q. Yin, F. Yin and X.-B. Yin, *Chem. Sci.*, 2019, **10**, 11103-11109.
13. S. K. Behera, A. Murkherjee, G. Sadhuragiri, P. Elumalai, M. Sathiyendiran, M. Kumar, B. B. Mandal and G. Krishnamoorthy, *Faraday Discuss.*, 2017, **196**, 71-90.
14. F. A. S. Chipem, S. K. Behera and G. Krishnamoorthy, *Photochem. Photobiol. Sci.*, 2014, **13**, 1297-1304.
15. A. Maity, F. Ali, H. Agarwalla, B. Anothumakkool and A. Das, *Chem. Commun.*, 2015, **51**, 2130-2133.
16. H.-Y. Fu, X.-J. Liu, H. Zha, X.-X. Li, Y. Xu, F. Yang and M. Xia, *Phys. Chem. Chem. Phys.*, 2019, **21**, 1399-1407.
17. J. Li, C. Yang, X. Peng, Y. Chen, Q. Qi, X. Luo, W.-Y. Lai and W. Huang, *J. Mater. Chem. C*, 2018, **6**, 19-28.
18. H. Naito, K. Nishino, Y. Morisaki, K. Tanaka and Y. Chujo, *Angew. Chem. Int. Ed.*, 2017, **56**, 254-259.
19. S. K. Behera, M. Pegu and G. Krishnamoorthy, *ChemistrySelect*, 2018, **3**, 4147-4155.
20. N. Dash, F. A. S. Chipem, R. Swaminathan and G. Krishnamoorthy, *Chem. Phys. Lett.*, 2008, **460**, 119-124.
21. D. R. Weinberg, C. J. Gagliardi, J. F. Hull, C. F. Murphy, C. A. Kent, B. C. Westlake, A. Paul, D. H. Ess, D. G. McCafferty and T. J. Meyer, *Chem. Rev.*, 2012, **112**, 4016-4093.
22. S. Hayashi, E. Tajkhorshid and K. Schulten, *Biophys. J.*, 2002, **83**, 1281-1297.
23. D. Jacquemin, J. Zúñiga, A. Requena and J. P. Ceron-Carrasco, *Acc. Chem. Res.*, 2014, **47**, 2467-2474.
24. P. J. Tonge and S. R. Meech, *J. Photochem. Photobiol. A*, 2009, **205**, 1-11.
25. Y. Zhang, K. de L. Harpe, A. A. Beckstead, L. Martínez-Fernández, R. Improta and B. Kohler, *J. Phys. Chem. Lett.*, 2016, **7**, 950-954.
26. A. Samanta and N. Guchhait, *J. Lumin.*, 2014, **151**, 176-187.

27. D. Ray, A. Pramanik and N. Guchhait, *J. Photochem. Photobiol. A*, 2015, **302**, 42-50.
28. C. Li, D. Li, Y. Shi and Y. Liu, *Org. Electron.*, 2018, **54**, 177-183.
29. W.-S. Yu, C.-C. Cheng, Y.-M. Cheng, P.-C. Wu, Y.-H. Song, Y. Chi, and P.-T. Chou, *J. Am. Chem. Soc.*, 2003, **125**, 10800-10801.
30. Z. Zhang, Y.-H. Hsu, Y.-A. Chen, C.-L. Chen, T.-C. Lin, J.-Y. Shen, and P.-T. Chou, *Chem. Commun.*, 2014, **50**, 15026-15029.
31. H. Yuan, S. Feng, K. Wen, X. Guo, and J. Zhang, *Spectrochim Acta A*, 2018, **191**, 421-426.
32. F.-Y Meng, Y.-H. Hsu, Z. Zhang, P.-J. Wu, Y.-T. Chen, Y.-A. Chen, C.-L. Chen, C.-M. Chao, K.-M. Liu, and P.-T. Chou, *Chem. Asian J.*, 2017, **12**, 3010-3015.
33. K.-C. Tang, C.-L. Chen, H.-H. Chuang, J.-L. Chen, Y.-J. Chen, Y.-C. Lin, J.-Y. Shen, W.-P. Hu and P.-T. Chou, *J. Phys. Chem. Lett.*, 2011, **2**, 3063-3068.
34. J. Zhao and Y. Zheng, *Sci. Rep.*, 2017, **7**, 44897-44905.
35. X. Liu, J. Zhao and Y. Zheng, *RSC Adv.*, 2017, **7**, 51318-51323.
36. C.-Y. Peng, J.-Y. Shen, Y.-T. Chen, P.-J. Wu, W.-Y. Hung, W.-P. Hu and P.-T. Chou, *J. Am. Chem. Soc.*, 2015, **137**, 14349-14357.
37. Y.-T. Chen, P.-J. Wu, C.-Y. Peng, J.-Y. Shen, C.-C. Tsai, W.-P. Hu and P.-T. Chou, *Phys. Chem. Chem. Phys.*, 2017, **19**, 28641-28646.
38. R. Wortmanna, S. Lebusa, H. Reisa, A. Grabowska, K. Kownacki and S. Jarosz, *Chem. Phys.*, 1999, **243**, 295-304.
39. Y. Zhang, M. Sun and Y. Li, *Sci. Rep.*, 2016, **6**, 25568-25574.
40. A. J. Stasyuk, Y. –T. Chen, C. –L. Chen, P. –J. Wu, and P. –T. Chou, *Phys. Chem. Chem. Phys.*, 2016, **18**, 24428-24436.
41. O. K. Abou-Zied, *J. Phys. Chem. B*, 2010, **114**, 1069-1076.
42. P. Zhou, M. R. Hoffmann, K. Han and G. He, *J. Phys. Chem. B*, 2015, **119**, 2125-2131.
43. S. Lazzaroni, D. Dondi, A. Mezzetti and S. Protti, *Photochem. Photobiol. Sci.*, 2018, **17**, 923-933.
44. C. A. Rumble, J. Breffke and M. Maroncelli, *J. Phys. Chem. B*, 2017, **121**, 630-637.
45. S. M. Aly, A. Usman, M. AlZayer, G. A. Hamdi, E. Alarousu and O. F. Mohammed, *J. Phys. Chem. B*, 2015, **119**, 2596-2603.
46. K. Sakai, T. Ishikawa and T. Akutagawa, *J. Mater. Chem. C*, 2013, **1**, 7866-7871.
47. F. A. S. Chipem, A. Malakar and G. Krishnamoorthy, *Photochem. Photobiol*, 2015, **91**, 298-305.
48. J. Zhao, H. Dong, H. Yang and Y. Zheng, *ACS Appl. Bio Mater.*, 2019, **2**, 2060-2068.
49. W. A. Muriel, R. Morales-Cueto and W. Rodriguez-Cordoba, *Phys. Chem. Chem. Phys.*, 2019, **21**, 915-928.
50. M. Krishnamurthy and S. K. Dogra, *J. Photochemistry*, 1986, **32**, 235-242.
51. G. Krishnamoorthy and S. K. Dogra, *J. Lumin.*, 2000, **92**, 103-114.
52. V. R. Mishra, C. W. Ghanavatkar and N. Sekar, *J. Lumin.*, 2019, **215**, 116689-116697.
53. Q. Q. Wang, L. Y. Zhou, L. P. Qiu, D. Q. Lu, Y. X. Wu and X. B. Zhang, *Analyst*, 2015, **140**, 5563-5569.
54. K.-I. Hong, S.-H. Park, S. M. Lee, I. Shin and W.-D. Jang, *Sens. Actuators B Chem.*, 2019, **286**, 148-153.

55. Z. Mao, L. Hu, C. Zhong, H. Zhang, B.-F. Liu, Z. Liu, *Sens. Actuators B Chem.*, 2015, **219**, 179-184.
56. J. F. Wang, Y. B. Li, N. G. Patel, G. Zhang, D. M. Zhou and Y. Pang, *Chem. Commun.*, 2014, **50**, 12258-12261.
57. M. Ebina, Y. Kondo, T. Iwasa and T. Taketsugu, *Inorg. Chem.*, 2019, **58**, 4686-4698.
58. Z. Xu, M. Zhang, R. Zhang, S. Liu and Y. Yang, *RSC Adv.*, 2019, **9**, 27937-27944.
59. M. Gupta, S. Sahana, V. Sharma and P. K Bharadwaj, *Dalton Trans.*, 2019, **48**, 7801-7808.
60. A. Micera, L. Bruno, A. Cacciamani, M. Rongioletti and R. Squitti, *Curr. Alzheimer Res.*, 2019, **16**, 1073-1083.
61. N. Gonzalez, T. Arcos-Lopez, A. Koenig, L. Quintanar, M. M. Marquez, T. F. Outeiro and C. O. Fernandez, *J. Neurochem.*, 2019, **150**, 507-521.
62. H. Rubin, *Bioessays*, 2005, **27**, 311-320.
63. J. M. Berg and Y. G. Shi, *Science*, 1996, **271**, 1081-1085.
64. S. L. Sensi, P. Paoletti, A. I. Bush and I. Sekler, *Nat. Rev. Neurosci.*, 2009, **10**, 780-791.
65. I. Caracelli, I. Haiduc, J. Zukerman-Schpector and E. R. T. Tiekink, Monographs in Supramolecular Chemistry, Aromatic Interactions: Frontiers in Knowledge and Application, 2017, **20**, 98-123.
66. A. J. Plajer, F. J. Rizzuto, H.-C. Niu, S. Lee, J. M. Goodman and D. S. Wright, *Angew. Chem. Int. Ed.*, 2019, **58**, 10655-10659.
67. G. Ju, M. Cheng, F. Guo, Q. Zhang and F. Shi, *Angew. Chem. Int. Ed.*, 2018, **57**, 8963-8967.
68. K. S. Mali, N. Pearce, S. D. Feyter and N. R. Champness, *Chem. Soc. Rev.*, 2017, **46**, 2520-2542.
69. M. Du, L. Yang, C. Liao, T. P. Diangha, Y. Ma, L. Zhang, Y. Lan and G. Chang, *Macromol. Rapid Commun.*, 2020, 41, e1900606.
70. A. C. Sedgwick, W.-T. Dou, J.-B. Jiao, L. Wu, G. T. Williams, A. T. A. Jenkins, S. D. Bull, J. L. Sessler, X.-P. He and T. D. James, *J. Am. Chem. Soc.*, 2018, **140**, 14267-14271.
71. S. Sahana, G. Mishra, S. Sivakumar and P. K. Bharadwaj, *Dalton Trans.*, 2015, **44**, 20139-20146.
72. K. Pramanik, P. Ghosh, D. Dey, P. Malpaharia, S. K. Chandra, S. K. Mukhopadhyay and P. Banerjee, *ChemistrySelect*, 2018, **3**, 1151-1156.
73. C. Wu, Y. Jin, D. Li, L. Ding, Y. Xing, K. Zhang and B. Song, *Soft Matter*, 2018, **14**, 4374-4379.
74. F. S. Santos, E. Ramasamy, V. Ramamurthy and F. S. Rodembusch, *J. Photochem. Photobiol. A*, 2016, **317**, 175-185.
75. F. A. S. Chipem, S. K. Behera and G. Krishnamoorthy, *J. Phys. Chem. A*, 2013, **117**, 20, 4084-4095.
76. M. Shaikh, S. Dutta Choudhury, J. Mohanty, A. C. Bhasikuttan, W. M. Nau and H. Pal, *Chem. Eur. J.*, 2009, **15**, 12362-12370.
77. R. Das, G. Duportail, L. Richert, A. Klymchenko and Y. Mely, *Langmuir*, 2012, **28**, 7147-7159.
78. S. Ghosh, J. Kuchlyan, S. Roychowdhury, D. Banik, N. Kundu, A. Roy, and N. Sarkar, *J. Phys. Chem. B*, 2014, **118**, 9329-9340.

79. M. Sarkar and P. K. Sengupta, *Chem. Phys. Lett.*, 1991, **179**, 68-72.
80. H. X. Zhang and O. Annunziata, *Langmuir*, 2008, **24**, 10680-10687.
81. P. A. Bhat, G. M. Rather and A. A. Dar, *J. Phys. Chem. B*, 2009, **113**, 997-1006.
82. M. H. M. Leung, H. Colangelo and T. W. Kee, Langmuir, 2008, **24**, 5672-5675.
83. R. Adhikary, P. J. Carlson, T. W. Kee and J. W. Petrich, *J. Phys. Chem. B*, 2010, **114**, 2997-3004.
84. S. Mondal, S. Basu and D. Mandal, *Chem. Phys. Lett.*, 2009, **479**, 218-223.
85. P. M. Gashnga, T. S. Singh, T. S. BasuBaul and S. Mitra. *J. Lumin.*, 2014, **148**, 134-142.
86. M. Gao, L. Wang, J. Chen, S. Li, G. Lu, L. Wang, Y. Wang, L. Ren, A. Qin, and B. Z. Tang, *Chem. Eur. J.*, 2016, **22**, 5107-5112.
87. X. He, F. Yang, S. Li, X. He, A. Yu, J. Chen, J. Xu and J. Wang, *J. Phys. Chem. A*, 2019, **123**, 6463-6471.
88. G. Ren, Q. Meng, J. Zhao and T. Chu, *J. Mol*, 2018, **264**, 48-53.
89. M. Savarese, P. A. Netti, N. Rega, C. Adamo and I. Ciofini, *Phys. Chem. Chem. Phys.*, 2014, **16**, 8661-8666.
90. T. Kumpulainen, B. H. Bakker, M. Hilbers and A. M. Brouwer, *J. Phys. Chem. B*, 2015, **119**, 2515-2524.
91. A. A. Awasthi and P. K. Singh, *ChemPhysChem*, 2018, **19**, 198-207.
92. M. Itoh, T. Adachi and K. Tokumura, *J. Am. Chem. Soc.*, 1984, **106**, 850-855.
93. K. Kerdpol, R. Daengngern, J. Meeprasert, S. Namuangruk and N. Kungwan, *Theor. Chem. Acc.*, 2016, **135**, 1-9.
94. M. Esboui, *J. Chem. Phys.*, 2015, **143**, 034306-034318.
95. R. Salaeh, C. Prommin, W. Chansen, K. Kerdpol, R. Daengngern and N. Kungwan, *J. Mol*, 2018, **252**, 428-438.
96. H. Matsumoto, S. Ikedu, T. Tosaka, Y. Nishimura and T. Arai, *Photochem. Photobiol. Sci.*, 2018, **17**, 561-569.
97. P. J. Pacheco-Linan, J. Fernandez-Sainz, I. Bravo, A. Garzon-Ruiz, C. Alonso-Moreno, F. Carrillo-Hermosilla, A. Antinolo and J. Albaladejo, *J. Phys. Chem. C*, 2018, **122**, 9363-9373.
98. S. K. Mondal, K. Sahu, S. Ghosh, P. Sen, and K. Bhattacharyya, *J. Phys. Chem. A*, 2006, **110**, 13646-13652.
99. M. Mukhopadhyay, D. Banerjee, A. Koll, A. Mandal, A. Filarowski, D. Fitzmaurice, R. Das and S. Mukherjee, *J. Photochem. Photobiol. A*, 2005, **175**, 94-99.
100. K. M. Solntsev, A. V. Popov, V. A. Solovyeva1, S. A. Al-Ainain, Y. V. Ilichev, R. Hernandez and M. G Kuzmin, *Methods Appl. Fluoresc.*, 2016, **4**, 014001.
101. N. Basilio, C. A. Laia and F. Pina, *J. Phys. Chem. B*, 2015, **119**, 2749-2757.
102. P. M. Gashnga, T. S. Singh and S. Mitra, *J. Mol*, 2016, **218**, 549-557.
103. J. Herbich and A. Kapturkiewicz, *J. Am. Chem. Soc.*, 1998, **120**, 1014-1029.
104. H. Park, H. Kim, G. Moon and W. Choi, *Energy Environ. Sci*., 2016, **9**, 411-433.
105. S. Sumalekshmy and K. R. Gopidas, *J. Phys. Chem. B*, 2004, **108**, 3705-3712.
106. M. M. Raikwar, E. Mathew, M. Varghese, I. H. Joe and S. N. Nethi, *Photochem. Photobiol.*, 2019, **95**, 931-945.

107. J. Su, W. Chen, F. Wu, X. Bai, W. Du, L. Fang, Y. Wu, X. Wen, H. Wang and X. Ba, *Dyes Pigm.*, 2019, **162**, 808-814.
108. Y. Wan, J. Li, X. Peng, C. Huang, Q. Qi, W.-Y. Lai and W. Huang, *RSC Adv.*, 2017, **7**, 35543-35548.
109. G. E. Collins, L.-S. Choi and J. H. Callahan, *J. Am. Chem. Soc.*, 1998, **120**, 1474-1478.
110. A. B. J. Parusel, G. Koehler and S. Grimme, *J. Phys. Chem. A*, 1998, **102**, 6297-6306.
111. A. L. Sobolewski and W. Domcke, *Chem. Phys. Lett.*, 1996, **259**, 119-127.
112. K. A. Zachariasse, S. I. Druzhinin, W. Bosch and R. Machinek, *J. Am. Chem. Soc.*, 2004, **126**, 1705-1715.
113. E. Lippert, W. Leder, F. Moll, W. Naegele, H. Boos, H. Prigge and I. Seibold-Blankenstein, *Angew. Chem. Int. Ed.*, 1961, **73**, 695-706.
114. W. Rettig, *Angew. Chem. Int. Ed.*, 1986, **25**, 971-988.
115. G. E. Purnell, M. T. McNally, P. R. Callis and R. A. Walker, *J. Am. Chem. Soc.*, 2020, **142**, 2375-2385.
116. D. Zuniga-Nunez, R. A. Zamora, P. Barrias, C. Tirapegui, H. Poblete, G. Cardenas-Jiron, E. I. Alarcon and A. Aspee, *Phys. Chem. Chem. Phys.*, 2018, **20**, 27621-27629.
117. Y. Li, X. Liu, J. Han, B. Cao, C. Sun, L. Diao, H. Yin and Y. Shi, *Spectrochim Acta A*, 2019, **222**, 117244-117250.
118. W. G. Santos, J. Pina, D. H. Burrows, M. D. E. Forbes and D. R. Cardoso, *Photochem. Photobiol. Sci.*, 2016, **15**, 1124-1137.
119. S. I. Druzhinin, V. A. Galievsky, A. Demeter, S. A. Kovalenko, T. Senyushkina, S. R. Dubbaka, P. Knochel, P. Mayer, C. Grosse, D. Stalke and K. A. Zachariasse, *J. Phys. Chem. A*, 2015, **119**, 11820-11836.
120. T. S. Singh and S. Mitra, *J. Lumin.*, 2007, **127**, 508-514.
121. F. A. S. Chipem, A. Mishra and G. Krishnamoorthy, *Phys. Chem. Chem. Phys.*, **14**, 8775-8790.
122. S. Biswas, I. Bhattacharya and T. Chakraborty, *J. Phys. Chem. A*, **123**, 10563-10570.
123. A. Mishra, S. Sahu, N. Dash, S. K. Behera and G. Krishnamoorthy, *J. Phys. Chem. B*, 2013, **117**, 9469-9477.
124. S. K. Behera and G. Krishnamoorthy, *Photochem. Photobiol. Sci.*, 2015, **14**, 2225-2237.
125. E. Fasani, A. Albini, P. Savarino, G. Viscardi and E. Barni, *J. Heterocycl. Chem.*, 1993, **30**, 1041-1044.
126. S. R. Vazquez, J. L. P. Lustres, F. Rodriguez-Prieto, M. Mosquera and M. C. R. Rodriguez, *J. Phys. Chem. B*, 2015, **119**, 2475-2489.
127. J. Zhou, H. Liu, B. Jin, X. Liu, H. Fu and D. Shangguan, *J. Mater. Chem. C*, 2013, **1**, 4427-4436.
128. P. Mahato, S. Saha and A. Das, *J. Phys. Chem. C*, 2012, **116**, 17448-17457.
129. B. Maity, A. Chatterjee, S. A. Ahmed and D. Seth, *J. Lumin.*, 2017, **183**, 238-250.
130. A. A. M. Prabhu and N. Rajendiran, *J. Fluoresc.*, 2012, **22**, 1461-1474.
131. S. Kundu, S. Maity, S. C. Bera and N. Chattopadhyay, *J. Mol.*, 1997, **405**, 231-238.
132. Y.-B. Jiang, J.-G. Xu and X.-Z. Huang, *Chem. J. Chinese U.*, 1994, **15**, 552-556.
133. S. S. Jaffer, M. Sowmiya, S. K. Saha and P. Purkayastha, *J. Colloid Interf. Sci.*, 2008, **325**, 236-242.

134. S. Wiedbrauk, B. Maerz, E. Samoylova, A. Reiner, F. Trommer, P. Mayer, W. Zinth, and H. Dube, *J. Am. Chem. Soc.*, 2016, **138**, 12219-12227.
135. C.-L. Chen, Y.-T. Chen, A. P. Demchenko and P.-T. Chou, *Nat. Rev. Chem.*, 2018, **2**, 131-143.
136. H.-W. Tseng, T.-C. Lin, C.-L. Chen, T.-C. Lin, Y.-A. Chen, J.-Q. Liu, C.-H. Hung, C.-M. Chao, K.-M. Liu and P.-T. Chou, *Chem. Commun.*, 2015, **51**, 16099-16102.
137. N. Kanlayakan, K. Kerdpol, C. Prommin, R. Salaeh, W. Chansen, C. Sattayanon and N. Kungwan, *New J. Chem.*, 2017, **41**, 8761-8771.
138. H.-W. Tseng, J.-Q. Liu, Y.-A. Chen, C.-M. Chao, K.-M. Liu, C.-L. Chen, T.-C. Lin, C.-H. Hung, Y.-L. Chou, T.-C. Lin, T.-L. Wang and P.-T. Chou, *J. Phys. Chem. Lett.*, 2015, **6**, 1477-1486.
139. T.-Y. Lin, K.-C. Tang, S.-H. Yang, J.-Y. Shen, Y.-M. Cheng, H.-A. Pan, Y. Chi, and P.-T. Chou, *J. Phys. Chem. A*, 2012, **116**, 4438-4444.
140. L. D. Mena, D. M. A. Vera, M. T. Baumgartnera and L. B. Jimenez, *Phys. Chem. Chem. Phys.*, 2019, **21**, 12231-12240.
141. S. Jana, S. Dalapati and N. Guchhait, *J. Phys. Chem. A*, 2013, **117**, 4367-4376.
142. S. R. Vazquez, M. C. R. Rodriguez, M. Mosquera and F. Rodríguez-Prieto, *J. Phys. Chem. A*, 2008, **112**, 376-387.
143. Y. Kim, M. Yoon and D. Kim, *J. Photochem. Photobiol. A*, 2001, **138**, 167-175.
144. Y. Kim and M. Yoon, *Bull. Korean Chem. Soc.*, 1998, **19**, 980-985.
145. S. Jana, S. Dalapati and Nikhil Guchhait, *J. Phys. Chem. A*, 2012, **116**, 10948-10958.
146. D. Gormin and M. Kasha, *Chem. Phys. Lett.*, 1988, **153**, 574-576.
147. M. A. El-Kemary, *Chem. Phys.*, 2003, **295**, 1-10.
148. R. Ghosh and D. K. Palit, *Photochem. Photobiol. Sci.*, 2013, **12**, 987-995.
149. A. Maliakal, G. Lem, N. J. Turro, R. Ravichandran, J. C. Suhadolnik, A. D. DeBellis, M. G. Wood and J. Lau, *J. Phys. Chem. A*, 2002, **106**, 7680-7689.
150. A. G. Jadhav and N. Sekar, *J. Solution Chem.*, 2017, **46**, 777-797.
151. K. –Y. Chen and J. –W. Hu, *J. Lumin.*, 2015, **159**, 171-177.
152. G. Krishnamoorthy and S. K. Dogra, *J. Org. Chem.*, 1999, **64**, 6566-6574.
153. D. L. Gourrierec, V. A Kharlanov, R. G Brown and W. Rettig, *J. Photochem. Photobiol. A*, 2000, **130**, 101-111.
154. X.-B. Zhang, J. Peng, C.-L. He, G.-L Shen and R.-Q. Yu, *Anal. Chim. Acta*, 2006, **567**, 189-195.
155. L.-N. Chen, C.-C. Kuo, Y.-C. Chiu and W.-C. Chen, *RSC Adv.*, 2014, **4**, 45345-45353.
156. Y. Tian, C.-Y. Chen, C.-C. Yang, A. C. Young, S.-H. Jang, W.-C. Chen and A, K.-Y. Jen, *Chem. Mater.*, 2008, **20**, 1977-1987.
157. A. S. Braegelman and M. J. Webber, *Theranostics*, 2019, **9**, 3017-3040.
158. M. J. Webber and R. Langer, *Chem. Soc. Rev.*, 2017, **46**, 6600-6620.
159. W.-C. Geng, J. L. Sessler and D.-S. Guo, *Chem. Soc. Rev.*, 2020, Advance Article. doi.org/10.1039/C9CS00622B
160. Z. Li, N. Song and Y.-W. Yang, *Matter*, 2019, **1**, 345-368.
161. S. Sahu, M. Das, A. K. Bharti and G. Krishnamoorthy, *Phys. Chem. Chem. Phys.*, 2018, **20**, 27131-27139.

162. E. Buncel, E. A. Symons, D. Dolman and R. Stewart, Can. *J. Chem.*, 1970, **48**, 3354-3357.
163. F. A. S. Chipem and G. Krishnamoorthy, *J. Phys. Chem. A*, 2009, **113**, 12063-12070.
164. S. Sahu, S. Dutta and G. Krishnamoorthy, *Phys. Chem. Chem. Phys.*, 2016, **18**, 29905-29913.
165. S. K. Behera, A. Karak and G. Krishnamoorthy, *J. Phys. Chem. B*, 2015, **119**, 2330-2344.
166. A. Malakar and G. Krishnamoorthy, *J. Colloid Interface Sci.*, 2015, **443**, 23-29.
167. F. A. S. Chipem, A. Mishra and G. Krishnamoorthy, *Phys. Chem. Chem. Phys.*, 2012, **14**, 8775-8790
168. A. M. Nowicka, A. Kowalczyk, M. Donten, P. Krysinski and Z. Stojek, *Anal. Chem.*, 2009, **81**, 7474-7483.
169. H. Xiao, Y. Chen and M. Alnaggar, *Micron*, 2019, **126**, 102750-102756.
170. S. Link and M. A. El-Sayed, *J. Phys. Chem. B*, 1999, **103**, 8410-8426.
171. W. Wu, M. Wu, Z. Sun, G. Li, Y. Ma, X. Liu, X. Wang and X. Chen, *J. Alloys Compd.*, 2013, **579**, 117-123.
172. S. Tokonamia, Y. Yamamoto, H. Shiigi and T. Nagaokab, *Anal. Chim. Acta*, 2012, **716**, 76-91.
173. N. Bhardwaj, B. Satpati and S. Mohapatra, *Appl. Surf. Sci.*, **504**, 144381-144388.
174. F. T. Torqueti, G. L. Freitas, D. C. Ferreira, R. V. Gelamo, L. D. A. Goncalves and E. A. A. Naves, *J. Food Saf.*, 2019, **39**, e12668- e12675.
175. P. Dutta and B. Wang, *Coord. Chem. Rev.*, 2019, **383**, 1-29.
176. V. Campos, A. Almaguer-Fiores, D. Yelasco-Aria, D. Diaz and S. E. Rodil, *J. Mater. Sci. Eng. A*, 2018, **8**, 142-146.
177. Shahid-ul-Islam, B. S. Butola and F. Mohammad, *RSC Adv.*, 2016, **6**, 44232-44247.
178. S. Selvaraj, R. Thangam and N. N. Fathima, *Int. J. Biol. Macromol.*, 2018, **120**, 1674-1681.
179. P. Xu, C. Cen, N. Chen, H. Lin, Q. Wang, N. Xu, J. Tang and Z. Teng, *J. Colloid Interf. Sci.*, 2018, **526**, 194-200.
180. V. Thamilselvi and K. V. Radha, *IOSR J. Pharm.*, 2017, **7**, 21-27.
181. B. Wiley, Y. Sun and Y. Xia. *Acc. Chem. Res.*, 2007, **40**, 1067-1076.
182. A. Loiseau, L. Zhang, D. Hu, M. Salmain, Y. Mazouzi, R. Flack, B. Liedberg and S. Boujday, *ACS Appl. Mater. Interfaces*, 2019, **11**, 46462-46471.
183. C. Lertvachirapaiboon, A. Baba, S. Ekgasit, C. Thammacharoen, K. Shinbo, K. Kato and F. Kaneko, *Plasmonics*, 2014, **9**, 899-905.
184. A. Malakar, *Ph.D Thesis*, IIT Guwahati, 2018.
185. I. E. Serdiuk, M. Reszka, A. Synak, B. Liberek and P. Bojarski, *Dyes Pigm.*, 2018, **149**, 224-228.
186. I. Pastoriza-Santos and L.M. Liz-Marzán. *Langmuir*, 1999, **15**, 948-951.
187. R. N. Shelke, D. N. Pansare, C. D. Pawar, A. K. Deshmukh, R. P. Pawar and S. R. Bembalkar, *Eur. J. Chem.*, 2017, **8**, 25-32.
188. C.-F. Lin, T.-H. Duh, W.-D. Lu, J.-L. Lee, C.-Y. Lee, C.-C. Chen and M.-J. Wu, *J. Chin. Chem. Soc- Taip*, 2004, **51**, 183-186.
189. M.J. Frisch, G.W. Trucks, H.B. Schlegel, G.E. Scuseria, M.A. Robb, J.R. Cheeseman, G. Scalmani, V. Barone, B. Mennucci, G.A. Petersson, H. Nakatsuji, M. Caricato, X. Li, H.P. Hratchian, A.F. Izmaylov, J. Bloino, G. Zheng, J.L. Sonnenberg, M. Hada, M. Ehara, K.

Toyota, R. Fukuda, J. Hasegawa, M. Ishida, T.Y. Nakajima, O. Honda, H. Kitao, T. Nakai, J.A. Vreven Montgomery Jr., J.E. Peralta, F.O. Ogliaro, M.J. Bearpark, J. Heyd, E.N. Brothers, K.N. Kudin, V.N. Staroverov, R. Kobayashi, J. Normand, K. Raghavachari, A.P. Rendell, J.C. Burant, S.S. Iyengar, J. Tomasi, M. Cossi, N. Rega, N.J. Millam, M. Klene, J.E. Knox, J.B. Cross, V. Bakken, C. Adamo, J. Jaramillo, R. Gomperts, R.E. Stratmann, O. Yazyev, A.J. Austin, R. Cammi, C. Pomelli, J.W. Ochterski, R.L. Martin, K. Morokuma, V.G. Zakrzewski, G.A. Voth, P. Salvador, J.J. Dannenberg, S. Dapprich, A.D. Daniels, Ã.D.N. Farkas, J.B. Foresman, J.V. Ortiz, J. Cioslowski and D.J. Fox, *Gaussian, Inc*., Wallingford, CT, USA, 2009.

190. P. Hohenberg and W. Kohn, *Phys. Rev*., 1964, **136**, B864-B871.
191. W. Kohn and L.J. Sham, *Phys. Rev*.,1965, **140**, A1133-A1138.
192. S. Miertus, E. Scrocco and J. Tomasi, *Chem. Phys*., 1981, **55**, 117-129.
193. A.D. Becke, *J. Chem. Phys*.,1993, **98**, 5648-5652.
194. C. Lee, W. Yang and R.G. Parr, *Phys. Rev. B*, 1988, **37**, 785-789.
195. A. Crosby and J. N. Demas, *J. Phys. Chem.*, 1971, **75**, 991-1024.
196. A. S. R. Koti, M. M. G. Krishna and N. Periasamy, *J. Phys. Chem. A*, 2001, **105**, 1767-1771.
197. M. J. Jorgenson and D. R. Hartter, *J. Am. Chem. Soc*., 1963, **85**, 878-883.
198. G. Yagil, *J. Phys. Chem.*, 1967, **71**, 1034-1044.
199. R. B. Saper and R. Rash, *Am. Fam. Physician*, 2009, **79**, 768-772.
200. N. Roohani, R. Hurrell, R. Kelishadi, and R. Schulin, *J Res Med Sci*., 2013, **18**, 144-157.
201. A. Sharma, B. Patni, D. Shankhdhar, and S. C. Shankhdhar, *Physiol Mol Biol Plants.*, 2013, **19**, 11-20.
202. C. C. Pfeiffer, and E. R. Braverman, *Biol. Psychiatry*, 1982, **17**, 513-532.
203. C. Rodríguez-Rodríguez, M. A. Telpoukhovskaia, J. Alí-Torres, L. Rodríguez-Santiago, Y. Manso, G. A. Bailey, J. Hidalgo, M. Sodupe and C. Orvig, *Metallomics*, 2015,**7**, 83-92.
204. W. Qin, S. O. Obare, C. J. Murphy and S. M. Angel, *Anal. Chem.*, 2002, **74**, 4757-4762.
205. A. Pla-Dalmau, *J. Org. Chem.*, 1995, **60**, 5468-5473.
206. W. Qin, S. O. Obare, C. J. Murphy and S. M. Angel, *Analyst*, 2001, **126**, 1499-1501.
207. M. M. Henary and C. J. Fahrni, *J. Phys. Chem. A*, 2002, **106**, 5210-5220.
208. F. S. Rodembusch, F. R. Brand, D. S. Correa, J. C. Pocos, M. Martinelli and V. Stefani, *Mater. Chem. Phys*., 2005, **92**, 389-393.
209. B. Gidwani and A. Vyas, *Biomed. Res. Int.*, 2015, **2015**, 198268-198282.
210. G. Y. Tonga, T. Mizuhara, K. Saha, Z. Jiang, S. Hou, R. Das and V. M. Rotello, *Tetrahedron Lett.*, 2015, 56, 3653-3657.
211. G. J. Woolfe, M. Melzig, S. Schneider and F. Dorr, *Chem. Phys.*, 1983, **77**, 213-221.
212. M. Itoh and Y. Fujimaza, *J. Am. Chem. Soc.*, 1985, **107**, 1561-1565.
213. E. L. Roberts, J. Dey, and I. M. Warner, *J. Phys. Chem.*, 1996, **100**, 19681-19686.
214. A. Niemczynowicz, G. Czernel, A. Matwijczuk, M. Makowski, K. Pustula, D. Karcz, A. Matwijczuk, A. Gorecki and A. I. Piotrowicz-Cieslak, *J. Lumin.*, 2019, **208**, 125-134.
215. G. Krishnamoorthy and S. K. Dogra, *J. Lumin.*, 2000, **92**, 91-102.
216. F. S. Rodembusch, F. P. Leusin, L. F. Campo and V. Stefani, *J. Lumin.*, 2007, **126**, 728-734.
217. C. Marquez, R. R. Hudgins and W. M. Nau, *J. Am. Chem. Soc.*, 2004, **126**, 5806-5816.
218. S. D. Choudhury, J. Mohanty, H. Pal and A. C. Bhasikuttan, *J. Am. Chem. Soc.*, 2010, **132**, 1395-1401.

219. S. D. Choudhury, J. Mohanty, H. P. Upadhyaya, A. C. Bhasikuttan and H. Pal, *J. Phys. Chem. B*, 2009, **113**, 1891-1898.
220. D. Banik, J. Kuchlyan, A. Roy, N. Kundu, and Nilmoni Sarkar, *J. Phys. Chem. B*, 2015, **119**, 2310-2322.
221. M. Das, S. Sahu and G. Krishnamoorthy, *Phys. Chem. Chem. Phys.*, 2019, **21**, 15669-15677.
222. S. Sahu, M. Das and G. Krishnamoorthy, *Phys. Chem. Chem. Phys*., 2016, **18**, 11081-11090.
223. T. Mutai, H. Tomoda, T. Ohkawa, Y. Yabe and K. Araki, *Angew. Chem. Int. Ed*. 2008, **47**, 9522-9524.
224. T. Hirayama, K. Okuda and H. Nagasawa, *Chem. Sci.*, 2013, **4**, 1250-1256.
225. B. Chen, Y. Ding, X. Li, W. Zhu, J. P. Hill, K. Ariga and Y. Xie, *Chem. Commun.*, 2013, **49**, 10136-10138.
226. Y. Yu, B. Jiao, Z. Wu, Z. Li, L. Ma, G. Zhou, W. Yu, S. K. So and X. Hou, *J. Mater. Chem. C*, 2014, **2**, 9375-9384.
227. F. A. S. Chipem and G. Krishnamoorthy, *J. Phys. Chem. B*, 2013, **117**, 14079-14088.
228. F. A. S Chipem, N. Dash and G. Krishnamoorthy, *J. Chem. Phys.*, 2011, **134**, 104308-104316.
229. R. Omidyan and M. Iravani, *J. Phys. Chem. A*, 2016, **120**, 1012-1019.
230. G. Krishnamoorthy and S. K. Dogra, *J. Lumin.*, 2001, **92**, 91-102.
231. Z. R. Grabowski, K. Rotkiewicz and W. Rettig, *Chem. Rev.*, 2003, **103**, 3899-4032.
232. Y. H. Kim, D. W. Cho, M. Yoon and D. Kim, *J. Phys. Chem.*, 1996, **100**, 15670-15676.
233. Y. Kim, H. W. Cheon, M. Yoon, N. W. Song and D. Kim, *Chem. Phys. Lett.*, 1997, **264**, 673-679.
234. L. Manna, E. C. Scher, and A. P. Alivisatos, *J. Am. Chem. Soc.*, 2000, **122**, 12700-12706.
235. J. Gao, C. M. Bender, and C. J. Murphy, *Langmuir*, 2003, **19**, 9065-9070.
236. Z. Cao, H. Fu, L. Kang, L. Huang, T. Zhai, Y. Ma and J. Yao, *J. Mater. Chem.*, 2008, **18**, 2673-2678.
237. B. Trappmann, K. Ludwig, M. R. Radowski, A. Shukla, A. Mohr, H. Rehage, C. Bottcher and R. Haag, *J. Am. Chem. Soc.*, 2010, **132**, 11119-11124.
238. Z. M. Sui, X. Chen, L. Y. Wang, L. M. Xu, W. C. Zhuang, Y. C. Chai and C. J. Yang, *Physica E Low Dimens Syst. Nanostruct.*, 2006, **33**, 308-314.
239. B. Nikoobakht and M. A. El-Sayed, *Langmuir*, 2001, **17**, 6368-6374.
240. Z.-J. Jiang, C.-Y. Liu and L.-W. Sun, *J. Phys. Chem. B*, 2005, **109**, 1730-1735.
241. P. Prema, Chemical Mediated Synthesis of Silver Nanoparticles and its Potential Antibacterial Application, Progress in Molecular and Environmental Bioengineering - From Analysis and Modeling to Technology Applications, Angelo Carpi, IntechOpen, 2011.
242. K. Mallick, M. Witcomb and M. Scurrell, *Mater. Chem. Phys.*, 2006, **97**, 283-287.
243. T. Das, A. Kumar, P. Ghosh, A. Maity, S. S. Jaffer, and P. Purkayastha, *J. Phys. Chem. C*, 2010, **114**, 19635-19640.
244. N. Dash, F. A. S. Chipem and G Krishnamoorthy, *Photochem. Photobiol. Sci.*, 2009, **8**, 1708-1715.

245. A. Mishra, A. Malakar, H. T. Biswal, M. K. Barman and G. Krishnamoorthy, *J. Mol. Recognit.*, 2015, **28**, 299-305.
246. N. Dash and G. Krishnamoorthy, *J. Fluoresc.*, 2010, **20**, 135-142.
247. K. Hofman, Imidazole and its Derivatives, Interscience Publishers: New York, 1953.
248. V. Lopez, J. Catalan, R. M. Claramunt, C. Lopez, E. Cayon and J. Elguero, *Can. J. Chem.*, 1990, **68**, 958-959.
249. J. Catalan, R. M. Claramunt, J. Elguero, J. Laynez, M. Menendez, F. Anvia, J. H. Quian, M. Taagepera and R. W. Taft, *J. Am. Chem. Soc.*, 1988, **110**, 4105-4111.
250. H. K. Sinha and S. K. Dogra, *Chem. Phys.*, 1986, **102**, 337-347.
251. S. K. Behera, G. Sadhuragiri, P. Elumalai, M. Sathiyendiran and G. Krishnamoorthy, *RSC Adv.*, 2016, **6**, 59708-59717.
252. J. K. Dey and S. K. Dogra, *J. Phys. Chem.*, 1994, **98**, 3638-3644.
253. A. Mishra and G. Krishnamoorthy, *Photochem. Photobiol. Sci*., 2012, **11**, 1356-1367.
254. S. K. Behera and G. Krishnamoorthy, *Phys. Chem. Chem. Phys.*, 2017, **19**, 19234-19242.
255. G. Krishnamoorthy and S. K. Dogra, *J. Lumin.*, 2001, **92**, 103-114.

Annexure-A

Table A1: The excitation energy (λ_{max}^{ex}) of HPBO–Zn^{2+} complex (in eV) calculated in water medium using different functional and basis set.

Functional	Basis set	λ_{max}^{ex}	Functional	Basis set	λ_{max}^{ex}
B3LYP	LANL2DZ	3.96	B3PW91	LANL2DZ	4.00
B3LYP	631G+DP	3.61	B3PW91	631G+DP	3.85
B3LYP	6311G++DP	3.72	B3PW91	6311G++DP	3.84
B3LYP	CCPVTZ	3.69	B3PW91	CCPVTZ	3.84
B3LYP	DGDZVP2	3.69	B3PW91	DGDZVP2	3.87
B3LYP	321g	4.04	B3PW91	321g	4.07
PBEPBE	LANL2DZ	3.63	MPW1PW91	LANL2DZ	4.08
PBEPBE	631G+DP	3.00	MPW1PW91	631G+DP	3.93
PBEPBE	6311G++DP	3.11	MPW1PW91	6311G++DP	3.91
PBEPBE	CCPVTZ	3.09	MPW1PW91	CCPVTZ	3.92
PBEPBE	DGDZVP2	3.07	MPW1PW91	DGDZVP2	3.95
PBEPBE	**321g**	**3.52**	MPW1PW91	321g	4.15
BPV86	LANL2DZ	3.62	WB97XD	LANL2DZ	4.36
BPV86	631G+DP	3.20	WB97XD	631G+DP	4.22
BPV86	6311G++DP	3.29	WB97XD	6311G++DP	4.20
BPV86	CCPVTZ	3.24	WB97XD	CCPVTZ	4.20
BPV86	DGDZVP2	3.23	WB97XD	DGDZVP2	4.24
BPV86	321g	3.54	WB97XD	321g	4.44

Table A2: XYZ coordinate of optimized trans-enol HPBO in water.

(a) in ground state

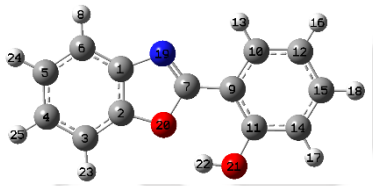

Center Number	Atomic Number	Coordinates (Angstroms) X	Y	Z
1	6	-1.9932	-0.84512	-6E-06
2	6	-1.93411	0.568194	0.000004
3	6	-3.05086	1.399396	0.000012
4	6	-4.29854	0.739237	0.000009
5	6	-4.3898	-0.67734	-1E-06
6	6	-3.24088	-1.49181	-9E-06
7	6	0.13561	-0.33093	-2E-06
8	1	-3.31203	-2.57469	-1.5E-05
9	6	1.590321	-0.28036	0
10	6	2.309454	-1.5058	0.000006
11	6	2.320914	0.943606	-3E-06
12	6	3.706991	-1.52276	0.000008
13	1	1.744679	-2.4332	0.000008
14	6	3.730473	0.920911	-1E-06
15	6	4.418868	-0.2997	0.000004
16	1	4.241364	-2.46778	0.000012
17	1	4.261817	1.86756	-4E-06
18	1	5.505428	-0.30165	0.000006
19	7	-0.67583	-1.36829	-7E-06
20	8	-0.56765	0.921794	-2E-06
21	8	1.726638	2.199282	-0.00001
22	1	0.740516	2.14391	-1.4E-05

(b) in excited state

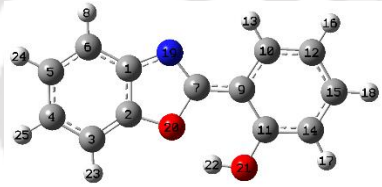

Center Number	Atomic Number	Coordinates (Angstroms) X	Y	Z
1	6	-1.97552	-0.85675	-1E-06
2	6	-1.92736	0.588837	0.000001
3	6	-3.03977	1.407379	0.000002
4	6	-4.30107	0.742926	0.000001
5	6	-4.39204	-0.68032	-1E-06
6	6	-3.25385	-1.49728	-2E-06
7	6	0.160798	-0.31675	-1E-06
8	1	-3.32669	-2.57989	-3E-06
9	6	1.562922	-0.29643	-1E-06
10	6	2.308872	-1.53361	0
11	6	2.34109	0.954359	0
12	6	3.703211	-1.52342	0
13	1	1.75469	-2.46599	-1E-06
14	6	3.741216	0.933881	0.000001
15	6	4.433206	-0.29562	0.000001
16	1	4.24562	-2.46521	0.000001
17	1	4.272129	1.88088	0.000001
18	1	5.519168	-0.30666	0.000002
19	7	-0.71395	-1.38859	-2E-06
20	8	-0.57039	0.956641	0.000001
21	8	1.719214	2.18094	-1E-06
22	1	0.726907	2.106628	-3E-06

23	1	-2.97271	2.480997	0.000018	23	1	-2.9665	2.489302	0.000003
24	1	-5.37197	-1.14144	-3E-06	24	1	-5.37719	-1.13864	-1E-06
25	1	-5.20967	1.330589	0.000014	25	1	-5.21129	1.335774	0.000002

Table A3: XYZ coordinate of optimized HPBO in water.

(a) cis-enol in ground state

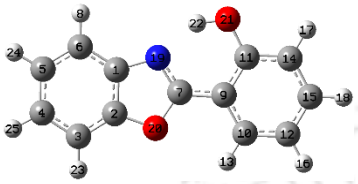

Center Number	Atomic Number	Coordinates (Angstroms) X	Y	Z
1	6	-1.91576	0.634126	-0.00007
2	6	-1.99221	-0.77891	0.000014
3	6	-3.18698	-1.49398	0.000102
4	6	-4.36323	-0.71399	0.000101
5	6	-4.31427	0.704652	0.000017
6	6	-3.09102	1.402528	-6.7E-05
7	6	0.144897	-0.13238	-8.1E-05
8	1	-3.05581	2.487026	-0.00013
9	6	1.586925	-0.24358	-4.8E-05
10	6	2.251648	-1.49529	-8.3E-05
11	6	2.353015	0.963641	0.000049
12	6	3.649735	-1.55332	-3.4E-05
13	1	1.661468	-2.40695	-0.00015
14	6	3.760492	0.896181	0.000096
15	6	4.400494	-0.35244	0.000053
16	1	4.156559	-2.5134	-5.9E-05
17	1	4.328965	1.821055	0.000163
18	1	5.486477	-0.39461	0.000093
19	7	-0.55064	1.002538	-0.00014
20	8	-0.66831	-1.27898	-1.8E-05
21	8	1.74684	2.203595	0.000076
22	1	0.735678	2.095317	-5.2E-05
23	1	-3.21534	-2.57804	0.000163
24	1	-5.24577	1.263541	0.000019
25	1	-5.32845	-1.21209	0.000162

(b) keto in excited state

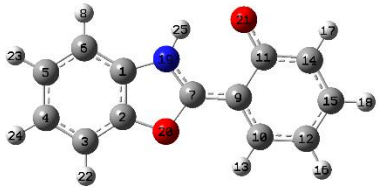

Center Number	Atomic Number	Coordinates (Angstroms) X	Y	Z
1	6	-1.96332	0.655936	-1.7E-05
2	6	-1.99623	-0.76437	0.000013
3	6	-3.17071	-1.50477	0.000037
4	6	-4.37637	-0.75552	0.00003
5	6	-4.36266	0.659991	0
6	6	-3.15871	1.397952	-2.4E-05
7	6	0.175326	-0.11452	-1.7E-05
8	1	-3.15608	2.482458	-4.6E-05
9	6	1.608196	-0.22256	-7E-06
10	6	2.256439	-1.46302	-2E-06
11	6	2.409194	1.015792	-6E-06
12	6	3.693991	-1.54727	0.000011
13	1	1.671611	-2.37837	-8E-06
14	6	3.83339	0.88938	0.000004
15	6	4.471607	-0.38295	0.000014
16	1	4.163574	-2.52673	0.000017
17	1	4.419145	1.805261	0.000009
18	1	5.555968	-0.44461	0.000023
19	7	-0.61962	1.010403	-3.6E-05
20	8	-0.66413	-1.24495	0.000013
21	8	1.804452	2.189121	-1.4E-05
22	1	-3.16702	-2.58913	0.00006
23	1	-5.30772	1.196097	-5E-06
24	1	-5.3264	-1.28142	0.000047
25	1	-0.15921	1.925778	-4.5E-05

Table A4: XYZ coordinate of optimized trans-enol HPBO in DMSO.

(a) in ground state

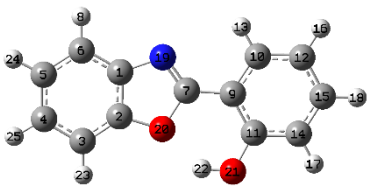

Center Number	Atomic Number	Coordinates (Angstroms) X	Y	Z
1	6	-1.99315	-0.84506	-6E-06
2	6	-1.93415	0.568259	0.000004
3	6	-3.05097	1.399355	0.000012
4	6	-4.2986	0.739127	0.000009

(b) in excited state

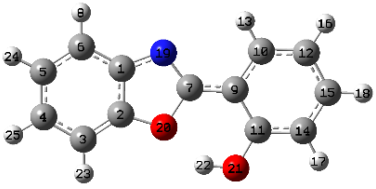

Center Number	Atomic Number	Coordinates (Angstroms) X	Y	Z
1	6	-1.97559	-0.8567	-1E-06
2	6	-1.92743	0.588785	0.000001
3	6	-3.03987	1.407352	0.000002
4	6	-4.30116	0.742941	0.000001

5	6	-4.38976	-0.67744	-1E-06
6	6	-3.24078	-1.49181	-9E-06
7	6	0.135622	-0.33087	-2E-06
8	1	-3.31175	-2.5747	-1.5E-05
9	6	1.590324	-0.2803	0
10	6	2.309354	-1.5058	0.000006
11	6	2.320985	0.94361	-3E-06
12	6	3.706872	-1.52284	0.000008
13	1	1.744425	-2.43311	0.000008
14	6	3.730537	0.920822	-1E-06
15	6	4.418824	-0.29983	0.000005
16	1	4.241185	-2.46789	0.000012
17	1	4.261826	1.867495	-4E-06
18	1	5.505393	-0.30185	0.000006
19	7	-0.6758	-1.36819	-7E-06
20	8	-0.56773	0.921987	-2E-06
21	8	1.726824	2.199298	-0.00001
22	1	0.740728	2.143946	-1.4E-05
23	1	-2.9729	2.480969	0.000018
24	1	-5.37189	-1.14162	-3E-06
25	1	-5.20979	1.330416	0.000014

5	6	-4.39207	-0.68026	-1E-06
6	6	-3.25384	-1.49721	-2E-06
7	6	0.160694	-0.31701	-1E-06
8	1	-3.32658	-2.57982	-3E-06
9	6	1.563043	-0.29661	-1E-06
10	6	2.308985	-1.53352	0
11	6	2.341069	0.95423	0
12	6	3.703461	-1.52312	0.000001
13	1	1.754902	-2.46596	-1E-06
14	6	3.741276	0.934044	0.000001
15	6	4.433367	-0.29534	0.000001
16	1	4.245912	-2.4649	0.000001
17	1	4.271892	1.881201	0.000002
18	1	5.519329	-0.30631	0.000002
19	7	-0.71389	-1.38858	-2E-06
20	8	-0.57043	0.956627	0.000001
21	8	1.719007	2.180612	-1E-06
22	1	0.726671	2.106004	-3E-06
23	1	-2.96656	2.489284	0.000003
24	1	-5.3772	-1.13864	-1E-06
25	1	-5.21139	1.335782	0.000002

Table A5: XYZ coordinate of optimized HPBO in DMSO.

(a) cis-enol in ground state

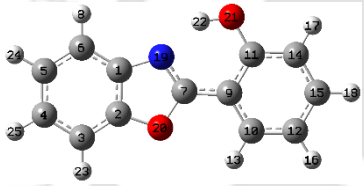

Center Number	Atomic Number	Coordinates (Angstroms) X	Y	Z
1	6	-1.91577	0.634155	-5.5E-05
2	6	-1.99219	-0.77888	0.000011
3	6	-3.18695	-1.49396	0.000081
4	6	-4.36322	-0.71401	0.000078
5	6	-4.31428	0.704613	0.000012
6	6	-3.09106	1.402502	-5.4E-05
7	6	0.144893	-0.13225	-6.5E-05
8	1	-3.05581	2.487	-0.0001
9	6	1.586891	-0.24351	-3.7E-05
10	6	2.251505	-1.49528	-6.4E-05
11	6	2.353063	0.963664	0.000038
12	6	3.649558	-1.55344	-2.6E-05
13	1	1.661177	-2.40684	-0.00011
14	6	3.76055	0.896037	0.000073
15	6	4.400412	-0.35261	0.00004
16	1	4.156314	-2.51356	-4.7E-05
17	1	4.328985	1.820927	0.000123
18	1	5.486401	-0.39489	0.000069
19	7	-0.55069	1.002637	-0.00011
20	8	-0.66831	-1.27893	-1.3E-05
21	8	1.747158	2.203637	0.000061
22	1	0.736056	2.095705	-2.7E-05
23	1	-3.21524	-2.57802	0.000129
24	1	-5.2458	1.263484	0.000013
25	1	-5.32843	-1.21214	0.000126

(b) keto in excited state

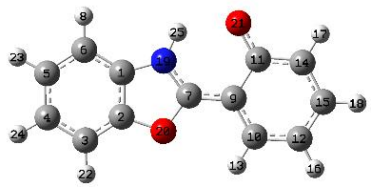

Center Number	Atomic Number	Coordinates (Angstroms) X	Y	Z
1	6	-1.96311	0.655752	-1.3E-05
2	6	-1.99632	-0.7645	0.000011
3	6	-3.17092	-1.50469	0.00003
4	6	-4.37647	-0.75518	0.000025
5	6	-4.36247	0.660267	0.000001
6	6	-3.15837	1,398021	-1.9E-05
7	6	0.175286	-0.11513	-1.5E-05
8	1	-3.15557	2.482533	-3.7E-05
9	6	1.608417	-0.22285	-6E-06
10	6	2.256916	-1.46296	-2E-06
11	6	2.408686	1.015742	-5E-06
12	6	3.694684	-1.54688	0.000009
13	1	1.672294	-2.37846	-8E-06
14	6	3.832863	0.889852	0.000004
15	6	4.471635	-0.38235	0.000012
16	1	4.164552	-2.5262	0.000014
17	1	4.418232	1.805967	0.000008
18	1	5.556036	-0.44346	0.000019
19	7	-0.61928	1.00987	-0.00003
20	8	-0.66424	-1.24535	0.00001
21	8	1.803453	2.188893	-1.2E-05
22	1	-3.16739	-2.58905	0.000049
23	1	-5.30742	1.196579	-2E-06
24	1	-5.3266	-1.2809	0.000039
25	1	-0.15793	1.924937	-3.7E-05

Table A6: XYZ coordinate of optimized HPBO–Zn^{2+} complex in water.

(a) in ground state

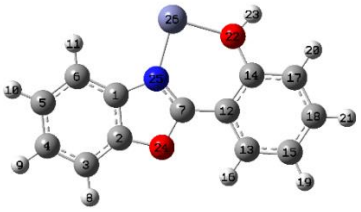

Center Number	Atomic Number	Coordinates (Angstroms) X	Y	Z
1	6	2.008609	0.055169	0.001055
2	6	2.025193	-1.353	0.030094
3	6	3.188657	-2.11728	0.051008
4	6	4.391638	-1.38195	0.040408
5	6	4.399202	0.038229	0.01059
6	6	3.206926	0.784485	-0.00943
7	6	-0.10049	-0.64103	0.009149
8	1	3.172513	-3.20084	0.073891
9	1	5.33683	-1.91596	0.055738
10	1	5.351594	0.559443	0.003415
11	1	3.212635	1.869334	-0.03149
12	6	-1.54292	-0.81007	0.00132
13	6	-2.07482	-2.12389	-0.10681
14	6	-2.45896	0.266401	0.100149
15	6	-3.45535	-2.34689	-0.1186
16	1	-1.38678	-2.95845	-0.18254
17	6	-3.84321	0.054202	0.085802
18	6	-4.34244	-1.25458	-0.02292
19	1	-3.84038	-3.35758	-0.20267
20	1	-4.52565	0.896864	0.157893
21	1	-5.41572	-1.41625	-0.03369
22	8	-1.97458	1.590938	0.226453
23	1	-2.68888	2.236787	0.410035
24	8	0.681315	-1.79108	0.035818
25	7	0.650607	0.463013	-0.01264
26	30	-0.06122	2.354263	-0.08971

(b) in excited state

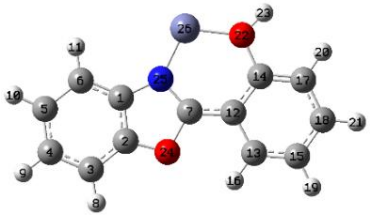

Center Number	Atomic Number	Coordinates (Angstroms) X	Y	Z
1	6	2.042754	0.19498	0.003788
2	6	2.081082	-1.20083	-0.00025
3	6	3.299851	-1.94569	-0.0062
4	6	4.520333	-1.22525	-0.00968
5	6	4.501878	0.16529	-0.0063
6	6	3.241291	0.907896	0.000524
7	6	-0.07878	-0.53341	0.002595
8	1	3.273316	-3.03524	-0.00835
9	1	5.46353	-1.7696	-0.01499
10	1	5.430743	0.73543	-0.00875
11	1	3.255068	1.99857	0.002096
12	6	-1.45794	-0.75547	-0.00095
13	6	-1.94391	-2.12184	0.009183
14	6	-2.47018	0.275058	-0.0121
15	6	-3.30058	-2.40696	0.010716
16	1	-1.20154	-2.91926	0.016785
17	6	-3.81927	-0.02677	-0.01104
18	6	-4.26044	-1.36846	0.001317
19	1	-3.62831	-3.44862	0.019548
20	1	-4.55219	0.784478	-0.02007
21	1	-5.32826	-1.58721	0.003067
22	8	-2.06812	1.654059	-0.02982
23	1	-2.85838	2.268903	-0.04986
24	8	0.801174	-1.71997	0.000802
25	7	0.699181	0.616488	0.00838
26	30	-0.29164	2.114438	0.01148

Table A7: XYZ coordinate of optimized HPBO–Zn^{2+} complex in DMSO.

(a) in ground state

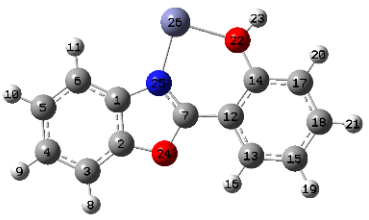

Center Number	Atomic Number	Coordinates (Angstroms) X	Y	Z
1	6	2.009518	0.05683	0.00215
2	6	2.026135	-1.35131	0.030019
3	6	3.189421	-2.11582	0.050038
4	6	4.392489	-1.38075	0.039969
5	6	4.400276	0.03943	0.011661
6	6	3.208155	0.785862	-0.0075
7	6	-0.09984	-0.64039	0.009579
8	1	3.172971	-3.19938	0.07187

(b) in excited state

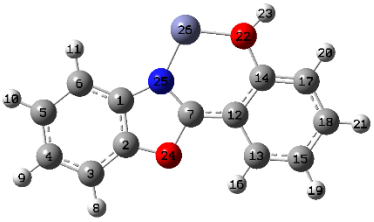

Center Number	Atomic Number	Coordinates (Angstroms) X	Y	Z
1	6	-2.04309	-0.19475	-0.00613
2	6	-2.08162	1.199868	0.001263
3	6	-3.30075	1.943793	0.010415
4	6	-4.52206	1.222568	0.014051
5	6	-4.5034	-0.16723	0.007576
6	6	-3.24266	-0.90839	-0.00288
7	6	0.078413	0.534728	-0.00279
8	1	-3.27519	3.033378	0.01521

9	1	5.337574	-1.91491	0.054578	9	1	-5.46505	1.767197	0.022251
10	1	5.352721	0.560506	0.004994	10	1	-5.43189	-0.73794	0.010472
11	1	3.214438	1.87063	-0.02823	11	1	-3.2555	-1.99905	-0.00683
12	6	-1.54209	-0.81001	0.001402	12	6	1.457804	0.755075	0.002048
13	6	-2.07334	-2.12405	-0.10757	13	6	1.944232	2.121177	-0.01343
14	6	-2.45886	0.26562	0.101002	14	6	2.469816	-0.27555	0.018189
15	6	-3.45377	-2.34764	-0.11925	15	6	3.300846	2.406048	-0.017
16	1	-1.38489	-2.95821	-0.18386	16	1	1.202039	2.918744	-0.02411
17	6	-3.84285	0.053127	0.086775	17	6	3.818945	0.025943	0.015197
18	6	-4.34142	-1.25593	-0.02265	18	6	4.260405	1.367364	-0.00401
19	1	-3.8383	-3.35845	-0.20387	19	1	3.628719	3.447578	-0.03041
20	1	-4.52577	0.895339	0.1596	20	1	4.551978	-0.78515	0.02802
21	1	-5.41459	-1.41819	-0.03323	21	1	5.328231	1.585903	-0.0079
22	8	-1.97529	1.591299	0.228125	22	8	2.068629	-1.65609	0.046188
23	1	-2.69063	2.235002	0.415206	23	1	2.860047	-2.26886	0.078759
24	8	0.682227	-1.7895	0.035525	24	8	-0.80106	1.719528	0.000766
25	7	0.650937	0.4644	-0.01145	25	7	-0.6998	-0.61632	-0.01266
26	30	-0.06395	2.352421	-0.09133	26	30	0.293112	-2.1113	-0.01692

Table A8: XYZ coordinate of optimized β-CD in the ground state.

(a) in water

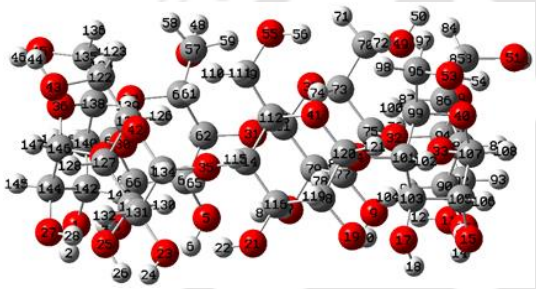

Center Number	Atomic Number	Coordinates (Angstroms) X	Y	Z
1	8	-5.62338	2.155823	-2.3282
2	1	-5.88259	1.611401	-3.10399
3	8	-4.29961	4.493267	-2.5782
4	1	-4.6908	3.576897	-2.46483
5	8	-1.60698	5.435321	-2.4828
6	1	-2.09951	5.163672	-3.28767
7	8	0.896732	6.413682	-2.39375
8	1	0.007506	5.947945	-2.40676
9	8	3.324579	4.886204	-2.40494
10	1	2.832262	5.217158	-3.18791
11	8	5.458129	3.244372	-2.5393
12	1	4.598454	3.757137	-2.46691
13	8	5.747624	0.39691	-2.53538
14	1	5.645072	0.975549	-3.32258
15	8	5.741391	-2.30407	-2.64578
16	1	5.626276	-1.31035	-2.57434
17	8	3.709585	-4.30719	-2.46852
18	1	4.023224	-3.87057	-3.29018
19	8	2.078417	-6.44044	-2.14857
20	1	2.553862	-5.56888	-2.26606
21	8	-0.84979	-6.25278	-2.31137
22	1	-1.70932	-5.7687	-2.44604
23	8	-3.40651	-5.17784	-2.61854
24	1	-3.9202	-5.79208	-3.18205
25	8	-5.04769	-2.77352	-2.50439
26	1	-4.60569	-3.0111	-3.3467
27	8	-6.58049	-0.54786	-2.30419

(b) in DMSO

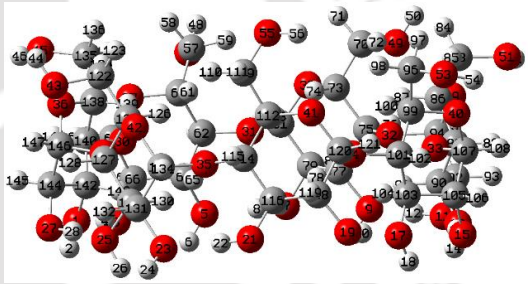

Center Number	Atomic Number	Coordinates (Angstroms) X	Y	Z
1	8	-5.62291	2.157214	-2.32713
2	1	-5.88566	1.612712	-3.10169
3	8	-4.29557	4.49224	-2.57936
4	1	-4.68923	3.577004	-2.46553
5	8	-1.60248	5.429319	-2.48292
6	1	-2.09802	5.160728	-3.28699
7	8	0.899593	6.411615	-2.3926
8	1	0.01047	5.945706	-2.40645
9	8	3.325427	4.883166	-2.40392
10	1	2.833697	5.217894	-3.18571
11	8	5.456663	3.240039	-2.54134
12	1	4.598312	3.754907	-2.46798
13	8	5.744445	0.393753	-2.53638
14	1	5.643615	0.973703	-3.32287
15	8	5.738876	-2.30666	-2.64617
16	1	5.624812	-1.31279	-2.57498
17	8	3.705459	-4.30732	-2.46755
18	1	4.021404	-3.87196	-3.28902
19	8	2.075882	-6.44249	-2.14509
20	1	2.55099	-5.57101	-2.264
21	8	-0.85218	-6.25468	-2.30799
22	1	-1.70908	-5.76724	-2.44641
23	8	-3.40513	-5.17171	-2.62172
24	1	-3.91805	-5.78585	-3.18606
25	8	-5.04185	-2.76597	-2.50591
26	1	-4.59751	-3.00189	-3.34742
27	8	-6.58088	-0.54524	-2.30287

28	1	-5.92464	-1.3045	-2.35434	28	1	-5.92417	-1.30106	-2.3541
29	8	-4.96908	-1.38215	-0.03327	29	8	-4.96906	-1.38005	-0.03091
30	8	-4.15036	3.032955	-0.04859	30	8	-4.15015	3.034537	-0.04707
31	8	-0.2092	5.120728	-0.01487	31	8	-0.20726	5.119493	-0.01277
32	8	3.893719	3.345012	-0.07955	32	8	3.895739	3.342549	-0.0781
33	8	5.032254	-0.97909	-0.14765	33	8	5.032876	-0.98132	-0.14599
34	8	2.350182	-4.56618	0.02451	34	8	2.348286	-4.5664	0.026915
35	8	-2.10063	-4.77755	-0.14873	35	8	-2.10275	-4.77573	-0.14733
36	8	-6.12406	0.168787	1.345674	36	8	-6.12467	0.170962	1.347233
37	8	-3.79722	5.094444	1.091217	37	8	-3.79647	5.09744	1.09001
38	8	1.595667	5.986617	1.265914	38	8	1.598288	5.984805	1.26733
39	8	5.752801	2.474239	1.119535	39	8	5.757323	2.472549	1.117673
40	8	5.588341	-2.95875	1.043191	40	8	5.588902	-2.9621	1.042846
41	8	1.073031	-5.99435	1.417975	41	8	1.069907	-5.99272	1.420933
42	8	-4.17651	-4.89359	1.020409	42	8	-4.18142	-4.8946	1.016541
43	8	-6.49208	-3.49131	2.227376	43	8	-6.50302	-3.49082	2.215931
44	1	-7.0077	-3.33459	3.044821	44	1	-7.02099	-3.34353	3.033628
45	8	-6.58013	2.539971	2.781426	45	8	-6.58694	2.539289	2.781359
46	1	-7.23626	1.815972	2.685891	46	1	-7.24015	1.812665	2.685709
47	8	-1.92358	7.087327	2.243083	47	8	-1.92089	7.093882	2.236045
48	1	-1.62286	7.56728	3.041827	48	1	-1.62419	7.576728	3.034539
49	8	4.257039	5.656115	2.490688	49	8	4.261576	5.654404	2.489125
50	1	4.806676	5.610232	3.299837	50	1	4.813608	5.607699	3.296572
51	8	7.319516	0.537274	2.426181	51	8	7.32919	0.539104	2.420454
52	1	7.597481	1.468142	2.284768	52	1	7.604778	1.470538	2.278088
53	8	5.106658	-5.38277	2.425192	53	8	5.107625	-5.38686	2.423389
54	1	6.006537	-5.04966	2.218208	54	1	6.007559	-5.05386	2.216531
55	8	-0.13993	-4.92316	3.751276	55	8	-0.14269	-4.91767	3.752716
56	1	0.738575	-5.36063	3.74888	56	1	0.735246	-5.35631	3.751446
57	6	-1.88519	5.640611	2.478873	57	6	-1.88598	5.648127	2.4777
58	1	-2.56015	5.361559	3.298473	58	1	-2.56353	5.373612	3.296706
59	1	-0.86381	5.323638	2.724579	59	1	-0.86574	5.330178	2.726967
60	6	-2.32676	4.927865	1.209376	60	6	-2.32621	4.931311	1.209877
61	1	-2.10709	3.85712	1.311614	61	1	-2.10655	3.860851	1.315394
62	6	-1.63233	5.46908	-0.06143	62	6	-1.6301	5.468883	-0.06157
63	1	-1.75291	6.557263	-0.11079	63	1	-1.74976	6.557005	-0.11344
64	6	-2.22864	4.818655	-1.30921	64	6	-2.22583	4.816259	-1.30842
65	1	-2.01384	3.74212	-1.31128	65	1	-2.01245	3.73943	-1.30782
66	6	-3.75052	5.04114	-1.35475	66	6	-3.74731	5.040635	-1.35582
67	1	-3.9538	6.118373	-1.37904	67	1	-3.9491	6.118111	-1.38148
68	6	-4.38584	4.467994	-0.07155	68	6	-4.38439	4.469914	-0.07238
69	1	-5.45568	4.689864	-0.01624	69	1	-5.45409	4.692674	-0.01839
70	6	3.166898	4.678952	2.565157	70	6	3.170739	4.678417	2.566104
71	1	2.49313	4.911692	3.400238	71	1	2.497777	4.913217	3.401309
72	1	3.571363	3.667388	2.695423	72	1	3.57426	3.666594	2.697608
73	6	2.377797	4.726428	1.265865	73	6	2.380575	4.724811	1.267328
74	1	1.677182	3.881303	1.248568	74	1	1.680021	3.879572	1.250966
75	6	3.272484	4.670339	0.007093	75	6	3.27469	4.668047	0.008187
76	1	4.044983	5.445594	0.069725	76	1	4.047228	5.443251	0.070353
77	6	2.424685	4.866744	-1.24919	77	6	2.426347	4.864375	-1.24766
78	1	1.72035	4.031297	-1.35731	78	1	1.721513	4.02923	-1.35511
79	6	1.644383	6.190986	-1.17326	79	6	1.646692	6.188956	-1.17179
80	1	2.353494	7.023445	-1.10122	80	1	2.356125	7.021144	-1.09979
81	6	0.769291	6.192411	0.098587	81	6	0.771736	6.190819	0.100124
82	1	0.274422	7.154982	0.252737	82	1	0.277272	7.153567	0.254428
83	6	5.857404	0.484937	2.442828	83	6	5.867358	0.483985	2.441207
84	1	5.462087	1.0282	3.311274	84	1	5.473451	1.026479	3.310802
85	1	5.593194	-0.57183	2.524022	85	1	5.605365	-0.57329	2.523109
86	6	5.260998	1.075263	1.166094	86	6	5.266474	1.073374	1.166019
87	1	4.165733	1.077741	1.233822	87	1	4.171386	1.075184	1.236853
88	6	5.691793	0.328794	-0.11589	88	6	5.693642	0.326095	-0.11671
89	1	6.782932	0.203207	-0.12423	89	1	6.784669	0.199622	-0.12763
90	6	5.247331	1.105245	-1.35528	90	6	5.246861	1.102321	-1.35537
91	1	4.151016	1.144154	-1.39695	91	1	4.15047	1.141641	-1.39475

92	6	5.812416	2.536883	-1.32665	92	6	5.812375	2.533804	-1.32847
93	1	6.907469	2.490449	-1.30935	93	1	6.907452	2.487037	-1.31257
94	6	5.339418	3.241662	-0.03748	94	6	5.341529	3.239384	-0.03894
95	1	5.800601	4.225752	0.082837	95	1	5.802887	4.223574	0.079989
96	6	4.189378	-4.24472	2.492934	96	6	4.190963	-4.2486	2.493159
97	1	4.455822	-3.58325	3.327728	97	1	4.458479	-3.588	3.328326
98	1	3.197724	-4.66644	2.66926	98	1	3.199308	-4.67013	2.670034
99	6	4.192032	-3.44018	1.194583	99	6	4.192561	-3.4429	1.19548
100	1	3.521324	-2.5771	1.29229	100	1	3.522493	-2.57946	1.294671
101	6	3.782575	-4.26632	-0.04701	101	6	3.780858	-4.2678	-0.04616
102	1	4.364282	-5.19716	-0.08171	102	1	4.361641	-5.19917	-0.0822
103	6	4.024835	-3.45616	-1.32172	103	6	4.022451	-3.45719	-1.3207
104	1	3.3692	-2.57538	-1.33337	104	1	3.367543	-2.57582	-1.33121
105	6	5.495061	-3.00524	-1.40258	105	6	5.493014	-3.00748	-1.40274
106	1	6.139707	-3.89169	-1.41975	106	1	6.136783	-3.89456	-1.42057
107	6	5.848025	-2.17983	-0.14879	107	6	5.847826	-2.18278	-0.149
108	1	6.912984	-1.9326	-0.11289	108	1	6.912958	-1.93616	-0.11415
109	6	-0.91455	-5.42736	2.619204	109	6	-0.91738	-5.42284	2.621198
110	1	-1.85334	-4.87096	2.621656	110	1	-1.8558	-4.8658	2.622808
111	1	-1.12877	-6.49891	2.745603	111	1	-1.13241	-6.49409	2.748879
112	6	-0.17692	-5.20348	1.301041	112	6	-0.17939	-5.2011	1.302877
113	1	0.087284	-4.14499	1.184803	113	1	0.085582	-4.14294	1.185407
114	6	-0.96357	-5.68493	0.070142	114	6	-0.96602	-5.68352	0.072412
115	1	-1.33228	-6.70897	0.231371	115	1	-1.3352	-6.70724	0.234736
116	6	-0.10928	-5.65499	-1.21561	116	6	-0.11145	-5.65562	-1.2132
117	1	0.133655	-4.60559	-1.44129	117	1	0.131939	-4.6066	-1.4402
118	6	1.192164	-6.45349	-1.00715	118	6	1.189766	-6.45425	-1.00379
119	1	0.932238	-7.50671	-0.84966	119	1	0.929521	-7.50727	-0.84537
120	6	1.928631	-5.9433	0.256018	120	6	1.926007	-5.94319	0.259178
121	1	2.789038	-6.57692	0.491072	121	1	2.786011	-6.577	0.4952
122	6	-5.08236	-3.15303	2.445594	122	6	-5.09333	-3.1582	2.442661
123	1	-4.65566	-3.76289	3.252403	123	1	-4.67224	-3.77343	3.248332
124	1	-4.98272	-2.09072	2.700943	124	1	-4.99171	-2.09744	2.703801
125	6	-4.31352	-3.42343	1.160844	125	6	-4.31928	-3.4249	1.160129
126	1	-3.31052	-2.98633	1.251133	126	1	-3.3167	-2.98787	1.255307
127	6	-5.00902	-2.84486	-0.09208	127	6	-5.01021	-2.8426	-0.09366
128	1	-6.04753	-3.19342	-0.12754	128	1	-6.04892	-3.19011	-0.13308
129	6	-4.27348	-3.27122	-1.3663	129	6	-4.27141	-3.26675	-1.36666
130	1	-3.26972	-2.82881	-1.3849	130	1	-3.26713	-2.82541	-1.38148
131	6	-4.16064	-4.80067	-1.41878	131	6	-4.16015	-4.7962	-1.422
132	1	-5.16205	-5.2462	-1.45143	132	1	-5.16207	-5.2405	-1.45668
133	6	-3.44204	-5.31659	-0.15475	133	6	-3.44398	-5.3149	-0.15774
134	1	-3.4331	-6.40953	-0.11537	134	1	-3.4351	-6.40793	-0.1206
135	6	-5.2384	1.975144	2.635991	135	6	-5.24312	1.979459	2.637096
136	1	-5.01675	1.290204	3.465072	136	1	-5.01915	1.296361	3.467114
137	1	-4.54866	2.821306	2.66923	137	1	-4.55667	2.828347	2.66941
138	6	-5.08538	1.228731	1.311677	138	6	-5.08715	1.23209	1.313545
139	1	-4.09357	0.762129	1.258913	139	1	-4.09472	0.76659	1.262305
140	6	-5.29436	2.126972	0.072068	140	6	-5.29498	2.129556	0.073228
141	1	-6.22381	2.701953	0.182184	141	1	-6.22418	2.705136	0.182296
142	6	-5.35589	1.270416	-1.19284	142	6	-5.3561	1.272415	-1.19122
143	1	-4.39127	0.769194	-1.34777	143	1	-4.39147	0.770965	-1.34539
144	6	-6.47134	0.216263	-1.07858	144	6	-6.47162	0.218361	-1.07697
145	1	-7.43592	0.721029	-0.9539	145	1	-7.43618	0.723134	-0.9521
146	6	-6.21642	-0.66053	0.165393	146	6	-6.21663	-0.65844	0.166988
147	1	-7.03928	-1.35376	0.357648	147	1	-7.03928	-1.35193	0.359263

Table A9: XYZ coordinate of optimized cis-enol HPBO–*β*-CD complex (benzoxazole moiety inside the cavity) in water.

(a) in ground state

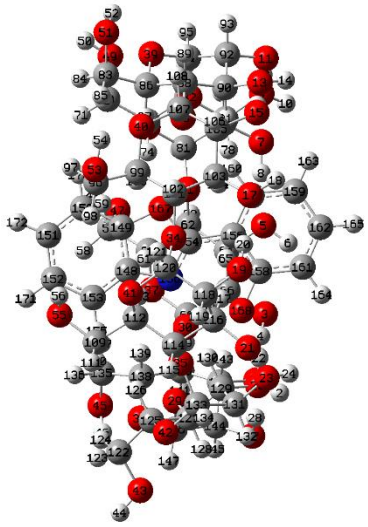

(b) in excited state

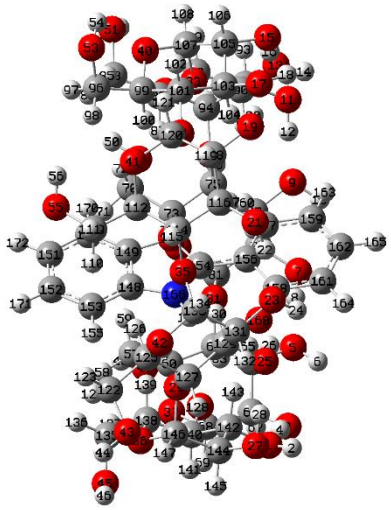

Center Number	Atomic Number	Coordinates (Angstroms)			Center Number	Atomic Number	Coordinates (Angstroms)		
		X	Y	Z			X	Y	Z
1	8	5.905503	1.2276	-2.23211	1	8	-4.70317	-3.6808	-2.19809
2	1	5.781485	1.794935	-3.02417	2	1	-4.33363	-4.17224	-2.96403
3	8	6.108844	-1.47298	-2.43366	3	8	-6.14934	-1.40194	-2.49241
4	1	5.920535	-0.49359	-2.33518	4	1	-5.52466	-2.17537	-2.36521
5	8	4.306075	-3.70402	-2.36329	5	8	-5.55264	1.411531	-2.49275
6	1	4.593087	-3.2244	-3.17043	6	1	-5.57888	0.832682	-3.28545
7	8	2.684166	-5.86264	-2.26941	7	8	-4.88712	4.038239	-2.50298
8	1	3.191481	-4.99723	-2.28611	8	1	-5.01773	3.044239	-2.47191
9	8	-0.19694	-5.81369	-2.36351	9	8	-2.25924	5.227562	-2.44459
10	1	0.409513	-5.85346	-3.1352	10	1	-2.75778	4.973394	-3.25154
11	8	-2.88454	-5.40321	-2.58706	11	8	0.259831	6.252056	-2.41864
12	1	-1.88951	-5.43513	-2.47269	12	1	-0.61483	5.762771	-2.3977
13	8	-4.75291	-3.22646	-2.51701	13	8	2.883113	5.087513	-2.34727
14	1	-4.33539	-3.60162	-3.32295	14	1	2.372019	5.316364	-3.15418
15	8	-6.31868	-1.01833	-2.52689	15	8	5.282523	3.842755	-2.36609
16	1	-5.645	-1.76018	-2.49385	16	1	4.342253	4.190359	-2.33813
17	8	-5.70293	1.768015	-2.37809	17	8	6.029721	1.084037	-2.3814
18	1	-5.76672	1.227418	-3.19546	18	1	5.862005	1.649907	-3.1665
19	8	-5.38103	4.439831	-2.12201	19	8	6.771734	-1.52664	-2.36908
20	1	-5.35387	3.445472	-2.2222	20	1	6.352428	-0.61959	-2.36412
21	8	-2.75717	5.73135	-2.35658	21	8	5.015801	-3.8832	-2.55256
22	1	-1.84132	5.509802	-2.68537	22	1	4.084105	-4.13456	-2.80748
23	8	-0.18383	5.174125	-2.87431	23	8	2.461449	-4.65614	-2.93544
24	1	0.295752	4.683646	-3.57557	24	1	1.78961	-4.42588	-3.6129
25	8	2.309954	3.820723	-2.47394	25	8	-0.35591	-4.46218	-2.47658
26	1	2.105249	2.838819	-2.48343	26	1	-0.63569	-3.4866	-2.52154
27	8	5.004988	3.987622	-2.22683	27	8	-2.68599	-5.74924	-2.10156
28	1	4.008216	3.939124	-2.35201	28	1	-1.80838	-5.28145	-2.26829
29	8	3.333084	3.766527	0.21604	29	8	-1.24441	-4.66196	0.267928
30	8	5.156285	-0.30392	0.06508	30	8	-4.78849	-1.90964	0.044412
31	8	2.884164	-4.13067	0.069254	31	8	-4.49876	2.483732	-0.07145
32	8	-1.54602	-4.76474	-0.1094	32	8	-0.75819	4.913722	-0.06631
33	8	-4.89223	-1.74047	-0.08929	33	8	3.604286	3.664999	0.005408
34	8	-4.59052	2.722097	0.078434	34	8	5.42896	-0.44174	-0.04913
35	8	-0.89823	5.115211	-0.11942	35	8	3.178255	-4.15608	-0.22498
36	8	5.265494	3.180819	1.422515	36	8	-3.22426	-4.96837	1.524558

37	8	5.909304	-2.23433	1.234177	37	8	-6.37526	-0.52634	1.1481
38	8	1.757173	-5.77521	1.363858	38	8	-4.28098	4.498393	1.169736
39	8	-3.59007	-5.0541	1.081082	39	8	0.918392	5.959574	1.263187
40	8	-6.38962	-0.38851	1.167211	40	8	5.508203	3.061529	1.293879
41	8	-4.25006	4.643266	1.424525	41	8	6.096987	-2.34399	1.203898
42	8	0.884818	6.616944	0.363547	42	8	2.181301	-6.21996	0.410302
43	8	3.714968	7.001019	1.259198	43	8	-0.2063	-7.66068	1.483837
44	1	4.217345	7.534721	1.908492	44	1	-0.43869	-8.30249	2.185927
45	8	7.041605	1.516796	2.814146	45	8	-5.6366	-4.36388	2.830272
46	1	7.159277	2.485686	2.708502	46	1	-5.26252	-5.26881	2.760419
47	8	5.312244	-4.89495	2.403368	47	8	-7.08925	2.135966	2.224336
48	1	5.295157	-5.44513	3.213263	48	1	-7.33509	2.670093	3.007319
49	8	-0.69271	-6.88206	2.538742	49	8	-2.56691	6.560944	2.394625
50	1	-1.20485	-7.12302	3.337751	50	1	-2.26295	7.016948	3.206035
51	8	-5.93916	-4.31091	2.44202	51	8	3.309535	6.218498	2.725023
52	1	-5.6699	-5.2412	2.281572	52	1	2.664938	6.947024	2.592811
53	8	-7.27851	1.895586	2.573585	53	8	7.294743	1.381417	2.673431
54	1	-7.84738	1.117052	2.389626	54	1	7.425362	2.347908	2.561523
55	8	-2.65713	4.465962	3.761353	55	8	4.808167	-2.99701	3.621735
56	1	-3.63477	4.379281	3.756787	56	1	5.659341	-2.51136	3.567074
57	6	4.521412	-3.67632	2.603308	57	6	-5.82579	1.433262	2.468205
58	1	4.930732	-3.07743	3.427281	58	1	-5.92133	0.743547	3.317002
59	1	3.477907	-3.93426	2.823813	59	1	-5.02456	2.154396	2.673153
60	6	4.562429	-2.85215	1.325514	60	6	-5.46027	0.639424	1.223212
61	1	3.818199	-2.04872	1.401321	61	1	-4.43375	0.266175	1.333015
62	6	4.281848	-3.68742	0.055614	62	6	-5.55844	1.471777	-0.07554
63	1	4.951802	-4.55448	0.032261	63	1	-6.54176	1.952748	-0.13177
64	6	4.484052	-2.83582	-1.1974	64	6	-5.33771	0.585782	-1.30158
65	1	3.736866	-2.03211	-1.22933	65	1	-4.30767	0.206714	-1.30823
66	6	5.897955	-2.22658	-1.21399	66	6	-6.32052	-0.5978	-1.29895
67	1	6.636016	-3.03724	-1.22242	67	1	-7.34677	-0.21398	-1.33188
68	6	6.111351	-1.39939	0.070717	68	6	-6.14648	-1.39231	0.012408
69	1	7.136988	-1.02643	0.147425	69	1	-6.87851	-2.20053	0.100182
70	6	-0.30457	-5.47022	2.594592	70	6	-2.3679	5.114401	2.523507
71	1	0.35892	-5.28313	3.449172	71	1	-2.96713	4.711538	3.350537
72	1	-1.19498	-4.83455	2.678984	72	1	-1.30772	4.892627	2.698953
73	6	0.429151	-5.11549	1.310288	73	6	-2.79941	4.445226	1.227622
74	1	0.579155	-4.0288	1.276573	74	1	-2.48878	3.392658	1.252817
75	6	-0.32251	-5.56369	0.0375	75	6	-2.21154	5.122313	-0.0304
76	1	-0.57718	-6.62697	0.116223	76	1	-2.43462	6.195256	-0.00512
77	6	0.540408	-5.31756	-1.19902	77	6	-2.79787	4.497221	-1.29503
78	1	0.721171	-4.24307	-1.32121	78	1	-2.50042	3.444291	-1.36659
79	6	1.891995	-6.03998	-1.06943	79	6	-4.3343	4.582755	-1.27958
80	1	1.722751	-7.11902	-0.97955	80	1	-4.64014	5.634779	-1.25221
81	6	2.601847	-5.55209	0.21315	81	6	-4.86342	3.889604	-0.00491
82	1	3.520792	-6.11094	0.409373	82	1	-5.94479	4.007494	0.105251
83	6	-4.73961	-3.47361	2.459626	83	6	2.599892	4.942961	2.625574
84	1	-4.09904	-3.73544	3.312159	84	1	1.880821	4.83608	3.448531
85	1	-5.09026	-2.44521	2.571218	85	1	3.362878	4.165595	2.706243
86	6	-3.93862	-3.61489	1.166466	86	6	1.861929	4.814992	1.294141
87	1	-3.01788	-3.02126	1.231734	87	1	1.294579	3.875545	1.272285
88	6	-4.72508	-3.1964	-0.09529	88	6	2.792823	4.883536	0.063813
89	1	-5.70503	-3.69225	-0.10606	89	1	3.440806	5.76721	0.138305
90	6	-3.93484	-3.56503	-1.3513	90	6	1.96247	4.953841	-1.2178
91	1	-3.00852	-2.97919	-1.38294	91	1	1.384549	4.028366	-1.33386
92	6	-3.59611	-5.06671	-1.36977	92	6	1.0051	6.159329	-1.17979
93	1	-4.52968	-5.64116	-1.38695	93	1	1.596322	7.079724	-1.11075
94	6	-2.82712	-5.44392	-0.08612	94	6	0.105661	6.072495	0.0713
95	1	-2.69401	-6.52547	0.001357	95	1	-0.48526	6.981677	0.208801
96	6	-5.8817	1.460459	2.593012	96	6	5.862276	1.093459	2.60226
97	1	-5.70499	0.766871	3.425576	97	1	5.334184	1.550717	3.449369
98	1	-5.28576	2.363235	2.742816	98	1	5.767879	0.007157	2.660648
99	6	-5.48501	0.7837	1.282111	99	6	5.251816	1.598988	1.296214
100	1	-4.44715	0.432514	1.344953	100	1	4.168722	1.421806	1.299644

101	6	-5.63852	1.699085	0.044703	101	6	5.86764	0.952642	0.033606
102	1	-6.6309	2.169511	0.049509	102	1	6.963693	1.006062	0.083018
103	6	-5.45468	0.885502	-1.23828	103	6	5.364929	1.672593	-1.21937
104	1	-4.42519	0.507339	-1.29183	104	1	4.279781	1.534044	-1.3152
105	6	-6.44146	-0.29574	-1.27731	105	6	5.687457	3.17614	-1.14565
106	1	-7.46601	0.092623	-1.25174	106	1	6.773528	3.30593	-1.07513
107	6	-6.23196	-1.18146	-0.03262	107	6	5.048221	3.775801	0.123109
108	1	-6.9844	-1.97252	0.034997	108	1	5.350289	4.815998	0.275411
109	6	-2.25407	5.244945	2.591849	109	6	4.666519	-3.81944	2.421407
110	1	-1.16263	5.247859	2.592334	110	1	3.682718	-4.28741	2.489946
111	1	-2.62154	6.278536	2.672531	111	1	5.440878	-4.60025	2.397277
112	6	-2.77307	4.613685	1.301663	112	6	4.75405	-2.96827	1.155606
113	1	-2.44957	3.567641	1.232514	113	1	3.99931	-2.17266	1.176777
114	6	-2.33831	5.372146	0.034918	114	6	4.600327	-3.78858	-0.13771
115	1	-2.51311	6.452286	0.153602	115	1	5.218275	-4.69805	-0.09212
116	6	-3.08197	4.878204	-1.22897	116	6	4.981911	-2.99062	-1.40807
117	1	-2.76887	3.842323	-1.42636	117	1	4.228548	-2.20276	-1.55405
118	6	-4.60623	4.914894	-0.9982	118	6	6.370687	-2.34095	-1.24352
119	1	-4.91523	5.956025	-0.84847	119	1	7.124108	-3.13372	-1.16857
120	6	-4.95958	4.119233	0.281194	120	6	6.408794	-1.51463	0.063075
121	1	-6.02339	4.208377	0.520674	121	1	7.408971	-1.11178	0.248472
122	6	2.682419	6.21189	1.94026	122	6	0.43348	-6.4771	2.068839
123	1	2.066315	6.849354	2.587039	123	1	1.279312	-6.76512	2.705975
124	1	3.147901	5.425421	2.548249	124	1	-0.29274	-5.91359	2.668384
125	6	1.79058	5.564612	0.891169	125	6	0.944191	-5.59191	0.941396
126	1	1.180174	4.791468	1.375722	126	1	1.205357	-4.60835	1.352639
127	6	2.57883	4.925083	-0.27682	127	6	-0.07232	-5.41359	-0.21048
128	1	3.26304	5.667596	-0.70191	128	1	-0.38532	-6.40211	-0.56425
129	6	1.600427	4.421006	-1.34517	129	6	0.567248	-4.6207	-1.35745
130	1	0.93738	3.668451	-0.90297	130	1	0.862506	-3.62726	-0.99982
131	6	0.74887	5.597019	-1.83952	131	6	1.820554	-5.36559	-1.83711
132	1	1.393399	6.393845	-2.23432	132	1	1.55223	-6.37863	-2.16591
133	6	-0.05065	6.16264	-0.64774	133	6	2.817081	-5.48462	-0.66677
134	1	-0.63389	7.043917	-0.92589	134	1	3.700696	-6.06805	-0.93862
135	6	5.61423	1.208659	2.727472	135	6	-4.54099	-3.3987	2.752508
136	1	5.072667	1.650208	3.57446	136	1	-3.87525	-3.50012	3.619633
137	1	5.535983	0.120086	2.773764	137	1	-5.00567	-2.41012	2.764705
138	6	5.009932	1.719735	1.420554	138	6	-3.72956	-3.57624	1.468876
139	1	3.928493	1.54035	1.414097	139	1	-2.88218	-2.88137	1.473567
140	6	5.634644	1.078228	0.163325	140	6	-4.56067	-3.34899	0.187771
141	1	6.730497	1.101699	0.234756	141	1	-5.51761	-3.88343	0.261035
142	6	5.17395	1.806276	-1.09934	142	6	-3.79804	-3.81683	-1.05153
143	1	4.101929	1.628692	-1.24582	143	1	-2.92371	-3.173	-1.21456
144	6	5.438424	3.31979	-1.01286	144	6	-3.34809	-5.28014	-0.89994
145	1	6.517226	3.500283	-0.9516	145	1	-4.22863	-5.92242	-0.78517
146	6	4.790639	3.89847	0.267436	146	6	-2.49072	-5.43478	0.378358
147	1	5.06511	4.94557	0.423535	147	1	-2.24964	-6.48144	0.582862
148	6	0.768389	0.453747	1.798471	148	6	-0.58621	-0.9805	1.920981
149	6	-0.02855	-0.69733	2.002079	149	6	-0.47104	0.423394	2.092117
150	6	-0.46479	-1.13062	3.251043	150	6	-0.34284	1.037244	3.330804
151	6	-0.06228	-0.33507	4.344688	151	6	-0.32876	0.171231	4.453644
152	6	0.7337	0.826519	4.166528	152	6	-0.43995	-1.2318	4.301779
153	6	1.162529	1.241469	2.891625	153	6	-0.5715	-1.83938	3.034476
154	6	0.38403	-0.44289	-0.1752	154	6	-0.65639	0.004342	-0.13071
155	1	1.762999	2.135208	2.758283	155	1	-0.65058	-2.91549	2.927533
156	6	0.354601	-0.68543	-1.60112	156	6	-0.67403	0.298874	-1.53857
157	6	-0.32985	-1.78074	-2.17838	157	6	-0.50893	1.60431	-2.01198
158	6	1.04138	0.237036	-2.44661	158	6	-0.85458	-0.78484	-2.50869
159	6	-0.33508	-1.95587	-3.5673	159	6	-0.53568	1.892734	-3.42322
160	1	-0.84698	-2.4807	-1.52948	160	1	-0.35577	2.416335	-1.30757
161	6	1.03649	0.058947	-3.83968	161	6	-0.86519	-0.47213	-3.8999
162	6	0.348226	-1.0335	-4.39411	162	6	-0.70911	0.86473	-4.35777
163	1	-0.86112	-2.79697	-4.00767	163	1	-0.41894	2.922187	-3.74921
164	1	1.565343	0.767391	-4.46946	164	1	-1.00406	-1.28957	-4.60253

165	1	0.3449	-1.16856	-5.47212	165	1	-0.72573	1.080519	-5.42134
166	7	1.008955	0.575488	0.412022	166	7	-0.69675	-1.19842	0.549912
167	8	-0.27784	-1.27694	0.732518	167	8	-0.51154	1.036824	0.819005
168	8	1.721141	1.313503	-1.89048	168	8	-1.00204	-2.0219	-2.05648
169	1	1.628101	1.281182	-0.85421	169	1	-0.81024	-2.07859	0.047862
170	1	-1.07876	-2.01494	3.378969	170	1	-0.2573	2.113329	3.432993
171	1	1.015605	1.410185	5.038039	171	1	-0.4229	-1.86141	5.186856
172	1	-0.37196	-0.618	5.346448	172	1	-0.22961	0.595421	5.44819

Table A10: XYZ coordinate of optimized cis-enol HPBO–*β*-CD complex (benzoxazole moiety inside the cavity) in DMSO.

(a) in ground state

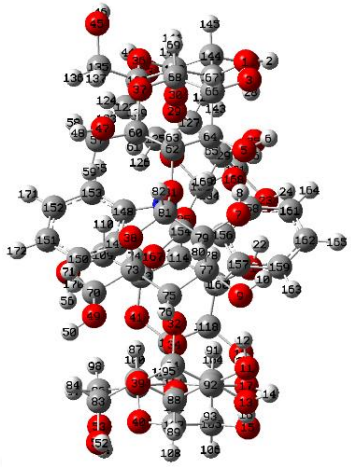

(b) in excited state

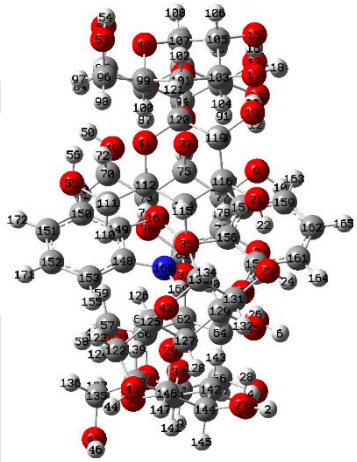

Center Number	Atomic Number	Coordinates (Angstroms) X	Y	Z	Center Number	Atomic Number	Coordinates (Angstroms) X	Y	Z
1	8	-5.89982	1.245656	2.23643	1	8	-4.70125	-3.68452	-2.20098
2	1	-5.77657	1.815667	3.026716	2	1	-4.33181	-4.17952	-2.96471
3	8	-6.10053	-1.45451	2.444278	3	8	-6.14281	-1.4023	-2.50397
4	1	-5.91493	-0.47487	2.343546	4	1	-5.52116	-2.1776	-2.37396
5	8	-4.30382	-3.68884	2.365742	5	8	-5.54988	1.411776	-2.49593
6	1	-4.58892	-3.2092	3.173553	6	1	-5.57428	0.83436	-3.28972
7	8	-2.7019	-5.86175	2.258327	7	8	-4.89908	4.042103	-2.49231
8	1	-3.20271	-4.99268	2.280626	8	1	-5.02578	3.047406	-2.46681
9	8	0.178628	-5.82069	2.356237	9	8	-2.27088	5.227929	-2.43718
10	1	-0.43074	-5.86807	3.125237	10	1	-2.77748	4.982459	-3.24187
11	8	2.863921	-5.40358	2.591364	11	8	0.25324	6.236847	-2.42339
12	1	1.869526	-5.44065	2.473126	12	1	-0.62542	5.754966	-2.3977
13	8	4.738819	-3.23424	2.522042	13	8	2.876843	5.078317	-2.34927
14	1	4.319424	-3.6093	3.327069	14	1	2.364543	5.305785	-3.15581
15	8	6.311543	-1.03065	2.532272	15	8	5.286915	3.855242	-2.35966
16	1	5.636363	-1.77104	2.498929	16	1	4.343778	4.195163	-2.33527
17	8	5.703529	1.756628	2.378942	17	8	6.039998	1.097968	-2.38098
18	1	5.766696	1.2164	3.196622	18	1	5.875315	1.667258	-3.16427
19	8	5.395431	4.430241	2.116173	19	8	6.776864	-1.51522	-2.37802
20	1	5.363429	3.436475	2.219771	20	1	6.359153	-0.6076	-2.36967
21	8	2.774439	5.728876	2.349734	21	8	5.022977	-3.87446	-2.56072
22	1	1.859196	5.508684	2.680769	22	1	4.091457	-4.12729	-2.81428
23	8	0.200504	5.174074	2.870185	23	8	2.467465	-4.65219	-2.94023
24	1	-0.28043	4.687285	3.573057	24	1	1.795977	-4.4262	-3.61944
25	8	-2.2967	3.827008	2.472214	25	8	-0.35065	-4.45966	-2.48094
26	1	-2.09469	2.844628	2.481548	26	1	-0.63392	-3.48515	-2.52649
27	8	-4.99155	4.002081	2.228765	27	8	-2.68004	-5.74767	-2.10089
28	1	-3.99477	3.950982	2.352679	28	1	-1.80259	-5.28025	-2.26904
29	8	-3.323	3.775112	-0.21673	29	8	-1.23787	-4.6509	0.264603

30	8	-5.15836	-0.28946	-0.06193	30	8	-4.79288	-1.91029	0.039662
31	8	-2.89522	-4.11965	-0.07451	31	8	-4.50599	2.478105	-0.06677
32	8	1.533818	-4.76646	0.108157	32	8	-0.763	4.907755	-0.06386
33	8	4.888599	-1.75244	0.091814	33	8	3.603807	3.666752	0.008781
34	8	4.598899	2.710873	-0.08149	34	8	5.436883	-0.43506	-0.05416
35	8	0.912901	5.112638	0.114495	35	8	3.186747	-4.14659	-0.23245
36	8	-5.25917	3.195105	-1.42012	36	8	-3.21612	-4.95985	1.524225
37	8	-5.92364	-2.21915	-1.22418	37	8	-6.38979	-0.5337	1.136835
38	8	-1.77018	-5.76136	-1.37361	38	8	-4.28223	4.487606	1.180733
39	8	3.580539	-5.06474	-1.0758	39	8	0.914135	5.960944	1.25959
40	8	6.392371	-0.4056	-1.16249	40	8	5.506803	3.064445	1.298624
41	8	4.26302	4.630901	-1.42996	41	8	6.108704	-2.33845	1.194982
42	8	-0.86681	6.618646	-0.36736	42	8	2.188609	-6.20746	0.409631
43	8	-3.6982	7.008425	-1.25938	43	8	-0.20303	-7.63747	1.495497
44	1	-4.19286	7.552295	-1.90612	44	1	-0.4275	-8.27953	2.19988
45	8	-7.04478	1.539489	-2.80721	45	8	-5.63131	-4.36919	2.827638
46	1	-7.15717	2.509037	-2.70179	46	1	-5.25059	-5.27149	2.759485
47	8	-5.33701	-4.88547	-2.3901	47	8	-7.1134	2.130464	2.20755
48	1	-5.33097	-5.43517	-3.20047	48	1	-7.36935	2.659045	2.991033
49	8	0.680779	-6.86776	-2.54899	49	8	-2.56173	6.543894	2.408143
50	1	1.189934	-7.10776	-3.35016	50	1	-2.2556	6.996666	3.220529
51	8	5.935935	-4.33449	-2.43029	51	8	3.305646	6.232753	2.716936
52	1	5.661741	-5.26308	-2.26829	52	1	2.658603	6.958692	2.582436
53	8	7.2913	1.874227	-2.56907	53	8	7.295826	1.386602	2.676289
54	1	7.857432	1.094005	-2.38381	54	1	7.423065	2.353992	2.568338
55	8	2.66958	4.454459	-3.76585	55	8	4.823665	-2.99535	3.614253
56	1	3.647031	4.365519	-3.76075	56	1	5.675374	-2.5106	3.559961
57	6	-4.54817	-3.66722	-2.59912	57	6	-5.85346	1.425552	2.4624
58	1	-4.96438	-3.06985	-3.42075	58	1	-5.95808	0.734162	3.308773
59	1	-3.50647	-3.92558	-2.82768	59	1	-5.05325	2.145266	2.67644
60	6	-4.57907	-2.84059	-1.32252	60	6	-5.47745	0.633492	1.219292
61	1	-3.83326	-2.03916	-1.40418	61	1	-4.4511	0.261766	1.335883
62	6	-4.29232	-3.67455	-0.05314	62	6	-5.56707	1.467539	-0.07896
63	1	-4.96336	-4.54056	-0.02469	63	1	-6.54941	1.949746	-0.14039
64	6	-4.48592	-2.82134	1.200047	64	6	-5.33988	0.583844	-1.30542
65	1	-3.73681	-2.01925	1.227381	65	1	-4.3095	0.205721	-1.30787
66	6	-5.89834	-2.20889	1.223644	66	6	-6.32131	-0.60084	-1.30976
67	1	-6.63814	-3.01793	1.236243	67	1	-7.34791	-0.21836	-1.34686
68	6	-6.11667	-1.38228	-0.0606	68	6	-6.15237	-1.39715	0.001067
69	1	-7.14163	-1.0064	-0.13193	69	1	-6.88245	-2.2077	0.083524
70	6	0.293753	-5.45568	-2.60027	70	6	-2.36468	5.096758	2.531102
71	1	-0.36911	-5.26502	-3.4546	71	1	-2.96259	4.691607	3.358015
72	1	1.184623	-4.82001	-2.68171	72	1	-1.30436	4.872529	2.702967
73	6	-0.44074	-5.10519	-1.31518	73	6	-2.80059	4.433267	1.23372
74	1	-0.58819	-4.01835	-1.2762	74	1	-2.49045	3.380365	1.253235
75	6	0.308203	-5.56134	-0.04367	75	6	-2.21646	5.115493	-0.02318
76	1	0.559969	-6.62493	-0.12703	76	1	-2.43987	6.188211	0.00707
77	6	-0.55573	-5.31808	1.19263	77	6	-2.80673	4.494906	-1.2881
78	1	-0.73388	-4.24362	1.318952	78	1	-2.51051	3.441918	-1.36368
79	6	-1.90906	-6.0363	1.058434	79	6	-4.34305	4.581543	-1.26818
80	1	-1.74276	-7.11544	0.964494	80	1	-4.64821	5.633634	-1.23631
81	6	-2.61601	-5.54139	-0.22315	81	6	-4.86909	3.884165	0.005503
82	1	-3.53605	-6.09702	-0.42323	82	1	-5.94995	4.002736	0.119696
83	6	4.740532	-3.49164	-2.45365	83	6	2.599801	4.95475	2.624265
84	1	4.101799	-3.752	-3.30807	84	1	1.882193	4.849415	3.448745
85	1	5.09648	-2.46511	-2.5658	85	1	3.365286	4.180084	2.707395
86	6	3.934355	-3.62699	-1.16301	86	6	1.860395	4.818767	1.294333
87	1	3.015868	-3.03028	-1.23257	87	1	1.295301	3.877752	1.277244
88	6	4.717971	-3.20797	0.100324	88	6	2.789949	4.883855	0.062787
89	1	5.696664	-3.70617	0.115105	89	1	3.436116	5.769219	0.132846
90	6	3.923049	-3.57214	1.354598	90	6	1.958096	4.946992	-1.21815
91	1	2.998419	-2.98343	1.38264	91	1	1.382123	4.019709	-1.32974
92	6	3.579462	-5.07268	1.374852	92	6	0.998411	6.150767	-1.18408
93	1	4.51119	-5.65009	1.395223	93	1	1.58836	7.072289	-1.11857

94	6	2.812654	-5.4498	0.08987	94	6	0.100012	6.067744	0.067988
95	1	2.676241	-6.53106	0.003847	95	1	-0.49162	6.976943	0.202293
96	6	5.893313	1.443388	-2.59135	96	6	5.86463	1.093748	2.602004
97	1	5.716415	0.749513	-3.42367	97	1	5.333582	1.546352	3.449799
98	1	5.300512	2.347863	-2.74345	98	1	5.774073	0.006917	2.656633
99	6	5.491473	0.769136	-1.28069	99	6	5.254434	1.601228	1.296534
100	1	4.452741	0.420875	-1.34559	100	1	4.171809	1.421084	1.297956
101	6	5.644362	1.685477	-0.04393	101	6	5.87348	0.959623	0.033119
102	1	6.637896	2.153465	-0.04685	102	1	6.969368	1.01458	0.08453
103	6	5.455448	0.873766	1.239502	103	6	5.371754	1.682044	-1.21878
104	1	4.424805	0.498407	1.291046	104	1	4.28706	1.54138	-1.31702
105	6	6.438916	-0.31016	1.281981	105	6	5.690625	3.186117	-1.14027
106	1	7.46456	0.075455	1.258177	106	1	6.776236	3.318334	-1.06732
107	6	6.229933	-1.19674	0.037837	107	6	5.047516	3.780744	0.128943
108	1	6.980465	-1.98984	-0.02717	108	1	5.346635	4.821293	0.284677
109	6	2.268159	5.235686	-2.59733	109	6	4.680645	-3.81583	2.412819
110	1	1.176714	5.240815	-2.5977	110	1	3.697245	-4.28455	2.482141
111	1	2.637682	6.268461	-2.6793	111	1	5.455372	-4.5962	2.386125
112	6	2.78607	4.604952	-1.30644	112	6	4.765736	-2.96252	1.148284
113	1	2.46011	3.559769	-1.23578	113	1	4.011023	-2.16694	1.172346
114	6	2.353588	5.366089	-0.04059	114	6	4.609349	-3.78056	-0.14607
115	1	2.530716	6.445684	-0.16088	115	1	5.226406	-4.69076	-0.10274
116	6	3.096729	4.872682	1.223836	116	6	4.989667	-2.98186	-1.41632
117	1	2.78128	3.837907	1.423305	117	1	4.235826	-2.1943	-1.56142
118	6	4.620974	4.905322	0.992284	118	6	6.378255	-2.33145	-1.25307
119	1	4.932394	5.945479	0.84084	119	1	7.132274	-3.12388	-1.18058
120	6	4.97169	4.106855	-0.28609	120	6	6.41794	-1.50715	0.054769
121	1	6.035638	4.192802	-0.52613	121	1	7.418057	-1.1037	0.239113
122	6	-2.6672	6.218609	-1.94182	122	6	0.443502	-6.45404	2.072964
123	1	-2.05013	6.855753	-2.58799	123	1	1.290714	-6.74235	2.708125
124	1	-3.1344	5.433675	-2.55052	124	1	-0.27842	-5.88504	2.672659
125	6	-1.77594	5.568755	-0.89373	125	6	0.95328	-5.57555	0.939855
126	1	-1.16825	4.793789	-1.37889	126	1	1.216403	-4.5901	1.345477
127	6	-2.5648	4.931614	0.275154	127	6	-0.06458	-5.40261	-0.21159
128	1	-3.24641	5.676204	0.70076	128	1	-0.37651	-6.39292	-0.56122
129	6	-1.58669	4.425168	1.342563	129	6	0.57355	-4.61354	-1.36208
130	1	-0.92595	3.670814	0.899953	130	1	0.868762	-3.61857	-1.00859
131	6	-0.73169	5.599118	1.835884	131	6	1.826876	-5.35937	-1.84032
132	1	-1.37391	6.397789	2.230755	132	1	1.558416	-6.37316	-2.16673
133	6	0.068366	6.162267	0.643321	133	6	2.824083	-5.47588	-0.67028
134	1	0.654018	7.042167	0.920724	134	1	3.706895	-6.06094	-0.94123
135	6	-5.61896	1.224084	-2.72342	135	6	-4.54271	-3.3964	2.748957
136	1	-5.07695	1.662215	-3.57194	136	1	-3.87691	-3.4913	3.61681
137	1	-5.54653	0.135066	-2.76902	137	1	-5.01457	-2.41119	2.758826
138	6	-5.0093	1.733077	-1.4181	138	6	-3.72919	-3.57073	1.466101
139	1	-3.92854	1.549507	-1.41406	139	1	-2.88581	-2.871	1.470482
140	6	-5.63336	1.09392	-0.15936	140	6	-4.56075	-3.34871	0.184405
141	1	-6.72929	1.120238	-0.22869	141	1	-5.51596	-3.88612	0.258272
142	6	-5.16837	1.821301	1.102094	142	6	-3.79615	-3.81583	-1.05393
143	1	-4.09665	1.640488	1.246944	143	1	-2.92379	-3.16946	-1.21775
144	6	-5.42823	3.335543	1.015308	144	6	-3.34164	-5.27742	-0.89956
145	1	-6.50654	3.519416	0.955176	145	1	-4.2202	-5.92199	-0.78212
146	6	-4.78022	3.911669	-0.26601	146	6	-2.48261	-5.42658	0.378234
147	1	-5.05143	4.959598	-0.42223	147	1	-2.23805	-6.47189	0.585141
148	6	-0.77056	0.447048	-1.80057	148	6	-0.58918	-1.00275	1.924492
149	6	0.020678	-0.70818	-2.00284	149	6	-0.4726	0.400068	2.102221
150	6	0.452821	-1.14654	-3.25145	150	6	-0.3425	1.008039	3.343588
151	6	0.052331	-0.3517	-4.34634	151	6	-0.32782	0.136765	4.46242
152	6	-0.73774	0.814109	-4.16958	152	6	-0.44055	-1.26532	4.304008
153	6	-1.16259	1.234069	-2.89497	153	6	-0.57422	-1.86685	3.033972
154	6	-0.38711	-0.44685	0.174499	154	6	-0.66091	-0.00801	-0.12241
155	1	-1.75819	2.131214	-2.76271	155	1	-0.65528	-2.9424	2.92216
156	6	-0.35669	-0.68714	1.600721	156	6	-0.68049	0.294706	-1.52911
157	6	0.323846	-1.78457	2.178623	157	6	-0.51758	1.602874	-1.99471

158	6	-1.03838	0.239469	2.445726	158	6	-0.8606	-0.7832	-2.50489
159	6	0.330056	-1.95777	3.567757	159	6	-0.54567	1.89987	-3.40469
160	1	0.837078	-2.48763	1.529976	160	1	-0.36542	2.411137	-1.2857
161	6	-1.03248	0.063315	3.839023	161	6	-0.87244	-0.46255	-3.89421
162	6	-0.34824	-1.03131	4.394106	162	6	-0.71822	0.877313	-4.3447
163	1	0.852919	-2.80055	4.008682	163	1	-0.43078	2.931426	-3.72462
164	1	-1.55745	0.774868	4.468537	164	1	-1.01077	-1.27608	-4.60146
165	1	-0.34415	-1.16486	5.472302	165	1	-0.73572	1.098945	-5.40704
166	7	-1.00833	0.573065	-0.41397	166	7	-0.70158	-1.214	0.552289
167	8	0.269542	-1.28592	-0.73248	167	8	-0.5143	1.019645	0.832135
168	8	-1.7142	1.318085	1.888957	168	8	-1.00678	-2.02304	-2.0596
169	1	-1.62264	1.284283	0.852844	169	1	-0.81666	-2.09234	0.047014
170	1	1.062703	-2.03394	-3.37807	170	1	-0.2559	2.083631	3.450499
171	1	-1.01794	1.397261	-5.04198	171	1	-0.42305	-1.89912	5.186077
172	1	0.359131	-0.63832	-5.34794	172	1	-0.22702	0.556139	5.45884

Table A11: XYZ coordinate of optimized cis-enol HPBO–*β*-CD complex (benzoxazole moiety outside the cavity) in ground state.

(a) in water

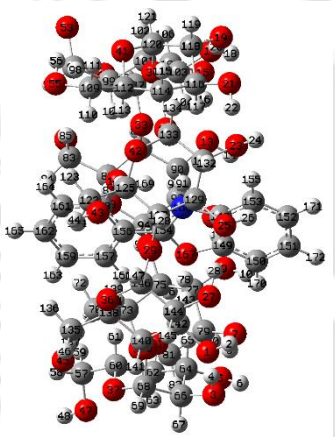

(b) in DMSO

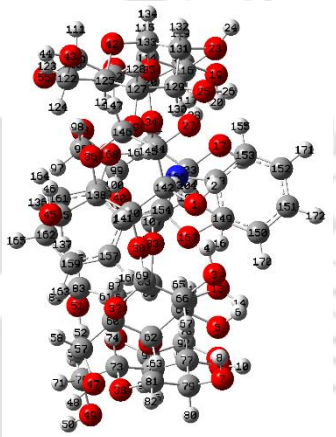

Center Number	Atomic Number	Coordinates (Angstroms)			Center Number	Atomic Number	Coordinates (Angstroms)		
		X	Y	Z			X	Y	Z
1	8	6.252936	0.722905	1.732309	1	8	0.099108	6.168707	1.885988
2	1	6.458807	0.142358	2.497736	2	1	0.767297	6.333081	2.588092
3	8	5.72116	3.340318	2.002867	3	8	-2.39846	5.429604	2.519565
4	1	5.814808	2.345175	1.90619	4	1	-1.44547	5.632921	2.279641
5	8	3.31556	4.803203	2.352286	5	8	-4.23046	3.27861	2.555816
6	1	3.946647	4.474956	3.031533	6	1	-3.70874	3.629408	3.310327
7	8	0.727905	5.090417	2.966943	7	8	-6.01661	1.281197	2.625532
8	1	1.697291	4.958623	2.738492	8	1	-5.27348	1.954409	2.568042
9	8	-2.01424	4.432408	2.669664	9	8	-5.47661	-1.52559	2.463363
10	1	-1.46047	4.202791	3.445902	10	1	-5.50074	-0.97896	3.278857
11	8	-4.66626	4.399346	2.369391	11	8	-5.1041	-4.18214	2.292816
12	1	-3.66945	4.335368	2.482252	12	1	-5.13288	-3.17953	2.340286
13	8	-5.81148	1.767904	2.159297	13	8	-2.55587	-5.4997	2.284734
14	1	-5.63582	2.261187	2.989988	14	1	-3.0991	-5.26802	3.069811
15	8	-6.79496	-0.72535	2.003521	15	8	-0.02889	-6.42631	2.43964
16	1	-6.32354	0.159506	2.054729	16	1	-0.92059	-5.97371	2.359597
17	8	-5.32985	-3.17934	2.196587	17	8	2.569181	-5.25229	2.414039
18	1	-5.71509	-2.66452	2.939334	18	1	2.014442	-5.4295	3.204891
19	8	-3.71849	-5.35428	2.490034	19	8	5.088634	-4.24848	2.338103
20	1	-4.1708	-4.47398	2.35623	20	1	4.111773	-4.45871	2.349756
21	8	-0.82511	-5.80368	2.676767	21	8	5.918248	-1.43211	2.401048
22	1	0.131434	-5.53439	2.733423	22	1	5.785168	-0.44678	2.445252
23	8	1.941203	-5.36276	2.833501	23	8	5.857775	1.365209	2.505473

24	1	2.309869	-5.9726	3.504872	24	1	6.591688	1.654358	3.08553
25	8	4.189357	-3.55464	2.358877	25	8	4.239415	3.759247	2.160863
26	1	3.740474	-3.49861	3.228008	26	1	4.250921	3.323859	3.038796
27	8	6.393999	-2.14198	1.745923	27	8	2.94702	6.061753	1.688445
28	1	5.524701	-2.59392	1.96415	28	1	3.3492	5.15772	1.859406
29	8	4.326967	-2.5262	-0.29026	29	8	2.986912	3.990949	-0.38756
30	8	4.741106	1.918381	-0.3868	30	8	-1.39935	4.855412	-0.19302
31	8	1.450617	4.814641	0.137244	31	8	-4.73615	1.94922	0.063016
32	8	-2.95869	4.151239	-0.02296	32	8	-4.54067	-2.5165	-0.04653
33	8	-5.22853	0.328596	-0.23648	33	8	-0.92703	-5.15324	-0.02845
34	8	-3.57556	-3.82257	0.054628	34	8	3.405974	-3.96801	0.011162
35	8	0.69765	-5.04842	0.343168	35	8	5.156123	0.12355	0.084141
36	8	5.69166	-1.39125	-1.85646	36	8	1.889231	5.488568	-1.85921
37	8	4.695855	3.996851	-1.54279	37	8	-3.57045	5.3455	-1.04429
38	8	-0.09553	6.546306	-0.39696	38	8	-6.35782	0.61084	-1.04815
39	8	-4.90146	3.899024	-1.33548	39	8	-4.36069	-4.47507	-1.37037
40	8	-5.99454	-1.4643	-1.58317	40	8	0.75742	-6.3261	-1.22606
41	8	-2.70045	-5.71888	-1.08573	41	8	5.30453	-3.36228	-1.28175
42	8	2.639247	-5.83717	-0.79861	42	8	6.035926	1.951713	-1.17421
43	8	5.167712	-5.20851	-2.24251	43	8	5.534609	4.534659	-2.58677
44	1	5.648716	-5.32288	-3.08775	44	1	5.624359	4.993707	-3.44701
45	8	6.570085	0.740969	-3.46506	45	8	-0.21774	6.645881	-3.29696
46	1	7.014611	-0.13307	-3.41829	46	1	0.705027	6.98117	-3.29456
47	8	3.240832	6.37403	-2.45251	47	8	-6.25102	4.384947	-1.88544
48	1	2.931513	6.920023	-3.20417	48	1	-6.90102	4.360024	-2.61729
49	8	-2.83432	7.31118	-1.332	49	8	-7.16127	-2.00064	-2.22268
50	1	-3.2938	7.821712	-2.02989	50	1	-7.46466	-2.45889	-3.03306
51	8	-6.80956	2.497584	-2.87687	51	8	-3.0811	-6.53743	-2.79046
52	1	-6.85476	3.462563	-2.70281	52	1	-4.05401	-6.46425	-2.68186
53	8	-5.86021	-3.92746	-2.94045	53	8	3.217217	-6.71009	-2.55077
54	1	-6.65807	-3.35611	-2.9136	54	1	2.558323	-7.42306	-2.40521
55	8	-1.3481	-5.42312	-3.53275	55	8	4.99423	-2.01956	-3.74613
56	1	-2.29454	-5.67241	-3.4588	56	1	5.103478	-2.99115	-3.66083
57	6	2.761981	4.997974	-2.59752	57	6	-4.96588	3.838279	-2.33091
58	1	3.159324	4.54175	-3.51382	58	1	-4.5734	4.409084	-3.18246
59	1	1.665239	4.975986	-2.62898	59	1	-5.08292	2.786408	-2.62089
60	6	3.231508	4.18729	-1.39925	60	6	-3.97419	3.923257	-1.18003
61	1	2.752976	3.20097	-1.43278	61	1	-3.08288	3.339324	-1.43971
62	6	2.907318	4.857804	-0.04365	62	6	-4.55375	3.40337	0.156526
63	1	3.254742	5.897818	-0.05163	63	1	-5.5157	3.890575	0.352314
64	6	3.568473	4.084667	1.098013	64	6	-3.58393	3.681089	1.304237
65	1	3.13134	3.081068	1.170733	65	1	-2.66432	3.097906	1.173365
66	6	5.084553	3.971526	0.86583	66	6	-3.23944	5.17835	1.366817
67	1	5.517285	4.975912	0.791149	67	1	-4.16215	5.755045	1.508133
68	6	5.321778	3.248799	-0.47553	68	6	-2.62505	5.608481	0.019296
69	1	6.384076	3.197816	-0.73154	69	1	-2.43332	6.684899	-0.01722
70	6	-1.9568	6.302814	-1.93601	70	6	-5.90625	-1.289	-2.48289
71	1	-1.25479	6.767328	-2.64024	71	1	-6.03723	-0.54699	-3.28138
72	1	-2.55491	5.550206	-2.46528	72	1	-5.12109	-1.99912	-2.77138
73	6	-1.16605	5.617033	-0.83139	73	6	-5.4792	-0.57302	-1.20966
74	1	-0.69524	4.717389	-1.247	74	1	-4.44655	-0.22483	-1.33279
75	6	-2.03501	5.217774	0.38233	75	6	-5.56374	-1.46951	0.045853
76	1	-2.59368	6.090899	0.73664	76	1	-6.56089	-1.91942	0.109052
77	6	-1.15749	4.663132	1.503208	77	6	-5.27768	-0.65279	1.304595
78	1	-0.70782	3.711931	1.193772	78	1	-4.23831	-0.29938	1.294711
79	6	-0.04507	5.655842	1.876744	79	6	-6.23267	0.551197	1.394057
80	1	-0.50377	6.587147	2.234665	80	1	-7.26508	0.18621	1.440772
81	6	0.782924	6.01	0.621979	81	6	-6.09157	1.414707	0.121995
82	1	1.507555	6.802802	0.828569	82	1	-6.82522	2.224957	0.096559
83	6	-5.41217	2.071657	-2.79235	83	6	-2.4987	-5.19933	-2.68563
84	1	-4.81823	2.538308	-3.58919	84	1	-2.82715	-4.56944	-3.52287
85	1	-5.4171	0.988351	-2.93278	85	1	-1.41613	-5.33573	-2.73642
86	6	-4.79813	2.421954	-1.4383	86	6	-2.87771	-4.52415	-1.36832
87	1	-3.74051	2.131052	-1.42349	87	1	-2.48111	-3.50135	-1.34687

88	6	-5.52485	1.764895	-0.24352	88	6	-2.38307	-5.29001	-0.12109
89	1	-6.60714	1.930804	-0.32854	89	1	-2.6606	-6.34994	-0.20106
90	6	-5.0094	2.340083	1.075528	90	6	-2.99002	-4.68755	1.146007
91	1	-3.95928	2.049506	1.212832	91	1	-2.62629	-3.66001	1.278307
92	6	-5.12389	3.874878	1.098965	92	6	-4.52715	-4.68393	1.063258
93	1	-6.17856	4.162764	1.0249	93	1	-4.88588	-5.71479	0.965407
94	6	-4.37794	4.470002	-0.116	94	6	-4.96764	-3.89782	-0.19036
95	1	-4.52405	5.55026	-0.20175	95	1	-6.04676	-3.95689	-0.35499
96	6	-4.67851	-3.08739	-2.74444	96	6	2.518472	-5.42468	-2.56819
97	1	-4.55312	-2.39552	-3.58782	97	1	1.840429	-5.36578	-3.42974
98	1	-3.82539	-3.76744	-2.70379	98	1	3.292488	-4.66043	-2.66301
99	6	-4.7658	-2.28826	-1.44612	99	6	1.722887	-5.19929	-1.28415
100	1	-3.89572	-1.62539	-1.35935	100	1	1.170291	-4.25342	-1.35109
101	6	-4.86562	-3.16908	-0.17941	101	6	2.597768	-5.18935	-0.00883
102	1	-5.65435	-3.92275	-0.31008	102	1	3.24777	-6.07487	0.00318
103	6	-5.17141	-2.29811	1.0398	103	6	1.707249	-5.18109	1.235069
104	1	-4.33413	-1.6111	1.221584	104	1	1.123773	-4.25145	1.268541
105	6	-6.46141	-1.48773	0.818904	105	6	0.751371	-6.38828	1.220413
106	1	-7.29802	-2.17794	0.661556	106	1	1.342041	-7.31189	1.205431
107	6	-6.30674	-0.62189	-0.4493	107	6	-0.10338	-6.34788	-0.06242
108	1	-7.23821	-0.10933	-0.70699	108	1	-0.71842	-7.24618	-0.16846
109	6	-0.65936	-5.85635	-2.31751	109	6	5.606253	-1.38057	-2.5823
110	1	0.373369	-5.51899	-2.41692	110	1	5.40478	-0.31268	-2.68127
111	1	-0.67605	-6.95365	-2.23895	111	1	6.694085	-1.5458	-2.58252
112	6	-1.29547	-5.2382	-1.07407	112	6	5.004668	-1.90786	-1.28118
113	1	-1.29111	-4.14497	-1.14762	113	1	3.918198	-1.76755	-1.27988
114	6	-0.62704	-5.67967	0.239139	114	6	5.621185	-1.26826	-0.02463
115	1	-0.51596	-6.7745	0.258869	115	1	6.719875	-1.28635	-0.08949
116	6	-1.42955	-5.23861	1.482995	116	6	5.187741	-1.98332	1.273753
117	1	-1.42098	-4.13957	1.530258	117	1	4.105608	-1.83367	1.405447
118	6	-2.88211	-5.74164	1.375786	118	6	5.49371	-3.49028	1.176298
119	1	-2.86734	-6.8383	1.37929	119	1	6.580195	-3.61902	1.105462
120	6	-3.49867	-5.27585	0.034251	120	6	4.855128	-4.07303	-0.10797
121	1	-4.48947	-5.71467	-0.11702	121	1	5.15553	-5.11441	-0.25774
122	6	3.858988	-4.59075	-2.48408	122	6	4.771082	3.292785	-2.7524
123	1	3.262902	-5.20022	-3.17551	123	1	5.251876	2.634859	-3.48775
124	1	3.987803	-3.58626	-2.90649	124	1	3.749207	3.519511	-3.08164
125	6	3.117438	-4.47858	-1.16041	125	6	4.708382	2.573849	-1.41314
126	1	2.246422	-3.8252	-1.29653	126	1	3.955544	1.77801	-1.47341
127	6	4.000838	-3.92911	-0.01814	127	6	4.367021	3.519383	-0.23947
128	1	4.918177	-4.52466	0.051278	128	1	5.059575	4.368803	-0.24184
129	6	3.248711	-3.96968	1.315822	129	6	4.457141	2.776915	1.096878
130	1	2.40315	-3.2723	1.285811	130	1	3.680129	2.005349	1.146061
131	6	2.735649	-5.38751	1.599915	131	6	5.838345	2.127811	1.251978
132	1	3.585583	-6.07033	1.715769	132	1	6.611105	2.905208	1.275441
133	6	1.869292	-5.88947	0.426852	133	6	6.125318	1.195205	0.057473
134	1	1.5959	-6.94078	0.554295	134	1	7.148074	0.808577	0.088342
135	6	5.158171	0.565103	-3.1245	135	6	-0.19289	5.214468	-2.99726
136	1	4.652377	-0.04718	-3.88268	136	1	0.300543	4.659975	-3.8064
137	1	4.721496	1.566214	-3.11551	137	1	-1.23658	4.901431	-2.92644
138	6	4.98903	-0.0883	-1.75402	138	6	0.52624	4.930605	-1.67917
139	1	3.924474	-0.26593	-1.55562	139	1	0.59613	3.84748	-1.51843
140	6	5.590436	0.74441	-0.59971	140	6	-0.156	5.584247	-0.45651
141	1	6.613282	1.053961	-0.85393	141	1	-0.37145	6.640325	-0.66894
142	6	5.594099	-0.07181	0.692745	142	6	0.746573	5.469244	0.772414
143	1	4.559299	-0.27464	0.998981	143	1	0.870674	4.41176	1.040398
144	6	6.344571	-1.40153	0.501897	144	6	2.124159	6.096369	0.497439
145	1	7.387835	-1.19605	0.237875	145	1	1.999966	7.157474	0.253838
146	6	5.697879	-2.19369	-0.65469	146	6	2.767876	5.392876	-0.71611
147	1	6.260942	-3.09711	-0.90311	147	1	3.703833	5.867744	-1.02129
148	6	0.679415	-0.68842	2.370801	148	6	1.123542	0.633346	2.445045
149	6	0.702655	0.721998	2.479562	149	6	-0.23922	0.922017	2.69248
150	6	0.819381	1.413373	3.682667	150	6	-0.76914	1.152729	3.959094
151	6	0.915625	0.606343	4.83637	151	6	0.151759	1.081327	5.025984

152	6	0.893639	-0.81105	4.757053	152	6	1.524072	0.793549	4.805089
153	6	0.775892	-1.48308	3.524986	153	6	2.033711	0.56513	3.512539
154	6	0.497438	0.126381	0.337324	154	6	0.092646	0.632089	0.503409
155	1	0.758759	-2.56707	3.469827	155	1	3.083542	0.344865	3.348119
156	6	0.353897	0.28374	-1.09337	156	6	-0.22222	0.540528	-0.90533
157	6	0.292379	1.558032	-1.71035	157	6	-1.53488	0.734217	-1.40193
158	6	0.263274	-0.89291	-1.89709	158	6	0.837833	0.239817	-1.81409
159	6	0.144467	1.665583	-3.09744	159	6	-1.79268	0.634927	-2.77401
160	1	0.36209	2.447286	-1.09062	160	1	-2.33708	0.960111	-0.70518
161	6	0.115655	-0.77734	-3.29315	161	6	0.570247	0.140884	-3.19354
162	6	0.056937	0.492844	-3.88607	162	6	-0.73522	0.338133	-3.66726
163	1	0.094967	2.64295	-3.56755	163	1	-2.79794	0.786767	-3.1554
164	1	0.047793	-1.68188	-3.88939	164	1	1.387461	-0.08866	-3.87011
165	1	-0.05794	0.573627	-4.96368	165	1	-0.93356	0.260827	-4.73289
166	7	0.55033	-1.02536	1.001793	166	7	1.292553	0.457665	1.051163
167	8	0.58564	1.25269	1.173153	167	8	-0.90929	0.924122	1.445938
168	8	0.314663	-2.15626	-1.34097	168	8	2.132822	0.040963	-1.37802
169	1	0.406435	-2.09786	-0.33287	169	1	2.187748	0.134972	-0.36914
170	1	0.834987	2.497766	3.727502	170	1	-1.81945	1.369717	4.119119
171	1	0.969676	-1.39058	5.672721	171	1	2.196277	0.747938	5.657138
172	1	1.008315	1.081785	5.808617	172	1	-0.19904	1.250178	6.039951

Table A12: XYZ coordinate of optimized trans-enol HPBO–*β*-CD complex (benzoxazole moiety inside the cavity) in water.

(a) in ground state

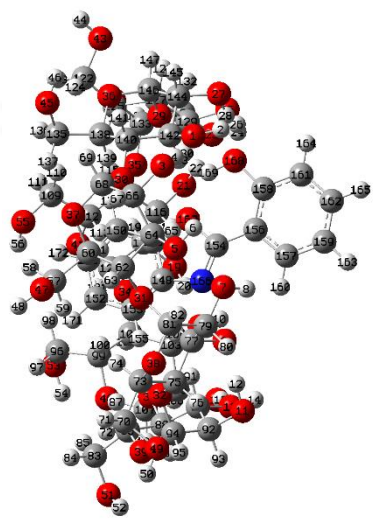

(b) in excited state

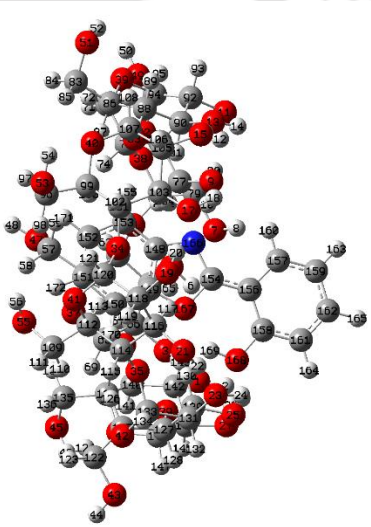

Center Number	Atomic Number	Coordinates (Angstroms) X	Y	Z	Center Number	Atomic Number	Coordinates (Angstroms) X	Y	Z
1	8	-5.72908	-1.93963	1.246144	1	8	5.677672	2.026148	1.247524
2	1	-5.84043	-1.72743	2.1975	2	1	5.789833	1.818027	2.199682
3	8	-5.88803	-4.34647	0.027537	3	8	5.795154	4.432278	0.028274
4	1	-5.75235	-3.48216	0.515143	4	1	5.674024	3.566118	0.516504
5	8	-3.65763	-6.21034	0.3497	5	8	3.528888	6.251493	0.336262
6	1	-4.41068	-6.1505	0.977513	6	1	4.279562	6.204687	0.968037
7	8	-1.20088	-4.47544	2.110636	7	8	1.107465	4.457527	2.075577
8	1	-0.88726	-4.05698	2.941075	8	1	0.790182	3.988382	2.878088
9	8	1.45654	-3.36646	2.240526	9	8	-1.52414	3.306049	2.198279
10	1	1.109237	-2.41447	2.14302	10	1	-1.16526	2.34879	2.073971
11	8	4.022126	-3.67308	2.852731	11	8	-4.07246	3.59855	2.843401
12	1	3.04284	-3.53631	2.63793	12	1	-3.09277	3.468298	2.61806
13	8	5.236003	-1.05588	2.613562	13	8	-5.24441	0.963418	2.628277
14	1	4.803915	-1.40927	3.421097	14	1	-4.81051	1.330678	3.428693

15	8	6.258266	1.414083	2.320201	15	8	-6.21398	-1.52947	2.359643
16	1	5.785294	0.532344	2.399383	16	1	-5.76005	-0.63696	2.429719
17	8	4.6461	3.752466	1.875215	17	8	-4.5528	-3.83179	1.897894
18	1	4.88416	3.377279	2.750575	18	1	-4.78715	-3.46142	2.776244
19	8	3.574576	6.136049	1.180049	19	8	-3.46718	-6.19912	1.166854
20	1	3.83442	5.213903	1.465304	20	1	-3.73284	-5.28356	1.467621
21	8	0.690964	6.619814	1.518627	21	8	-0.57582	-6.63709	1.510648
22	1	-0.14727	6.269933	1.934197	22	1	0.247913	-6.2699	1.939949
23	8	-1.70031	5.739557	2.404926	23	8	1.78256	-5.69948	2.423794
24	1	-1.98465	5.339535	3.255878	24	1	2.057013	-5.2978	3.277081
25	8	-3.67434	3.814041	2.798641	25	8	3.73556	-3.75042	2.822157
26	1	-3.593	2.86492	3.05932	26	1	3.638116	-2.80459	3.08616
27	8	-5.90419	0.755584	2.296913	27	8	5.928209	-0.65887	2.301121
28	1	-4.96473	0.946294	2.549736	28	1	4.996949	-0.88165	2.553694
29	8	-4.34877	2.217846	0.37039	29	8	4.395829	-2.15361	0.387008
30	8	-4.2727	-2.1979	-1.2059	30	8	4.231932	2.248332	-1.21267
31	8	-1.07815	-4.86244	-0.70985	31	8	0.978951	4.861592	-0.74403
32	8	3.199001	-3.91162	0.013393	32	8	-3.29137	3.847335	-0.01162
33	8	5.307751	-0.0197	-0.06401	33	8	-5.32969	-0.08383	-0.04704
34	8	3.305366	3.91252	-0.64618	34	8	-3.23769	-3.95768	-0.64005
35	8	-1.01035	4.985886	-0.26772	35	8	1.103479	-4.96195	-0.25674
36	8	-5.66821	1.269245	-1.40992	36	8	5.694402	-1.1923	-1.40237
37	8	-3.75795	-3.69765	-2.96326	37	8	3.695662	3.736293	-2.97368
38	8	0.561616	-6.56368	-0.38951	38	8	-0.68781	6.534185	-0.41224
39	8	5.466266	-3.72298	-0.60149	39	8	-5.56298	3.614419	-0.59165
40	8	6.230174	1.684052	-1.41605	40	8	-6.23498	-1.81499	-1.37512
41	8	2.176856	5.313295	-2.17896	41	8	-2.07282	-5.31759	-2.17917
42	8	-3.21035	5.587241	-0.95707	42	8	3.313866	-5.54573	-0.92772
43	8	-6.02826	4.800246	-1.48663	43	8	6.129326	-4.7258	-1.43626
44	1	-6.73887	4.865699	-2.1571	44	1	6.845461	-4.79148	-2.10079
45	8	-6.33171	-0.3657	-3.64421	45	8	6.334909	0.44724	-3.63932
46	1	-6.92095	0.350616	-3.32331	46	1	6.935923	-0.25736	-3.31432
47	8	-1.91512	-5.63156	-4.15388	47	8	1.822901	5.629429	-4.18089
48	1	-1.40797	-5.84387	-4.96437	48	1	1.310691	5.831742	-4.99077
49	8	3.468045	-7.29465	-0.31415	49	8	-3.60351	7.227443	-0.3266
50	1	4.089856	-7.95112	-0.69025	50	1	-4.23293	7.878963	-0.69862
51	8	7.773246	-2.444	-1.63313	51	8	-7.86087	2.297326	-1.58925
52	1	7.776873	-3.36973	-1.30678	52	1	-7.87338	3.223293	-1.26379
53	8	6.125773	4.001373	-3.07783	53	8	-6.09162	-4.14419	-3.02442
54	1	6.971857	3.569644	-2.83078	54	1	-6.94677	-3.73815	-2.76529
55	8	0.542427	3.982755	-4.14751	55	8	-0.4327	-3.87292	-4.09703
56	1	1.490034	4.185033	-4.30343	56	1	-1.37653	-4.06993	-4.28001
57	6	-1.52938	-4.31077	-3.64982	57	6	1.459191	4.303702	-3.67332
58	1	-1.67455	-3.54363	-4.42204	58	1	1.622349	3.536567	-4.44196
59	1	-0.47766	-4.31267	-3.33596	59	1	0.406206	4.287314	-3.36427
60	6	-2.39759	-3.96842	-2.44772	60	6	2.327826	3.982443	-2.46575
61	1	-2.01521	-3.04568	-1.9948	61	1	1.961223	3.054033	-2.01123
62	6	-2.38522	-5.06986	-1.35795	62	6	2.288687	5.087439	-1.38035
63	1	-2.42962	-6.06565	-1.81469	63	1	2.321274	6.08221	-1.8404
64	6	-3.52674	-4.92192	-0.34092	64	6	3.424908	4.960557	-0.35453
65	1	-3.25487	-4.14049	0.379922	65	1	3.161987	4.175212	0.365389
66	6	-4.87676	-4.56684	-0.99129	66	6	4.78552	4.630462	-0.9965
67	1	-5.232	-5.42268	-1.5757	67	1	5.126808	5.492291	-1.58051
68	6	-4.72692	-3.37389	-1.95027	68	6	4.665386	3.433586	-1.95516
69	1	-5.6605	-3.15637	-2.47823	69	1	5.606246	3.235289	-2.47776
70	6	2.769618	-6.58385	-1.39181	70	6	-2.89841	6.530235	-1.40883
71	1	2.292482	-7.29253	-2.08076	71	1	-2.43191	7.248004	-2.0957
72	1	3.477715	-5.95908	-1.95104	72	1	-3.59974	5.898978	-1.96937
73	6	1.697648	-5.69394	-0.77921	73	6	-1.81393	5.651251	-0.80259
74	1	1.349061	-4.98804	-1.54474	74	1	-1.45814	4.953117	-1.572
75	6	2.194729	-4.8939	0.449652	75	6	-2.29679	4.840177	0.424547
76	1	2.638754	-5.5836	1.176125	76	1	-2.74614	5.521397	1.155635
77	6	1.020796	-4.13431	1.077675	77	6	-1.11013	4.092671	1.042564
78	1	0.600989	-3.44529	0.336618	78	1	-0.68357	3.417361	0.291891

79	6	-0.07504	-5.13884	1.474472	79	6	-0.0273	5.109767	1.443423
80	1	0.34705	-5.89533	2.152639	80	1	-0.45881	5.856079	2.12713
81	6	-0.5673	-5.8587	0.204679	81	6	0.452678	5.844036	0.177254
82	1	-1.31705	-6.61901	0.426259	82	1	1.190407	6.61511	0.401911
83	6	6.423249	-2.11177	-2.08752	83	6	-6.51216	1.983733	-2.06034
84	1	6.138844	-2.73774	-2.94342	84	1	-6.24859	2.610921	-2.92202
85	1	6.457427	-1.06635	-2.40308	85	1	-6.53476	0.936854	-2.372
86	6	5.394099	-2.28979	-0.97226	86	6	-5.47119	2.18171	-0.9594
87	1	4.393582	-2.06709	-1.36083	87	1	-4.47225	1.975112	-1.36101
88	6	5.670049	-1.40379	0.263365	88	6	-5.7147	1.29395	0.282031
89	1	6.729656	-1.47087	0.54306	89	1	-6.77174	1.34117	0.575099
90	6	4.791501	-1.818	1.443784	90	6	-4.82895	1.728262	1.449758
91	1	3.750253	-1.55257	1.222872	91	1	-3.78594	1.480478	1.216733
92	6	4.879485	-3.32603	1.737053	92	6	-4.938	3.235663	1.739557
93	1	5.897705	-3.57578	2.055559	93	1	-5.95634	3.469932	2.069526
94	6	4.57653	-4.13625	0.455454	94	6	-4.66584	4.047067	0.451345
95	1	4.751598	-5.20609	0.598868	95	1	-4.85855	5.114009	0.5942
96	6	5.054878	3.005038	-3.03035	96	6	-5.05249	-3.11391	-3.00201
97	1	5.226583	2.217415	-3.77568	97	1	-5.2639	-2.33563	-3.74694
98	1	4.13517	3.53948	-3.27803	98	1	-4.1212	-3.61965	-3.26645
99	6	4.932426	2.369424	-1.6474	99	6	-4.92397	-2.46766	-1.62451
100	1	4.128405	1.623302	-1.65349	100	1	-4.14037	-1.70062	-1.6484
101	6	4.671234	3.394074	-0.51879	101	6	-4.6164	-3.47879	-0.49529
102	1	5.397686	4.214228	-0.58827	102	1	-5.31874	-4.32063	-0.55116
103	6	4.781856	2.718472	0.848991	103	6	-4.72673	-2.80268	0.872239
104	1	3.971773	1.986198	0.963739	104	1	-3.93317	-2.05097	0.975712
105	6	6.141588	2.010662	1.005693	105	6	-6.10098	-2.12766	1.045588
106	1	6.943036	2.755534	0.94629	106	1	-6.88502	-2.89177	0.999637
107	6	6.339649	1.002131	-0.14593	107	6	-6.33976	-1.12876	-0.10677
108	1	7.338752	0.556759	-0.12734	108	1	-7.34818	-0.70585	-0.0742
109	6	0.024486	4.901318	-3.1331	109	6	0.073079	-4.83697	-3.11808
110	1	-1.01	4.600971	-2.95842	110	1	1.108534	-4.55094	-2.92665
111	1	0.04428	5.936511	-3.50414	111	1	0.048108	-5.85571	-3.53123
112	6	0.826681	4.802605	-1.83904	112	6	-0.73532	-4.78501	-1.82549
113	1	0.91742	3.754892	-1.53063	113	1	-0.84934	-3.74544	-1.49662
114	6	0.24529	5.633986	-0.68347	114	6	-0.14129	-5.62416	-0.68213
115	1	0.040111	6.661822	-1.01836	115	1	0.079938	-6.64382	-1.03132
116	6	1.197418	5.681585	0.534908	116	6	-1.09594	-5.70014	0.533078
117	1	1.256331	4.66705	0.958323	117	1	-1.17394	-4.69033	0.964745
118	6	2.605723	6.141758	0.105809	118	6	-2.495	-6.18023	0.09557
119	1	2.543431	7.185248	-0.22431	119	1	-2.4148	-7.21989	-0.2427
120	6	3.11652	5.293106	-1.08494	120	6	-3.01762	-5.33035	-1.08959
121	1	4.050857	5.700442	-1.4829	121	1	-3.94121	-5.7534	-1.49609
122	6	-4.81907	4.224477	-2.08992	122	6	4.917507	-4.17264	-2.05534
123	1	-4.47277	4.84194	-2.92854	123	1	4.586966	-4.80287	-2.8908
124	1	-5.0238	3.207446	-2.43522	124	1	5.110742	-3.15617	-2.4089
125	6	-3.71973	4.193853	-1.03388	125	6	3.808461	-4.14765	-1.00902
126	1	-2.90494	3.549076	-1.38672	126	1	2.989922	-3.51447	-1.37382
127	6	-4.18838	3.693744	0.363496	127	6	4.259014	-3.63173	0.388845
128	1	-5.14555	4.162086	0.619011	128	1	5.221597	-4.08343	0.6537
129	6	-3.14857	4.00752	1.452697	129	6	3.217347	-3.95368	1.474123
130	1	-2.26084	3.380646	1.295238	130	1	2.323389	-3.33744	1.311038
131	6	-2.71947	5.477623	1.397615	131	6	2.805515	-5.429	1.422787
132	1	-3.58956	6.12122	1.583058	132	1	3.681955	-6.06155	1.616302
133	6	-2.16162	5.819022	0.010364	133	6	2.260624	-5.78284	0.033484
134	1	-1.90951	6.879397	-0.07742	134	1	2.019259	-6.84595	-0.05039
135	6	-4.9517	-0.04122	-3.28253	135	6	4.959931	0.099152	-3.28076
136	1	-4.62382	0.875257	-3.79032	136	1	4.650246	-0.82495	-3.78616
137	1	-4.34385	-0.87981	-3.62911	137	1	4.338005	0.925459	-3.63189
138	6	-4.79053	0.13258	-1.77309	138	6	4.797452	-0.07244	-1.77122
139	1	-3.74741	0.384436	-1.5414	139	1	3.758347	-0.34203	-1.54163
140	6	-5.21899	-1.10817	-0.96389	140	6	5.19957	1.179054	-0.96468
141	1	-6.23406	-1.40607	-1.2564	141	1	6.209291	1.496428	-1.25541
142	6	-5.1768	-0.78867	0.529925	142	6	5.159248	0.861168	0.529738

143	1	-4.12917	-0.65175	0.8301	143	1	4.113913	0.695806	0.824368
144	6	-6.00057	0.469131	0.877233	144	6	6.01429	-0.37474	0.879877
145	1	-7.05794	0.247348	0.701007	145	1	7.06591	-0.12953	0.701082
146	6	-5.64264	1.68133	-0.01647	146	6	5.679303	-1.5975	-0.00697
147	1	-6.40581	2.460642	0.056645	147	1	6.456333	-2.36271	0.068842
148	6	0.552103	-0.5171	0.305166	148	6	-0.56559	0.495062	0.306232
149	6	-0.39656	0.497502	0.062376	149	6	0.458024	-0.4879	0.047056
150	6	-0.51314	1.19079	-1.13729	150	6	0.585044	-1.18321	-1.13459
151	6	0.395537	0.813017	-2.14735	151	6	-0.37291	-0.87812	-2.14621
152	6	1.34777	-0.21749	-1.9375	152	6	-1.37991	0.11224	-1.93882
153	6	1.442762	-0.90156	-0.71154	153	6	-1.49402	0.811881	-0.73328
154	6	-0.60996	-0.29858	2.163184	154	6	0.655551	0.351636	2.153427
155	1	2.161968	-1.70026	-0.56365	155	1	-2.24644	1.579335	-0.58869
156	6	-1.21306	-0.36449	3.485652	156	6	1.238148	0.499795	3.415817
157	6	-0.57797	-1.12683	4.501489	157	6	0.636245	1.366116	4.41006
158	6	-2.42826	0.304187	3.803701	158	6	2.470393	-0.19641	3.804087
159	6	-1.13118	-1.21988	5.782515	159	6	1.200637	1.491495	5.675662
160	1	0.35836	-1.62793	4.277349	160	1	-0.27998	1.891806	4.16217
161	6	-2.98519	0.212197	5.087946	161	6	3.015628	-0.05747	5.076052
162	6	-2.3387	-0.54738	6.075335	162	6	2.387521	0.782145	6.025029
163	1	-0.63104	-1.80351	6.548577	163	1	0.729572	2.137677	6.410795
164	1	-3.91285	0.734057	5.299941	164	1	3.927168	-0.59355	5.321601
165	1	-2.77264	-0.61327	7.068654	165	1	2.815825	0.889557	7.01702
166	7	0.383497	-0.98821	1.63613	166	7	-0.44634	0.985565	1.582761
167	8	-1.15222	0.644071	1.248485	167	8	1.247464	-0.58111	1.208278
168	8	-3.14272	1.069418	2.863885	168	8	3.150825	-1.00111	2.885166
169	1	-2.69089	1.110502	1.982042	169	1	2.689634	-1.04855	2.002099
170	1	-1.24515	1.974588	-1.28757	170	1	1.357546	-1.92538	-1.29171
171	1	2.021278	-0.48401	-2.74678	171	1	-2.07459	0.324991	-2.74597
172	1	0.366812	1.332366	-3.10078	172	1	-0.33497	-1.42365	-3.08504

Table A13: XYZ coordinate of optimized trans-enol HPBO–*β*-CD complex (benzoxazole moiety inside the cavity) in DMSO.

(a) in ground state

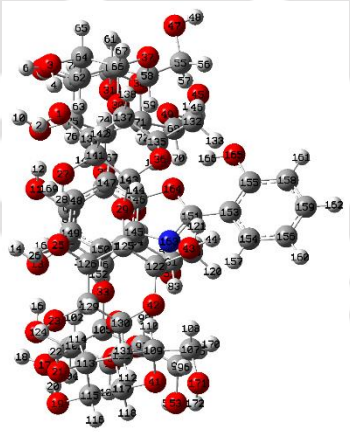

Center Number	Atomic Number	Coordinates (Angstroms) X	Y	Z
1	8	4.897785	-2.98715	-3.07103
2	1	5.168947	-2.48165	-3.86853
3	8	3.267832	-5.14421	-3.1887
4	1	3.775657	-4.28244	-3.11836
5	8	0.452521	-5.6177	-2.97228
6	1	0.955751	-5.46233	-3.80117
7	8	-2.20094	-6.04225	-2.80916
8	1	-1.23574	-5.76991	-2.84257

9	8	-4.38309	-4.19113	-2.62469
10	1	-3.98849	-4.55075	-3.44917
11	8	-6.32865	-2.32033	-2.5318
12	1	-5.52887	-2.92578	-2.54996
13	8	-6.17901	0.544693	-2.52312
14	1	-6.24787	-0.03707	-3.31172
15	8	-5.71651	3.211336	-2.66073
16	1	-5.76649	2.212736	-2.58692
17	8	-3.39378	4.895798	-2.62872
18	1	-3.81987	4.522913	-3.43077
19	8	-1.40244	6.739517	-2.41341
20	1	-2.0192	5.957934	-2.49728
21	8	1.4579	6.093442	-2.74162
22	1	2.224852	5.483569	-2.91552
23	8	3.815807	4.63356	-3.17344
24	1	4.39229	5.17741	-3.74827
25	8	5.114101	2.02311	-3.1781
26	1	4.683314	2.34849	-3.99678
27	8	6.241978	-0.4472	-3.11892
28	1	5.728113	0.413267	-3.10881
29	8	4.929352	0.585537	-0.74232
30	8	3.456683	-3.63405	-0.69674
31	8	-0.77513	-5.03015	-0.46311
32	8	-4.57659	-2.66722	-0.22315
33	8	-5.04423	1.775157	-0.22195
34	8	-1.83598	4.899704	-0.2518
35	8	2.552932	4.388163	-0.67201
36	8	5.945421	-1.12829	0.553446
37	8	2.812376	-5.58347	0.508949
38	8	-2.62421	-5.66689	0.898711
39	8	-6.16571	-1.53554	1.131216
40	8	-5.19883	3.802992	1.007021
41	8	-0.28328	6.079354	1.088208
42	8	4.660909	4.141063	0.425509
43	8	6.806179	2.39466	1.500949
44	1	7.325806	2.133056	2.288483
45	8	6.130169	-3.54966	1.962616
46	1	6.880198	-2.93153	1.824357
47	8	0.692402	-7.20478	1.783601
48	1	0.35534	-7.61452	2.606508
49	8	-5.17707	-5.01689	2.249495
50	1	-5.66169	-4.97002	3.09895
51	8	-7.29447	0.598858	2.565041
52	1	-7.71648	-0.28112	2.458377
53	8	-4.22567	6.097628	2.359503
54	1	-5.18127	5.917005	2.226548
55	6	0.895614	-5.7669	1.980232
56	1	1.637158	-5.5822	2.768293
57	1	-0.05154	-5.28341	2.250522
58	6	1.398923	-5.16471	0.677025
59	1	1.373592	-4.07103	0.761242
60	6	0.573262	-5.60466	-0.55409
61	1	0.511685	-6.69868	-0.57833
62	6	1.218662	-5.09101	-1.84116
63	1	1.191988	-3.99443	-1.86786
64	6	2.678415	-5.56936	-1.9355
65	1	2.696457	-6.66545	-1.94337
66	6	3.45092	-5.08808	-0.69033
67	1	4.470311	-5.48404	-0.66715
68	6	-3.94686	-4.22365	2.325134
69	1	-3.28512	-4.60554	3.113452
70	1	-4.18486	-3.17169	2.527375
71	6	-3.2263	-4.315	0.987904
72	1	-2.41802	-3.5722	0.974786

73	6	-4.16112	-4.07307	-0.21846
74	1	-5.03781	-4.72609	-0.13982
75	6	-3.42325	-4.34123	-1.52929
76	1	-2.61441	-3.61158	-1.66155
77	6	-2.83723	-5.76381	-1.53872
78	1	-3.65503	-6.48766	-1.44588
79	6	-1.90448	-5.9426	-0.32201
80	1	-1.55341	-6.9735	-0.22882
81	6	-5.84541	0.437911	2.443578
82	1	-5.4529	-0.15971	3.276939
83	1	-5.42425	1.444785	2.488249
84	6	-5.46472	-0.228	1.122099
85	1	-4.38122	-0.39834	1.089535
86	6	-5.89123	0.584382	-0.12069
87	1	-6.94643	0.875947	-0.03037
88	6	-5.68686	-0.24231	-1.39058
89	1	-4.61746	-0.44688	-1.5324
90	6	-6.45754	-1.57157	-1.29883
91	1	-7.52694	-1.36077	-1.18355
92	6	-5.98187	-2.34806	-0.05288
93	1	-6.57283	-3.25235	0.115699
94	6	-3.50258	4.825435	2.351571
95	1	-3.80868	4.202288	3.202245
96	1	-2.44458	5.078176	2.451235
97	6	-3.736	4.053017	1.054508
98	1	-3.2071	3.092429	1.095503
99	6	-3.29814	4.823598	-0.21174
100	1	-3.7305	5.833027	-0.19895
101	6	-3.75413	4.080991	-1.4686
102	1	-3.24311	3.111316	-1.53303
103	6	-5.27762	3.859316	-1.44156
104	1	-5.77954	4.833619	-1.41555
105	6	-5.66218	3.08721	-0.16297
106	1	-6.7471	3.006784	-0.04893
107	6	1.654735	5.209509	2.178458
108	1	2.547383	4.586737	2.093555
109	6	0.820599	5.106802	0.901764
110	1	0.403281	4.096558	0.811564
111	6	1.595711	5.4682	-0.37842
112	1	2.138943	6.41123	-0.22616
113	6	0.682832	5.604702	-1.61517
114	1	0.254716	4.617674	-1.84567
115	6	-0.45817	6.598321	-1.32684
116	1	-0.02655	7.595166	-1.18062
117	6	-1.19259	6.188477	-0.02733
118	1	-1.92955	6.94323	0.26258
119	6	5.371996	2.257777	1.773095
120	1	5.070515	2.907136	2.605324
121	1	5.130925	1.216044	2.018918
122	6	4.596994	2.661048	0.527037
123	1	3.54907	2.361098	0.65387
124	6	5.165924	2.030996	-0.76411
125	1	6.240865	2.235955	-0.82738
126	6	4.455723	2.591162	-2.0003
127	1	3.400943	2.292722	-1.99393
128	6	4.554217	4.122215	-2.01385
129	1	5.606404	4.423968	-2.07778
130	6	3.965269	4.702891	-0.71164
131	1	4.129296	5.782105	-0.64746
132	6	4.882545	-2.78812	1.906488
133	1	4.821758	-2.08507	2.747774
134	1	4.077001	-3.52131	1.986182
135	6	4.75758	-2.0157	0.594303
136	1	3.849533	-1.40086	0.607314

137	6	4.736679	-2.92356	-0.65574
138	1	5.568033	-3.64021	-0.61146
139	6	4.843225	-2.07716	-1.92477
140	1	3.956363	-1.43667	-2.01729
141	6	6.10775	-1.20022	-1.88862
142	1	6.993567	-1.84269	-1.83073
143	6	6.070745	-0.30734	-0.63077
144	1	6.996686	0.25852	-0.5002
145	6	0.80056	0.638739	0.219114
146	6	0.314926	-0.68077	0.362045
147	6	-0.275	-1.41501	-0.66288
148	6	-0.37717	-0.74847	-1.90285
149	6	0.099487	0.576996	-2.07641
150	6	0.698185	1.290944	-1.02108
151	6	1.189666	0.07672	2.300458
152	1	1.071584	2.301134	-1.15258
153	6	1.560993	-0.02867	3.703843
154	6	2.173879	1.090865	4.328311
155	6	1.336665	-1.20586	4.475871
156	6	2.55277	1.049723	5.672705
157	1	2.337289	1.985749	3.735817
158	6	1.722504	-1.243	5.83091
159	6	2.324869	-0.12639	6.425871
160	1	3.018405	1.914564	6.135059
161	1	1.540062	-2.15237	6.394958
162	1	2.6161	-0.16875	7.471766
163	7	1.342337	1.075438	1.455235
164	8	0.556325	-1.06426	1.699414
165	8	0.7464	-2.35921	3.973064
166	1	0.485753	-2.2593	3.025974
167	1	-0.62471	-2.43309	-0.52594
168	1	0.001434	1.048871	-3.04997
169	1	-0.8283	-1.26498	-2.74525
170	1	1.052042	4.872221	3.032436
171	8	2.133202	6.574856	2.397029
172	1	1.360078	7.180029	2.384754

Table A14: XYZ coordinate of optimized CB-7 in the ground state.

(a) in water

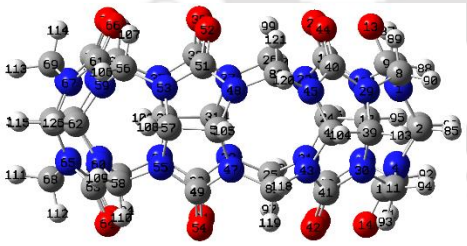

(b) in DMSO

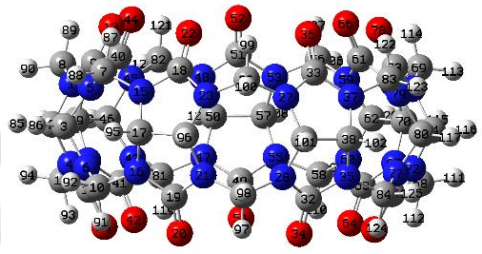

Center Number	Atomic Number	Coordinates (Angstroms) X	Y	Z	Center Number	Atomic Number	Coordinates (Angstroms) X	Y	Z
1	7	5.173629	-1.37635	1.221852	1	7	-5.19863	1.054897	1.247413
2	6	5.849414	-1.02852	-0.03117	2	6	-5.90111	0.670817	0.019933
3	6	5.914631	0.542711	0.009163	3	6	-5.86729	-0.90176	0.05366
4	7	5.100515	-1.30405	-1.2637	4	7	-5.22356	0.996746	-1.24086
5	7	5.215921	0.877083	1.25637	5	7	-5.10717	-1.19871	1.273741
6	7	5.245977	0.946455	-1.23148	6	7	-5.21862	-1.25713	-1.21133
7	6	5.192045	2.216248	1.835034	7	6	-5.00861	-2.53302	1.857718
8	6	5.097229	-2.73426	1.752764	8	6	-5.19623	2.411401	1.787256
9	6	4.824849	-0.25366	1.969908	9	6	-4.75759	-0.04738	1.977712
10	6	5.281831	2.304858	-1.76707	10	6	-5.16728	-2.61514	-1.74404
11	6	4.97021	-2.63498	-1.84853	11	6	-5.18219	2.337504	-1.81506

12	6	4.790992	-0.14384	-1.97092	12	6	-4.86765	-0.13901	-1.9652
13	8	4.302757	-0.2603	3.112523	13	8	-4.19782	-0.01208	3.100887
14	8	4.248643	-0.09412	-3.10273	14	8	-4.37303	-0.15246	-3.11944
15	7	4.205753	3.129908	1.264507	15	7	-3.99165	-3.40293	1.274899
16	7	4.288573	3.223744	-1.2192	16	7	-4.10412	-3.46073	-1.21037
17	6	4.447159	3.927459	0.056932	17	6	-4.20179	-4.19252	0.055675
18	6	3.089363	3.565808	1.976058	18	6	-2.85377	-3.79768	1.976979
19	6	3.21075	3.699876	-1.96244	19	6	-2.99584	-3.84182	-1.96441
20	8	2.89688	3.33756	-3.12355	20	8	-2.714	-3.43711	-3.11937
21	7	2.580974	4.694558	-1.2173	21	7	-2.29213	-4.80076	-1.23904
22	8	2.706659	3.125887	3.08851	22	8	-2.49115	-3.36214	3.09746
23	7	2.509572	4.617398	1.268329	23	7	-2.22629	-4.80681	1.248576
24	6	3.25991	4.959231	0.055476	24	6	-2.95371	-5.15012	0.023363
25	6	1.532793	5.547497	-1.76907	25	6	-1.18725	-5.5629	-1.81141
26	6	1.461269	5.461737	1.833746	26	6	-1.13344	-5.60848	1.791519
27	7	0.1331	5.288269	1.253678	27	7	0.185296	-5.33944	1.227834
28	7	0.193046	5.323975	-1.23332	28	7	0.132235	-5.2697	-1.25902
29	7	4.022103	-3.56058	1.21199	29	7	-4.19335	3.310084	1.22436
30	7	3.925041	-3.47573	-1.27213	30	7	-4.16539	3.227273	-1.26162
31	6	-0.29943	5.930817	0.006364	31	6	0.658012	-5.89839	-0.04326
32	6	-0.82272	4.721703	-1.97302	32	6	1.116814	-4.59502	-1.97924
33	6	-0.93084	4.744289	1.970324	33	6	1.206942	-4.74072	1.961971
34	8	-0.69735	4.194839	-3.10611	34	8	0.965235	-4.03967	-3.09528
35	7	-2.014	4.863167	-1.26432	35	7	2.315767	-4.70339	-1.27613
36	8	-0.86322	4.232199	3.115301	36	8	1.104819	-4.27164	3.122206
37	7	-2.09211	4.925749	1.221717	37	7	2.376848	-4.81405	1.208755
38	6	-1.84568	5.643261	-0.03189	38	6	2.184341	-5.5176	-0.06279
39	6	4.110374	-4.28287	-0.06092	39	6	-4.36281	4.023027	-0.04622
40	6	2.911311	-3.93708	1.963996	40	6	-3.10813	3.780443	1.961041
41	6	2.772761	-3.82417	-1.97464	41	6	-3.03773	3.621099	-1.98008
42	8	2.420574	-3.3616	-3.08795	42	8	-2.67946	3.171044	-3.09604
43	7	2.114044	-4.82097	-1.25665	43	7	-2.41551	4.650429	-1.27546
44	8	2.636216	-3.54127	3.123742	44	8	-2.79252	3.419574	3.121754
45	7	2.19341	-4.8777	1.229076	45	7	-2.47485	4.768503	1.209551
46	6	2.84068	-5.21153	-0.04419	46	6	-3.15248	5.027865	-0.06392
47	7	-0.30577	-5.31132	-1.24417	47	7	-0.02169	5.258514	-1.26513
48	7	-0.24145	-5.28644	1.242693	48	7	-0.07529	5.353151	1.220858
49	6	-1.31951	-4.68766	-1.96765	49	6	1.030403	4.679488	-1.97295
50	6	-0.78528	-5.88374	0.019278	50	6	0.426933	5.919385	-0.03331
51	6	-1.20608	-4.59252	1.971562	51	6	0.927055	4.739704	1.969892
52	8	-1.03584	-4.05012	3.091641	52	8	0.792061	4.240143	3.113876
53	7	-2.40902	-4.66179	1.270481	53	7	2.119383	4.838196	1.254987
54	8	-1.21091	-4.2015	-3.12087	54	8	0.951251	4.143629	-3.10592
55	7	-2.48938	-4.75519	-1.2144	55	7	2.197122	4.857248	-1.23166
56	6	-3.68143	-4.24543	1.852759	56	6	3.412358	4.495165	1.838847
57	6	-2.30289	-5.47154	0.050878	57	6	1.966444	5.600082	0.009639
58	6	-3.79342	-4.37363	-1.74766	58	6	3.523481	4.561109	-1.76425
59	7	-4.27729	-3.04587	1.271541	59	7	4.068037	3.321023	1.271442
60	7	-4.35333	-3.13594	-1.21309	60	7	4.170193	3.373919	-1.21411
61	6	-4.38666	-1.84851	1.976533	61	6	4.211736	2.128884	1.979717
62	6	-5.0915	-3.05496	0.050126	62	6	4.894723	3.358327	0.060622
63	6	-4.44884	-1.96628	-1.96398	63	6	4.376008	2.215786	-1.96112
64	8	-3.97979	-1.78796	-3.11544	64	8	3.953107	2.002941	-3.1242
65	7	-5.20934	-1.05111	-1.23989	65	7	5.187671	1.362871	-1.21584
66	8	-3.87899	-1.60584	3.0996	66	8	3.691143	1.86455	3.0912
67	7	-5.20931	-0.99195	1.247181	67	7	5.086105	1.308291	1.269236
68	6	-5.68005	0.205121	-1.8142	68	6	5.759096	0.138195	-1.76747
69	6	-5.72072	0.263738	1.789861	69	6	5.649934	0.085713	1.833437
70	6	-5.71556	-1.61117	0.01884	70	6	5.604834	1.954238	0.059207
71	7	-5.1336	1.476023	1.227327	71	7	5.160592	-1.15961	1.251251
72	7	-5.07892	1.414258	-1.25915	72	7	5.21428	-1.108	-1.23609
73	6	-4.30241	2.318878	1.962301	73	6	4.377557	-2.06146	1.969147
74	6	-5.56165	2.074657	-0.04198	74	6	5.679623	-1.73426	0.003698
75	6	-4.18307	2.205094	-1.97622	75	6	4.375631	-1.9419	-1.97374

76	8	-3.67612	1.921506	-3.08988	76	8	3.889246	-1.68835	-3.10337
77	7	-3.99769	3.393447	-1.27204	77	7	4.223718	-3.13394	-1.26703
78	8	-3.86955	2.100764	3.121092	78	8	3.901599	-1.87343	3.116101
79	7	-4.08912	3.473417	1.212248	79	7	4.271432	-3.23098	1.219002
80	6	-4.81982	3.461767	-0.05865	80	6	5.023638	-3.16359	-0.03658
81	6	1.006831	-5.59212	-1.81563	81	6	-1.34376	5.457171	-1.85093
82	6	1.070604	-5.62246	1.789113	82	6	-1.41153	5.609998	1.749452
83	6	-3.42461	4.654935	1.753888	83	6	3.684867	-4.45813	1.749506
84	6	-3.31386	4.547387	-1.84802	84	6	3.599566	-4.31611	-1.85302
85	1	6.83296	-1.51001	-0.07377	85	1	-6.91357	1.090481	0.020375
86	1	6.935253	0.941182	0.032747	86	1	-6.86	-1.36319	0.108764
87	1	4.962433	2.106385	2.898122	87	1	-4.76323	-2.40855	2.915762
88	1	6.187957	2.665735	1.725428	88	1	-5.98539	-3.0275	1.769971
89	1	4.936693	-2.6561	2.83123	89	1	-5.00116	2.33862	2.860441
90	1	6.05503	-3.23679	1.564725	90	1	-6.1906	2.84998	1.629114
91	1	5.104257	2.238802	-2.84365	91	1	-5.01039	-2.53672	-2.82302
92	1	6.281824	2.722008	-1.59039	92	1	-6.13209	-3.10296	-1.55281
93	1	4.736965	-2.50279	-2.90834	93	1	-4.97687	2.226388	-2.88311
94	1	5.931415	-3.15749	-1.75377	94	1	-6.16536	2.808683	-1.68369
95	1	5.437156	4.395225	0.107778	95	1	-5.16118	-4.71972	0.110971
96	1	3.584717	6.005107	0.097503	96	1	-3.21437	-6.21486	0.027611
97	1	1.49285	5.358259	-2.84496	97	1	-1.15534	-5.33465	-2.88007
98	1	1.805769	6.596804	-1.59636	98	1	-1.39028	-6.63357	-1.67603
99	1	1.384438	5.222369	2.89762	99	1	-1.07528	-5.40273	2.863598
100	1	1.761058	6.512078	1.721492	100	1	-1.3719	-6.66956	1.639067
101	1	-0.04977	6.997705	0.027774	101	1	0.47327	-6.97857	-0.06963
102	1	-2.46162	6.548655	-0.07391	102	1	2.854191	-6.38347	-0.11753
103	1	5.057203	-4.83186	-0.11688	103	1	-5.34298	4.513062	-0.07381
104	1	3.076916	-6.2812	-0.07639	104	1	-3.45394	6.080255	-0.12162
105	1	-0.62306	-6.96756	0.026689	105	1	0.200698	6.990873	-0.07901
106	1	-4.39705	-5.07305	1.759635	106	1	4.086435	5.356033	1.73537
107	1	-3.50464	-4.04143	2.912059	107	1	3.244853	4.295956	2.900616
108	1	-2.98994	-6.32358	0.105196	108	1	2.600819	6.493501	0.035955
109	1	-4.50251	-5.18948	-1.55641	109	1	4.171555	5.429747	-1.58731
110	1	-3.67845	-4.24146	-2.82663	110	1	3.417604	4.403401	-2.84073
111	1	-6.76879	0.266278	-1.68548	111	1	6.843058	0.146	-1.59141
112	1	-5.44575	0.18138	-2.88169	112	1	5.56789	0.147713	-2.8438
113	1	-6.80728	0.293045	1.634353	113	1	6.742095	0.122081	1.723301
114	1	-5.51033	0.26888	2.862552	114	1	5.396854	0.067363	2.896854
115	1	-6.8115	-1.60439	0.018999	115	1	6.698394	2.01317	0.105652
116	1	-6.65404	2.158329	-0.06833	116	1	6.775347	-1.75257	0.026501
117	1	-5.49543	4.322945	-0.11148	117	1	5.751739	-3.98159	-0.08216
118	1	1.227051	-6.66029	-1.68802	118	1	-1.61449	6.517308	-1.75601
119	1	0.950771	-5.36239	-2.88295	119	1	-1.27195	5.198497	-2.9107
120	1	1.246835	-6.69532	1.634986	120	1	-1.66485	6.661094	1.558336
121	1	1.044819	-5.41209	2.861563	121	1	-1.376	5.437601	2.828339
122	1	-3.32252	4.505658	2.831924	122	1	3.565563	-4.3246	2.827907
123	1	-4.05959	5.531137	1.56809	123	1	4.380116	-5.28692	1.562236
124	1	-3.15172	4.336184	-2.90836	124	1	3.430667	-4.10307	-2.9119
125	1	-3.96632	5.425382	-1.75123	125	1	4.293717	-5.1624	-1.76198
126	1	-5.83714	-3.85662	0.101898	126	1	5.590459	4.20406	0.107247

Table A15: XYZ coordinate of optimized cis-enol HPBO–CB-7 complex (benzoxazole moiety inside the cavity) in water.

(a) in ground state

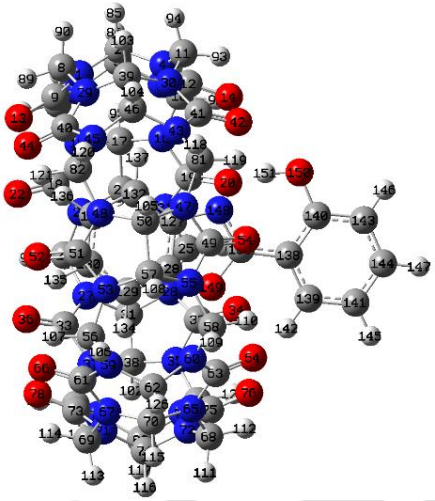

(b) in excited state

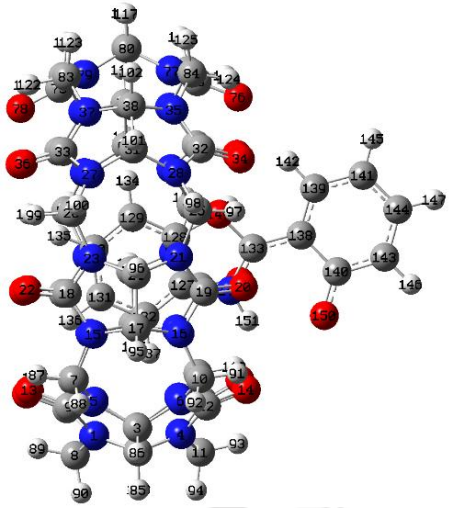

Center Number	Atomic Number	Coordinates (Angstroms) X	Y	Z	Center Number	Atomic Number	Coordinates (Angstroms) X	Y	Z
1	7	5.219924	-0.97226	-1.63699	1	7	-5.04374	1.814146	-1.58932
2	6	5.759909	-1.58572	-0.41713	2	6	-5.43976	2.476473	-0.34159
3	6	5.133536	-3.02952	-0.42814	3	6	-4.58983	3.801135	-0.34184
4	7	5.286099	-1.01491	0.847308	4	7	-5.02326	1.808946	0.895385
5	7	4.370805	-3.06125	-1.67925	5	7	-3.82035	3.711137	-1.58776
6	7	4.344068	-3.06477	0.810638	6	7	-3.81639	3.711753	0.902026
7	6	3.809642	-4.27891	-2.25816	7	6	-3.06699	4.829079	-2.15088
8	6	5.69757	0.296246	-2.18112	8	6	-5.75592	0.671426	-2.15923
9	6	4.446264	-1.86125	-2.38227	9	6	-4.12021	2.563222	-2.31826
10	6	3.724858	-4.2737	1.34811	10	6	-3.04079	4.816418	1.459122
11	6	5.799201	0.228256	1.41931	11	6	-5.67663	0.623857	1.437227
12	6	4.491803	-1.90546	1.568703	12	6	-4.10662	2.56048	1.628553
13	8	3.949348	-1.63584	-3.51351	13	8	-3.67717	2.275818	-3.45788
14	8	4.03031	-1.71399	2.719868	14	8	-3.66403	2.271524	2.767612
15	7	2.507596	-4.67997	-1.73533	15	7	-1.72997	5.029724	-1.60126
16	7	2.443721	-4.6435	0.751839	16	7	-1.7123	5.005562	0.884996
17	6	2.326016	-5.42409	-0.48441	17	6	-1.46365	5.752666	-0.35114
18	6	1.344173	-4.62776	-2.50021	18	6	-0.57435	4.81504	-2.35003
19	6	1.234827	-4.5523	1.441689	19	6	-0.53994	4.717106	1.581718
20	8	1.064171	-4.01761	2.565602	20	8	-0.46603	4.148252	2.699345
21	7	0.260954	-5.21443	0.695302	21	7	0.532035	5.225632	0.850424
22	8	1.240037	-4.13773	-3.6521	22	8	-0.52235	4.301381	-3.49502
23	7	0.333972	-5.27251	-1.79008	23	7	0.504397	5.327771	-1.63302
24	6	0.807358	-5.82986	-0.5194	24	6	0.099392	5.932891	-0.36174
25	6	-1.06285	-5.52748	1.228603	25	6	1.882792	5.316665	1.398119
26	6	-0.96597	-5.5846	-2.37591	26	6	1.83901	5.46771	-2.20658
27	7	-2.09321	-4.81866	-1.85208	27	7	2.843488	4.540135	-1.69573
28	7	-2.17487	-4.79129	0.633686	28	7	2.870889	4.42938	0.790825
29	7	5.110624	1.492932	-1.58473	29	7	-5.36342	-0.6374	-1.64169
30	7	5.187723	1.450112	0.903091	30	7	-5.26808	-0.64478	0.834865
31	6	-2.818	-5.17393	-0.62882	31	6	3.589042	4.745263	-0.44929
32	6	-2.91629	-3.85166	1.346868	32	6	3.436559	3.355455	1.475529
33	6	-2.74379	-3.83234	-2.59021	33	6	3.37249	3.510894	-2.47095
34	8	-2.65282	-3.4305	2.500332	34	8	3.093863	2.941724	2.610887
35	7	-4.03248	-3.51147	0.584296	35	7	4.490811	2.860489	0.709099
36	8	-2.38491	-3.38826	-3.70899	36	8	2.984645	3.176984	-3.61816
37	7	-3.8981	-3.4697	-1.89937	37	7	4.44696	2.958649	-1.77789

38	6	-4.09547	-4.2567	-0.67717	38	6	4.713714	3.646188	-0.51056
39	6	5.600394	2.103391	-0.3429	39	6	-5.86799	-1.19965	-0.38299
40	6	4.255228	2.336832	-2.29139	40	6	-4.68406	-1.58037	-2.41213
41	6	4.338682	2.248656	1.668034	41	6	-4.45335	-1.5622	1.490569
42	8	3.923907	1.987637	2.824123	42	8	-3.81975	-1.34849	2.557135
43	7	4.081769	3.414618	0.950232	43	7	-4.48839	-2.75872	0.786378
44	8	3.775838	2.112195	-3.43064	44	8	-4.23371	-1.40017	-3.57026
45	7	4.072177	3.495147	-1.53947	45	7	-4.64322	-2.77413	-1.69477
46	6	4.852016	3.486671	-0.29763	46	6	-5.34116	-2.68296	-0.40824
47	7	2.057314	4.83004	0.948355	47	7	-2.72544	-4.48794	0.712501
48	7	2.091898	4.969622	-1.53403	48	7	-2.85106	-4.47753	-1.76992
49	6	0.863353	4.588908	1.627022	49	6	-1.51243	-4.522	1.397007
50	6	1.864564	5.648307	-0.25254	50	6	-2.68837	-5.2543	-0.53807
51	6	0.931367	4.868414	-2.29797	51	6	-1.68832	-4.44867	-2.53972
52	8	0.85527	4.420449	-3.46894	52	8	-1.56673	-3.92198	-3.67328
53	7	-0.11829	5.408409	-1.55878	53	7	-0.70295	-5.16135	-1.85757
54	8	0.744912	3.974216	2.716088	54	8	-1.29671	-4.03891	2.536011
55	7	-0.16831	5.203593	0.918652	55	7	-0.60244	-5.24061	0.625335
56	6	-1.44502	5.637569	-2.12142	56	6	0.567129	-5.54023	-2.47104
57	6	0.317156	5.930906	-0.26076	57	6	-1.19937	-5.75495	-0.61111
58	6	-1.50786	5.378913	1.474175	58	6	0.701397	-5.65872	1.133195
59	7	-2.49547	4.74876	-1.6338	59	7	1.751418	-4.8824	-1.92679
60	7	-2.5595	4.581551	0.849063	60	7	1.852421	-4.96951	0.557451
61	6	-3.05541	3.743994	-2.41937	61	6	2.48198	-3.94171	-2.64985
62	6	-3.24081	4.971226	-0.39219	62	6	2.458256	-5.33966	-0.72564
63	6	-3.22906	3.564151	1.526712	63	6	2.647532	-4.09075	1.290505
64	8	-2.94443	3.131429	2.670756	64	8	2.418488	-3.68985	2.458627
65	7	-4.30615	3.157024	0.740327	65	7	3.773018	-3.78671	0.526614
66	8	-2.666	3.395251	-3.56156	66	8	2.155628	-3.45134	-3.75922
67	7	-4.16258	3.235513	-1.7435	67	7	3.664968	-3.69053	-1.95779
68	6	-5.34304	2.247586	1.223031	68	6	4.920929	-3.062	1.067708
69	6	-5.10952	2.322603	-2.37418	69	6	4.764943	-2.9189	-2.52625
70	6	-4.43089	3.947239	-0.48815	70	6	3.795257	-4.51079	-0.74951
71	7	-5.12238	0.966234	-1.83431	71	7	4.986569	-1.60754	-1.92368
72	7	-5.32118	0.905433	0.64571	72	7	5.102463	-1.70357	0.562923
73	6	-4.65897	-0.12998	-2.56062	73	6	4.722412	-0.42077	-2.60342
74	6	-5.90393	0.569723	-0.65825	74	6	5.774024	-1.39309	-0.70394
75	6	-4.98559	-0.22678	1.384895	75	6	4.898124	-0.57151	1.349833
76	8	-4.58608	-0.23728	2.575149	76	8	4.451672	-0.55805	2.523163
77	7	-5.22834	-1.34762	0.59384	77	7	5.33299	0.539044	0.628255
78	8	-4.044	-0.08196	-3.65492	78	8	4.154488	-0.31934	-3.7191
79	7	-5.04611	-1.28701	-1.88937	79	7	5.252648	0.630155	-1.85777
80	6	-5.84443	-1.00204	-0.69276	80	6	5.948098	0.169622	-0.65228
81	6	3.367782	4.549022	1.529061	81	6	-3.95539	-4.00631	1.329544
82	6	3.416365	4.685006	-2.07628	82	6	-4.14601	-4.02228	-2.27
83	6	-4.92498	-2.61534	-2.48356	83	6	5.354029	1.988868	-2.38122
84	6	-5.1374	-2.71198	1.108884	84	6	5.436707	1.870919	1.219541
85	1	6.85552	-1.58058	-0.4459	85	1	-6.52225	2.646906	-0.3326
86	1	5.878699	-3.83313	-0.42176	86	1	-5.19771	4.712936	-0.34082
87	1	3.689253	-4.1076	-3.331	87	1	-2.95366	4.640944	-3.22169
88	1	4.521043	-5.10001	-2.10041	88	1	-3.64844	5.749146	-2.00564
89	1	5.452041	0.30767	-3.24635	89	1	-5.56278	0.666352	-3.23512
90	1	6.788348	0.342336	-2.06199	90	1	-6.83118	0.810599	-1.98665
91	1	3.555305	-4.1033	2.414373	91	1	-2.91223	4.616965	2.526171
92	1	4.421268	-5.11374	1.224265	92	1	-3.61069	5.745813	1.331506
93	1	5.609183	0.197548	2.49543	93	1	-5.43369	0.578524	2.501819
94	1	6.881644	0.274605	1.24339	94	1	-6.76221	0.727366	1.316703
95	1	3.009926	-6.27985	-0.45413	95	1	-2.01827	6.698157	-0.33813
96	1	0.639992	-6.91289	-0.49915	96	1	0.424086	6.978829	-0.32215
97	1	-1.0508	-5.29129	2.295873	97	1	1.822578	5.06189	2.459486
98	1	-1.24497	-6.60256	1.098634	98	1	2.232653	6.352358	1.295989
99	1	-0.89773	-5.3784	-3.44725	99	1	1.753032	5.293803	-3.28242
100	1	-1.17119	-6.65254	-2.22553	100	1	2.187444	6.494142	-2.03361
101	1	-3.04501	-6.24613	-0.62426	101	1	3.976388	5.769857	-0.40809

102	1	-5.03697	-4.81447	-0.7371	102	1	5.730498	4.055619	-0.51127
103	1	6.692018	2.193859	-0.37573	103	1	-6.95947	-1.11856	-0.33987
104	1	5.525488	4.351082	-0.27254	104	1	-6.13475	-3.43596	-0.35264
105	1	2.478594	6.554122	-0.19363	105	1	-3.42563	-6.06445	-0.5039
106	1	-1.74037	6.673956	-1.91234	106	1	0.692741	-6.62624	-2.36961
107	1	-1.36967	5.494478	-3.20256	107	1	0.508346	-5.28278	-3.5318
108	1	0.061461	6.993453	-0.17823	108	1	-1.10245	-6.84605	-0.64917
109	1	-1.77833	6.440572	1.39755	109	1	0.814626	-6.73689	0.958783
110	1	-1.4672	5.093188	2.5286	110	1	0.711171	-5.46565	2.209106
111	1	-6.32336	2.700301	1.024101	111	1	5.829961	-3.63968	0.854073
112	1	-5.20934	2.138936	2.302533	112	1	4.784083	-2.9928	2.15
113	1	-6.11992	2.744114	-2.2904	113	1	5.687941	-3.50669	-2.43694
114	1	-4.83766	2.252138	-3.43075	114	1	4.54145	-2.75835	-3.58424
115	1	-5.41789	4.422164	-0.52884	115	1	4.696391	-5.13108	-0.81284
116	1	-6.92029	0.973205	-0.73044	116	1	6.721752	-1.94015	-0.76851
117	1	-6.82825	-1.47767	-0.77674	117	1	6.993527	0.498008	-0.67392
118	1	3.990796	5.447622	1.43014	118	1	-4.72691	-4.7819	1.235987
119	1	3.220039	4.329623	2.5898	119	1	-3.74161	-3.83798	2.38804
120	1	4.065179	5.552212	-1.89663	120	1	-4.88689	-4.81153	-2.08699
121	1	3.301035	4.539157	-3.15346	121	1	-4.04453	-3.86518	-3.34698
122	1	-4.6749	-2.48158	-3.53931	122	1	5.123141	1.94677	-3.4489
123	1	-5.89517	-3.1228	-2.40372	123	1	6.385775	2.33925	-2.24957
124	1	-5.00805	-2.64103	2.192035	124	1	5.254166	1.76516	2.292274
125	1	-6.07752	-3.23559	0.890621	125	1	6.456081	2.247749	1.063624
126	1	-3.56401	6.016816	-0.33021	126	1	2.61092	-6.42412	-0.76993
127	6	0.777542	-0.01545	0.736312	127	6	-0.9178	0.008183	0.93548
128	6	-0.60487	0.138053	0.478542	128	6	0.483425	0.081223	0.729443
129	6	-1.14208	0.356162	-0.78726	129	6	1.074642	0.289274	-0.50976
130	6	-0.20958	0.412416	-1.84426	130	6	0.185496	0.429741	-1.60578
131	6	1.182244	0.260067	-1.61445	131	6	-1.2155	0.368106	-1.42227
132	6	1.698246	0.046646	-0.32193	132	6	-1.7978	0.160704	-0.15291
133	6	-0.26555	-0.16754	2.663159	133	6	0.116368	-0.25294	2.942317
134	1	-2.20618	0.481622	-0.95101	134	1	2.15079	0.347923	-0.62885
135	1	-0.56619	0.579816	-2.85629	135	1	0.589841	0.593918	-2.59998
136	1	1.865376	0.316216	-2.45679	136	1	-1.86538	0.494001	-2.28378
137	1	2.764556	-0.05424	-0.14986	137	1	-2.87335	0.140436	-0.0294
138	6	-0.58558	-0.2983	4.068811	138	6	0.481195	-0.37633	4.33056
139	6	-1.91899	-0.22933	4.545662	139	6	1.824818	-0.48123	4.714668
140	6	0.488107	-0.49272	4.991238	140	6	-0.5731	-0.38861	5.355417
141	6	-2.18283	-0.34163	5.916209	141	6	2.184832	-0.57631	6.106045
142	1	-2.73027	-0.09937	3.835271	142	1	2.607039	-0.49469	3.960627
143	6	0.210441	-0.60195	6.369208	143	6	-0.17402	-0.49761	6.724274
144	6	-1.11393	-0.52533	6.825969	144	6	1.197312	-0.5848	7.098152
145	1	-3.2047	-0.28876	6.280356	145	1	3.235986	-0.64538	6.37301
146	1	1.037224	-0.74703	7.058058	146	1	-0.95725	-0.49232	7.478763
147	1	-1.31676	-0.6107	7.890552	147	1	1.469388	-0.66065	8.147302
148	7	0.949624	-0.20757	2.12726	148	7	-1.10194	-0.20853	2.300697
149	8	-1.28321	0.037575	1.71307	149	8	1.124111	-0.08825	1.972903
150	8	1.802607	-0.58072	4.58309	150	8	-1.83566	-0.29415	4.989615
151	1	1.8844	-0.50886	3.577315	151	1	-1.98701	-0.35805	2.796159

Table A16: XYZ coordinate of optimized cis-enol HPBO–CB-7 complex (benzoxazole moiety inside the cavity) in DMSO.

(a) in ground state

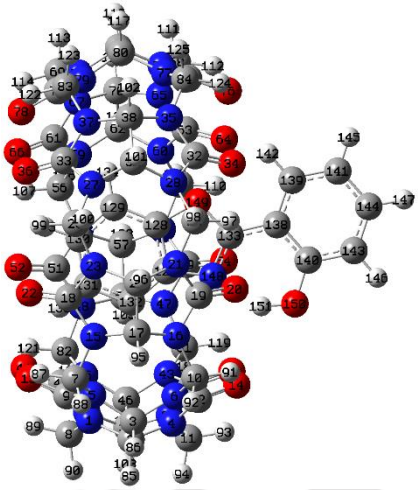

(b) in excited state

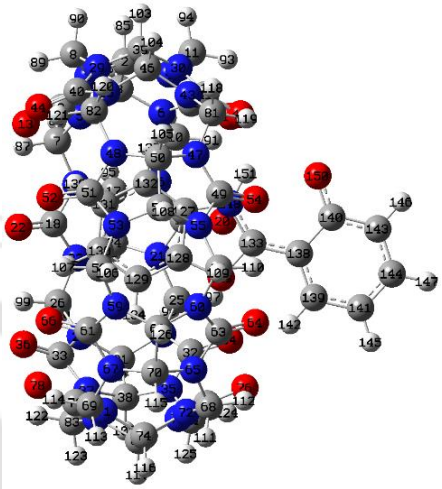

Center Number	Atomic Number	Coordinates (Angstroms) X	Y	Z	Center Number	Atomic Number	Coordinates (Angstroms) X	Y	Z
1	7	-5.111	1.486493	-1.61947	1	7	5.031066	-1.83093	-1.5962
2	6	-5.60038	2.134619	-0.39719	2	6	5.424915	-2.49753	-0.3505
3	6	-4.83475	3.50958	-0.3825	3	6	4.570112	-3.81926	-0.3534
4	7	-5.2033	1.507929	0.867472	4	7	5.012133	-1.83189	0.888576
5	7	-4.04031	3.47232	-1.61473	5	7	3.79684	-3.72095	-1.5964
6	7	-4.08272	3.464815	0.876894	6	7	3.802806	-3.73324	0.894093
7	6	-3.36674	4.639112	-2.17851	7	6	3.03858	-4.83411	-2.16241
8	6	-5.70765	0.280859	-2.18717	8	6	5.748853	-0.69127	-2.16478
9	6	-4.23507	2.298214	-2.33946	9	6	4.101398	-2.57296	-2.32507
10	6	-3.35366	4.601904	1.430381	10	6	3.023792	-4.83631	1.449494
11	6	-5.83161	0.305827	1.410147	11	6	5.66998	-0.6504	1.432692
12	6	-4.35423	2.318618	1.620546	12	6	4.09677	-2.58432	1.623054
13	8	-3.75131	2.038834	-3.4689	13	8	3.658624	-2.28088	-3.46324
14	8	-3.95084	2.082268	2.785136	14	8	3.659772	-2.29854	2.764659
15	7	-2.04361	4.924856	-1.63399	15	7	1.703485	-5.03516	-1.60956
16	7	-2.03509	4.845882	0.852218	16	7	1.693754	-5.02002	0.877986
17	6	-1.82062	5.630654	-0.36641	17	6	1.4386	-5.76055	-0.36057
18	6	-0.87972	4.80477	-2.39073	18	6	0.546602	-4.8154	-2.35529
19	6	-0.84944	4.597602	1.543173	19	6	0.524175	-4.72637	1.577874
20	8	-0.7478	4.008953	2.64766	20	8	0.45546	-4.16303	2.698116
21	7	0.197159	5.17591	0.825425	21	7	-0.55192	-5.22613	0.846443
22	8	-0.80126	4.339036	-3.55427	22	8	0.493614	-4.30041	-3.4992
23	7	0.169325	5.352608	-1.6552	23	7	-0.53161	-5.32809	-1.63717
24	6	-0.26988	5.894292	-0.3669	24	6	-0.12557	-5.93427	-0.36715
25	6	1.5351	5.339679	1.38698	25	6	-1.90215	-5.30772	1.396185
26	6	1.497329	5.576422	-2.21791	26	6	-1.86772	-5.46312	-2.20807
27	7	2.549908	4.697979	-1.71674	27	7	-2.86858	-4.53185	-1.6972
28	7	2.584221	4.535433	0.767103	28	7	-2.88651	-4.41605	0.789565
29	7	-5.24153	-0.97781	-1.6113	29	7	5.364851	0.618922	-1.64487
30	7	-5.32542	-0.95612	0.875593	30	7	5.268389	0.621117	0.832063
31	6	3.278565	4.926255	-0.46603	31	6	-3.61017	-4.73002	-0.44756
32	6	3.24233	3.512121	1.447768	32	6	-3.44375	-3.33756	1.474526
33	6	3.126567	3.69631	-2.49511	33	6	-3.39442	-3.50107	-2.47281
34	8	2.935041	3.064673	2.579942	34	8	-3.09582	-2.92441	2.608054
35	7	4.339127	3.119295	0.681404	35	7	-4.49878	-2.83899	0.710822
36	8	2.757413	3.349264	-3.64398	36	8	-3.01008	-3.17268	-3.62241
37	7	4.22613	3.193476	-1.80294	37	7	-4.46357	-2.94165	-1.77667

38	6	4.475158	3.908356	-0.54575	38	6	-4.72935	-3.62496	-0.507
39	6	-5.79015	-1.55632	-0.37795	39	6	5.871462	1.175001	-0.38451
40	6	-4.4793	-1.89426	-2.33513	40	6	4.693045	1.568244	-2.41455
41	6	-4.53624	-1.82935	1.623984	41	6	4.457459	1.541589	1.488989
42	8	-4.09149	-1.61538	2.777649	42	8	3.822723	1.32991	2.554843
43	7	-4.3776	-3.00298	0.890088	43	7	4.499946	2.739173	0.786953
44	8	-3.98672	-1.70554	-3.47463	44	8	4.245366	1.394379	-3.57426
45	7	-4.41138	-3.07521	-1.59967	45	7	4.659156	2.760638	-1.69433
46	6	-5.16871	-3.00183	-0.34777	46	6	5.35343	2.661651	-0.4067
47	7	-2.47485	-4.57903	0.853716	47	7	2.743179	4.474503	0.712253
48	7	-2.56032	-4.70915	-1.62849	48	7	2.874162	4.472259	-1.7701
49	6	-1.25809	-4.45541	1.525041	49	6	1.529526	4.511856	1.395875
50	6	-2.36842	-5.40602	-0.35258	50	6	2.711021	5.24454	-0.53587
51	6	-1.40251	-4.68003	-2.40294	51	6	1.711949	4.446179	-2.54125
52	8	-1.30658	-4.22744	-3.57055	52	8	1.59101	3.923542	-3.6764
53	7	-0.38738	-5.30133	-1.67881	53	7	0.727161	5.159201	-1.85802
54	8	-1.07522	-3.8653	2.618378	54	8	1.311024	4.027612	2.533339
55	7	-0.29272	-5.15605	0.801918	55	7	0.623857	5.237448	0.62526
56	6	0.912074	-5.62241	-2.25885	56	6	-0.54164	5.541121	-2.47166
57	6	-0.84989	-5.81376	-0.38541	57	6	1.223553	5.749928	-0.61023
58	6	1.026286	-5.46904	1.347685	58	6	-0.67776	5.661092	1.133664
59	7	2.038778	-4.84467	-1.75142	59	7	-1.72841	4.888668	-1.92671
60	7	2.149149	-4.7661	0.734063	60	7	-1.83237	4.97838	0.558067
61	6	2.683835	-3.86979	-2.50949	61	6	-2.46311	3.951495	-2.65054
62	6	2.772343	-5.18084	-0.52911	62	6	-2.43392	5.349648	-0.72647
63	6	2.926396	-3.84571	1.435105	63	6	-2.63435	4.106712	1.292466
64	8	2.698528	-3.42506	2.595878	64	8	-2.41213	3.71012	2.462932
65	7	4.033333	-3.52779	0.648626	65	7	-3.75961	3.806695	0.526218
66	8	2.31655	-3.44342	-3.63216	66	8	-2.13958	3.46185	-3.76067
67	7	3.844742	-3.49769	-1.83355	67	7	-3.64759	3.705575	-1.95862
68	6	5.158016	-2.73643	1.142195	68	6	-4.911	3.087142	1.066185
69	6	4.873486	-2.66719	-2.44887	69	6	-4.74982	2.937388	-2.52714
70	6	4.058785	-4.27902	-0.6096	70	6	-3.77533	4.527645	-0.7514
71	7	5.029725	-1.33527	-1.87122	71	7	-4.97783	1.627735	-1.92357
72	7	5.256492	-1.37969	0.60835	72	7	-5.09691	1.728745	0.563715
73	6	4.670938	-0.17714	-2.559	73	6	-4.72232	0.439213	-2.60416
74	6	5.854801	-1.05457	-0.69135	74	6	-5.76656	1.418307	-0.70374
75	6	5.03026	-0.24669	1.386961	75	6	-4.89511	0.597058	1.352285
76	8	4.645683	-0.23835	2.582167	76	8	-4.45337	0.583673	2.527019
77	7	5.366123	0.872664	0.629085	77	7	-5.33	-0.51352	0.630151
78	8	4.049123	-0.13125	-3.64913	78	8	-4.16007	0.334091	-3.72195
79	7	5.172408	0.915844	-1.85528	79	7	-5.25648	-0.6085	-1.85624
80	6	5.942603	0.516705	-0.67306	80	6	-5.94624	-0.14374	-0.64961
81	6	-3.75052	-4.19501	1.452875	81	6	3.970258	3.987614	1.330372
82	6	-3.86472	-4.31371	-2.14831	82	6	4.168049	4.012137	-2.26751
83	6	5.175822	2.267057	-2.4087	83	6	-5.3664	-1.96705	-2.37819
84	6	5.378553	2.223707	1.183479	84	6	-5.43735	-1.844	1.223573
85	1	-6.69072	2.238057	-0.43875	85	1	6.506961	-2.67196	-0.34263
86	1	-5.49787	4.382324	-0.39183	86	1	5.174811	-4.73335	-0.35928
87	1	-3.24392	4.462091	-3.25024	87	1	2.921346	-4.63915	-3.23163
88	1	-4.00805	5.517835	-2.0288	88	1	3.618976	-5.75624	-2.02518
89	1	-5.46173	0.263731	-3.2522	89	1	5.554282	-0.68295	-3.24046
90	1	-6.79795	0.339456	-2.06948	90	1	6.823576	-0.83728	-1.99342
91	1	-3.21664	4.407212	2.497339	91	1	2.897659	-4.63799	2.517077
92	1	-3.96062	5.508093	1.303579	92	1	3.590247	-5.76756	1.319363
93	1	-5.65042	0.301438	2.488276	93	1	5.425325	-0.60573	2.496976
94	1	-6.91223	0.358278	1.223899	94	1	6.755431	-0.75873	1.313898
95	1	-2.42417	6.545181	-0.33549	95	1	1.989015	-6.70875	-0.35276
96	1	-0.00255	6.95495	-0.2945	96	1	-0.45403	-6.97915	-0.32687
97	1	1.485235	5.054306	2.44109	97	1	-1.83769	-5.05023	2.456752
98	1	1.816145	6.399088	1.312598	98	1	-2.25885	-6.3416	1.297486
99	1	1.425077	5.416962	-3.29703	99	1	-1.78269	-5.29013	-3.28419
100	1	1.788569	6.617058	-2.02386	100	1	-2.21934	-6.48836	-2.03369
101	1	3.595566	5.973805	-0.40182	101	1	-4.00305	-5.75256	-0.4029

102	1	5.4602	4.388288	-0.57476	102	1	-5.74837	-4.02928	-0.50376
103	1	-6.88574	-1.54922	-0.4148	103	1	6.962598	1.087509	-0.34107
104	1	-5.91714	-3.80204	-0.31468	104	1	6.151569	3.409724	-0.34766
105	1	-3.0531	-6.25908	-0.28414	105	1	3.450802	6.052445	-0.49713
106	1	1.120673	-6.68671	-2.08751	106	1	-0.66358	6.627946	-2.37255
107	1	0.841607	-5.4374	-3.33396	107	1	-0.48366	5.281078	-3.53187
108	1	-0.68223	-6.89561	-0.32884	108	1	1.130196	6.841552	-0.6478
109	1	1.192385	-6.55048	1.251554	109	1	-0.78554	6.740164	0.960111
110	1	1.017516	-5.19983	2.40717	110	1	-0.68839	5.466785	2.209424
111	1	6.087687	-3.27411	0.913941	111	1	-5.81765	3.667936	0.850207
112	1	5.048791	-2.65035	2.226488	112	1	-4.77569	3.019135	2.148803
113	1	5.836637	-3.19092	-2.38542	113	1	-5.67069	3.529101	-2.43996
114	1	4.602516	-2.53889	-3.50018	114	1	-4.52525	2.774484	-3.58461
115	1	4.992049	-4.84882	-0.68691	115	1	-4.67316	5.152754	-0.81738
116	1	6.828812	-1.54775	-0.78942	116	1	-6.71258	1.968356	-0.77062
117	1	6.966218	0.901378	-0.74664	117	1	-6.99327	-0.46793	-0.6681
118	1	-4.44535	-5.04046	1.359331	118	1	4.744736	4.760651	1.238786
119	1	-3.57111	-3.99452	2.512365	119	1	3.754128	3.818521	2.388298
120	1	-4.58018	-5.1246	-1.959	120	1	4.912036	4.79784	-2.08145
121	1	-3.75428	-4.17463	-3.22695	121	1	4.068118	3.857318	-3.34503
122	1	4.919183	2.188372	-3.46856	122	1	-5.13772	-1.92686	-3.44646
123	1	6.188261	2.681154	-2.31402	123	1	-6.39992	-2.31145	-2.24353
124	1	5.241153	2.130197	2.263929	124	1	-5.24883	-1.73687	2.295205
125	1	6.356654	2.680067	0.981627	125	1	-6.45941	-2.2163	1.073457
126	1	2.988005	-6.2554	-0.50447	126	1	-2.58097	6.435057	-0.77176
127	6	-0.79519	-0.05296	0.729466	127	6	0.917154	-0.01626	0.943914
128	6	0.583623	-0.18493	0.443577	128	6	-0.48504	-0.07619	0.740981
129	6	1.107321	-0.27827	-0.84273	129	6	-1.08073	-0.276	-0.49741
130	6	0.164581	-0.2272	-1.89057	130	6	-0.19546	-0.42125	-1.59575
131	6	-1.22372	-0.08899	-1.63276	131	6	1.206414	-0.37194	-1.41549
132	6	-1.72601	-0.00127	-0.32032	132	6	1.793272	-0.17308	-0.14693
133	6	0.270419	-0.08349	2.650239	133	6	-0.11011	0.248589	2.953433
134	1	2.169096	-0.38913	-1.02764	134	1	-2.15756	-0.32532	-0.6142
135	1	0.510834	-0.29433	-2.9176	135	1	-0.60352	-0.57959	-2.58934
136	1	-1.9146	-0.05523	-2.46978	136	1	1.852827	-0.50099	-2.27921
137	1	-2.78841	0.104654	-0.12814	137	1	2.869238	-0.16133	-0.02598
138	6	0.602789	-0.07529	4.058906	138	6	-0.47099	0.375152	4.34251
139	6	1.941885	-0.14282	4.518158	139	6	-1.81225	0.502116	4.72792
140	6	-0.46798	0.002672	5.002099	140	6	0.584004	0.36634	5.366499
141	6	2.214893	-0.13522	5.891687	141	6	-2.16992	0.598397	6.119914
142	1	2.750821	-0.19541	3.79526	142	1	-2.59439	0.529767	3.974144
143	6	-0.18113	0.007751	6.382322	143	6	0.187798	0.477455	6.735828
144	6	1.149845	-0.06059	6.82119	144	6	-1.18186	0.58652	7.111217
145	1	3.241433	-0.18558	6.24293	145	1	-3.21968	0.683805	6.387754
146	1	-1.00553	0.066129	7.086656	146	1	0.971387	0.45553	7.48969
147	1	1.360617	-0.05518	7.887714	147	1	-1.45177	0.662975	8.16095
148	7	-0.95109	0.005839	2.133776	148	7	1.10614	0.194971	2.309466
149	8	1.27575	-0.20257	1.674423	149	8	-1.1213	0.096316	1.986234
150	8	-1.78701	0.072071	4.606323	150	8	1.84481	0.251134	4.999772
151	1	-1.86372	0.066816	3.594827	151	1	1.993404	0.335568	2.803023

Table A17: XYZ coordinate of optimized cis-enol HPBO–CB-7 complex (benzoxazole moiety outside the cavity) in ground state.

(a) in water

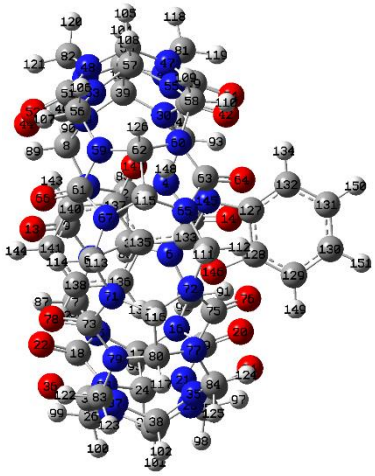

(b) in DMSO

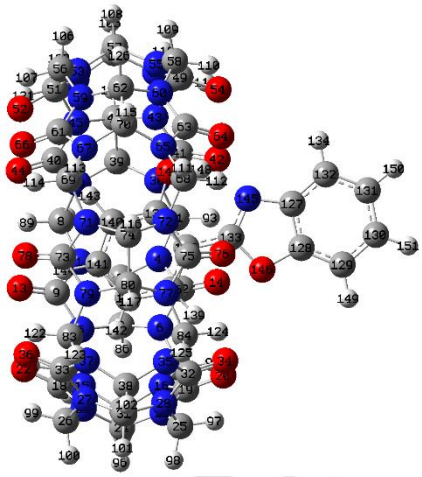

Center Number	Atomic Number	Coordinates (Angstroms) X	Y	Z	Center Number	Atomic Number	Coordinates (Angstroms) X	Y	Z
1	7	0.961769	-5.16031	-1.43802	1	7	-0.31516	-5.26646	-1.78525
2	6	0.571273	-5.82293	-0.191	2	6	-0.76014	-5.77703	-0.48607
3	6	-0.99952	-5.77306	-0.22428	3	6	-2.288	-5.40641	-0.45133
4	7	0.908388	-5.10833	1.046383	4	7	-0.21473	-5.09425	0.69386
5	7	-1.2913	-5.03926	-1.46245	5	7	-2.49615	-4.70451	-1.72276
6	7	-1.34726	-5.0857	1.021107	6	7	-2.41616	-4.59068	0.759284
7	6	-2.62499	-4.96232	-2.05372	7	6	-3.81058	-4.34183	-2.24217
8	6	2.316616	-5.20232	-1.98065	8	6	0.985985	-5.5688	-2.37098
9	6	-0.13607	-4.71797	-2.17455	9	6	-1.34289	-4.65977	-2.50357
10	6	-2.70367	-5.03566	1.5583	10	6	-3.7033	-4.25488	1.363367
11	6	2.244192	-5.11127	1.637653	11	6	1.109795	-5.38177	1.24351
12	6	-0.22396	-4.70927	1.755891	12	6	-1.19929	-4.42584	1.422731
13	8	-0.09572	-4.17494	-3.30664	13	8	-1.26015	-4.20718	-3.67215
14	8	-0.23062	-4.15633	2.883816	14	8	-1.0292	-3.83064	2.515122
15	7	-3.50596	-3.9426	-1.49213	15	7	-4.3967	-3.12718	-1.68115
16	7	-3.56251	-3.99617	0.999515	16	7	-4.3731	-3.081	0.810715
17	6	-4.28985	-4.13259	-0.26542	17	6	-5.15956	-3.09155	-0.43085
18	6	-3.93418	-2.84019	-2.23011	18	6	-4.50188	-1.94153	-2.4053
19	6	-3.98899	-2.89905	1.7447	19	6	-4.57456	-1.92255	1.556084
20	8	-3.62057	-2.61581	2.911488	20	8	-4.14225	-1.70558	2.714713
21	7	-4.94329	-2.21296	0.996124	21	7	-5.38773	-1.06687	0.81504
22	8	-3.53635	-2.52275	-3.37811	22	8	-4.01601	-1.72583	-3.54265
23	7	-4.92554	-2.189	-1.49778	23	7	-5.29284	-1.05624	-1.67269
24	6	-5.26631	-2.8988	-0.26085	24	6	-5.82743	-1.66589	-0.44797
25	6	-5.73112	-1.11106	1.543956	25	6	-5.91395	0.184551	1.354802
26	6	-5.72018	-1.09255	-2.04373	26	6	-5.78862	0.198332	-2.23418
27	7	-5.42169	0.22702	-1.49143	27	7	-5.20935	1.410696	-1.66115
28	7	-5.41881	0.208849	1.001852	28	7	-5.29777	1.399394	0.826023
29	7	3.251151	-4.229	-1.42237	29	7	2.104302	-4.7773	-1.86719
30	7	3.191544	-4.15927	1.065123	30	7	2.225628	-4.67882	0.616709
31	6	-5.99521	0.735586	-0.23885	31	6	-5.69982	2.041258	-0.42869
32	6	-4.75162	1.187589	1.73726	32	6	-4.42255	2.18736	1.572043
33	6	-4.81347	1.231351	-2.24226	33	6	-4.35091	2.242719	-2.38007
34	8	-4.27714	1.047687	2.890637	34	8	-3.98879	1.922376	2.720235
35	7	-4.76165	2.367491	0.993384	35	7	-4.15781	3.344777	0.844978
36	8	-4.35707	1.105961	-3.40603	36	8	-3.87122	2.002044	-3.5152
37	7	-4.85087	2.409074	-1.49981	37	7	-4.16702	3.41155	-1.64445
38	6	-5.56601	2.249349	-0.23029	38	6	-4.93744	3.418177	-0.39762

39	6	3.964229	-4.4171	-0.15433	39	6	2.843197	-5.10366	-0.64605
40	6	3.774397	-3.17983	-2.17646	40	6	2.745186	-3.80539	-2.63369
41	6	3.677209	-3.06721	1.782575	41	6	3.015619	-3.76365	1.312868
42	8	3.278599	-2.70027	2.915772	42	8	2.802884	-3.35078	2.479003
43	7	4.721316	-2.49936	1.054593	43	7	4.114706	-3.44605	0.515603
44	8	3.427725	-2.86973	-3.34325	44	8	2.370707	-3.38529	-3.75623
45	7	4.791046	-2.58174	-1.43574	45	7	3.9101	-3.43187	-1.96717
46	6	5.03365	-3.26255	-0.16063	46	6	4.130319	-4.20382	-0.73905
47	7	5.418248	-0.12532	1.020386	47	7	5.332291	-1.28967	0.465832
48	7	5.456528	-0.20369	-1.47363	48	7	5.068261	-1.25627	-2.01171
49	6	4.857531	0.933939	1.728377	49	6	5.092241	-0.16003	1.244452
50	6	6.046231	0.309441	-0.23523	50	6	5.90248	-0.95628	-0.84326
51	6	4.828409	0.789358	-2.21663	51	6	4.667851	-0.10832	-2.69111
52	8	4.299704	0.639792	-3.34802	52	8	4.032817	-0.0765	-3.77421
53	7	4.956928	1.992464	-1.53035	53	7	5.152042	0.996337	-1.99408
54	8	4.36581	0.87083	2.883572	54	8	4.722657	-0.15675	2.444743
55	7	4.994415	2.089497	0.963197	55	7	5.408698	0.964223	0.485346
56	6	4.587827	3.271789	-2.12386	56	6	5.105521	2.345964	-2.54561
57	6	5.723864	1.850611	-0.28775	57	6	5.9584	0.617202	-0.82905
58	6	4.667946	3.416554	1.477114	58	6	5.395226	2.315904	1.036569
59	7	3.39781	3.908875	-1.56355	59	7	4.139952	3.243157	-1.92054
60	7	3.461377	4.029492	0.92383	60	7	4.318695	3.185227	0.56226
61	6	2.213669	4.061448	-2.28326	61	6	3.010316	3.708648	-2.58908
62	6	3.431013	4.743085	-0.35748	62	6	4.396704	3.970699	-0.67261
63	6	2.305157	4.237453	1.674415	63	6	3.233565	3.552755	1.356919
64	8	2.10433	3.841863	2.849668	64	8	2.979381	3.121573	2.508146
65	7	1.43366	5.019358	0.917636	65	7	2.51439	4.537163	0.6787
66	8	1.960988	3.560952	-3.4071	66	8	2.624098	3.343262	-3.72652
67	7	1.380211	4.920506	-1.56737	67	7	2.42361	4.699441	-1.80357
68	6	0.218379	5.608171	1.473312	68	6	1.447728	5.303455	1.316466
69	6	0.170618	5.501898	-2.14375	69	6	1.351875	5.560752	-2.29254
70	6	2.022576	5.440871	-0.35678	70	6	3.16991	4.949938	-0.56863
71	7	-1.08796	5.048374	-1.55899	71	7	0.03467	5.317721	-1.71344
72	7	-1.03695	5.09959	0.926323	72	7	0.108933	5.109842	0.764008
73	6	-2.0171	4.291079	-2.27034	73	6	-1.02111	4.77441	-2.44217
74	6	-1.64284	5.592961	-0.31348	74	6	-0.38859	5.837062	-0.41069
75	6	-1.90852	4.299185	1.662861	75	6	-0.91694	4.496846	1.483749
76	8	-1.67284	3.798042	2.789865	76	8	-0.7897	3.884821	2.57291
77	7	-3.10857	4.203875	0.960411	77	7	-2.1177	4.740249	0.816515
78	8	-1.84305	3.788856	-3.4086	78	8	-0.95696	4.330187	-3.61497
79	7	-3.19371	4.241015	-1.52471	79	7	-2.17403	4.871292	-1.66534
80	6	-3.09938	4.999051	-0.27413	80	6	-1.93543	5.55372	-0.38815
81	6	5.589673	-1.45545	1.598067	81	6	5.242999	-2.6479	0.995259
82	6	5.669308	-1.55259	-1.98611	82	6	4.92839	-2.59061	-2.58491
83	6	-4.44376	3.69928	-2.05082	83	6	-3.50422	4.590328	-2.19594
84	6	-4.32167	3.643688	1.551127	84	6	-3.42316	4.471954	1.412667
85	1	0.979691	-6.83924	-0.16147	85	1	-0.56549	-6.85386	-0.4195
86	1	-1.47118	-6.76171	-0.25326	86	1	-2.95154	-6.27667	-0.39021
87	1	-2.49901	-4.73315	-3.11526	87	1	-3.70039	-4.18705	-3.31869
88	1	-3.10953	-5.94307	-1.95366	88	1	-4.5021	-5.17609	-2.06548
89	1	2.247514	-5.00644	-3.05396	89	1	0.908405	-5.38299	-3.44548
90	1	2.721627	-6.21112	-1.8241	90	1	1.208689	-6.63073	-2.20193
91	1	-2.62676	-4.84994	2.632765	91	1	-3.53042	-4.0554	2.424232
92	1	-3.17941	-6.01186	1.392624	92	1	-4.3683	-5.12336	1.264172
93	1	2.131836	-4.86229	2.69622	93	1	1.098711	-5.09243	2.297727
94	1	2.664382	-6.12221	1.548733	94	1	1.286654	-6.46354	1.167917
95	1	-4.80463	-5.09982	-0.29827	95	1	-5.8822	-3.91541	-0.40868
96	1	-6.32644	-3.1781	-0.27097	96	1	-6.92233	-1.69375	-0.4897
97	1	-5.54086	-1.07761	2.619949	97	1	-5.7387	0.172669	2.433773
98	1	-6.79538	-1.31882	1.37298	98	1	-6.99358	0.226131	1.162722
99	1	-5.52491	-1.04679	-3.11831	99	1	-5.55117	0.194913	-3.30141
100	1	-6.78297	-1.31319	-1.88005	100	1	-6.87873	0.234783	-2.10691
101	1	-7.08147	0.58803	-0.23897	101	1	-6.79034	2.141691	-0.46726
102	1	-6.41227	2.944714	-0.1882	102	1	-5.60218	4.289344	-0.37193

103	1	4.401567	-5.4217	-0.11526	103	1	3.058874	-6.17818	-0.61382
104	1	6.068851	-3.62074	-0.11889	104	1	5.062358	-4.77558	-0.81838
105	1	7.118785	0.084134	-0.20999	105	1	6.884816	-1.42983	-0.9557
106	1	5.434051	3.964477	-2.02305	106	1	6.106006	2.791804	-2.46878
107	1	4.394483	3.094527	-3.18498	107	1	4.830757	2.259811	-3.60036
108	1	6.616418	2.485921	-0.32409	108	1	6.971786	1.022898	-0.93033
109	1	5.519072	4.08335	1.28656	109	1	6.354663	2.799461	0.810652
110	1	4.519229	3.322672	2.556028	110	1	5.285953	2.220821	2.120137
111	1	0.249576	6.694791	1.314918	111	1	1.696159	6.371921	1.254328
112	1	0.218674	5.400779	2.546661	112	1	1.416647	5.002041	2.366929
113	1	0.228206	6.594553	-2.0457	113	1	1.630516	6.605833	-2.10272
114	1	0.151891	5.237914	-3.20435	114	1	1.2671	5.399836	-3.37055
115	1	2.073443	6.534977	-0.40173	115	1	3.453659	6.007614	-0.51023
116	1	-1.61376	6.688446	-0.33591	116	1	-0.13314	6.900031	-0.32924
117	1	-3.8859	5.761284	-0.23555	117	1	-2.54916	6.459902	-0.32695
118	1	6.633664	-1.76622	1.462669	118	1	6.170996	-3.18278	0.75374
119	1	5.375772	-1.37514	2.667229	119	1	5.147094	-2.56496	2.081115
120	1	6.710895	-1.83964	-1.79353	120	1	5.897617	-3.10271	-2.52003
121	1	5.497628	-1.52431	-3.06535	121	1	4.65475	-2.46973	-3.63647
122	1	-4.3158	3.566599	-3.12822	122	1	-3.39569	4.433163	-3.2723
123	1	-5.24486	4.427294	-1.86827	123	1	-4.146	5.46388	-2.02102
124	1	-4.12258	3.481107	2.613658	124	1	-3.26462	4.250977	2.471548
125	1	-5.13324	4.376032	1.444656	125	1	-4.03861	5.376785	1.320909
126	1	4.269943	5.446736	-0.41283	126	1	5.364701	4.482228	-0.72945
127	6	0.607285	0.249718	3.304367	127	6	1.149526	-0.11461	4.806626
128	6	-0.80525	0.187054	3.344986	128	6	-0.2332	-0.08829	5.107085
129	6	-1.55175	0.210923	4.520276	129	6	-0.74706	-0.09718	6.401412
130	6	-0.80073	0.288197	5.712442	130	6	0.210479	-0.13523	7.438017
131	6	0.618649	0.345984	5.698532	131	6	1.602779	-0.16221	7.162729
132	6	1.348246	0.331595	4.494377	132	6	2.095716	-0.1526	5.843304
133	6	-0.10303	0.131045	1.228205	133	6	0.070559	-0.058	2.894455
134	1	2.431213	0.389218	4.467925	134	1	3.159868	-0.17321	5.632688
135	6	-0.16317	0.068835	-0.21404	135	6	-0.26501	-0.02947	1.488622
136	6	-1.38283	-0.04637	-0.92472	136	6	-1.60434	0.024348	1.035861
137	6	1.069385	0.126627	-0.93431	137	6	0.799144	-0.05914	0.536436
138	6	-1.3824	-0.10162	-2.3224	138	6	-1.88682	0.044719	-0.33333
139	1	-2.31432	-0.09699	-0.36836	139	1	-2.40245	0.052832	1.769261
140	6	1.063186	0.072615	-2.34145	140	6	0.505802	-0.03905	-0.84169
141	6	-0.15523	-0.04106	-3.02421	141	6	-0.82772	0.011421	-1.27087
142	1	-2.31466	-0.19203	-2.86656	142	1	-2.91499	0.087184	-0.67569
143	1	2.009804	0.129294	-2.86874	143	1	1.326937	-0.0627	-1.55137
144	1	-0.15507	-0.08234	-4.1105	144	1	-1.04624	0.025331	-2.33526
145	7	1.010239	0.215538	1.951312	145	7	1.297291	-0.09452	3.40251
146	8	-1.26748	0.108879	2.008449	146	8	-0.93572	-0.05288	3.881572
147	8	2.279972	0.234908	-0.27993	147	8	2.119685	-0.10935	0.923296
148	1	2.125249	0.249494	0.72922	148	1	2.204952	-0.12105	1.933176
149	1	-2.63448	0.188507	4.506016	149	1	-1.81239	-0.07631	6.603386
150	1	1.151538	0.407601	6.643751	150	1	2.303082	-0.19099	7.992964
151	1	-1.32219	0.309143	6.665623	151	1	-0.12719	-0.14383	8.470525

Table A18: XYZ coordinate of optimized trans-enol HPBO–CB-7 complex (benzoxazole moiety inside the cavity) in water.

(a) in ground state

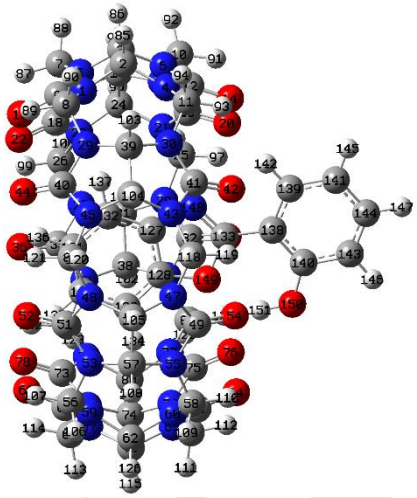

(b) in excited state

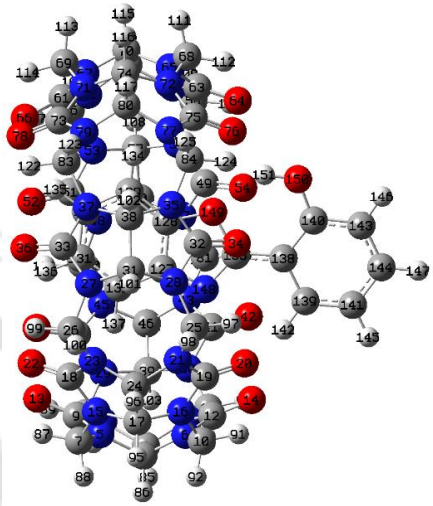

Center Number	Atomic Number	Coordinates (Angstroms) X	Y	Z	Center Number	Atomic Number	Coordinates (Angstroms) X	Y	Z
1	7	5.207321	1.290734	-1.72499	1	7	-5.19606	-1.25857	-1.71348
2	6	5.936359	0.889047	-0.51956	2	6	-5.9267	-0.86364	-0.50644
3	6	5.94345	-0.68208	-0.59982	3	6	-5.93173	0.70784	-0.57758
4	7	5.271515	1.159293	0.762174	4	7	-5.26531	-1.14325	0.774658
5	7	5.165229	-0.96173	-1.81298	5	7	-5.16165	0.99404	-1.79386
6	7	5.337769	-1.09404	0.671126	6	7	-5.31721	1.111211	0.691894
7	6	5.089949	-2.27802	-2.43973	7	6	-5.09208	2.313374	-2.41445
8	6	5.160566	2.660269	-2.22766	8	6	-5.15268	-2.62484	-2.22456
9	6	4.785181	0.200316	-2.48124	9	6	-4.77909	-0.16403	-2.4669
10	6	5.316129	-2.47482	1.149372	10	6	-5.29207	2.489392	1.177264
11	6	5.183906	2.487312	1.364167	11	6	-5.18816	-2.47434	1.371631
12	6	5.004495	-0.00683	1.477738	12	6	-4.99166	0.018646	1.495139
13	8	4.209054	0.254039	-3.59623	13	8	-4.20424	-0.21228	-3.58291
14	8	4.592653	-0.06442	2.662491	14	8	-4.5849	0.069699	2.681513
15	7	4.094686	-3.18025	-1.87376	15	7	-4.09394	3.213582	-1.85097
16	7	4.24745	-3.31261	0.607114	16	7	-4.22694	3.329842	0.63205
17	6	4.333836	-4.00334	-0.68481	17	6	-4.32313	4.028871	-0.6548
18	6	2.941503	-3.55214	-2.56119	18	6	-2.94536	3.588245	-2.54431
19	6	3.176113	-3.76221	1.377835	19	6	-3.15097	3.77617	1.398148
20	8	2.927809	-3.42953	2.562833	20	8	-2.89483	3.437681	2.579906
21	7	2.464902	-4.69615	0.626336	21	7	-2.44533	4.714976	0.647328
22	8	2.548288	-3.07436	-3.65438	22	8	-2.56154	3.117752	-3.64394
23	7	2.336401	-4.59069	-1.85628	23	7	-2.3331	4.620375	-1.83649
24	6	3.099649	-4.97825	-0.66568	24	6	-3.0882	5.003005	-0.63918
25	6	1.387707	-5.50567	1.188895	25	6	-1.36637	5.523852	1.207664
26	6	1.249263	-5.39005	-2.41403	26	6	-1.24519	5.418296	-2.3943
27	7	-0.06193	-5.17818	-1.80941	27	7	0.067436	5.197888	-1.79591
28	7	0.049445	-5.2231	0.674066	28	7	-0.02964	5.241291	0.688695
29	7	4.127313	3.503603	-1.63929	29	7	-4.12735	-3.47658	-1.63482
30	7	4.12216	3.346907	0.843714	30	7	-4.13158	-3.33964	0.849966
31	6	-0.48697	-5.81282	-0.55658	31	6	0.502824	5.828751	-0.54504
32	6	-0.93306	-4.59123	1.433903	32	6	0.955166	4.610328	1.44601
33	6	-1.12087	-4.59065	-2.49795	33	6	1.118519	4.602371	-2.48926
34	8	-0.76788	-4.05968	2.560044	34	8	0.795649	4.086413	2.576502
35	7	-2.14562	-4.7081	0.754518	35	7	2.163896	4.719124	0.758663
36	8	-1.05995	-4.06592	-3.63745	36	8	1.048096	4.078448	-3.62853
37	7	-2.2728	-4.74336	-1.72782	37	7	2.275553	4.746872	-1.72498

38	6	-2.02302	-5.48188	-0.48629	38	6	2.03758	5.48976	-0.48355
39	6	4.272208	4.186327	-0.35073	39	6	-4.28361	-4.16781	-0.35199
40	6	3.008824	3.930024	-2.35093	40	6	-3.01135	-3.90963	-2.34624
41	6	2.988355	3.677425	1.585325	41	6	-3.00504	-3.68773	1.594719
42	8	2.661885	3.183502	2.693059	42	8	-2.68266	-3.21182	2.711388
43	7	2.314151	4.696922	0.914373	43	7	-2.33339	-4.70297	0.914715
44	8	2.698619	3.579817	-3.51666	44	8	-2.6945	-3.55334	-3.50835
45	7	2.330971	4.861682	-1.56778	45	7	-2.34599	-4.85464	-1.56865
46	6	3.015471	5.130934	-0.2983	46	6	-3.0356	-5.12409	-0.30208
47	7	-0.09925	5.233836	0.946934	47	7	0.078661	-5.2456	0.939713
48	7	-0.08818	5.365633	-1.53593	48	7	0.068649	-5.37688	-1.54364
49	6	-1.13098	4.63035	1.663463	49	6	1.109714	-4.63882	1.65458
50	6	-0.57951	5.907118	-0.26718	50	6	0.559081	-5.91847	-0.27436
51	6	-1.09016	4.73713	-2.27307	51	6	1.072305	-4.75488	-2.28345
52	8	-0.9627	4.241014	-3.42007	52	8	0.946643	-4.26461	-3.43319
53	7	-2.27478	4.812028	-1.5415	53	7	2.256239	-4.82894	-1.55105
54	8	-1.02234	4.078847	2.786638	54	8	1.000503	-4.0855	2.776743
55	7	-2.31318	4.80318	0.945761	55	7	2.292102	-4.81056	0.936683
56	6	-3.5729	4.467256	-2.11437	56	6	3.55421	-4.48319	-2.12303
57	6	-2.11413	5.564173	-0.29004	57	6	2.09398	-5.57591	-0.29683
58	6	-3.62733	4.479695	1.492348	58	6	3.60628	-4.48729	1.483945
59	7	-4.20954	3.274513	-1.56041	59	7	4.187945	-3.28845	-1.57002
60	7	-4.2649	3.292485	0.929984	60	7	4.244769	-3.30088	0.920947
61	6	-4.3723	2.104286	-2.29832	61	6	4.346141	-2.1174	-2.30741
62	6	-5.01313	3.279574	-0.33126	62	6	4.991856	-3.29109	-0.3413
63	6	-4.42593	2.11773	1.658674	63	6	4.41402	-2.12779	1.650719
64	8	-3.98144	1.897376	2.811834	64	8	3.977734	-1.90759	2.807188
65	7	-5.21797	1.249838	0.907844	65	7	5.205722	-1.26211	0.896958
66	8	-3.89083	1.876975	-3.43583	66	8	3.86093	-1.88957	-3.44334
67	7	-5.20839	1.250137	-1.57877	67	7	5.182956	-1.26214	-1.5899
68	6	-5.73326	-0.00358	1.447696	68	6	5.724706	-0.00938	1.433577
69	6	-5.76888	0.027326	-2.15142	69	6	5.74461	-0.04201	-2.16689
70	6	-5.69568	1.86138	-0.33751	70	6	5.67578	-1.87374	-0.35092
71	7	-5.22077	-1.22004	-1.62172	71	7	5.204166	1.207897	-1.6351
72	7	-5.16071	-1.21451	0.860728	72	7	5.153863	1.203006	0.846576
73	6	-4.43484	-2.07908	-2.38981	73	6	4.418629	2.070903	-2.39938
74	6	-5.66455	-1.83967	-0.36685	74	6	5.657519	1.825465	-0.38286
75	6	-4.26425	-2.03127	1.541835	75	6	4.265448	2.0255	1.529966
76	8	-3.72519	-1.76831	2.646384	76	8	3.728515	1.765284	2.636764
77	7	-4.10721	-3.20736	0.819728	77	7	4.114325	3.203362	0.810629
78	8	-4.01621	-1.85158	-3.55134	78	8	3.990593	1.844298	-3.55767
79	7	-4.24302	-3.25275	-1.66435	79	7	4.238632	3.2465	-1.67404
80	6	-4.95312	-3.24384	-0.38235	80	6	4.955036	3.234109	-0.39568
81	6	1.224502	5.455804	1.52222	81	6	-1.24488	-5.46891	1.51552
82	6	1.230153	5.670114	-2.0843	82	6	-1.25307	-5.67127	-2.08887
83	6	-3.60749	-4.43788	-2.2353	83	6	3.605057	4.434367	-2.24162
84	6	-3.42564	-4.3777	1.369967	84	6	3.445105	4.379224	1.365527
85	1	6.938233	1.333422	-0.52283	85	1	-6.92925	-1.3065	-0.51485
86	1	6.947009	-1.11334	-0.69225	86	1	-6.93538	1.140792	-0.66071
87	1	4.833994	-2.12476	-3.49139	87	1	-4.84288	2.165972	-3.46857
88	1	6.075944	-2.75653	-2.37336	88	1	-6.07831	2.790053	-2.33928
89	1	4.966627	2.610585	-3.30229	89	1	-4.95114	-2.56881	-3.29753
90	1	6.139108	3.128361	-2.05807	90	1	-6.13463	-3.08962	-2.0654
91	1	5.18815	-2.44307	2.2345	91	1	-5.1568	2.451545	2.261341
92	1	6.280588	-2.94285	0.912062	92	1	-6.25789	2.959623	0.949421
93	1	4.999629	2.345024	2.432255	93	1	-5.00479	-2.33791	2.440662
94	1	6.144399	3.002672	1.230453	94	1	-6.1523	-2.98198	1.233815
95	1	5.298981	-4.51541	-0.77113	95	1	-5.28861	4.542099	-0.73008
96	1	3.375192	-6.03756	-0.72532	96	1	-3.36329	6.062728	-0.69227
97	1	1.372964	-5.32181	2.266325	97	1	-1.34797	5.338781	2.284844
98	1	1.610791	-6.56521	1.005909	98	1	-1.59031	6.58356	1.026549
99	1	1.162898	-5.13605	-3.47372	99	1	-1.16424	5.169096	-3.45556
100	1	1.513772	-6.45134	-2.31808	100	1	-1.50456	6.480211	-2.2916
101	1	-0.26791	-6.88629	-0.58573	101	1	0.289457	6.903401	-0.57208

102	1	-2.66363	-6.3698	-0.44128	102	1	2.683081	6.374484	-0.44505
103	1	5.228069	4.721107	-0.31399	103	1	-5.24416	-4.69462	-0.32329
104	1	3.267761	6.19512	-0.2257	104	1	-3.29806	-6.18633	-0.23568
105	1	-0.36816	6.980994	-0.20914	105	1	0.347517	-6.99233	-0.21668
106	1	-4.25255	5.319848	-1.98361	106	1	4.235569	-5.33407	-1.99015
107	1	-3.42112	4.290465	-3.18234	107	1	3.402972	-4.30848	-3.19142
108	1	-2.76329	6.447088	-0.29706	108	1	2.742864	-6.45907	-0.29984
109	1	-4.28957	5.34182	1.341461	109	1	4.267962	-5.35008	1.33393
110	1	-3.50405	4.303539	2.564058	110	1	3.482803	-4.31054	2.555524
111	1	-6.82164	-0.03337	1.309019	111	1	6.812744	0.01834	1.29165
112	1	-5.50567	-0.01419	2.516823	112	1	5.500209	0.003092	2.503316
113	1	-6.85514	0.032997	-1.99239	113	1	6.83177	-0.05138	-2.01382
114	1	-5.56108	0.041076	-3.22462	114	1	5.531028	-0.05607	-3.23895
115	1	-6.79078	1.900203	-0.34264	115	1	6.770795	-1.9137	-0.3619
116	1	-6.75787	-1.89881	-0.33827	116	1	6.751311	1.877488	-0.35834
117	1	-5.64627	-4.09056	-0.32695	117	1	5.653655	4.076425	-0.34378
118	1	1.463162	6.525333	1.44921	118	1	-1.48534	-6.5375	1.435058
119	1	1.172729	5.17043	2.576224	119	1	-1.19154	-5.19103	2.571438
120	1	1.450463	6.727917	-1.88936	120	1	-1.48148	-6.72745	-1.89478
121	1	1.183998	5.504566	-3.1638	121	1	-1.20753	-5.50476	-3.16827
122	1	-3.51796	-4.27147	-3.31191	122	1	3.506889	4.267217	-3.31738
123	1	-4.25602	-5.3049	-2.05615	123	1	4.259354	5.29818	-2.06801
124	1	-3.23815	-4.17849	2.428199	124	1	3.262925	4.18149	2.424917
125	1	-4.09473	-5.24359	1.279655	125	1	4.12068	5.239542	1.270733
126	1	-5.72662	4.111173	-0.35372	126	1	5.704476	-4.12352	-0.36225
127	6	0.499753	-0.14751	0.30814	127	6	-0.53092	0.097414	0.320296
128	6	-0.89245	-0.18632	0.549433	128	6	0.896389	0.188772	0.523008
129	6	-1.8539	-0.10616	-0.45415	129	6	1.826063	0.119093	-0.49651
130	6	-1.35941	0.004379	-1.77102	130	6	1.304893	-0.03218	-1.81426
131	6	0.032855	0.033617	-2.04087	131	6	-0.09754	-0.11011	-2.05381
132	6	0.983814	-0.03859	-1.00645	132	6	-1.03019	-0.05089	-1.011
133	6	0.257466	-0.3223	2.475258	133	6	-0.21714	0.307792	2.490194
134	1	-2.91689	-0.11765	-0.24494	134	1	2.892984	0.162505	-0.31359
135	1	-2.06176	0.073637	-2.59576	135	1	1.994144	-0.09572	-2.65081
136	1	0.368271	0.119055	-3.07035	136	1	-0.44587	-0.22417	-3.07649
137	1	2.048487	-0.01063	-1.21043	137	1	-2.09681	-0.11885	-1.19298
138	6	0.424674	-0.40727	3.919641	138	6	-0.38373	0.392998	3.879258
139	6	1.743509	-0.25685	4.433409	139	6	-1.7153	0.254318	4.434818
140	6	-0.64978	-0.61764	4.832399	140	6	0.721726	0.593588	4.830228
141	6	1.992567	-0.2901	5.808218	141	6	-1.91546	0.254318	5.813346
142	1	2.558733	-0.11346	3.729925	142	1	-2.54671	0.135865	3.747939
143	6	-0.38579	-0.63963	6.220961	143	6	0.482997	0.575125	6.214173
144	6	0.91659	-0.47592	6.707662	144	6	-0.82159	0.401647	6.719584
145	1	3.005287	-0.16996	6.181884	145	1	-2.92197	0.136633	6.207634
146	1	-1.22256	-0.79558	6.895309	146	1	1.329861	0.719481	6.878558
147	1	1.095706	-0.49754	7.77953	147	1	-0.99282	0.396265	7.792327
148	7	1.184883	-0.23227	1.541407	148	7	-1.193	0.164977	1.51367
149	8	-1.06869	-0.30492	1.944762	149	8	1.115209	0.334703	1.903577
150	8	-1.97663	-0.80648	4.491968	150	8	2.017284	0.814994	4.448413
151	1	-2.19797	-0.93475	3.536643	151	1	2.229593	0.942266	3.484675

Table A19: XYZ coordinate of optimized trans-enol HPBO–CB-7 complex (benzoxazole moiety inside the cavity) in DMSO.

(a) in ground state

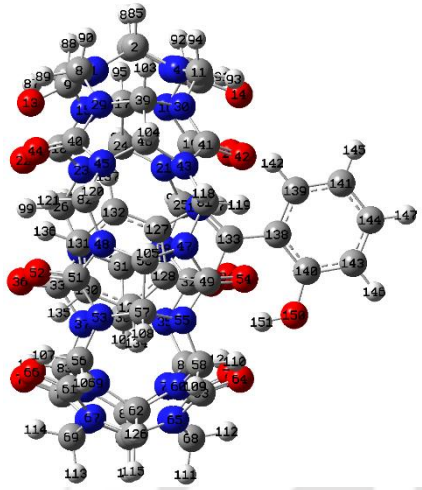

(b) in excited state

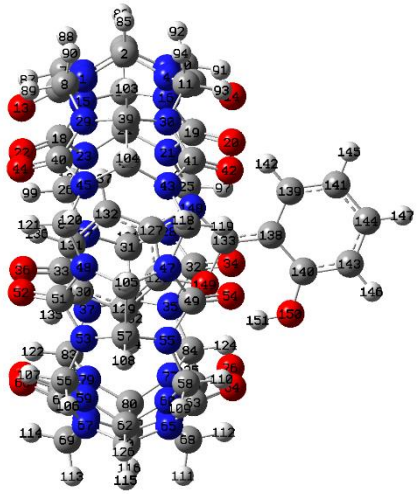

Center Number	Atomic Number	Coordinates (Angstroms) X	Y	Z	Center Number	Atomic Number	Coordinates (Angstroms) X	Y	Z
1	7	5.204073	1.25602	-1.73048	1	7	5.204645	1.187489	-1.71911
2	6	5.934344	0.85126	-0.52703	2	6	5.928489	0.78195	-0.51179
3	6	5.9312	-0.72004	-0.6056	3	6	5.910404	-0.78947	-0.58272
4	7	5.277316	1.127132	0.757005	4	7	5.272564	1.070911	0.769599
5	7	5.151402	-0.9963	-1.81808	5	7	5.136277	-1.06455	-1.79872
6	7	5.324603	-1.1266	0.666392	6	7	5.291949	-1.18397	0.687132
7	6	5.071173	-2.31211	-2.44506	7	6	5.050681	-2.38285	-2.41943
8	6	5.165109	2.62497	-2.23458	8	6	5.182141	2.55403	-2.23055
9	6	4.775742	0.167422	-2.48635	9	6	4.772312	0.099005	-2.47319
10	6	5.292675	-2.507	1.144361	10	6	5.248221	-2.56143	1.172498
11	6	5.200573	2.455844	1.358526	11	6	5.213778	2.402507	1.366867
12	6	5.002918	-0.0365	1.474104	12	6	4.983887	-0.08683	1.491017
13	8	4.200012	0.223797	-3.60103	13	8	4.201833	0.155628	-3.59071
14	8	4.597724	-0.08986	2.660953	14	8	4.582827	-0.13179	2.679062
15	7	4.072261	-3.21074	-1.88098	15	7	4.042502	-3.27132	-1.85631
16	7	4.219531	-3.3378	0.601054	16	7	4.172704	-3.38819	0.627871
17	6	4.303561	-4.03154	-0.68924	17	6	4.259522	-4.08807	-0.65911
18	6	2.917168	-3.57572	-2.56919	18	6	2.888003	-3.6292	-2.54908
19	6	3.144231	-3.77929	1.37148	19	6	3.091182	-3.82075	1.394814
20	8	2.89692	-3.44367	2.555419	20	8	2.839692	-3.48076	2.576799
21	7	2.429542	-4.71167	0.621003	21	7	2.374262	-4.75123	0.643883
22	8	2.530012	-3.09958	-3.66481	22	8	2.512332	-3.1559	-3.64992
23	7	2.303957	-4.60817	-1.86219	23	7	2.26109	-4.65173	-1.84007
24	6	3.062968	-4.9986	-0.67004	24	6	3.011358	-5.04544	-0.64347
25	6	1.348821	-5.51532	1.184538	25	6	1.286571	-5.54752	1.204892
26	6	1.210367	-5.39885	-2.41876	26	6	1.160807	-5.43261	-2.397
27	7	-0.09875	-5.17825	-1.81318	27	7	-0.14735	-5.1961	-1.7955
28	7	0.011618	-5.22691	0.671167	28	7	-0.04772	-5.24862	0.68969
29	7	4.141753	3.477234	-1.64261	29	7	4.171464	3.422723	-1.64056
30	7	4.144358	3.323396	0.840984	30	7	4.171127	3.283355	0.844441
31	6	-0.52797	-5.81039	-0.56082	31	6	-0.58916	-5.824	-0.54547
32	6	-0.96693	-4.59108	1.433094	32	6	-1.02234	-4.60478	1.449708
33	6	-1.15339	-4.58201	-2.50114	33	6	-1.1915	-4.58563	-2.48661
34	8	-0.79887	-4.06515	2.561083	34	8	-0.85482	-4.08606	2.581036
35	7	-2.18018	-4.69984	0.753112	35	7	-2.2333	-4.69633	0.76333
36	8	-1.08951	-4.05975	-3.64121	36	8	-1.11638	-4.06294	-3.62571
37	7	-2.30616	-4.72566	-1.73001	37	7	-2.34927	-4.7158	-1.72041

38	6	-2.06189	-5.46914	-0.49031	38	6	-2.11924	-5.46446	-0.48103
39	6	4.296196	4.159555	-0.35512	39	6	4.336849	4.109504	-0.3567
40	6	3.02451	3.911927	-2.3514	40	6	3.061802	3.872445	-2.35188
41	6	3.014652	3.66198	1.585707	41	6	3.050125	3.6487	1.589749
42	8	2.68841	3.172075	2.694831	42	8	2.720479	3.176716	2.705442
43	7	2.346335	4.686268	0.915583	43	7	2.396384	4.676959	0.911206
44	8	2.709322	3.564004	-3.5161	44	8	2.741598	3.523378	-3.51493
45	7	2.356839	4.850103	-1.56702	45	7	2.409477	4.825483	-1.57275
46	6	3.046748	5.113917	-0.29945	46	6	3.103627	5.085058	-0.30665
47	7	-0.06342	5.238973	0.952489	47	7	-0.00673	5.257702	0.941581
48	7	-0.05843	5.372845	-1.53162	48	7	0.002099	5.380743	-1.54356
49	6	-1.09687	4.642569	1.672738	49	6	-1.046	4.673547	1.663674
50	6	-0.543	5.914314	-0.26045	50	6	-0.47956	5.931198	-0.27503
51	6	-1.06676	4.754817	-2.26936	51	6	-1.01062	4.770316	-2.28109
52	8	-0.94706	4.267618	-3.42064	52	8	-0.89392	4.280281	-3.43148
53	7	-2.24841	4.832242	-1.53278	53	7	-2.19215	4.858544	-1.54586
54	8	-0.98989	4.096948	2.798453	54	8	-0.94549	4.134499	2.793062
55	7	-2.27925	4.818251	0.955763	55	7	-2.22581	4.85301	0.94327
56	6	-3.54986	4.496321	-2.10297	56	6	-3.495	4.529627	-2.11638
57	6	-2.07976	5.579362	-0.27962	57	6	-2.01906	5.608116	-0.29474
58	6	-3.59285	4.498216	1.50474	58	6	-3.54247	4.542587	1.490907
59	7	-4.19267	3.306252	-1.55085	59	7	-4.14498	3.344617	-1.56207
60	7	-4.23717	3.31592	0.940497	60	7	-4.19289	3.362155	0.929461
61	6	-4.36436	2.138778	-2.2914	61	6	-4.32421	2.176529	-2.29967
62	6	-4.99005	3.311854	-0.31783	62	6	-4.94377	3.359512	-0.33018
63	6	-4.40085	2.138894	1.665433	63	6	-4.36678	2.188599	1.657868
64	8	-3.95082	1.910031	2.814439	64	8	-3.92295	1.960488	2.809536
65	7	-5.20479	1.280324	0.915997	65	7	-5.17435	1.333159	0.908616
66	8	-3.88947	1.912218	-3.43152	66	8	-3.84894	1.942495	-3.43826
67	7	-5.20272	1.287373	-1.57061	67	7	-5.17087	1.33383	-1.57817
68	6	-5.72849	0.030352	1.45496	68	6	-5.70797	0.08872	1.449457
69	6	-5.77203	0.068893	-2.14356	69	6	-5.75377	0.121866	-2.15123
70	6	-5.68173	1.898133	-0.32597	70	6	-5.64574	1.951126	-0.33529
71	7	-5.23137	-1.18335	-1.61753	71	7	-5.22916	-1.13637	-1.62311
72	7	-5.16795	-1.18428	0.864931	72	7	-5.16157	-1.13244	0.858339
73	6	-4.45194	-2.04629	-2.38847	73	6	-4.45883	-2.01046	-2.39083
74	6	-5.67746	-1.80249	-0.36344	74	6	-5.68313	-1.74637	-0.36774
75	6	-4.27813	-2.00992	1.544419	75	6	-4.28539	-1.97111	1.538568
76	8	-3.73812	-1.75435	2.649746	76	8	-3.7396	-1.72106	2.642872
77	7	-4.1312	-3.18574	0.81958	77	7	-4.16043	-3.15211	0.819375
78	8	-4.03443	-1.82012	-3.55034	78	8	-4.03413	-1.79103	-3.55144
79	7	-4.26707	-3.22258	-1.6651	79	7	-4.29137	-3.18803	-1.66535
80	6	-4.9764	-3.21203	-0.38295	80	6	-5.00365	-3.16645	-0.38488
81	6	1.262906	5.452305	1.524682	81	6	1.321883	5.461549	1.512588
82	6	1.261351	5.666666	-2.08164	82	6	1.326563	5.6557	-2.09176
83	6	-3.63815	-4.41006	-2.23792	83	6	-3.67484	-4.38396	-2.23448
84	6	-3.4581	-4.36174	1.367722	84	6	-3.50835	-4.33839	1.371638
85	1	6.939253	1.289126	-0.53493	85	1	6.937708	1.209846	-0.52035
86	1	6.932258	-1.15753	-0.69815	86	1	6.90793	-1.23672	-0.6667
87	1	4.816417	-2.15738	-3.49686	87	1	4.802689	-2.23203	-3.4734
88	1	6.055535	-2.7942	-2.37819	88	1	6.031456	-2.87108	-2.34476
89	1	4.964508	2.574693	-3.30805	89	1	4.977689	2.500045	-3.30315
90	1	6.148377	3.085828	-2.07153	90	1	6.171916	3.003032	-2.07345
91	1	5.163328	-2.47391	2.229341	91	1	5.11339	-2.52141	2.256597
92	1	6.254367	-2.98189	0.908551	92	1	6.207944	-3.04451	0.944781
93	1	5.017246	2.314783	2.426973	93	1	5.02606	2.267575	2.435375
94	1	6.16485	2.96396	1.222666	94	1	6.185761	2.896126	1.231449
95	1	5.265545	-4.55045	-0.77241	95	1	5.217913	-4.61495	-0.73366
96	1	3.331623	-6.0599	-0.72818	96	1	3.271926	-6.10888	-0.69828
97	1	1.335608	-5.33029	2.261827	97	1	1.272639	-5.36361	2.282367
98	1	1.567022	-6.57617	1.002021	98	1	1.497608	-6.60972	1.021632
99	1	1.124802	-5.14286	-3.47809	99	1	1.080977	-5.17864	-3.45728
100	1	1.466943	-6.46237	-2.32399	100	1	1.405428	-6.49856	-2.29817
101	1	-0.31629	-6.88544	-0.59139	101	1	-0.3904	-6.90145	-0.57637

102	1	-2.7085	-6.35313	-0.44877	102	1	-2.77659	-6.3407	-0.44391
103	1	5.256243	4.687337	-0.32223	103	1	5.305406	4.621651	-0.32628
104	1	3.307535	6.176369	-0.22802	104	1	3.382838	6.143327	-0.24165
105	1	-0.32622	6.987314	-0.20216	105	1	-0.25468	7.00277	-0.22117
106	1	-4.2242	5.352754	-1.96857	106	1	-4.16446	5.39016	-1.98392
107	1	-3.40137	4.321079	-3.17171	107	1	-3.34694	4.351509	-3.18471
108	1	-2.72425	6.466046	-0.28284	108	1	-2.6567	6.499725	-0.30157
109	1	-4.25245	5.363421	1.358872	109	1	-4.19669	5.41118	1.340909
110	1	-3.46654	4.31792	2.57547	110	1	-3.41918	4.365426	2.562505
111	1	-6.81762	0.010178	1.31945	111	1	-6.79769	0.078404	1.317012
112	1	-5.49737	0.01592	2.523358	112	1	-5.474	0.072637	2.517197
113	1	-6.85798	0.081199	-1.98154	113	1	-6.83971	0.14739	-1.99046
114	1	-5.56688	0.083201	-3.21732	114	1	-5.54725	0.13288	-3.22476
115	1	-6.77665	1.944311	-0.32776	115	1	-6.74027	2.005321	-0.33782
116	1	-6.77129	-1.85417	-0.33362	116	1	-6.77761	-1.78135	-0.33574
117	1	-5.67609	-4.05372	-0.33022	117	1	-5.71604	-3.99738	-0.3332
118	1	1.508469	6.520377	1.450834	118	1	1.579454	6.525978	1.428232
119	1	1.211144	5.167452	2.578862	119	1	1.266781	5.187818	2.569526
120	1	1.490506	6.722957	-1.88793	120	1	1.569697	6.709327	-1.90078
121	1	1.2117	5.50032	-3.16095	121	1	1.276319	5.486848	-3.17067
122	1	-3.54597	-4.24119	-3.31399	122	1	-3.57597	-4.21684	-3.31024
123	1	-4.29268	-5.27338	-2.06175	123	1	-4.34094	-5.23885	-2.06057
124	1	-3.26966	-4.1656	2.42638	124	1	-3.32117	-4.14443	2.430867
125	1	-4.13325	-5.22291	1.275286	125	1	-4.19698	-5.1885	1.276886
126	1	-5.69828	4.148271	-0.33424	126	1	-5.64568	4.201162	-0.35009
127	6	0.509123	-0.13797	0.306757	127	6	0.541596	-0.10983	0.308326
128	6	-0.88272	-0.18247	0.549314	128	6	-0.88565	-0.18582	0.51854
129	6	-1.84541	-0.0979	-0.45268	129	6	-1.82017	-0.10408	-0.49552
130	6	-1.35285	0.023934	-1.76919	130	6	-1.30493	0.044067	-1.81583
131	6	0.038973	0.059462	-2.0403	131	6	0.097075	0.106038	-2.06305
132	6	0.991225	-0.01738	-1.0075	132	6	1.034695	0.034544	-1.02573
133	6	0.270092	-0.3269	2.472733	133	6	0.237309	-0.31801	2.479523
134	1	-2.90809	-0.11319	-0.24216	134	1	-2.8864	-0.1354	-0.30615
135	1	-2.05623	0.098152	-2.5927	135	1	-1.99798	0.118193	-2.64847
136	1	0.373129	0.154069	-3.06935	136	1	0.441074	0.218203	-3.08735
137	1	2.0555	0.017036	-1.21249	137	1	2.100769	0.090883	-1.21401
138	6	0.439218	-0.41939	3.916447	138	6	0.407064	-0.40135	3.868247
139	6	1.758465	-0.26992	4.428669	139	6	1.741919	-0.27562	4.419373
140	6	-0.63328	-0.63697	4.829456	140	6	-0.69731	-0.58848	4.822626
141	6	2.010127	-0.31227	5.802839	141	6	1.946741	-0.2786	5.797001
142	1	2.571296	-0.12053	3.723694	142	1	2.571333	-0.16579	3.728775
143	6	-0.36687	-0.66879	6.217347	143	6	-0.45383	-0.57369	6.205643
144	6	0.936213	-0.50665	6.702855	144	6	0.854566	-0.41522	6.706875
145	1	3.023372	-0.19274	6.17539	145	1	2.955858	-0.17148	6.187761
146	1	-1.20244	-0.83038	6.891911	146	1	-1.30027	-0.70813	6.872713
147	1	1.117286	-0.53564	7.774292	147	1	1.029328	-0.41236	7.779141
148	7	1.196112	-0.22903	1.538599	148	7	1.209758	-0.18534	1.498105
149	8	-1.05724	-0.31035	1.944075	149	8	-1.09878	-0.33078	1.89991
150	8	-1.96039	-0.82497	4.489742	150	8	-1.99718	-0.79335	4.44476
151	1	-2.18294	-0.93474	3.532663	151	1	-2.21093	-0.91151	3.480601

Annexure-B

Table B1: The optimized Cartesian coordinates of optimized bis-HPTA in DMF.

(a) bis-HPTA-I.

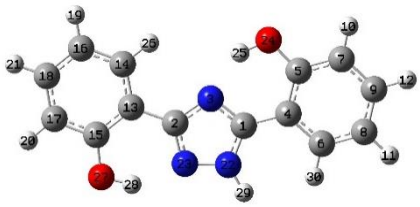

Atom Number	Atomic Number	Coordinates (Angstroms) X	Y	Z
1	6	-1.123671	-0.595629	-0.00001
2	6	1.015478	-0.439764	0.000029
3	7	-0.131157	0.303794	0.000221
4	6	-2.542928	-0.261487	0.00013
5	6	-2.935378	1.102898	-0.000299
6	6	-3.541965	-1.2555	0.000665
7	6	-4.299285	1.431681	-0.000376
8	6	-4.890427	-0.921486	0.000602
9	6	-5.264997	0.430959	0.000051
10	1	-4.57635	2.480955	-0.000739
11	1	-5.643456	-1.702192	0.001017
12	1	-6.316156	0.70327	0.000004
13	6	2.370619	0.113688	0.000105
14	6	2.566418	1.507349	0.0003
15	6	3.506428	-0.732942	-0.000067
16	6	3.844194	2.057507	0.000351
17	6	4.792126	-0.174393	0.00001
18	6	4.959624	1.207881	0.000221
19	1	3.972492	3.135	0.000491
20	1	5.646332	-0.84411	-0.000084
21	1	5.962598	1.624289	0.000272
22	7	-0.578096	-1.833064	-0.000362
23	7	0.776806	-1.751662	-0.000665
24	8	-2.043494	2.121915	-0.000604
25	1	-1.126474	1.743618	-0.000089
26	1	1.694597	2.152909	0.000406
27	8	3.417499	-2.090529	-0.000193
28	1	2.471495	-2.360073	-0.000053
29	1	-1.02638	-2.738687	-0.000625
30	1	-3.26103	-2.30412	0.001145

(b) bis-HPTA-Ia.

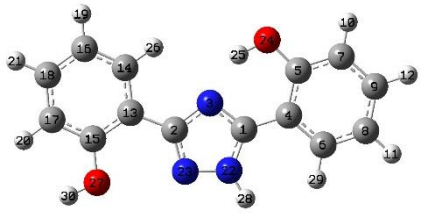

Atom Number	Atomic Number	Coordinates (Angstroms) X	Y	Z
1	6	-1.137491	-0.644689	-0.000263
2	6	1.01066	-0.548762	-0.000591
3	7	-0.124375	0.226234	0.000446
4	6	-2.549776	-0.27756	0.000107
5	6	-2.909352	1.095453	0.000552
6	6	-3.572508	-1.24636	-0.000095
7	6	-4.26426	1.458507	0.000504
8	6	-4.913114	-0.87924	0.000073
9	6	-5.254812	0.481568	0.000311
10	1	-4.515553	2.514346	0.000755
11	1	-5.68497	-1.641469	-0.000048
12	1	-6.299018	0.779613	0.000379
13	6	2.354264	0.052858	-0.000423
14	6	2.457276	1.458061	-0.001237
15	6	3.555246	-0.693162	0.000653
16	6	3.687021	2.110059	-0.001077
17	6	4.794103	-0.036748	0.000889
18	6	4.864139	1.354335	0.000009
19	1	3.726391	3.194473	-0.001762
20	1	5.704178	-0.631629	0.001772
21	1	5.834123	1.842233	0.000185
22	7	-0.615864	-1.891579	-0.001421
23	7	0.742415	-1.853981	-0.001339
24	8	-1.988552	2.089374	0.000773
25	1	-1.083109	1.680308	0.00068
26	1	1.542385	2.038753	-0.002049
27	8	3.493945	-2.05711	0.001684
28	1	-1.086768	-2.785368	-0.002292
29	1	-3.316863	-2.301578	-0.000288
30	1	4.392461	-2.418427	0.002731

(c) bis-HPTA-Ib.

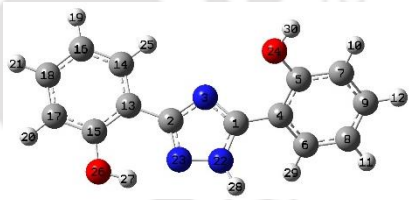

Atom Number	Atomic Number	Coordinates (Angstroms) X	Y	Z
1	6	1.0766	-0.44056	0.047724
2	6	-1.049484	-0.357309	0.035997
3	7	0.067716	0.400051	-0.173902
4	6	2.519182	-0.186237	-0.080234
5	6	3.117128	0.990732	0.41955
6	6	3.337594	-1.143571	-0.706722
7	6	4.496779	1.186956	0.28023
8	6	4.710741	-0.949299	-0.842648
9	6	5.287346	0.224038	-0.346355
10	1	4.947596	2.094891	0.67235
11	1	5.319904	-1.698433	-1.337095
12	1	6.354926	0.394646	-0.445927
13	6	-2.423687	0.136487	-0.093979
14	6	-2.661305	1.474306	-0.459318
15	6	-3.534331	-0.709522	0.144628
16	6	-3.955286	1.97061	-0.587061
17	6	-4.836299	-0.206565	0.014832
18	6	-5.045253	1.12195	-0.347719
19	1	-4.115616	3.006063	-0.869817
20	1	-5.670201	-0.875361	0.203776

21	1	-6.060244	1.49633	-0.443731
22	7	0.574694	-1.656239	0.37835
23	7	-0.777789	-1.621833	0.376576
24	8	2.325112	1.902723	1.052694
25	1	-1.805889	2.1164	-0.640604
26	8	-3.403278	-2.016611	0.50247
27	1	-2.44749	-2.245917	0.559707
28	1	1.066346	-2.497865	0.648738
29	1	2.880557	-2.041265	-1.112213
30	1	2.86474	2.635661	1.382788

(d) bis-HPTA-Ic.

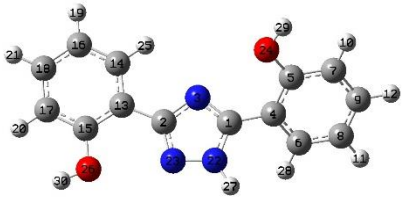

Atom Number	Atomic Number	Coordinates (Angstroms) X	Y	Z
1	6	1.087425	-0.487097	0.06146
2	6	-1.045728	-0.462752	0.067004
3	7	0.058036	0.32543	-0.149221
4	6	2.523989	-0.200962	-0.076394
5	6	3.105254	0.980788	0.431283
6	6	3.356041	-1.13485	-0.719848
7	6	4.47958	1.205194	0.282828
8	6	4.724655	-0.91374	-0.8647
9	6	5.283664	0.264599	-0.360701
10	1	4.915734	2.117621	0.681257
11	1	5.343466	-1.646322	-1.371987
12	1	6.346971	0.456629	-0.467085
13	6	-2.409666	0.079177	-0.074699
14	6	-2.551963	1.436757	-0.424362
15	6	-3.590523	-0.673517	0.118485
16	6	-3.799363	2.035604	-0.579375
17	6	-4.847205	-0.071751	-0.038535
18	6	-4.955934	1.273341	-0.384596
19	1	-3.868204	3.084548	-0.849338
20	1	-5.74086	-0.672229	0.114237
21	1	-5.93903	1.719614	-0.50058
22	7	0.610384	-1.712783	0.390826
23	7	-0.743829	-1.720784	0.402666
24	8	2.302463	1.871988	1.082268
25	1	-1.649006	2.017527	-0.573061
26	8	-3.493723	-1.993305	0.459896
27	1	1.12466	-2.543848	0.650984
28	1	2.912556	-2.036949	-1.130778
29	1	2.832913	2.610906	1.413836
30	1	-4.38262	-2.364768	0.558207

(e) bis-HPTA-II.

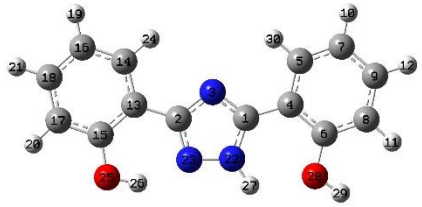

Atom Number	Atomic Number	Coordinates (Angstroms) X	Y	Z
1	6	1.053121	-0.203343	-0.000009
2	6	-1.075727	-0.224327	0.00004
3	7	-0.003003	0.615892	0.000027
4	6	2.455775	0.218685	-0.00005
5	6	2.753498	1.594272	-0.000312
6	6	3.529001	-0.69716	0.000179
7	6	4.068216	2.0498	-0.000351
8	6	4.851431	-0.242872	0.000141
9	6	5.119635	1.125187	-0.000125
10	1	4.273519	3.115131	-0.000561
11	1	5.663887	-0.964386	0.000318
12	1	6.150321	1.466056	-0.000155
13	6	-2.475824	0.211104	0.000072
14	6	-2.790083	1.582529	0.000322
15	6	-3.536295	-0.728042	-0.000157
16	6	-4.110495	2.022698	0.000341
17	6	-4.865062	-0.281413	-0.000145
18	6	-5.150053	1.081966	0.000101
19	1	-4.329991	3.085555	0.000535
20	1	-5.659388	-1.021298	-0.000321
21	1	-6.184942	1.411562	0.000116
22	7	0.615395	-1.485158	-0.000096
23	7	-0.73641	-1.519268	-0.000032
24	1	-1.9729	2.296129	0.000502
25	8	-3.330602	-2.073806	-0.000422
26	1	-2.362303	-2.256189	-0.000376
27	1	1.17583	-2.327846	0.000031
28	8	3.229122	-2.034424	0.000465
29	1	4.035672	-2.570184	0.000474
30	1	1.927425	2.296555	-0.00049

(f) bis-HPTA-IIa.

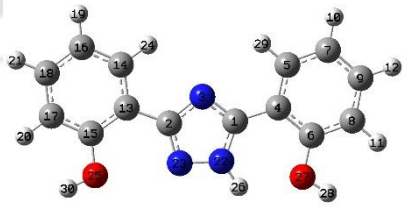

Atom Number	Atomic Number	Coordinates (Angstroms) X	Y	Z
1	6	-1.063513	-0.258436	-0.000893
2	6	1.06944	-0.341877	-0.001242
3	7	0.011766	0.529046	0.000278
4	6	-2.456	0.199483	0.000482
5	6	-2.719736	1.581882	0.004737
6	6	-3.553251	-0.687237	-0.002198
7	6	-4.022331	2.072108	0.006317
8	6	-4.863575	-0.19871	-0.000257

9	6	-5.097624	1.175686	0.00387
10	1	-4.199383	3.142578	0.00951
11	1	-5.694088	-0.899309	-0.001917
12	1	-6.119307	1.54271	0.005231
13	6	2.461476	0.144724	-0.001245
14	6	2.677655	1.536976	-0.006538
15	6	3.599734	-0.693663	0.003978
16	6	3.955638	2.08959	-0.006813
17	6	4.887501	-0.138226	0.00383
18	6	5.069127	1.243056	-0.001531
19	1	4.08125	3.167611	-0.0111
20	1	5.748042	-0.803144	0.008116
21	1	6.075126	1.651762	-0.001594
22	7	-0.651049	-1.5487	-0.003009
23	7	0.700171	-1.627404	-0.002967
24	1	1.807162	2.182698	-0.010525
25	8	3.431084	-2.050193	0.009337
26	1	-1.230573	-2.377797	-0.00452
27	8	-3.290113	-2.033077	-0.00657
28	1	-4.112066	-2.544907	-0.010882
29	1	-1.875603	2.262476	0.006752
30	1	4.298208	-2.48124	0.013702

(g) bis-HPTA-III.

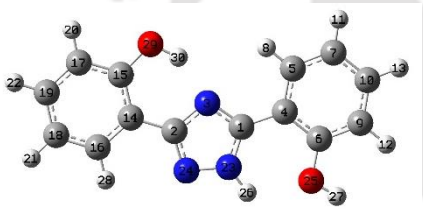

Atom Number	Atomic Number	Coordinates (Angstroms) X	Y	Z
1	6	0.996875	-0.425405	-0.000003
2	6	-1.135605	-0.643984	-0.000017
3	7	-0.133993	0.290315	0.000001
4	6	2.355282	0.118008	0.000006
5	6	2.536538	1.513846	0.000023
6	6	3.502083	-0.704205	-0.000002
7	6	3.808369	2.077992	0.000031
8	1	1.657717	2.148776	0.000029
9	6	4.781686	-0.14066	0.000007
10	6	4.933809	1.245086	0.000023
11	1	3.923012	3.15678	0.000044
12	1	5.651829	-0.791809	0.000001
13	1	5.931983	1.671687	0.00003
14	6	-2.555009	-0.274673	-0.000009
15	6	-2.946694	1.086826	-0.000021
16	6	-3.555493	-1.264731	0.000021
17	6	-4.309564	1.420426	0.000002
18	6	-4.905815	-0.92964	0.000043
19	6	-5.279902	0.422313	0.000034
20	1	-4.583999	2.470788	-0.000009
21	1	-5.660367	-1.709665	0.000068
22	1	-6.330506	0.697847	0.00005
23	7	0.658289	-1.733835	-0.000021
24	7	-0.686137	-1.899666	-0.000012
25	8	3.314388	-2.061166	-0.000017
26	1	1.291358	-2.523361	-0.000031
27	1	4.162845	-2.527406	-0.000022
28	1	-3.251819	-2.306605	0.000032
29	8	-2.0497	2.109087	-0.000067
30	1	-1.136018	1.724702	-0.000129

(h) bis-HPTA-IIIa.

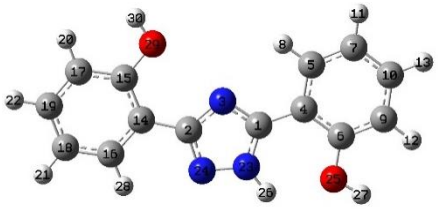

Atom Number	Atomic Number	Coordinates (Angstroms) X	Y	Z
1	6	-1.03133	-0.382102	0.000003
2	6	1.095217	-0.534392	0.000007
3	7	0.072254	0.370218	-0.000009
4	6	-2.405848	0.126303	-0.000009
5	6	-2.618953	1.517431	-0.000041
6	6	-3.534926	-0.719404	0.000012
7	6	-3.903043	2.054554	-0.000053
8	1	-1.750405	2.166524	-0.000057
9	6	-4.826768	-0.184025	0
10	6	-5.010477	1.198174	-0.000032
11	1	-4.040895	3.130818	-0.000079
12	1	-5.682248	-0.854281	0.000018
13	1	-6.017975	1.602486	-0.000041
14	6	2.537394	-0.217021	-0.000003
15	6	3.062904	1.095159	0.000034
16	6	3.457519	-1.285792	-0.000052
17	6	4.451632	1.300212	0.000018
18	6	4.833917	-1.08281	-0.000065
19	6	5.334436	0.224024	-0.000031
20	1	4.832404	2.318825	0.000046
21	1	5.508432	-1.933057	-0.000104
22	1	6.404703	0.407236	-0.000042
23	7	-0.665534	-1.685725	0.000026
24	7	0.678514	-1.808904	0.00003
25	8	-3.319991	-2.074058	0.000044
26	1	-1.274103	-2.493906	0.000042
27	1	-4.159889	-2.555522	0.000059
28	1	3.063237	-2.295674	-0.000081
29	8	2.212463	2.165528	0.000088
30	1	2.730269	2.983796	0.000119

(i) bis-HPTA-IV.

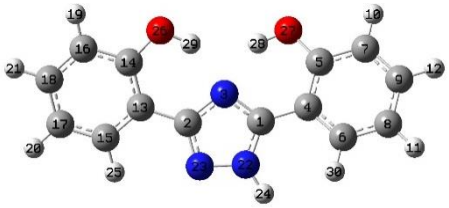

Atom Number	Atomic Number	Coordinates (Angstroms) X	Y	Z
1	6	1.070569	-0.736291	0.033438
2	6	-1.080644	-0.781401	-0.026363
3	7	-0.001338	0.070861	0.016869
4	6	2.467238	-0.311437	0.050499

5	6	2.810358	1.013636	-0.315451
6	6	3.498776	-1.204605	0.403825
7	6	4.155643	1.4058	-0.333889
8	6	4.830914	-0.808742	0.3887
9	6	5.155665	0.503293	0.014472
10	1	4.392586	2.424518	-0.623115
11	1	5.608794	-1.510232	0.670462
12	1	6.192891	0.823894	-0.000057
13	6	-2.4751	-0.324422	-0.03749
14	6	-2.817755	1.002399	0.312902
15	6	-3.508486	-1.218154	-0.378867
16	6	-4.161659	1.401709	0.316521
17	6	-4.840939	-0.819264	-0.376197
18	6	-5.164768	0.499382	-0.02559
19	1	-4.395606	2.425185	0.592038
20	1	-5.620202	-1.524072	-0.647398
21	1	-6.200875	0.824635	-0.021292
22	7	0.627163	-2.010046	-0.005093
23	7	-0.728554	-2.063483	-0.035411
24	1	1.160834	-2.867894	-0.040333
25	1	-3.243645	-2.234342	-0.651864
26	8	-1.893227	1.936744	0.671906
27	8	1.885999	1.942551	-0.671824
28	1	0.989047	1.559348	-0.574685
29	1	-0.998011	1.548034	0.590317
30	1	3.252255	-2.216162	0.711659

(j) bis-HPTA-IVa.

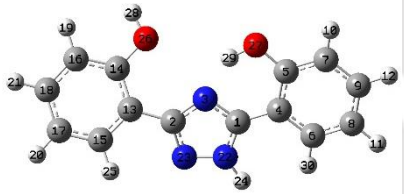

Atom Number	Atomic Number	Coordinates (Angstroms) X	Y	Z
1	6	-1.105453	-0.761329	0.094928
2	6	1.039465	-0.750563	0.107424
3	7	-0.055239	0.053435	-0.056764
4	6	-2.496508	-0.331706	0.006893
5	6	-2.779605	1.037801	-0.240256
6	6	-3.569776	-1.230502	0.162299
7	6	-4.113472	1.464497	-0.325718
8	6	-4.88855	-0.799447	0.075934
9	6	-5.15556	0.555883	-0.169944
10	1	-4.307452	2.515378	-0.515492
11	1	-5.700866	-1.508024	0.198057
12	1	-6.182032	0.903386	-0.239644
13	6	2.441308	-0.316033	-0.016873
14	6	2.87203	0.986468	0.315886
15	6	3.402557	-1.236906	-0.473026
16	6	4.221812	1.337869	0.179409
17	6	4.74569	-0.890986	-0.602842
18	6	5.153685	0.406782	-0.276325
19	1	4.53573	2.34536	0.440714
20	1	5.463334	-1.621077	-0.962636
21	1	6.194979	0.697992	-0.375932
22	7	-0.63875	-2.006623	0.337788
23	7	0.718996	-2.020329	0.355463
24	1	-1.148605	-2.861051	0.514064
25	1	3.071537	-2.236303	-0.734862
26	8	1.955175	1.882735	0.789956
27	8	-1.807061	1.967025	-0.398071
28	1	2.398951	2.712369	1.018088
29	1	-0.92107	1.518354	-0.311913
30	1	-3.370198	-2.280814	0.352337

(k) bis-HPTA-IVb.

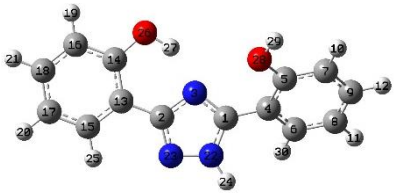

Atom Number	Atomic Number	Coordinates (Angstroms) X	Y	Z
1	6	-1.023312	-0.66561	-0.103291
2	6	1.116572	-0.766158	-0.131877
3	7	0.062728	0.085805	0.081622
4	6	-2.434079	-0.28695	0.041602
5	6	-2.920143	0.962445	-0.401722
6	6	-3.338769	-1.191974	0.627201
7	6	-4.275934	1.278474	-0.250689
8	6	-4.688009	-0.878126	0.773492
9	6	-5.153246	0.364854	0.332106
10	1	-4.638787	2.24185	-0.59909
11	1	-5.364635	-1.58904	1.23548
12	1	-6.200722	0.628287	0.441904
13	6	2.510296	-0.324826	-0.01926
14	6	2.814545	1.021076	0.303594
15	6	3.570864	-1.225847	-0.229499
16	6	4.154032	1.426796	0.405408
17	6	4.89732	-0.818856	-0.127144
18	6	5.185299	0.516331	0.192426
19	1	4.36182	2.463063	0.653418
20	1	5.699618	-1.530534	-0.293422
21	1	6.216479	0.847192	0.275443
22	7	-0.613993	-1.916461	-0.41668
23	7	0.73856	-2.005884	-0.442202
24	1	-1.178549	-2.71915	-0.661504
25	1	3.33366	-2.255881	-0.475618
26	8	1.855916	1.959802	0.523243
27	1	0.965917	1.531615	0.421991
28	8	-2.04547	1.826441	-0.991368
29	1	-2.512943	2.623261	-1.281441
30	1	-2.969116	-2.144601	0.994592

(l) bis-HPTA-IVc.

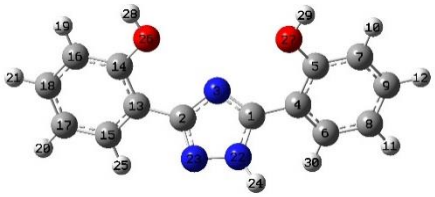

Atom Number	Atomic Number	Coordinates (Angstroms) X	Y	Z
1	6	1.053551	-0.54092	0.243209

2	6	-1.072786	-0.586521	0.290896
3	7	-0.011467	0.120689	-0.204765
4	6	2.475462	-0.274766	-0.027026
5	6	3.022728	1.02322	0.059172
6	6	3.32598	-1.340545	-0.371799
7	6	4.383025	1.228808	-0.202967
8	6	4.680969	-1.137281	-0.628636
9	6	5.206116	0.155824	-0.544777
10	1	4.793883	2.232471	-0.130317
11	1	5.314838	-1.97475	-0.900393
12	1	6.258003	0.334666	-0.745737
13	6	-2.49128	-0.291419	0.007059
14	6	-3.014878	1.018357	0.022437
15	6	-3.366784	-1.353035	-0.280073
16	6	-4.369325	1.239963	-0.25913
17	6	-4.716978	-1.137021	-0.554385
18	6	-5.21569	0.169255	-0.547471
19	1	-4.757642	2.255301	-0.241533
20	1	-5.368158	-1.975454	-0.779601
21	1	-6.262439	0.359953	-0.764644
22	7	0.631176	-1.599707	0.977725
23	7	-0.720886	-1.644963	1.025005
24	1	1.181847	-2.268357	1.499993
25	1	-2.963694	-2.360515	-0.294712
26	8	-2.178617	2.051503	0.344616
27	8	2.20026	2.049055	0.42431
28	1	-2.674961	2.882425	0.357684
29	1	2.705493	2.872773	0.483386
30	1	2.907265	-2.338635	-0.460344

(a)

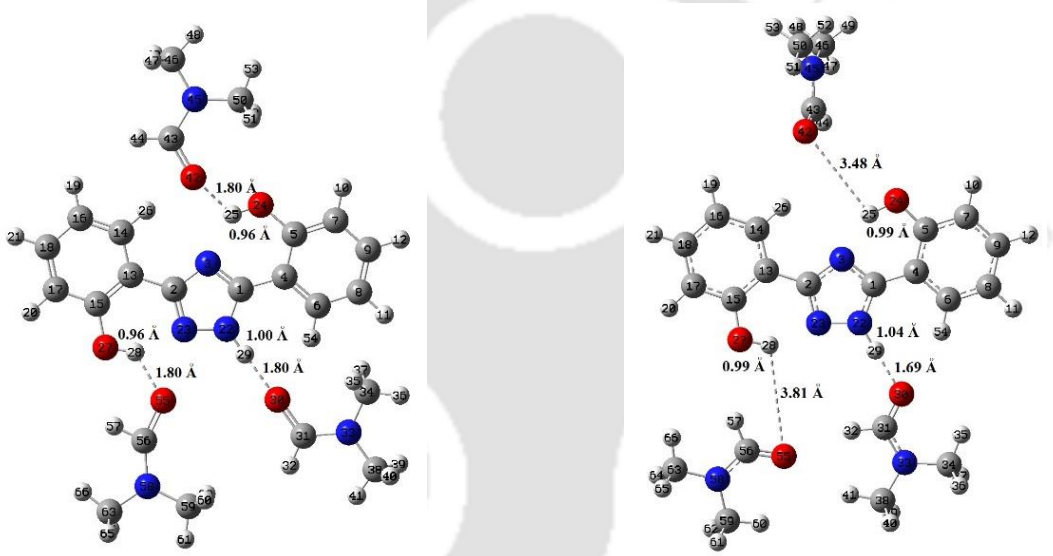

(b)

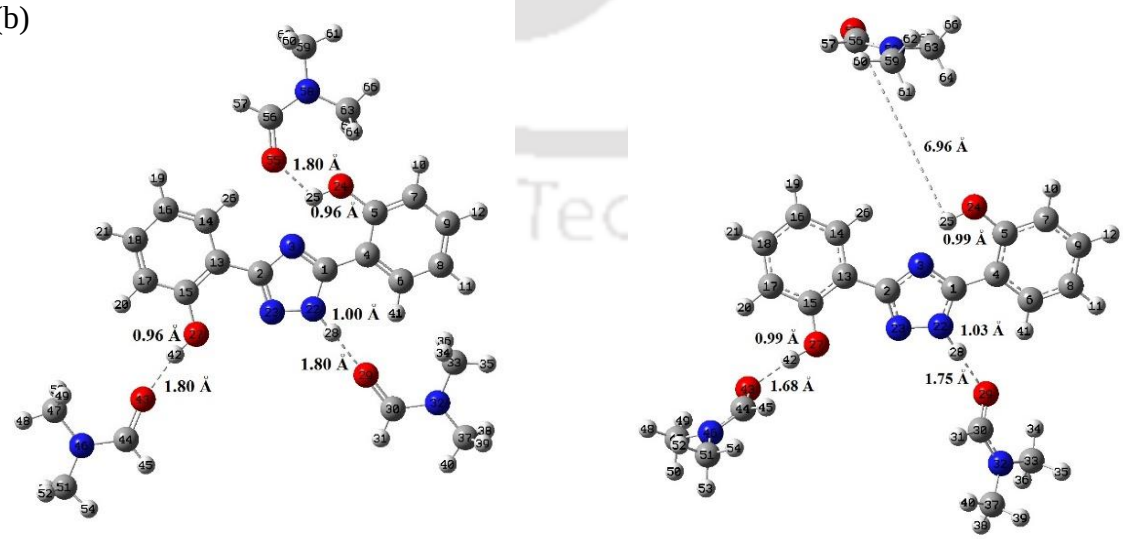

(c)

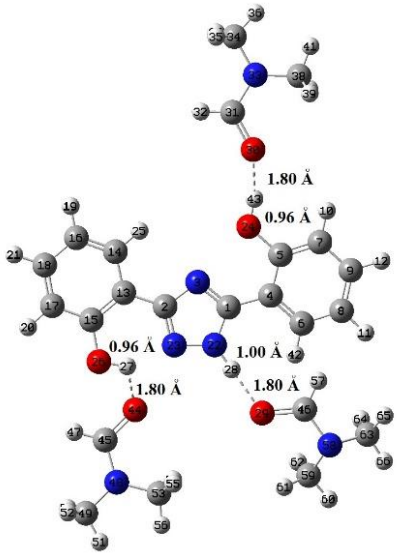

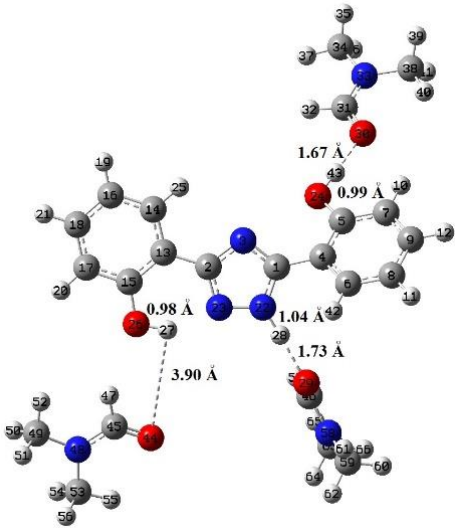

(d)

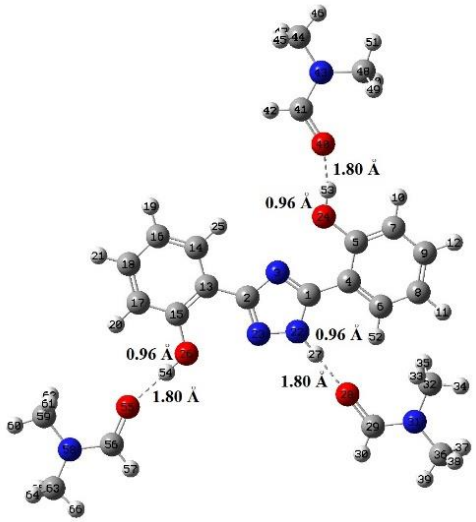

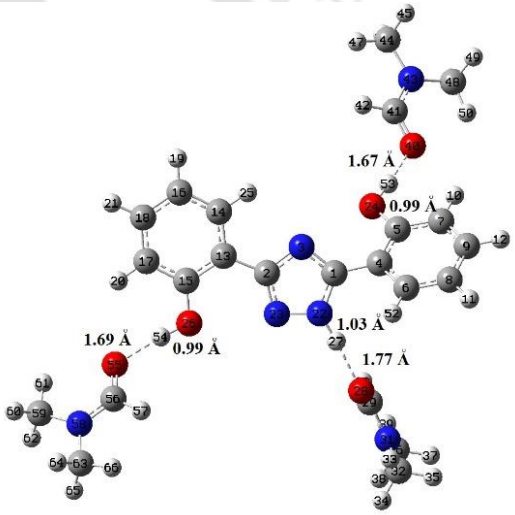

(e)

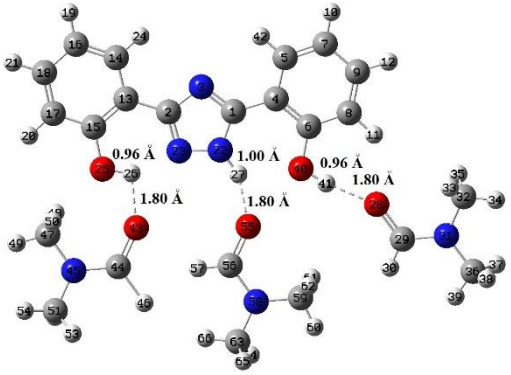

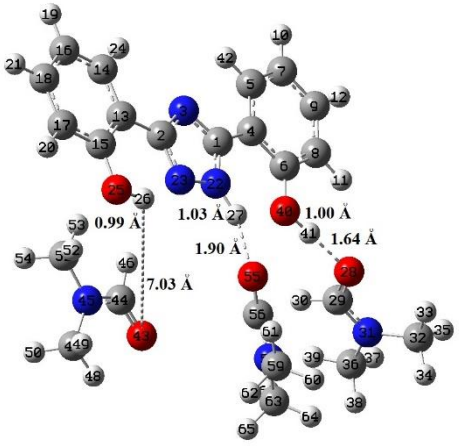

(f)

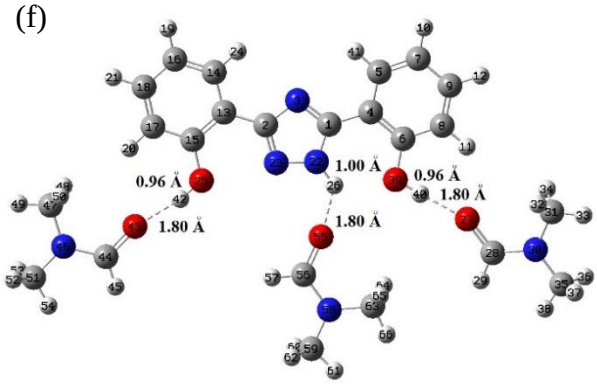

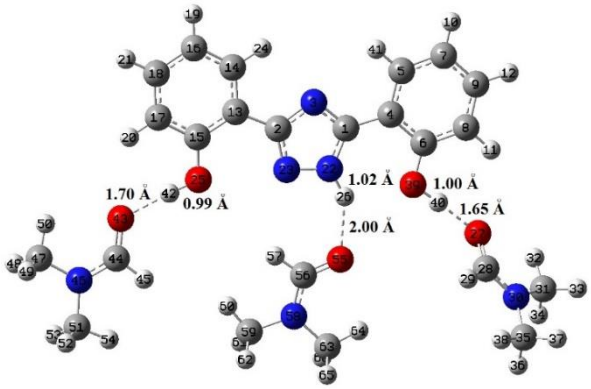

(g)

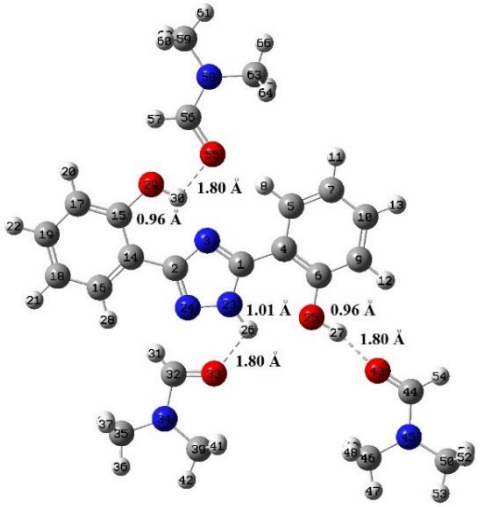

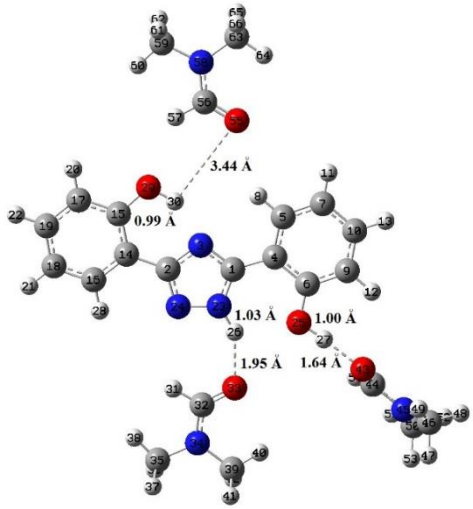

(h)

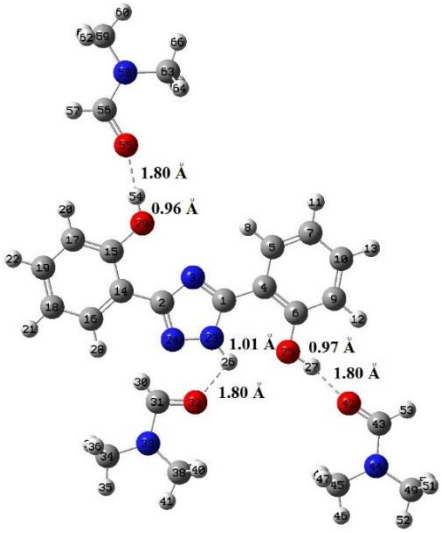

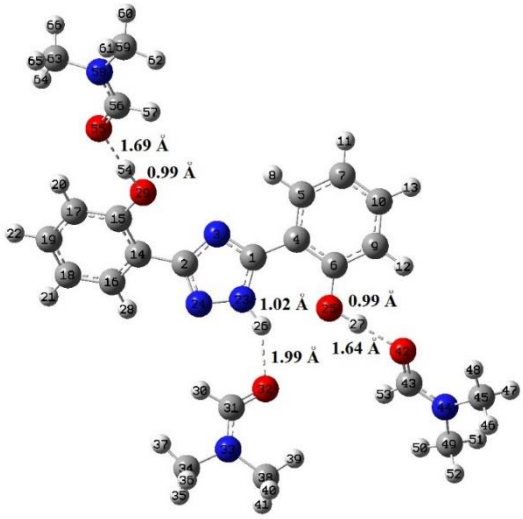

(i)

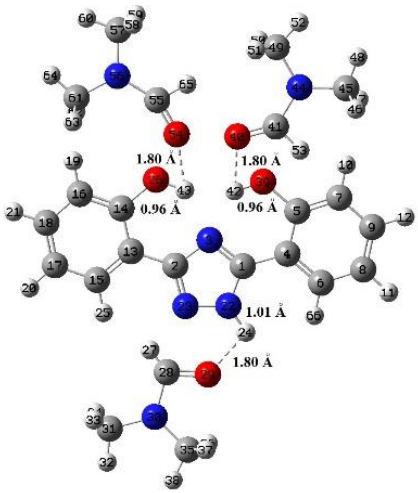
1.80 Å
1.80 Å
0.96 Å
0.96 Å
1.01 Å
1.80 Å

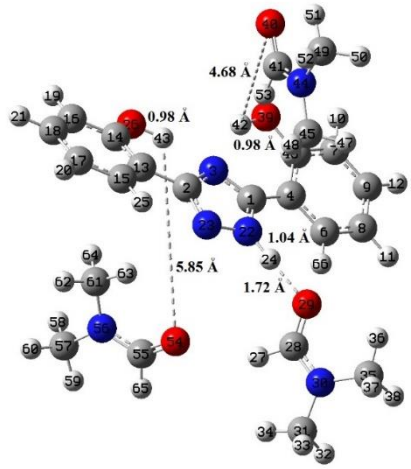
4.68 Å
0.98 Å
0.98 Å
1.04 Å
5.85 Å
1.72 Å

(j)

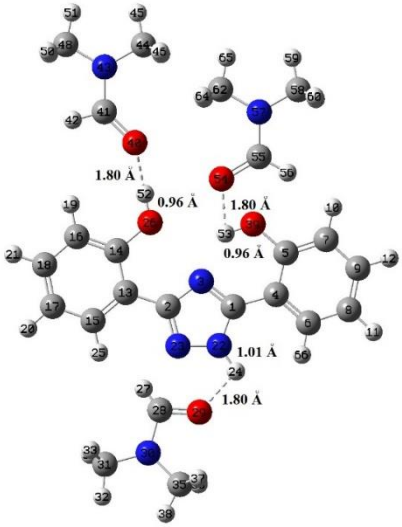
1.80 Å
0.96 Å
1.80 Å
0.96 Å
1.01 Å
1.80 Å

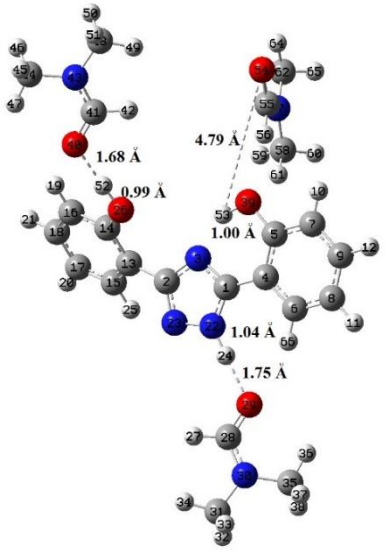
1.68 Å
4.79 Å
0.99 Å
1.00 Å
1.04 Å
1.75 Å

(k)

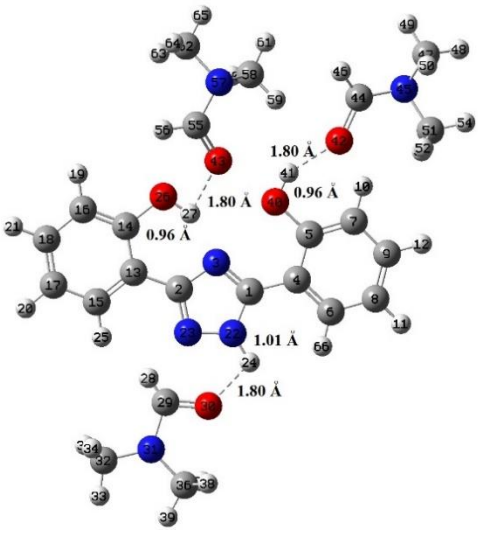
1.80 Å
1.80 Å
0.96 Å
0.96 Å
1.01 Å
1.80 Å

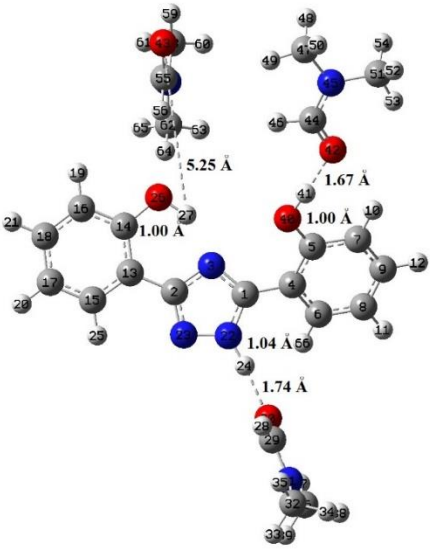
5.25 Å
1.67 Å
1.00 Å
1.00 Å
1.04 Å
1.74 Å

(l)

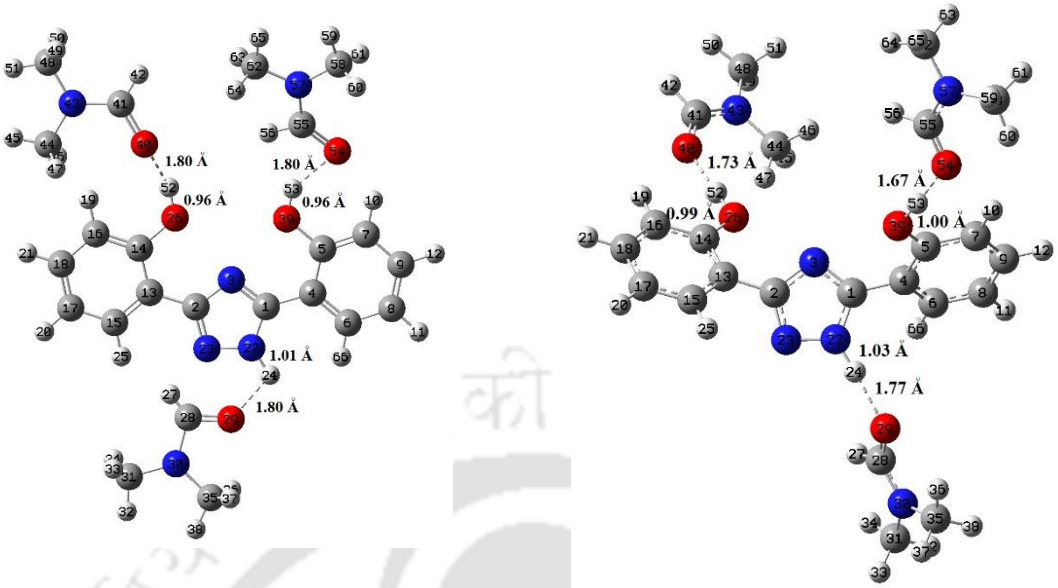

Figure B1: The input (left) and output (right) structures of bis-HPTA DMF complexes. (a) bis-HPTA-I, (b) bis-HPTA-Ia, (c) bi-HPTA-Ib, (d) bis-HPTA-Ic, (e) bis-HPTA-II, (f) bis-HPTA-IIa, (g) bis-HPTA-III, (h) bis-HPTA-IIIa, (i) bis-HPTA-IV, (j) bis-HPTA-IVa, (k) bis-HPTA-IVb, (l) bis-HPTA-IVc.

Table B2: The optimized Cartesian coordinates of optimized bis-HPTA DMF complexes.

(a) bis-HPTA-I DMF complex.

Atom Number	Atomic Number	Coordinates (Angstroms) X	Y	Z
1	6	0.671062	1.471032	-0.22195
2	6	0.526642	-0.663539	-0.287598
3	7	1.426816	0.361555	-0.27481
4	6	1.207489	2.829003	-0.189733
5	6	2.61311	3.023787	-0.20668
6	6	0.364877	3.957693	-0.141492
7	6	3.134225	4.32601	-0.174695
8	6	0.890387	5.244693	-0.110233
9	6	2.28165	5.424506	-0.12676
10	1	4.212337	4.45062	-0.188589
11	1	0.225428	6.101311	-0.073392
12	1	2.701195	6.425903	-0.102607
13	6	0.86582	-2.087739	-0.337628
14	6	2.210352	-2.501975	-0.376771
15	6	-0.151606	-3.074744	-0.343784
16	6	2.545516	-3.852756	-0.419528
17	6	0.19196	-4.432747	-0.387606
18	6	1.529799	-4.81878	-0.424673
19	1	3.588467	-4.151283	-0.44954
20	1	-0.606063	-5.168638	-0.391361
21	1	1.780502	-5.87508	-0.458021
22	7	-0.631245	1.118029	-0.204543
23	7	-0.736451	-0.233352	-0.245409
24	8	3.493965	1.994616	-0.253258
25	1	2.985295	1.141391	-0.275408
26	1	2.995964	-1.752792	-0.374074
27	8	-1.477157	-2.765309	-0.307861
28	1	-1.579015	-1.78399	-0.277477
29	1	-1.494625	1.701234	-0.158291
30	8	-2.874962	2.683051	-0.083492
31	6	-4.032176	2.229077	0.059636
32	1	-4.22139	1.149669	0.131709
33	7	-5.13819	2.979658	0.13826
34	6	-5.085974	4.436318	0.06096
35	1	-4.051204	4.751334	-0.063009
36	1	-5.680167	4.785737	-0.78986
37	1	-5.49511	4.873002	0.978005
38	6	-6.453554	2.366002	0.310621
39	1	-6.911671	2.717865	1.241053
40	1	-7.10622	2.638096	-0.525613
41	1	-6.349196	1.280606	0.347972
42	8	5.559373	-1.190138	-0.502314
43	6	6.220532	-0.933612	0.512494
44	1	5.741974	-0.547557	1.427256
45	7	7.555577	-1.081012	0.643899
46	6	8.238546	-0.749323	1.88873
47	1	7.51343	-0.399086	2.625871
48	1	8.751234	-1.630903	2.288902
49	1	8.979584	0.039611	1.719475
50	6	8.376504	-1.578891	-0.453446
51	1	7.737845	-1.771529	-1.314609
52	1	9.137409	-0.837544	-0.721108
53	1	8.880464	-2.505694	-0.157575
54	1	-0.7119	3.821382	-0.128588

55	8	-5.25701	-0.983253	0.320907
56	6	-5.160375	-2.215002	0.213681
57	1	-4.189983	-2.699424	0.02291
58	7	-6.177655	-3.094349	0.311139
59	6	-7.544244	-2.652755	0.563739
60	1	-7.554226	-1.567872	0.660179
61	1	-8.196654	-2.951978	-0.263974
62	1	-7.920967	-3.105321	1.487487
63	6	-5.958142	-4.528889	0.164528
64	1	-6.26313	-5.055728	1.075209
65	1	-6.539969	-4.91922	-0.677588
66	1	-4.89968	-4.723763	-0.017812

(b) bis-HPTA-Ia DMF complex.

Atom Number	Atomic Number	Coordinates (Angstroms) X	Y	Z
1	6	-0.496945	1.934465	-0.005962
2	6	0.090972	-0.094073	-0.390652
3	7	-0.973402	0.682624	-0.006406
4	6	-1.282443	3.113493	0.351141
5	6	-2.636543	2.952842	0.744604
6	6	-0.734545	4.410722	0.316334
7	6	-3.398704	4.078636	1.089428
8	6	-1.497645	5.522298	0.659403
9	6	-2.834629	5.350579	1.04709
10	1	-4.432104	3.93162	1.387314
11	1	-1.057786	6.5137	0.62536
12	1	-3.438378	6.212238	1.316435
13	6	-0.035188	-1.553387	-0.548759
14	6	-1.325203	-2.094062	-0.713676
15	6	1.066906	-2.443935	-0.529739
16	6	-1.539898	-3.461849	-0.864613
17	6	0.845532	-3.82488	-0.682839
18	6	-0.442132	-4.329698	-0.849413
19	1	-2.547004	-3.844188	-0.997055
20	1	1.701147	-4.492951	-0.665251
21	1	-0.58559	-5.400021	-0.967685
22	7	0.799698	1.901127	-0.376408
23	7	1.190456	0.623185	-0.624101
24	8	-3.237337	1.738226	0.803499
25	1	-2.574499	1.047888	0.526869
26	1	-2.167984	-1.411556	-0.729205
27	8	2.317581	-1.956104	-0.352633
28	1	1.482026	2.672948	-0.482081
29	8	2.597754	3.999598	-0.718587
30	6	3.755291	4.000942	-0.254454
31	1	4.117845	3.173877	0.372066
32	7	4.663191	4.965743	-0.450513
33	6	4.363148	6.144095	-1.259321
34	1	3.344779	6.067779	-1.636865
35	1	4.462789	7.048844	-0.650835
36	1	5.062466	6.205865	-2.099412
37	6	5.999371	4.881416	0.132934
38	1	6.756583	4.886321	-0.657734
39	1	6.175817	5.734643	0.79577
40	1	6.094112	3.959352	0.708912
41	1	0.300206	4.545129	0.015731
42	1	2.99073	-2.687807	-0.318267
43	8	4.23942	-3.818361	-0.297745
44	6	4.860348	-4.076355	0.753637
45	1	4.608358	-3.577049	1.699567
46	7	5.864797	-4.954712	0.857322
47	6	6.340376	-5.711136	-0.298172
48	1	6.245527	-6.784263	-0.103844
49	1	5.745219	-5.44319	-1.169616
50	1	7.393529	-5.478872	-0.487142
51	6	6.53638	-5.194073	2.132006
52	1	6.435915	-6.245858	2.418299
53	1	7.600478	-4.950744	2.048857
54	1	6.089618	-4.571106	2.908555
55	8	-7.770519	-2.960073	-1.797638
56	6	-7.519164	-3.069723	-0.590004
57	1	-7.233398	-4.038462	-0.148697
58	7	-7.55545	-2.072617	0.318256
59	6	-7.23682	-2.309678	1.721344
60	1	-6.989927	-3.362511	1.871491
61	1	-6.37996	-1.699247	2.026552
62	1	-8.092846	-2.053924	2.35534
63	6	-7.911962	-0.710816	-0.062279
64	1	-7.084049	-0.028281	0.15876
65	1	-8.12786	-0.686124	-1.129635
66	1	-8.794999	-0.382728	0.49698

(c) bi-HPTA-Ib DMF complex.

Atom Number	Atomic Number	Coordinates (Angstroms) X	Y	Z
1	6	0.91246	0.156356	-1.366961
2	6	-0.460199	-1.445752	-1.119504
3	7	0.844438	-1.177151	-1.411838
4	6	2.076589	1.011434	-1.656693
5	6	3.33716	0.781947	-1.056719
6	6	1.929437	2.09335	-2.542285
7	6	4.413648	1.629443	-1.371425
8	6	2.999055	2.933495	-2.84884
9	6	4.244338	2.691647	-2.258784
10	1	5.377432	1.448661	-0.90597
11	1	2.864564	3.757938	-3.541391
12	1	5.090796	3.332869	-2.487748
13	6	-1.043416	-2.789975	-1.049199
14	6	-0.251927	-3.923339	-1.30904
15	6	-2.408115	-2.978351	-0.71843
16	6	-0.783546	-5.2088	-1.246434
17	6	-2.940566	-4.273438	-0.655866
18	6	-2.135337	-5.379955	-0.917438
19	1	-0.153936	-6.068737	-1.451702
20	1	-3.989043	-4.390293	-0.399879
21	1	-2.563171	-6.376913	-0.86509
22	7	-0.303948	0.663172	-1.061071
23	7	-1.190468	-0.346021	-0.898536
24	8	3.465573	-0.235479	-0.174317
25	1	0.792068	-3.772469	-1.562913
26	8	-3.24936	-1.940877	-0.451491
27	1	-2.75185	-1.09172	-0.535846
28	1	-0.594835	1.648317	-0.901743
29	8	-1.169373	3.257454	-0.636169
30	8	5.896501	-0.374178	0.91243
31	6	6.168895	-1.272294	1.735749
32	1	5.428663	-2.037029	2.008175
33	7	7.343633	-1.40999	2.361178
34	6	7.574446	-2.492171	3.314619
35	1	8.408288	-3.117081	2.979416
36	1	7.815301	-2.080445	4.299907
37	1	6.67886	-3.110051	3.397316
38	6	8.44845	-0.484213	2.12501

39	1	9.317714	-1.032627	1.748183
40	1	8.139984	0.259977	1.392795
41	1	8.723469	0.012813	3.060933
42	1	0.96214	2.261344	-3.006651
43	1	4.3833	-0.27159	0.212339
44	8	-5.538553	0.83747	1.393955
45	6	-6.026551	-0.268958	1.121969
46	6	-1.366357	3.673652	0.522824
47	1	-5.424166	-1.058868	0.64631
48	7	-7.301938	-0.643933	1.357932
49	6	-7.78163	-1.973645	1.000637
50	1	-8.133198	-2.505036	1.891944
51	1	-8.609814	-1.901956	0.286948
52	1	-6.973152	-2.548115	0.544556
53	6	-8.258612	0.262067	1.981704
54	1	-8.634055	-0.170166	2.915924
55	1	-7.763872	1.209293	2.192943
56	1	-9.107455	0.434899	1.310841
57	1	-1.160657	3.03976	1.397016
58	7	-1.831936	4.889361	0.837498
59	6	-2.165096	5.869341	-0.19262
60	1	-1.551138	6.766943	-0.065594
61	1	-1.977049	5.434095	-1.172739
62	1	-3.220331	6.149711	-0.111711
63	6	-2.030791	5.290309	2.227624
64	1	-3.082981	5.537321	2.401978
65	1	-1.743551	4.474428	2.892971
66	1	-1.419112	6.168648	2.457695

(d) bis-HPTA-Ic DMF complex.

Atom Number	Atomic Number	Coordinates (Angstroms) X	Y	Z
1	6	0.933059	0.45452	-1.021483
2	6	-0.702883	-0.866485	-0.665736
3	7	0.616387	-0.838553	-1.045503
4	6	2.210934	1.08592	-1.396887
5	6	3.453287	0.613574	-0.911055
6	6	2.19777	2.201578	-2.252668
7	6	4.638405	1.260506	-1.302375
8	6	3.375276	2.842472	-2.636635
9	6	4.598316	2.361589	-2.157172
10	1	5.586344	0.893277	-0.921308
11	1	3.338743	3.697337	-3.304105
12	1	5.527365	2.844515	-2.446654
13	6	-1.443807	-2.139803	-0.57228
14	6	-0.75373	-3.327973	-0.886142
15	6	-2.804923	-2.247348	-0.189265
16	6	-1.362901	-4.579142	-0.833217
17	6	-3.41713	-3.513524	-0.136523
18	6	-2.707373	-4.668713	-0.455368
19	1	-0.796993	-5.47109	-1.083668
20	1	-4.460158	-3.57266	0.159832
21	1	-3.204187	-5.633671	-0.40686
22	7	-0.152444	1.169213	-0.644737
23	7	-1.204448	0.347277	-0.410347
24	8	3.466592	-0.436686	-0.057474
25	1	0.286766	-3.244453	-1.178438
26	8	-3.505969	-1.131773	0.127519
27	1	-0.245244	2.18507	-0.474758
28	8	-0.522161	3.907813	-0.144483
29	6	-0.268228	4.379674	0.980302
30	1	0.155293	3.752178	1.777917
31	7	-0.468242	5.653134	1.348626
32	6	-1.02637	6.635792	0.424265
33	1	-1.231669	6.1519	-0.529284
34	1	-1.954446	7.04737	0.83439
35	1	-0.314131	7.453937	0.275061
36	6	-0.137752	6.11763	2.692838
37	1	0.606371	6.919241	2.642691
38	1	-1.034618	6.49981	3.191086
39	1	0.269514	5.293283	3.280671
40	8	5.905633	-1.118289	0.782579
41	6	6.175171	-2.323437	0.965702
42	1	5.439329	-3.109492	0.747002
43	7	7.340814	-2.78808	1.430017
44	6	7.57033	-4.218929	1.612791
45	1	8.411112	-4.547282	0.993423
46	1	7.800331	-4.431209	2.661761
47	1	6.678016	-4.777339	1.325339
48	6	8.439044	-1.88962	1.776183
49	1	9.315672	-2.120853	1.162441
50	1	8.129102	-0.861229	1.598261
51	1	8.703578	-2.01675	2.830861
52	1	1.244091	2.55658	-2.632266
53	1	4.393238	-0.667095	0.226087
54	1	-4.452242	-1.349051	0.340058
55	8	-6.09333	-1.555136	0.714128
56	6	-6.92248	-0.753519	0.237483
57	1	-6.604304	0.072134	-0.414295
58	7	-8.243725	-0.794599	0.448733
59	6	-8.85189	-1.821242	1.290691
60	1	-9.590191	-2.385828	0.712221
61	1	-8.075334	-2.494814	1.649141
62	1	-9.355221	-1.353961	2.14351
63	6	-9.139293	0.191706	-0.14967
64	1	-9.871517	-0.306466	-0.793142
65	1	-9.672554	0.740062	0.633506
66	1	-8.563576	0.899021	-0.748824

(e) bis-HPTA-II DMF complex.

Atom Number	Atomic Number	Coordinates (Angstroms) X	Y	Z
1	6	1.323244	1.812728	-0.212055
2	6	3.168779	0.779999	-0.460845
3	7	2.639771	1.941073	0.00845
4	6	0.331061	2.837606	0.128126
5	6	0.786555	4.07452	0.624114
6	6	-1.061424	2.63811	-0.017914
7	6	-0.0994	5.09099	0.966787
8	6	-1.953931	3.666534	0.328547
9	6	-1.476451	4.881069	0.815456
10	1	0.27619	6.036411	1.344707
11	1	-3.019273	3.498908	0.207873
12	1	-2.181677	5.664937	1.076213
13	6	4.596117	0.441594	-0.443164
14	6	5.532973	1.339852	0.098773
15	6	5.062485	-0.787731	-0.970875
16	6	6.892911	1.041945	0.122862
17	6	6.432193	-1.085117	-0.945416
18	6	7.340178	-0.178074	-0.403242
19	1	7.598073	1.750351	0.545912
20	1	6.763565	-2.033596	-1.356747
21	1	8.398253	-0.423198	-0.391292
22	7	1.084446	0.611589	-0.792603

23	7	2.250584	-0.05643	-0.957271
24	1	5.168724	2.279218	0.501387
25	8	4.228846	-1.716903	-1.514251
26	1	3.300005	-1.383962	-1.466823
27	1	0.211163	0.173694	-1.112458
28	8	-4.116282	1.232798	-0.726993
29	6	-4.814805	0.738767	0.183707
30	1	-4.36229	0.400145	1.125656
31	7	-6.139653	0.569287	0.127738
32	6	-6.913107	0.965166	-1.046692
33	1	-6.240011	1.379914	-1.795084
34	1	-7.431333	0.093993	-1.459852
35	1	-7.657181	1.716855	-0.764217
36	6	-6.878782	-0.014485	1.244544
37	1	-7.620082	0.698997	1.61824
38	1	-7.395597	-0.922541	0.918442
39	1	-6.190478	-0.267842	2.052327
40	8	-1.493246	1.446226	-0.492345
41	1	-2.491086	1.399292	-0.549173
42	1	1.855679	4.219335	0.731617
43	8	-1.778492	-2.614872	3.248859
44	6	-0.603245	-2.22372	3.253119
45	7	0.481975	-2.980001	2.988367
46	1	-0.347347	-1.177051	3.48493
47	6	0.360125	-4.394703	2.656849
48	1	-0.69322	-4.671904	2.668309
49	1	0.777954	-4.585966	1.662372
50	1	0.905784	-5.001523	3.387794
51	6	1.827108	-2.417216	3.019865
52	1	2.305702	-2.518011	2.039773
53	1	1.778102	-1.358165	3.280393
54	1	2.440212	-2.936427	3.764601
55	8	-0.66547	-1.242488	-2.033929
56	6	-1.678314	-1.822832	-1.609106
57	1	-2.147036	-1.529755	-0.658141
58	7	-2.308514	-2.839236	-2.22326
59	6	-1.836652	-3.367912	-3.49898
60	1	-2.615698	-3.259361	-4.261232
61	1	-0.94842	-2.817009	-3.804714
62	1	-1.591905	-4.430488	-3.396536
63	6	-3.49124	-3.464089	-1.640327
64	1	-4.342231	-3.37674	-2.324004
65	1	-3.303487	-4.525641	-1.447115
66	1	-3.74244	-2.972951	-0.698645

(f) bis-HPTA-IIa DMF complex.

Atom Number	Atomic Number	Coordinates (Angstroms) X	Y	Z
1	6	1.097179	-2.263354	0.046177
2	6	-1.038683	-2.192992	0.001218
3	7	0.023448	-3.056714	-0.001659
4	6	2.484006	-2.743069	0.062634
5	6	2.721541	-4.130127	0.019722
6	6	3.59511	-1.870045	0.121573
7	6	4.013468	-4.648223	0.034191
8	6	4.898387	-2.394313	0.137316
9	6	5.104746	-3.771594	0.093566
10	1	4.169849	-5.7217	0.000405
11	1	5.738588	-1.708602	0.184441
12	1	6.119197	-4.159704	0.106607
13	6	-2.427666	-2.691344	-0.041304
14	6	-2.623175	-4.086868	-0.074387
15	6	-3.577948	-1.862499	-0.051417
16	6	-3.890987	-4.661042	-0.116757
17	6	-4.858111	-2.446273	-0.094697
18	6	-5.016443	-3.829501	-0.12723
19	1	-3.999235	-5.740958	-0.141051
20	1	-5.725347	-1.793269	-0.102393
21	1	-6.016112	-4.253637	-0.160205
22	7	0.682223	-0.973842	0.075551
23	7	-0.672487	-0.907363	0.047558
24	1	-1.742595	-4.718883	-0.065976
25	8	-3.439462	-0.514039	-0.018826
26	1	1.221187	-0.104469	0.11775
27	8	5.53745	0.957977	0.302321
28	6	5.707105	1.892591	-0.508858
29	1	4.998909	2.066402	-1.330403
30	7	6.726424	2.757683	-0.478821
31	6	7.765326	2.678844	0.545293
32	1	7.554484	1.838199	1.204074
33	1	8.742376	2.53917	0.071872
34	1	7.784615	3.606002	1.127139
35	6	6.847787	3.825523	-1.46808
36	1	6.835336	4.800977	-0.971504
37	1	7.78769	3.721827	-2.019426
38	1	6.015696	3.77495	-2.17212
39	8	3.360106	-0.53719	0.164546
40	1	4.203576	-0.001807	0.199262
41	1	1.864804	-4.793431	-0.02526
42	1	-4.324924	-0.065513	-0.041836
43	8	-5.807958	0.772871	-0.083948
44	6	-5.872553	2.016821	-0.148857
45	1	-4.963199	2.633511	-0.166749
46	7	-7.006321	2.7271	-0.202299
47	6	-8.315371	2.079678	-0.191819
48	1	-8.899876	2.43801	0.661613
49	1	-8.856078	2.317357	-1.113845
50	1	-8.180219	1.002051	-0.115591
51	6	-6.986476	4.185446	-0.279844
52	1	-7.47898	4.520558	-1.198307
53	1	-7.511641	4.614985	0.579263
54	1	-5.95532	4.542252	-0.279752
55	8	1.246236	1.889838	0.207431
56	6	0.150538	2.455979	0.357397
57	1	-0.785796	1.879233	0.36945
58	7	-0.027827	3.780473	0.516642
59	6	-1.358881	4.350865	0.691189
60	1	-2.107032	3.556657	0.662376
61	1	-1.427949	4.867534	1.654591
62	1	-1.572797	5.068675	-0.108006
63	6	1.099489	4.706084	0.527926
64	1	2.021428	4.14413	0.38481
65	1	0.989764	5.441176	-0.276747
66	1	1.140071	5.237782	1.48481

(g) bis-HPTA-III DMF complex.

Atom Number	Atomic Number	Coordinates (Angstroms) X	Y	Z
1	6	-0.314886	-0.081072	-0.147252
2	6	-1.330722	1.80647	-0.072733
3	7	-1.54414	0.456523	-0.10788
4	6	-0.032274	-1.517131	-0.195526
5	6	-1.108384	-2.42617	-0.171723
6	6	1.285943	-2.026135	-0.269468

7	6	-0.892764	-3.800327	-0.219978
8	1	-2.122013	-2.043996	-0.11403
9	6	1.498259	-3.413605	-0.320236
10	6	0.417193	-4.291692	-0.295145
11	1	-1.736781	-4.482049	-0.199891
12	1	2.515849	-3.786236	-0.37948
13	1	0.598729	-5.361938	-0.334525
14	6	-2.432624	2.774268	-0.025506
15	6	-3.778542	2.332267	-0.009955
16	6	-2.177575	4.15773	0.004514
17	6	-4.821222	3.270091	0.035074
18	6	-3.214249	5.085292	0.049103
19	6	-4.542135	4.634107	0.064209
20	1	-5.843936	2.905943	0.04608
21	1	-2.993691	6.147781	0.071401
22	1	-5.360711	5.347227	0.098653
23	7	0.583106	0.93039	-0.135002
24	7	-0.039661	2.135225	-0.087379
25	8	2.310837	-1.14341	-0.291102
26	1	1.608741	0.905954	-0.151093
27	1	3.202987	-1.593455	-0.347586
28	1	-1.1454	4.492721	-0.008363
29	8	-4.115378	1.014826	-0.037035
30	1	-3.278345	0.479194	-0.069666
31	1	2.38088	3.660682	-0.04414
32	6	3.322494	3.092205	-0.053303
33	8	3.319554	1.850367	-0.10483
34	7	4.42017	3.868023	-0.004193
35	6	4.320002	5.322297	0.056341
36	1	4.793209	5.697753	0.96991
37	1	4.818672	5.773677	-0.808016
38	1	3.270159	5.620803	0.053966
39	6	5.76123	3.293589	-0.006509
40	1	5.682913	2.208983	-0.064681
41	1	6.327235	3.666518	-0.866822
42	1	6.291655	3.573813	0.910064
43	8	4.697023	-2.248628	-0.499294
44	6	5.540653	-2.143084	0.416083
45	7	6.786904	-2.624939	0.368324
46	6	7.286201	-3.338879	-0.804373
47	1	8.164983	-2.823625	-1.20504
48	1	7.571803	-4.358198	-0.525207
49	1	6.505115	-3.372304	-1.562002
50	6	7.709174	-2.460359	1.489271
51	1	7.216476	-1.918932	2.29844
52	1	8.028847	-3.439703	1.859169
53	1	8.592288	-1.897858	1.170064
54	1	5.297903	-1.626361	1.354476
55	8	-4.701064	-2.65377	0.062824
56	6	-5.767606	-2.024903	0.113459
57	1	-5.782957	-0.924568	0.073931
58	7	-6.997993	-2.570611	0.219835
59	6	-8.195017	-1.739835	0.270157
60	1	-7.915825	-0.686301	0.208322
61	1	-8.860996	-1.978583	-0.566427
62	1	-8.737171	-1.907459	1.207412
63	6	-7.187717	-4.014297	0.290142
64	1	-6.214567	-4.502138	0.249513
65	1	-7.69215	-4.283399	1.224833
66	1	-7.802967	-4.356255	-0.549572

(h) bis-HPTA-IIIa DMF complex.

Atom Number	Atomic Number	Coordinates (Angstroms) X	Y	Z
1	6	-0.136188	-0.686858	-0.771293
2	6	1.275133	0.899034	-0.954996
3	7	1.133236	-0.445699	-1.124624
4	6	-0.7624	-2.013815	-0.783833
5	6	0.016894	-3.126614	-1.153613
6	6	-2.117499	-2.223979	-0.437431
7	6	-0.517102	-4.411822	-1.18226
8	1	1.055014	-2.957774	-1.417543
9	6	-2.65455	-3.521791	-0.465461
10	6	-1.860462	-4.605508	-0.835047
11	1	0.10488	-5.253386	-1.470135
12	1	-3.695795	-3.664237	-0.194058
13	1	-2.292012	-5.602234	-0.850529
14	6	2.493813	1.671583	-1.274997
15	6	3.786509	1.252316	-0.881812
16	6	2.366364	2.88061	-1.980324
17	6	4.903807	2.036196	-1.219552
18	6	3.474927	3.661747	-2.308514
19	6	4.7489	3.228435	-1.926742
20	1	5.890293	1.703904	-0.910658
21	1	3.346815	4.58762	-2.860421
22	1	5.626716	3.817796	-2.176756
23	7	-0.718183	0.482336	-0.409475
24	7	0.167099	1.503818	-0.517423
25	8	-2.861806	-1.149768	-0.081422
26	1	-1.664024	0.676702	-0.069238
27	1	-3.808432	-1.39541	0.126076
28	1	1.3719	3.197423	-2.279262
29	8	3.918251	0.111428	-0.16014
30	1	-1.490322	3.398289	0.723282
31	6	-2.539224	3.132866	0.921316
32	8	-2.975583	2.003532	0.641626
33	7	-3.252417	4.130821	1.474591
34	6	-2.645686	5.425117	1.76638
35	1	-3.16616	6.22027	1.221914
36	1	-2.703131	5.638747	2.839134
37	1	-1.59705	5.418334	1.463581
38	6	-4.662038	3.965922	1.811558
39	1	-4.970823	2.952046	1.560695
40	1	-4.814188	4.140614	2.882021
41	1	-5.270056	4.683533	1.24991
42	8	-5.372847	-1.738283	0.505334
43	6	-6.307129	-1.11092	-0.036752
44	7	-7.607554	-1.325868	0.189005
45	6	-8.062779	-2.353399	1.122171
46	1	-8.670686	-1.895931	1.90922
47	1	-8.671085	-3.093346	0.591988
48	1	-7.197201	-2.842364	1.565933
49	6	-8.636006	-0.545215	-0.494268
50	1	-8.168197	0.176465	-1.165671
51	1	-9.283493	-1.207151	-1.077956
52	1	-9.247723	-0.007169	0.236876
53	1	-6.107482	-0.310924	-0.76253
54	1	4.867439	-0.058745	0.080991
55	8	6.450055	-0.450774	0.527703
56	6	6.666518	-1.395315	1.313957
57	1	5.839208	-1.968101	1.755359
58	7	7.878154	-1.811758	1.701545
59	6	8.036926	-2.926446	2.631863

60	1	8.613056	-3.729806	2.161771
61	1	8.564327	-2.593506	3.531533
62	1	7.05733	-3.313289	2.917542
63	6	9.097671	-1.17042	1.21733
64	1	8.831334	-0.378671	0.519095
65	1	9.655002	-0.746142	2.0589
66	1	9.729234	-1.908541	0.712715

(i) bis-HPTA-IV DMF complex.

Atom Number	Atomic Number	Coordinates (Angstroms) X	Y	Z
1	6	0.232286	0.372302	0.867242
2	6	0.595397	-1.207466	-0.544282
3	7	0.710436	-0.883101	0.786003
4	6	0.160247	1.179071	2.084421
5	6	0.850292	0.771724	3.252928
6	6	-0.575058	2.381215	2.119183
7	6	0.791232	1.559034	4.410908
8	6	-0.631641	3.157293	3.271525
9	6	0.055889	2.740465	4.420496
10	1	1.330608	1.224011	5.29106
11	1	-1.207564	4.076777	3.277923
12	1	0.016666	3.338274	5.326157
13	6	0.98554	-2.50863	-1.102073
14	6	1.18487	-3.635701	-0.271325
15	6	1.145205	-2.663838	-2.492312
16	6	1.531348	-4.871697	-0.834411
17	6	1.489285	-3.891293	-3.050174
18	6	1.682539	-4.999091	-2.212712
19	1	1.67553	-5.719431	-0.171945
20	1	1.610557	-3.985406	-4.124501
21	1	1.953997	-5.962377	-2.634379
22	7	-0.139632	0.764574	-0.366806
23	7	0.073783	-0.223583	-1.271591
24	1	-0.552549	1.664389	-0.684865
25	1	0.996705	-1.797422	-3.128452
26	8	1.0375	-3.589819	1.083217
27	1	-2.924829	2.334961	-1.987152
28	6	-2.294597	3.223938	-1.846271
29	8	-1.198673	3.150895	-1.253134
30	7	-2.816586	4.343575	-2.360821
31	6	-4.109438	4.337503	-3.040304
32	1	-4.808879	5.00297	-2.524294
33	1	-3.992563	4.680431	-4.073248
34	1	-4.52023	3.326605	-3.046064
35	6	-2.119679	5.623896	-2.268925
36	1	-1.179972	5.481617	-1.737892
37	1	-1.919398	6.010859	-3.273326
38	1	-2.740571	6.346758	-1.73
39	8	1.59495	-0.363857	3.308815
40	8	5.798589	-0.320394	0.595888
41	6	4.923856	0.319502	-0.003192
42	1	1.530314	-0.828158	2.446161
43	1	0.8407	-2.66774	1.348606
44	7	5.141002	1.305943	-0.898069
45	6	4.036355	1.998996	-1.550388
46	1	3.085873	1.593258	-1.1991
47	1	4.069731	3.069827	-1.321459
48	1	4.094526	1.871328	-2.636919
49	6	6.491317	1.724269	-1.254975
50	1	6.633235	2.783922	-1.015672
51	1	7.207726	1.125646	-0.693792
52	1	6.658363	1.583053	-2.328533
53	1	3.852523	0.119177	0.159587
54	8	-4.50337	-0.579128	0.216761
55	6	-5.331816	-1.480806	0.401378
56	7	-5.056057	-2.79736	0.504767
57	6	-6.109616	-3.781404	0.724103
58	1	-5.935019	-4.324837	1.659159
59	1	-7.077505	-3.279984	0.783993
60	1	-6.13548	-4.502345	-0.100304
61	6	-3.689974	-3.297401	0.401731
62	1	-3.608921	-4.002084	-0.433125
63	1	-3.016725	-2.457562	0.234958
64	1	-3.407029	-3.814828	1.324995
65	1	-6.407551	-1.260952	0.499134
66	1	-1.107886	2.706065	1.231088

(j) bis-HPTA-IVa DMF complex.

Atom Number	Atomic Number	Coordinates (Angstroms) X	Y	Z
1	6	-1.724491	0.362447	-0.097747
2	6	-0.840902	-1.393531	0.753782
3	7	-0.535952	-0.177785	0.208275
4	6	-1.885948	1.677363	-0.713444
5	6	-0.729206	2.437665	-1.029379
6	6	-3.154259	2.214479	-1.00738
7	6	-0.869383	3.700879	-1.622873
8	6	-3.283973	3.46877	-1.59575
9	6	-2.134181	4.211054	-1.902579
10	1	0.028212	4.264488	-1.857098
11	1	-4.269795	3.866089	-1.81447
12	1	-2.225418	5.1909	-2.362063
13	6	0.13697	-2.349421	1.30436
14	6	1.402057	-2.570677	0.709557
15	6	-0.203757	-3.082786	2.45503
16	6	2.286037	-3.499502	1.286924
17	6	0.672272	-4.007398	3.02156
18	6	1.924935	-4.209245	2.431177
19	1	3.252712	-3.661511	0.819754
20	1	0.386211	-4.554743	3.914095
21	1	2.62472	-4.921057	2.859981
22	7	-2.697148	-0.502689	0.256928
23	7	-2.153769	-1.625312	0.795802
24	1	-3.725266	-0.429938	0.150388
25	1	-1.173999	-2.905356	2.907956
26	8	1.724861	-1.900415	-0.422814
27	1	-5.785144	-2.233433	-0.433669
28	6	-6.192722	-1.219554	-0.315797
29	8	-5.453546	-0.25611	-0.031014
30	7	-7.516288	-1.146342	-0.505578
31	6	-8.303386	-2.331804	-0.834286
32	1	-9.062642	-2.50523	-0.064933
33	1	-8.802703	-2.196164	-1.798981
34	1	-7.651445	-3.204962	-0.892179
35	6	-8.23607	0.119391	-0.393233
36	1	-7.52969	0.911521	-0.150361
37	1	-8.733886	0.348858	-1.340954
38	1	-8.993265	0.048354	0.394366
39	8	0.525954	1.988886	-0.779288
40	8	4.135892	-2.489841	-1.410664
41	6	4.867113	-1.547991	-1.780673
42	1	4.548065	-0.502946	-1.665622
43	7	6.075874	-1.685582	-2.337985

44	6	6.665866	-3.001311	-2.570498
45	1	6.858123	-3.138986	-3.639482
46	1	7.613431	-3.084024	-2.028459
47	1	5.976857	-3.768676	-2.221628
48	6	6.862921	-0.523347	-2.742283
49	1	6.317253	0.392803	-2.511017
50	1	7.818455	-0.512773	-2.208399
51	1	7.059944	-0.558159	-3.818545
52	1	2.63184	-2.149139	-0.749678
53	1	0.457189	1.082296	-0.363463
54	8	4.348011	3.791387	0.312459
55	6	3.306159	3.53854	0.935643
56	1	2.412891	3.14254	0.427555
57	7	3.127263	3.703473	2.263824
58	6	1.858467	3.374777	2.903099
59	1	2.002671	2.597523	3.661767
60	1	1.434276	4.261317	3.387498
61	1	1.153053	3.009941	2.154334
62	6	4.190816	4.215182	3.119077
63	1	4.436764	3.482164	3.895454
64	1	5.072966	4.409063	2.509979
65	1	3.871209	5.143808	3.605035
66	1	-4.044852	1.639963	-0.771173

(k) bis-HPTA-IVb DMF complex.

Atom Number	Atomic Number	Coordinates (Angstroms) X	Y	Z
1	6	1.576979	0.131345	0.446834
2	6	1.149289	2.097523	-0.284775
3	7	0.555823	0.934639	0.127951
4	6	1.523245	-1.22854	0.998279
5	6	0.511751	-2.149306	0.627977
6	6	2.508515	-1.636803	1.917541
7	6	0.515032	-3.438183	1.190525
8	6	2.508652	-2.916348	2.467335
9	6	1.501945	-3.816198	2.098612
10	1	-0.262482	-4.137431	0.899618
11	1	3.275404	-3.20351	3.179336
12	1	1.482041	-4.817142	2.520103
13	6	0.362413	3.252771	-0.729982
14	6	-1.052361	3.17836	-0.778878
15	6	0.988834	4.450037	-1.121435
16	6	-1.794125	4.287073	-1.21399
17	6	0.249092	5.548246	-1.550908
18	6	-1.149894	5.461176	-1.596265
19	1	-2.876169	4.205354	-1.245728
20	1	0.753624	6.462159	-1.847984
21	1	-1.739168	6.31027	-1.930352
22	7	2.729013	0.804031	0.226003
23	7	2.48055	2.054078	-0.239129
24	1	3.711144	0.483301	0.323083
25	1	2.072167	4.503221	-1.081983
26	8	-1.738589	2.060646	-0.417944
27	1	-1.079197	1.368406	-0.133475
28	1	5.662714	-0.23872	-1.507423
29	6	6.094056	-0.208864	-0.496664
30	8	5.39427	0.076079	0.495171
31	7	7.40057	-0.501954	-0.460804
32	6	8.141512	-0.823626	-1.677361
33	1	8.955687	-0.10649	-1.823307
34	1	8.566449	-1.829908	-1.604474
35	1	7.474008	-0.782356	-2.539645
36	6	8.146842	-0.510355	0.794381
37	1	7.471574	-0.264455	1.612319
38	1	8.581449	-1.501137	0.961849
39	1	8.955607	0.226508	0.751817
40	8	-0.422085	-1.774511	-0.273924
41	1	-1.070279	-2.509584	-0.458644
42	8	-2.210314	-3.675302	-0.803541
43	8	-6.330605	1.224095	-0.013779
44	6	-3.181446	-3.406068	-1.541012
45	7	-4.177633	-4.248285	-1.837073
46	1	-3.280577	-2.418096	-2.011039
47	6	-5.276248	-3.848776	-2.713123
48	1	-6.228636	-3.923452	-2.178758
49	1	-5.133553	-2.817736	-3.040587
50	1	-5.312352	-4.500208	-3.592124
51	6	-4.215335	-5.606741	-1.301732
52	1	-4.201978	-6.330464	-2.12309
53	1	-3.348056	-5.763122	-0.662572
54	1	-5.131393	-5.750499	-0.719922
55	6	-5.301836	1.549532	0.597341
56	1	-4.334983	1.661548	0.082538
57	7	-5.220534	1.802609	1.92066
58	6	-6.388513	1.710755	2.787497
59	1	-7.254023	1.430645	2.188259
60	1	-6.223705	0.957053	3.565678
61	1	-6.576043	2.675842	3.271268
62	6	-3.954291	2.175972	2.54194
63	1	-3.675254	1.442997	3.307322
64	1	-3.170401	2.213816	1.783037
65	1	-4.039734	3.159886	3.016626
66	1	3.275533	-0.928467	2.214322

(l) bis-HPTA-IVc DMF complex.

Atom Number	Atomic Number	Coordinates (Angstroms) X	Y	Z
1	6	-1.133191	-0.09102	-0.029203
2	6	-0.166758	-1.509189	-1.283146
3	7	0.072328	-0.410795	-0.505757
4	6	-1.476129	0.985378	0.917962
5	6	-1.035864	2.316637	0.728986
6	6	-2.273047	0.686904	2.037116
7	6	-1.39282	3.30128	1.666571
8	6	-2.629211	1.66729	2.96284
9	6	-2.179968	2.978127	2.771413
10	1	-1.052577	4.320448	1.511269
11	1	-3.239699	1.410412	3.822478
12	1	-2.443113	3.755716	3.482937
13	6	0.85446	-2.214689	-2.086105
14	6	2.102424	-2.606378	-1.550192
15	6	0.573575	-2.526382	-3.427206
16	6	3.033017	-3.273426	-2.364209
17	6	1.494529	-3.195222	-4.23462
18	6	2.731144	-3.563551	-3.695049
19	1	3.986899	-3.568387	-1.937289
20	1	1.25361	-3.41748	-5.269426
21	1	3.464932	-4.080065	-4.307523
22	7	-2.048102	-0.965854	-0.5074
23	7	-1.450274	-1.879023	-1.31087
24	1	-3.071955	-0.994797	-0.36255
25	1	-0.386167	-2.22367	-3.83453
26	8	2.363112	-2.350472	-0.241353
27	1	-4.881963	-2.933915	0.592254

28	6	-5.433682	-2.049839	0.24121
29	8	-4.837879	-1.061876	-0.228711
30	7	-6.763098	-2.159892	0.374975
31	6	-7.37344	-3.360916	0.937525
32	1	-7.946312	-3.107802	1.835536
33	1	-8.047538	-3.819725	0.206925
34	1	-6.597371	-4.080529	1.203919
35	6	-7.662856	-1.08648	-0.037319
36	1	-7.074044	-0.258861	-0.429781
37	1	-8.34687	-1.449672	-0.811424
38	1	-8.251578	-0.744193	0.820075
39	8	-0.301127	2.613777	-0.36819
40	8	4.795362	-3.273966	0.540256
41	6	5.588873	-3.18666	1.496466
42	1	6.654096	-3.416274	1.354024
43	7	5.283532	-2.834019	2.753061
44	6	3.92123	-2.496871	3.157153
45	1	3.652423	-3.073401	4.047337
46	1	3.848876	-1.429798	3.393249
47	1	3.229876	-2.735493	2.351373
48	6	6.317434	-2.735186	3.780978
49	1	6.088386	-3.41123	4.61078
50	1	7.286771	-3.00626	3.359474
51	1	6.371035	-1.711003	4.164304
52	1	3.248725	-2.696769	0.023177
53	1	-0.063877	3.58074	-0.399029
54	8	0.371298	5.189189	-0.555027
55	6	1.549158	5.491126	-0.83795
56	1	2.313432	4.716073	-0.987492
57	7	2.008161	6.739054	-0.9875
58	6	1.135838	7.899431	-0.826614
59	1	1.118877	8.482395	-1.753118
60	1	0.128884	7.559604	-0.59011
61	1	1.508519	8.535313	-0.01703
62	6	3.406956	6.999179	-1.318021
63	1	3.873734	7.600706	-0.531472
64	1	3.947229	6.055769	-1.411049
65	1	3.4744	7.542961	-2.265655
66	1	-2.601631	-0.337582	2.185472

Table B3: The optimized Cartesian coordinates of excited state optimized bis-HPTA-II and bis-HPTA-III DMF complexes.

(a) bis-HPTA-II DMF complex.

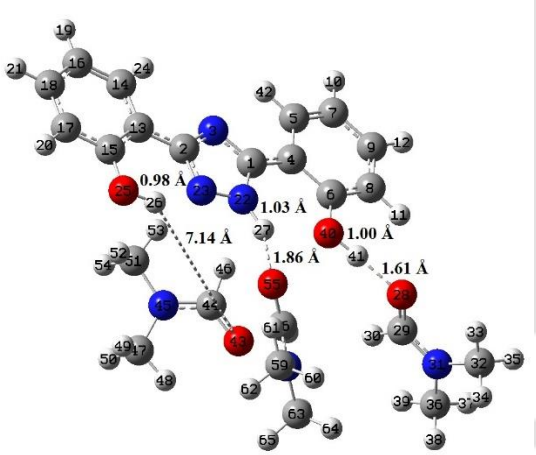

Atom Number	Atomic Number	Coordinates (Angstroms) X	Y	Z
1	6	1.348748	1.490882	-0.655314
2	6	3.206022	0.405983	-0.695971
3	7	2.704463	1.646963	-0.500689
4	6	0.400734	2.522753	-0.540932
5	6	0.859354	3.870614	-0.269467
6	6	-1.035447	2.336986	-0.685325
7	6	-0.036721	4.920781	-0.172568
8	6	-1.914415	3.414491	-0.585649
9	6	-1.42742	4.714785	-0.331181
10	1	0.33531	5.922335	0.027321
11	1	-2.977852	3.233506	-0.703983
12	1	-2.1198	5.547117	-0.25385
13	6	4.595005	0.033814	-0.639621
14	6	5.574368	1.022975	-0.355293
15	6	5.038275	-1.314515	-0.862282
16	6	6.919427	0.701034	-0.291844
17	6	6.40384	-1.624435	-0.79426
18	6	7.336251	-0.629847	-0.512044
19	1	7.653651	1.469729	-0.073281
20	1	6.708281	-2.65145	-0.966542
21	1	8.39084	-0.882773	-0.462423
22	7	1.111387	0.132102	-0.946688
23	7	2.251824	-0.532215	-0.967724
24	1	5.235433	2.039166	-0.189333
25	8	4.189641	-2.324159	-1.140434
26	1	3.263319	-1.980171	-1.160104
27	1	0.23569	-0.381243	-1.129144
28	8	-4.043621	0.783175	-1.223217
29	6	-4.801411	0.572545	-0.251248
30	1	-4.415042	0.560784	0.776699
31	7	-6.11531	0.346679	-0.34095
32	6	-6.802625	0.327522	-1.630228
33	1	-6.076447	0.486898	-2.425457
34	1	-7.296707	-0.638924	-1.77094
35	1	-7.559351	1.118146	-1.659382
36	6	-6.930063	0.117792	0.850074
37	1	-7.708947	0.883217	0.924615
38	1	-7.405703	-0.866457	0.795553
39	1	-6.303303	0.16077	1.742107
40	8	-1.460284	1.080652	-0.91255
41	1	-2.460497	1.017998	-1.003978
42	1	1.923458	4.033591	-0.151873
43	8	-1.91321	-0.428099	3.510767
44	6	-0.734924	-0.04652	3.527385
45	7	0.327249	-0.78189	3.916257
46	1	-0.456037	0.970836	3.208383
47	6	0.171944	-2.156999	4.375472
48	1	-0.87896	-2.435825	4.309854

49	1	0.768949	-2.831156	3.751791
50	1	0.510414	-2.249809	5.413475
51	6	1.678203	-0.232797	3.904395
52	1	2.324891	-0.826449	3.249263
53	1	1.655497	0.795461	3.538661
54	1	2.101994	-0.240047	4.91468
55	8	-0.660591	-1.952065	-1.581053
56	6	-1.639281	-2.389123	-0.951441
57	1	-2.076927	-1.825282	-0.114822
58	7	-2.263585	-3.553343	-1.195748
59	6	-1.827977	-4.441361	-2.268927
60	1	-2.644952	-4.59563	-2.981705
61	1	-0.978218	-3.991241	-2.779938
62	1	-1.535088	-5.412388	-1.855658
63	6	-3.403687	-3.987027	-0.394594
64	1	-4.287098	-4.113632	-1.029266
65	1	-3.181794	-4.941952	0.093428
66	1	-3.621876	-3.24123	0.371715

(b) bis-HPTA-III DMF complex.

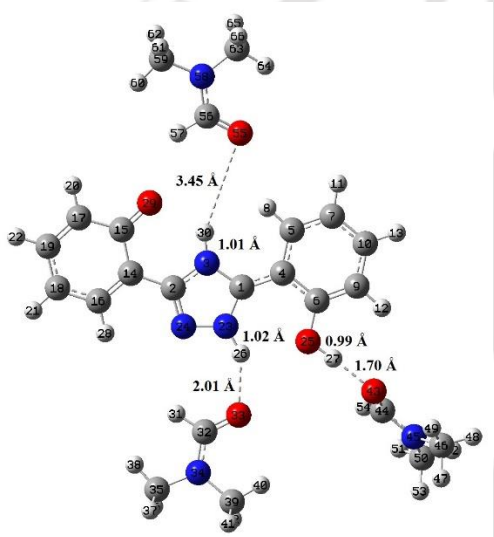

Atom Number	Atomic Number	Coordinates (Angstroms) X	Y	Z
1	6	-0.272535	-0.207465	-0.005759
2	6	-1.377532	1.74178	0.074098
3	7	-1.529261	0.380069	0.068897
4	6	-0.002774	-1.58647	-0.046612
5	6	-1.066061	-2.557612	0.002555
6	6	1.339376	-2.103446	-0.14144
7	6	-0.800101	-3.921269	-0.034484
8	1	-2.099201	-2.232097	0.070433
9	6	1.580449	-3.467589	-0.177445
10	6	0.516025	-4.398628	-0.122939
11	1	-1.63081	-4.621086	0.006445
12	1	2.608021	-3.812172	-0.251651
13	1	0.723921	-5.463115	-0.15196
14	6	-2.496257	2.697229	0.130938
15	6	-3.88442	2.229826	0.164631
16	6	-2.237927	4.058278	0.148755
17	6	-4.926744	3.236823	0.21387
18	6	-3.281976	4.998279	0.196036
19	6	-4.628764	4.580534	0.228404
20	1	-5.949702	2.877327	0.238175
21	1	-3.043276	6.055793	0.207872
22	1	-5.422113	5.319676	0.264759
23	7	0.575801	0.890295	-0.006112
24	7	-0.117853	2.083514	0.022627
25	8	2.345804	-1.177812	-0.198858
26	1	1.587679	0.913507	-0.118435
27	1	3.236179	-1.607538	-0.280528
28	1	-1.210149	4.402392	0.124435
29	8	-4.183091	1.00026	0.150304
30	1	-2.437786	-0.065351	0.082116
31	1	2.247752	3.728993	-0.008063
32	6	3.212153	3.225831	-0.173523
33	8	3.281649	1.989409	-0.264349
34	7	4.252235	4.075946	-0.261408
35	6	4.066974	5.517488	-0.136367
36	1	4.644531	5.903014	0.710727
37	1	4.40069	6.024273	-1.048225
38	1	3.010946	5.741442	0.025434
39	6	5.611762	3.595981	-0.483238
40	1	5.595532	2.510147	-0.566364
41	1	6.016199	4.027372	-1.405291
42	1	6.255823	3.889552	0.352866
43	8	4.815464	-2.215412	-0.47987
44	6	5.660555	-2.115779	0.43169
45	7	6.920419	-2.565659	0.366736
46	6	7.431217	-3.23624	-0.82581
47	1	8.295122	-2.689845	-1.217909
48	1	7.743284	-4.255494	-0.575487
49	1	6.646872	-3.269319	-1.580263
50	6	7.842367	-2.409314	1.488369
51	1	7.339897	-1.901004	2.313014
52	1	8.186651	-3.389987	1.832309
53	1	8.711489	-1.81793	1.182647
54	1	5.412468	-1.63146	1.386638
55	8	-4.677121	-2.696631	0.114526
56	6	-5.729504	-2.045888	0.042103
57	1	-5.72153	-0.945653	0.074633
58	7	-6.968517	-2.568791	-0.081893
59	6	-8.148094	-1.715548	-0.157488
60	1	-7.84932	-0.667247	-0.097779
61	1	-8.678057	-1.878705	-1.102538
62	1	-8.832683	-1.935568	0.669235
63	6	-7.184721	-4.008928	-0.146767
64	1	-6.221671	-4.514725	-0.08832
65	1	-7.819179	-4.334355	0.685228
66	1	-7.679778	-4.274201	-1.087579

Table B4: The optimized Cartesian coordinates of excited state optimized anion of bis-HPTA-II.

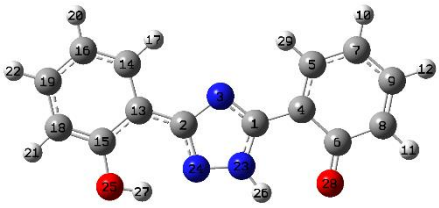

Atom Number	Atomic Number	Coordinates (Angstroms) X	Y	Z
1	6	-1.067124	-0.207537	-0.000002
2	6	1.082489	-0.233335	-0.000002
3	7	-0.022966	0.614902	-0.000001
4	6	-2.474177	0.202814	0
5	6	-2.794553	1.554899	0.000005
6	6	-3.556685	-0.789807	-0.000003
7	6	-4.128548	1.985525	0.000008
8	6	-4.920778	-0.294058	0.000001
9	6	-5.19259	1.052708	0.000006
10	1	-4.345083	3.047984	0.000012
11	1	-5.709879	-1.038193	-0.000001
12	1	-6.218127	1.40715	0.000009
13	6	2.434164	0.202879	-0.000001
14	6	2.785436	1.608632	-0.000004
15	6	3.540066	-0.72681	0.000002
16	6	4.111639	2.024789	-0.000003
17	1	1.982763	2.338479	-0.000006
18	6	4.852522	-0.295451	0.000003
19	6	5.170785	1.097844	0.000001
20	1	4.329128	3.091674	-0.000005
21	1	5.640134	-1.045061	0.000006
22	1	6.205728	1.423964	0.000001
23	7	-0.660155	-1.491791	-0.000005
24	7	0.701518	-1.561458	-0.000005
25	8	3.308411	-2.091502	0.000006
26	1	-1.262331	-2.304994	-0.000008
27	1	2.334683	-2.243151	0.000006
28	8	-3.327363	-2.03216	-0.000007
29	1	-1.990064	2.281299	0.000007

Annexure-C

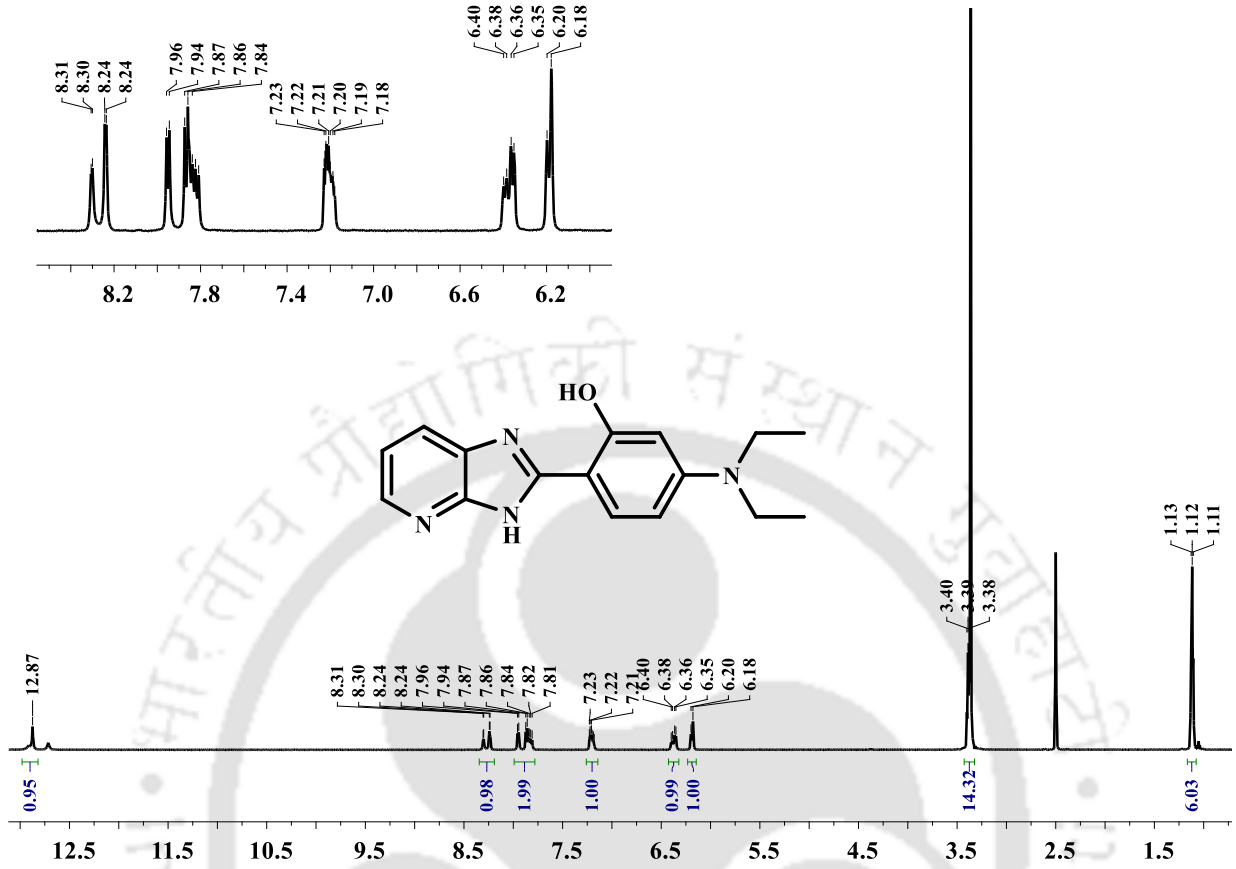

Figure C1: ^{1}H NMR spectra of DEAHPIP-b in DMSO-d_6.

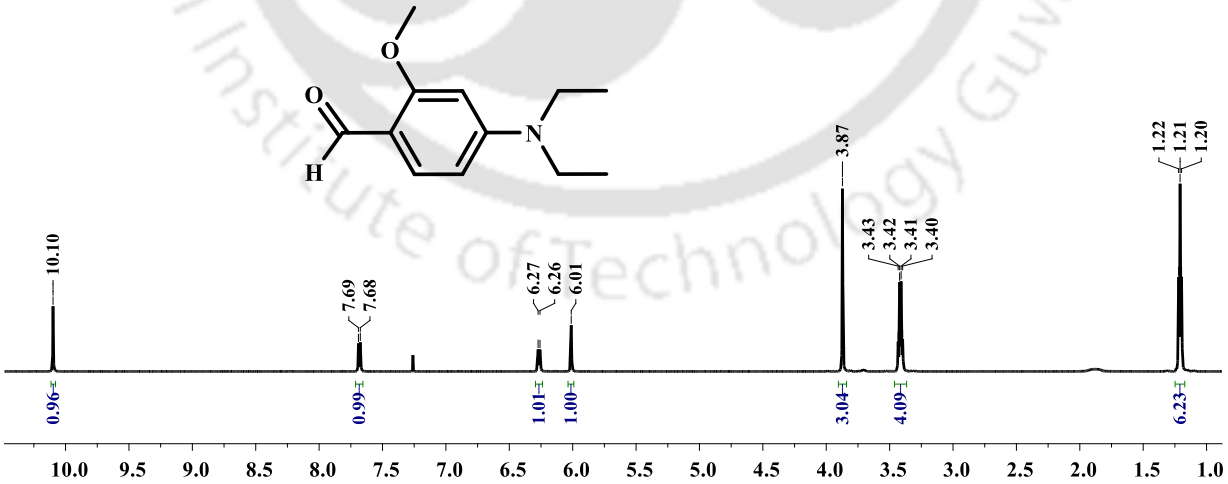

Figure C2: ^{1}H NMR spectra of 4-*N*,*N*-Diethylamino-2-methoxybenzaldehyde in $CDCl_3$.

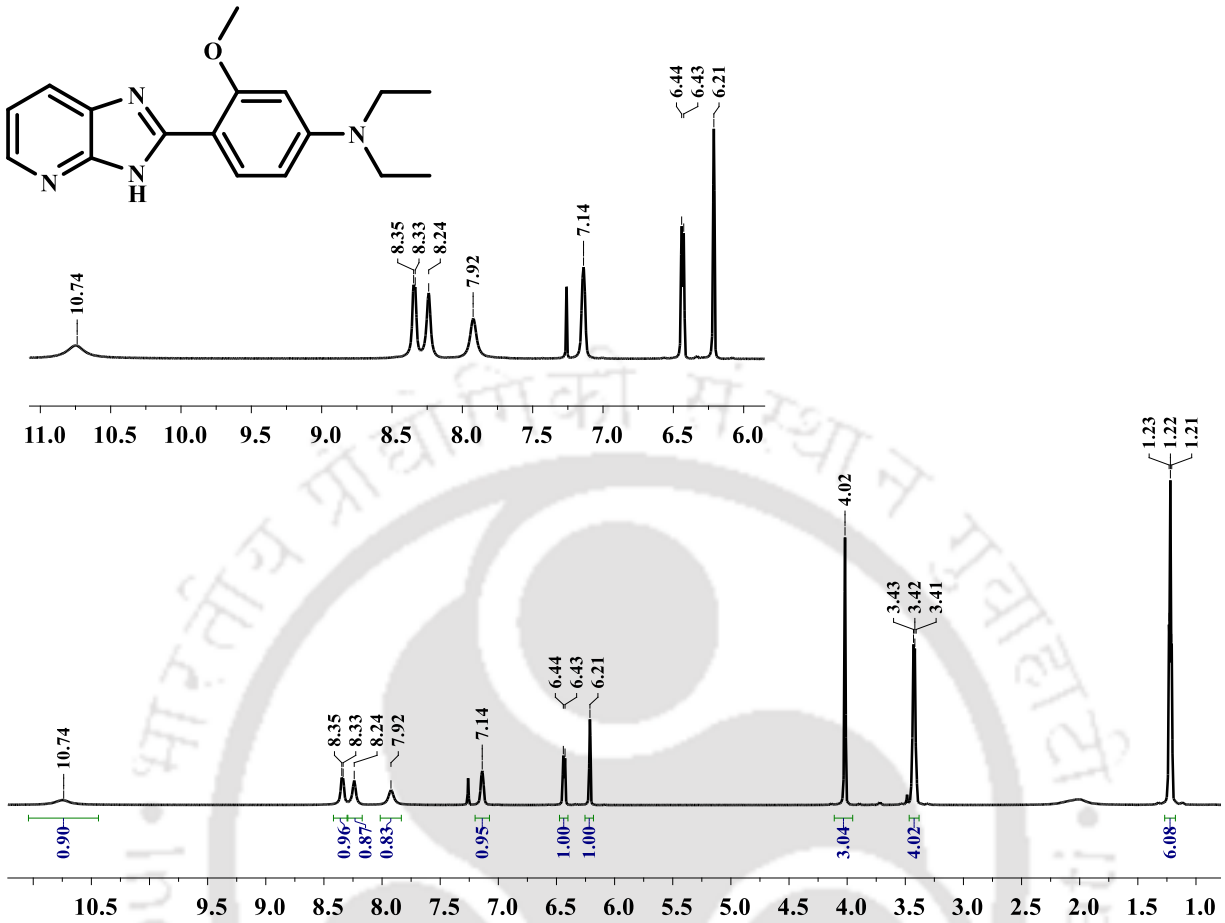

Figure C3: ^{1}H NMR spectra of DEAMPIP-b in $CDCl_3$.

Table C1: XYZ coordinate of optimized cis-enol DEAHPIP-b in ether.

(a) in the ground state

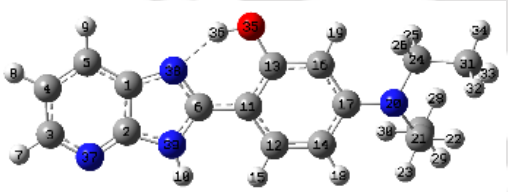

Center Number	Atomic Number	Coordinates (Angstroms) X	Y	Z
1	6	-3.74579	0.612768	-0.11519
2	6	-3.82127	-0.78095	0.118507
3	6	-6.05802	-0.82535	0.051801
4	6	-6.11409	0.554569	-0.18395
5	6	-4.9418	1.307049	-0.27277
6	6	-1.70245	-0.09535	0.072835
7	1	-6.97522	-1.401	0.11893
8	1	-7.08058	1.030281	-0.29673
9	1	-4.96049	2.37502	-0.4548
10	1	-2.21588	-2.14941	0.402463
11	6	-0.25854	-0.11212	0.123644
12	6	0.486735	-1.28722	0.338103
13	6	0.476787	1.087656	-0.05826
14	6	1.863385	-1.29792	0.380893
15	1	-0.0277	-2.23191	0.477735
16	6	1.869337	1.083846	-0.01886

(b) in the excited state

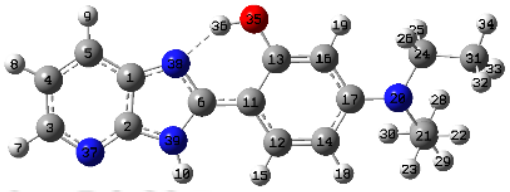

Center Number	Atomic Number	Coordinates (Angstroms) X	Y	Z
1	6	3.731657	0.618853	0.115205
2	6	3.821922	-0.78676	-0.12725
3	6	6.067394	-0.80719	-0.05269
4	6	6.110466	0.572878	0.189692
5	6	4.943495	1.337246	0.283827
6	6	1.686307	-0.11961	-0.08878
7	1	6.992008	-1.3712	-0.11893
8	1	7.080326	1.043952	0.305654
9	1	4.957344	2.402753	0.472602
10	1	2.25499	-2.17288	-0.42427
11	6	0.264677	-0.13707	-0.12947
12	6	-0.49605	-1.31624	-0.35226
13	6	-0.48099	1.088051	0.071585
14	6	-1.87617	-1.30288	-0.38703
15	1	0.011216	-2.26091	-0.50577
16	6	-1.86131	1.091	0.037337

17	6	2.606739	-0.09394	0.216147	17	6	-2.60713	-0.09309	-0.19675
18	1	2.361871	-2.24013	0.549509	18	1	-2.38855	-2.23406	-0.57584
19	1	2.352534	2.033003	-0.19265	19	1	-2.34451	2.037901	0.224124
20	7	3.987809	-0.08015	0.305048	20	7	-3.99028	-0.073	-0.25468
21	6	4.741293	-1.32683	0.123514	21	6	-4.75673	-1.31264	-0.09946
22	1	5.733145	-1.18215	0.548037	22	1	-5.74595	-1.14966	-0.52029
23	1	4.282911	-2.10869	0.728765	23	1	-4.3007	-2.09293	-0.70818
24	6	4.691146	1.192339	0.072895	24	6	-4.69275	1.212469	-0.10898
25	1	4.614881	1.488091	-0.98408	25	1	-4.62567	1.551533	0.935888
26	1	4.172519	1.958808	0.651188	26	1	-4.15312	1.944524	-0.71146
27	6	4.859742	-1.78161	-1.33606	27	6	-4.87514	-1.77568	1.360286
28	1	5.373677	-1.03143	-1.94305	28	1	-5.37996	-1.02504	1.973131
29	1	5.431604	-2.71215	-1.39504	29	1	-5.45744	-2.69989	1.405286
30	1	3.875524	-1.95782	-1.77666	30	1	-3.89028	-1.96662	1.792033
31	6	6.156954	1.207737	0.500238	31	6	-6.15356	1.217104	-0.55038
32	1	6.274961	0.899717	1.542444	32	1	-6.26645	0.868111	-1.57965
33	1	6.792096	0.577107	-0.12499	33	1	-6.79883	0.622011	0.098167
34	1	6.52784	2.23171	0.410452	34	1	-6.5119	2.248197	-0.50684
35	8	-0.13052	2.272114	-0.28749	35	8	0.153753	2.249675	0.309202
36	1	-1.11179	2.120196	-0.29282	36	1	1.139883	2.076986	0.304678
37	7	-4.91651	-1.51777	0.206848	37	7	4.922448	-1.52818	-0.21766
38	7	-2.42352	1.006034	-0.13817	38	7	2.432802	0.999078	0.133627
39	7	-2.51044	-1.20014	0.233444	39	7	2.526593	-1.21773	-0.25033

Table C2: XYZ coordinate of optimized trans-enol DEAHPIP-b in ether.

(a) in the ground state

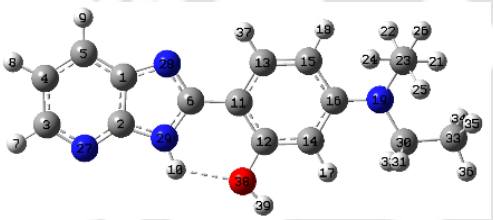

Center Number	Atomic Number	Coordinates (Angstroms) X	Y	Z
1	6	-3.75205	-0.84455	0.130588
2	6	-3.83501	0.551577	-0.10325
3	6	-6.07284	0.565192	-0.17348
4	6	-6.12383	-0.81786	0.053905
5	6	-4.94932	-1.55386	0.21165
6	6	-1.725	-0.12261	0.072097
7	1	-6.99347	1.127027	-0.29457
8	1	-7.08937	-1.3065	0.105409
9	1	-4.96455	-2.62309	0.388511
10	1	-2.18911	1.920719	-0.28227
11	6	-0.26921	-0.06832	0.107831
12	6	0.491995	1.101018	-0.06503
13	6	0.459695	-1.25385	0.319855
14	6	1.88231	1.085881	-0.02168
15	6	1.836561	-1.28992	0.368658
16	6	2.604586	-0.10446	0.214868
17	1	2.39583	2.021941	-0.19198
18	1	2.316238	-2.24279	0.534007
19	7	3.985131	-0.10966	0.311006
20	6	4.718143	-1.3703	0.139738
21	1	5.710114	-1.24024	0.568586
22	1	4.242286	-2.13969	0.747481
23	6	4.835271	-1.8359	-1.31637
24	1	3.850411	-1.99651	-1.76125
25	1	5.367277	-1.09975	-1.92512
26	1	5.38922	-2.77765	-1.36626
27	7	-4.93564	1.274756	-0.2563

(b) in the excited state

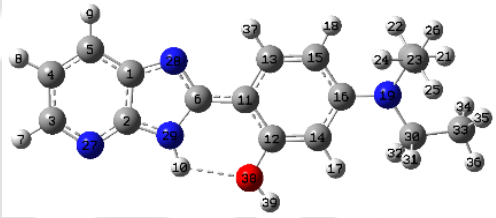

Center Number	Atomic Number	Coordinates (Angstroms) X	Y	Z
1	6	3.727126	-0.85122	-0.14212
2	6	3.836096	0.559712	0.100079
3	6	6.082029	0.528965	0.158267
4	6	6.110655	-0.85495	-0.07538
5	6	4.934497	-1.59185	-0.23359
6	6	1.699593	-0.07655	-0.06753
7	1	7.014346	1.072088	0.277026
8	1	7.075664	-1.34659	-0.13115
9	1	4.935748	-2.65942	-0.41377
10	1	2.246454	1.960896	0.296651
11	6	0.28481	-0.04249	-0.09417
12	6	-0.51138	1.140674	0.091321
13	6	-0.45034	-1.25205	-0.31114
14	6	-1.88606	1.111587	0.047066
15	6	-1.82362	-1.28229	-0.35709
16	6	-2.60093	-0.09866	-0.18943
17	1	-2.41454	2.038321	0.223384
18	1	-2.30418	-2.23295	-0.53478
19	7	-3.98143	-0.11595	-0.26738
20	6	-4.70939	-1.38128	-0.1278
21	1	-5.70045	-1.24613	-0.55442
22	1	-4.22394	-2.13947	-0.74211
23	6	-4.82345	-1.86514	1.325184
24	1	-3.83658	-2.02628	1.764339
25	1	-5.36084	-1.14074	1.942255
26	1	-5.37224	-2.81036	1.354992
27	7	4.948707	1.275898	0.253239

28	7	-2.43464	-1.23278	0.234617	28	7	2.434346	-1.21943	-0.24146
29	7	-2.52875	0.980969	-0.13506	29	7	2.550854	1.011911	0.139352
30	6	4.708697	1.150752	0.081041	30	6	-4.72483	1.145339	-0.11841
31	1	4.637142	1.450663	-0.97554	31	1	-4.68111	1.481171	0.92929
32	1	4.204608	1.924895	0.663175	32	1	-4.20562	1.898795	-0.7132
33	6	6.175221	1.142237	0.506207	33	6	-6.18055	1.108192	-0.57579
34	1	6.289611	0.831976	1.548019	34	1	-6.27085	0.760956	-1.60781
35	1	6.798136	0.500925	-0.12025	35	1	-6.81361	0.489278	0.062359
36	1	6.563303	2.159773	0.415831	36	1	-6.57225	2.127141	-0.53087
37	1	-0.1015	-2.17052	0.4495	37	1	0.117202	-2.16233	-0.44557
38	8	-0.17401	2.280708	-0.29595	38	8	0.169556	2.304515	0.329745
39	1	0.451795	3.009921	-0.37523	39	1	-0.44263	3.044465	0.422255

Table C3: XYZ coordinate of optimized cis-enol DEAHPIP-b in acetonitrile.

(a) in the ground state

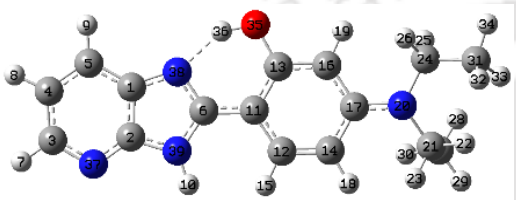

Center Number	Atomic Number	Coordinates (Angstroms) X	Y	Z
1	6	3.747299	0.61152	0.113277
2	6	3.821842	-0.78315	-0.11604
3	6	6.060772	-0.82443	-0.05157
4	6	6.115955	0.556118	0.179635
5	6	4.942784	1.307666	0.267309
6	6	1.703435	-0.09962	-0.0699
7	1	6.978756	-1.3988	-0.11781
8	1	7.082043	1.032997	0.289836
9	1	4.961904	2.376228	0.445936
10	1	2.216448	-2.1536	-0.39413
11	6	0.259378	-0.1149	-0.11864
12	6	-0.48908	-1.29052	-0.32391
13	6	-0.47454	1.086872	0.055983
14	6	-1.8657	-1.29799	-0.36596
15	1	0.022098	-2.23775	-0.45525
16	6	-1.86632	1.087798	0.016954
17	6	-2.60786	-0.09101	-0.21087
18	1	-2.36571	-2.24118	-0.52389
19	1	-2.34879	2.038803	0.183386
20	7	-3.98611	-0.07383	-0.29998
21	6	-4.74441	-1.32234	-0.145
22	1	-5.73187	-1.16823	-0.57555
23	1	-4.28203	-2.0956	-0.75793
24	6	-4.68913	1.199645	-0.06367
25	1	-4.60627	1.492116	0.993249
26	1	-4.17425	1.967512	-0.6436
27	6	-4.8773	-1.79768	1.306343
28	1	-5.39375	-1.05402	1.919097
29	1	-5.4539	-2.72618	1.344777
30	1	-3.89809	-1.98637	1.753116
31	6	-6.15746	1.215789	-0.48116
32	1	-6.28302	0.914793	-1.5245
33	1	-6.78699	0.580446	0.14469
34	1	-6.52721	2.239198	-0.38172
35	8	0.138597	2.273149	0.277608
36	1	1.119895	2.114814	0.283618
37	7	4.918971	-1.51868	-0.20314

(b) in the excited state

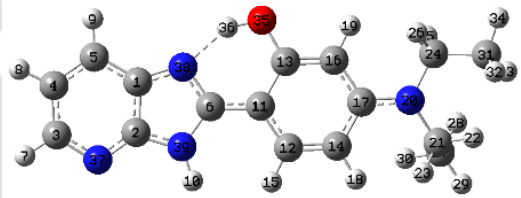

Center Number	Atomic Number	Coordinates (Angstroms) X	Y	Z
1	6	3.737897	0.616916	0.104116
2	6	3.822186	-0.79578	-0.111
3	6	6.072447	-0.81587	-0.05661
4	6	6.119289	0.567911	0.157255
5	6	4.953217	1.335767	0.246281
6	6	1.687504	-0.12242	-0.06611
7	1	6.995601	-1.38252	-0.12041
8	1	7.090637	1.040242	0.254284
9	1	4.971569	2.405238	0.411778
10	1	2.250081	-2.18285	-0.3698
11	6	0.269343	-0.13581	-0.09897
12	6	-0.49837	-1.31993	-0.28621
13	6	-0.47448	1.095888	0.069144
14	6	-1.87598	-1.30268	-0.32672
15	1	0.00437	-2.27172	-0.40416
16	6	-1.8525	1.104552	0.029839
17	6	-2.60521	-0.08337	-0.17919
18	1	-2.39034	-2.23933	-0.47805
19	1	-2.33366	2.058443	0.183008
20	7	-3.98184	-0.0554	-0.24647
21	6	-4.75962	-1.2974	-0.19531
22	1	-5.73008	-1.1018	-0.64404
23	1	-4.28239	-2.04205	-0.83145
24	6	-4.68219	1.230968	-0.07377
25	1	-4.57815	1.558367	0.970731
26	1	-4.16359	1.968918	-0.6883
27	6	-4.9423	-1.84335	1.228391
28	1	-5.46317	-1.12242	1.862787
29	1	-5.53781	-2.7593	1.192016
30	1	-3.97975	-2.07586	1.68909
31	6	-6.15651	1.240606	-0.4634
32	1	-6.30606	0.927252	-1.49923
33	1	-6.7749	0.620897	0.188048
34	1	-6.51467	2.268519	-0.37209
35	8	0.166482	2.264904	0.276598
36	1	1.150276	2.087186	0.274165
37	7	4.922677	-1.53876	-0.19669

38	7	2.42466	1.004051	0.136661	38	7	2.442589	1.000947	0.127216
39	7	2.511621	-1.20341	-0.22795	39	7	2.526835	-1.22572	-0.21229

Table C4: XYZ coordinate of optimized trans-enol DEAHPIP-b in acetonitrile.

(a) in the ground state

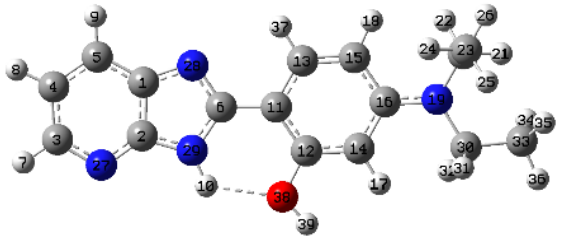

(b) in the excited state

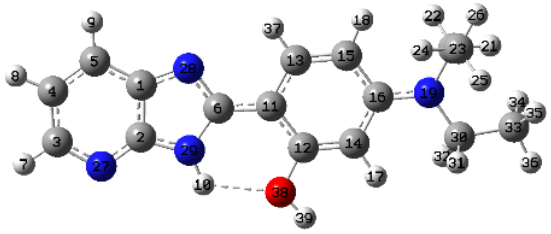

Center Number	Atomic Number	Coordinates (Angstroms) X	Y	Z	Center Number	Atomic Number	Coordinates (Angstroms) X	Y	Z
1	6	-3.75519	-0.84556	0.128894	1	6	3.733236	-0.85638	-0.12522
2	6	-3.83415	0.551211	-0.10252	2	6	3.838211	0.558764	0.091701
3	6	-6.07423	0.568759	-0.171	3	6	6.089088	0.53326	0.140734
4	6	-6.1276	-0.81407	0.054132	4	6	6.119168	-0.85277	-0.0685
5	6	-4.95387	-1.55261	0.209761	5	6	4.942653	-1.59617	-0.20861
6	6	-1.72429	-0.12672	0.070329	6	6	1.701033	-0.08587	-0.05671
7	1	-6.99394	1.132196	-0.2904	7	1	7.020591	1.08053	0.245591
8	1	-7.09381	-1.30107	0.10567	8	1	7.08491	-1.34359	-0.12002
9	1	-4.97316	-2.62217	0.384868	9	1	4.947949	-2.66692	-0.37002
10	1	-2.18352	1.916872	-0.2797	10	1	2.243981	1.958136	0.269059
11	6	-0.26964	-0.07302	0.105156	11	6	0.285869	-0.05038	-0.08134
12	6	0.49027	1.100108	-0.06359	12	6	-0.50509	1.140918	0.083808
13	6	0.462655	-1.25873	0.310599	13	6	-0.4555	-1.25956	-0.2748
14	6	1.87995	1.087531	-0.02013	14	6	-1.87889	1.117785	0.037391
15	6	1.839326	-1.29281	0.357754	15	6	-1.82841	-1.28567	-0.32174
16	6	2.605491	-0.10333	0.210345	16	6	-2.60052	-0.09288	-0.17959
17	1	2.390996	2.025763	-0.18385	17	1	-2.40206	2.050997	0.19074
18	1	2.321045	-2.24596	0.515067	18	1	-2.31273	-2.23831	-0.4755
19	7	3.982963	-0.10528	0.305698	19	7	-3.97541	-0.10162	-0.25708
20	6	4.721285	-1.36617	0.153222	20	6	-4.71503	-1.36684	-0.19505
21	1	5.709635	-1.22807	0.587107	21	1	-5.69126	-1.20525	-0.64496
22	1	4.243485	-2.1311	0.764919	22	1	-4.21474	-2.10106	-0.82583
23	6	4.850683	-1.84402	-1.29755	23	6	-4.87949	-1.90784	1.232482
24	1	3.869914	-2.01528	-1.7478	24	1	-3.90971	-2.10375	1.695027
25	1	5.382777	-1.10999	-1.90853	25	1	-5.42521	-1.20063	1.861564
26	1	5.410517	-2.78278	-1.33367	26	1	-5.44299	-2.84418	1.203662
27	7	-4.93434	1.276278	-0.25349	27	7	4.951283	1.280391	0.227566
28	7	-2.43803	-1.23682	0.231627	28	7	2.440583	-1.22952	-0.21272
29	7	-2.52712	0.977609	-0.13434	29	7	2.552979	1.007382	0.128338
30	6	4.705992	1.157783	0.07541	30	6	-4.71426	1.163682	-0.08913
31	1	4.631097	1.455179	-0.98083	31	1	-4.63588	1.492297	0.957439
32	1	4.202314	1.931766	0.65764	32	1	-4.21068	1.917987	-0.69637
33	6	6.173212	1.150071	0.496762	33	6	-6.1826	1.131827	-0.5003
34	1	6.291262	0.84411	1.53948	34	1	-6.30774	0.811268	-1.53717
35	1	6.794098	0.506734	-0.12947	35	1	-6.79279	0.496687	0.143922
36	1	6.559144	2.167836	0.401172	36	1	-6.5711	2.149426	-0.4173
37	1	-0.09324	-2.1794	0.435237	37	1	0.103543	-2.17781	-0.38949
38	8	-0.17932	2.276643	-0.2888	38	8	0.182158	2.303362	0.300893
39	1	0.442199	3.009266	-0.3784	39	1	-0.42417	3.049612	0.389018

Table C5: XYZ coordinate of optimized keto tautomer DEAHPIP-b in the excited state.

(a) in ether

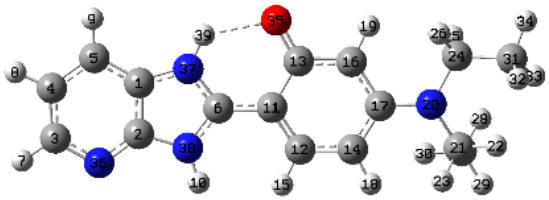

Center Number	Atomic Number	Coordinates (Angstroms) X	Y	Z
1	6	3.831982	0.623291	0.080701
2	6	3.857757	-0.7748	-0.08223
3	6	6.105785	-0.86154	-0.038
4	6	6.194791	0.513483	0.125892
5	6	5.040909	1.326614	0.194049
6	6	1.696602	-0.10136	-0.05252
7	1	7.007934	-1.46128	-0.0867
8	1	7.17632	0.966577	0.20291
9	1	5.088131	2.398778	0.321869
10	1	2.242622	-2.13799	-0.27069
11	6	0.252103	-0.10051	-0.09798
12	6	-0.49872	-1.2428	-0.28711
13	6	-0.47772	1.145343	0.074194
14	6	-1.91933	-1.25997	-0.32553
15	1	-0.00658	-2.20174	-0.41341
16	6	-1.90603	1.108737	0.029566
17	6	-2.66558	-0.08387	-0.19505
18	1	-2.39663	-2.21887	-0.4562
19	1	-2.38116	2.063495	0.193892
20	7	-4.04416	-0.04452	-0.28387
21	6	-4.79584	-1.30255	-0.25677
22	1	-5.77034	-1.12143	-0.70653
23	1	-4.30088	-2.01568	-0.91765
24	6	-4.75965	1.201793	0.049553
25	1	-4.7159	1.389941	1.131921
26	1	-4.23793	2.025254	-0.4377
27	6	-4.97401	-1.90058	1.144656
28	1	-5.53023	-1.21957	1.794271
29	1	-5.53288	-2.83854	1.082879
30	1	-4.01141	-2.10879	1.617293
31	6	-6.21334	1.249532	-0.41529
32	1	-6.29932	1.048634	-1.48623
33	1	-6.85818	0.553825	0.124877
34	1	-6.59612	2.256333	-0.23188
35	8	0.119722	2.252077	0.267382
36	7	4.929513	-1.55672	-0.14685
37	7	2.504555	0.987778	0.091608
38	7	2.533349	-1.17885	-0.16025
39	1	2.083761	1.905654	0.204757

(b) in acetonitrile

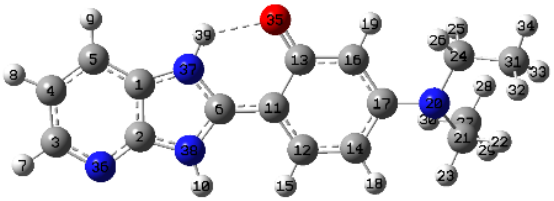

Center Number	Atomic Number	Coordinates (Angstroms) X	Y	Z
1	6	3.804724	0.619923	0.153816
2	6	3.850293	-0.75596	-0.16447
3	6	6.100085	-0.80989	-0.12452
4	6	6.167779	0.544322	0.191248
5	6	5.003904	1.323297	0.345269
6	6	1.685426	-0.1153	-0.07576
7	1	7.013175	-1.38425	-0.237
8	1	7.142381	1.000514	0.319276
9	1	5.032084	2.375754	0.590409
10	1	2.26121	-2.10763	-0.53282
11	6	0.247761	-0.13384	-0.10768
12	6	-0.48003	-1.29475	-0.32925
13	6	-0.50801	1.113587	0.107714
14	6	-1.88792	-1.29932	-0.39094
15	1	0.022114	-2.24424	-0.47407
16	6	-1.92767	1.060539	0.054266
17	6	-2.65005	-0.12137	-0.2108
18	1	-2.37008	-2.24218	-0.60438
19	1	-2.42705	1.998467	0.248495
20	7	-4.0394	-0.13632	-0.3446
21	6	-4.7829	-1.33815	0.063064
22	1	-5.7626	-1.30114	-0.41195
23	1	-4.29353	-2.21764	-0.35323
24	6	-4.74676	1.147764	-0.24464
25	1	-4.74896	1.520058	0.791918
26	1	-4.18056	1.871269	-0.83391
27	6	-4.94006	-1.49604	1.580474
28	1	-5.48747	-0.65554	2.015142
29	1	-5.49595	-2.41071	1.805026
30	1	-3.96602	-1.56074	2.072489
31	6	-6.17725	1.122457	-0.77982
32	1	-6.21356	0.715893	-1.79395
33	1	-6.85812	0.5475	-0.1494
34	1	-6.55289	2.148114	-0.81307
35	8	0.109	2.199924	0.355574
36	7	4.938784	-1.50478	-0.3132
37	7	2.478947	0.962718	0.198745
38	7	2.539259	-1.16697	-0.29457
39	1	2.034798	1.860788	0.383936

Table C6: XYZ coordinate of optimized trans DEAMPIP-b in ether.

(a) in the ground state

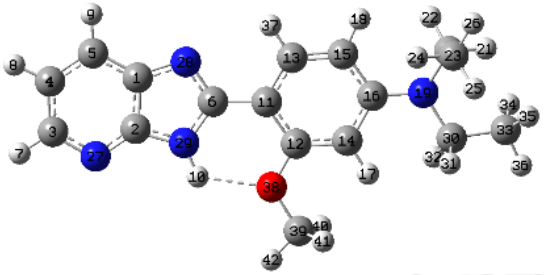

Center Number	Atomic Number	Coordinates (Angstroms) X	Y	Z
1	6	-3.78325	-1.00904	0.111199
2	6	-3.8636	0.395973	-0.06512
3	6	-6.10192	0.418091	-0.12661
4	6	-6.15559	-0.97284	0.044351
5	6	-4.98238	-1.71776	0.167469
6	6	-1.75394	-0.28946	0.07583
7	1	-7.02148	0.986756	-0.22119
8	1	-7.12223	-1.46082	0.079544
9	1	-5.00008	-2.79333	0.30033
10	1	-2.20675	1.763243	-0.19189
11	6	-0.29749	-0.24186	0.11092
12	6	0.475552	0.935126	-0.00675
13	6	0.41505	-1.4428	0.265812
14	6	1.866708	0.894983	0.040814
15	6	1.792358	-1.50064	0.314765
16	6	2.570381	-0.3191	0.221704
17	1	2.409692	1.816571	-0.07739
18	1	2.259067	-2.46679	0.433133
19	7	3.95146	-0.34349	0.32263
20	6	4.670606	-1.60471	0.106501
21	1	5.661856	-1.50331	0.544715
22	1	4.182552	-2.39164	0.681529
23	6	4.790453	-2.01585	-1.36594
24	1	3.806315	-2.14665	-1.82198
25	1	5.335078	-1.26372	-1.94322
26	1	5.332876	-2.96199	-1.4491
27	7	-4.96288	1.127566	-0.18465
28	7	-2.46701	-1.40432	0.195203
29	7	-2.55646	0.822166	-0.0837
30	6	4.693617	0.91614	0.156253
31	1	4.633762	1.266409	-0.88546
32	1	4.19686	1.669408	0.771003
33	6	6.157111	0.868124	0.58944
34	1	6.260506	0.507092	1.615885
35	1	6.77623	0.249437	-0.06301
36	1	6.558768	1.88368	0.550191
37	1	-0.15853	-2.35712	0.349708
38	8	-0.20857	2.109203	-0.17993
39	6	0.507558	3.340583	-0.3027
40	1	1.095045	3.544599	0.596324
41	1	1.158075	3.331057	-1.18116
42	1	-0.2523	4.110251	-0.42252

(b) in the excited state

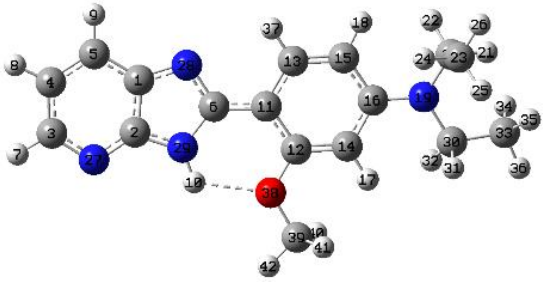

Center Number	Atomic Number	Coordinates (Angstroms) X	Y	Z
1	6	3.759543	-1.01733	-0.11632
2	6	3.866027	0.4032	0.054798
3	6	6.112609	0.380933	0.104321
4	6	6.143423	-1.01236	-0.06044
5	6	4.967995	-1.75913	-0.17596
6	6	1.729707	-0.24408	-0.0724
7	1	7.044119	0.931492	0.19122
8	1	7.10936	-1.50414	-0.09623
9	1	4.97109	-2.83447	-0.30189
10	1	2.268756	1.806259	0.187869
11	6	0.31326	-0.21741	-0.09805
12	6	-0.49504	0.973472	0.025454
13	6	-0.40591	-1.44352	-0.25002
14	6	-1.87186	0.921941	-0.022
15	6	-1.77898	-1.49286	-0.2978
16	6	-2.56763	-0.3105	-0.19743
17	1	-2.426	1.837199	0.098827
18	1	-2.24775	-2.45753	-0.42344
19	7	-3.94791	-0.34904	-0.28355
20	6	-4.66089	-1.61731	-0.10069
21	1	-5.65106	-1.5105	-0.53741
22	1	-4.16295	-2.39181	-0.68425
23	6	-4.7787	-2.04971	1.368133
24	1	-3.79303	-2.18398	1.818834
25	1	-5.32745	-1.30935	1.955544
26	1	-5.31749	-2.99921	1.429393
27	7	4.977624	1.129299	0.167418
28	7	2.466473	-1.39255	-0.19183
29	7	2.579638	0.853354	0.076867
30	6	-4.70987	0.906897	-0.1924
31	1	-4.67511	1.288971	0.839626
32	1	-4.19963	1.641235	-0.81801
33	6	-6.16303	0.829739	-0.65298
34	1	-6.24412	0.434269	-1.66827
35	1	-6.79091	0.232443	0.010403
36	1	-6.5682	1.844421	-0.65646
37	1	0.172851	-2.35285	-0.3327
38	8	0.199573	2.132595	0.201364
39	6	-0.50872	3.367584	0.33242
40	1	-1.09688	3.576506	-0.56544
41	1	-1.15903	3.352489	1.211278
42	1	0.254379	4.1329	0.456102

Table C7: XYZ coordinate of optimized trans DEAMPIP-b in acetonitrile.

(a) in the ground state

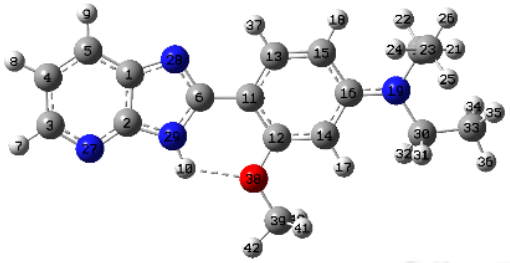

Center Number	Atomic Number	Coordinates (Angstroms) X	Y	Z
1	6	-3.78607	-1.01005	0.109986
2	6	-3.86227	0.395378	-0.06496
3	6	-6.10282	0.42119	-0.12557
4	6	-6.15898	-0.9693	0.0443
5	6	-4.98661	-1.71652	0.166292
6	6	-1.75297	-0.29357	0.07471
7	1	-7.0214	0.991292	-0.21938
8	1	-7.12629	-1.45563	0.079571
9	1	-5.00839	-2.79223	0.298287
10	1	-2.20095	1.759343	-0.19044
11	6	-0.29768	-0.24681	0.109026
12	6	0.474002	0.933536	-0.00594
13	6	0.418651	-1.44736	0.258995
14	6	1.86467	0.895958	0.041171
15	6	1.795771	-1.50288	0.30653
16	6	2.572093	-0.31772	0.217905
17	1	2.405174	1.819376	-0.07374
18	1	2.264762	-2.46863	0.418595
19	7	3.950054	-0.3386	0.317636
20	6	4.674259	-1.6009	0.119116
21	1	5.662328	-1.49181	0.561857
22	1	4.184705	-2.38364	0.698405
23	6	4.804674	-2.02403	-1.34867
24	1	3.824004	-2.16486	-1.80949
25	1	5.349056	-1.27392	-1.92853
26	1	5.352579	-2.96792	-1.4187
27	7	-4.96111	1.128573	-0.18338
28	7	-2.47015	-1.40828	0.193283
29	7	-2.55436	0.818696	-0.08334
30	6	4.691298	0.923839	0.150014
31	1	4.627781	1.27082	-0.89175
32	1	4.194797	1.677179	0.764459
33	6	6.155589	0.877607	0.579258
34	1	6.262906	0.522276	1.607337
35	1	6.772662	0.256131	-0.07232
36	1	6.554912	1.893692	0.533295
37	1	-0.14947	-2.36551	0.33931
38	8	-0.21242	2.104307	-0.17542
39	6	0.500513	3.340636	-0.29958
40	1	1.088982	3.544628	0.598151
41	1	1.148655	3.331899	-1.17917
42	1	-0.26333	4.106256	-0.41721

(b) in the excited state

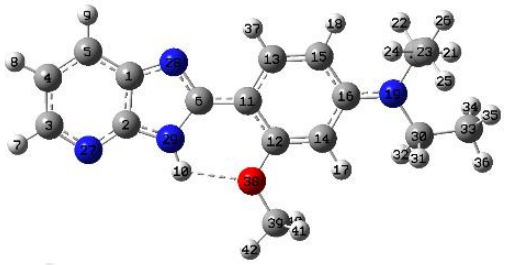

Center Number	Atomic Number	Coordinates (Angstroms) X	Y	Z
1	6	3.763807	-1.01962	-0.11012
2	6	3.865143	0.402304	0.05404
3	6	6.116339	0.384589	0.102458
4	6	6.149816	-1.00781	-0.05593
5	6	4.974751	-1.75889	-0.16728
6	6	1.729019	-0.25185	-0.06894
7	1	7.046503	0.937762	0.186466
8	1	7.11672	-1.49789	-0.09026
9	1	4.982685	-2.83493	-0.28864
10	1	2.262213	1.800579	0.180559
11	6	0.312713	-0.22494	-0.09448
12	6	-0.49191	0.97086	0.021618
13	6	-0.41173	-1.44893	-0.23793
14	6	-1.86788	0.92404	-0.02716
15	6	-1.78454	-1.49484	-0.28497
16	6	-2.56946	-0.30705	-0.19399
17	1	-2.41823	1.84257	0.084443
18	1	-2.25652	-2.459	-0.40036
19	7	-3.9451	-0.33937	-0.27464
20	6	-4.6659	-1.60972	-0.13472
21	1	-5.6484	-1.4875	-0.58347
22	1	-4.16127	-2.37161	-0.72833
23	6	-4.80898	-2.07245	1.32223
24	1	-3.83161	-2.22384	1.785546
25	1	-5.36249	-1.34104	1.9159
26	1	-5.35493	-3.01912	1.351827
27	7	4.976599	1.13149	0.162639
28	7	2.471624	-1.39887	-0.18267
29	7	2.578598	0.848106	0.074583
30	6	-4.70409	0.920852	-0.17418
31	1	-4.6488	1.298383	0.857379
32	1	-4.20179	1.654264	-0.80711
33	6	-6.16457	0.847928	-0.60852
34	1	-6.26578	0.468799	-1.62812
35	1	-6.77911	0.241045	0.058403
36	1	-6.56728	1.863252	-0.58863
37	1	0.159365	-2.3637	-0.31386
38	8	0.206758	2.126691	0.190201
39	6	-0.4981	3.367317	0.319141
40	1	-1.08643	3.574306	-0.57831
41	1	-1.14676	3.35522	1.198604
42	1	0.269203	4.128568	0.439376

Table C8: XYZ coordinate of optimized DEAHPIP-b – 2 methanol complex in the ground state in methanol.

(a) cis-enol methanol complex

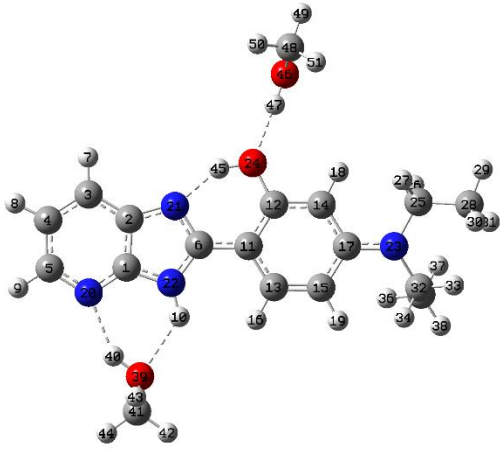

Center Number	Atomic Number	Coordinates (Angstroms) X	Y	Z
1	6	3.657615	-0.00043	0.106055
2	6	3.256681	1.355482	0.09473
3	6	4.254413	2.324987	0.138236
4	6	5.571851	1.863219	0.189074
5	6	5.848478	0.4909	0.194804
6	6	1.447873	0.153422	0.018555
7	1	4.023418	3.383538	0.133122
8	1	6.396052	2.56456	0.224736
9	1	6.874084	0.141262	0.234204
10	1	2.485177	-1.75392	0.045538
11	6	0.05032	-0.20758	-0.03959
12	6	-0.94604	0.798805	-0.09081
13	6	-0.3989	-1.54226	-0.03593
14	6	-2.2965	0.47459	-0.14556
15	6	-1.73424	-1.87582	-0.08935
16	1	0.321801	-2.3505	0.01482
17	6	-2.73811	-0.86722	-0.16638
18	1	-2.99236	1.299346	-0.15959
19	1	-1.99865	-2.92196	-0.07568
20	7	4.900168	-0.46249	0.153712
21	7	1.879689	1.418129	0.039745
22	7	2.494742	-0.73666	0.058084
23	7	-4.07595	-1.18506	-0.27627
24	8	-0.61683	2.118205	-0.08009
25	6	-5.06293	-0.08992	-0.28376
26	1	-5.11266	0.385192	0.706601
27	1	-4.70116	0.66909	-0.97943
28	6	-6.46806	-0.48764	-0.7278
29	1	-7.06613	0.422532	-0.81632
30	1	-6.45818	-0.97762	-1.70482
31	1	-6.97321	-1.14053	-0.01356
32	6	-4.54008	-2.53618	0.065469
33	1	-5.50904	-2.68476	-0.40702
34	1	-3.8785	-3.26616	-0.40059
35	6	-4.64992	-2.79905	1.571688
36	1	-3.68212	-2.6874	2.06665
37	1	-5.35521	-2.1092	2.042694
38	1	-5.00617	-3.81798	1.747606
39	8	3.999113	-3.18512	0.143539

(b) open-enol methanol complex

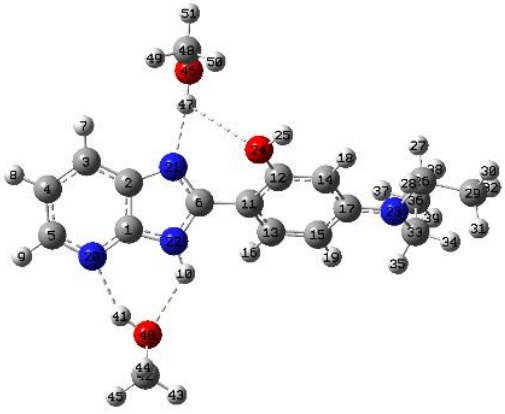

Center Number	Atomic Number	Coordinates (Angstroms) X	Y	Z
1	6	-3.30945	0.541666	0.137301
2	6	-3.22483	-0.86839	0.176235
3	6	-4.41694	-1.58299	0.271445
4	6	-5.59394	-0.83325	0.312775
5	6	-5.55257	0.566123	0.258525
6	6	-1.19585	-0.13135	0.030334
7	1	-4.43278	-2.66577	0.309253
8	1	-6.55518	-1.32644	0.386088
9	1	-6.47249	1.139625	0.287186
10	1	-1.75802	1.959988	-0.06659
11	6	0.25506	0.004617	-0.02689
12	6	1.099761	-0.91394	-0.68146
13	6	0.885684	1.101622	0.59049
14	6	2.480456	-0.73591	-0.70505
15	6	2.252246	1.29121	0.577942
16	1	0.278087	1.819484	1.129952
17	6	3.105751	0.374154	-0.09245
18	1	3.066301	-1.48855	-1.21411
19	1	2.652961	2.148424	1.096878
20	7	-4.41528	1.277007	0.170977
21	7	-1.8998	-1.25556	0.110991
22	7	-2.01179	0.982298	0.048277
23	7	4.471658	0.563353	-0.16022
24	8	0.533484	-1.97788	-1.31906
25	1	1.22009	-2.4926	-1.76049
26	6	5.295473	-0.47633	-0.80264
27	1	5.28538	-1.39707	-0.20128
28	1	4.82777	-0.71915	-1.75886
29	6	6.739747	-0.07461	-1.08956
30	1	7.205561	-0.87564	-1.66863
31	1	6.793221	0.841468	-1.68331
32	1	7.333528	0.05991	-0.18353
33	6	5.12444	1.500294	0.763186
34	1	6.09215	1.763976	0.341328
35	1	4.556416	2.430557	0.781667
36	6	5.308228	0.956062	2.18457
37	1	4.348102	0.708213	2.643486
38	1	5.927791	0.05528	2.184342
39	1	5.801338	1.704926	2.810793

40	1	4.617955	-2.42887	0.136278	40	8	-2.95493	3.72356	-0.05994
41	6	4.384905	-4.12318	-0.86313	41	1	-3.71166	3.107517	0.001481
42	1	3.655269	-4.93345	-0.85164	42	6	-3.17518	4.638221	-1.13465
43	1	4.387544	-3.66791	-1.85969	43	1	-2.30234	5.289274	-1.19491
44	1	5.376376	-4.54205	-0.66107	44	1	-3.28995	4.117389	-2.09195
45	1	0.379421	2.19021	-0.02927	45	1	-4.06141	5.257653	-0.95951
46	8	-2.17552	4.39954	0.690676	46	8	-1.21025	-3.90334	0.936761
47	1	-1.66368	3.611894	0.443906	47	1	-1.36929	-3.00047	0.584127
48	6	-2.41843	5.163595	-0.48894	48	6	-1.31007	-4.83284	-0.13445
49	1	-2.99199	6.044448	-0.19637	49	1	-2.30345	-4.81717	-0.60109
50	1	-1.48547	5.49743	-0.958	50	1	-0.55941	-4.64354	-0.91117
51	1	-3.00091	4.600018	-1.22726	51	1	-1.14089	-5.83195	0.272618

Table C9: XYZ coordinate of optimized trans-enol DEAHPIP-b – 2 methanol complex in methanol.

(a) in the ground state

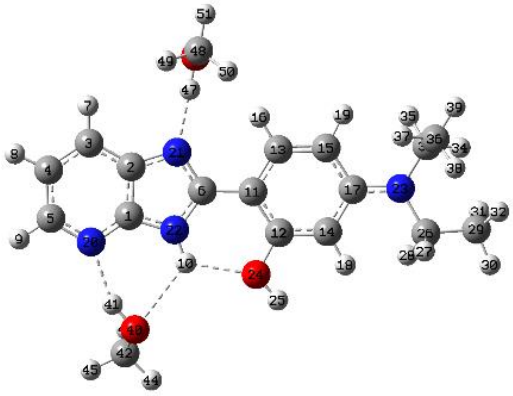

(b) in the excited state

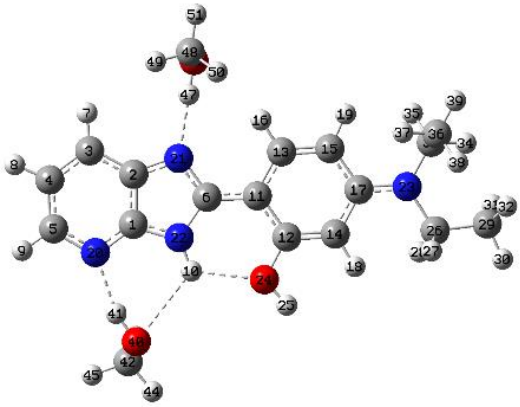

Center Number	Atomic Number	Coordinates (Angstroms) X	Y	Z	Center Number	Atomic Number	Coordinates (Angstroms) X	Y	Z
1	6	-3.31064	-0.24622	0.052756	1	6	-3.28866	-0.22843	0.07726
2	6	-3.12082	1.134019	-0.18819	2	6	-3.07037	1.159678	-0.17094
3	6	-4.25782	1.933183	-0.29005	3	6	-4.211	1.997932	-0.27908
4	6	-5.48943	1.291587	-0.14473	4	6	-5.44824	1.356428	-0.13058
5	6	-5.5534	-0.08718	0.092121	5	6	-5.54033	-0.01854	0.10999
6	6	-1.14924	0.240634	-0.09431	6	6	-1.10516	0.213855	-0.06797
7	1	-4.19242	2.999023	-0.47413	7	1	-4.12884	3.060675	-0.4662
8	1	-6.41164	1.854935	-0.21384	8	1	-6.36793	1.92634	-0.20135
9	1	-6.51386	-0.5779	0.203753	9	1	-6.51237	-0.48689	0.220234
10	1	-1.81554	-1.75676	0.274097	10	1	-1.84821	-1.76598	0.304951
11	6	0.292427	0.056278	-0.12075	11	6	0.307716	0.037713	-0.09336
12	6	0.938014	-1.1716	0.131295	12	6	0.967608	-1.22005	0.130702
13	6	1.136514	1.148725	-0.40722	13	6	1.167301	1.147867	-0.34789
14	6	2.32125	-1.29661	0.090635	14	6	2.33701	-1.34592	0.08125
15	6	2.509009	1.044392	-0.4539	15	6	2.536005	1.027754	-0.39592
16	1	0.683683	2.112606	-0.60085	16	1	0.71922	2.11766	-0.51367
17	6	3.158186	-0.20061	-0.22208	17	6	3.179165	-0.23079	-0.19346
18	1	2.738638	-2.2675	0.317803	18	1	2.758319	-2.32204	0.275965
19	1	3.079448	1.933403	-0.67518	19	1	3.115617	1.915913	-0.59588
20	7	-4.47014	-0.8771	0.194846	20	7	-4.4641	-0.85236	0.221852
21	7	-1.77172	1.40777	-0.27383	21	7	-1.74228	1.410419	-0.25695
22	7	-2.04853	-0.78374	0.107615	22	7	-2.05153	-0.78869	0.136905
23	7	4.52553	-0.33968	-0.31332	23	7	4.545	-0.36809	-0.26426
24	8	0.160667	-2.25777	0.436215	24	8	0.165689	-2.29034	0.406803
25	1	0.709275	-3.03873	0.577723	25	1	0.691218	-3.08853	0.543311
26	6	5.127671	-1.64114	0.030933	26	6	5.149726	-1.69183	-0.01591
27	1	5.013425	-1.83777	1.106528	27	1	5.007173	-1.95421	1.041664

28	1	4.561331	-2.41329	-0.49362	28	1	4.589723	-2.42246	-0.60311
29	6	6.59369	-1.80225	-0.3611	29	6	6.624914	-1.82402	-0.37681
30	1	6.887284	-2.83476	-0.15723	30	1	6.912883	-2.86438	-0.20998
31	1	6.748976	-1.61482	-1.42648	31	1	6.809248	-1.59273	-1.42821
32	1	7.261244	-1.1543	0.209964	32	1	7.272232	-1.20198	0.243418
33	6	5.385949	0.85058	-0.32449	33	6	5.413411	0.813499	-0.31645
34	1	6.342971	0.565411	-0.75661	34	1	6.356909	0.513887	-0.76522
35	1	4.965542	1.582704	-1.014	35	1	4.977012	1.543653	-0.99709
36	6	5.605379	1.479349	1.056412	36	6	5.665034	1.444192	1.06086
37	1	4.661526	1.802839	1.501871	37	1	4.73155	1.775858	1.520514
38	1	6.080124	0.77132	1.740906	38	1	6.14985	0.735618	1.736332
39	1	6.257178	2.353122	0.968893	39	1	6.320865	2.31115	0.946869
40	8	-3.44696	-3.49267	0.625945	40	8	-3.6812	-3.50227	0.636561
41	1	-4.0229	-2.71242	0.490784	41	1	-4.13293	-2.63616	0.504141
42	6	-3.76677	-4.47868	-0.35341	42	6	-4.04293	-4.37383	-0.42969
43	1	-3.64189	-4.09529	-1.3731	43	1	-3.78786	-3.94992	-1.40893
44	1	-3.08267	-5.31712	-0.21392	44	1	-3.48753	-5.30521	-0.30425
45	1	-4.79333	-4.84619	-0.23995	45	1	-5.11455	-4.60821	-0.42082
46	8	-0.99007	4.131911	-0.55829	46	8	-0.90963	4.102551	-0.61397
47	1	-1.2437	3.187037	-0.46645	47	1	-1.19278	3.167773	-0.49433
48	6	-0.92187	4.706897	0.742014	48	6	-0.92232	4.742674	0.656914
49	1	-1.8879	4.66522	1.260353	49	1	-1.92392	4.746336	1.104674
50	1	-0.16943	4.213276	1.369812	50	1	-0.22864	4.267938	1.362373
51	1	-0.63901	5.755204	0.629115	51	1	-0.60817	5.778285	0.512976

Table C10: XYZ coordinate of optimized cis-enol DEAHPIP-b – methanol complex in methanol.

(a) in the ground state

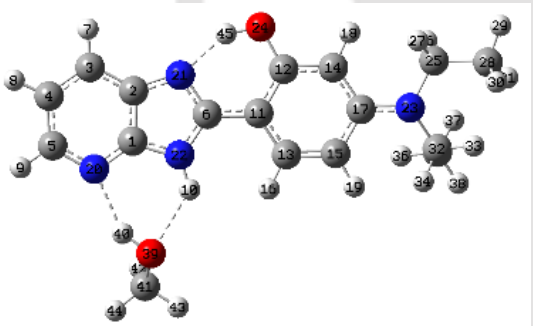

Center Number	Atomic Number	Coordinates (Angstroms) X	Y	Z
1	6	-3.45139	-0.14364	-0.06973
2	6	-3.20793	-1.52314	0.125309
3	6	-4.31138	-2.36089	0.258949
4	6	-5.56843	-1.75514	0.186923
5	6	-5.68613	-0.37449	-0.011
6	6	-1.2716	-0.55134	-0.0373
7	1	-4.20315	-3.42825	0.410872
8	1	-6.4683	-2.34966	0.283241
9	1	-6.66563	0.087159	-0.06667
10	1	-2.08351	1.443872	-0.3134
11	6	0.15827	-0.35216	-0.08511
12	6	1.040596	-1.45519	0.049889
13	6	0.748342	0.915656	-0.25527
14	6	2.420626	-1.27772	0.003629
15	6	2.112334	1.100115	-0.30267
16	1	0.117334	1.792111	-0.35192
17	6	3.003534	-0.00705	-0.19225
18	1	3.021892	-2.1645	0.134832
19	1	2.487193	2.103972	-0.42951
20	7	-4.63369	0.453645	-0.14259

(b) in the intermolecular PT induced TICT state

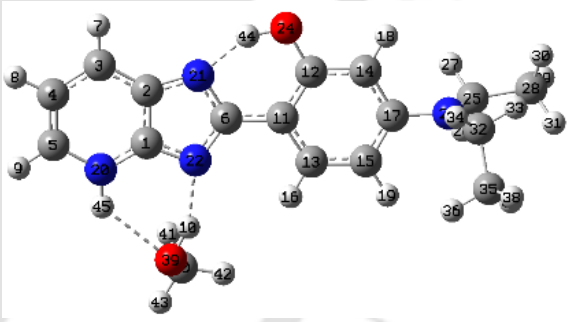

Center Number	Atomic Number	Coordinates (Angstroms) X	Y	Z
1	6	3.409338	0.009839	0.111283
2	6	3.302269	-1.4065	0.011346
3	6	4.467014	-2.19974	-0.02034
4	6	5.704902	-1.51349	0.051468
5	6	5.785947	-0.14473	0.146834
6	6	1.340348	-0.47805	0.037381
7	1	4.426773	-3.27824	-0.09519
8	1	6.632481	-2.0727	0.031834
9	1	6.716835	0.39835	0.202852
10	1	2.507267	2.398343	0.229253
11	6	-0.0936	-0.3652	0.019551
12	6	-0.90803	-1.53753	-0.09351
13	6	-0.75363	0.881491	0.108696
14	6	-2.29359	-1.437	-0.11035
15	6	-2.13751	0.989525	0.090522
16	1	-0.15401	1.779264	0.188718
17	6	-2.89787	-0.1759	-0.01848
18	1	-2.88962	-2.33788	-0.19393
19	1	-2.61571	1.959004	0.152122
20	7	4.629627	0.625635	0.177221

21	7	-1.84648	-1.74472	0.141173	21	7	1.972322	-1.69199	-0.03441
22	7	-2.21105	0.445235	-0.16945	22	7	2.204221	0.589102	0.127407
23	7	4.370761	0.153388	-0.29219	23	7	-4.33254	-0.11029	-0.03844
24	8	0.584545	-2.71596	0.237418	24	8	-0.35525	-2.77026	-0.18552
25	6	5.233653	-1.02575	-0.09673	25	6	-4.97766	0.12673	-1.32445
26	1	5.190924	-1.35988	0.949998	26	1	-4.66265	1.135056	-1.62617
27	1	4.821595	-1.83501	-0.70226	27	1	-4.48431	-0.54826	-2.03025
28	6	6.690842	-0.83812	-0.51045	28	6	-6.48959	-0.01516	-1.37193
29	1	7.192606	-1.8057	-0.43291	29	1	-6.80903	0.190015	-2.39481
30	1	6.775001	-0.49993	-1.54637	30	1	-6.80969	-1.02764	-1.12025
31	1	7.230382	-0.13887	0.131161	31	1	-6.99758	0.695225	-0.71852
32	6	4.967608	1.486339	-0.13837	32	6	-5.06653	-0.20766	1.214211
33	1	5.95862	1.461443	-0.58713	33	1	-6.04614	-0.63343	1.010274
34	1	4.399911	2.199221	-0.73619	34	1	-4.50543	-0.88314	1.857891
35	6	5.066216	1.965029	1.314807	35	6	-5.21194	1.170497	1.894786
36	1	4.080047	2.021949	1.781881	36	1	-4.23782	1.58592	2.150628
37	1	5.686592	1.290349	1.910768	37	1	-5.74728	1.873985	1.256467
38	1	5.518445	2.960147	1.35111	38	1	-5.78242	1.025854	2.811781
39	8	-3.43548	3.014987	-0.58677	39	8	3.008694	3.244903	0.291936
40	1	-4.13215	2.346039	-0.43587	40	6	2.745076	4.024417	-0.87105
41	6	-3.66664	4.142461	0.259819	41	1	3.011889	3.488905	-1.79043
42	1	-3.67149	3.858898	1.318148	42	1	1.690763	4.319658	-0.93302
43	1	-2.85362	4.84952	0.091846	43	1	3.352353	4.929382	-0.81154
44	1	-4.61445	4.636001	0.019971	44	1	0.646711	-2.64778	-0.14962
45	1	-0.40876	-2.68378	0.251921	45	1	4.663891	1.636527	0.24223

Table C11: XYZ coordinate of optimized DEAHPIP-b – 2 ethanol complex in the ground state in ethanol.

(a) cis-enol ethanol complex

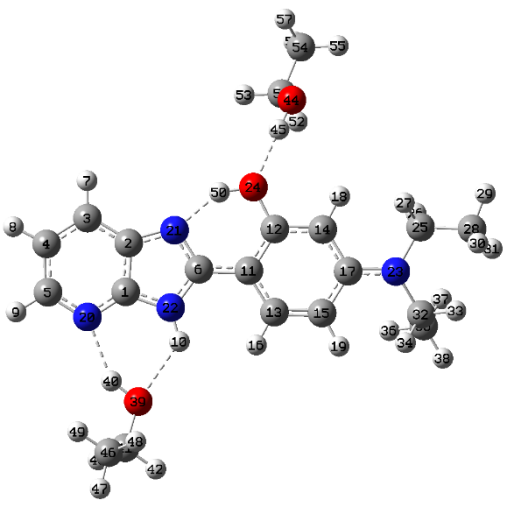

Center Number	Atomic Number	Coordinates (Angstroms) X	Y	Z
1	6	-3.4581	0.787487	-0.04839
2	6	-2.77033	1.992871	0.223641
3	6	-3.52362	3.159092	0.322299
4	6	-4.90261	3.028967	0.141326
5	6	-5.4733	1.778546	-0.12396
6	6	-1.28084	0.413141	0.147092
7	1	-3.06568	4.119079	0.528875
8	1	-5.54685	3.896931	0.205211
9	1	-6.54475	1.686368	-0.26246
10	1	-2.69431	-1.17403	-0.26182
11	6	-0.00575	-0.26427	0.189066

(b) open-enol ethanol complex

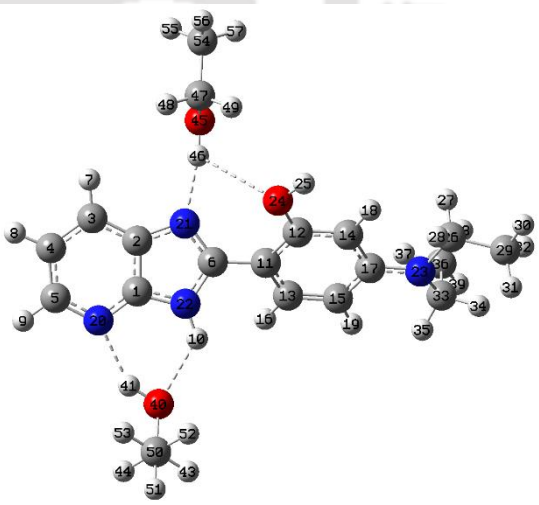

Center Number	Atomic Number	Coordinates (Angstroms) X	Y	Z
1	6	-3.16203	-0.41516	-0.29906
2	6	-2.9999	0.986119	-0.21062
3	6	-4.14897	1.772303	-0.26031
4	6	-5.36396	1.09638	-0.38658
5	6	-5.39945	-0.30254	-0.45733
6	6	-1.01736	0.127428	-0.10176
7	1	-4.1045	2.853437	-0.20295
8	1	-6.2953	1.647146	-0.43076
9	1	-6.34879	-0.81829	-0.55202
10	1	-1.69404	-1.93035	-0.2003
11	6	0.422621	-0.09375	-0.03467

12	6	1.182968	0.463652	0.445438	12	6	1.307183	0.73428	0.685082
13	6	0.135324	-1.64814	-0.02933	13	6	1.002013	-1.18505	-0.71003
14	6	2.421136	-0.16697	0.481118	14	6	2.674804	0.474293	0.718897
15	6	1.356382	-2.28449	0.00678	15	6	2.355028	-1.45417	-0.68885
16	1	-0.74155	-2.25042	-0.23865	16	1	0.365653	-1.83266	-1.30253
17	6	2.552082	-1.55945	0.281797	17	6	3.246807	-0.63216	0.051097
18	1	3.278707	0.463151	0.660336	18	1	3.293565	1.160539	1.279963
19	1	1.381485	-3.34745	-0.17689	19	1	2.71489	-2.30072	-1.25333
20	7	-4.76444	0.639507	-0.22317	20	7	-4.30512	-1.08163	-0.41597
21	7	-1.42165	1.72747	0.339695	21	7	-1.6577	1.291922	-0.09154
22	7	-2.49166	-0.19348	-0.09216	22	7	-1.89207	-0.93348	-0.23013
23	7	3.776467	-2.18944	0.369301	23	7	4.597875	-0.90774	0.132205
24	8	1.157497	1.806217	0.660102	24	8	0.793283	1.792645	1.373536
25	6	4.982635	-1.36392	0.563236	25	1	1.501856	2.242354	1.849832
26	1	5.184241	-0.76858	-0.3388	26	6	5.467396	0.035053	0.858042
27	1	4.768608	-0.65661	1.366046	27	1	5.539505	0.987596	0.312875
28	6	6.240221	-2.13502	0.955662	28	1	4.986237	0.254077	1.813146
29	1	7.022744	-1.40955	1.190426	29	6	6.870856	-0.48324	1.162025
30	1	6.075283	-2.74848	1.845066	30	1	7.369354	0.244459	1.806933
31	1	6.617522	-2.77332	0.154574	31	1	6.841144	-1.43727	1.694575
32	6	3.94117	-3.54929	-0.16162	32	1	7.485776	-0.60067	0.267798
33	1	4.822982	-3.98354	0.305334	33	6	5.218519	-1.80621	-0.84993
34	1	3.106212	-4.16281	0.17626	34	1	6.152907	-2.16907	-0.426
35	6	4.07308	-3.61883	-1.68738	35	1	4.592726	-2.69081	-0.96449
36	1	3.189354	-3.20914	-2.18243	36	6	5.482911	-1.1575	-2.2137
37	1	4.947235	-3.06199	-2.03514	37	1	4.555601	-0.81006	-2.67569
38	1	4.188668	-4.65919	-2.00412	38	1	6.157339	-0.30231	-2.11914
39	8	-4.50318	-2.16674	-0.67012	39	1	5.948728	-1.88142	-2.88829
40	1	-4.94565	-1.30387	-0.54353	40	8	-2.93441	-3.61278	-0.43292
41	6	-5.46711	-3.22576	-0.65703	41	1	-3.687	-2.98998	-0.40852
42	1	-4.91437	-4.13247	-0.91324	42	6	-3.25824	-4.80149	0.300093
43	1	-6.21197	-3.0605	-1.44547	43	1	-2.42499	-5.48815	0.134598
44	8	3.347878	3.659921	0.447525	44	1	-4.15616	-5.26569	-0.12549
45	1	2.608361	3.034092	0.519288	45	8	-0.8267	3.967896	-0.68889
46	6	-6.15259	-3.38546	0.694324	46	1	-1.02962	3.05182	-0.39881
47	1	-6.85309	-4.22574	0.665747	47	6	-0.87745	4.834608	0.442668
48	1	-5.41874	-3.57584	1.482152	48	1	-1.87156	4.794971	0.909821
49	1	-6.71683	-2.48585	0.95799	49	1	-0.14823	4.514712	1.198628
50	1	0.211099	2.117952	0.592845	50	6	-3.44911	-4.54774	1.790244
51	6	3.365153	4.197211	-0.8798	51	1	-3.65929	-5.48798	2.309243
52	1	3.506891	3.391281	-1.61182	52	1	-2.54933	-4.10752	2.228253
53	1	2.40651	4.683305	-1.10332	53	1	-4.28819	-3.86927	1.969838
54	6	4.497152	5.203461	-0.98723	54	6	-0.57419	6.254832	-0.00423
55	1	5.459643	4.727268	-0.78044	55	1	-1.3046	6.592658	-0.7448
56	1	4.534311	5.627493	-1.99444	56	1	-0.60845	6.939739	0.847783
57	1	4.357016	6.021812	-0.2756	57	1	0.421676	6.31523	-0.45233

Table C12: XYZ coordinate of optimized trans-enol DEAHPIP-b – 2 ethanol complex in ethanol.

(a) in the ground state

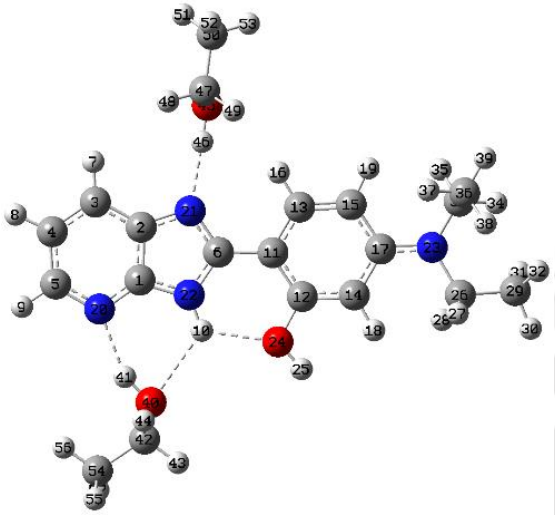

Center Number	Atomic Number	Coordinates (Angstroms) X	Y	Z
1	6	-3.0925	0.067029	-0.27459
2	6	-2.73101	1.431683	-0.35477
3	6	-3.76058	2.368679	-0.41805
4	6	-5.06422	1.869118	-0.39641
5	6	-5.29997	0.49101	-0.31437
6	6	-0.88468	0.30125	-0.27937
7	1	-3.56215	3.431941	-0.48296
8	1	-5.9099	2.54384	-0.44377
9	1	-6.31555	0.111155	-0.299
10	1	-1.80068	-1.62975	-0.16852
11	6	0.526117	-0.05042	-0.26184
12	6	1.012193	-1.36999	-0.16185
13	6	1.504099	0.961711	-0.34407
14	6	2.372899	-1.65318	-0.15391
15	6	2.856502	0.700918	-0.33904
16	1	1.175493	1.990339	-0.41793
17	6	3.345771	-0.63293	-0.26126
18	1	2.664476	-2.68883	-0.04954
19	1	3.535699	1.537336	-0.40225
20	7	-4.32325	-0.43075	-0.25179
21	7	-1.35677	1.547655	-0.35475
22	7	-1.90597	-0.62225	-0.2276
23	7	4.692968	-0.92056	-0.30603
24	8	0.099414	-2.38629	-0.05792
25	1	0.545089	-3.24088	-0.01499
26	6	5.121965	-2.32187	-0.14641
27	1	4.929411	-2.66391	0.880675
28	1	4.499261	-2.93088	-0.80452
29	6	6.578442	-2.59909	-0.50934
30	1	6.738115	-3.67927	-0.46983
31	1	6.811356	-2.26328	-1.52293
32	1	7.285667	-2.13945	0.183511
33	6	5.677965	0.142741	-0.06812
34	1	6.627288	-0.18181	-0.48945
35	1	5.393235	1.022591	-0.64475
36	6	5.861655	0.50706	1.409605
37	1	4.926832	0.859953	1.851776
38	1	6.208402	-0.35347	1.987892

(b) in the excited state

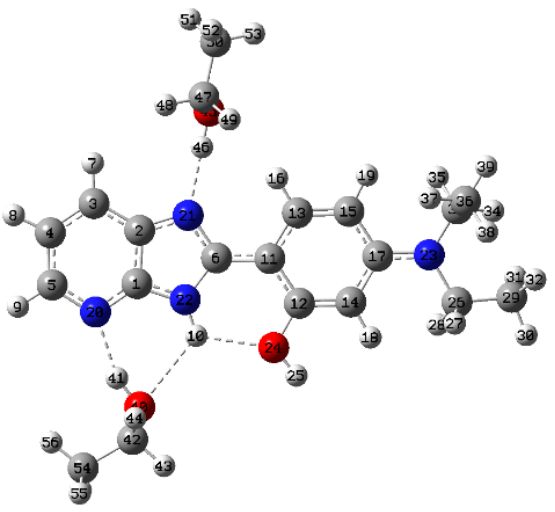

Center Number	Atomic Number	Coordinates (Angstroms) X	Y	Z
1	6	-3.07013	0.048335	-0.32753
2	6	-2.68767	1.421615	-0.3927
3	6	-3.72198	2.39119	-0.467
4	6	-5.0278	1.882375	-0.46886
5	6	-5.28243	0.508271	-0.40031
6	6	-0.8475	0.250804	-0.29489
7	1	-3.51414	3.451827	-0.52204
8	1	-5.87424	2.557679	-0.52515
9	1	-6.30449	0.145009	-0.40427
10	1	-1.82965	-1.66217	-0.21267
11	6	0.536987	-0.0798	-0.25961
12	6	1.044048	-1.42321	-0.18088
13	6	1.524389	0.94979	-0.30037
14	6	2.393027	-1.69545	-0.16822
15	6	2.872978	0.682508	-0.28723
16	1	1.193482	1.977792	-0.35032
17	6	3.365089	-0.65663	-0.23297
18	1	2.695428	-2.73006	-0.08882
19	1	3.554771	1.518364	-0.32565
20	7	-4.31265	-0.45031	-0.32642
21	7	-1.33786	1.526952	-0.37102
22	7	-1.90749	-0.65361	-0.26771
23	7	4.711378	-0.9369	-0.24956
24	8	0.116504	-2.42277	-0.11033
25	1	0.543401	-3.28785	-0.07376
26	6	5.157368	-2.3418	-0.17806
27	1	4.94465	-2.73366	0.826638
28	1	4.546194	-2.91388	-0.87836
29	6	6.622696	-2.58859	-0.52027
30	1	6.785068	-3.66874	-0.51609
31	1	6.874619	-2.21783	-1.51636
32	1	7.309977	-2.15223	0.206202
33	6	5.699309	0.13118	-0.05986
34	1	6.637635	-0.20066	-0.49674
35	1	5.393081	1.003064	-0.63664
36	6	5.91161	0.507845	1.413596
37	1	4.984793	0.864105	1.868292
38	1	6.273642	-0.34589	1.991028

39	1	6.606073	1.302124	1.508348	39	1	6.656709	1.304924	1.479271
40	8	-3.5685	-3.18382	-0.14338	40	8	-3.71949	-3.18692	-0.15574
41	1	-4.08505	-2.35239	-0.15888	41	1	-4.14289	-2.29929	-0.21223
42	6	-3.9711	-3.96409	0.986806	42	6	-4.13381	-3.82096	1.056085
43	1	-3.25308	-4.78488	1.057547	43	1	-3.47285	-4.6809	1.194222
44	1	-3.88129	-3.37012	1.905682	44	1	-3.97439	-3.14708	1.90851
45	8	-0.25568	4.184165	-0.48351	45	8	-0.18328	4.13319	-0.44681
46	1	-0.61791	3.272261	-0.4356	46	1	-0.58067	3.233784	-0.41554
47	6	-0.24421	4.739904	0.83234	47	6	-0.28251	4.723175	0.849784
48	1	-1.2598	4.747746	1.250937	48	1	-1.33525	4.797402	1.154958
49	1	0.379894	4.128349	1.498428	49	1	0.23024	4.097427	1.59329
50	6	0.300013	6.15674	0.770456	50	6	0.344668	6.106382	0.817429
51	1	-0.32324	6.78302	0.126105	51	1	-0.16786	6.746905	0.094301
52	1	0.317078	6.602794	1.768801	52	1	0.277831	6.57916	1.801321
53	1	1.31946	6.163831	0.374814	53	1	1.399994	6.04719	0.53674
54	6	-5.38699	-4.51187	0.851937	54	6	-5.58802	-4.27856	1.017556
55	1	-5.64038	-5.12983	1.719079	55	1	-5.85341	-4.78791	1.949517
56	1	-6.11767	-3.69969	0.792133	56	1	-6.26341	-3.4268	0.894135
57	1	-5.48097	-5.12634	-0.04754	57	1	-5.75376	-4.97143	0.187977

Table C13: XYZ coordinate of optimized cis-enol DEAHPIP-b – ethanol complex in ethanol.

(a) in the ground state

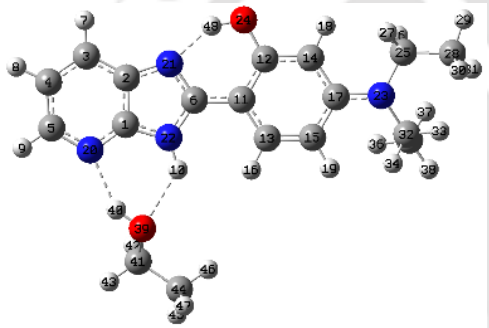

(b) in the intermolecular PT induced TICT state

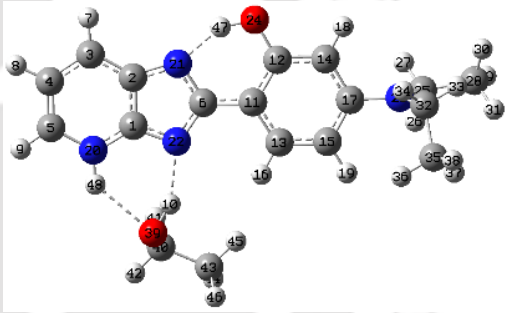

Center Number	Atomic Number	Coordinates (Angstroms) X	Y	Z	Center Number	Atomic Number	Coordinates (Angstroms) X	Y	Z
1	6	-3.31532	-0.56922	-0.06658	1	6	3.31535	-0.34169	0.155154
2	6	-2.99554	-1.93374	0.123356	2	6	3.156729	-1.74396	-0.03638
3	6	-4.0508	-2.83174	0.255304	3	6	4.291249	-2.57714	-0.11005
4	6	-5.33951	-2.29618	0.186947	4	6	5.553115	-1.94478	0.016105
5	6	-5.53354	-0.92341	-0.00585	5	6	5.683818	-0.58883	0.200396
6	6	-1.11621	-0.85575	-0.03821	6	6	1.231163	-0.74511	0.034061
7	1	-3.88346	-3.892	0.403231	7	1	4.211328	-3.64627	-0.25507
8	1	-6.20505	-2.93982	0.282189	8	1	6.459312	-2.53644	-0.03182
9	1	-6.53714	-0.51629	-0.0585	9	1	6.633878	-0.08638	0.29921
10	1	-2.03782	1.092998	-0.30494	10	1	2.546412	2.10103	0.393809
11	6	0.300601	-0.57837	-0.08657	11	6	-0.19786	-0.58059	0.018539
12	6	1.242076	-1.63119	0.049806	12	6	-1.05263	-1.71345	-0.1741
13	6	0.820414	0.719635	-0.25758	13	6	-0.81424	0.679477	0.190774
14	6	2.610269	-1.37763	0.005882	14	6	-2.43372	-1.5627	-0.18733
15	6	2.1723	0.978859	-0.30446	15	6	-2.19336	0.837801	0.176707
16	1	0.142249	1.559894	-0.35572	16	1	-0.18319	1.546976	0.334918
17	6	3.122865	-0.07746	-0.19168	17	6	-2.9937	-0.28984	-0.01257
18	1	3.259337	-2.2293	0.140391	18	1	-3.06079	-2.43441	-0.33136
19	1	2.490999	2.001769	-0.43278	19	1	-2.63748	1.816999	0.304388
20	7	-4.52886	-0.03787	-0.13587	20	7	4.557366	0.221236	0.270325
21	7	-1.62396	-2.07964	0.136815	21	7	1.817935	-1.97542	-0.11102
22	7	-2.10949	0.08799	-0.16546	22	7	2.132599	0.281483	0.198454
23	7	4.479681	0.156634	-0.29144	23	7	-4.42525	-0.17209	-0.02913
24	8	0.856295	-2.91511	0.23712	24	8	-0.54349	-2.95609	-0.34615
25	6	5.404835	-0.97389	-0.09391	25	6	-5.05869	0.170119	-1.29698

26	1	5.380815	-1.30772	0.953563	26	1	-4.70915	1.185	-1.53152
27	1	5.036652	-1.80556	-0.69739	27	1	-4.58672	-0.47338	-2.04546
28	6	6.849741	-0.70935	-0.50897	28	6	-6.57452	0.083376	-1.35412
29	1	7.40199	-1.64904	-0.43188	29	1	-6.88435	0.364237	-2.36187
30	1	6.915059	-0.3672	-1.54494	30	1	-6.92958	-0.93158	-1.16762
31	1	7.352159	0.017263	0.132318	31	1	-7.05942	0.767482	-0.65663
32	6	5.003712	1.519877	-0.14069	32	6	-5.1652	-0.3228	1.21481
33	1	5.993017	1.548467	-0.59313	33	1	-6.15996	-0.6967	0.984324
34	1	4.395922	2.200203	-0.73696	34	1	-4.6315	-1.05958	1.812934
35	6	5.082087	2.005133	1.311603	35	6	-5.25877	1.012555	1.983938
36	1	4.096322	2.010355	1.783059	36	1	-4.2698	1.372805	2.265158
37	1	5.739803	1.365236	1.905874	37	1	-5.76614	1.776114	1.393595
38	1	5.48097	3.022926	1.344986	38	1	-5.83551	0.830405	2.890282
39	8	-3.46592	2.592341	-0.58023	39	8	3.141854	2.875057	0.51926
40	1	-4.12562	1.886782	-0.43029	40	6	3.016095	3.75694	-0.59989
41	6	-3.7757	3.722269	0.24862	41	1	3.10935	3.19216	-1.5367
42	1	-3.79541	3.418277	1.302656	42	1	3.867001	4.441155	-0.54621
43	1	-4.77025	4.107068	-0.00717	43	6	1.710645	4.544228	-0.59058
44	6	-2.72508	4.795167	0.029917	44	1	1.677078	5.234873	-1.4392
45	1	-2.9422	5.668403	0.65086	45	1	0.847832	3.876074	-0.66575
46	1	-1.7309	4.425544	0.295468	46	1	1.61638	5.126385	0.330165
47	1	-2.70785	5.113882	-1.01573	47	1	0.462351	-2.87207	-0.29557
48	1	-0.13736	-2.93796	0.249752	48	1	4.624321	1.225225	0.399754

Table C14: XYZ coordinate of optimized keto DEAHPIP-b – ethanol complex in ethanol.

(a) in the excited state

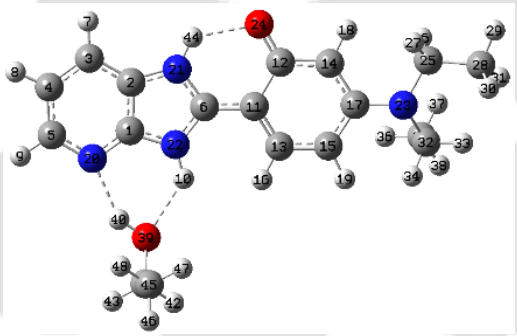

Center Number	Atomic Number	Coordinates (Angstroms)		
		X	Y	Z
1	6	3.274504	-0.53285	-0.2024
2	6	2.99581	-1.90494	-0.06586
3	6	4.055202	-2.8296	-0.0451
4	6	5.335018	-2.24628	-0.16826
5	6	5.505506	-0.87283	-0.29978
6	6	1.044958	-0.77562	-0.05061
7	1	3.90443	-3.89482	0.056494
8	1	6.215645	-2.87787	-0.16209
9	1	6.501676	-0.45548	-0.39308
10	1	2.000845	1.139505	-0.26807
11	6	-0.36966	-0.4966	0.006956
12	6	-1.33186	-1.59712	0.164428
13	6	-0.87737	0.787255	-0.09287
14	6	-2.71873	-1.28102	0.221021
15	6	-2.25889	1.061579	-0.02131
16	1	-0.21371	1.633616	-0.22704
17	6	-3.2189	0.037419	0.155677
18	1	-3.37532	-2.13403	0.305356
19	1	-2.55951	2.09583	-0.09777
20	7	4.479143	0.034731	-0.32199
21	7	1.628684	-2.00609	0.022583

22	7	2.061757	0.124386	-0.18916
23	7	-4.57231	0.327096	0.290562
24	8	-0.92614	-2.80179	0.230351
25	6	-5.5028	-0.80053	0.453334
26	1	-5.58721	-1.37627	-0.48136
27	1	-5.06743	-1.47251	1.195055
28	6	-6.89676	-0.41326	0.941443
29	1	-7.44492	-1.32884	1.17649
30	1	-6.84656	0.192074	1.850333
31	1	-7.47666	0.12913	0.192315
32	6	-5.10476	1.569763	-0.28505
33	1	-6.07215	1.760187	0.176527
34	1	-4.473	2.403454	0.021889
35	6	-5.24951	1.546692	-1.81153
36	1	-4.28466	1.384108	-2.29866
37	1	-5.9311	0.754825	-2.13339
38	1	-5.65151	2.5008	-2.16379
39	8	3.335319	2.608063	-0.60052
40	1	4.031754	1.925364	-0.49128
41	6	3.734281	3.833128	0.02746
42	1	2.973574	4.568791	-0.24373
43	1	4.68591	4.172926	-0.39865
44	1	1.034657	-2.82647	0.127123
45	6	3.844031	3.717428	1.542806
46	1	4.117967	4.68436	1.975936
47	1	2.891889	3.403476	1.978967
48	1	4.610549	2.991071	1.827664

भारतीय प्रौद्योगिकी संस्थान गुवाहाटी
Indian Institute of Technology Guwahati

Annexure-D

Table D1: XYZ coordinate of optimized DA of DEAHPIP-b in the ground state in water.

(a) in ground state

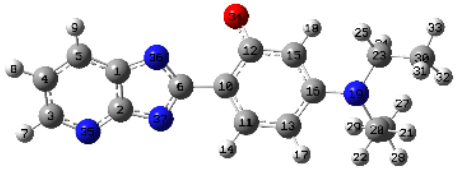

Center Number	Atomic Number	Coordinates (Angstroms) X	Y	Z
1	6	-3.81865	0.638307	0.24318
2	6	-3.75742	-0.74616	-0.14295
3	6	-6.02183	-0.9361	-0.13406
4	6	-6.18743	0.40265	0.250592
5	6	-5.06864	1.220184	0.447233
6	6	-1.77178	0.048958	0.016352
7	1	-6.89925	-1.5601	-0.28647
8	1	-7.1896	0.792237	0.391554
9	1	-5.17541	2.259593	0.743994
10	6	-0.29448	0.065391	0.049628
11	6	0.362318	-1.00263	0.678022
12	6	0.508978	1.104824	-0.55647
13	6	1.742808	-1.09809	0.810873
14	1	-0.25178	-1.78713	1.110303
15	6	1.932688	0.981286	-0.38845
16	6	2.561135	-0.07201	0.278739
17	1	2.168484	-1.92748	1.360656
18	1	2.517621	1.762095	-0.85853
19	7	3.967755	-0.11679	0.475703
20	6	4.631421	-1.40408	0.212622
21	1	5.610551	-1.38782	0.69491
22	1	4.067825	-2.19158	0.710991
23	6	4.7352	1.072981	0.096333
24	1	4.805495	1.191195	-0.99772
25	1	4.181192	1.939078	0.462793
26	6	4.791315	-1.75596	-1.27362
27	1	5.417072	-1.02854	-1.79782
28	1	5.263516	-2.73738	-1.37857
29	1	3.819431	-1.79169	-1.77336
30	6	6.141728	1.117277	0.696292
31	1	6.11234	0.966611	1.779285
32	1	6.8118	0.370891	0.26397
33	1	6.581209	2.099469	0.50228
34	8	0.028685	2.073482	-1.25528
35	7	-4.83291	-1.52939	-0.3341
36	7	-2.54191	1.120458	0.340378
37	7	-2.44925	-1.09976	-0.28084

(b) in excited state

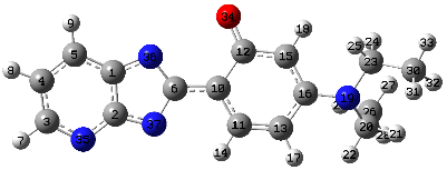

Center Number	Atomic Number	Coordinates (Angstroms) X	Y	Z
1	6	-3.83188	-0.65087	0.024571
2	6	-3.75695	0.783327	-0.08524
3	6	-6.03345	0.978827	-0.14977
4	6	-6.2103	-0.41144	-0.05128
5	6	-5.11127	-1.28267	0.044583
6	6	-1.7637	-0.04415	0.02926
7	1	-6.91459	1.614714	-0.21582
8	1	-7.2246	-0.80065	-0.04498
9	1	-5.22864	-2.35778	0.129727
10	6	-0.32443	-0.04625	-0.00334
11	6	0.357587	1.145962	-0.37381
12	6	0.534157	-1.21344	0.328126
13	6	1.735927	1.235586	-0.48588
14	1	-0.24479	2.014664	-0.60489
15	6	1.952689	-1.07142	0.164
16	6	2.577684	0.116053	-0.22317
17	1	2.167595	2.170104	-0.82298
18	1	2.530357	-1.94687	0.431069
19	7	3.971228	0.227022	-0.42918
20	6	4.640833	1.414745	0.128226
21	1	5.604658	1.527265	-0.37094
22	1	4.060194	2.296473	-0.14058
23	6	4.750775	-1.01398	-0.40149
24	1	4.859936	-1.40581	0.623409
25	1	4.178182	-1.7598	-0.95567
26	6	4.840957	1.382943	1.650184
27	1	5.476412	0.548745	1.959357
28	1	5.321341	2.308108	1.98187
29	1	3.882476	1.293315	2.168534
30	6	6.133422	-0.89189	-1.0426
31	1	6.064861	-0.4718	-2.05001
32	1	6.819154	-0.27502	-0.45794
33	1	6.577288	-1.88814	-1.11929
34	8	0.060441	-2.29735	0.788625
35	7	-4.83591	1.62302	-0.16382
36	7	-2.5827	-1.15527	0.094713
37	7	-2.46199	1.151408	-0.09231

Table D2: XYZ coordinate of optimized MA2 of DEAHPIP-b in water.

(a) in ground state

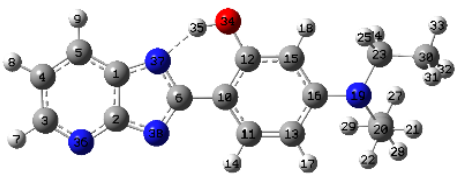

(b) in excited state

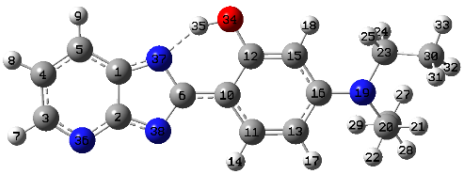

Center Number	Atomic Number	Coordinates (Angstroms) X	Y	Z
1	6	-3.74668	0.610892	-0.12109
2	6	-3.77864	-0.80237	0.131472
3	6	-6.04646	-0.84043	0.057065
4	6	-6.11791	0.538441	-0.19233
5	6	-4.94716	1.296163	-0.28674
6	6	-1.74783	-0.15294	0.087444
7	1	-6.96516	-1.41709	0.12753
8	1	-7.0892	1.004904	-0.31047
9	1	-4.97772	2.363755	-0.47963
10	6	-0.28585	-0.14088	0.137373
11	6	0.4626	-1.30601	0.370988
12	6	0.447873	1.05238	-0.05892
13	6	1.845013	-1.31357	0.419682
14	1	-0.07599	-2.23453	0.520115
15	6	1.844426	1.056654	-0.0176
16	6	2.584784	-0.1146	0.238021
17	1	2.345998	-2.25183	0.607953
18	1	2.327713	2.004405	-0.20341
19	7	3.976197	-0.09472	0.341915
20	6	4.727155	-1.32843	0.075113
21	1	5.72606	-1.20811	0.492105
22	1	4.277735	-2.14511	0.639155
23	6	4.668329	1.17891	0.094617
24	1	4.598681	1.466376	-0.96615
25	1	4.14167	1.948853	0.660978
26	6	4.824951	-1.70326	-1.40911
27	1	5.330153	-0.92196	-1.98357
28	1	5.396107	-2.6288	-1.52596
29	1	3.834115	-1.85844	-1.84331
30	6	6.13177	1.206988	0.531724
31	1	6.243414	0.895744	1.573947
32	1	6.775379	0.58081	-0.08919
33	1	6.497086	2.23348	0.446733
34	8	-0.17293	2.234462	-0.3067
35	1	-1.16257	2.047749	-0.3039
36	7	-4.90522	-1.52732	0.220702
37	7	-2.43451	1.002426	-0.145
38	7	-2.49908	-1.26375	0.260138

Center Number	Atomic Number	Coordinates (Angstroms) X	Y	Z
1	6	3.731723	0.615492	0.114223
2	6	3.760241	-0.8157	-0.13665
3	6	6.038532	-0.84978	-0.06854
4	6	6.111483	0.536909	0.177498
5	6	4.954257	1.319251	0.278766
6	6	1.717336	-0.15254	-0.08722
7	1	6.96544	-1.41502	-0.13798
8	1	7.092568	0.987455	0.288341
9	1	4.987952	2.385518	0.469603
10	6	0.306911	-0.1465	-0.12406
11	6	-0.46743	-1.33096	-0.34795
12	6	-0.44969	1.076502	0.076121
13	6	-1.84339	-1.31307	-0.38485
14	1	0.06193	-2.26371	-0.49265
15	6	-1.82893	1.083072	0.038631
16	6	-2.58018	-0.10295	-0.20155
17	1	-2.35887	-2.24506	-0.56649
18	1	-2.31397	2.029822	0.224965
19	7	-3.96383	-0.0792	-0.28314
20	6	-4.73082	-1.31737	-0.10527
21	1	-5.71865	-1.16393	-0.53428
22	1	-4.27298	-2.10811	-0.6987
23	6	-4.6665	1.199927	-0.09536
24	1	-4.62049	1.504525	0.961863
25	1	-4.12168	1.955161	-0.66282
26	6	-4.85885	-1.75876	1.359275
27	1	-5.36829	-0.99967	1.958447
28	1	-5.44064	-2.68288	1.416725
29	1	-3.87679	-1.94322	1.800875
30	6	-6.11958	1.219506	-0.56392
31	1	-6.21156	0.896474	-1.60404
32	1	-6.77674	0.605534	0.054483
33	1	-6.48052	2.248828	-0.49945
34	8	0.195615	2.238118	0.319566
35	1	1.188222	2.039155	0.308285
36	7	4.901185	-1.56038	-0.22952
37	7	2.449586	1.013302	0.141209
38	7	2.505832	-1.27571	-0.25977

Table D3: XYZ coordinate of optimized MA1 of DEAHPIP-b in water.

(a) in ground state

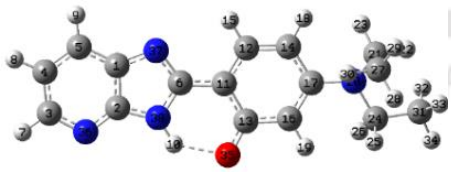

(b) in excited state

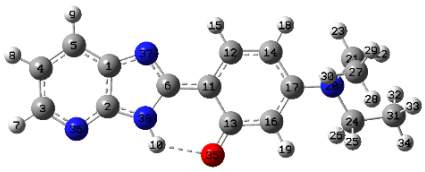

Center Number	Atomic Number	Coordinates (Angstroms) X	Y	Z
1	6	-3.77857	-0.82504	0.162954
2	6	-3.77406	0.57012	-0.13055
3	6	-6.01572	0.707561	-0.22844
4	6	-6.14945	-0.65618	0.054817
5	6	-5.01849	-1.45368	0.257568
6	6	-1.71088	-0.21952	0.099842
7	1	-6.89972	1.317813	-0.38414
8	1	-7.14205	-1.08664	0.115178
9	1	-5.10402	-2.51193	0.47858

Center Number	Atomic Number	Coordinates (Angstroms) X	Y	Z
1	6	3.777769	-0.81575	-0.17621
2	6	3.808658	0.57364	0.13323
3	6	6.063013	0.649922	0.232725
4	6	6.16052	-0.71064	-0.06551
5	6	5.01746	-1.50273	-0.28305
6	6	1.71237	-0.1524	-0.10526
7	1	6.968089	1.228272	0.394406
8	1	7.149745	-1.15285	-0.12686
9	1	5.075868	-2.559	-0.51428

10	1	-1.9407	1.795158	-0.33251	10	1	2.080963	1.860582	0.361749
11	6	-0.26862	-0.16488	0.137166	11	6	0.277102	-0.13089	-0.14468
12	6	0.478034	-1.32842	0.404187	12	6	-0.45158	-1.29998	-0.4298
13	6	0.435136	1.076945	-0.09732	13	6	-0.48544	1.110012	0.110326
14	6	1.855519	-1.34122	0.457602	14	6	-1.84006	-1.3098	-0.47843
15	1	-0.06372	-2.251	0.583829	15	1	0.092393	-2.21467	-0.62919
16	6	1.862529	1.025725	-0.0393	16	6	-1.90648	1.044262	0.061464
17	6	2.589077	-0.13573	0.240849	17	6	-2.60783	-0.13268	-0.22546
18	1	2.360521	-2.26744	0.690979	18	1	-2.33545	-2.23219	-0.74938
19	1	2.364078	1.961232	-0.24576	19	1	-2.42163	1.968109	0.285494
20	7	3.987925	-0.13019	0.359496	20	7	-4.00461	-0.17645	-0.34639
21	6	4.733662	-1.31855	-0.08149	21	6	-4.71823	-1.34515	0.193854
22	1	5.726504	-1.27838	0.366876	22	1	-5.70008	-1.38849	-0.27807
23	1	4.262196	-2.207	0.334838	23	1	-4.19924	-2.25029	-0.11784
24	6	4.680234	1.157234	0.219284	24	6	-4.7274	1.099902	-0.30784
25	1	4.661534	1.513871	-0.82292	25	1	-4.75241	1.514829	0.712566
26	1	4.119461	1.886985	0.805398	26	1	-4.15751	1.805427	-0.9148
27	6	4.855452	-1.46255	-1.60418	27	6	-4.86828	-1.34062	1.721129
28	1	5.380571	-0.61194	-2.04719	28	1	-5.43746	-0.47451	2.06858
29	1	5.416866	-2.36821	-1.85203	29	1	-5.39821	-2.24098	2.044754
30	1	3.869749	-1.53572	-2.07134	30	1	-3.89072	-1.3268	2.210376
31	6	6.12168	1.15571	0.728083	31	6	-6.14986	1.029444	-0.86223
32	1	6.181489	0.764103	1.747342	32	1	-6.16351	0.57766	-1.85778
33	1	6.79762	0.577525	0.094921	33	1	-6.83039	0.469551	-0.21781
34	1	6.488953	2.185166	0.739962	34	1	-6.5432	2.045742	-0.94571
35	8	-0.17223	2.187657	-0.36044	35	8	0.123547	2.196497	0.385953
36	7	-4.83273	1.345241	-0.32629	36	7	4.887974	1.347435	0.344839
37	7	-2.48997	-1.2901	0.300583	37	7	2.489747	-1.24133	-0.31888
38	7	-2.44733	0.916482	-0.16308	38	7	2.498884	0.955821	0.169079

Table D4: XYZ coordinate of optimized neutral species of DEAHPIP-b in water.

(a) cis-enol in ground state

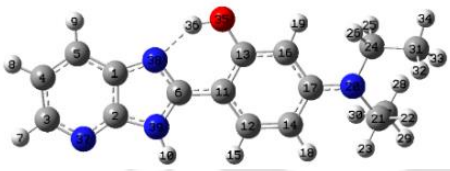

Center Number	Atomic Number	Coordinates (Angstroms) X	Y	Z
1	6	-3.74742	0.611374	-0.1133
2	6	-3.82198	-0.78332	0.115891
3	6	-6.06108	-0.82425	0.051767
4	6	-6.11613	0.556339	-0.17929
5	6	-4.94287	1.307711	-0.26708
6	6	-1.70355	-0.10013	0.06948
7	1	-6.97918	-1.39843	0.118103
8	1	-7.08218	1.03333	-0.28927
9	1	-4.96197	2.376299	-0.44558
10	1	-2.21669	-2.15403	0.393638
11	6	-0.25948	-0.11525	0.118109
12	6	0.489361	-1.29089	0.322508
13	6	0.474287	1.086728	-0.05569
14	6	1.865963	-1.29802	0.364564
15	1	-0.02146	-2.23838	0.45306
16	6	1.866004	1.088164	-0.01656
17	6	2.607981	-0.0907	0.210514
18	1	2.366138	-2.24127	0.521546
19	1	2.348308	2.03942	-0.18213
20	7	3.985973	-0.07322	0.299571

(b) keto in excited state

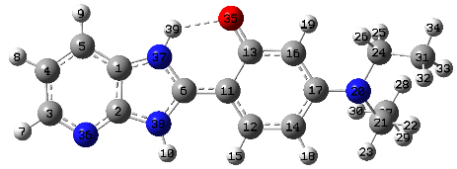

Center Number	Atomic Number	Coordinates (Angstroms) X	Y	Z
1	6	-3.80211	0.621187	-0.15141
2	6	-3.84953	-0.75602	0.163573
3	6	-6.09939	-0.80735	0.118592
4	6	-6.16509	0.548079	-0.19413
5	6	-5.00034	1.325859	-0.34386
6	6	-1.6842	-0.117	0.079818
7	1	-7.01343	-1.38091	0.227612
8	1	-7.13899	1.005477	-0.32315
9	1	-5.0268	2.378858	-0.58695
10	1	-2.26322	-2.11073	0.529687
11	6	-0.2476	-0.13626	0.113587
12	6	0.478626	-1.29757	0.346747
13	6	0.509443	1.110606	-0.11059
14	6	1.884958	-1.30196	0.406948
15	1	-0.02516	-2.24422	0.503365
16	6	1.928533	1.055699	-0.05827
17	6	2.647694	-0.12523	0.212066
18	1	2.36845	-2.2411	0.634023
19	1	2.430613	1.991044	-0.25875
20	7	4.038101	-0.14497	0.345034

21	6	4.744761	-1.32183	0.146731	21	6	4.778636	-1.3382	-0.09375
22	1	5.731855	-1.16675	0.577696	22	1	5.756324	-1.31988	0.386803
23	1	4.282128	-2.09445	0.760276	23	1	4.28199	-2.22692	0.292868
24	6	4.688999	1.200348	0.063045	24	6	4.746586	1.139369	0.26367
25	1	4.605516	1.492661	-0.99383	25	1	4.755438	1.523555	-0.76855
26	1	4.174571	1.968278	0.643285	26	1	4.176669	1.856337	0.857399
27	6	4.878957	-1.79886	-1.30388	27	6	4.9417	-1.45271	-1.61451
28	1	5.395643	-1.05576	-1.91713	28	1	5.494457	-0.60285	-2.02325
29	1	5.456016	-2.72714	-1.34054	29	1	5.494647	-2.36309	-1.86247
30	1	3.900241	-1.98871	-1.75125	30	1	3.969257	-1.49951	-2.11171
31	6	6.157563	1.216318	0.47952	31	6	6.173973	1.105174	0.806832
32	1	6.283868	0.915709	1.522884	32	1	6.203391	0.68528	1.815757
33	1	6.786508	0.580618	-0.14654	33	1	6.857382	0.536898	0.17312
34	1	6.527342	2.239653	0.379425	34	1	6.55134	2.129585	0.85549
35	8	-0.13937	2.273188	-0.27656	35	8	-0.10851	2.195176	-0.3649
36	1	-1.12063	2.114351	-0.28283	36	7	-4.9395	-1.50371	0.307741
37	7	-4.9193	-1.51867	0.203066	37	7	-2.47667	0.962911	-0.19278
38	7	-2.42475	1.003739	-0.13685	38	7	-2.53989	-1.16868	0.29503
39	7	-2.51183	-1.20375	0.227593	39	1	-2.02998	1.859832	-0.37911

Table D5: XYZ coordinate of optimized trans-enol DEAHPIP-b in ground state in water.

Center Number	Atomic Number	Coordinates (Angstroms)		
		X	Y	Z
1	6	3.755515	-0.84567	-0.12857
2	6	3.834136	0.551213	0.10228
3	6	6.074409	0.569131	0.170453
4	6	6.12798	-0.81373	-0.05416
5	6	4.954308	-1.55254	-0.20934
6	6	1.724276	-0.12709	-0.07002
7	1	6.994036	1.132749	0.289497
8	1	7.094247	-1.30059	-0.10567
9	1	4.973962	-2.62217	-0.38404
10	1	2.1831	1.916586	0.279231
11	6	0.269716	-0.07349	-0.10476
12	6	-0.46285	-1.2592	-0.3097
13	6	-0.49012	1.099959	0.063647
14	6	-1.83951	-1.29313	-0.35679
15	1	0.09257	-2.18023	-0.43387
16	6	-1.87974	1.0876	0.019986
17	6	-2.60553	-0.10331	-0.21007
18	1	-2.32133	-2.24635	-0.51339
19	1	-2.39058	2.026011	0.183142
20	7	-3.98275	-0.10495	-0.30547
21	6	-4.72161	-1.36576	-0.15451
22	1	-5.70954	-1.22702	-0.5891
23	1	-4.24352	-2.13048	-0.76622
24	6	-4.70568	1.158412	-0.07529
25	1	-4.63019	1.455855	0.980807
26	1	-4.2022	1.932265	-0.65783
27	6	-4.85248	-1.84432	1.29587
28	1	-5.38484	-1.11037	1.906698
29	1	-5.41277	-2.78283	1.330818
30	1	-3.87218	-2.01634	1.746899
31	6	-6.1731	1.150645	-0.49582
32	1	-6.29189	0.844626	-1.53843

33	1	-6.79357	0.507416	0.13093
34	1	-6.55873	2.168488	-0.40004
35	8	0.179731	2.276177	0.2886
36	7	4.934285	1.276475	0.252844
37	7	2.438364	-1.23722	-0.23103
38	7	2.527035	0.977341	0.13416
39	1	-0.44143	3.009076	0.379032

Table D6: XYZ coordinate of optimized MC1 of DEAHPIP-b in water.

(a) cis-enol in ground state

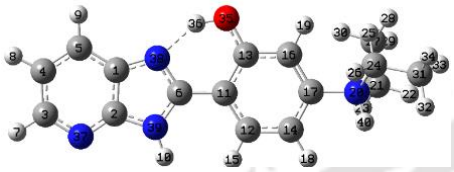

Center Number	Atomic Number	Coordinates (Angstroms) X	Y	Z
1	6	3.697903	0.650877	-0.05508
2	6	3.860245	-0.75057	0.027893
3	6	6.093532	-0.6348	0.074669
4	6	6.060198	0.766952	-0.00567
5	6	4.844592	1.442552	-0.07266
6	6	1.711018	-0.21056	-0.05279
7	1	7.048143	-1.14755	0.126702
8	1	6.994174	1.3146	-0.01443
9	1	4.79189	2.52279	-0.13459
10	1	2.349582	-2.24948	0.081213
11	6	0.257059	-0.31253	-0.07683
12	6	-0.4088	-1.54543	-0.03205
13	6	-0.51782	0.87459	-0.14985
14	6	-1.79241	-1.62656	-0.05038
15	1	0.155213	-2.46818	0.014199
16	6	-1.91601	0.794401	-0.16875
17	6	-2.52851	-0.44459	-0.11595
18	1	-2.27957	-2.59357	-0.01661
19	1	-2.47132	1.719365	-0.23138
20	7	-4.00904	-0.55285	-0.10977
21	6	-4.59986	-0.47519	1.309477
22	1	-5.62794	-0.82116	1.216592
23	1	-4.04437	-1.21489	1.884377
24	6	-4.68988	0.353036	-1.13281
25	1	-4.57442	1.377786	-0.79003
26	1	-4.11581	0.228712	-2.04992
27	6	-4.52687	0.896301	1.95227
28	1	-5.10318	1.647209	1.410154
29	1	-4.96292	0.808358	2.949642
30	1	-3.5007	1.244779	2.070839
31	6	-6.14972	-0.00944	-1.34577
32	1	-6.26682	-1.05735	-1.63286
33	1	-6.76785	0.192812	-0.47064
34	1	-6.52884	0.602651	-2.16624
35	8	0.02882	2.098619	-0.20336
36	1	1.021947	1.996227	-0.18202
37	7	5.004111	-1.41686	0.093017
38	7	2.352577	0.952095	-0.10355
39	7	2.580747	-1.26821	0.027166
40	1	-4.2146	-1.5056	-0.42045

(b) keto in excited state

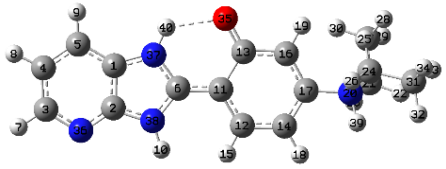

Center Number	Atomic Number	Coordinates (Angstroms) X	Y	Z
1	6	3.781067	0.665424	-0.08203
2	6	3.875828	-0.74283	0.057764
3	6	6.121608	-0.70311	0.098309
4	6	6.141714	0.687356	-0.03746
5	6	4.951653	1.421744	-0.13283
6	6	1.690217	-0.17925	-0.03933
7	1	7.053461	-1.25274	0.17076
8	1	7.096619	1.197141	-0.06843
9	1	4.941877	2.498255	-0.23774
10	1	2.344199	-2.19627	0.17292
11	6	0.267375	-0.27698	-0.05363
12	6	-0.39513	-1.50368	0.050513
13	6	-0.54703	0.948922	-0.18569
14	6	-1.8016	-1.58468	0.046946
15	1	0.156089	-2.43091	0.136551
16	6	-1.96992	0.821712	-0.18606
17	6	-2.57284	-0.43058	-0.06442
18	1	-2.26858	-2.55929	0.132275
19	1	-2.53384	1.737442	-0.2957
20	7	-4.04642	-0.57364	-0.0445
21	6	-4.66741	-0.33556	1.344206
22	1	-5.68332	-0.72279	1.279656
23	1	-4.10126	-0.97963	2.015842
24	6	-4.73558	0.174988	-1.18384
25	1	-4.6238	1.238227	-0.98823
26	1	-4.15913	-0.07323	-2.07404
27	6	-4.65092	1.106429	1.814622
28	1	-5.23152	1.767521	1.169289
29	1	-5.11355	1.128339	2.80385
30	1	-3.63867	1.498592	1.91532
31	6	-6.19335	-0.2216	-1.34426
32	1	-6.3063	-1.30094	-1.47432
33	1	-6.81393	0.103642	-0.50875
34	1	-6.57412	0.262045	-2.24589
35	8	0.008588	2.081232	-0.29808
36	7	4.991589	-1.44815	0.14888
37	7	2.447739	0.96284	-0.13679
38	7	2.585851	-1.2205	0.079669
39	1	-4.22585	-1.56283	-0.23196
40	1	1.987469	1.86388	-0.23454

Table D7: XYZ coordinate of optimized MC2 of DEAHPIP-b in water.

(a) in ground state

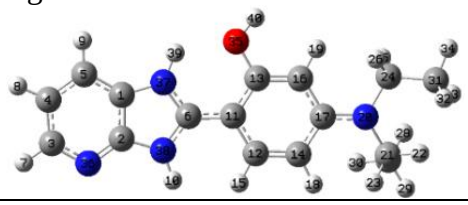

Center Number	Atomic Number	Coordinates (Angstroms) X	Y	Z
1	6	3.816337	0.598739	0.090251
2	6	3.806726	-0.79177	-0.097
3	6	6.038733	-0.93312	-0.07005
4	6	6.162704	0.449747	0.117792
5	6	5.030221	1.259792	0.203293
6	6	1.674641	-0.07401	-0.0453
7	1	6.927001	-1.5513	-0.13475
8	1	7.150202	0.885467	0.196012
9	1	5.096876	2.330258	0.347815
10	1	2.152184	-2.11518	-0.30424
11	6	0.24663	-0.06495	-0.07848
12	6	-0.49169	-1.26015	-0.25902
13	6	-0.51309	1.123472	0.071924
14	6	-1.86087	-1.28601	-0.30042
15	1	0.026501	-2.20465	-0.37085
16	6	-1.89435	1.113944	0.032872
17	6	-2.62511	-0.08422	-0.17381
18	1	-2.34707	-2.23952	-0.43331
19	1	-2.40348	2.055314	0.177695
20	7	-3.9857	-0.08265	-0.25436
21	6	-4.73886	-1.34636	-0.23868
22	1	-5.70383	-1.1629	-0.70459
23	1	-4.23611	-2.06384	-0.88636
24	6	-4.71342	1.189817	-0.05373
25	1	-4.61235	1.506746	0.992225
26	1	-4.22233	1.947385	-0.66749
27	6	-4.93755	-1.92729	1.164707
28	1	-5.48734	-1.23192	1.803917
29	1	-5.51077	-2.85614	1.10244
30	1	-3.98162	-2.14879	1.645149
31	6	-6.18922	1.169896	-0.43756
32	1	-6.33533	0.874298	-1.47915
33	1	-6.78792	0.518952	0.201896
34	1	-6.57583	2.185234	-0.32322
35	8	0.173856	2.284361	0.268337
36	7	4.864644	-1.57632	-0.18039
37	7	2.489991	0.996609	0.116806
38	7	2.472429	-1.16642	-0.17584
39	1	2.124861	1.934146	0.236229
40	1	-0.42498	3.037828	0.349658

(b) in excited state

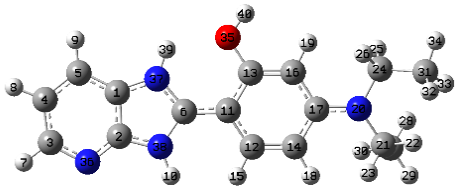

Center Number	Atomic Number	Coordinates (Angstroms) X	Y	Z
1	6	3.823125	0.604172	0.122654
2	6	3.808023	-0.79414	-0.13151
3	6	6.050007	-0.93661	-0.1009
4	6	6.177335	0.433834	0.151878
5	6	5.049862	1.258031	0.273069
6	6	1.670211	-0.05862	-0.06183
7	1	6.938491	-1.55187	-0.19072
8	1	7.169682	0.855569	0.253184
9	1	5.122359	2.319461	0.46698
10	1	2.180549	-2.09755	-0.43306
11	6	0.245198	-0.06078	-0.07875
12	6	-0.48983	-1.26593	-0.24284
13	6	-0.53017	1.1365	0.068054
14	6	-1.86789	-1.2886	-0.29157
15	1	0.031873	-2.20906	-0.33517
16	6	-1.90674	1.118454	0.02486
17	6	-2.62855	-0.09083	-0.16969
18	1	-2.35241	-2.24255	-0.43026
19	1	-2.42529	2.056327	0.16044
20	7	-4.00563	-0.09554	-0.23846
21	6	-4.75088	-1.35557	-0.1845
22	1	-5.72384	-1.18711	-0.63774
23	1	-4.24878	-2.09295	-0.80995
24	6	-4.73653	1.179552	-0.11975
25	1	-4.63343	1.549163	0.910894
26	1	-4.2354	1.903407	-0.76604
27	6	-4.92532	-1.89272	1.245922
28	1	-5.46843	-1.17993	1.869951
29	1	-5.49669	-2.82353	1.209466
30	1	-3.95916	-2.09685	1.711751
31	6	-6.21237	1.140782	-0.49773
32	1	-6.36189	0.792994	-1.52218
33	1	-6.81042	0.528738	0.178996
34	1	-6.5918	2.162997	-0.4352
35	8	0.167879	2.293552	0.256207
36	7	4.867897	-1.58319	-0.24891
37	7	2.520458	1.008299	0.156774
38	7	2.491413	-1.15813	-0.23304
39	1	2.172753	1.946016	0.311512
40	1	-0.42305	3.053036	0.338747

Table D8: XYZ coordinate of optimized MC3 of DEAHPIP-b in water.

(a) in ground state

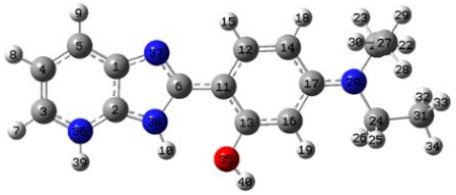

Center Number	Atomic Number	Coordinates (Angstroms) X	Y	Z
1	6	-3.70689	-0.86861	0.129611
2	6	-3.7619	0.531224	-0.09395
3	6	-6.09825	0.497219	-0.17238
4	6	-6.09943	-0.86555	0.045382
5	6	-4.89995	-1.5766	0.200449
6	6	-1.67469	-0.15307	0.083914
7	1	-6.99402	1.085684	-0.29898
8	1	-7.05061	-1.37698	0.09342
9	1	-4.90517	-2.64601	0.369677
10	1	-2.13057	1.908603	-0.25328
11	6	-0.23393	-0.08794	0.11531
12	6	0.507659	-1.27553	0.299576
13	6	0.515118	1.098281	-0.04283
14	6	1.88069	-1.29772	0.334233
15	1	-0.03969	-2.20244	0.413929
16	6	1.900944	1.096389	-0.00939
17	6	2.637396	-0.09608	0.196843
18	1	2.372562	-2.24848	0.470076
19	1	2.40482	2.039854	-0.16169
20	7	4.006812	-0.0892	0.271342
21	6	4.758816	-1.34904	0.180706
22	1	5.739601	-1.18356	0.620613
23	1	4.27918	-2.09259	0.816651
24	6	4.72509	1.182482	0.05523
25	1	4.627545	1.49315	-0.99409
26	1	4.229189	1.944111	0.659977
27	6	4.910731	-1.87871	-1.24918
28	1	5.441822	-1.16126	-1.88008
29	1	5.482072	-2.81099	-1.2419
30	1	3.938263	-2.07914	-1.70516
31	6	6.1999	1.17345	0.446327
32	1	6.341638	0.868183	1.486032
33	1	6.80769	0.532238	-0.19457
34	1	6.580661	2.192308	0.34334
35	8	-0.17312	2.264874	-0.24407
36	7	-4.923	1.182891	-0.24003
37	7	-2.3963	-1.25625	0.23451
38	7	-2.48698	0.968303	-0.11862
39	1	-4.94222	2.18448	-0.4056
40	1	0.430726	3.012474	-0.33547

(b) in excited state

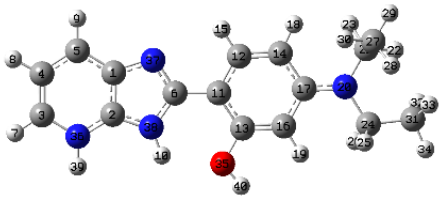

Center Number	Atomic Number	Coordinates (Angstroms) X	Y	Z
1	6	3.708539	-0.85896	-0.10193
2	6	3.78512	0.517887	0.086265
3	6	6.141664	0.44305	0.137074
4	6	6.101707	-0.92319	-0.04941
5	6	4.895682	-1.63878	-0.1764
6	6	1.683125	-0.10315	-0.05876
7	1	7.059605	1.001861	0.236024
8	1	7.049553	-1.44467	-0.0966
9	1	4.871361	-2.70904	-0.32132
10	1	2.186676	1.942664	0.226972
11	6	0.219696	-0.05138	-0.08943
12	6	-0.49945	-1.24941	-0.25379
13	6	-0.53406	1.145653	0.042536
14	6	-1.87449	-1.28172	-0.29673
15	1	0.060573	-2.16932	-0.35023
16	6	-1.91484	1.134029	0.004181
17	6	-2.63371	-0.07724	-0.17393
18	1	-2.36081	-2.23546	-0.42504
19	1	-2.43255	2.073534	0.125646
20	7	-3.99948	-0.08641	-0.22176
21	6	-4.74877	-1.35039	-0.2637
22	1	-5.705	-1.14992	-0.73803
23	1	-4.22698	-2.04795	-0.91544
24	6	-4.73971	1.18573	-0.05441
25	1	-4.57969	1.536434	0.972144
26	1	-4.27927	1.917592	-0.72059
27	6	-4.9675	-1.95975	1.128169
28	1	-5.52543	-1.27934	1.774551
29	1	-5.54231	-2.88271	1.024088
30	1	-4.01758	-2.1959	1.61173
31	6	-6.23236	1.135594	-0.35197
32	1	-6.43597	0.831274	-1.38048
33	1	-6.78176	0.485599	0.330251
34	1	-6.62099	2.148032	-0.22409
35	8	0.165503	2.300448	0.212505
36	7	4.971963	1.19362	0.208084
37	7	2.380282	-1.22447	-0.1894
38	7	2.507976	0.990294	0.111883
39	1	5.00905	2.190182	0.359765
40	1	-0.42164	3.064359	0.282253

Table D9: XYZ coordinate of optimized DC1 of DEAHPIP-b in water.

(a) in ground state

Center Number	Atomic Number	Coordinates (Angstroms) X	Y	Z
1	6	-3.87769	0.562626	0.057647
2	6	-3.83585	-0.83158	-0.07528
3	6	-6.05888	-1.01931	-0.11185
4	6	-6.21618	0.372224	0.019806
5	6	-5.10858	1.207297	0.10835
6	6	-1.73247	-0.07114	0.0132
7	1	-6.93484	-1.65439	-0.1796
8	1	-7.21488	0.787358	0.05099
9	1	-5.19817	2.280865	0.209579
10	1	-2.15247	-2.12721	-0.1976
11	6	-0.27982	-0.03284	0.029422
12	6	0.461679	-1.22655	-0.01652
13	6	0.424594	1.190755	0.088463
14	6	1.844394	-1.22619	-0.0125
15	1	-0.03939	-2.1843	-0.05096
16	6	1.820862	1.198095	0.093206
17	6	2.506064	-0.00193	0.040846
18	1	2.381382	-2.16346	-0.05543
19	1	2.349063	2.143327	0.139186
20	7	3.983304	0.03379	0.049834
21	6	4.536615	-0.58929	1.338486
22	1	3.968092	-0.12971	2.146021
23	1	4.286955	-1.6477	1.292528
24	6	4.597607	-0.55248	-1.24148
25	1	5.006983	-1.52531	-0.97596
26	1	3.769364	-0.7017	-1.9297
27	6	6.026716	-0.36368	1.516011
28	1	6.278987	0.69899	1.525011
29	1	6.307422	-0.77909	2.485887
30	1	6.622349	-0.87109	0.756643
31	6	5.640124	0.373424	-1.84614
32	1	5.20332	1.334919	-2.12644
33	1	6.484743	0.546331	-1.17868
34	1	6.021077	-0.09591	-2.75542
35	8	-0.28921	2.337089	0.139623
36	7	-4.87555	-1.64272	-0.16173
37	7	-2.56134	0.985887	0.107551
38	7	-2.49309	-1.18052	-0.09876
39	1	-2.22014	1.937465	0.194872
40	1	4.25129	1.020302	0.074239
41	1	0.274077	3.122007	0.169533

(b) in excited state

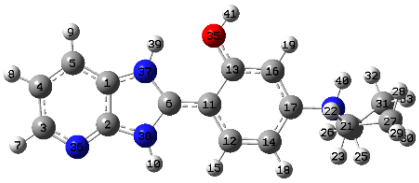

Center Number	Atomic Number	Coordinates (Angstroms) X	Y	Z
1	6	3.88273	0.580812	-0.0429
2	6	3.819843	-0.85095	0.067023
3	6	6.046189	-1.05444	0.1099
4	6	6.221181	0.348101	0.001829
5	6	5.127746	1.206228	-0.07734
6	6	1.708847	-0.04121	-0.0176
7	1	6.917762	-1.69623	0.170676
8	1	7.228064	0.744392	-0.01712
9	1	5.234147	2.27929	-0.15892
10	1	2.158872	-2.13173	0.165673
11	6	0.315598	-0.01784	-0.03734
12	6	-0.45221	-1.23119	0.024388
13	6	-0.44441	1.224876	-0.11447
14	6	-1.82576	-1.21453	0.02342
15	1	0.045538	-2.18924	0.069371
16	6	-1.83051	1.223487	-0.11662
17	6	-2.51492	0.012111	-0.04416
18	1	-2.36524	-2.151	0.079313
19	1	-2.36266	2.166027	-0.17609
20	7	-3.98568	0.028015	-0.04827
21	6	-4.54504	-0.61141	-1.32912
22	1	-3.98653	-0.15251	-2.14376
23	1	-4.28449	-1.66694	-1.27584
24	6	-4.59569	-0.55513	1.249453
25	1	-5.00452	-1.53002	0.990007
26	1	-3.76347	-0.69909	1.934241
27	6	-6.03908	-0.40142	-1.49811
28	1	-6.30064	0.658953	-1.51606
29	1	-6.32265	-0.82924	-2.46191
30	1	-6.6251	-0.90601	-0.72941
31	6	-5.63663	0.372836	1.853864
32	1	-5.20003	1.336931	2.125568
33	1	-6.48456	0.539915	1.188987
34	1	-6.0124	-0.09085	2.768329
35	8	0.272189	2.355791	-0.18077
36	7	4.853883	-1.67152	0.144046
37	7	2.599638	1.026495	-0.08931
38	7	2.500732	-1.18559	0.076928
39	1	2.29264	1.988203	-0.16332
40	1	-4.26536	1.011162	-0.07902
41	1	-0.28425	3.147784	-0.22172

Table D10: XYZ coordinate of optimized DC2 of DEAHPIP-b in water.

(a) in ground state

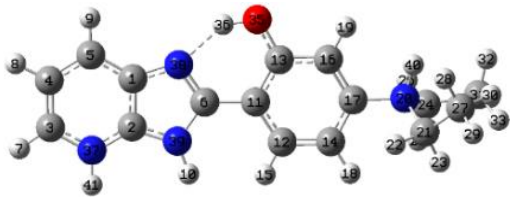

Center Number	Atomic Number	Coordinates (Angstroms) X	Y	Z
1	6	-3.76816	0.59804	-0.05284
2	6	-3.79032	-0.80739	0.072675
3	6	-6.12239	-0.8243	0.117894
4	6	-6.15261	0.552589	-0.00425
5	6	-4.96886	1.293963	-0.09249
6	6	-1.71597	-0.08713	-0.02984
7	1	-7.00914	-1.43579	0.188634
8	1	-7.11406	1.045286	-0.03071
9	1	-4.98876	2.371966	-0.18842
10	1	-2.18367	-2.18243	0.169926
11	6	-0.26429	-0.07896	-0.04823
12	6	0.492749	-1.26079	0.024538
13	6	0.415582	1.164522	-0.13394
14	6	1.875654	-1.241	0.023824
15	1	0.001017	-2.22328	0.082273
16	6	1.817248	1.183368	-0.13438
17	6	2.516326	-0.00357	-0.05307
18	1	2.428957	-2.1676	0.089233
19	1	2.31853	2.1417	-0.19779
20	7	3.995347	0.056512	-0.0483
21	6	4.602779	-0.4776	1.26617
22	1	3.770148	-0.60256	1.954008
23	1	5.01563	-1.45947	1.041852
24	6	4.57398	-0.59452	-1.3089
25	1	4.340789	-1.65517	-1.23572
26	1	4.007541	-0.16872	-2.13618
27	6	5.639619	0.471234	1.845062
28	1	5.198569	1.441146	2.087157
29	1	6.014958	0.036579	2.773706
30	1	6.488582	0.622758	1.17808
31	6	6.062635	-0.35151	-1.47891
32	1	6.298834	0.714324	-1.51596
33	1	6.658154	-0.82702	-0.69904
34	1	6.360228	-0.79029	-2.43336
35	8	-0.2101	2.345476	-0.21348
36	1	-1.18911	2.192302	-0.20272
37	7	-4.94006	-1.49113	0.155251
38	7	-2.45602	1.005847	-0.11381
39	7	-2.50204	-1.22598	0.086494
40	1	4.243327	1.047383	-0.10048
41	1	-4.94422	-2.50334	0.246105

(b) in excited state

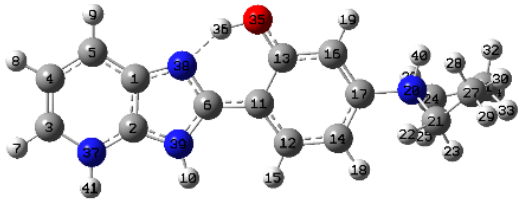

Center Number	Atomic Number	Coordinates (Angstroms) X	Y	Z
1	6	-3.74701	0.60015	-0.05034
2	6	-3.82978	-0.79661	0.069197
3	6	-6.18326	-0.70588	0.101808
4	6	-6.13796	0.667755	-0.01612
5	6	-4.93083	1.381061	-0.0962
6	6	-1.71641	-0.20202	-0.0195
7	1	-7.09923	-1.2718	0.164681
8	1	-7.08161	1.196748	-0.04627
9	1	-4.90072	2.456539	-0.18746
10	1	-2.29894	-2.25708	0.164182
11	6	-0.27445	-0.20321	-0.037
12	6	0.522541	-1.33646	0.020085
13	6	0.396899	1.090323	-0.11799
14	6	1.921704	-1.24464	0.016836
15	1	0.081047	-2.32249	0.0705
16	6	1.814252	1.169073	-0.1214
17	6	2.552062	0.011109	-0.05032
18	1	2.501577	-2.15607	0.074954
19	1	2.265418	2.151693	-0.17973
20	7	4.0228	0.091452	-0.04892
21	6	4.647658	-0.47198	1.25043
22	1	3.818925	-0.65525	1.930529
23	1	5.099399	-1.42639	0.98752
24	6	4.609349	-0.51577	-1.33306
25	1	4.392737	-1.58186	-1.28979
26	1	4.035954	-0.073	-2.14643
27	6	5.644544	0.494518	1.867579
28	1	5.167447	1.438781	2.139899
29	1	6.029807	0.040946	2.782979
30	1	6.491273	0.697674	1.211419
31	6	6.093878	-0.24439	-1.49247
32	1	6.312335	0.825561	-1.50326
33	1	6.695789	-0.7299	-0.72387
34	1	6.39893	-0.65481	-2.45712
35	8	-0.28088	2.1968	-0.18957
36	1	-1.31097	1.957051	-0.17398
37	7	-5.01314	-1.45471	0.147161
38	7	-2.42554	0.933443	-0.10167
39	7	-2.56291	-1.28386	0.087039
40	1	4.257866	1.086805	-0.0744
41	1	-5.05751	-2.46015	0.237648

Table D11: XYZ coordinate of optimized keto-DC2 of DEAHPIP-b in the excited state in water.

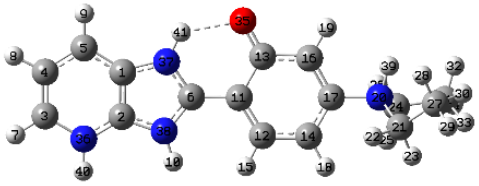

Center Number	Atomic Number	Coordinates (Angstroms)		
		X	Y	Z
1	6	-3.8372	0.597706	-0.02053
2	6	-3.82013	-0.78574	0.048366
3	6	-6.17048	-0.84448	0.052638
4	6	-6.21038	0.52996	-0.01565
5	6	-5.04703	1.322996	-0.05603
6	6	-1.70923	-0.10349	0.009075
7	1	-7.05233	-1.46462	0.083665
8	1	-7.18354	1.001861	-0.03876
9	1	-5.077	2.400058	-0.11036
10	1	-2.19343	-2.15545	0.099344
11	6	-0.24654	-0.07491	0.003346
12	6	0.500854	-1.22257	0.12748
13	6	0.426391	1.217059	-0.13201
14	6	1.916313	-1.1949	0.115138
15	1	0.03207	-2.19142	0.241855
16	6	1.866664	1.206905	-0.14403
17	6	2.569695	0.024757	-0.02184
18	1	2.458153	-2.12449	0.22121
19	1	2.361833	2.164383	-0.25303
20	7	4.047942	0.066072	-0.05008
21	6	4.688728	-0.49651	1.237665
22	1	3.875949	-0.63146	1.9472
23	1	5.091507	-1.47486	0.982182
24	6	4.581376	-0.57362	-1.33929
25	1	4.330275	-1.63115	-1.27521
26	1	3.999534	-0.12434	-2.14302
27	6	5.744711	0.437881	1.804942
28	1	5.314272	1.404448	2.077306
29	1	6.143766	-0.01623	2.714136
30	1	6.575375	0.598317	1.117272
31	6	6.068298	-0.35351	-1.54711
32	1	6.321337	0.708512	-1.57819
33	1	6.677386	-0.84938	-0.79088
34	1	6.330324	-0.78506	-2.5152
35	8	-0.21126	2.297567	-0.23167
36	7	-4.96076	-1.52514	0.085321
37	7	-2.50793	0.97414	-0.04167
38	7	-2.51006	-1.19521	0.065593
39	1	4.306255	1.054938	-0.09391
40	1	-4.94273	-2.53499	0.128495
41	1	-2.09565	1.906237	-0.10784

Table D12: XYZ coordinate of optimized DC3 of DEAHPIP-b in water.

(a) in ground state

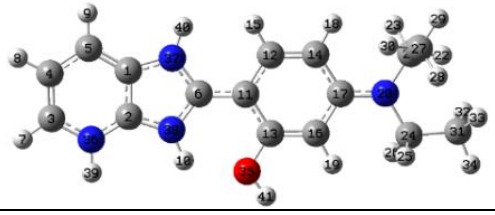

Center Number	Atomic Number	Coordinates (Angstroms) X	Y	Z
1	6	3.755696	-0.85913	-0.12302
2	6	3.746605	0.526482	0.090085
3	6	6.081196	0.562416	0.151254
4	6	6.126452	-0.80026	-0.05968
5	6	4.950365	-1.55026	-0.20254
6	6	1.622734	-0.13566	-0.05565
7	1	6.959022	1.179017	0.268914
8	1	7.091169	-1.28402	-0.11195
9	1	4.982421	-2.61918	-0.36618
10	1	2.088043	1.882724	0.257767
11	6	0.212768	-0.1074	-0.07461
12	6	-0.54598	-1.30272	-0.21588
13	6	-0.53127	1.102737	0.053337
14	6	-1.90961	-1.30633	-0.24995
15	1	-0.04187	-2.25803	-0.29058
16	6	-1.90719	1.112497	0.018694
17	6	-2.6563	-0.08391	-0.15608
18	1	-2.41367	-2.25455	-0.34599
19	1	-2.40428	2.063105	0.1396
20	7	-4.00759	-0.06484	-0.22916
21	6	-4.78413	-1.3173	-0.24771
22	1	-5.73239	-1.10975	-0.73603
23	1	-4.27623	-2.03547	-0.88972
24	6	-4.72141	1.225821	-0.06781
25	1	-4.59817	1.571346	0.965314
26	1	-4.22911	1.954177	-0.71471
27	6	-5.02757	-1.90371	1.14563
28	1	-5.57983	-1.20323	1.776547
29	1	-5.61685	-2.82013	1.059073
30	1	-4.08867	-2.14806	1.647816
31	6	-6.20296	1.210519	-0.42546
32	1	-6.37148	0.903378	-1.45994
33	1	-6.79487	0.574908	0.235077
34	1	-6.57681	2.231291	-0.31848
35	8	0.180809	2.249263	0.216336
36	7	4.887181	1.211339	0.223467
37	7	2.425657	-1.22365	-0.20784
38	7	2.454793	0.943183	0.124917
39	1	4.87528	2.215153	0.384176
40	1	2.099459	-2.16512	-0.37409
41	1	-0.39436	3.023349	0.279275

(b) in excited state

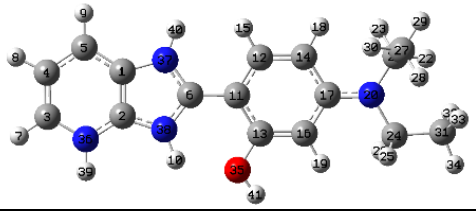

Center Number	Atomic Number	Coordinates (Angstroms) X	Y	Z
1	6	3.770578	-0.83313	-0.17278
2	6	3.766956	0.505637	0.173066
3	6	6.116244	0.52361	0.230361
4	6	6.140777	-0.81088	-0.11198
5	6	4.968533	-1.56028	-0.33457
6	6	1.64796	-0.11008	-0.05718
7	1	7.007434	1.107579	0.400092
8	1	7.10848	-1.28415	-0.21126
9	1	4.984612	-2.60378	-0.6083
10	1	2.106904	1.856407	0.434351
11	6	0.18461	-0.09168	-0.07992
12	6	-0.54198	-1.29042	-0.1529
13	6	-0.54375	1.121763	-0.02162
14	6	-1.91991	-1.3062	-0.20168
15	1	-0.02772	-2.24198	-0.16488
16	6	-1.9277	1.124044	-0.06313
17	6	-2.65636	-0.08665	-0.16602
18	1	-2.41647	-2.26072	-0.26287
19	1	-2.43349	2.075413	-0.0017
20	7	-4.02694	-0.07995	-0.21804
21	6	-4.79044	-1.33274	-0.20474
22	1	-5.74212	-1.14239	-0.69183
23	1	-4.27187	-2.06867	-0.81585
24	6	-4.74744	1.209964	-0.14167
25	1	-4.55091	1.641369	0.847786
26	1	-4.29295	1.877647	-0.87742
27	6	-5.02547	-1.86971	1.217354
28	1	-5.57752	-1.1504	1.824457
29	1	-5.61307	-2.78761	1.149017
30	1	-4.0818	-2.09598	1.71687
31	6	-6.24829	1.159777	-0.38837
32	1	-6.4893	0.792696	-1.38768
33	1	-6.7824	0.564671	0.353292
34	1	-6.6188	2.184201	-0.31547
35	8	0.173131	2.268013	0.08363
36	7	4.919596	1.206316	0.377586
37	7	2.43317	-1.17638	-0.30517
38	7	2.462631	0.925925	0.235247
39	1	4.912158	2.1823	0.637969
40	1	2.101282	-2.09155	-0.57833
41	1	-0.39263	3.051154	0.109876

Table D13: XYZ coordinate of optimized TC of DEAHPIP-b in water.

(a) in ground state

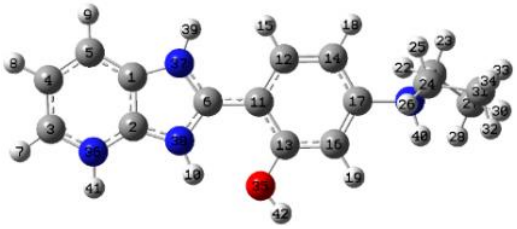

Center Number	Atomic Number	Coordinates (Angstroms) X	Y	Z
1	6	-3.78569	-0.89148	0.082898
2	6	-3.80974	0.498428	-0.04915
3	6	-6.13681	0.493495	-0.00752
4	6	-6.15207	-0.88696	0.12343
5	6	-4.96473	-1.61738	0.172005
6	6	-1.68482	-0.12907	-0.02128
7	1	-7.03272	1.094598	-0.04844
8	1	-7.10709	-1.38803	0.188126
9	1	-4.9662	-2.69438	0.274681
10	1	-2.17534	1.893375	-0.19662
11	6	-0.24151	-0.07515	-0.04615
12	6	0.514826	-1.26211	0.013805
13	6	0.444852	1.160249	-0.12327
14	6	1.894504	-1.24014	0.010972
15	1	0.027769	-2.22646	0.060314
16	6	1.840899	1.185505	-0.12753
17	6	2.539518	-0.00489	-0.05621
18	1	2.444958	-2.16863	0.066894
19	1	2.356872	2.136559	-0.1859
20	7	4.014868	0.048945	-0.05098
21	6	4.615653	-0.48866	1.269733
22	1	3.780329	-0.60554	1.955966
23	1	5.021077	-1.47347	1.045731
24	6	4.591418	-0.61042	-1.31265
25	1	4.355167	-1.66991	-1.23494
26	1	4.027221	-0.18414	-2.14116
27	6	5.657101	0.455245	1.846939
28	1	5.221774	1.427621	2.08887
29	1	6.028633	0.01778	2.775763
30	1	6.507398	0.600321	1.180428
31	6	6.080613	-0.37188	-1.47931
32	1	6.32034	0.692892	-1.51993
33	1	6.672767	-0.84802	-0.69748
34	1	6.377023	-0.81498	-2.4321
35	8	-0.2859	2.290707	-0.19082
36	7	-4.96815	1.169667	-0.09332
37	7	-2.4461	-1.23341	0.096151
38	7	-2.52143	0.938422	-0.11034
39	1	-2.09775	-2.17881	0.193444
40	1	4.273426	1.037156	-0.10427
41	1	-4.98519	2.182629	-0.1912
42	1	0.258267	3.089738	-0.22255

(b) in excited state

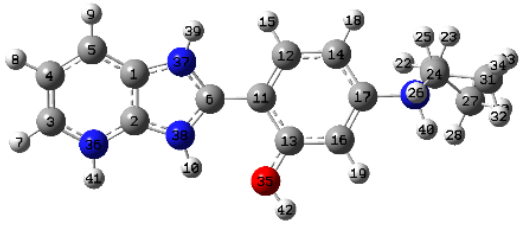

Center Number	Atomic Number	Coordinates (Angstroms) X	Y	Z
1	6	-3.80973	-0.89122	0.020976
2	6	-3.84618	0.511448	0.073589
3	6	-6.19475	0.466113	0.165482
4	6	-6.18463	-0.90762	0.110104
5	6	-4.98552	-1.64398	0.031661
6	6	-1.70685	-0.08717	-0.06074
7	1	-7.09539	1.056792	0.224165
8	1	-7.13414	-1.42432	0.126544
9	1	-4.97681	-2.72262	-0.01724
10	1	-2.28677	1.943079	0.028802
11	6	-0.25979	-0.05442	-0.02934
12	6	0.485779	-1.14658	0.370074
13	6	0.480772	1.121182	-0.42285
14	6	1.900795	-1.12898	0.351944
15	1	0.006488	-2.04945	0.721952
16	6	1.896983	1.151941	-0.41785
17	6	2.593953	0.023562	-0.04031
18	1	2.427702	-2.02084	0.663552
19	1	2.396934	2.063375	-0.72393
20	7	4.063621	0.027644	-0.05436
21	6	4.671716	-0.22383	1.351551
22	1	3.835507	-0.24083	2.046693
23	1	5.117525	-1.21575	1.319347
24	6	4.608578	-0.92177	-1.13912
25	1	4.340614	-1.92812	-0.82139
26	1	4.052135	-0.6757	-2.04246
27	6	5.668398	0.854965	1.733483
28	1	5.195058	1.838526	1.772401
29	1	6.043735	0.626094	2.732802
30	1	6.521489	0.892533	1.055123
31	6	6.10349	-0.77124	-1.35046
32	1	6.373348	0.245173	-1.6444
33	1	6.6857	-1.06279	-0.47594
34	1	6.383152	-1.43808	-2.16851
35	8	-0.23477	2.160899	-0.79162
36	7	-5.01474	1.182367	0.146169
37	7	-2.47736	-1.21488	-0.05377
38	7	-2.57583	0.971545	0.021184
39	1	-2.12631	-2.156	-0.17091
40	1	4.356624	0.967717	-0.335
41	1	-5.03944	2.193926	0.180499
42	1	0.292992	2.938951	-1.04284

Table D14: XYZ coordinate of optimized MA2 of DEAMPIP-b in water.

(a) in ground state

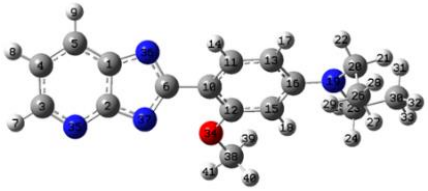

Center Number	Atomic Number	Coordinates (Angstroms) X	Y	Z
1	6	3.811202	-0.79944	-0.49192
2	6	3.824007	0.249032	0.490432
3	6	6.088102	0.195165	0.641004
4	6	6.182111	-0.82758	-0.31708
5	6	5.025665	-1.34588	-0.90528
6	6	1.811972	-0.17179	-0.07919
7	1	6.996488	0.586967	1.092089
8	1	7.160314	-1.20703	-0.59031
9	1	5.075453	-2.13821	-1.64622
10	6	0.333806	-0.17269	-0.11867
11	6	-0.34691	-1.39472	-0.20071
12	6	-0.47515	0.984393	-0.09257
13	6	-1.72936	-1.50354	-0.23982
14	1	0.246444	-2.30114	-0.22556
15	6	-1.87007	0.894964	-0.12494
16	6	-2.53964	-0.3467	-0.21351
17	1	-2.16414	-2.491	-0.2911
18	1	-2.44064	1.806677	-0.08296
19	7	-3.93049	-0.41855	-0.3061
20	6	-4.60407	-1.66356	0.083119
21	1	-5.60541	-1.64917	-0.34483
22	1	-4.09964	-2.50248	-0.39601
23	6	-4.70151	0.829075	-0.1946
24	1	-4.63613	1.243128	0.823788
25	1	-4.23772	1.559996	-0.85944
26	6	-4.69038	-1.89383	1.597253
27	1	-5.25325	-1.09496	2.087908
28	1	-5.19899	-2.83977	1.805031
29	1	-3.6962	-1.93678	2.049007
30	6	-6.16975	0.713802	-0.60013
31	1	-6.27552	0.281204	-1.59861
32	1	-6.76152	0.121328	0.100376
33	1	-6.60039	1.718024	-0.62168
34	8	0.16567	2.190609	-0.06418
35	7	4.937683	0.74475	1.057473
36	7	2.512129	-1.05284	-0.83997
37	7	2.539036	0.632903	0.737891
38	6	-0.60165	3.39229	-0.08036
39	1	-1.21427	3.465494	-0.98438
40	1	-1.24301	3.471061	0.802874
41	1	0.124029	4.203899	-0.06988

(b) in excited state

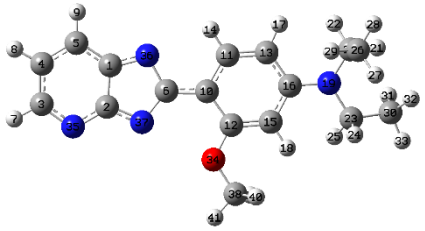

Center Number	Atomic Number	Coordinates (Angstroms) X	Y	Z
1	6	3.767448	-1.00639	-0.09891
2	6	3.85812	0.443312	0.00821
3	6	6.136383	0.37211	-0.00014
4	6	6.154035	-1.03629	-0.10165
5	6	4.964675	-1.77055	-0.15319
6	6	1.787389	-0.13817	-0.03289
7	1	7.086544	0.901247	0.037473
8	1	7.11637	-1.53666	-0.13778
9	1	4.954599	-2.8524	-0.22922
10	6	0.372101	-0.13666	-0.03859
11	6	-0.32827	-1.38944	-0.18422
12	6	-0.49572	1.022821	0.089952
13	6	-1.6967	-1.48943	-0.26057
14	1	0.275156	-2.28335	-0.25129
15	6	-1.87139	0.913093	0.00853
16	6	-2.52776	-0.3365	-0.19201
17	1	-2.12816	-2.47205	-0.39104
18	1	-2.46212	1.804112	0.136772
19	7	-3.907	-0.41572	-0.34457
20	6	-4.59921	-1.6723	-0.03464
21	1	-5.56846	-1.65249	-0.52944
22	1	-4.05482	-2.50008	-0.48779
23	6	-4.70184	0.820368	-0.31122
24	1	-4.77226	1.205661	0.718605
25	1	-4.16033	1.568821	-0.89036
26	6	-4.78259	-1.92331	1.468825
27	1	-5.37937	-1.13405	1.933445
28	1	-5.29957	-2.87426	1.625233
29	1	-3.81737	-1.97006	1.978834
30	6	-6.10537	0.699943	-0.9027
31	1	-6.07873	0.280807	-1.91188
32	1	-6.77752	0.096333	-0.29023
33	1	-6.53535	1.702612	-0.96556
34	8	0.118472	2.211522	0.317787
35	7	5.031013	1.142513	0.0579
36	7	2.480716	-1.3621	-0.12818
37	7	2.626632	0.96297	0.046955
38	6	-0.66779	3.394762	0.443771
39	1	-1.24365	3.588303	-0.46656
40	1	-1.34652	3.333814	1.300117
41	1	0.043171	4.203611	0.602371

Table D15: XYZ coordinate of optimized neutral species of DEAMPIP-b in water.

(a) in ground state

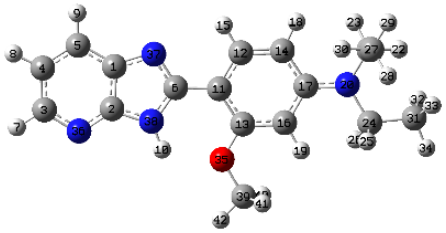

Center Number	Atomic Number	Coordinates (Angstroms) X	Y	Z
1	6	3.786319	-1.01012	-0.1098
2	6	3.862049	0.395346	0.065053
3	6	6.102778	0.421626	0.12585
4	6	6.159267	-0.96883	-0.04395
5	6	4.987033	-1.71632	-0.16597
6	6	1.752839	-0.29403	-0.07478
7	1	7.021232	0.991912	0.219688
8	1	7.126672	-1.45494	-0.07914
9	1	5.009281	-2.79204	-0.29791
10	1	2.200214	1.758905	0.190324
11	6	0.29768	-0.24737	-0.10931
12	6	-0.41903	-1.44783	-0.25919
13	6	-0.47386	0.933251	0.005593
14	6	-1.79614	-1.50308	-0.30654
15	1	0.148546	-2.36634	-0.33951
16	6	-1.86449	0.895962	-0.0413
17	6	-2.5723	-0.3176	-0.21784
18	1	-2.26536	-2.46873	-0.41851
19	1	-2.40469	1.819568	0.073528
20	7	-3.94997	-0.33816	-0.31704
21	6	-4.67465	-1.60051	-0.11994
22	1	-5.66257	-1.4906	-0.56272
23	1	-4.18522	-2.38289	-0.6998
24	6	-4.69109	0.92453	-0.14893
25	1	-4.62726	1.270885	0.892942
26	1	-4.19457	1.678009	-0.76311
27	6	-4.80553	-2.02477	1.347448
28	1	-5.34925	-1.27464	1.92786
29	1	-5.35436	-2.96819	1.41643
30	1	-3.82503	-2.16706	1.808199
31	6	-6.15543	0.878708	-0.57793
32	1	-6.26308	0.524138	-1.60624
33	1	-6.77251	0.256952	0.073382
34	1	-6.55436	1.894905	-0.53116
35	8	0.212819	2.103694	0.174821
36	7	4.960789	1.12874	0.183547
37	7	2.470453	-1.40868	-0.19319
38	7	2.554042	0.818341	0.08324
39	6	-0.49976	3.340505	0.298996
40	1	-1.08851	3.544342	-0.59853
41	1	-1.14752	3.332053	1.178821
42	1	0.264514	4.105745	0.416111

(b) in excited state

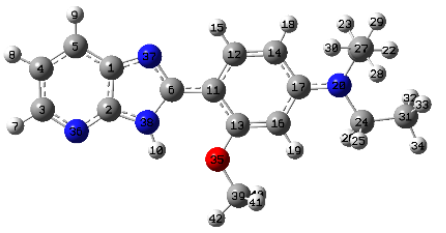

Center Number	Atomic Number	Coordinates (Angstroms) X	Y	Z
1	6	3.764345	-1.01999	-0.10869
2	6	3.865243	0.402157	0.054055
3	6	6.116841	0.384807	0.102601
4	6	6.150538	-1.0076	-0.05443
5	6	4.975486	-1.75908	-0.16509
6	6	1.729119	-0.25261	-0.06842
7	1	7.046881	0.93825	0.186138
8	1	7.117515	-1.49757	-0.08827
9	1	4.983839	-2.83526	-0.28547
10	1	2.261838	1.800125	0.179041
11	6	0.312859	-0.22564	-0.09424
12	6	-0.41211	-1.44948	-0.23653
13	6	-0.49139	0.970692	0.02049
14	6	-1.78489	-1.49504	-0.2837
15	1	0.158253	-2.36482	-0.31134
16	6	-1.86726	0.924344	-0.02856
17	6	-2.56942	-0.30667	-0.19412
18	1	-2.2572	-2.45919	-0.3977
19	1	-2.41724	1.843268	0.081426
20	7	-3.94462	-0.33819	-0.27428
21	6	-4.66637	-1.60871	-0.14058
22	1	-5.64747	-1.48464	-0.59184
23	1	-4.16018	-2.36883	-0.73504
24	6	-4.70287	0.922601	-0.17137
25	1	-4.64206	1.300329	0.859691
26	1	-4.20336	1.655542	-0.80711
27	6	-4.81409	-2.07564	1.314528
28	1	-5.36901	-1.34562	1.908559
29	1	-5.36071	-3.02205	1.33943
30	1	-3.83824	-2.22904	1.780394
31	6	-6.16552	0.850051	-0.59792
32	1	-6.27244	0.473556	-1.6179
33	1	-6.77605	0.241368	0.071031
34	1	-6.56816	1.865283	-0.57327
35	8	0.207659	2.126322	0.18783
36	7	4.976691	1.131634	0.161988
37	7	2.47224	-1.3996	-0.18089
38	7	2.578692	0.847624	0.074064
39	6	-0.49693	3.367487	0.315973
40	1	-1.08531	3.573844	-0.58154
41	1	-1.14546	3.356059	1.195483
42	1	0.270727	4.128459	0.435528

Table D16: XYZ coordinate of optimized MC1 of DEAHPIP-b in water.

(a) in ground state

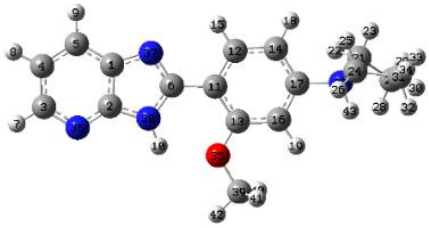

Center Number	Atomic Number	Coordinates (Angstroms) X	Y	Z
1	6	-3.79594	-1.06451	0.047858
2	6	-3.92141	0.344888	-0.01372
3	6	-6.15903	0.297782	-0.00786
4	6	-6.16577	-1.10631	0.05345
5	6	-4.97	-1.81848	0.082629
6	6	-1.79597	-0.27854	0.008847
7	1	-7.09953	0.838638	-0.02999
8	1	-7.11603	-1.62522	0.077563
9	1	-4.95064	-2.90102	0.12938
10	1	-2.31683	1.774767	-0.07999
11	6	-0.33059	-0.1992	-0.00119
12	6	0.394295	-1.39707	0.045408
13	6	0.389908	1.01787	-0.05485
14	6	1.781318	-1.42357	0.037404
15	1	-0.1599	-2.32476	0.088874
16	6	1.789098	1.001931	-0.06587
17	6	2.457485	-0.21222	-0.02013
18	1	2.305544	-2.36882	0.080161
19	1	2.345506	1.927875	-0.11001
20	7	3.938873	-0.19339	-0.04444
21	6	4.566089	-0.79497	1.229787
22	1	3.745401	-0.95266	1.924799
23	1	4.972864	-1.76525	0.950388
24	6	4.470528	-0.80832	-1.34245
25	1	4.208539	-1.86423	-1.30461
26	1	3.897358	-0.33585	-2.1392
27	6	5.616914	0.121764	1.835168
28	1	5.184761	1.081871	2.127786
29	1	6.006105	-0.35576	2.736662
30	1	6.455497	0.299967	1.161184
31	6	5.961117	-0.59873	-1.53875
32	1	6.225202	0.461245	-1.54244
33	1	6.56116	-1.11735	-0.7903
34	1	6.226081	-1.0096	-2.515
35	8	-0.32568	2.167468	-0.09396
36	7	-5.04812	1.047374	-0.0425
37	7	-2.46586	-1.42101	0.060581
38	7	-2.63039	0.81485	-0.03718
39	6	0.352732	3.434413	-0.13851
40	1	0.971142	3.571757	0.750839
41	1	0.958623	3.516207	-1.04323
42	1	-0.43593	4.182246	-0.15623
43	1	4.214236	0.790918	-0.06356

(b) in excited state

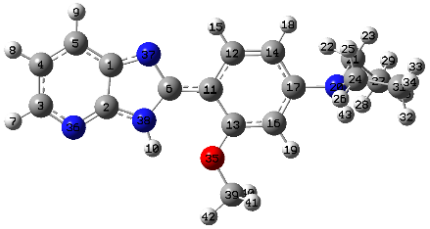

Center Number	Atomic Number	Coordinates (Angstroms) X	Y	Z
1	6	-3.76205	-1.07854	0.030774
2	6	-3.90918	0.3643	-0.01291
3	6	-6.14688	0.276102	-0.01482
4	6	-6.14206	-1.13572	0.028041
5	6	-4.95268	-1.84886	0.051962
6	6	-1.75891	-0.2353	0.007777
7	1	-7.09299	0.806403	-0.03291
8	1	-7.09442	-1.65162	0.041833
9	1	-4.92429	-2.93067	0.084584
10	1	-2.3454	1.814556	-0.05423
11	6	-0.36076	-0.17964	0.005755
12	6	0.385593	-1.41667	0.039384
13	6	0.411591	1.051804	-0.03019
14	6	1.757332	-1.43037	0.032871
15	1	-0.17157	-2.34173	0.069395
16	6	1.798082	1.022228	-0.03641
17	6	2.461835	-0.21337	-0.00344
18	1	2.284563	-2.37614	0.059938
19	1	2.364614	1.942801	-0.06559
20	7	3.935367	-0.21741	-0.04689
21	6	4.586861	-0.91116	1.17122
22	1	3.768323	-1.23046	1.810773
23	1	5.097999	-1.79591	0.795953
24	6	4.456442	-0.7495	-1.38889
25	1	4.204774	-1.80886	-1.41092
26	1	3.868147	-0.23601	-2.14809
27	6	5.526472	0.023884	1.913328
28	1	4.996621	0.901918	2.290368
29	1	5.937195	-0.51075	2.772244
30	1	6.361782	0.350544	1.291325
31	6	5.942628	-0.50597	-1.58615
32	1	6.186311	0.558332	-1.54427
33	1	6.55771	-1.04303	-0.86301
34	1	6.21122	-0.86866	-2.58057
35	8	-0.30487	2.191554	-0.0543
36	7	-5.03633	1.051878	-0.03591
37	7	-2.47418	-1.42656	0.042588
38	7	-2.63413	0.846824	-0.02584
39	6	0.363422	3.465047	-0.0928
40	1	0.984013	3.59536	0.79595
41	1	0.968056	3.549463	-0.99802
42	1	-0.43033	4.207103	-0.10467
43	1	4.225114	0.762141	-0.00634

Table D17: XYZ coordinate of optimized MC2 of DEAMPIP-b in water.

(a) in ground state

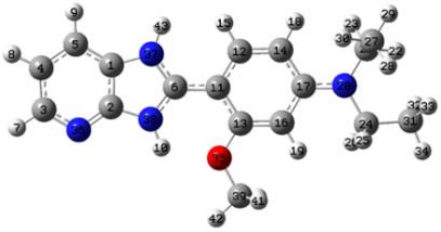

(b) in excited state

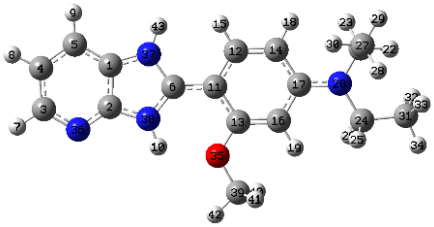

Center Number	Atomic Number	Coordinates (Angstroms) X	Y	Z
1	6	3.829069	-1.00327	-0.08882
2	6	3.845233	0.393298	0.049006
3	6	6.080767	0.480537	0.105146
4	6	6.177372	-0.91052	-0.0297
5	6	5.029001	-1.69631	-0.13138
6	6	1.699536	-0.2713	-0.06191
7	1	6.981206	1.079325	0.183254
8	1	7.155837	-1.37224	-0.05445
9	1	5.075532	-2.77249	-0.2363
10	1	2.161397	1.743643	0.149341
11	6	0.272133	-0.25887	-0.09465
12	6	-0.45989	-1.4618	-0.22931
13	6	-0.49069	0.940601	0.011667
14	6	-1.8293	-1.49847	-0.26932
15	1	0.061798	-2.40811	-0.3051
16	6	-1.87406	0.916164	-0.0306
17	6	-2.59565	-0.29662	-0.19001
18	1	-2.3102	-2.45895	-0.36551
19	1	-2.405	1.845849	0.07426
20	7	-3.95724	-0.30459	-0.27014
21	6	-4.70279	-1.57063	-0.19176
22	1	-5.67209	-1.41477	-0.65865
23	1	-4.20005	-2.31435	-0.80921
24	6	-4.69341	0.970776	-0.12719
25	1	-4.59841	1.334456	0.904096
26	1	-4.20518	1.703778	-0.77212
27	6	-4.88783	-2.08702	1.238458
28	1	-5.43764	-1.36605	1.848629
29	1	-5.45493	-3.02159	1.224007
30	1	-3.92679	-2.27915	1.721258
31	6	-6.16783	0.925382	-0.51448
32	1	-6.30886	0.581502	-1.54188
33	1	-6.76569	0.301639	0.152303
34	1	-6.55999	1.942904	-0.44819
35	8	0.214421	2.090686	0.164081
36	7	4.919745	1.154537	0.1468
37	7	2.49433	-1.37172	-0.15384
38	7	2.520053	0.800136	0.061413
39	6	-0.47222	3.347985	0.290018
40	1	-1.06035	3.556163	-0.60568
41	1	-1.11093	3.349806	1.175247
42	1	0.311397	4.093587	0.398874
43	1	2.158601	-2.31848	-0.24753

Center Number	Atomic Number	Coordinates (Angstroms) X	Y	Z
1	6	3.830282	-1.00382	-0.12949
2	6	3.853255	0.400456	0.089561
3	6	6.098967	0.457216	0.165585
4	6	6.186596	-0.9227	-0.04871
5	6	5.033234	-1.70652	-0.20611
6	6	1.696789	-0.24949	-0.0857
7	1	7.006244	1.03981	0.28382
8	1	7.16546	-1.38381	-0.09211
9	1	5.073874	-2.77423	-0.37357
10	1	2.216125	1.759738	0.238441
11	6	0.271706	-0.25168	-0.09996
12	6	-0.455	-1.46482	-0.2154
13	6	-0.50977	0.955679	0.001486
14	6	-1.83411	-1.49716	-0.26205
15	1	0.070062	-2.40911	-0.26858
16	6	-1.88765	0.923688	-0.04179
17	6	-2.59961	-0.30012	-0.18654
18	1	-2.31309	-2.45866	-0.36221
19	1	-2.426	1.850946	0.053387
20	7	-3.97689	-0.3179	-0.25191
21	6	-4.71217	-1.58056	-0.13925
22	1	-5.68964	-1.43916	-0.59215
23	1	-4.20941	-2.33972	-0.73775
24	6	-4.7175	0.955274	-0.18109
25	1	-4.61064	1.370102	0.831778
26	1	-4.22793	1.65517	-0.86184
27	6	-4.87177	-2.05906	1.313028
28	1	-5.41965	-1.32713	1.910278
29	1	-5.43167	-2.99757	1.320867
30	1	-3.90022	-2.231	1.780752
31	6	-6.1957	0.888252	-0.54582
32	1	-6.34964	0.495074	-1.55306
33	1	-6.78333	0.300657	0.161116
34	1	-6.584	1.908874	-0.52447
35	8	0.206281	2.100215	0.143563
36	7	4.939751	1.152699	0.239746
37	7	2.512822	-1.36017	-0.22528
38	7	2.552334	0.814299	0.108168
39	6	-0.4773	3.358482	0.255124
40	1	-1.0655	3.557045	-0.64343
41	1	-1.11824	3.370704	1.139429
42	1	0.305738	4.105671	0.356444
43	1	2.183642	-2.2963	-0.40805

Table D18: XYZ coordinate of optimized MC3 of DEAMPIP-b in water.

(a) in ground state

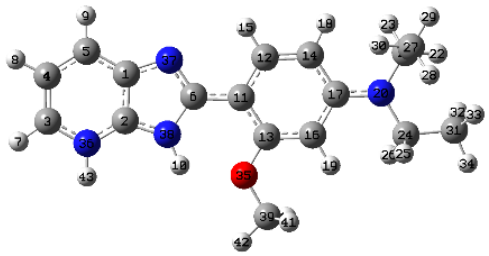

(b) in excited state

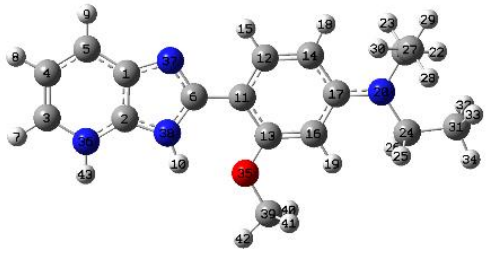

Center Number	Atomic Number	Coordinates (Angstroms) X	Y	Z
1	6	3.737114	-1.03391	-0.1033
2	6	3.788538	0.375698	0.052558
3	6	6.125605	0.35382	0.122168
4	6	6.130405	-1.01786	-0.02904
5	6	4.932856	-1.74001	-0.14451
6	6	1.702358	-0.32208	-0.08433
7	1	7.019801	0.950772	0.21546
8	1	7.083176	-1.5279	-0.05651
9	1	4.941792	-2.81631	-0.262
10	1	2.144715	1.749531	0.155121
11	6	0.261658	-0.26252	-0.11757
12	6	-0.46499	-1.46266	-0.25848
13	6	-0.4986	0.930053	-0.00481
14	6	-1.83824	-1.50445	-0.29676
15	1	0.094181	-2.38632	-0.33659
16	6	-1.88586	0.904441	-0.04416
17	6	-2.60491	-0.30761	-0.20806
18	1	-2.31803	-2.46553	-0.39845
19	1	-2.41866	1.832486	0.067404
20	7	-3.97485	-0.31749	-0.28756
21	6	-4.71254	-1.58204	-0.15573
22	1	-5.69423	-1.44366	-0.60292
23	1	-4.22249	-2.34123	-0.76481
24	6	-4.70984	0.952593	-0.1236
25	1	-4.61964	1.306004	0.912792
26	1	-4.22234	1.696113	-0.75697
27	6	-4.86127	-2.06466	1.291047
28	1	-5.40311	-1.33312	1.896102
29	1	-5.42036	-3.00408	1.314382
30	1	-3.88723	-2.23636	1.75524
31	6	-6.18347	0.910401	-0.51694
32	1	-6.31928	0.564645	-1.54468
33	1	-6.78499	0.28655	0.146615
34	1	-6.57678	1.927726	-0.45304
35	8	0.202892	2.089861	0.153772
36	7	4.947695	1.037898	0.16175
37	7	2.428002	-1.43006	-0.18465
38	7	2.512524	0.808551	0.061619
39	6	-0.49279	3.338737	0.285966
40	1	-1.0846	3.548951	-0.60737
41	1	-1.13212	3.333986	1.171284
42	1	0.283415	4.092102	0.397951
43	1	4.963737	2.046667	0.27618

Center Number	Atomic Number	Coordinates (Angstroms) X	Y	Z
1	6	3.740508	-1.02039	-0.09256
2	6	3.812052	0.360311	0.065737
3	6	6.168614	0.295129	0.118563
4	6	6.133672	-1.07494	-0.03823
5	6	4.929938	-1.79733	-0.14984
6	6	1.712019	-0.27052	-0.06765
7	1	7.08476	0.859003	0.205173
8	1	7.083415	-1.59388	-0.07411
9	1	4.909341	-2.87059	-0.27177
10	1	2.202182	1.779318	0.172701
11	6	0.247303	-0.22771	-0.10117
12	6	-0.45598	-1.43668	-0.22673
13	6	-0.5198	0.972926	-0.00981
14	6	-1.83159	-1.48701	-0.27045
15	1	0.114707	-2.35279	-0.29148
16	6	-1.90202	0.939946	-0.05433
17	6	-2.60322	-0.28832	-0.19051
18	1	-2.30633	-2.45022	-0.3674
19	1	-2.44536	1.864762	0.029473
20	7	-3.96877	-0.31739	-0.23923
21	6	-4.70133	-1.59205	-0.22579
22	1	-5.66306	-1.42396	-0.70159
23	1	-4.17459	-2.30834	-0.85307
24	6	-4.72461	0.951116	-0.12434
25	1	-4.55817	1.354934	0.881526
26	1	-4.28242	1.656151	-0.83111
27	6	-4.90317	-2.14856	1.190179
28	1	-5.46425	-1.44913	1.813194
29	1	-5.4675	-3.08184	1.128412
30	1	-3.94701	-2.35375	1.675743
31	6	-6.22019	0.867799	-0.39935
32	1	-6.43365	0.514927	-1.41022
33	1	-6.75155	0.24191	0.318899
34	1	-6.62142	1.879675	-0.31169
35	8	0.189511	2.119255	0.12507
36	7	4.996693	1.042889	0.173624
37	7	2.413285	-1.39251	-0.17292
38	7	2.53292	0.828015	0.079892
39	6	-0.49892	3.376899	0.230108
40	1	-1.08576	3.569431	-0.67039
41	1	-1.1405	3.390356	1.113685
42	1	0.282064	4.126286	0.329246
43	1	5.030432	2.04292	0.301633

Table D19: XYZ coordinate of optimized DC1 of DEAMPIP-b in water.

(a) in ground state

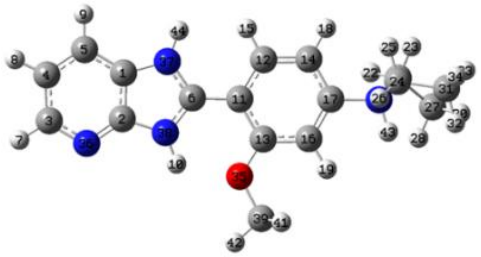

(b) in excited state

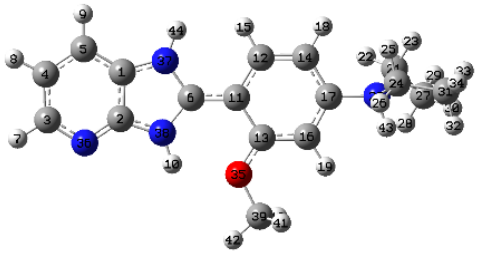

Center Number	Atomic Number	Coordinates (Angstroms) X	Y	Z
1	6	-3.84996	-1.05349	0.017873
2	6	-3.89933	0.346999	0.025817
3	6	-6.1312	0.39069	0.051374
4	6	-6.19586	-1.0143	0.044254
5	6	-5.03528	-1.77912	0.026701
6	6	-1.75045	-0.27465	-0.00229
7	1	-7.04747	0.969968	0.065162
8	1	-7.16481	-1.4959	0.052817
9	1	-5.0551	-2.86093	0.020971
10	1	-2.24855	1.739731	0.005748
11	6	-0.29817	-0.22931	-0.01053
12	6	0.44066	-1.42091	0.059787
13	6	0.405131	1.0019	-0.08237
14	6	1.824389	-1.42467	0.05403
15	1	-0.06107	-2.37644	0.130556
16	6	1.804077	1.000589	-0.09127
17	6	2.484382	-0.20319	-0.02331
18	1	2.359869	-2.36153	0.118371
19	1	2.347286	1.933285	-0.14872
20	7	3.962712	-0.17032	-0.03719
21	6	4.581382	-0.74558	1.256327
22	1	3.756716	-0.88206	1.951418
23	1	4.983114	-1.72399	0.999447
24	6	4.508651	-0.80707	-1.32205
25	1	4.255721	-1.86417	-1.26472
26	1	3.937656	-0.35367	-2.13133
27	6	5.633129	0.180394	1.844838
28	1	5.203277	1.147052	2.11806
29	1	6.017401	-0.28165	2.756444
30	1	6.474266	0.341989	1.170231
31	6	5.99856	-0.58819	-1.50959
32	1	6.254208	0.473523	-1.53044
33	1	6.596594	-1.08995	-0.74837
34	1	6.272755	-1.01413	-2.47676
35	8	-0.32352	2.130983	-0.13863
36	7	-4.99166	1.09203	0.042174
37	7	-2.5076	-1.39363	-0.00013
38	7	-2.58357	0.782122	0.011916
39	6	0.326921	3.418142	-0.21951
40	1	0.942831	3.587057	0.664724
41	1	0.923167	3.48426	-1.13047
42	1	-0.4824	4.142055	-0.25221
43	1	4.232414	0.815416	-0.07215
44	1	-2.15109	-2.33869	-0.02766

Center Number	Atomic Number	Coordinates (Angstroms) X	Y	Z
1	6	-3.83402	-1.06465	0.027149
2	6	-3.90285	0.367217	-0.0061
3	6	-6.14113	0.362682	-0.01005
4	6	-6.18563	-1.04963	0.021546
5	6	-5.01486	-1.80385	0.040841
6	6	-1.72544	-0.23774	0.010027
7	1	-7.06818	0.924703	-0.02435
8	1	-7.15095	-1.53892	0.031109
9	1	-5.01974	-2.88509	0.065095
10	1	-2.32773	1.790523	-0.0387
11	6	-0.32882	-0.214	0.014531
12	6	0.43108	-1.42743	0.06716
13	6	0.438959	1.032852	-0.03625
14	6	1.80691	-1.4189	0.054446
15	1	-0.06826	-2.38393	0.125452
16	6	1.830315	1.020778	-0.04812
17	6	2.503588	-0.19708	-0.00534
18	1	2.341034	-2.35941	0.097806
19	1	2.379383	1.951035	-0.09221
20	7	3.97456	-0.19493	-0.05041
21	6	4.626404	-0.86271	1.185249
22	1	3.808893	-1.16518	1.834756
23	1	5.133344	-1.75649	0.826959
24	6	4.491931	-0.75562	-1.38467
25	1	4.247525	-1.81672	-1.381
26	1	3.899065	-0.26191	-2.15332
27	6	5.568481	0.088472	1.902654
28	1	5.041863	0.976818	2.25901
29	1	5.976384	-0.42813	2.77382
30	1	6.40528	0.395951	1.27324
31	6	5.975739	-0.50665	-1.5877
32	1	6.212654	0.559649	-1.57059
33	1	6.594408	-1.02479	-0.85421
34	1	6.243435	-0.89053	-2.57423
35	8	-0.28685	2.148116	-0.07082
36	7	-5.01006	1.090076	-0.0244
37	7	-2.51353	-1.39122	0.037564
38	7	-2.61899	0.822387	-0.01661
39	6	0.342073	3.449144	-0.12146
40	1	0.965163	3.594371	0.761965
41	1	0.930768	3.540312	-1.03537
42	1	-0.47876	4.159608	-0.12713
43	1	4.262953	0.785876	-0.03061
44	1	-2.15403	-2.33424	0.032599

Table D20: XYZ coordinate of optimized DC2 of DEAMPIP-b in water.

(a) in ground state

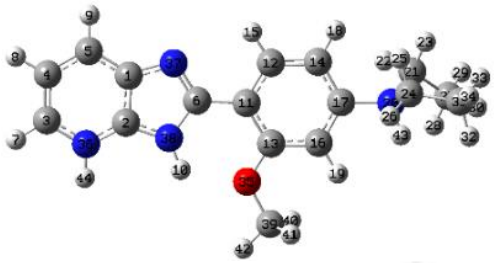

Center Number	Atomic Number	Coordinates (Angstroms) X	Y	Z
1	6	-3.75176	-1.07989	0.047731
2	6	-3.85037	0.330079	-0.01377
3	6	-6.18145	0.232958	-0.00391
4	6	-6.14025	-1.14837	0.056042
5	6	-4.91961	-1.83274	0.082664
6	6	-1.74979	-0.30441	0.009625
7	1	-7.09909	0.80105	-0.02568
8	1	-7.07565	-1.68918	0.082134
9	1	-4.88621	-2.91393	0.129078
10	1	-2.25878	1.76437	-0.07706
11	6	-0.29028	-0.21583	-0.00057
12	6	0.438629	-1.41203	0.045927
13	6	0.417644	1.008396	-0.05469
14	6	1.824105	-1.42691	0.037008
15	1	-0.10824	-2.34396	0.089918
16	6	1.816958	1.0013	-0.06681
17	6	2.490908	-0.20904	-0.02129
18	1	2.355818	-2.36767	0.080169
19	1	2.367458	1.9306	-0.11167
20	7	3.971185	-0.18336	-0.04525
21	6	4.598425	-0.78182	1.231726
22	1	3.777842	-0.93618	1.927727
23	1	5.003522	-1.75331	0.954404
24	6	4.505164	-0.79961	-1.34318
25	1	4.246133	-1.85609	-1.3034
26	1	3.931388	-0.32943	-2.14087
27	6	5.650064	0.136001	1.833601
28	1	5.218822	1.0971	2.124162
29	1	6.038863	-0.33999	2.736071
30	1	6.488583	0.311506	1.158984
31	6	5.995209	-0.58655	-1.53807
32	1	6.257142	0.473875	-1.54268
33	1	6.595712	-1.10387	-0.78918
34	1	6.261029	-0.99776	-2.51395
35	8	-0.30814	2.148559	-0.09295
36	7	-5.03503	0.958704	-0.03929
37	7	-2.42559	-1.43607	0.060378
38	7	-2.58773	0.805495	-0.03719
39	6	0.355089	3.427028	-0.13715
40	1	0.972761	3.567648	0.751518
41	1	0.955781	3.515169	-1.04405
42	1	-0.44413	4.16322	-0.15113
43	1	4.244025	0.80169	-0.06575
44	1	-5.08973	1.971931	-0.08501

(b) in excited state

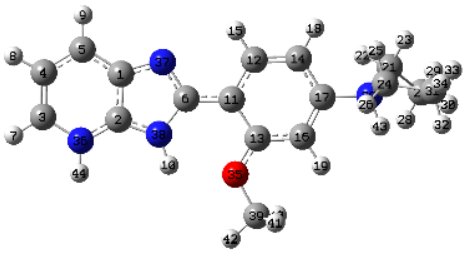

Center Number	Atomic Number	Coordinates (Angstroms) X	Y	Z
1	6	-3.73327	-1.07921	0.037402
2	6	-3.85158	0.333395	-0.0161
3	6	-6.19951	0.194573	-0.01235
4	6	-6.13002	-1.18626	0.041005
5	6	-4.9115	-1.87506	0.067411
6	6	-1.72901	-0.25005	0.007662
7	1	-7.12778	0.744693	-0.0337
8	1	-7.06466	-1.73141	0.062251
9	1	-4.86141	-2.95395	0.108597
10	1	-2.32472	1.805057	-0.06738
11	6	-0.3085	-0.19571	0.0018
12	6	0.429303	-1.40663	0.033713
13	6	0.455216	1.042889	-0.03541
14	6	1.805601	-1.4114	0.024261
15	1	-0.11737	-2.33769	0.064706
16	6	1.855905	1.026978	-0.04405
17	6	2.511813	-0.18907	-0.01547
18	1	2.335475	-2.35467	0.051646
19	1	2.410071	1.954432	-0.07584
20	7	3.983299	-0.20336	-0.0504
21	6	4.61383	-0.88905	1.187492
22	1	3.786781	-1.18428	1.828428
23	1	5.110658	-1.78724	0.826474
24	6	4.500092	-0.76491	-1.38519
25	1	4.246341	-1.8238	-1.38639
26	1	3.916467	-0.26254	-2.15531
27	6	5.562711	0.044517	1.918115
28	1	5.044233	0.934684	2.281404
29	1	5.960834	-0.48592	2.78536
30	1	6.405385	0.348621	1.295048
31	6	5.9871	-0.52894	-1.57784
32	1	6.233713	0.535039	-1.55738
33	1	6.59607	-1.0546	-0.84168
34	1	6.256856	-0.9136	-2.56342
35	8	-0.26293	2.156295	-0.05942
36	7	-5.04824	0.965518	-0.04249
37	7	-2.42695	-1.41515	0.05027
38	7	-2.60478	0.833803	-0.03339
39	6	0.363516	3.462946	-0.09743
40	1	0.983235	3.599546	0.788958
41	1	0.951441	3.561472	-1.01032
42	1	-0.461	4.168592	-0.0978
43	1	4.285065	0.773411	-0.02243
44	1	-5.11571	1.974047	-0.08394

Table D21: XYZ coordinate of optimized DC3 of DEAMPIP-b in the ground state in water.

(a) in ground state

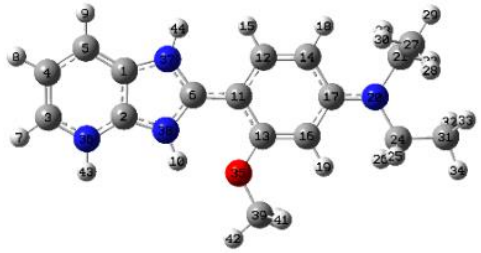

Center Number	Atomic Number	Coordinates (Angstroms) X	Y	Z
1	6	3.783897	-1.02812	-0.06572
2	6	3.77103	0.370966	0.030696
3	6	6.1063	0.419591	0.071251
4	6	6.155181	-0.95575	-0.0207
5	6	4.980785	-1.71927	-0.09219
6	6	1.648005	-0.30706	-0.05285
7	1	6.982596	1.046915	0.126605
8	1	7.121302	-1.43924	-0.03802
9	1	5.015948	-2.79814	-0.16535
10	1	2.099337	1.72592	0.103442
11	6	0.239259	-0.28028	-0.08265
12	6	-0.50768	-1.48325	-0.20815
13	6	-0.51378	0.93536	0.01362
14	6	-1.8711	-1.50263	-0.24898
15	1	0.006007	-2.43395	-0.2775
16	6	-1.89208	0.924463	-0.02548
17	6	-2.6263	-0.28613	-0.17518
18	1	-2.3651	-2.45681	-0.33755
19	1	-2.41488	1.859781	0.067735
20	7	-3.97819	-0.28079	-0.24694
21	6	-4.74115	-1.54158	-0.26026
22	1	-5.69253	-1.3461	-0.74742
23	1	-4.22624	-2.25587	-0.90125
24	6	-4.70514	1.004931	-0.10308
25	1	-4.56511	1.376121	0.918831
26	1	-4.23538	1.724198	-0.77679
27	6	-4.97623	-2.12757	1.134734
28	1	-5.53671	-1.43261	1.764427
29	1	-5.55405	-3.05155	1.050731
30	1	-4.0341	-2.35897	1.636943
31	6	-6.19375	0.96438	-0.4275
32	1	-6.38179	0.641454	-1.45371
33	1	-6.76173	0.329843	0.25471
34	1	-6.57901	1.981442	-0.32552
35	8	0.207021	2.073451	0.150816
36	7	4.909786	1.068712	0.096267
37	7	2.455044	-1.40285	-0.11532
38	7	2.478444	0.783983	0.038886
39	6	-0.45981	3.345476	0.274595
40	1	-1.04865	3.554712	-0.6197
41	1	-1.09144	3.357952	1.164131
42	1	0.337261	4.077486	0.374539
43	1	4.896227	2.083234	0.1637
44	1	2.131698	-2.35797	-0.17276

(b) in excited state

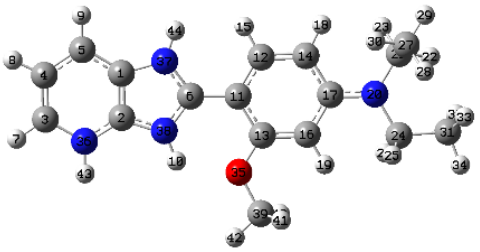

Center Number	Atomic Number	Coordinates (Angstroms) X	Y	Z
1	6	3.800541	-1.01537	-0.04577
2	6	3.79576	0.365302	0.022435
3	6	6.144456	0.397502	0.074979
4	6	6.170412	-0.97883	0.007648
5	6	4.999134	-1.75919	-0.05547
6	6	1.675782	-0.28691	-0.05646
7	1	7.035774	1.003624	0.123727
8	1	7.138752	-1.46112	0.004381
9	1	5.017085	-2.83681	-0.10699
10	1	2.121992	1.732178	0.062587
11	6	0.212924	-0.26877	-0.09705
12	6	-0.50423	-1.46496	-0.23445
13	6	-0.52605	0.945684	0.000919
14	6	-1.88325	-1.49114	-0.28051
15	1	0.013821	-2.41126	-0.31199
16	6	-1.91065	0.933307	-0.04402
17	6	-2.62848	-0.28074	-0.19017
18	1	-2.37076	-2.44645	-0.38617
19	1	-2.43675	1.867719	0.041206
20	7	-3.99837	-0.28408	-0.23813
21	6	-4.75242	-1.54262	-0.28123
22	1	-5.70471	-1.33798	-0.76161
23	1	-4.22866	-2.24691	-0.92417
24	6	-4.73074	0.993684	-0.09627
25	1	-4.53421	1.379425	0.911817
26	1	-4.28677	1.701019	-0.80081
27	6	-4.98617	-2.14396	1.114558
28	1	-5.54443	-1.45636	1.752213
29	1	-5.56702	-3.0623	1.00546
30	1	-4.04182	-2.38518	1.605974
31	6	-6.23202	0.940762	-0.34072
32	1	-6.47251	0.618905	-1.35564
33	1	-6.75791	0.305506	0.372947
34	1	-6.61258	1.956772	-0.21825
35	8	0.198169	2.077682	0.138227
36	7	4.947755	1.095177	0.084213
37	7	2.462851	-1.38119	-0.09341
38	7	2.490558	0.786248	0.015749
39	6	-0.46665	3.351233	0.268972
40	1	-1.05221	3.567143	-0.62598
41	1	-1.09954	3.358354	1.157769
42	1	0.331921	4.080206	0.375497
43	1	4.941223	2.105029	0.128738
44	1	2.134169	-2.33601	-0.13977

Table D22: XYZ coordinate of optimized TC of DEAMPIP-b in water.

(a) in ground state

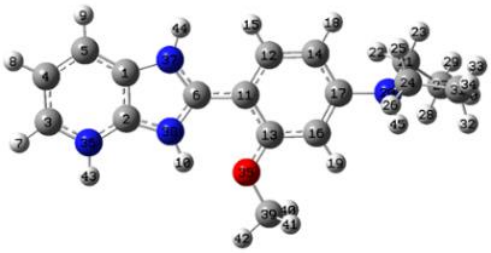

(b) in excited state

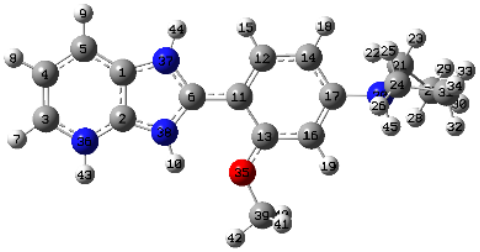

Center Number	Atomic Number	Coordinates (Angstroms) X	Y	Z
1	6	-3.80812	-1.06472	0.056543
2	6	-3.82497	0.329628	-0.02232
3	6	-6.15227	0.336726	0.010745
4	6	-6.17514	-1.04745	0.086818
5	6	-4.99176	-1.78616	0.112315
6	6	-1.70268	-0.30866	-0.01281
7	1	-7.04472	0.943956	-0.00903
8	1	-7.13295	-1.5457	0.12743
9	1	-5.00058	-2.86637	0.172495
10	1	-2.17351	1.716222	-0.11557
11	6	-0.26029	-0.25524	-0.03319
12	6	0.487196	-1.44706	-0.00897
13	6	0.431978	0.986505	-0.07214
14	6	1.867858	-1.43648	-0.01165
15	1	-0.00676	-2.40899	0.007739
16	6	1.830849	0.995497	-0.07568
17	6	2.517961	-0.20463	-0.0427
18	1	2.412155	-2.36984	0.015894
19	1	2.367176	1.933398	-0.10334
20	7	3.994334	-0.16109	-0.04348
21	6	4.600805	-0.7458	1.253881
22	1	3.767482	-0.89821	1.935446
23	1	5.015763	-1.71682	0.990915
24	6	4.560209	-0.78059	-1.32957
25	1	4.317823	-1.84071	-1.28657
26	1	3.994912	-0.32329	-2.14071
27	6	5.634506	0.18463	1.866248
28	1	5.191714	1.144054	2.143956
29	1	6.010296	-0.28395	2.778058
30	1	6.483446	0.361114	1.205328
31	6	6.050102	-0.54512	-1.49479
32	1	6.295826	0.519018	-1.50162
33	1	6.642706	-1.04956	-0.73113
34	1	6.340618	-0.95849	-2.46264
35	8	-0.30474	2.107485	-0.10324
36	7	-4.97911	1.008983	-0.04329
37	7	-2.47023	-1.41403	0.060437
38	7	-2.53487	0.764213	-0.06323
39	6	0.329125	3.409691	-0.13434
40	1	0.936067	3.551817	0.759954
41	1	0.927258	3.513335	-1.03984
42	1	-0.49191	4.120492	-0.14556
43	1	-4.989	2.025374	-0.09741
44	1	-2.12792	-2.36429	0.123813
45	1	4.258974	0.82639	-0.06518

Center Number	Atomic Number	Coordinates (Angstroms) X	Y	Z
1	6	-3.82774	-1.06512	0.067455
2	6	-3.86558	0.333041	-0.05365
3	6	-6.2144	0.286113	-0.08612
4	6	-6.20331	-1.0844	0.033431
5	6	-5.00283	-1.81706	0.115879
6	6	-1.72092	-0.26091	0.038872
7	1	-7.11681	0.873762	-0.15006
8	1	-7.15312	-1.59987	0.064524
9	1	-4.99277	-2.8927	0.210997
10	1	-2.29752	1.757189	-0.13575
11	6	-0.27655	-0.23142	0.020937
12	6	0.464369	-1.402	0.018883
13	6	0.475462	1.010626	0.002512
14	6	1.873989	-1.3941	0.003717
15	1	-0.01602	-2.36976	0.022876
16	6	1.888868	1.016825	-0.01991
17	6	2.573385	-0.18316	-0.01965
18	1	2.393861	-2.34286	0.012846
19	1	2.417998	1.95942	-0.0366
20	7	4.042639	-0.18069	-0.06368
21	6	4.687384	-0.88289	1.160841
22	1	3.867082	-1.18904	1.805479
23	1	5.182232	-1.77361	0.77971
24	6	4.554642	-0.71242	-1.4153
25	1	4.304447	-1.77223	-1.43713
26	1	3.965584	-0.19525	-2.17123
27	6	5.639638	0.042198	1.896845
28	1	5.121245	0.921739	2.284972
29	1	6.050098	-0.50477	2.747858
30	1	6.473767	0.362047	1.27044
31	6	6.039319	-0.46767	-1.609
32	1	6.28265	0.596373	-1.56954
33	1	6.653498	-1.00685	-0.8873
34	1	6.303827	-0.83204	-2.60361
35	8	-0.24319	2.11057	0.00608
36	7	-5.03578	1.000985	-0.13083
37	7	-2.49421	-1.38561	0.119904
38	7	-2.59505	0.79116	-0.0675
39	6	0.343987	3.44517	-0.01823
40	1	0.950366	3.586084	0.875855
41	1	0.931129	3.562712	-0.92844
42	1	-0.50681	4.117446	-0.01826
43	1	-5.06137	2.009468	-0.22045
44	1	-2.14486	-2.32831	0.223587
45	1	4.335635	0.798451	-0.01981

List of publications

1. Light-driven switching between intramolecular proton-transfer and charge-transfer states. **M. Das**, M. Brahma, G. Krishnamoorthy, Journal of Physical Chemistry B, 125, 2021, 2339-2350.
2. Tweaking the proton transfer triggered proton transfer of 3,5-bis(2-hydroxyphenyl)-1H-1,2,4-triazole. **M. Das**, S. Sahu, G. Krishnamoorthy, Physical Chemistry Chemical Physics, 21, 2019, 15669-15677.
3. Chlorin e6 decorated doxorubicin encapsulated chitosan nanoparticles for photo-controlled cancer drug delivery. A. Bhatta, G. Krishnamoorthy, N. Marimuthu, A. Dihingia, P. Manna, H. T. Biswal, **M. Das**, G. Krishnamoorthy, International Journal of Biological Macromolecules, 136, 2019, 951-961. #
4. Proton transfer triggered proton transfer: a self-assisted twin excited state intramolecular proton transfer. S. Sahu, **M. Das**, G. Krishnamoorthy, Physical Chemistry Chemical Physics, 20, 2018, 27131-27139. #
5. Switching between cis- and trans- anions of 2-(2'-hydroxyphenyl)benzimidazole: A molecular rotation perturbed by chemical stabilization. S. Sahu, **M. Das**, G. Krishnamoorthy, Physical Chemistry Chemical Physics, 18, 2016, 11081-11090. #
6. A single fluorophore to address multiple logic gates. S. Sahu, T. B. Sil, **M. Das**, G. Krishnamoorthy, Analyst, 140, 2015, 6114-6123. #
7. Zn^{2+} transport by an ESIPT active fluorophore 2-(2'-hydroxyphenyl) benzoxazole with the help of Host-Guest Interaction. (Manuscript under preparation)
8. Nanoparticle and surfactant controlled switching between proton transfer and charge transfer reaction coordinates. (Manuscript communicated)
9. Controlling the photoswitching of 2-(4′-diethylamino-2′-hydroxyphenyl)-1H-imidazo-[4,5-b]pyridine by pH. (Manuscript communicated)

List of conference proceedings

1. **M. Das**, S. Sahu, G. Krishnamoorthy, Construction of full subtractor and fuzzy logic gate using molecular fluorophore, NSFAC-2015, ICT Mumbai. #

2. **M. Das**, G. Krishnamoorthy, Photophysical Study of 2-(4′-amino-2′-hydroxy phenyl)-1H-imidazo-[4,5-b] pyridine and its derivatives, FICS-2016, IIT Guwahati.

3. **M. Das**, G. Krishnamoorthy, Switching between ESIPT and TICT: Effect of Zn^{2+} on 2-(4′-diethylamino-2′-hydroxyphenyl)-1H-imidazo-[4,5-b] pyridine, ICSIMR-2017, IIT Guwahati. #

4. **M. Das**, G. Krishnamoorthy, Zn^{2+} induced twisted intramolecular charge transfer of amino and ethylated amino derivatives of 2-(2′-Hydroxyphenyl) pyridine imidazole, EAS8-2017, CSIR- NIIST, Kerala. #

5. **M. Das**, G. Krishnamoorthy, Excited state intramolecular proton transfer in 2-(2'-hydroxynaphthalen-1-yl)-1H-benzo[d]imidazole-5-carbonitrile and its sensitivity towards anions, FCS-2017, IIT Guwahati. #

6. **M. Das**, G. Krishnamoorthy, Delivery of Zn^{2+} by an ESIPT active molecule 2-(2'-Hydroxyphenyl) benzoxazole (HPBO) with the help of Host-Guest Interaction, FICS-2018, IIT Guwahati.

 # = not part of thesis